# A YEAR IN REVIEW: DISCUSSIONS IN IMMUNOLOGICAL MEMORY

EDITED BY: Scott N. Mueller
PUBLISHED IN: Frontiers in Immunology

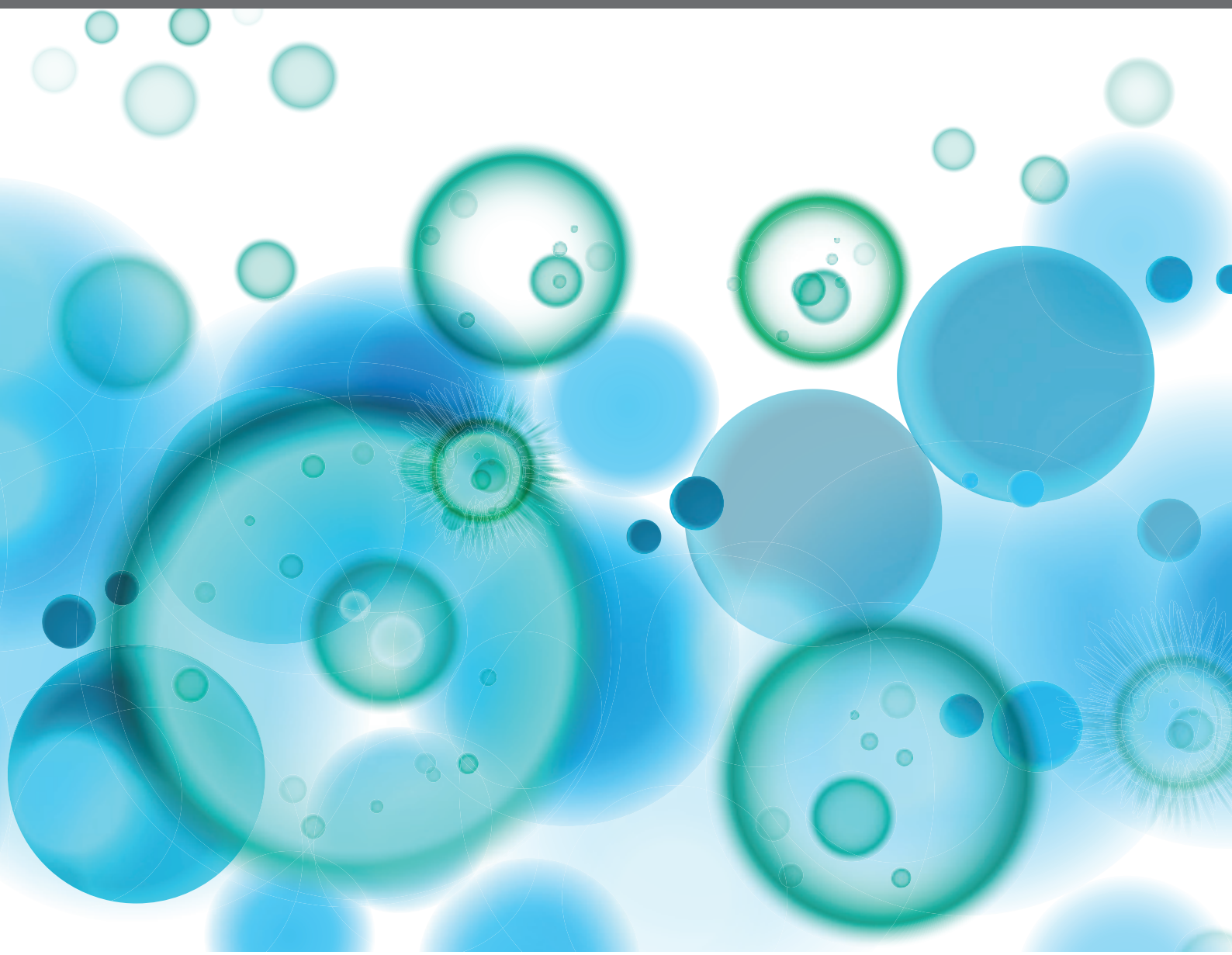

frontiers Research Topics

ISSN 1664-8714
ISBN 978-2-83250-781-0
DOI 10.3389/978-2-83250-781-0

## About Frontiers

Frontiers is more than just an open-access publisher of scholarly articles: it is a pioneering approach to the world of academia, radically improving the way scholarly research is managed. The grand vision of Frontiers is a world where all people have an equal opportunity to seek, share and generate knowledge. Frontiers provides immediate and permanent online open access to all its publications, but this alone is not enough to realize our grand goals.

## Frontiers Journal Series

The Frontiers Journal Series is a multi-tier and interdisciplinary set of open-access, online journals, promising a paradigm shift from the current review, selection and dissemination processes in academic publishing. All Frontiers journals are driven by researchers for researchers; therefore, they constitute a service to the scholarly community. At the same time, the Frontiers Journal Series operates on a revolutionary invention, the tiered publishing system, initially addressing specific communities of scholars, and gradually climbing up to broader public understanding, thus serving the interests of the lay society, too.

## Dedication to Quality

Each Frontiers article is a landmark of the highest quality, thanks to genuinely collaborative interactions between authors and review editors, who include some of the world's best academicians. Research must be certified by peers before entering a stream of knowledge that may eventually reach the public - and shape society; therefore, Frontiers only applies the most rigorous and unbiased reviews.
Frontiers revolutionizes research publishing by freely delivering the most outstanding research, evaluated with no bias from both the academic and social point of view. By applying the most advanced information technologies, Frontiers is catapulting scholarly publishing into a new generation.

## What are Frontiers Research Topics?

Frontiers Research Topics are very popular trademarks of the Frontiers Journals Series: they are collections of at least ten articles, all centered on a particular subject. With their unique mix of varied contributions from Original Research to Review Articles, Frontiers Research Topics unify the most influential researchers, the latest key findings and historical advances in a hot research area! Find out more on how to host your own Frontiers Research Topic or contribute to one as an author by contacting the Frontiers Editorial Office: frontiersin.org/about/contact

# A YEAR IN REVIEW: DISCUSSIONS IN IMMUNOLOGICAL MEMORY

Topic Editor:
**Scott N. Mueller,** The University of Melbourne, Australia

**Citation:** Mueller, S. N., ed. (2022). A Year in Review: Discussions in Immunological Memory. Lausanne: Frontiers Media SA. doi: 10.3389/978-2-83250-781-0

# Table of Contents

frontiers in Immunology

ORIGINAL RESEARCH
published: 17 March 2021
doi: 10.3389/fimmu.2021.613810

# Göttingen Minipigs as a Model to Evaluate Longevity, Functionality, and Memory of Immune Response Induced by Pertussis Vaccines

*Céline Vaure, Véronique Grégoire-Barou, Virginie Courtois, Emilie Chautard, Cyril Dégletagne and Yuanqing Liu**

*Research and External Innovation, Sanofi Pasteur, Marcy l'Etoile, France*

Evaluation of the short-term and long-term immunological responses in a preclinical model that simulates the targeted age population with a relevant vaccination schedule is essential for human vaccine development. A Göttingen minipig model was assessed, using pertussis vaccines, to demonstrate that vaccine antigen-specific humoral and cellular responses, including IgG titers, functional antibodies, Th polarization and memory B cells can be assessed in a longitudinal study. A vaccination schedule of priming with a whole cell (DTwP) or an acellular (DTaP) pertussis vaccine was applied in neonatal and infant minipigs followed by boosting with a Tdap acellular vaccine. Single cell RNAsequencing was used to explore the long-term maintenance of immune memory cells and their functionality for the first time in this animal model. DTaP but not DTwP vaccination induced pertussis toxin (PT) neutralizing antibodies. The cellular immune response was also characterized by a distinct Th polarization, with a Th-2-biased response for DTaP and a Th-1/Th-17-biased response for DTwP. No difference in the maintenance of pertussis-specific memory B cells was observed in DTaP- or DTwP-primed animals 6 months post Tdap boost. However, an increase in pertussis-specific T cells was still observed in DTaP primed minipigs, together with up-regulation of genes involved in antigen presentation and interferon pathways. Overall, the minipig model reproduced the humoral and cellular immune responses induced in humans by DTwP vs. DTaP priming, followed by Tdap boosting. Our data suggest that the Göttingen minipig is an attractive preclinical model to predict the long-term immunogenicity of human vaccines against *Bordetella pertussis* and potentially also vaccines against other pathogens.

**Keywords: Göttingen minipigs, longitudinal study, pertussis vaccines, antibody response, T helper polarization, memory cells, single cell RNA sequencing**

OPEN ACCESS

***Edited by:***
*Peter Katsikis, Erasmus University Rotterdam, Netherlands*

***Reviewed by:***
*Rustom Antia, Emory University, United States*
*Matthew Williams, The University of Utah, United States*

****Correspondence:***
*Yuanqing Liu*
*yuanqing.liu@sanofi.com*

***Specialty section:***
*This article was submitted to Immunological Memory, a section of the journal Frontiers in Immunology*

***Received:*** *03 October 2020*
***Accepted:*** *22 February 2021*
***Published:*** *17 March 2021*

***Citation:***
*Vaure C, Grégoire-Barou V, Courtois V, Chautard E, Dégletagne C and Liu Y (2021) Göttingen Minipigs as a Model to Evaluate Longevity, Functionality, and Memory of Immune Response Induced by Pertussis Vaccines. Front. Immunol. 12:613810. doi: 10.3389/fimmu.2021.613810*

## INTRODUCTION

Although the mouse is traditionally the species of choice for preclinical evaluation of vaccines, the results have limited translatability to humans since they do not always predict results in humans (1, 2). To overcome the limitation of using only mice, non-human primates (NHPs) can be used. But ethical and financial concerns, and the availability of suitable animal facilities for NHPs, limit

their use in preclinical studies. Also it is difficult to perform suitable-sized NHP studies to evaluate pediatric vaccines in neonatal and infant animals. There are as well differences in vaccine responses between humans and NHPs, notably in newborns (3).

Pigs, and more particularly minipigs, offer many advantages as an alternative model for preclinical vaccine evaluation as they can be housed in large groups in standard animal facilities, despite being large animals. Delivery routes commonly used in humans can be used; and large volumes of blood can be drawn, unlike in mice (4, 5). Pigs are a large animal model that can be used to evaluate vaccines in special populations such as in neonates (5). Mimicking pediatric primary series followed by adolescent booster vaccination is more practical in minipigs than NHPs because pigs have relatively large litters; and are considered to be neonates to infant before 1 month of age and adolescent between 3 and 5 months of age, whereas NHPs are considered to be adolescent between 3 and 4 years of age (6). Longitudinal follow up of the immune response can be performed in the same individual animals, unlike in mice. The pig immune system is probably the best characterized system, after murine and primate immune systems and its development is very similar to that of humans (4, 7–9). The porcine immune system has been reported to be closer to humans than the mouse system. For example, the conservation of many immune-related gene families has been reported to be three-times greater, in terms of synteny, between humans and pigs than between humans and mice. The overall identity with human immune proteins is significantly higher in pigs than in mice and there is an increasing number of tools available to conduct immunological studies in pigs (10, 11). Minipigs have been used as an immunosafety model, showing good similarity with effects seen in humans, suggesting a good translatability to humans (7).

The objective of this study was to evaluate minipigs as a preclinical model for assessing short-term and long-term vaccine immunogenicity, using pertussis vaccines as an example.

Introduction of whole cell pertussis vaccine (wP) combined with diphtheria and tetanus antigens (DTwP) in the 1940's, followed by a less reactogenic acellular pertussis vaccine (aP) also combined with diphtheria and tetanus antigens (DTaP) in the 1990's led to a drastic decline in the incidence of reported cases of whooping cough. Despite of the fact that both wP and aP vaccines elicit an antibody response in vaccinees, DTwP or DTaP vaccines do not elicit the same profile of immune responses. For instance, DTwP induces T helper (Th)-1/Th-17 effector cells whereas DTaP induces Th-2 cells (12). Moreover, some reports suggest a difference in the longevity and memory of responses elicited by DTwP and DTaP vaccines (13).

We compared the humoral and cellular immune responses in Göttingen minipigs after priming with DTwP or DTaP, followed by a boost with modified acellular Tdap vaccine, 3 months later. The antibody response was monitored by Meso Scale Discovery (MSD) technology, functional antibodies by a pertussis toxin (PT) neutralization assay, and the Th profile and memory B cells by FLUOROSPOT. Finally, we, for the first time, used single cell RNA sequencing (scRNAseq) of minipig peripheral blood mononuclear cells (PBMCs) to phenotype the immune cells and explore their long term functionality after immunization. The results from these various evaluations provided a comprehensive, long-term study of the immune response elicited by the pertussis vaccines in the Göttingen minipig.

**Abbreviations:** DTwP, whole cell pertussis vaccine; DTaP, acellular pertussis vaccine; Tdap, booster acellular pertussis vaccine; SCs, secreting cells; MSD, MesoScaleDiscovery; HD, human dose; scRNAseq, single cell RNA sequencing; DT, diphteria toxoid; TT, tetanus toxoid; PT, pertussis toxin; PTxd, pertussis toxoid; PRN, pertactin; FIM, fimbria; FHA, filamentous hemagglutinin.

# MATERIALS AND METHODS

## Vaccines

The whole cell pertussis vaccine (DTwP; D.T.COQ/D.T.P®, Sanofi-Pasteur Ltd.) contained ≥4 I.U. of heat-inactivated *Bordetella pertussis* (Bp), ≥60 I.U. of tetanus toxoid (TT) and ≥30 I.U of diphtheria toxoid (DT). The five-component acellular pertussis vaccine (DTaP; DTaP5cp-IPV-Hib, PEDIACEL®, Sanofi-Pasteur Ltd.), contained 20 μg chemically-detoxified pertussis toxin (PTxd), 20 μg filamentous hemagglutinin (FHA), 3 μg pertactin (PRN), 5 μg fimbriae 2/3 (FIM), 5 Lf TT, 15 Lf DT and 1.5 mg aluminum phosphate per dose. The modified acellular pertussis booster vaccine (Tdap) contained 10 μg PTxd, 5 μg FHA, 5 μg PRN, 7.5 μg FIM, 5 Lf TT, 2 Lf DT and 1.5 mg aluminum phosphate per dose.

## Animals

Pregnant Göttingen minipig sows were purchased from Ellegaard Göttingen Minipigs A/S and their piglets were born in Sanofi Pasteur's animal facilities. Piglets were labeled individually using transponders and visual identification. They were housed with their mother until weaning on D36. Males and females were then housed separately. This project was approved by Sanofi Pasteur's animal ethics committee and complied with European guidelines for animal care.

## Study Schedules

In the first study, 4–6-day old neonate minipigs from three different litters received an intramuscular (IM) injection of either DTaP or DTwP at ½ human dose (HD) (seven animals per group) (**Figure 1A**). A second injection of 1HD of DTaP or DTwP was administered on D22. Both groups were boosted with 1 HD of Tdap 3 months later (M4). A negative control group of three minipigs received three injections of tris buffer saline (TBS). Minipigs of different sexes and litters were allocated to the groups to minimize any genetic or gender effect on immune response to vaccination (14, 15).

In the second study, in which memory B cell assessments and scRNAseq analyses were performed, 3-week old infant minipigs from four different litters received an IM injection with 1 HD of either DTaP or DTwP (five animals per group) (**Figure 1B**). A second injection of 1 HD of DTaP or DTwP was administered 4 weeks later (D28). Both groups were boosted with 1 HD of Tdap at month 4 (M4). A negative control group of three minipigs received TBS on D0, D28 and M4.

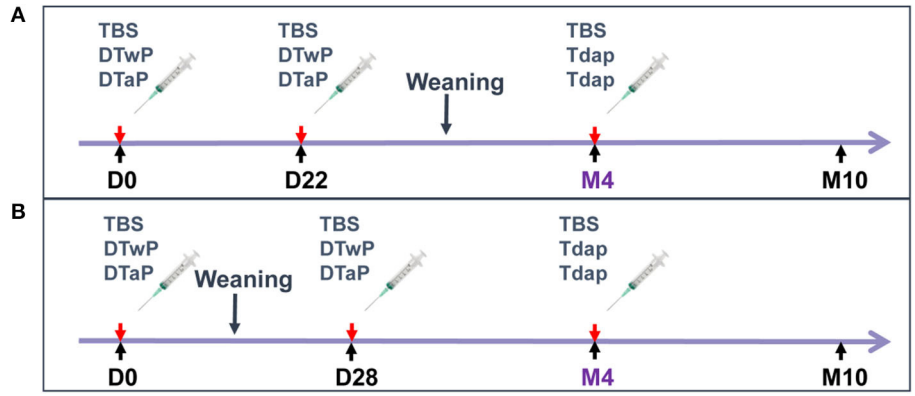


**FIGURE 1 |** Study design. **(A)** First study: 4–6-day-old neonate minipigs from three different litters received intramuscular (IM) injections of DTaP or DTwP at ½ human dose (HD) or TBS (seven animals per group), followed by a second IM injection of 1HD of DTaP, DTwP or TBS on D22 and a booster injection with 1 HD of Tdap or TBS 3 months later (M4). **(B)** Second study: 3-week old infant minipigs from four different litters received an IM injection with 1 HD of DTaP or DTwP or TBS (five animals per group), followed by a second IM injection of 1 HD of DTaP or DTwP or TBS 4 weeks later (D28) and a booster injection with 1 HD of Tdap or TBS at month 4 (M4).

## Blood Samples

Blood samples were collected from the cranial vena cava under anesthesia with IM Zoletil 50® (0.2 mL/kg) in serum-separation tubes (BD Vacutainer # BD366882) for antibody assessment or in sodium heparin plasma tubes (BD Vacutainer # BD368480) for PBMC isolation for the analysis of T cell and memory B cell FLUOROSPOT and scRNAseq assays.

## Analytical Assays

### IgG Assay

Antigen-specific Immunoglobulin G (IgG) titers were determined using MSD electrochemical luminescence (MSD-ECL) assays according to the manufacturer's instructions. The MSD-ECL plates were printed with FHA, FIM2/3, PRN, PTxd, TT, DT antigens (multi-spot® 96-well-7 spot plates) by the manufacturer (Meso Scale Discovery). Serum IgG was detected using goat anti-pig IgG (Fc) biotin conjugate (Biorad #AAI41B) followed by Streptavidin-Sulfo-Tag® (MSD #R32AD-1).

### Pertussis Toxin Neutralization Antibody Titers

PT neutralizing antibody titers were assessed in a Chinese hamster ovary (CHO) cell assay, as previously described (16). Briefly, CHO cells were incubated for 48 h with a mixture of sera and PT (pre-incubated for 2–3 h). CHO cells were then fixed with methanol and stained with Giemsa before reading the cell clusters. Samples with titers below the assay cut-off of 20 were arbitrarily attributed a titer of 10 (50% of the cut-off).

### Memory B Cell FLUOROSPOT

PBMCs were stimulated for 4 days with R848 (InvivoGen #tlrl-r848-5) and recombinant porcine IL-2 (R&Dsystems #652-P2) and then incubated for 5 h on ELISPOT plates (Millipore #S5EJ104I07) previously coated with a pool of pertussis antigens (PTxd, PRN, FIM2/3, FHA), purified anti-porcine IgG mAb MT421 (Mabtech #3151-3-250) as positive control or medium alone as negative control. Memory B cells were detected using biotinylated anti-porcine IgG mAb MT424 (Mabtech # 3151-6-250) followed by streptavidin-PE (Southern Biotech #7100-09L). Positive spots were counted with an automatic ELISPOT fluorescent plate reader (Microvision). Data shown after correction for background by subtraction of the counts from negative control wells.

### T Cell FLUOROSPOT

ELISPOT plates (Millipore #S5EJ104I07) were coated with mouse anti-pig IFN-γ (ThermoFisher #MP700), goat anti-porcine IL-4 (R&Dsystems #AF654), or rabbit anti-swine IL-17A (KingFisher Biotech #PB0158S-100). After blocking with RPMI medium supplemented with glutamine, streptomycin, penicillin, β mercaptoethanol and 10% fetal bovine serum, PBMCs were added and stimulated for 48 h with a pool of pertussis antigens (PTxd, PRN, FIM2/3) or heat inactivated whole cell *B. pertussis* (hk*Bp*). IFN-γ, IL-4 and IL-17 secreting cells were detected using biotin mouse anti-pig IFN-γ (BD Biosciences #559958), goat anti-porcine IL-4 (R&Dsystems #BAF654) and rabbit anti-swine IL-17A (KingFisher Biotech #PBB0270S-050), respectively, followed by streptavidin-PE (Southern Biotech #7100-09L). Data shown after correction for background by subtracting count from negative control wells.

### Single Cell RNA Sequencing (scRNAseq)

PBMCs from control minipigs and DTaP-primed minipigs were incubated at +37°C for 16 h in a 5% $CO_2$ atmosphere with PBS ($n = 2$ per group) and PBMCs from DTaP-primed minipigs were incubated with a pool of pertussis antigens ($n = 2$). Cells were washed with PBS and the number of live cells was determined with a NucleoCounter NC 200 (Chemometec). The cells were resuspended in PBS with 0.04% BSA to obtain an expected cell recovery population of 10,000 cells per channel, loaded on 10X chip and run on the Chromium Controller system (10XGenomics) to be used directly for single-cell sequencing. scRNAseq libraries were generated with the Chromium Single Cell 3′ v3 assay (10X Genomics, PN-1000075) and sequenced on

the NovaSeq 6000 platform (Illumina, S2 flowcell, # 20012862) to obtain around 30,000 reads per cell.

### *Sample Preprocessing*

The Cellranger Single-Cell Software Suite (v3.0.2) was used to perform sample demultiplexing, alignment to the closest available genome, the pig genome (Sscrofa11.1, Ensembl release 98), barcode assignment for each cell, and gene counting by unique molecular identifier (UMI) counts. Data were analyzed in RStudio (v1.1.383, R v3.6.1) using the Seurat (v3.1.0) package (17). Only cells with at least 500 molecules, 200 unique genes detected, and <20% of reads that mapped to the mitochondrial genome were used. Data were normalized using the scran package (v1.12.1) (18). Variable genes were determined for each sample using Seurat's FindVariableGenes function with default parameters and merged using Seurat integration strategy based on "anchors." Scaled values were calculated using ScaleData function with default settings.

### *Clustering*

Principal component analysis (PCA) was performed on the first 60 principal components (PCs). Clusters in the resulting subspace were then identified using the FindClusters function with the resolution set to 0.6 and mapped using the RunUMAP function. Specific marker genes for clusters were identified using the FindAllMarkers function to identify cell phenotypes. Clusters containing all activated T cells were split according to CD8A, CD8B and CD4 expression to enable CD4 and CD8 activated T cells to be distinguished. A similar strategy based on CD2 expression was used to isolate γδ non-terminally differentiated T cells from other γδ T naive cells. Cell phenotypes were checked by comparing the mean expression of key marker genes in each cell type with the overall mean expression and results were visualized using the corrplot R package (v0.84).

### *Differential Gene Expression and Functional Enrichment Analysis*

Gene expression under different experimental conditions for each cell type was assessed using Seurat FindMarker function, and analyzed using Wilcoxon rank testing. Only genes with absolute log-fold changes higher than 0.2 and adjusted *P*-value <0.05 were retained. Ortholog pig and human genes were determined using the BiomaRt R package (v2.40.3), keeping only 1-to-1 orthologs for which only one copy was found in each species, and *Sus scrofa* gene names were replaced by their corresponding human Ensembl ortholog identifiers before being processed in Ingenuity Pathway Analysis (IPA) software using default parameters (19, 20).

## Statistical Analysis

The normal distribution of log-transformed data was confirmed before analysis. Differences between TBS- and DTaP- or DTwP-primed groups, as well as differences between DTaP- and DTwP-primed groups were assessed with one-way analysis of variance (ANOVA). Analyses were not performed when there were more than 50% of non-responders. The residuals were assessed to verify the model's validity. All analyses were done on SAS v9.4®. Differences were considered significant at a $p$-value $< 0.05$.

# RESULTS

## Antigen Specific IgG Responses Can Be Monitored in Minipigs Immunized With DTaP, DTwP and Tdap Vaccines

Both DTaP- and DTwP-priming induced statistically-significant IgG responses against non-pertussis antigens (TT and DT) after the first injection and against the pertussis antigens (PT, PRN, FIM2/3, FHA) after the second injection, as compared to the TBS control group (**Figure 2**). DTaP priming induced a significantly more rapid and stronger anti-PT IgG response ($p < 0.001$), and to a lesser extent, the anti-FHA IgG response ($p < 0.05$), whereas DTwP priming induced a more rapid and stronger anti-FIM IgG response ($p < 0.05$ or $< 0.001$, depending on the time-point). The anti-PRN IgG responses were similar in the two groups. A boost by Tdap increased the IgG titers against all antigens in both DTaP and DTwP primed groups.

## PT Neutralizing Antibodies Were Measured Post-boost in DTaP- but Not DTwP-Primed Minipigs

To evaluate the functionality of pertussis-specific antibodies, PT neutralizing antibodies were assessed. Two vaccinations in neonatal minipigs (before weaning) induced no detectable PT neutralizing antibody in either group (**Figure 3**). After boosting minipigs with Tdap, PT neutralizing antibodies were detected in those primed with DTaP, but not in those primed with DTwP. The PT neutralizing antibodies peaked 1 month after the Tdap boost and decreased to a low level at M8 and then stabilized for the following 2 months. PT neutralization titers were below the limit of detection in the control (TBS) group. No statistical analyses were performed between groups because of the high number of non responders in the TBS and DTwP groups.

When 3-week old infant minipigs were primed, the induction of the IgG and PT neutralization responses was more rapid than in neonatal minipigs (data not shown). Particularly, the first prime injection induced IgG responses against all antigens. PT neutralizing antibodies were induced after the 2nd prime in DTaP-primed minipigs, reaching a geometric mean titer (GMT) of 90 on day 42 and 640 at 3-weeks post-Tdap boost, compared with GMTs of <20 and 210, respectively, in neonatal DTaP-primed minipigs. The induced PT neutralization response reached a titer of 120 from M5 to M7 after the Tdap boost in DTwP-primed minipigs.

## Pertussis-Specific Memory B Cells Were Detected Up to at Least 6 Months Post-Tdap Boost

The pertussis-specific circulating memory B cells were assessed in the minipigs that received their first dose of vaccine at 3-weeks old. Memory B cells, specific for a pool of pertussis antigens (PTxd, PRN, FIM2/3, FHA) were found to persist at a low but detectable level 6 months after the Tdap boost (**Figure 4**).

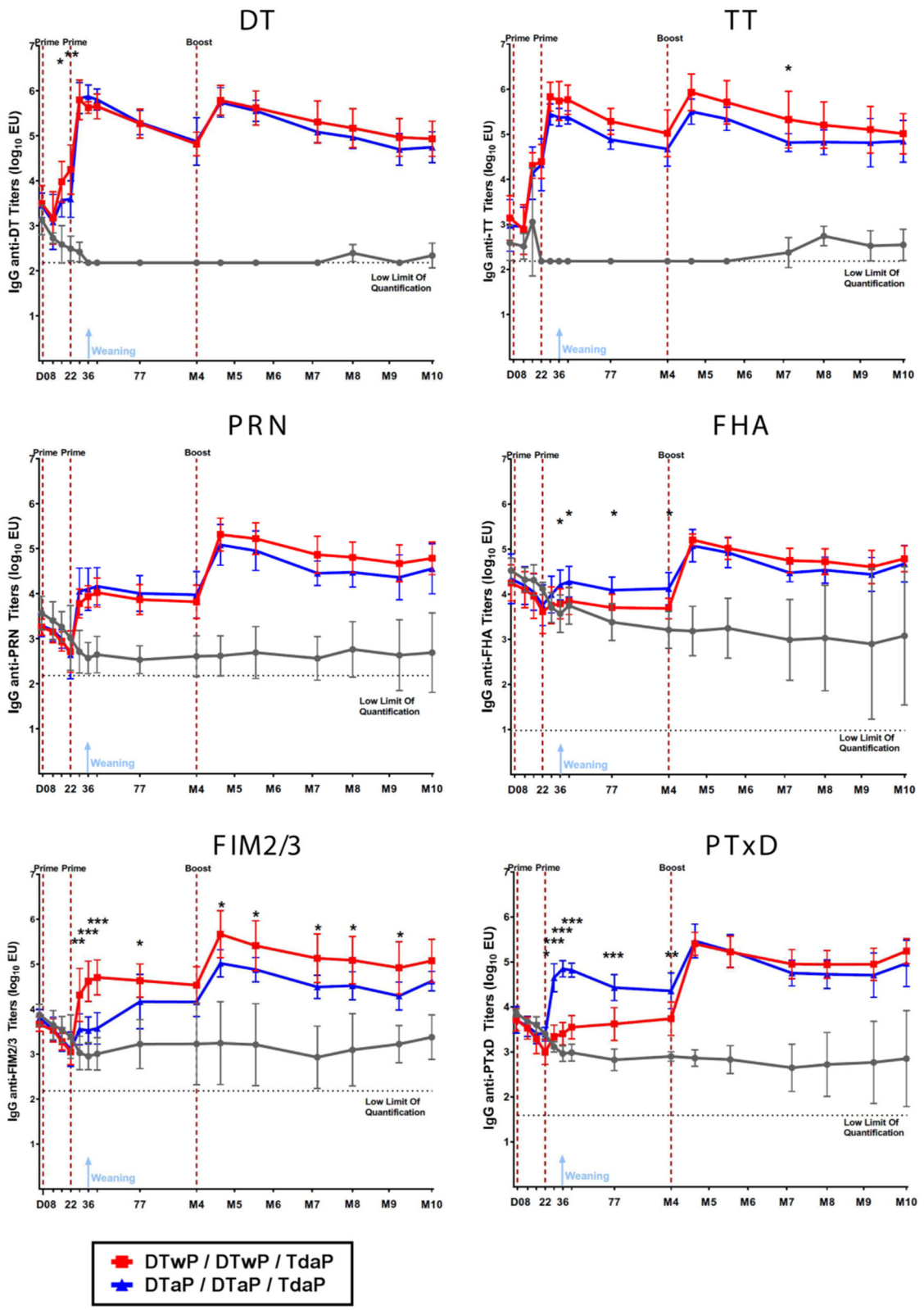


**FIGURE 2 |** IgG titers against DT, TT, PRN, FHA, FIM2/3 and PT measured by the MSD-ECL assay in neonatal minipigs primed with either DTwP ($n = 7$) or DTaP ($n = 7$) and boosted with Tdap vaccine and in control (TBS-injected) minipigs ($n = 3$). Data are shown as $\log_{10}$ geometric mean titers with standard deviations. *$p$-value $< 0.05$, **$p$-value $< 0.01$, and ***$p$-value $< 0.001$ for comparison between the DTaP- and DTwP primed groups.

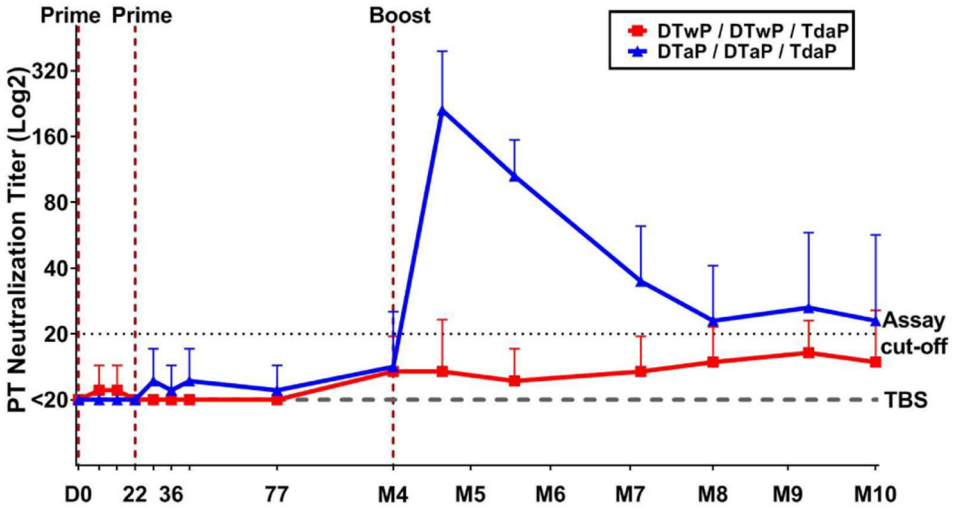


**FIGURE 3 |** Functional antibodies measured by PT neutralization assay in neonatal minipigs primed with either DTwP ($n = 7$) or DTaP ($n = 7$) and boosted with Tdap vaccine. Data are shown as geometric mean titers with standard deviations for the DTwP and DTaP groups. The geometric mean titer for the control group ($n = 3$) that received TBS injections is shown (dashed line). All values below the assay cut-off were arbitrarily attributed a titer of 50% of the cut-off value.

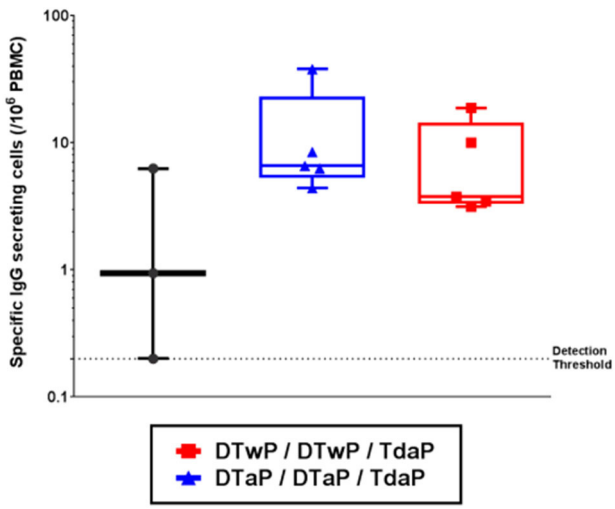


**FIGURE 4 |** Memory B cells specific for a pool of pertussis antigens (PTxd, PRN, FIM2/3, FHA) measured by FLUOROSPOT 6 months post-Tdap boost in infant minipigs primed with either DTwP or DTaP vaccine (first dose at 3-weeks old) and boosted with Tdap vaccine. Data shown as box and whisker plots with median and min/max ($n = 5$ for DTwP and DTaP groups and $n = 3$ for TBS group).

No statistical difference was found between DTwP- and DTaP-primed groups.

## DTaP and DTwP Priming Induced Th-2 and Th-1/Th-17 Biased Profiles, Respectively, That Were Sustained After a Tdap Boost

To characterize the Th profile induced by DTaP- and DTwP-priming in the minipigs, the number of IFN-γ, IL-4, and IL-17 secreting cells were counted in a FluoroSpot assay to determine Th-1, Th-2, and Th-17 responses, respectively. DTaP-priming induced mainly a Th-2 biased response, whereas DTwP-priming induced a Th-1/Th-17 biased response to the pool of pertussis antigens (**Supplementary Figure 1**). This Th-2 vs. Th-1/Th-17 bias persisted after a Tdap boost (**Figure 5A**). While the IL-4 and IFN-γ responses to the pool of pertussis antigens were stable, the IL-17 response in the DTwP primed group appeared to be transient after Tdap boost, and decreased to baseline level at M10, that is, 6 months post boost.

Following stimulation with hk*Bp*, both the IFN-γ and IL-17 responses were significantly stronger in DTwP-primed minipigs than in DTaP-primed minipigs ($p < 0.05$), with a peak at M6 to M7, and little or no decrease up to M10 (**Figure 5B**). The frequency of IL-4 secreting cells was at a similarly low level in both the DTwP- and DTaP-primed groups.

In addition, we observed a consistent Th-2 profile in the DTaP-primed infant minipigs, with a higher level of response (geometric mean titers between 30 and 70 IL-4 secreting cells/$10^6$ PBMCs) than in the DTaP-primed neonatal minipigs. However, we observed a low IFN-γ response in the DTwP-primed group and a few to undetectable number of IL-17-secreting cells in infant minipigs in both the DTwP- and DTaP-primed groups.

## Pertussis-Specific T Cells Were Detected 6 Months Post-Tdap Boost in DTaP-Primed Minipigs by scRNAseq

We used single cell RNA sequencing (scRNAseq) on a 10X Genomics platform to phenotype minipig PBMCs 6 months post-Tdap boost (M10), when T cell and memory B cell FluoroSpot assays were also performed. The final dataset that passed quality control contained 15,286 cells from the TBS control

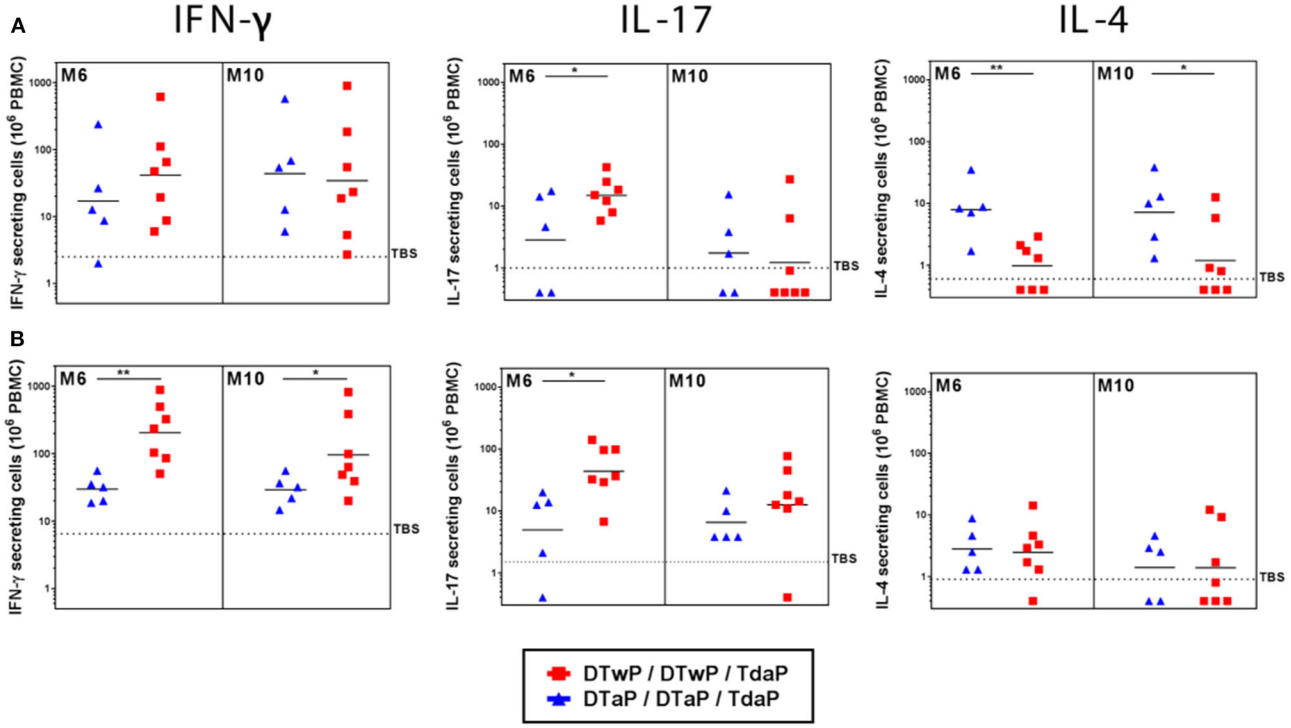


**FIGURE 5 |** IFN-γ (Th-1), IL-17 (Th-17) and IL-4 (Th-2) secreting cells measured by FluoroSpot assay at M6 and M10 on PBMCs from neonatal minipigs primed with either DTwP or DTaP and boosted with Tdap vaccine, stimulated for 48 h with **(A)** a pool of pertussis antigens (PTxd, PRN, FIM2/3) and **(B)** heat-killed B. pertussis (hk*Bp*). Data are shown for DTwP ($n = 7$) and DTaP ($n = 7$) groups as individual and geometric mean titers, after correction for background levels of cytokine secreting cells in the negative control wells (media alone). Data for the control group (TBS, $n = 3$) are shown as the geometric mean titer for all minipigs at all time-points. *$p$-value $< 0.05$ and **$p$-value $< 0.01$ for statistical comparison of DTaP- and DTwP primed groups.

group incubated with medium, 15,189 cells from the DTaP-primed group incubated with medium and 18,421 cells from the DTaP-primed group incubated overnight with the pool of pertussis antigens.

The analysis showed 30 different clusters composed of major immune cell types including $CD4^+$, $CD8^+$and γδ T cells (21, 19, and 34% of all isolated cells, respectively), monocytes (8%) and dendritic cells (DCs, 0.5%), as well as B cells (6%) and natural killer cells (NK, 3.5%) (**Figure 6A**). These populations were identified by their specific gene signature as CD3D and CD3E (T cells), NKG7 (NK cells), MS4A1 i.e., CD20 (B cells), CD14 and FCGR3A i.e., CD16A (monocytes) or FLT3 (DCs) (**Figure 6B**). T cell populations were split according to the expression of CD4 (T $CD4^+$), CD8B and CD8A (T $CD8^+$) as well as TRDC and BLK (γδ T cells). Combinations of specific markers were then used to distinguish subpopulations in $CD4^+$ T cells (naïve, memory $S100A4^+$/SELL, regulatory $FOXP3^+$/$IL2RA^+$), γδ T cells (naïve with no or low CD2 expression, non terminally differentiated $GATA3^-$/$CD2^+$, as well as terminally differentiated $TBX21^+$), B cells (naïve $IGHM^+$, memory $IGHG^+$), monocytes ($CD14^+$ or $CD14^-$) and DCs (plasmacytoid DC $BLNK^+$/$LRP8^+$, and conventional DC $NAV1^+$) (**Figures 6A,B**). Our analysis revealed a high expression of IRF1, ISG15 and STAT1 in some specific clusters of T cell subpopulations that were, therefore, categorized as "activated."

Cell frequencies within a population did not appear to change drastically in the three groups analyzed, but no statistical test was performed to compare between the groups due to the low number of individuals in each group ($n = 2$ per group). However, the numbers of activated T cells ($CD4^+$, $CD8^+$ and γδ T cells) were much higher in the samples from the DTaP-primed group incubated with the pool of pertussis antigens than in those from the DTaP-primed or TBS groups incubated with medium (**Figure 7**).

## Genes Involved in Antigen Presentation and Interferon Pathways Were Up-Regulated in DTaP Primed/Tdap Boosted Minipigs After *in-vitro* Stimulation With Pertussis Antigens

Gene expression within each cell population showed limited quantitative differences between the DTaP-primed group and the TBS control, both incubated with medium, and between the DTaP-primed group incubated with the pool of pertussis antigens and the DTaP-primed group incubated with medium (**Supplementary Figure 2**). In the first comparison, DTaP-primed vs. TBS control, the majority of genes were up-regulated, mainly in the NK cells and monocytes (51 and 35 upregulated genes, respectively), and to a lesser extent in B cells (21

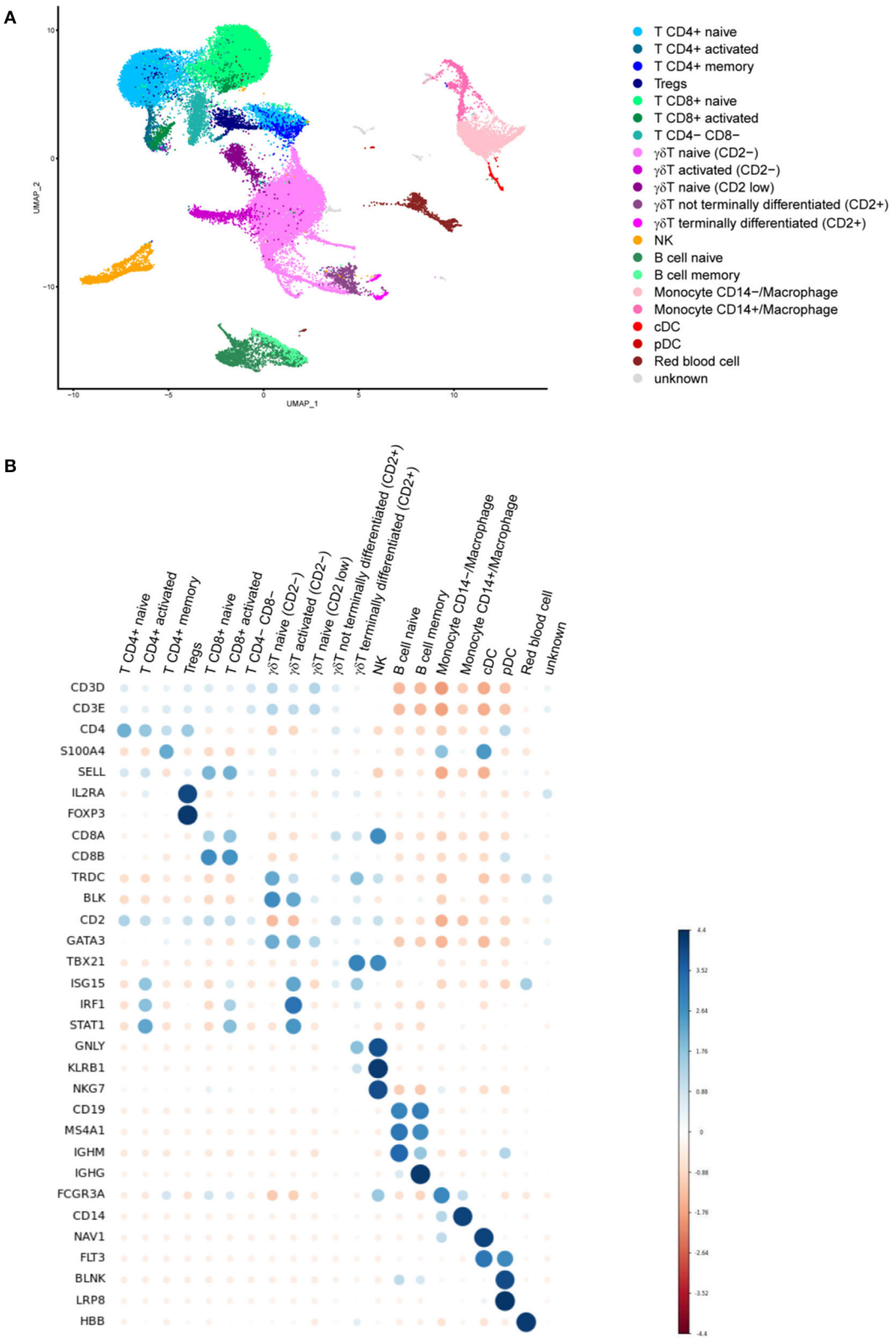


**FIGURE 6 | (A)** Uniform manifold approximation and projection (UMAP) plot showing the results of single cell RNA sequencing (scRNAseq) of minipig PBMC populations. The plot shows scRNAseq results for PBMC immune cells from control minipigs incubated with medium ($n = 2$) and from DTaP-primed minipigs incubated with medium ($n = 2$) or a pool of pertussis antigens (PTxd, PRN, FIM2/3) ($n = 2$). **(B)** Dot plot showing the expression marker genes in each cell population. Blue dots indicate that the expression was higher than the average expression in the entire dataset in this population and red dots indicate that it was lower (MS4A1 = CD20 and FCGR3A = CD16A).

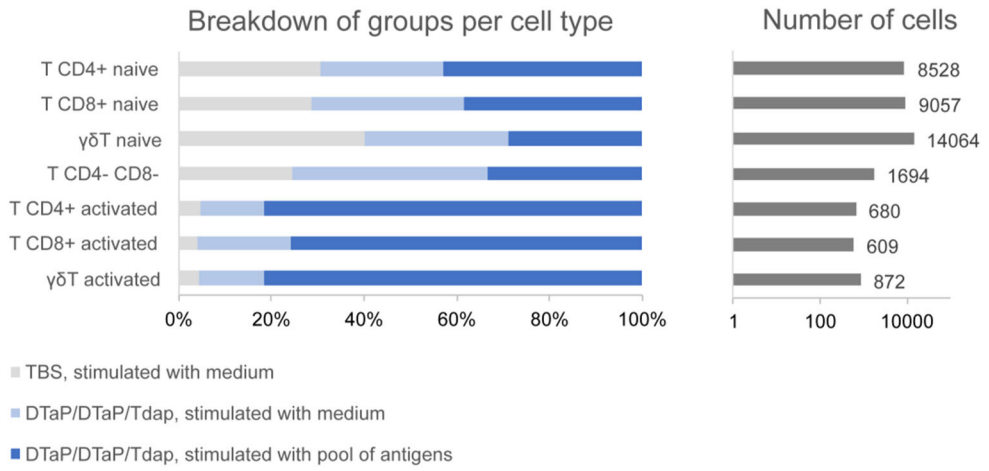


**FIGURE 7 |** Group distribution of activated and non-activated T cell subpopulations within the entire set of T cells obtained by scRNAseq for the control TBS group incubated with medium ($n = 2$), DTaP-primed group stimulated with medium ($n = 2$) and DTaP-primed group stimulated with a pool of pertussis antigens (PTxd, PRN, FIM2/3) ($n = 2$).

upregulated genes). The results from the IPA analysis showed, in NK cells, a coordinated overexpression of genes involved in NK cell signaling ($p$-value adjusted by BH test = 0.002), such as KLRB1, KLRK1, NCR1 (NKp46), PIK3R1 or TYROBP in the DTaP-primed group compared with the TBS control group, when both were incubated overnight with medium. For the second comparison, with DTaP-primed groups incubated with the pool of pertussis antigens vs. medium, there was a majority of down-regulated genes. Among the up-regulated genes, the IPA analysis showed an activation of the antigen presentation pathway ($p$-value adjusted by BH test = 8E-5) in monocytes (CALR, CIITA, HLA-DRA, LMP2, TAP1) and a stimulation of the interferon pathway supported by an increase of STAT1 or IRF1 expression, amongst others, in monocytes, T and γδ T cells ($p$-value adjusted by BH test $< 0.01$). Down-regulated genes for each comparison did not appear to be linked with particular intra cellular pathways.

## DISCUSSION

In this study, we evaluated the Göttingen minipig as a preclinical model for vaccine immunogenicity. This evaluation was based on common readouts such as vaccine antigen-specific IgG and functional antibody titers, the T helper cytokine profile and memory B cell response, as well as the emergent scRNAseq approach to investigate further in depth the immune response. We showed that IgG titers against DT, TT, FHA, FIM, PRN and PT and pertussis toxin neutralizing antibodies, can be measured in minipigs. The responses were shown to be similar, but stronger when the first vaccination dose was administered in infant rather than in neonatal minipigs.

Measurement of total IgG level against vaccine antigens is the only immune assessment accepted by regulatory authorities for licensing acellular pertussis vaccines. We evalutated the IgG titers against the pertussis and non-pertussis antigens in the acellular vaccines in the sera from minipigs. Elevated initial IgG antibody titers against DT, TT, FHA, FIM, PRN and PT were observed on D0 in the control TBS group, which gradually decreased during the first 40 days after birth. These elevated IgG antibodies might be partially due to maternal antibodies acquired by the neonates from colostrum. Due to the epitheliochorial structure of the porcine placenta, piglets are born agammaglobulinemic and depend on receiving antibodies from colostrum which is richer in immunoglobulins, notably IgG, than human colostrum (21, 22). Pertussis-specific antibodies (FHA, FIM, PRN, PT) were detected in the sow sera (data not shown), probably due to the exposure to *B. bronchiseptica* that was present in Ellegaard barriers. Down-selection of the sows free of *B.bronchiseptica* could be a solution to avoid interference by *B.bronchiseptica* carriage to the immune response, but this was not done in our studies. The high anti-PT IgG in the sows was an unexpected finding because *B. pertussis* is thought by many to be the only bacterial species to produce the pertussis toxin. Some authors have reported that *B. bronchiseptica* does not have a PT gene (23), while others have indicated that *B. bronchiseptica* has a PT gene but that it was probably not expressed in their experimental conditions (24–26). Evidence suggests that certain genes from pathogenic organisms may be transcriptionally silent during growth on a rich laboratory medium, but can subsequently be induced during infection (27). If the PT expression in *B. bronchiseptica* were to be induced during infection, it could explain the observed anti-PT IgG titers in sera as a result of an anti-*B. bronchiseptica* immune response in the sows. Nevertheless, the elevated IgG titers against DT and TT up to D36 in the piglets suggest that *B. bronchiseptica* cross-reactive maternal antibodies are not the only explanation. Background IgG due to maternal antibodies and cross-reactive antibodies in piglets have been reported, and this could also explain the background levels observed in our study for specific pertussis and non-pertussis IgG titers (28).

For all antigens, the IgG responses peaked 1 month post-Tdap boost, i.e., M5, followed by a decline over the time. Noticeably, the IgG antibodies fell rapidly during the initial couple of months after M5, depending on the antigen, before reaching a stable level. The IgG titers to all antigens remained higher than those measured prior to vaccination, 6 months post-Tdap boost. This pattern of non-linear IgG decline after pertussis vaccination is in agreement with the observations in humans and baboons (29–31). We observed differences in the onset of IgG responses against the pertussis antigens (PT, FHA, FIM, PRN) and the non-pertussis antigens (DT and TT). These differences were consistent with the fact that TT is a strong immunogen whereas FHA, FIM, PRN and PT antigens are relatively weak, and that the immunogenicity of DT is intermediate (32). In addition, presence of maternal antibodies may impact the immune response to priming vaccination. We observed that the higher the antibody titer against a pertussis-specific antigen in a sow, the lower the neonatal antibody response to this antigen in the piglets born to the sow (data not shown). This interference from maternal antibodies present at time of immunization (known as blunting) has been observed in neonatal mice as well as in humans (33–35). The ratio of the maternal antibodies to vaccine antigens determines the extent of the inhibition, because there may be sufficient B cell epitopes free from maternal antibodies to be bound by the infants' B cells (36).

Since PT is a major *B.pertussis* virulence factor and antibody-mediated neutralization of PT was reported to be essential to control pertussis disease, it was important to monitor the total anti-PT IgG and functional PT neutralizing antibodies (37). There was a stronger and faster total IgG response to PT in the DTaP-primed group than in the DTwP-primed group; but only the DTaP-primed neonatal minipigs mounted a functional PT neutralizing antibody response. In agreement, the propensity of higher anti-PT responses induced by DTaP than DTwP was reported in humans (38). This may be attributed to a higher PT content in DTaP than in DTwP vaccines (39). The PT concentration in the DTaP vaccine is well defined (20 μg/HD), whereas the PT concentration in the DTwP vaccine is batch specific and not documented but is estimated to be lower. In our studies, priming 4–6-day old neonatal minipigs with DTwP induced anti-PT IgG but no anti-PT functional antibodies at any time. In contrast, 3-week-old infant minipigs primed with DTwP produced the functional anti-PT antibodies after a Tdap boost. Moreover, a PT neutralizing response was induced after the 2nd priming dose in DTaP-primed 3-week-old infant minipigs but not in 4–6-day old neonatal minipigs. These data altogether suggest a better antibody maturation when immunization is performed in older piglets, in agreement with the notion of immature neonatal immune system (40–43). The possibly longer time required for neonatal immune system to fully develop in pigs and humans may partially explain the disparity observed in baboons in terms of the anti-PT antibody responses. In pre-adult baboon, DTwP induced similar or higher anti-PT IgG and PT neutralizing antibodies than DTaP (31). The anti-PT IgG and PT neutralizing antibodies peaked 1 month post-Tdap boost in the minipigs, and then waned over time, as previously described in humans (37).

In addition to the humoral response, the cellular contributors to the immune response are crucial to establish an efficient immune response against *B. pertussis* (12, 44). Th-1, Th-2 and Th-17 FluoroSpot assays were developed to investigate cellular immune responses. IFN-γ secreting cell measurement has been previously described in minipigs (45). But to the best of our knowledge, it is the first time that Th-1, Th-2 and Th-17 profiles were monitored simultaneously in the minipig model using FluoroSpot assays. Our assessment of the T cell immune response focused on the post-Tdap boost period to mirror the same period that Th responses have been measured in many human studies (46, 47).

The importance of T helper response in the immunity against *B.pertussis* infection and colonization has recently been reviewed (12). In our minipig model we observed a Th-1/Th-17 biased profile in DTwP-primed minipigs and a Th-2 biased profile in DTaP-primed minipigs, as previously described in humans and baboons (31, 48, 49). These characteristic Th profiles were observed after priming and persisted during the post-Tdap boost period, highlighting a potential imprinting effect of DTaP vs. DTwP priming in the minipig model, with a Th-2 biased response for DTaP and a Th-1/Th-17 biased response for DTwP, similar to that reported in humans and baboons (31, 46, 48). The observed Th-2 profile was similar in the studies with neonatal and infant primed minipigs unlike the Th-1 and Th-17 profiles that showed some differences. This could be caused by variabilities in the batches of DTwP vaccine used in the studies, or heterogeneity between the minipigs. Alternatively, the T cell FluoroSpot assay may not be sufficiently robust in minipigs with batch variations of anti-cytokine antibody reagents. Although, human neonates have prefentially Th-2 biased responses, the Th response in neonatal and infant minipigs has not been fully characterized, to the best of our knowledge (42).

IFN-γ, IL-4 and IL-17 were still detectable 6 months post-Tdap boost. Moreover, the Th-2 biased profile associated with DTaP priming, and the Th-1/Th-17 biased profile associated with a DTwP priming were still observed several months post-Tdap boost, as reported in humans (46). Thus, the minipig model can be used to evaluate the longevity of the cellular immune response induced by vaccines.

To monitor the immune memory response, we developed a memory B cell FluoroSpot assay specific for pertussis antigens. This enabled us to detect antigen-specific memory B cells 6 months after the last vaccine dose, demonstrating that the minipig model can be used to monitor long-term immune memory responses. The number of IgG memory B cells specific for the pool of pertussis antigens was low, but the level is consistent with what has been reported in humans (46, 50). No difference was observed in circulating pertussis antigen specific memory B cells in DTaP and DTwP primed minipigs or human subjects several months post-Tdap boost. In baboons, DTwP priming resulted in significantly more longterm memory B cells than DTaP priming although these antigen specific memory B cells were detected at an order of $10^1$-$10^2/10^6$ PBMC (31, 46, 50).

Single-cell RNA-sequencing technology has been used to characterize immune cell responses by investigating the immune cell populations in various animal models, including pigs (51, 52), and in this study, to the best of our knowledge, for the first time in Göttingen minipigs PBMCs. Our objective was to assess the impact of the Tdap booster on PBMCs of minipigs primed with DTaP and to characterize the long-term immune memory response 6 months after the last vaccine dose, when T cell and memory B cell FluoroSpot assays were also performed. Major cell populations were characterized successfully based on their transcriptomic profile, and scRNAseq-based overall estimation of the major cell population frequencies was similar to what has been previously observed using cytometry-based methods in pigs (53–55). More importantly, low frequency populations (e.g., pDC) or those with a transitionary transcriptomic profile, such as the non-terminally differentiated γδ T cells were well-identified. Regarding the evaluation of long-term immune memory response, our scRNAseq analyses showed that the Tdap booster increased the numbers of T cells with an "activated" state after *in vitro* stimulation with a pool of pertussis antigens. It was accompanied by stimulation of the interferon pathway in the T cells and monocytes/macrophages, which is compatible with the IFN-γ production in PBMCs from DTaP-primed minipigs observed by FluoroSpot, even 6-months post-Tdap booster. Taken together, these results suggest that DTaP priming followed by Tdap boost induces a long-term memory T cell response against pertussis antigens. This memory response is probably reinforced by the activation of antigen presentation pathways in the monocyte/macrophage population, i.e., cells able to specifically stimulate T cells when exposed to pathogens. Altogether, T cell Fluorospot and scRNAseq provided complementary information in characterizing the cellular immune response. Indeed, our T cell FluoroSpot assay is sensitive in quantifying antigen-specific cytokine-secreting cells in PBMCs from pertussis vaccinated minipigs, therefore determining the Th response profile induced by vaccination. scRNAseq allowed a deep analysis of intracellular pathways involved in activation of the immune response at a single cell level. Such analysis could not otherwise be performed using a Fluorospot assay alone.

We also detected memory B cells using scRNAseq assays in our samples. The cell frequencies were similar irrespective of the vaccination received. However, these cells represented all memory B cells and not just *B. pertussis* specific memory B cells. A deeper analysis would be needed, either by increasing the total number of B cells, or by sorting B cells specific for pertussis antigens to characterize pertussis-specific memory B cells and by using new methods such as LIBRA-Seq (56).

Cell populations such as $CD4^+CD8^+$ T cells, known as activated and memory T cells, were not identified in the scRNAseq assay since the cells expressing these two markers were not in the same cluster (57). This may be due to differences observed between mRNA and protein expression, or to the fact that these cells have few differences in their transcriptomic profile, compared with $CD4^+$ or $CD8^+$ T cells. Currently, with the droplet-based scRNAseq assay, the genes studied represent the most expressed transcripts, i.e., only a partial view of the total transcriptome, and therefore may not always be sufficient to make a clear separation of cell types. Genes encoding cell surface markers were not always sufficiently detected to enable cell types sharing very close transcriptional patterns to be distinguished. The results that we presented could potentially be reinforced using a technology coupling detection of mRNA and protein expression such as CITE-seq or REAP-seq (58).

One of the limitations of minipig models is that although porcine IgG subclasses and their predicted functional properties have been previously described, based on their genomic sequences, their exact functionality in relation to human IgG subclasses is unknown (59). The route of maternal antibody transfer in pigs is different from that in humans, and therefore it is important to be cautious when interpreting results from the pig model for the influence of maternal antibodies (21, 22). Pigs are "high" γδT cell species and although porcine γδT cells share some similarities with human γδT cells, little is known about their biological function (8, 60). There are an increasing number of tools available to monitor porcine immune response. As shown in this study, commercial reagents are sensitive to assess cytokine-secreting Th-1 (IFN-γ), Th-2 (IL-4), Th-17 (IL-17) cells and antibody-secreting memory B cells by FluoroSpot. In our experience, antibodies for detecting antigen specific porcine total IgG, IgG1, IgG2, IgA in ELISA are also available. In addition, functional antibody assays such as pertussis toxin neutralization assay can be implemented. ELISA kits for cytokine quantification and fluorochrome-conjugated antibodies for identifying major immune cells such as $CD4^+$ and $CD8^+$ T cells, γδT cells, B cells, NK cells, monocytes and dendritic cells are also commercially available. Moreover, scRNAseq being a generic technology does not have species limitations. Regarding the scRNAseq data analysis, the pig genome is available and sufficiently annotated. However, reagents for the characterization of lymphocyte activation and differentiation are yet needed. It will also be important to have reliable multiplex cytokine detection methods for use in minipigs. Finally, the use of the minipig model for a combined evaluation of pertussis vaccine immunogenicity and protective efficacy, is limited by their resistance to *B. pertussis* infection from 4 to 5 weeks of age, and the fact that a *B. pertussis* challenge can only be done through an invasive intra-pulmonary *B. pertussis* inoculation (61, 62). Thus, vaccine efficacy could not be assessed in our study, particularly under an immunization schedule that mimicked the human pediatric priming, adolescent boosting pertussis vaccination scheme. Nevertheless, the protective immunity of other vaccines against their respective pathogens may be assessed in this preclinical model, as already described for example for Influenza (63, 64), *Chlamydia trachomatis* (65) or *B. parapertussis* (66). A combined immunogenicity and challenge model will be useful for identifying correlates and thresholds of immune protection.

In conclusion, our results demonstrated that this Göttingen minipig model can be used to characterize vaccine-induced immune responses, including IgG titers, functional antibodies, Th-1, Th-2, Th-17 profiles, memory B cells, and the longevity of the response. In addition, advanced analytical tools such

as scRNAseq can be used with this model to investigate the characteristics of cell populations, study the interactions between immune components, and monitor the long-term memory response after vaccination. In addition to ethical and financial concerns when compared to NHPs, the minipig model displays particular advantages for vaccine evaluation. Notably, it is practical to evaluate a pediatric vaccine in neonatal minipigs due to their large litter size and ontogeny. Moreover, the magnitude and the kinetics of the response can be assessed in the same individuals, in a longitudinal study using immunization schedules similar to those used for humans, that are otherwise difficult to model in mice and NHPs. The onset, kinetics and longevity of the immune responses induced by DTwP and DTaP priming followed by Tdap boosting in the Göttingen minipig model were shown to be very similar to human immune responses. Therefore, our data, along with data from previous studies in pigs or minipigs support the use of pigs, particularly, Göttingen minipigs as a useful preclinical model for assessing the long-term immunogenicity of pertussis vaccines, and candidate human vaccines against other pathogens (45, 67, 68).

## DATA AVAILABILITY STATEMENT

The datasets presented in this study can be found in online repositories. The names of the repository/repositories and accession number(s) can be found at: https://www.ncbi.nlm.nih.gov/geo/query/acc.cgi?acc=GSE164263.

## ETHICS STATEMENT

The animal study was reviewed and approved by Sanofi Pasteur's animal ethics committee.

## AUTHOR CONTRIBUTIONS

CV and YL developed the study design. VC, EC, and CD developed the scRNAseq experimental study. CV, VG-B, and CD performed the experiments. CV, VG-B, VC, EC, CD, and YL participated in the data analysis and interpretation, drafted the manuscript and prepared the figures and revised the manuscript. All authors contributed to the article and approved the submitted version.

## FUNDING

This work was funded by Sanofi Pasteur.

## ACKNOWLEDGMENTS

We would like to thank Christelle Serraille for performing functional antibody assessment, Stéphanie Husson for performing scRNASeq experiments, Julie Piolat for statistical analysis, and Catherine Caillet and Catherine Hessler for critical review of the manuscript, all from Sanofi Pasteur, Marcy l'Etoile, France. We thank everyone at Sanofi Pasteur's animal facility (Marcy l'Etoile, France), especially Kevin Thibault-Duprey. We also thank Catherine Meunier and Michel Didier from Sanofi (Chilly-Mazarin, France) for scRNAseq library sequencing on the NovaSeq 6000 system. Additionally, we acknowledge editorial services from Margaret Haugh, MediCom Consult, Villeurbanne, France funded by Sanofi Pasteur.

## SUPPLEMENTARY MATERIAL

The Supplementary Material for this article can be found online at: https://www.frontiersin.org/articles/10.3389/fimmu.2021.613810/full#supplementary-material

**Supplementary Figure 1 |** IFN-γ (Th-1), IL-17 (Th-17), and IL-4 (Th-2) secreting cells measured by FluoroSpot assay pre-boost (D77) on PBMCs stimulated with a pool of pertussis antigens (PTxd, PRN, FIM2/3) or heat-killed *B. pertussis* (hk*Bp*) for 24 h. Data for the DTwP ($n = 7$) and DTaP ($n = 7$) groups are shown as individual and geometric mean titers, after correction for background levels of cytokine secreting cells in the negative control wells (media alone). Data for the control group (TBS, $n = 3$) are shown as the geometric mean titer for all minipigs on D77, irrespective of the stimulation. $^{*}p$-value $< 0.05$ and $^{***}p$-value $< 0.001$ for statistical comparison of DTaP- and DTwP primed groups, NP = Not Performed because of too much non responders.

**Supplementary Figure 2 |** Heatmap representing differentially expressed genes between **(A)** DTaP-primed and TBS groups both incubated with medium or **(B)** DTaP-primed group stimulated either with a pool of pertussis antigens or with medium. The differentially expressed genes (in rows) are represented for each major cell population (in columns). Down-regulated genes are indicated in blue (negative fold changes) whereas the upregulated genes are in red (positive fold changes).

## REFERENCES

1. World Health Organization. Recommendations to assure the quality, safety and efficacy of acellular pertussis vaccines. In: *WHO Expert Committee on Biological Standardization. Sixty-second Report*. (WHO Technical Report Series, No. 979), Annex 4. Geneva: World Health Organization (2013).
2. Masopust D, Sivula CP, Jameson SC. Of mice, dirty mice, and men: using mice to understand human immunology. *J Immunol.* (2017) 199:383–8. doi: 10.4049/jimmunol.1700453
3. Polack FP, Lydy SL, Lee S-H, Rota PA, Bellini WJ, Adams RJ, et al. Poor immune responses of newborn rhesus macaques to measles virus DNA vaccines expressing the hemagglutinin and fusion glycoproteins. *Clin Vaccine Immunol.* (2013) 20:205–10. doi: 10.1128/CVI.00394-12
4. Meurens F, Summerfield A, Nauwynck H, Saif L, Gerdts V. The pig: a model for human infectious diseases. *Trends Microbiol.* (2012) 20:50–7. doi: 10.1016/j.tim.2011.11.002
5. Gerdts V, Wilson HL, Meurens F, van Drunen Littel-van den Hurk S, Wilson D, Walker S, et al. Large animal models for vaccine development and testing. *ILAR J.* (2015) 56:53–62. doi: 10.1093/ilar/ilv009
6. Kimmel CA, Buelke-Sam J. Reproductive and developmental toxicology. In: Bingham E, Cohrssen B, Powell CH, editors. *Patty's Toxicology*. (2001). doi: 10.1002/0471435139.tox003
7. Rubic-Schneider T, Christen B, Brees D, Kammüller M. Minipigs in translational immunosafety sciences: a perspective. *Toxico Pathol.* (2016) 44:315–24. doi: 10.1177/0192623315621628

8. Mair KH, Sedlak C, Kaser T, Pasternak A, Levast B, Gerner W, et al. The porcine innate immune system: an update. *Dev Comp Immunol.* (2014) 45:321–43. doi: 10.1016/j.dci.2014.03.022
9. Descotes J, Allais L, Ancian P, Pedersen HD, Friry-Santini C, Iglesias A, et al. Nonclinical evaluation of immunological safety in Göttingen Minipigs: The CONFIRM initiative. *Regul Toxicol Pharmacol.* (2018) 94:271–5. doi: 10.1016/j.yrtph.2018.02.015
10. Dawson HD. A comparative assessment of the pig, mouse and human genomes : Structural and functional analysis of genes involved in immunity and inflammation. In: McAnulty PA, Dayan AD, Ganderup N-C, Hastings KL, editors. *The Minipig in Biomedical Research*. Boca Raton, FL: CRC Press, Taylor & Francis Group (2011). p. 323–42.
11. Dawson HD, Chen C, Loveland JE, Gilbert JGR, Carvalho-Silva D, Hunt T, et al. Structural and functional annotation of the porcine immunome. *BMC Genomics.* (2013) 14:332. doi: 10.1186/1471-2164-14-332
12. Kapil P, Merkel TJ. Pertussis vaccines and protective immunity. *Curr Opin Immunol.* (2019) 59:72–8. doi: 10.1016/j.coi.2019.03.006
13. Brummelman J, Wilk MM, Han WGH, Van Els CACM, Mills KHG. Roads to the development of improved pertussis vaccines paved by immunology. *Pathog Dis.* (2015) 73:ftv067. doi: 10.1093/femspd/ftv067
14. Fish EN. The X-files in immunity: sex-based differences predispose immune responses. *Nat Rev Immunol.* (2008) 8:737–44. doi: 10.1038/nri2394
15. Klein SL, Jedlicka A, Pekosz A. The Xs and Y of immune responses to viral vaccines. *Lancet Infect Dis.* (2010) 10:338–49. doi: 10.1016/S1473-3099(10)70049-9
16. Hewlett EL, Sauer KT, Myers GA, Cowell JL, Guerrant RL. Induction of a novel morphological response in Chinese hamster ovary cells by pertussis toxin. *Infect Immunity.* (1983) 40:1198–203. doi: 10.1128/IAI.40.3.1198-1203.1983
17. Butler A, Hoffman P, Smibert P, Papalexi E, Satija R. Integrating single-cell transcriptomic data across different conditions, technologies, and species. *Nat Biotechnol.* (2018) 36:411–20. doi: 10.1038/nbt.4096
18. Lun ATL, McCarthy DJ, Marioni JC. A step-by-step workflow for low-level analysis of single-cell RNA-seq data with Bioconductor [version 2; referees: 1 approved, 4 approved with reservations]. *F1000Research.* (2016) 5:2122. doi: 10.12688/f1000research.9501.2
19. Krämer A, Green J, Pollard JJ, Tugendreich S. Causal analysis approaches in ingenuity pathway analysis. *Bioinformatics.* (2014) 30:523–4. doi: 10.1093/bioinformatics/btt703
20. QIAGEN. *Ingenuity Pathway Analysis (IPA).* (2020). Available from: https://digitalinsights.qiagen.com/products-overview/discovery-insights-portfolio/analysis-and-visualization/qiagen-ipa/
21. Nechvatalova K, Kudlackova H, Leva L, Babickova K, Faldyna M. Transfer of humoral and cell-mediated immunity via colostrum in pigs. *Vet Immunol Immunopathol.* (2011) 142:95–100. doi: 10.1016/j.vetimm.2011.03.022
22. Hurley WL, Theil PK. Perspectives on immunoglobulins in colostrum and milk. *Nutrients.* (2011) 3:442–74. doi: 10.3390/nu3040442
23. Antoine R, Raze D, Locht C. Genomics of Bordetella pertussis toxins. *Int J Med Microbiol.* (2000) 290:301–5. doi: 10.1016/S1438-4221(00)80026-0
24. Arico B, Rappuoli R. *Bordetella parapertussis* and *Bordetella bronchiseptica* contain transcriptionally silent pertussis toxin genes. *J Bacteriol.* (1987) 169:2847–53. doi: 10.1128/JB.169.6.2847-2853.1987
25. Marchitto KS, Smith SG, Locht C, Keith JM. Nucleotide sequence homology to pertussis toxin gene in *Bordetella bronchiseptica* and *Bordetella parapertussis*. *Infect Immunity.* (1987) 55:497–501. doi: 10.1128/IAI.55.3.497-501.1987
26. Hausman SZ, Cherry JD, Heininger U, Wirsing Von KÖNig CH, Burns DL. Analysis of proteins encoded by the ptx and ptl genes of *Bordetella bronchiseptica* and *Bordetella parapertussis*. *Infect Immunity.* (1996) 64:4020–6. doi: 10.1128/IAI.64.10.4020-4026.1996
27. Camilli A, Mekalanos JJ. Use of recombinase gene fusions to identify Vibrio cholerae genes induced during infection. *Mol Microbiol.* (1995) 18:671–83. doi: 10.1111/j.1365-2958.1995.mmi_18040671.x
28. Christoforidou Z, Mora Ortiz M, Poveda C, Abbas M, Walton G, Bailey M, et al. Sexual dimorphism in immune development and in response to nutritional intervention in neonatal piglets. *Front Immunol.* (2019) 10:1–17. doi: 10.3389/fimmu.2019.02705
29. McIntyre PB, Turnbull FM, Egan A-M, Burgess MA, Wolter JM, Schuerman LM. High levels of antibody in adults three years after vaccination with a reduced antigen content diphtheria-tetanus-acellular pertussis vaccine. *Vaccine.* (2004) 23:380–5. doi: 10.1016/j.vaccine.2004.05.030
30. Aase A, Herstad TK, Jorgensen SB, Leegaard TM, Berbers G, Steinbakk M, et al. Anti-pertussis antibody kinetics following DTaP-IPV booster vaccination in Norwegian children 7-8 years of age. *Vaccine.* (2014) 32:5931–6. doi: 10.1016/j.vaccine.2014.08.069
31. Cole LE, Zhang J, Pacheco KM, Lhéritier P, Anosova NG, Piolat J, et al. Immunological distinctions between acellular and whole-cell pertussis immunizations of baboons persist for at least one year after acellular vaccine boosting. *Vaccines.* (2020) 8:729. doi: 10.3390/vaccines8040729
32. European Centre for Disease Prevention and Control. *ECDC GUIDANCE Scientific Panel on Childhood Immunisation Schedule: Diphtheria-Tetanus-Pertussis (DTP) Vaccination.* (2009). Available from: https://www.ecdc.europa.eu/en/publications-data/expert-opinion-childhood-immunisation-schedule-diphtheria-tetanus-pertussis-dtp
33. Niewiesk S. Maternal antibodies: Clinical significance, mechanism of interference with immune responses, and possible vaccination strategies. *Front Immunol.* (2014) 5(SEP):446. doi: 10.3389/fimmu.2014.00446
34. Kandeil W, Savic M, Ceregido MA, Guignard A, Kuznetsova A, Mukherjee P. Immune interference (blunting) in the context of maternal immunization with Tdap-containing vaccines: is it a class effect? *Exp Rev Vaccines.* (2020) 19:341–52. doi: 10.1080/14760584.2020.1749597
35. Martin Aispuro P, Ambrosis N, Zurita ME, Gaillard ME, Bottero D, Hozbor DF. Use of a neonatal-mouse model to characterize vaccines and strategies for overcoming the high susceptibility and severity of pertussis in early life. *Front Microbiol.* (2020) 11:723. doi: 10.3389/fmicb.2020.00723
36. Siegrist CA. Vaccination in the neonatal period and early infancy. *Int Rev Immunol.* (2000) 19:195–219. doi: 10.3109/08830180009088505
37. Pitisuttithum P, Chokephaibulkit K, Sirivichayakul C, Sricharoenchai S, Dhitavat J, Pitisuthitham A, et al. Antibody persistence after vaccination of adolescents with monovalent and combined acellular pertussis vaccines containing genetically inactivated pertussis toxin: a phase 2/3 randomised, controlled, non-inferiority trial. *Lancet Infect Dis.* (2018) 18:1260–8. doi: 10.1016/S1473-3099(18)30375-X
38. Auerbach, Lake, Wilson, Willingham, Shematek, Moulton, et al. Dose–response to a two-component acellular pertussis vaccine in infants and comparison with whole-cell vaccine. *Biologicals.* (1998) 26:145–53. doi: 10.1006/biol.1998.9999
39. Edwards KM, Meade BD, Decker MD, Reed GF, Rennels MB, Steinhoff MC, et al. Comparison of 13 acellular pertussis vaccines: overview and serologic response. *Pediatrics.* (1995) 96(3 Part 2):548–57.
40. Adkins B, Leclerc C, Marshall-Clarke S. Neonatal adaptive immunity comes of age. *Nat Rev Immunol.* (2004) 4:553–64. doi: 10.1038/nri1394
41. Siegrist C-A. Neonatal and early life vaccinology. *Vaccine.* (2001) 19:3331–46. doi: 10.1016/S0264-410X(01)00028-7
42. Mohr E, Siegrist C-A. Vaccination in early life: standing up to the challenges. *Curr Opin Immunol.* (2016) 41:1–8. doi: 10.1016/j.coi.2016.04.004
43. Dowling DJ, Levy O. Ontogeny of early life immunity. *Trends Immunol.* (2014) 35:299–310. doi: 10.1016/j.it.2014.04.007
44. Allen AC, Mills KH. Improved pertussis vaccines based on adjuvants that induce cell-mediated immunity. *Expert Rev Vaccines.* (2014) 13:1253–4. doi: 10.1586/14760584.2014.936391
45. Overgaard NH, Frosig TM, Jakobsen JT, Buus S, Andersen MH, Jungersen G. Low antigen dose formulated in CAF09 adjuvant Favours a cytotoxic T-cell response following intraperitoneal immunization in Gottingen minipigs. *Vaccine.* (2017) 35:5629–36. doi: 10.1016/j.vaccine.2017.08.057
46. van der Lee S, Hendrikx LH, Sanders EAM, Berbers GAM, Buisman AM. Whole-cell or acellular pertussis primary immunizations in infancy determines adolescent cellular immune profiles. *Front Immunol.* (2018) 9(JAN):51. doi: 10.3389/fimmu.2018.00051
47. Bancroft T, Dillon MBC, da Silva Antunes R, Paul S, Peters B, Crotty S, et al. Th1 versus Th2 T cell polarization by whole-cell and acellular childhood pertussis vaccines persists upon re-immunization in adolescence and adulthood. *Cell Immunol.* (2016) 304–5:35–43. doi: 10.1016/j.cellimm.2016.05.002
48. Da Silva Antunes R, Babor M, Carpenter C, Khalil N, Seumois G, Vijayanand P, et al. Th1/Th17 polarization persists following whole-cell

pertussis vaccination despite repeated acellular boosters. *J Clin Investig.* (2018) 128:3853–65. doi: 10.1172/JCI121309
49. Warfel JM, Zimmerman LI, Merkel TJ. Acellular pertussis vaccines protect against disease but fail to prevent infection and transmission in a nonhuman primate model. *Proc Natl Acad Sci USA.* (2014) 111:787–92. doi: 10.1073/pnas.1314688110
50. Schure R-M, Hendrikx LH, de Rond LGH, Öztürk K, Sanders EAM, Berbers GAM, et al. Differential T- and B-Cell responses to pertussis in acellular vaccine-primed versus whole-cell vaccine-primed children 2 years after preschool acellular booster vaccination. *Clin Vaccine Immunol.* (2013) 20:1388–95. doi: 10.1128/CVI.00270-13
51. Villani AC, Satija R, Sarkizova S, Shekhar K, Li W, De Jager PL, et al. Single-cell RNA-seq reveals new types of human blood dendritic cells, monocytes, and progenitors. *Science.* (2017) 356:eaah4573. doi: 10.1126/science.aah4573
52. Crinier A, Milpied P, Escalière B, Galluso J, Balsamo A, Spinelli L, et al. High-dimensional single-cell analysis identifies organ-specific signatures and conserved NK cell subsets in humans and mice. *Immunity.* (2018) 49:971–86.e5. doi: 10.1016/j.immuni.2018.09.009
53. Gerner W, Käser T, Saalmüller A. Porcine T lymphocytes and NK cells – An update. *Dev Comp Immunol.* (2009) 33:310–20. doi: 10.1016/j.dci.2008.06.003
54. Summerfield A, Guzylack-Piriou L, Schaub A, Carrasco CP, Tâche V, McCullough KC, et al. Porcine peripheral blood dendritic cells and natural interferon-producing cells. *Immunology.* (2003) 110:440–9. doi: 10.1111/j.1365-2567.2003.01755.x
55. Mair KH, Essler SE, Patzl M, Storset AK, Saalmller A, Gerner W. NKp46 expression discriminates porcine NK cells with different functional properties. *Eur J Immunol.* (2012) 42:1261–71. doi: 10.1002/eji.201141989
56. Setliff I, Shiakolas AR, Pilewski KA, Murji AA, Raju N, Qin JS, et al. High-Throughput mapping of B cell receptor sequences to antigen specificity. *Cell.* (2019) 179:1636–46.e15. doi: 10.1016/j.cell.2019.11.003
57. Saalmüller A, Gerner W. The immune system of swine. In: Ratcliffe MJH, editor. *Encyclopedia of Immunobiology*. Oxford: Academic Press (2016). p. 538–48.
58. Stoeckius M, Hafemeister C, Stephenson W, Houck-Loomis B, Chattopadhyay PK, Swerdlow H, et al. Simultaneous epitope and transcriptome measurement in single cells. *Nat Methods.* (2017) 14:865–8. doi: 10.1038/nmeth.4380
59. Butler JE, Wertz N, Deschacht N, Kacskovics I. Porcine IgG: structure, genetics, and evolution. *Immunogenetics.* (2009) 61:209–30. doi: 10.1007/s00251-008-0336-9
60. Rodríguez-Gómez IM, Talker SC, Käser T, Stadler M, Reiter L, Ladinig A, et al. Expression of T-Bet, eomesodermin, and GATA-3 correlates with distinct phenotypes and functional properties in porcine γδ T cells. *Front Immunol.* (2019) 10:396. doi: 10.3389/fimmu.2019.00396
61. Elahi S, Buchanan RM, Attah-Poku S, Townsend HGG, Babiuk LA, Gerdts V. The host defense peptide beta-defensin 1 confers protection against *Bordetella pertussis* in newborn piglets. *Infect Immunity.* (2006) 74:2338–52. doi: 10.1128/IAI.74.4.2338-2352.2006
62. Elahi S, Babiuk LA, Thompson DR, Van Kessel J, Gerdts V. Protective role of passively transferred maternal cytokines against *Bordetella pertussis* infection in newborn piglets. *Infect Immunity.* (2017) 85:e01063-16. doi: 10.1128/IAI.01063-16
63. Khatri M, Dwivedi V, Krakowka S, Manickam C, Ali A, Wang L, et al. Swine influenza H1N1 virus induces acute inflammatory immune responses in pig lungs: a potential animal model for human H1N1 influenza virus. *J Virol.* (2010) 84:11210–8. doi: 10.1128/JVI.01211-10
64. Skovgaard K, Cirera S, Vasby D, Podolska A, Breum SØ, Dürrwald R, et al. Expression of innate immune genes, proteins and microRNAs in lung tissue of pigs infected experimentally with influenza virus (H1N2). *Innate Immunity.* (2013) 19:531–44. doi: 10.1177/1753425912473668
65. Erneholm K, Lorenzen E, Bøje S, Olsen AW, Jungersen G, Jensen HE, et al. Genital Infiltrations of CD4+ and CD8+ T lymphocytes, IgA+ and IgG+ plasma cells and intra-mucosal lymphoid follicles associate with protection against genital chlamydiatrachomatis infection in minipigs intramuscularly immunized with UV-inactivated bacteria adjuvanted with CAF01. *Front Microbiol.* (2019) 10:197. doi: 10.3389/fmicb.2019.00197
66. Elahi S, Thompson DR, Strom S, Babiuk LA, Gerdts V, O'Connor B. Infection with *Bordetella parapertussis* but not *Bordetella pertussis* causes pertussis-like disease in older pigs. *J Infect Dis.* (2008) 198:384–92. doi: 10.1086/589713
67. Lorenzen E, Follmann F, Bøje S, Erneholm K, Olsen AW, Agerholm JS, et al. Intramuscular priming and intranasal boosting induce strong genital immunity through secretory IgA in minipigs infected with Chlamydia trachomatis. *Front Immunol.* (2015) 6:628. doi: 10.3389/fimmu.2015.00628
68. Smith AJ, Li Y, Bazin HG, St-Jean JR, Larocque D, Evans JT, et al. Evaluation of novel synthetic TLR7/8 agonists as vaccine adjuvants. *Vaccine.* (2016) 34:4304–12. doi: 10.1016/j.vaccine.2016.06.080

**Conflict of Interest:** CV, VG-B, VC, EC, and YL are all employed by Sanofi Pasteur, Marcy l'Etoile, France. They hold shares/stock options as part of their remuneration package. CD was on a mission with Sanofi Pasteur from Kelly Services, Paris, France.

frontiers in Immunology

ORIGINAL RESEARCH
published: 24 May 2021
doi: 10.3389/fimmu.2021.642807

# Stable Epigenetic Programming of Effector and Central Memory CD4 T Cells Occurs Within 7 Days of Antigen Exposure *In Vivo*

*Sarah L. Bevington[1], Remi Fiancette[2], Dominika W. Gajdasik[2], Peter Keane[1], Jake K. Soley[1], Claire M. Willis[2], Daniel J. L. Coleman[1], David R. Withers[2*†] and Peter N. Cockerill[1*†]*

[1] Institute of Cancer and Genomic Sciences, College of Medical and Dental Sciences, University of Birmingham, Birmingham, United Kingdom, [2] Institute of Immunology and Immunotherapy, College of Medical and Dental Sciences, University of Birmingham, Birmingham, United Kingdom

OPEN ACCESS

**Edited by:**
Kim Good-Jacobson,
Monash University, Australia

**Reviewed by:**
Christine R. Keenan,
Walter and Eliza Hall Institute of Medical Research, Australia
Jasmine Li,
Peter MacCallum Cancer Centre, Australia
Sebastian Scheer,
Monash University, Australia

***Correspondence:**
Peter N. Cockerill
p.n.cockerill@bham.ac.uk
David R. Withers
d.withers@bham.ac.uk

†These authors share last authorship

**Specialty section:**
This article was submitted to Immunological Memory, a section of the journal Frontiers in Immunology

**Received:** 16 December 2020
**Accepted:** 05 May 2021
**Published:** 24 May 2021

**Citation:**
Bevington SL, Fiancette R, Gajdasik DW, Keane P, Soley JK, Willis CM, Coleman DJL, Withers DR and Cockerill PN (2021) Stable Epigenetic Programming of Effector and Central Memory CD4 T Cells Occurs Within 7 Days of Antigen Exposure In Vivo. Front. Immunol. 12:642807. doi: 10.3389/fimmu.2021.642807

T cell immunological memory is established within days of an infection, but little is known about the *in vivo* changes in gene regulatory networks accounting for their ability to respond more efficiently to secondary infections. To decipher the timing and nature of immunological memory we performed genome-wide analyses of epigenetic and transcriptional changes in a mouse model generating antigen-specific T cells. Epigenetic reprogramming for Th differentiation and memory T cell formation was already established by the peak of the T cell response after 7 days. The Th memory T cell program was associated with a gain of open chromatin regions, enriched for RUNX, ETS and T-bet motifs, which remained stable for 56 days. The epigenetic programs for both effector memory, associated with T-bet, and central memory, associated with TCF-1, were established in parallel. Memory T cell-specific regulatory elements were associated with greatly enhanced inducible Th1-biased responses during secondary exposures to antigen. Furthermore, memory T cells responded *in vivo* to re-exposure to antigen by rapidly reprograming the entire ETS factor gene regulatory network, by suppressing *Ets1* and activating *Etv6* expression. These data show that gene regulatory networks are epigenetically reprogrammed towards memory during infection, and undergo substantial changes upon re-stimulation.

**Keywords: memory T CD4+ cells, gene regulatory networks, epigenetics (chromatin remodelling), immunological memory responses, T cell activation**

## INTRODUCTION

During primary immune responses, effector T cells arise from naïve T cells (TN) when their antigen (Ag) -specific TCRs recognize Ag on Ag presenting cells (APCs) for the first time and undergo transformation over a 1-2 day period to become rapidly dividing T blast cells (TB) (1). During this process, the combination of TCR, CD28 and IL-2 signaling promotes the extensive reprograming of the T cell gene regulatory network, rendering immune response genes much more receptive to

reactivation and enabling further differentiation to specialized Th cells (2–5). Systemic bacterial or viral infections *in vivo* typically establish a Th1-polarizing environment whereby additional cytokines such as IL-12 induce expression of the Th1-lineage-defining transcription factor (TF) T-bet, and T-bet target genes such as *Ifng* (IFN-γ), which reinforce Th1 status (6–8).

Secondary immune responses are dependent upon pools of long lived Ag-specific memory T cells (TM) that remain as a reservoir to fight future infections long after primary infections have resolved (9). In the absence of TCR signaling, long-term TM cells are dependent upon the homeostatic cytokines IL-2, IL-7 and/or IL-15, which each signal *via* a common gamma chain (10–12). CD4 and CD8 TM cells have retained their reprogramed status to respond much faster and more efficiently when re-exposed to Ag than naive T cells (TN) (3, 13–17). *In vitro* studies demonstrated that T cell memory is stable for at least 60 d in the absence of Ag (18). TM cells can be subdivided into two major subtypes based on their surface markers, gene expression profiles, and the nature of their responses to secondary infections (19, 20). Effector memory T cells (Tem) retain many of the properties of differentiated T cells and rapidly resume their original programed effector T cell response when reactivated. Tem cells are rapidly recruited during secondary infections and they maintain expression of differentiation inducing genes, such as *Tbx21* (T-bet) in Th1-type Tem cells. In contrast, central memory T cells (Tcm) have yet to undergo effector T cell differentiation and remain plastic and receptive to following different paths of T cell differentiation when reactivated. Thus, the transcriptional networks in Tcm cells are closer to TN cells and follicular helper T cells (Tfh), expressing factors such as *Bach2* (21–23), which represses the AP-1 responses downstream of TCR signaling (24), and *Bcl6* which polarizes cells towards Tcm or Tfh (25, 26). CD4 Tem and Tcm can also be differentiated on the basis of expression of the chemokine receptors CCR7 and CXCR5, enabling Tcm to circulate through lymphoid tissues. Tem lack expression of both CCR7 and CXCR5 and instead express receptors that enable them to traffic through non-lymphoid tissues (25–28).

The reprograming of the gene regulatory network in TB and TM cells is associated with the stable acquisition of thousands of highly accessible active chromatin regions defined as DNase I Hypersensitive Sites (DHSs) that maintain a long term transcriptional memory of their previous activation (2, 3, 29). Once formed during TB-transformation, these epigenetically primed DHSs (pDHSs) are maintained by cooperation between constitutively expressed TFs such as ETS1 and RUNX1 (2, 3), and IL-2/IL-7-inducible TFs such as STAT5 and JUND (4, 5). pDHSs play a critical role in maintaining immunological memory by maintaining broad active chromatin domains marked by the active chromatin modifications histone H3 K4me2 and H3 K27ac. These epigenetically primed domains typically encompass the inducible enhancers and promoters that mediate reactivation of immune response genes during secondary responses (2, 3).

Our understanding of CD4 TM populations has been significantly advanced by studies tracking antigen-specific responses *in vivo* (30), and in particular a model Th1 infection using an attenuated strain of *Listeria monocytogenes* (Lm) expressing the highly immunogenic peptide 2W1S (6, 26). In this acute infection, TM cells biased towards Th1 are established in lymphoid organs within 3-4 d of infection, and the T cell response reaches a peak after 6-7 d, before contracting ~7-10-fold by day 20 and then gradually subsiding further over the following months (6, 26). Interestingly, these studies demonstrated that CXCR5-ve Tem and CXCR5+ve Tcm and Tfh were established in parallel, with 90% of the CXCR5+ve cells resembling Tcm cells (26). Furthermore, the level of CXCR5 expression negatively correlated with *Il2ra* expression. *Il2ra*-deficient T cells were able to efficiently generate $CXCR5^{+}$ $PD\text{-}1^{-}$ Tcm cells, but they only produced 10% of the normal proportion of $T\text{-}bet^{high}$ $CXCR5^{-}$ Th1 cells (5, 26). Whilst the development of these memory cell populations was characterised in fine detail, the molecular basis underlying the establishment and stable maintenance of memory in Tem and Tcm cells *in vivo* was never established.

Although it is clear that the epigenetic program associated with long term immunological memory can be established within 2-3 d *in vitro*, it remains unknown how fast this is established during *in vivo* responses, or how stable it is. Most previous epigenetic analyses of TM cells formed *in vivo* have used polyclonal populations where it has not been possible to establish how recently epigenetic memory had formed or how stable it was in long-term memory cells (3). The goal of the present study was to use the Lm-2W1S as a highly tractable *in vivo* model to study the time-course and stability of epigenetic reprograming in Ag-specific TM cells, and to investigate the role of this program in secondary Ag responses. We established that (i) the TM-epigenetic program is established in both Tcm and Tem cells within 7 days and is stable for at least 56 days, (ii) epigenetic reprograming primes immune response genes for rapid secondary responses in TM cells, and (iii) Ag-stimulation of TM cells *in vivo* leads to extensive rewiring of the ETS TF gene regulation network, with suppression of *Ets1* and ETS1-regulated genes such as *Lef1* and *Tcf7* in parallel with upregulation of the ETS family repressor *Etv6*.

# MATERIALS AND METHODS

## Mice

C42 transgenic mice were used for the M7, M28 and M56 ATAC-seq and RNA-seq experiments. C42 mice have been extensively backcrossed onto a C57BL/6 background and contain a 130 kb DNA fragment of the human *IL3/CSF2* locus which can be used as a reporter of human cytokine gene activity (3). In previous studies the transgene did not have any detectable impact on the responses of these mice. WT C57BL/6 mice were used in experiments from which CXCR5+ and CXCR5- 2W1S-specific CD4 T cells were isolated. Mice were housed at 21°C +/- 2°C, 55% humidity (+/- 10%) with 12 hr light dark/cycle in 7-7 IVC caging with environmental enrichment of plastic houses plus paper bedding.

## Antigen-Specific Th Memory T Cell Generation and Purification

Mice were intravenously injected in the tail vein with $10^7$ *actA*-deficient *L. monocytogenes* expressing OVA-2W1S (*Lm*-2W1S, a kind gift from Dr. M. Jenkins) as described previously (5). To recover 2W1S-specific CD4 T cells, spleens were taken at 7, 28 or 56 days post infection, cells isolated by manual crushing of the tissue, depleted of red blood cells and then incubated with 2W1S:$A^b$-APC for 1 hour at room temperature. The 2W1S-specific population was enriched as described by the Jenkins Laboratory (31) using anti-APC microbeads (Miltenyi Biotech #130-090-855). Following enrichment the cells were stained with antibodies to detect CD3, CD4, CD44, B220, CD11c and CD11b. $CD44^{hi}$ 2W1S-specific CD4 T cells were sort purified using a BD FACSAria Fusion cell sorter (BD) to greater than 95% purity. For the re-stimulation mice were injected with 100 µg 2W1S peptide and 2.5 µg LPS 28 or 56 days post infection and purified as above 3 hours after injection. For the purification of the CXCR5 populations the cells were stained with CXCR5-PeCy7 at the same time as the 2W1S:$A^b$-APC staining. Naïve CD4 T cells were purified as $CD44^{lo}$, $CD62L^{hi}$.

## Assay for Transposase Accessible Chromatin Using Sequencing (ATAC-Seq)

FACS purified cells were resuspended in 50 µl ATAC transposition reaction mix containing 25 µl 2x Tagment DNA Buffer (Illumina), 2.5 µl Tn5 transposase (Illumina), 0.5 µl 1% Digitonin (Promega #G9441) and incubated for 20-30 minute at 37°C with gentle agitation. For the M28Ag_1, M56Ag_1 and the CXCR5pos and CXCR5neg samples 16.5 µl PBS and 0.5 µl 10% Tween-20 were added to the transposition mix to reduce the level of background obtained in the sequencing as described by Corces et al. (32). DNA was purified using the MinElute Reaction Clean up kit (Qiagen #28204) before performing 5 cycles of PCR amplification using Nextera custom primers. The number of additional PCR cycles required to generate adequate material for sequencing was calculated using a qPCR side reaction as described (32). Amplified DNA was purified using Ampure Beads (Beckman Coulter) and libraries were validated by qPCR. Samples were sequenced on NextSeq® 500/550 High Output kit v2 75 cycles (Illumina, FC 404-2005) at the Genomics Birmingham sequencing facility. Two biological replicates were sequenced for each time point.

## RNA-Sequencing (RNA-seq)

RNA was extracted using the RNeasy Plus Micro Kit (Qiagen# 74034). cDNA was generated from 0.5-3 ng of RNA using the Smart-Seq™ v4 Ultra™ Low Input RNA Kit for Sequencing (Clontech) according to the manufacturer's instructions. Following 11 cycles of PCR amplification the number of additional cycles was calculated for each individual sample based on the quantity of cDNA which was determined using the Agilent 2100 Bioanalyzer (High Sensitivity DNA Kit #5067-4626). Libraries were prepared from 150 pg of cDNA using the Nextera XT library prep kit (Illumina FC-131-1024) and the Nextera XT index kit (Illumina FC-131-1001) according to the manufacturer's instructions. Samples were sequenced on NextSeq® 500/550 High Output Kit v2 (150 cycles) (FC-404-2002) at the Genomics Birmingham sequencing facility. Three biological replicates were sequenced for each time point.

## Data Analysis

### Alignment, Coverage and Peak Detection of DNase-Seq, ATAC-Seq and ChIP-Seq Data Sets

Raw DNA sequencing reads were aligned to the NCBI Mouse Genome Sequencing Consortium version mm10 using *bowtie2* (Galaxy Version 2.3.2.2) (33) with the preset –very-sensitive-local. BedGraph files were generated with MACS2 callpeak (Galaxy version 2.1.1) using the default parameters (34) and were converted to bigwig files using the Wig/BedGraph-to-bigWig converter (Galaxy v1.1.1) in order to visualize on the UCSC genome browser. The statistics for ATAC-Seq read counts and peaks are shown in **Table 1**.

### Normalization of ATAC-Seq Data Sets

To determine a complete set of peaks with the most accurate coordinates the BAM files from the N, M7, M28, M56, M28Ag, M56Ag ATAC-Seq samples were merged using BamTools (Galaxy Version 0.0.2) (35). MACS2 callpeak (Galaxy Version 2.1.1) was then used to generate a master set of 107467 peaks. The DNA sequence tags +/- 200 bp from the peak summit were counted for each individual sample using the annotatePeaks function of the HOMER package (36). The samples were normalized to one another using a correction factor based on the median of the top 30,000 peaks. These correction factors were then used to normalize genome browser scales, average tag density plots and contrast levels in tag density profiles.

### Fold Change Analysis of ATAC-Seq Peaks

To generate a high confidence set of summits which could be used in downstream analyses the top 35000 peaks of the two replicate samples were intersected using BEDTools v2.26.0 intersect function (37). This generated peak groups for N, M7, M28, M56, M28Ag and M56Ag. These peaks sets were then merged to give a total of 48202 peaks which represent all the cell stages.

**TABLE 1** | Summary of statistics for ATAC-Seq data.

| Samples | Read count | Mapped reads | Peaks |
|---|---|---|---|
| N1 | 55009838 | 50182216 | 30339 |
| N2 | 28765208 | 19577334 | 30426 |
| M7 1 | 122567768 | 109756779 | 28005 |
| M7 2 | 26498877 | 20348656 | 29989 |
| M28 1 | 20348656 | 10627634 | 29207 |
| M28 2 | 59235548 | 38423698 | 27260 |
| M56 1 | 26141267 | 15532278 | 27392 |
| M56 2 | 42375252 | 38644631 | 28321 |
| M28Ag 1 | 25179335 | 15311639 | 31629 |
| M28Ag 2 | 55496446 | 47132970 | 36630 |
| M56Ag 1 | 21467935 | 19320998 | 33110 |
| M56Ag 2 | 23568973 | 18665342 | 32249 |
| CXCR5neg_1 | 17313607 | 14127739 | 34792 |
| CXCR5neg_2 | 16043618 | 15828665 | 32863 |
| CXCR5pos_1 | 19033264 | 18030772 | 34598 |
| CXCR5pos_2 | 17160597 | 16891953 | 33325 |

The sequencing reads were counted using featurecounts (38) and Deseq2 (Galaxy version 2.11) (39) was used to calculate the fold change and adjusted p-values between samples. A peak was considered to be significantly differentially enriched if it had a greater than 3-fold change between samples, an adjusted p-value < 0.05 and a normalized read count >20 in both of the replicates.

### Unions of ATAC-Seq Samples

The normalized counts from the Deseq2 analysis were used to determine a set of peaks for each sample. The peaks were filtered to only include sites with a read count >20 resulting in ~30,000 peaks/sample. The union of two samples was generated using the sort and merge function of the BEDtools package (37). The data were visualized as sequence tag density plots and ordered according to the fold change difference in tag density of one sample compared to the other.

### DNA Sequence Tag Density Profiles

Tag density profiles were produced using the annotatePeaks function of the HOMER package (36). with -hist 10 -ghist -size 2000 as parameters. The peak summit files generated from the union of the ATAC-seq samples and the bedGraph coverage files produced by MACS2 callpeak (Galaxy Version 2.1.1) (34) were used as inputs. Images were visualized using Java Treeview (http://jtreeview.sourceforge.net/).

### Average DNA Sequence Tag Density Plots

Average ATAC-Seq and ChIP-Seq tag density profiles were generated around the DHS summit using annotatePeaks from the HOMER package (36) with –hist 10 –size 2000 as parameters. The average sequence tag density was plotted for duplicate samples.

### Annotation and Intersection of Peaks

The closest gene to the peak was determined using the annotatePeaks function of the HOMER package (36). Peak groups were overlapped to generate Venn diagrams using BEDtools v2.26.0 intersect function (37).

### Motif Discovery

*De novo* DNA motif analysis was performed using the findMotifsGenome.pl function of the HOMER package (36). Motifs were identified +/- 100 bp from the peak summit.

### Wellington Footprinting of ATAC Data to Identify Occupied TF Motifs

Aligned reads from ATAC-Seq replicates were combined to create a single bam file using the merge function in samtools v1.9 (40). These bam files were then used to plot the positions of the Tn5 integration sites on the forward and reverse strands separately using the dnase_wig_tracks.py function in Wellington, which is part of the pyDNase python package v0.3.0 (41). This tool was run in ATAC-Seq mode by specifying the -A parameter. The resulting tracks were then visualized on the UCSC genome browser (42).

Average ATAC-Seq cut profiles for individual motifs were created by first extracting the positions for each motif in the peak set being considered using the annotatePeaks.pl function in Homer v4.9.1 (36) with the options -m -mbed. The resulting bed file was then filtered to retain only motifs that were found within footprinted regions using the intersect function in bedtools v2.29.2 (37). Footprints were identified using the wellington_footprints.py function in pyDNase, which was run in ATAC-Seq mode using the options -A -fdrlimit -10. The average ATAC-Seq cut profile was then plotted around the footprinted motifs using the dnase_average_profile.py function in pyDNase using the -A parameter.

### RNA-Seq Data Analyses

Paired-end sequence reads were processed with Trimmomatic (Galaxy version 0.38.0) (43) before alignment to the mouse genome (version mm10) using Hisat2 (Galaxy v2.1.0) (44) with default parameters. Gene expression levels were calculated with htseq-count (Galaxy version 0.9.1) (45) using RefSeq gene models as the reference transcriptome. Adjusted p-values and normalized counts were generated using Deseq2 (Galaxy version 2.11) (39). The log2 expression levels were calculated from the average of the normalized counts and the log2 FC between samples determined from these values. A gene was considered to be significantly differentially expressed if it had a greater than 3-fold change between experimental conditions, and an adjusted p-value < 0.05. The statistics for RNA-Seq read counts are shown in **Table 2**.

### KEGG Pathway Analysis

Kyoto Enyclopedia of Genes and Genomes (KEGG) pathway analysis was conducted using the ClueGO package v2.5.7 (46) in Cytoscape v3.8.2 (47). This was done using a right-sided (enrichment) test and p-values were corrected for multiple testing using the Benjamini-Hochberg method. A pathway was deemed to be significantly enriched if it had an adjusted p-value < 0.05.

### Public Datasets

All genome-wide sequencing data generated in this study are available *via* GEO accession number GSE165348. Previously published data sets are available as follows:

**TABLE 2** | Summary of statistics for RNA-Seq data.

| Samples | Read count | Mapped reads |
|---|---|---|
| N1 | 41708821 | 38753290 |
| N2 | 26210529 | 24937718 |
| N3 | 40189419 | 38236520 |
| M28_1 | 33360739 | 3150331 |
| M28_2 | 49159947 | 44957133 |
| M28_3 | 20466143 | 19511654 |
| M56_1 | 21657845 | 20588197 |
| M56_2 | 21089217 | 20098353 |
| M56_3 | 22704067 | 21612454 |
| M28Ag_1 | 73075749 | 69382406 |
| M28Ag_2 | 48663357 | 45860315 |
| M28Ag_3 | 16508204 | 15822670 |
| CXCR5neg_1 | 32335684 | 28473099 |
| CXCR5neg_2 | 19723427 | 18651578 |
| CXCR5neg_3 | 31192312 | 29610572 |
| CXCR5pos_1 | 20604093 | 18708539 |
| CXCR5pos_2 | 43553731 | 41214422 |
| CXCR5pos_3 | 45222585 | 42356577 |

ChIP-seq - TCF-1 thymocytes: GSE46662 (48).

ChIP-seq -T-BET Th1: GSE40623 (49).

ChIP-seq -JUNB TB PI (PMA+ Calcium ionophore A23187), ETS1 TB, RUNX1 TB, RUNX1 TB PI and gene expression microarray data - CD4 Naïve, Naïve PI, Memory and Memory PI: GSE67465 (3).

DNase-seq – TB IL-2, TB IL-2nil, ATAC-seq – TM $Il7r^{f/f,}$TM CD4Cre $Il7r^{f/f}$ and RNA-seq TB IL-2, TB IL-2nil: GSE147294 (5).

# RESULTS

## The Memory T Cell Chromatin Signature Is Established Within 7 of a Single Episode of Acute Infection

The aim of this study was to decipher the gene regulatory networks and chromatin signatures associated with the initial acquisition and long-term maintenance of immunological memory in 2W1S-specific TM cells, and with the recall response of TM cells re-challenged with the 2W1S peptide. We performed detailed genome-wide analyses of 2W1S-specific TM cells at the peak of the T cell response after 7 days, and then again at 28 and 56 d post-infection when the primary response and the infection had resolved and memory populations established (M7, M28 and M56), in parallel with TM cells harvested at days 28 and 56 but 3 hours after a second challenge with Ag (**Figure 1A**). Due to the tiny numbers of 2W1S-specific TN cells present in the first few days of the infection it was not possible to examine the initial Ag-inducible responses during blast cell transformation. Previous studies of BL6 mice estimated an average of just 190 2W1S-specific CD4 TN cells per mouse (31), making such analyses impractical.

To identify potential gene regulatory elements associated with immunological memory, we performed genome-wide sequencing assays of transposase-accessible chromatin (ATAC-Seq) (50). Principle component analysis of all of the ATAC data confirmed that the replicates were highly reproducible and suggested that the differences between M7, M28 and M56 were actually quite modest, with these three groups clustering closely together (**Supplementary Figure 1A**). By far the biggest differences were seen in the responses to Ag stimulation for M28Ag and M56Ag compared to non-stimulated cells.

We defined the subset of DHSs which represent immunologically primed DHSs in TM cells (mDHSs) by very rigid criteria on the basis that the average signal of the ATAC peak in M7, M28 or M56 was at least 3-fold the average value of the peak in TN with a p value of less than 0.05. In addition the peaks were filtered to have at least 20 reads in each of the 2 replicates. These analyses revealed 840 M7 ATAC peaks, 984 M28 ATAC peaks 1010 M56 ATAC peaks that were at least 3-fold greater than in TN CD4 T cells, with 508 of these mDHSs being defined by the same strict criteria in all three subsets (**Figure 1B**). Once formed at day 7, these mDHSs were remarkably persistent. Although 186 of the M7 mDHSs were not strictly defined as mDHSs in M28 and M56, they still retained a higher signal than TN at these DHSs in M28, with all except 17 DHSs being at least 2-fold higher than TN in either M28 or M56 (**Supplementary Table 1**). Furthermore, some of these transiently appearing mDHSs were detected at day 7 only by virtue of the fact that M7 cells still retained a faint activation signature from the primary infection at day 7, which subsided by day 28. For example, one weak M7-restricted mDHS located between the *Txnl4a* and *Hsbp1l1* genes was also clearly a strongly induced iDHS that recruits AP-1 and T-bet in stimulated T cells (**Supplementary Figure 2A**). KEGG pathway analysis of the genes linked to the 508 consistently identified mDHSs revealed a strong link to cytokines, cytokine and TCR signalling, and Th cell differentiation (**Supplementary Table 2**). A subset of these genes and pathways were also identified linked to the M7-specific mDHSs, including *Ifng*, *Il10*, *Il21*, and *Rora*, whereas *Il1b* and *Maf* were linked in M7 only.

By day 28, the mDHSs had largely stabilized whereby the fold increases in ATAC signals mostly remained the same within a factor of 2 at day 56 (grey dashed lines, **Figures 1B, C**). Of the 984 mDHSs detected as 3-fold higher at day 28, 820 still had an ATAC signal 3-fold higher than TN at day 56 (83%) and 959 peaks (97.5%) were still at least 2-fold higher (**Supplementary Table 1**). These highly stable mDHSs included peaks which had increased by at least 10-fold relative to TN at archetypal Th1 immune response genes including *Ifng*, *Cxcr3, Nkg7* and *Ccl5* (**Figure 1C**). The biggest differences between the three mDHS subsets were seen in the direct comparisons between the signals seen at day 28 or day 56 and the signal seen at day 7, whereby some ATAC signals continued to increase after day 7 (**Supplementary Figure 1C**). However, even then, no ATAC signals were more than 3-fold higher at either day 28 or day 56 than at day 7 (**Supplementary Table 1**).

In parallel with the establishment of mDHSs, similar numbers of TN-specific ATAC peaks (nDHSs) were lost during the acquisition of immunological memory (**Figures 1D, E** and **Supplementary Figure 1B**) at genes including *Cnn3*, *Bach2, Atp1b1* and *AcvrI1* (**Figure 1E**). The loss of sites at the *Bach2* locus is significant because it represents the suppression of a pathway that inhibits TCR-inducible AP-1 activity (24). Some of these sites continued to diminish with time, as the signals were lower in M28 and M56 than in M7 (**Supplementary Figure 1D**, **Supplementary Table 1**). In addition, 47% of the nDHSs (538/1153) which were suppressed at day 7 represented transient changes, most likely again due to the persistence of a weak activation signature at day 7, as they had increased in magnitude again by day 28 (**Figure 1D**). For example, several weak DHSs at the *Adarb2*/*Wdr37* locus were defined as nDHSs in M7, reappeared in M28 and M56, but were then suppressed by Ag in M28Ag and M56Ag (**Supplementary Figure 2B**). Two of these nDHSs bind either TCF-1 or ETS1.

To correlate the most stable changes in chromatin accessibility with changes in gene expression we performed parallel analyses of RNA-Seq data for M28 and M56 relative to TN (**Figures 1F–I** and **Supplementary Table 3**). These analyses

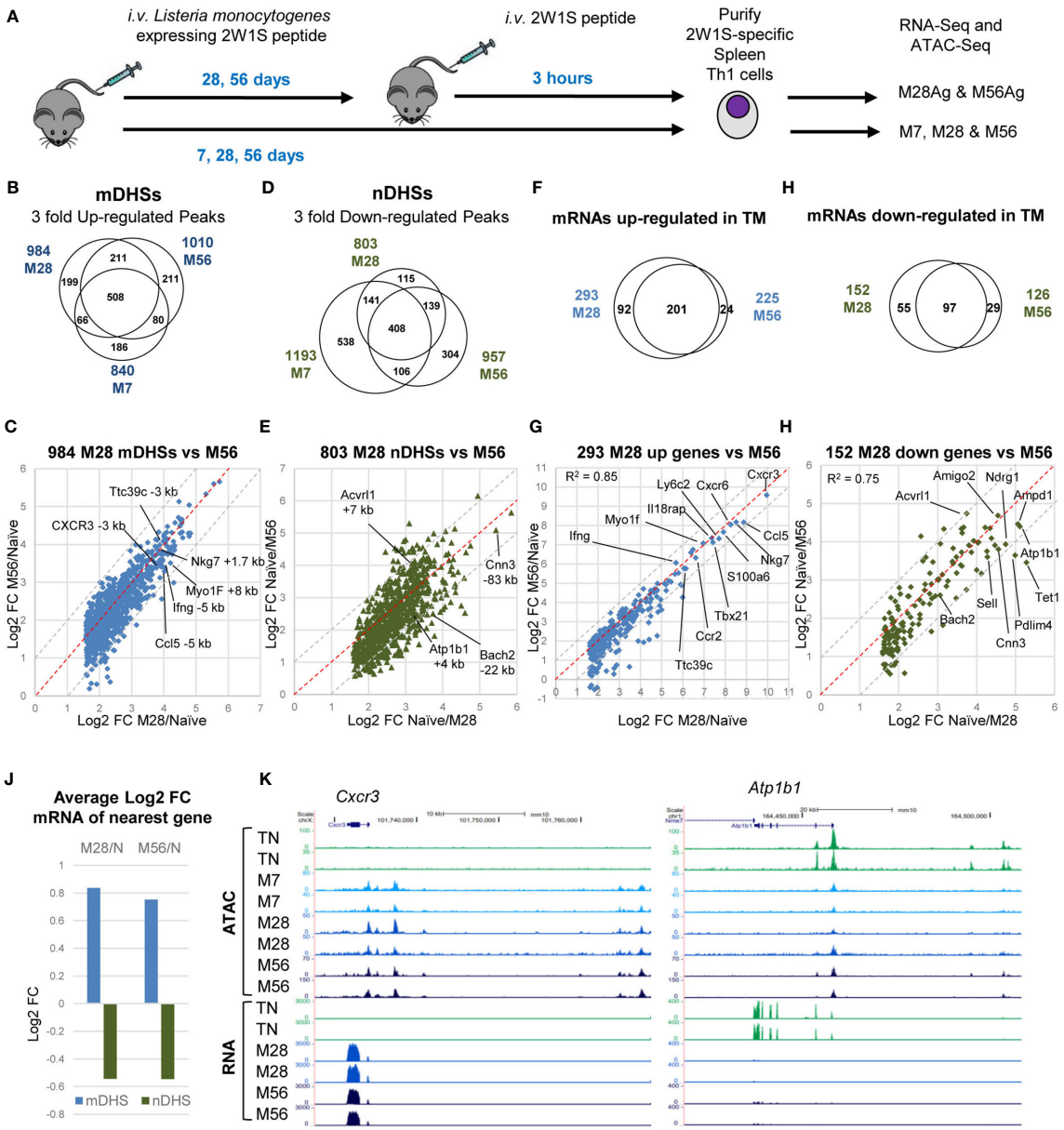


**FIGURE 1** | Establishment and maintenance of immunological memory in Th cells. **(A)** Protocol for the immunization of mice with Lm-2W1S. **(B–E)** Deseq2 analyses of duplicate ATAC-seq samples showing peaks which were either 3-fold up-regulated **(B, C)** or 3-fold down-regulated **(D, E)** (adj p<0.05) in M7, M28 or M56 compared to naïve CD4+, CD62L low T cells. **(F–I)** Deseq2 analyses of triplicate RNA-Seq samples showing genes which were either 3-fold up-regulated **(F, G)** or 3-fold down-regulated **(H, I)** (adj p<0.05) in M7, M28 or M56 compared to naïve CD4+, CD62L low T cells. The red dashed lines represent the equivalence points. The grey dashed lines indicate the boundaries of values that are 2-fold different. **(J)** Average log2 fold change in gene expression for genes adjacent to mDHSs or nDHSs. **(K)** UCSC browser screen shots of ATAC-seq and RNA-Seq data for the TM-specific *Cxcr3* gene and the TN-specific *Atp1b1* gene.

identified consistent changes in 201 genes that were upregulated and 97 genes that were downregulated in M28 and M56 compared to TN. The magnitude of increase in mRNA values also remained remarkably consistent from day 28 to day 56 for genes including *Ifng*, *Cxcr3*, and *Ccl5*, which are known to be regulated by T-bet in Th1 cells (**Figure 1G**), and where parallel chromatin changes were observed (**Figure 1C**). The expression of the genes *Cnn3*, *Bach2, Atp1b1* and *AcvrI1* also decreased in parallel with the loss of nDHSs (**Figures 1E, I**). Strongly down-regulated genes included the archetypal TN-associated gene *Sell* encoding for L-Selectin (CD62L) that functions to localise T cells in lymph nodes (51). Globally there were substantial changes in mRNA levels for genes associated with either mDHSs or nDHSs (**Figure 1J**). Examples of ATAC-Seq and RNA-Seq data are depicted for the TM-specific *Cxcr3* gene and the TN-specific *Atp1b1* gene (**Figure 1K**).

## The Acquisition of Immunological Memory Is Associated With Changes in Gene Regulatory Networks

To investigate the underlying basis of the TM and TN gene regulatory networks we performed HOMER *de novo* DNA motif-finding analyses of the TM-specific mDHSs detected in M28 and the TN-specific nDHSs that were lost in M28 (**Figures 2A, B**). The Th-specific mDHSs were enriched for binding sites for the Th1 lineage-defining factor T-bet (*Tbx21*), and for the constitutively expressed factors ETS-1 and RUNX1 that function globally to support immunological memory in bulk TM cells (3). These sites were also enriched for the inducible TF motif for AP-1 which may be one of the factors needed to initially open up mDHSs during the acute phase of infection (3). The nDHSs were characterized by TCF/LEF motifs, consistent with a shutdown of the *Lef1*/*Tcf7* (TCF-1)-associated TN program when naïve T cells are transformed to effector T cells. Analyses of gene expression for transcription factors (TFs) linked to the differentially regulated motifs (**Figure 2C**) indicated that *Tbx21*, and the AP-1 genes *Jun*, *Junb*, *Fos* and *Fosb* were all upregulated in M28 and M56 Th memory T cells as well as in data from purified bulk naturally arising CD4 memory T cells analysed in a previous study, which had been defined as "memory phenotype" on the basis of being CD4 and CD44 positive but CD62L negative (3). The loss of the TN program was reflected by down regulation of *Lef1* and upregulation of *Id2*, an inhibitor of HLH family proteins (**Figure 2C**), which may account for the decrease in nDHSs containing E-Box motifs for HLH TFs (**Figure 2B**). These changes in mRNA were also reflected in changes in the ATAC profiles at the *Tbx21* and *Lef1* loci (**Figure 2D**).

Global analyses of ATAC and TF DNA motif profiles were performed for all DHSs present in either TN or M28, ranked according to their relative ATAC-seq signals, and displayed alongside the ATAC signals for the same DNA elements in M7 and M56 cells (**Figure 2E**). These data confirmed that the TM-specific mDHSs were enriched for RUNX, ETS, AP-1 and T-bet motifs, whereas the naïve-specific nDHSs were enriched for ETS and in TCF/LEF motifs. Parallel analyses of published chromatin immunoprecipitation (ChIP) data for T-bet in Th1 cells (49), and for TCF-1 in thymus derived naïve T cells (48), confirmed binding of T-bet to the mDHSs and TCF-1 to the nDHSs (**Figures 2E, F**). Examples of these patterns of regulation are depicted for T-bet binding to TM-specific *Ccl5* (**Figure 2G**) and for TCF-1 binding to TN-specific *Cnn3* (**Figure 2H**).

To find indirect evidence that the above motifs were potentially occupied by the predicted families of TFs, we reanalysed the ATAC data using the Wellington footprinting algorithm (41) to plot average profiles of TF motifs. For this purpose we combined the ATAC replicates and plotted the cumulative merged ATAC profiles on the forward and reverse strand sequence reads for the ATAC profiles centred over each motif, to generate average profiles for the mDHSs and nDHSs in both TM and TN (**Supplementary Figure 3**). For the 984 mDHSs, these data revealed strong protection of ETS motifs, and modest protection of AP-1, T-bet and TCF/LEF motifs in TM cells, whereas these footprints were not seen in TN cells where the DHSs were absent. For the 803 nDHSs, these data revealed strong protection of ETS and TCF/LEF motifs, and poor protection of AP-1and T-bet motifs in TN cells, whereas these footprints were not seen in TM cells where the ATAC signal was much lower.

## Lm-2W1S-Specific Memory T Cells Respond Robustly to Re-Exposure to 2W1S

We next investigated the relationships between epigenetic priming in M28 and M56, and the responses of these cells to a second challenge with Ag. M28 and M56 mice were injected *i.v.* with the 2W1S peptide 3 hours prior to purification of 2W1S-specific T cells (**Figure 1A**). 1538 genes were at least 3-fold upregulated by this *in vivo* stimulation (red dots, **Figure 3A**, **Supplementary Table 3**). Strikingly, most of these inducible genes were maintained in homeostasis at the same levels in both TN and M28 in the absence of stimulation (black dots, **Figure 3A**). The exceptions to this were the 77/1538 genes (5%) that were already 3-fold upregulated in M28 relative to TN, and were then further upregulated by at least 3-fold by Ag, including genes such as *Tbx21, Gzmb, Ifng, Tnfsf14*, and *Il2* (**Figure 3A**). 30 of these genes were already associated with mDHSs prior to re-stimulation (**Supplementary Table 3**), and many of these Ag-primed genes were previously found to be non-inducible by PMA+ Calcium ionophore A23187 (PI) in TN cells where they lack priming (3). There were also 1568 genes which were at least 3-fold downregulated after a 3 hour *in vivo* exposure to 2W1S (blue dots, **Figure 3B** and **Supplementary Table 3**). These genes were also mostly maintained at the same levels of expression in TN and M28 cells under homeostatic conditions, (black dots, **Figure 3B**). Genes strongly downregulated by Ag in M28 T cells included *Tcf7, Ets1, Nkg7, Malat1, Ccr7* and *Il7r*.

Re-stimulation of TM cells with Ag induced global changes in accessible chromatin profiles. Analyses of the ATAC profiles revealed 6703 DHSs induced at day 28 (iDHSs), and 1935 diminished DHSs (dDHSs) that were rapidly suppressed by Ag at day 28 (**Figure 3C** and **Supplementary Table 1**). HOMER *de novo* DNA motif finding analyses found that the iDHSs were dominated by the archetypal inducible AP-1, NFAT, EGR and NR4A motifs classically associated with activation of TCR signalling throughout the T cell lineage (**Figure 3D**), as seen in previous studies (3, 52, 53), in combination with a lower level of RUNX and ETS motifs. The dDHSs were much more highly enriched for RUNX and ETS motifs, which maintain immunological memory at mDHSs in TM cells during homeostasis (3), in addition to KLF and TCT/LEF motifs (**Figure 3E**) which were also associated with TN-specific DHSs (**Figure 2B**). The enrichment of motifs specifically in iDHSs and dDHSs was reflected by parallel changes in mRNA levels of the associated TFs (**Figure 3F**).

Global analyses were performed for ATAC and TF DNA motif profiles of all DHSs present either before or after

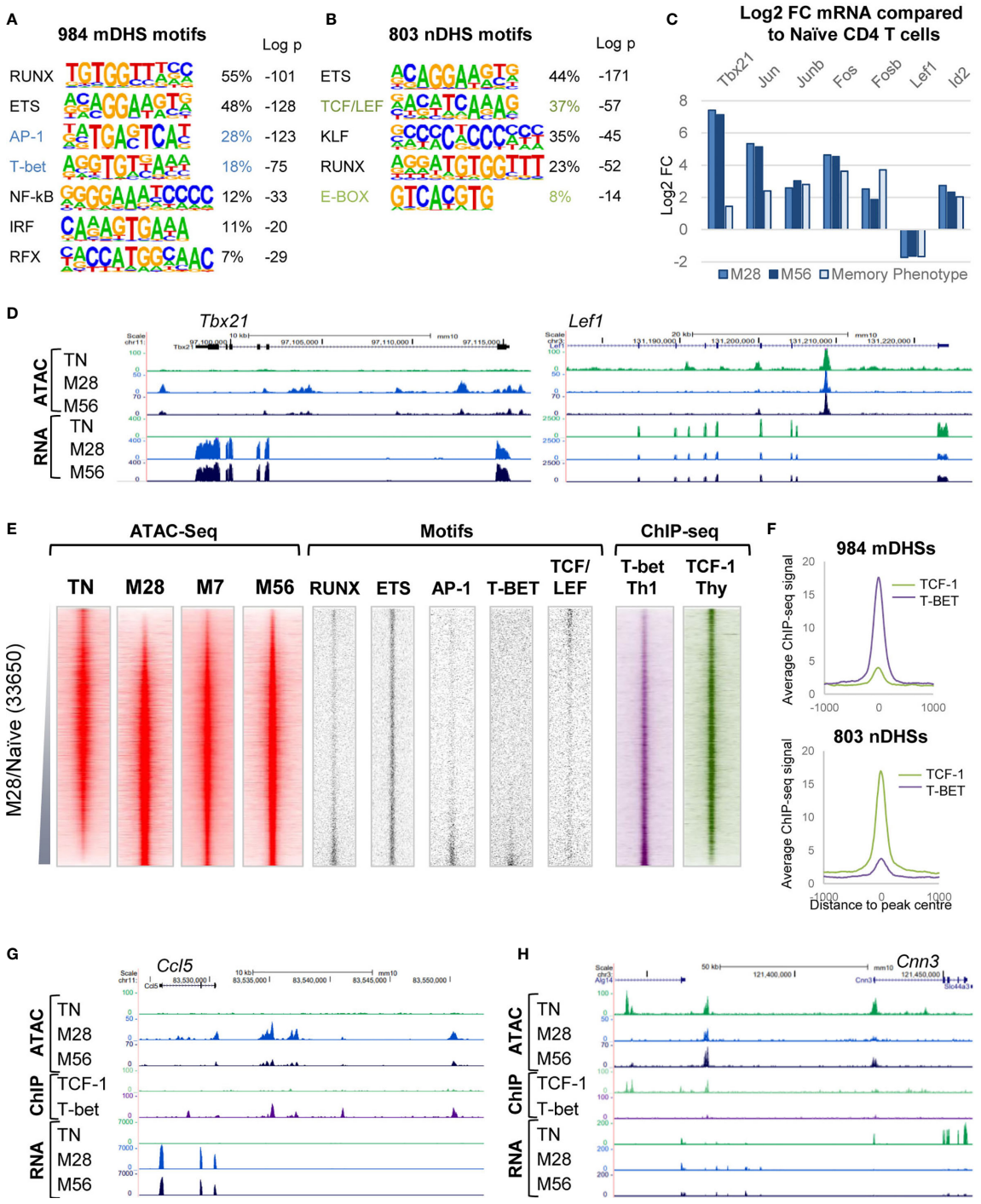


**FIGURE 2** | Gene regulatory networks associated with immunological memory in T cells. **(A, B)** HOMER *de novo* DNA motif analyses of TF motifs that are enriched in mDHSs that are gained **(A)** or nDHSs that are lost **(B)** during the acquisition of immunological memory. **(C)** Log2 values of the fold change (FC) in mRNA expression of TF genes associated with motifs enriched in the mDHSs and nDHSs. Data are shown for M28 or M56 TM cells relative to TN and for previously published microarray data for CD4 memory phenotype cells compared to naïve T cells (3). **(D)** UCSC browser screen shots of ATAC-seq and RNA-Seq data for the TM-specific *Tbx21* gene and the TN-specific *Lef1* gene. **(E)** Global analyses of all DHSs present in either TN or M28 TM cells (replicate 1), ranked according to fold increase in ATAC-seq signal. Shown alongside on the same coordinates are ATAC-seq signals for M7 and M56 TM cells (replicate 1), TF motifs associated with mDHSs and nDHSs, and published ChIP-Seq data for T-bet in Th1 cells (49) and TCF-1 in thymocytes (48). **(F)** Average TCF-1 and T-bet ChIP-Seq profiles for the mDHSs and nDHSs as displayed in **(E)**. **(G, H)** UCSC browser screen shots of ATAC-seq, ChIP-Seq and RNA-Seq data for the TM-specific *Ccl5* gene **(G)** and the TN-specific *Cnn3* gene **(H)**.

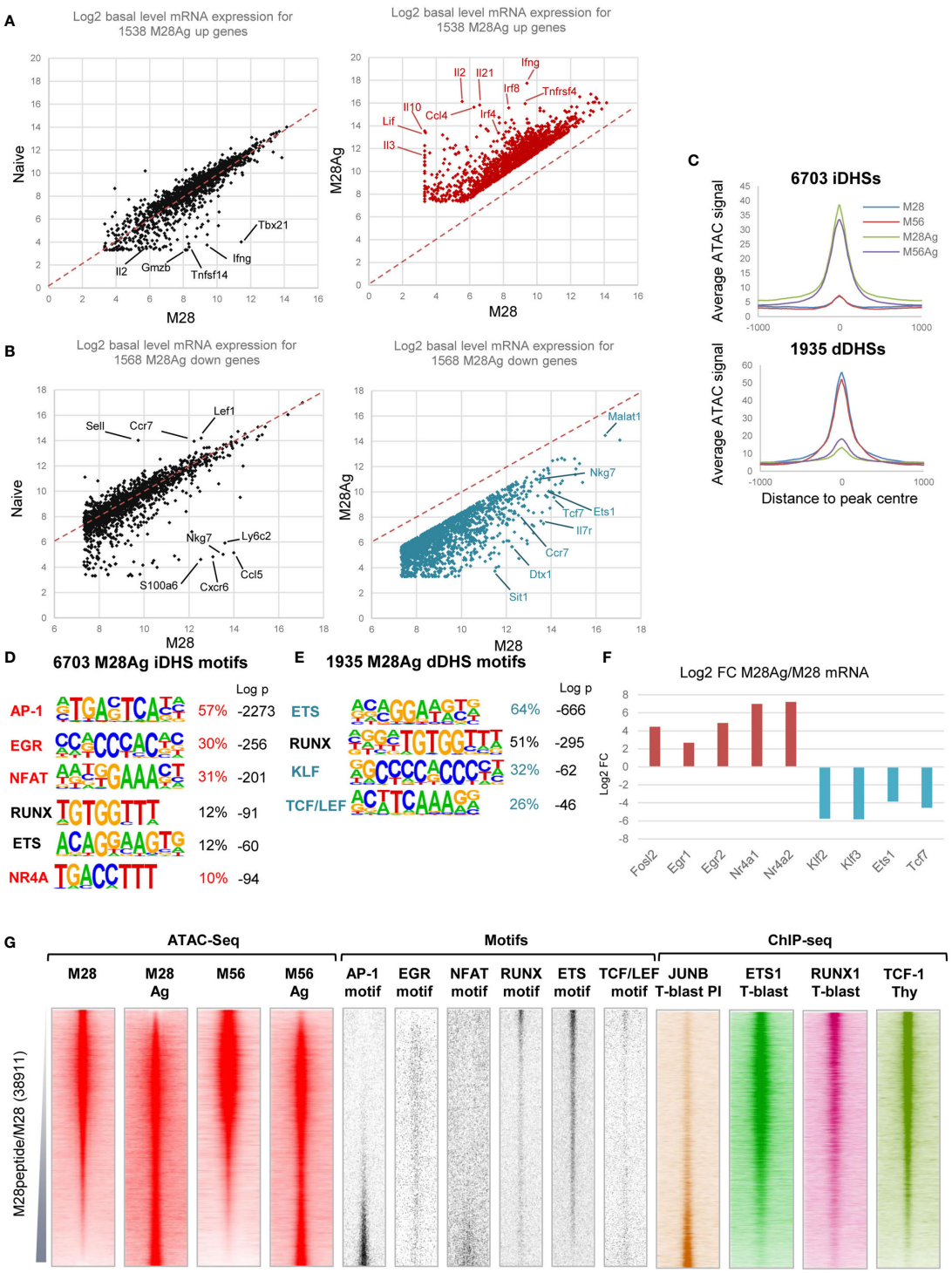


**FIGURE 3** | Gene regulatory networks associated with inducible genes in TM cells. **(A)** RNA-seq data for 3-fold inducible genes in M28 TM cells plotted versus Ag-stimulated M28 TM cells (M28Ag, red) or TN cells (black). **(B)** RNA-seq data for 3-fold inhibited genes in M28 TM cells plotted versus M28Ag TM cells (blue) or TN cells (black). **(C)** Average ATAC-Seq profiles for DHSs which are either 3-fold induced (iDHSs) or 3-fold diminished (dDHSs) in M28Ag. Data are shown as an average of the two replicates **(D, E)** HOMER *de novo* DNA motif analyses of TF motifs that are enriched in iDHSs **(D)** or dDHSs **(E)**. **(F)** Log2 values of the fold change (FC) in mRNA expression of TF genes associated with motifs enriched in iDHSs or dDHSs. **(G)** Global analyses of all DHSs present in either M28 TM cells or M28Ag TM cells (replicate 2), ranked according to fold increase in ATAC-seq signal. Shown alongside on the same coordinates are ATAC-seq signals for M56 and M56Ag TM cells (replicate 2), TF motifs associated with iDHSs and dDHSs, and published ChIP-Seq data for JUNB in PI-stimulated TB cells, ETS1 and RUNX1 in TB cells (3) and TCF-1 in thymocytes (48).

stimulation in M28, ranked according to their relative ATAC signals. Displayed alongside are the signals for the same DNA elements in M56 and M56Ag cells confirming that these regulatory regions were also induced at the later time point (**Figure 3G**). These data confirmed that the iDHSs were highly enriched for AP-1 and NFAT motifs, but not for RUNX, ETS or TCF/LEF motifs which were instead highly enriched in the dDHSs present in non-stimulated cells (**Figure 3G**). In contrast, the Ag-suppressed dDHSs were devoid of AP-1 motifs (**Figure 3G**), consistent with previous studies of dDHSs which disappear following *in vitro* activation of TCR signalling in T cells (2, 3). Published ChIP-Seq data also confirmed that the AP-1 factor JUNB bound to the iDHSs in T-blast cells stimulated with PI whereas TCF-1, ETS-1 and RUNX1 were enriched at the dDHSs in either TB cells or thymocytes (**Figure 3G**). The EGR motif was not, however, concentrated in the iDHSs, perhaps owing to its similarity to the widely distributed Sp1 motif which shares the sequence CCGCCC.

Here we again used Wellington to look for evidence of occupancy or loss of occupancy of the motifs of interest before and after Ag stimulation. This time we plotted average ATAC profiles for motifs in the iDHSs and dDHSs using the accumulated merged ATAC signals in all M28 and M56 samples compared to all M28Ag and M56Ag samples (**Supplementary Figure 4**). For the 6703 iDHSs, these data revealed strong protection of the inducible AP-1 and NFAT motifs, and moderate protection of ETS and TCF/LEF motifs in Ag-stimulated TM cells, with much weaker ATAC activity before stimulation. For the 1935 dDHSs, the ETS motifs showed very strong ATAC activity and footprint protection before stimulation and much less activity after stimulation. In addition, the dDHSs showed a complete absence of AP-1 footprints, and weak NFAT footprints prior to stimulation, consistent with the motif plots in **Figure 3G**. The footprints seen at TCF/LEF motifs in TM cells also diminished following stimulation. Overall, these data suggest that dDHSs are unresponsive to inducible factors but have a strong dependence on ETS factors which are no longer able to sustain them following stimulation. Due to the very low numbers of TM cells which can be purified it is technically not possible for us to perform ChIP assays to confirm loss of binding of ETS1 at the dDHSs, however the loss of open chromatin makes it highly unlikely that many TFs could remain bound at these sites.

The global loss of DHSs with protected TCF/LEF and ETS motifs in response to Ag stimulation was also accompanied by substantial decreases in mRNA expression and ATAC-seq signals at the *Tcf7* and *Lef1* loci (**Figure 4A**), and striking changes in expression of most of the ETS family TFs expressed in Ag-stimulated M28 cells (**Figures 4B, C**). These observations were supported by ChIP-Seq data from TB cells cultured *in vitro* showing binding of ETS1 and RUNX1 at ATAC peaks which are reduced upon stimulation with PI or Ag (**Figure 4A**). In response to *in vivo* activation by Ag, the expression of *Ets1* was suppressed by ~15-fold, while conversely the expression of *Etv6*, a repressor of ETS activity, was induced more than 10-fold. These changes were mirrored by extensive changes in the ATAC-Seq profiles at both the *Etv6* and *Ets1* loci, which included iDHSs bound by the AP-1 TF JUNB and RUNX1 in PI-stimulated TB cells at *Etv6*, and a binding site for TCF-1, ETS1 and RUNX1 at +45 kb ATAC peak in the *Ets1* locus which disappeared upon stimulation (**Figure 4D**). This +45 kb *Ets1* peak encompassed 3 ETS motifs, TCF/LEF and KLF motifs (**Figure 4E**), suggesting that its disappearance is linked to the downregulation of TFs such as *Ets1, Fli1, Elf1, Klf2, Klf3*,*Tcf7* and *Lef1* (**Figures 2C**, **3F**, **4C**). The +45 kb DHS also had 4 ideal GATA motifs, suggesting a potential alternate mode of regulation in Th2 cells that express GATA3. The inducible changes in ETS family gene expression were not, however, limited to TM cells as similar trends were observed to a smaller degree in published RNA micro-array data for PI-stimulated TN cells (**Figure 4C**). For example, *Ets1* and *Fli1* expression is suppressed 3-4 fold by PI in TN cells. Overall, it would appear that ETS1 plays a bigger role in maintaining the homeostatic T cell program, and immunological memory at mDHSs, than in activating inducible genes in Th1 cells. This is similar to the role previously defined for the IL-2/IL-7 inducible AP-1 family member JUND, which may maintain epigenetic priming without actually activating many AP-1 target genes which have low steady state levels of mRNA in TM cells (4, 5).

## TM-Specific and Inducible DHSs Cooperate in the Memory Recall Response

Previous *in vitro* studies suggested that much of the inducible gene expression program in memory T cells is dependent upon epigenetic priming of immune response genes (2, 3). Here we investigated the extent to which epigenetic reprograming was associated with the *in vivo* responses of memory T cells by looking for correlations between the inducibility of genes and their association with just mDHSs, just iDHSs, or iDHSs together with mDHSs. Global analyses of average mRNA expression revealed that genes which are associated with both iDHSs and mDHSs are more highly inducible by Ag in M28, or by PI in previously published data on bulk TM cells (3) than the other subsets (**Figure 5A**, green bars). Furthermore the same genes showed little response to stimulation by PI in TN cells which lack these mDHSs and genes with dDHSs actually went down in expression after activation. Taken together these data support the published model proposing that memory specific mDHSs aid the induction of proximal iDHSs and subsequent gene expression (2, 3). Examples of these concepts can be seen for: (i) Genes such as *Gfi1, Rel* and *Tnf*, where iDHSs appeared in both naïve and memory cells and which were induced in each of TN PI, TM PI and M28 Ag, with (**Figure 5B**, and **Supplementary Figure 5A**). These loci have pre-existing DHSs in TN and lack memory specific mDHSs accounting for the induction in both cell types. (ii) Genes such as *Il10*, *Il21* and *Ifng*, which have both mDHSs and iDHSs, showed higher levels of inducibility in M28 cells, and were PI-inducible in TM cells but not in TN cells where they lack pre-existing DHSs (**Figure 5C** and **Supplementary Figure 5B**). (iii) Genes with mDHSs only were, on average, expressed at a higher level in M28 and M56 cells than TN cells, but were not

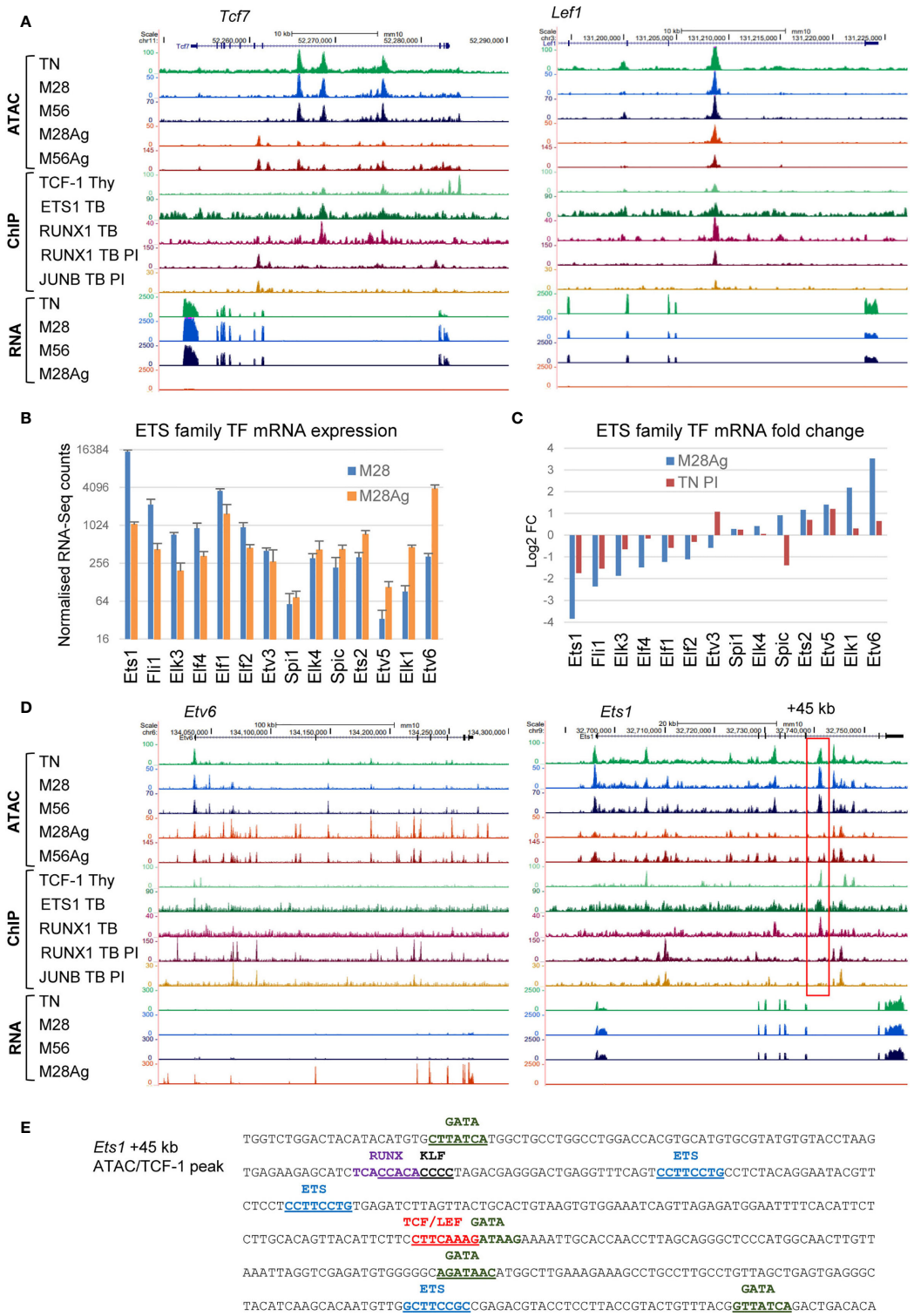


**FIGURE 4** | Rewiring or the ETS and TCF/LEF gene regulatory networks in response to Ag. **(A)** UCSC browser screen shots for *Tcf7* and *Lef1* showing ATAC-seq and RNA-Seq data in M28 and M56 TM cells, before or after Ag-stimulation. Also depicted are published ChIP-Seq data for TCF-1 in thymocytes (48), and ETS1, RUNX1 and JUNB, in TB cells before or after PI-stimulation (3). **(B)** RNA-seq data for all ETS family genes expressed in M28 or M28Ag. The standard deviation is shown for 3 replicates. **(C)** Log2 fold changes in gene expression for the data shown in **(B)**, in parallel with equivalent published data for naïve T cells treated with PI (3). **(D)** UCSC browser screen shots for *Etv6* and *Ets1*, the same data is depicted as for **(A)**. The red box highlights a DHS at + 45 kb which is suppressed in response to Ag. **(E)** DNA sequence of the *Ets1* +45 kb dDHS showing relevant TF motifs.

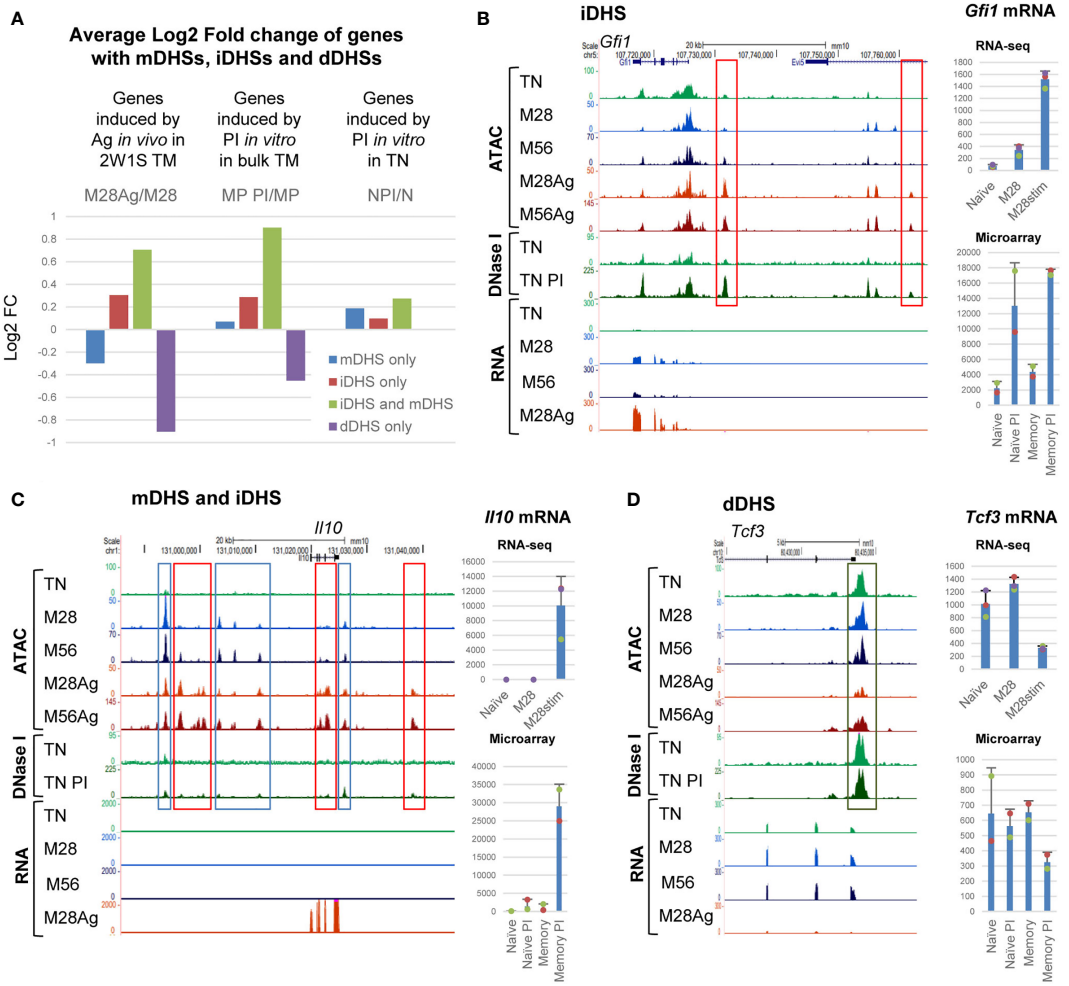


**FIGURE 5** | Inducible TM-specific genes have primed mDHSs associated with iDHSs. **(A)** Average Log2 values of the fold change (FC) in mRNA expression of genes associated with just mDHSs, just iDHSs, both mDHSs and iDHSs, or just dDHSs. Values are shown for mRNA changes following Ag-stimulation of M28 TM cells. Also shown are published microarray data for responses to PI-stimulation of CD4 memory phenotype cells (MP) and naïve T cells (N) (3). **(B–D)** UCSC browser screen shots showing ATAC-Seq, DNase-Seq and RNA-Seq data for representative genes with iDHSs **(B)**, mDHSs and iDHSs **(C)**, or dDHSs **(D)**. Tracks include published DNase-Seq data for naïve CD4 T cells (TN) before and after PI-stimulation (3). Red boxes highlight iDHSs, blue boxes highlight mDHSs, and the dark green box highlights a dDHS. Shown at the right are RNA-Seq data for TN, M28 and M28 Ag (top) and published microarray data for responses to PI-stimulation of CD4 memory phenotype cells and naïve T cells (bottom) (3). The standard deviation is shown for 3 replicates for the RNA-seq data and 2 replicates for the microarray data.

induced by Ag, and actually decreased in expression (**Supplementary Figure 5C**). On the other side of the spectrum, genes that have dDHSs which were lost after stimulation, such as *Tcf3* and *Pik3r5*, were expressed at a lower level in M28Ag than M28, but were not suppressed by PI-stimulation in TN cells (**Figures 5A, D** and **Supplementary Figure 5D**).

KEGG pathway analysis of the subsets of genes defined in **Figure 5A** consistently identified a strong link to cytokines, cytokine and TCR signalling, and Th cell differentiation in genes with mDHSs and/or iDHSs (**Supplementary Table 2**). KEGG analysis of genes with just dDHSs identified just 3 pathways, including endocytosis and apoptosis.

## The Epigenetic Programs for Central Memory and Effector Memory Are Both Established Within 7 Days of an Acute Episode of Infection

To investigate mechanisms involved in establishing both central and effector memory, we analysed Ag-specific TM cells soon after they had formed, 7 days after infection with Lm-2W1S, and separated 2W1S-specific CD4 T cells into CXCR5-ve Tem and CXCR5+ve Tcm cells (**Figure 6A**). Comparisons of ATAC-Seq data from these two populations identified 784 mDHSs that were 2-fold greater in Tem cells and 612 mDHSs that were 2-fold greater in Tcm cells (**Supplementary Table 4**). DNA motif analyses determined that these two subsets of DHSs had

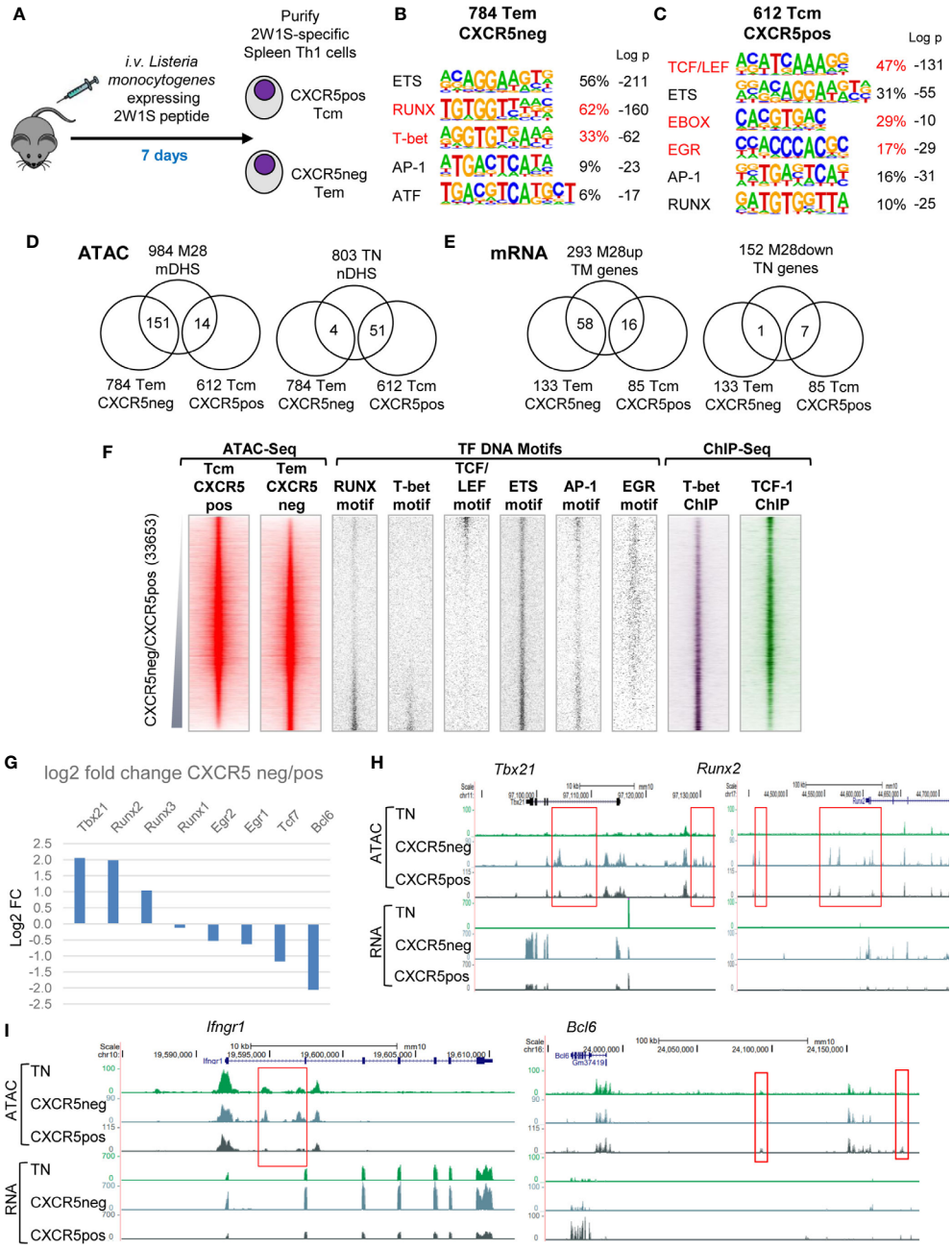


**FIGURE 6** | Tem and Tcm cells establish distinct chromatin and mRNA profiles. **(A)** Protocol for the immunization of mice with Lm-2W1S to generate Tem and Tcm cells. **(B, C)** HOMER *de novo* DNA motif analyses of TF motifs that are enriched in Tem **(B)** and Tcm **(C)**-specific DHSs. **(D, E)** Venn diagrams showing overlaps between Tem and Tcm-specific mDHSs identified by ATAC-Seq **(D)** and genes identified by RNA-Seq **(E)** and the corresponding TM and TN-specific DHSs and genes. **(F)** Global analyses of all DHSs present in either Tcm or Tem cells (replicate 1), ranked according to fold change in ATAC-seq signal. Shown alongside on the same coordinates are TF motifs associated with Tem and Tcm-specific DHSs, and published ChIP-Seq data for T-bet in Th1 cells (49) and TCF-1 in thymocytes (48). **(G)** Log2 values of the fold change (FC) in mRNA expression of selected differentially regulated TF genes. **(H, I)** UCSC browser screen shots showing ATAC-Seq and RNA-Seq data for TN, CXCR5-ve Tem and CXCR5+ve Tcm cells, showing representative examples of Tem-specific and Tcm-specific genes **(E)**. Red boxes highlight differentially regulated DHSs.

distinct gene regulation signatures. The Tem subgroup was enriched for T-bet motifs, similar the M28 mDHSs, whereas the Tcm subgroup was enriched for TCF/LEF and E-box motifs, similar to the TN-specific nDHSs (**Figures 6B, C**). However, despite these overall similarities with other DHS subsets, there was relatively little overlap between the Tem-specific and M28-

specific mDHSs (151/984 mDHSs) and genes (58/293) (**Figures 6D, E** and **Supplementary Table 1**). There was even less overlap between the Tcm-specific and TN-specific DHSs (51/803 nDHSs) and genes (7/152) (**Figures 6D, E**). Hence, the split between Tem and Tcm programs is not simply a reversion of Tcm cells to a more primitive state closer to the TN gene regulatory network. What is more likely is that Tcm and TN share a part of the cell quiescence program defined by TCF-1 and LEF1, whereas recently activated Tem develop a stronger commitment to Th1 differentiation, and that these two pathways of Ag response develop in parallel. KEGG pathway analysis of the subsets of genes linked to the Tem and Tcm-specific mDHSs identified in **Figure 6D** revealed a strong link to cytokines, cytokine and TCR signalling and Th cell differentiation in both subsets, whereas genes such as *Nfkb1* and *Mapk14* also had Tem-specific mDHSs linked to pathways associated with intracellular infections that drive Th1 responses (Human immunodeficiency virus 1 infection and Tuberculosis, **Supplementary Table 2**).

More detailed global analyses of the gene regulatory networks underlying the above-defined Tem-specific and Tcm-specific DHS subsets (**Figure 6F**) further confirmed the notion that Tem-specific sites were the regulatory elements showing the strongest commitment to Th1 differentiation, being most enriched for T-bet motifs. Conversely, the Tcm-specific DHSs revealed a lack of Th1 commitment and were heavily biased to the TCF/LEF program associated with dormant TN cells or thymocytes. These patterns were reflected by the published ChIP-Seq data for T-bet from Th1 cells and TCF1 from thymocytes (**Figure 6F**). Although AP-1 and EGR family TFs are both MAPK inducible, and AP-1 motifs were enriched in both Tem and Tcm-specific DHSs, the EGR motif was found in Tcm but not Tem-specific DHSs.

Closer inspection of the TF gene expression profiles confirmed that the Th1-defining TF *Tbx21* and the Th1-inducing IFN-g receptor gene *Ifngr1* were more highly expressed in Tem, and had Tem-specific DHSs (**Figures 6G–I**). The upregulation of *Runx2* and *Runx3* expression might partially account for the enrichment of RUNX motifs in Tem-specific DHSs (**Figure 6G**). Conversely, the Tfh-associated TF gene *Bcl6* was upregulated in Tcm, but not TN or Tem, as further evidence that Tcm cells had also moved beyond the TN stage (**Figure 6I**). Bcl6 is already known to play a major role in steering recently activated T cells towards Tcm fate, and is downregulated during secondary responses when Tcm cells are recruited as effector T cells (26).

## The Choice of Cytokine Receptors Influences the Decision Between Tem and Tcm Commitment

Sometimes, branches in lineage commitment are decided by stochastic choices in gene expression programs at differentiation branch points. This is in essence the cornerstone of the Waddington model of the role of epigenetics in differentiation (54). This may also be what separates the choices between Tem and Tcm fate. In this model, the cell fates are determined according to which cytokine receptors a recently activated T cell expresses. In this study, Tem cells exhibit much higher expression of the *Il7r*, *IL2ra* and *Il2b* genes than Tcm cells (**Figures 7A–C**) consistent with the previous observation that Tcm cells lack IL-2Rα expression (5, 26). This is highly significant because we recently demonstrated that IL-2/IL-7 signalling *via* the common gamma chain plays a crucial role in maintaining accessible sites in lineage-specific genes prior to T cell differentiation (5). Without this priming for T cell differentiation, Tcm cells may be left in limbo, unable to differentiate, but progress towards an equally important fate of establishing and maintaining a plastic memory of TCR activation, before any lineage-commitment decision has been made. Evidence suggests that IL-2 and IL-7 play major roles in determining Tem versus Tcm fate because recently activated T cells have DHSs which are biased towards Tem fate in the presence of IL-2 or when they express the IL-7 receptor (**Figure 7D**), but Tcm fate in the absence of IL-2 or when the *Il7r* is deleted (**Figure 7E**). Furthermore, expression of *Tcf7*, encoding TCF-1, is strongly down-regulated in the presence of IL-2, supporting a model where TCF-1 maintains "stemness" and quiescence (**Figure 7F**).

# DISCUSSION

## Immunological Memory Is Established Within 7 Days and Remains Stable

Previous *in vitro* studies suggested that the epigenetic and gene expression program underlying T cell memory is established within 2-3 d of activation of TCR signaling in naïve T cells (3, 13). This program relies on epigenetic priming of inducible genes that can be rapidly re-activated in a TM-specific manner. Mouse studies of Ag-specific memory T cells demonstrated that the mRNA expression program for immunological memory in response to acute episodes of bacterial infections is already established at the peak of the Th1 response within 7 d of infection (20). Here we used the same model system to confirm that epigenetic priming also forms the underlying basis of the acquisition of immunological memory in Th cells. Acute infection by Lm-2W1S triggered Th differentiation associated with stable expression of the Th1 lineage-defining factor T-bet and the epigenetic priming of hundreds of inducible genes. As seen in previous global studies of TM cells (20), this program was predominantly maintained by binding of the constitutively expressed TFs ETS1 and RUNX1 to sites which had previously been inaccessible in TN cells. These DNA elements also contained a high proportion of motifs for AP-1 which is thought to both support the initial opening up of mDHSs during the activation phase (3), and bind IL-2/IL-7-inducible JUND and STAT5 (5), to keep genes accessible for lineage-defining factors including T-bet during differentiation (5). Once immunological memory has been established in T cells, it is remarkably stable in the absence of further TCR activation. In rapidly dividing cells cultured with IL-2 or IL-7, mDHSs recruit TFs that include ETS1, RUNX1, JUND and STAT5 which maintain an open chromatin environment rendered more accessible by histone H3K4me2 and H3K9ac (3, 5). In the context of immune homeostasis, immunological priming of

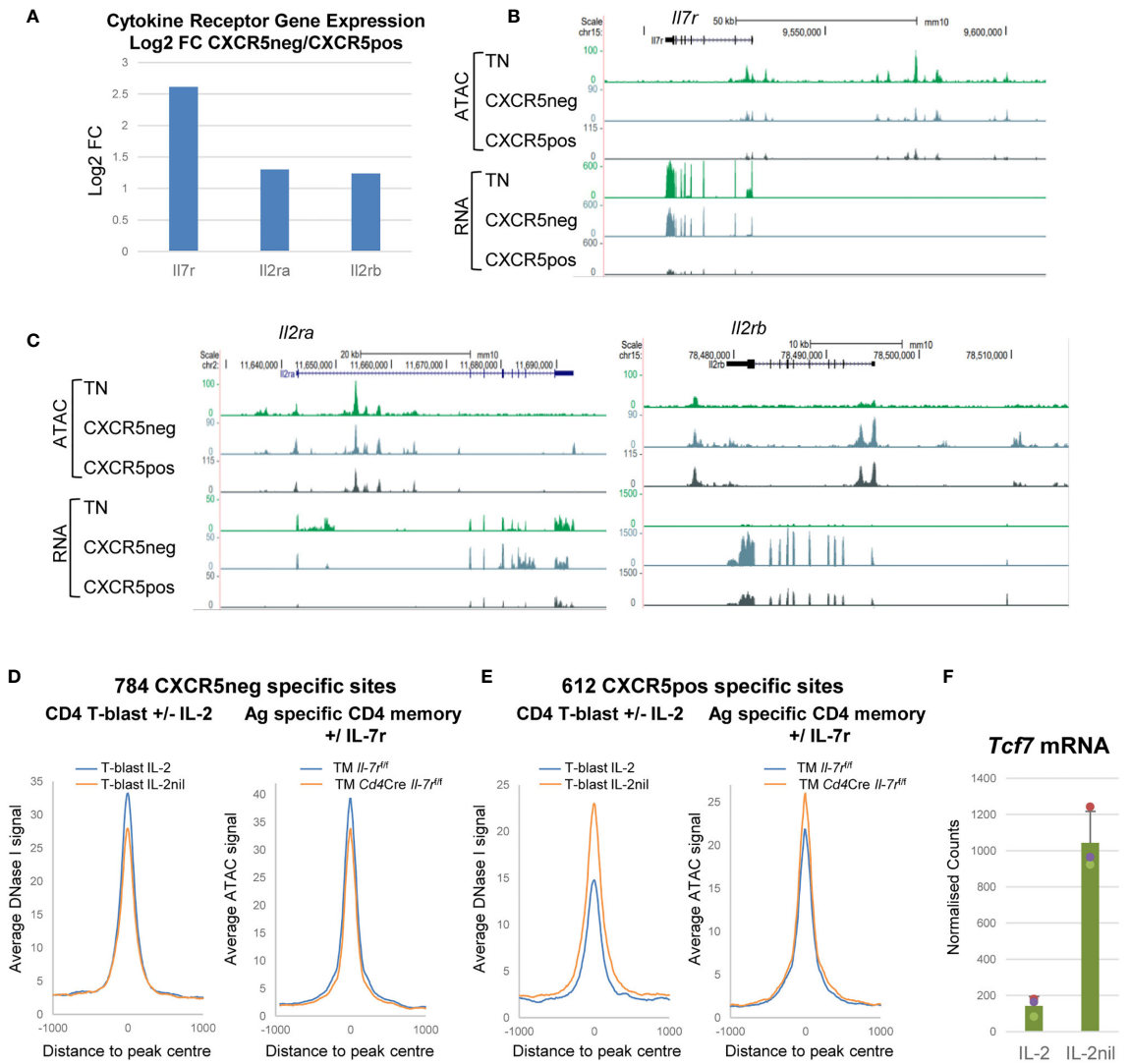


**FIGURE 7** | Cytokine receptor genes are differentially regulated in Tem and Tcm cells. **(A)** Log2 values of the fold change (FC) in mRNA expression of selected cytokine receptor genes in Tem relative to Tcm cells. **(B, C)** UCSC browser screen shots showing ATAC-Seq and RNA-Seq data for TN, CXCR5-ve Tem and CXCR5+ve Tcm cells, for IL-7 **(B)** and IL-2 **(B)** receptor genes. **(D, E)** Published data (5) depicting average DNase-Seq and ATAC-seq profiles for TB cells cultured in the presence or absence of IL-2 (left panels) and for Ag-specific Th TM cells before or after *in vivo* deletion of the *Il7r* gene (right panels) for Tem-specific **(D)** and Tcm-specific **(E)** DHSs. **(F)** Published mRNA-Seq data (5) for *Tcf7* expression in TB cells cultured in the presence or absence of IL-2.

TM cells is likely to remain stable for decades in quiescent TM cells in the presence of lymph node derived IL-7 or tissue-derived IL-15 (5, 10–12).

In this study we also showed the Th1 program developed in parallel with the transcriptional and epigenetic silencing of genes regulated by a TCF/LEF-dependent network in TN cells such as *Lef1*, *Bach2*, *Sell*, *Atp1b1*, *Ndgr1* and *Cnn3*. These changes may reflect a shut-down of a quiescent homeostatic program in TN cells where BACH2 silences the inducible AP-1 network (24). Some of these down regulated genes are known to control cell behavior and migration whereby L-Selectin (*Sell*) facilitates migration into lymph nodes, Calponin 3 (*Cnn3*) regulates actin in the cytoskeleton (55) where it can control contraction of actin stress fibers (56), and NDRG1 functions as a metastasis suppressor and blocks signaling to NF-κB (57, 58). NDRG1 is a T cell anergy factor that is suppressed by CD28 and IL-2 signaling, and NDRG1-deficient mice show T-cell hyper-responsiveness (59). NDRG1 is also likely to help maintain the TCF/LEF network by interacting with b-Catenin (60).

## The Th Tem and Tcm Programs Develop in Parallel

One of the key questions in memory T cell biology is whether memory T cells evolve in parallel with effector T cells, or

represent effector T cells that have returned to a quiescent state. Studies of the acute response to Lm2W1S suggested that these two mechanisms operate in parallel, producing both Tem cells and Tcm cells within the same time frame (26). Previous studies of Ag-specific T cells studies revealed that a systemic Lm-2W1S infection initiates a Th1-biased T cell response where (i) some TN cells differentiate as CXCR5-ve cells, expressing T-bet and CD25 (IL-2Rα), which support the Th1 program and revert to Tem memory T cells once the infection is cleared, and (ii) CXCR5+ve cells which expand in response to TCR signaling, but evade Th1 differentiation and develop as Tcm cells lacking CD25 expression (26). Here we established that (i) the Tem program is supported by a Th1-like gene regulatory network dominated by epigenetic priming maintained by T-bet, ETS and RUNX factors, and (ii) the Tcm program involves establishment of a different epigenetic program, but one maintained by a gene regulatory network involving TCF/LEF and HLH E-box-binding TFs. The choices between these two fates may well be stochastic whereby cells are biased towards either a Th1 pathway in Tem supported by IL-2 and IL-7 receptor signaling, or a Tcm pathway in cells with low IL-2 and IL-7 receptor expression and high BCL6 expression, which maintain the TCF/LEF network and thereby evade Th1 differentiation. However, in this study we did not track cell fate during the primary response, and so we have not been able formally identify the direct precursors of Tem and Tcm cells. Furthermore, a recent single cell analysis of CD4 T cell clones developing from malarial infection identified considerable heterogeneity in cell fates, and proposed that TM cells gradually arise from a pool of effector T cells rather than bypassing this stage (61). A similar study of CD8 T cells also found that viral infection leads to a heterogeneous population of responding cells that includes early arising effector T cells, that have an activation phenotype and have silenced genes associated with T cell memory (62). Following cell division, these effector T cells could subsequently generate distinct sub-populations of cells exhibiting either a Tem, Tcm or a Th1 cell phenotype, exhibiting differential expression of genes such as *Tbx21*, *Tcf7* and *Id2*.

### The Ag Recall Response Involves Extensive Rewiring of the ETS TF Network

Here we confirmed the previously proposed epigenetic priming model (2, 3) as the basis of the acquisition of immunological memory in T cells. We showed that a stable Ag recall response in *bona fide* long term Ag-specific memory T cells was indeed associated with epigenetic priming of gene regulatory elements within inducible effector T cell-specific genes. We demonstrated global epigenetic priming at DNA elements associated with greatly enhanced Ag responses in TM cells but not TN cells. In addition, a subset of these primed mDHSs were associated with genes that have increased steady state expression in Th1 cells such as *Tbx21* and *Ccl5*. In each case, the gene regulatory networks were supported by T-bet and ETS and RUNX factors.

One striking observation made here was that reactivation of TM cells by Ag resulted in a very rapid and global rewiring of the ETS gene regulatory networks. Previous studies conclusively established that ETS factors played crucial roles at every stage of hematopoietic, thymocyte and T cell development (63, 64). Early thymocyte development is associated with progressive down-regulation of the repressive ETS factor ETV6 and upregulation of the transcriptional activator ETS1 (65). ETS1 cooperates with LEF-1 and RUNX1 to activate expression of TCR genes (66–69). ETS1 is also essential for the development of a Th1 response in cells able to express IFN-γ (70). Paradoxically, we found that Ag-stimulation *in vivo* results in the almost immediate shutdown of the *Ets1* gene and activation of the *Etv6* gene. Taken together, these data suggest that TFs such as ETS1 are essential for driving T cell development and differentiation, and for maintaining immunological memory during homeostasis without activating transcription of immune response genes. In parallel with this switch in the role of ETS factors, we previously described opposing roles for different AP-1 proteins whereby (i) JUND maintains IL-2/IL-7-dependent priming during homeostasis, without activating transcription, and (ii) other TCR-inducible AP-1 proteins such as FOS, JUN and JUNB which drive reactivation of the immune response (5). Furthermore, previous studies found that depletion of *Ets1* or *JunD* in mice led to an increase in the number of activated T cells, and defects in Treg cells, suggesting that both ETS1 and JUND help to maintain homeostasis (71, 72).

In conclusion, the rewiring of the gene regulation program during T cell development, differentiation and activation involves many more levels than were previously fully appreciated. The memory T cell homeostasis program is holding genes in a poised receptive state, ready to be activated at a moment's notice, and this program itself has to be shut down during an immune response to recall Ags.

## DATA AVAILABILITY STATEMENT

The datasets presented in this study can be found in online repositories. The names of the repository/repositories and accession number(s) are: GEO, accessed via GSE165348.

## ETHICS STATEMENT

The animal study was reviewed and approved by UK Home Office.

## AUTHOR CONTRIBUTIONS

SB, RF, DG, JS, CW, and DC performed the experiments. SB and PK analyzed the data. SB, DW, and PC wrote the manuscript. All authors contributed to the article and approved the submitted version.

## FUNDING

This study was supported by funding from the Medical Research Council (MR/P001319/1).

## ACKNOWLEDGMENTS

We thank Genomics Birmingham at the University of Birmingham for assistance with DNA sequencing. We thank Csilla Varnai for assistance preparing the GEO submission of the genome-wide sequencing data. The following tetramer was obtained through the NIH Tetramer Facility: 2W1S:I-$A^b$.

## SUPPLEMENTARY MATERIAL

The Supplementary Material for this article can be found online at: https://www.frontiersin.org/articles/10.3389/fimmu.2021.642807/full#supplementary-material

## REFERENCES

1. Jenkins MK, Khoruts A, Ingulli E, Mueller DL, McSorley SJ, Reinhardt RL, et al. In Vivo Activation of Antigen-Specific CD4 T Cells. *Annu Rev Immunol* (2001) 19:23–45. doi: 10.1146/annurev.immunol.19.1.23
2. Bevington SL, Cauchy P, Cockerill PN. Chromatin Priming Elements Establish Immunological Memory in T Cells Without Activating Transcription: T Cell Memory Is Maintained by DNA Elements Which Stably Prime Inducible Genes Without Activating Steady State Transcription. *BioEssays: News Rev Mol Cell Dev Biol* (2017) 39:1–12. doi: 10.1002/bies.201600184
3. Bevington SL, Cauchy P, Piper J, Bertrand E, Lalli N, Jarvis RC, et al. Inducible Chromatin Priming Is Associated With the Establishment of Immunological Memory in T Cells. *EMBO J* (2016) 35:515–35. doi: 10.15252/embj.201592534
4. Bevington SL, Cauchy P, Withers DR, Lane PJ, Cockerill PN. T Cell Receptor and Cytokine Signaling Can Function at Different Stages to Establish and Maintain Transcriptional Memory and Enable T Helper Cell Differentiation. *Front Immunol* (2017) 8:204. doi: 10.3389/fimmu.2017.00204
5. Bevington SL, Keane P, Soley JK, Tauch S, Gajdasik DW, Fiancette R, et al. Il-2/IL-7-Inducible Factors Pioneer the Path to T Cell Differentiation in Advance of Lineage-Defining Factors. *EMBO J* (2020) 39:e105220. doi: 10.15252/embj.2020105220
6. Pepper M, Linehan JL, Pagan AJ, Zell T, Dileepan T, Cleary PP, et al. Different Routes of Bacterial Infection Induce Long-Lived TH1 Memory Cells and Short-Lived TH17 Cells. *Nat Immunol* (2010) 11:83–9. doi: 10.1038/ni.1826
7. Zhu J, Yamane H, Paul WE. Differentiation of Effector CD4 T Cell Populations (*). *Annu Rev Immunol* (2010) 28:445–89. doi: 10.1146/annurev-immunol-030409-101212
8. Vahedi G, Takahashi H, Nakayamada S, Sun HW, Sartorelli V, Kanno Y, et al. Stats Shape the Active Enhancer Landscape of T Cell Populations. *Cell* (2012) 151:981–93. doi: 10.1016/j.cell.2012.09.044
9. Ahmed R, Gray D. Immunological Memory and Protective Immunity: Understanding Their Relation. *Science* (1996) 272:54–60. doi: 10.1126/science.272.5258.54
10. Read KA, Powell MD, McDonald PW, Oestreich KJ. Il-2, IL-7, and IL-15: Multistage Regulators of CD4(+) T Helper Cell Differentiation. *Exp Hematol* (2016) 44:799–808. doi: 10.1016/j.exphem.2016.06.003
11. Mackay LK, Wynne-Jones E, Freestone D, Pellicci DG, Mielke LA, Newman DM, et al. T-Box Transcription Factors Combine With the Cytokines TGF-Beta and IL-15 to Control Tissue-Resident Memory T Cell Fate. *Immunity* (2015) 43:1101–11. doi: 10.1016/j.immuni.2015.11.008
12. Surh CD, Sprent J. Homeostasis of Naive and Memory T Cells. *Immunity* (2008) 29:848–62. doi: 10.1016/j.immuni.2008.11.002
13. Rogers PR, Dubey C, Swain SL. Qualitative Changes Accompany Memory T Cell Generation: Faster, More Effective Responses at Lower Doses of Antigen. *J Immunol* (2000) 164:2338–46. doi: 10.4049/jimmunol.164.5.2338
14. Sprent J, Surh CD. T Cell Memory. *Annu Rev Immunol* (2002) 20:551–79. doi: 10.1146/annurev.immunol.20.100101.151926
15. Curtsinger JM, Lins DC, Mescher MF. CD8+ Memory T Cells (CD44high, Ly-6C+) Are More Sensitive Than Naive Cells to (CD44low, Ly-6C-) to TCR/CD8 Signaling in Response to Antigen. *J Immunol* (1998) 160:3236–43.
16. Kaech SM, Wherry EJ, Ahmed R. Effector and Memory T-cell Differentiation: Implications for Vaccine Development. *Nat Rev Immunol* (2002) 2:251–62. doi: 10.1038/nri778
17. Pihlgren M, Dubois PM, Tomkowiak M, Sjogren T, Marvel J. Resting Memory CD8+ T Cells Are Hyperreactive to Antigenic Challenge *In Vitro*. *J Exp Med* (1996) 184:2141–51. doi: 10.1084/jem.184.6.2141
18. McKinstry KK, Golech S, Lee WH, Huston G, Weng NP, Swain SL. Rapid Default Transition of CD4 T Cell Effectors to Functional Memory Cells. *J Exp Med* (2007) 204:2199–211. doi: 10.1084/jem.20070041
19. Sallusto F, Geginat J, Lanzavecchia A. Central Memory and Effector Memory T Cell Subsets: Function, Generation, and Maintenance. *Annu Rev Immunol* (2004) 22:745–63. doi: 10.1146/annurev.immunol.22.012703.104702
20. Pepper M, Jenkins MK. Origins of CD4(+) Effector and Central Memory T Cells. *Nat Immunol* (2011) 12:467–71. doi: 10.1038/ni.2038
21. Tsukumo S, Unno M, Muto A, Takeuchi A, Kometani K, Kurosaki T, et al. Bach2 Maintains T Cells in a Naive State by Suppressing Effector Memory-Related Genes. *Proc Natl Acad Sci USA* (2013) 110:10735–40. doi: 10.1073/pnas.1306691110
22. Roychoudhuri R, Hirahara K, Mousavi K, Clever D, Klebanoff CA, Bonelli M, et al. BACH2 Represses Effector Programs to Stabilize T(reg)-Mediated Immune Homeostasis. *Nature* (2013) 498:506–10. doi: 10.1038/nature12199
23. Kuwahara M, Suzuki J, Tofukuji S, Yamada T, Kanoh M, Matsumoto A, et al. The Menin-Bach2 Axis Is Critical for Regulating CD4 T-Cell Senescence and Cytokine Homeostasis. *Nat Commun* (2014) 5:3555. doi: 10.1038/ncomms4555
24. Roychoudhuri R, Clever D, Li P, Wakabayashi Y, Quinn KM, Klebanoff CA, et al. BACH2 Regulates CD8(+) T Cell Differentiation by Controlling Access of AP-1 Factors to Enhancers. *Nat Immunol* (2016) 17:851–60. doi: 10.1038/ni.3441
25. Crotty S. Follicular Helper CD4 T Cells (TFH). *Annu Rev Immunol* (2011) 29:621–63. doi: 10.1146/annurev-immunol-031210-101400
26. Pepper M, Pagan AJ, Igyarto BZ, Taylor JJ, Jenkins MK. Opposing Signals From the Bcl6 Transcription Factor and the Interleukin-2 Receptor Generate T Helper 1 Central and Effector Memory Cells. *Immunity* (2011) 35:583–95. doi: 10.1016/j.immuni.2011.09.009
27. Sallusto F, Lenig D, Forster R, Lipp M, Lanzavecchia A. Two Subsets of Memory T Lymphocytes With Distinct Homing Potentials and Effector Functions. *Nature* (1999) 401:708–12. doi: 10.1038/44385
28. Campbell JJ, Butcher EC. Chemokines in Tissue-Specific and Microenvironment-Specific Lymphocyte Homing. *Curr Opin Immunol* (2000) 12:336–41. doi: 10.1016/S0952-7915(00)00096-0
29. Barski A, Cuddapah S, Kartashov AV, Liu C, Imamichi H, Yang W, et al. Rapid Recall Ability of Memory T Cells Is Encoded in Their Epigenome. *Sci Rep* (2017) 7:39785. doi: 10.1038/srep39785
30. Moon JJ, Chu HH, Pepper M, McSorley SJ, Jameson SC, Kedl RM, et al. Naive CD4(+) T Cell Frequency Varies for Different Epitopes and Predicts Repertoire Diversity and Response Magnitude. *Immunity* (2007) 27:203–13. doi: 10.1016/j.immuni.2007.07.007
31. Moon JJ, Chu HH, Hataye J, Pagan AJ, Pepper M, McLachlan JB, et al. Tracking Epitope-Specific T Cells. *Nat Protoc* (2009) 4:565–81. doi: 10.1038/nprot.2009.9
32. Corces MR, Trevino AE, Hamilton EG, Greenside PG, Sinnott-Armstrong NA, Vesuna S, et al. An Improved ATAC-seq Protocol Reduces Background

and Enables Interrogation of Frozen Tissues. *Nat Methods* (2017) 14:959–62. doi: 10.1038/nmeth.4396
33. Langmead B, Salzberg SL. Fast Gapped-Read Alignment With Bowtie 2. *Nat Methods* (2012) 9:357–9. doi: 10.1038/nmeth.1923
34. Zhang Y, Liu T, Meyer CA, Eeckhoute J, Johnson DS, Bernstein BE, et al. Model-Based Analysis of ChIP-Seq (Macs). *Genome Biol* (2008) 9:R137. doi: 10.1186/gb-2008-9-9-r137
35. Barnett DW, Garrison EK, Quinlan AR, Stromberg MP, Marth GT. BamTools: A C++ API and Toolkit for Analyzing and Managing BAM Files. *Bioinformatics* (2011) 27:1691–2. doi: 10.1093/bioinformatics/btr174
36. Heinz S, Benner C, Spann N, Bertolino E, Lin YC, Laslo P, et al. Simple Combinations of Lineage-Determining Transcription Factors Prime Cis-Regulatory Elements Required for Macrophage and B Cell Identities. *Mol Cell* (2010) 38:576–89. doi: 10.1016/j.molcel.2010.05.004
37. Quinlan AR, Hall IM. Bedtools: A Flexible Suite of Utilities for Comparing Genomic Features. *Bioinformatics* (2010) 26:841–2. doi: 10.1093/bioinformatics/btq033
38. Liao Y, Smyth GK, Shi W. featureCounts: An Efficient General Purpose Program for Assigning Sequence Reads to Genomic Features. *Bioinformatics* (2014) 30:923–30. doi: 10.1093/bioinformatics/btt656
39. Love MI, Huber W, Anders S. Moderated Estimation of Fold Change and Dispersion for RNA-seq Data With Deseq2. *Genome Biol* (2014) 15:550. doi: 10.1186/s13059-014-0550-8
40. Li H, Handsaker B, Wysoker A, Fennell T, Ruan J, Homer N, et al. The Sequence Alignment/Map Format and Samtools. *Bioinformatics* (2009) 25:2078–9. doi: 10.1093/bioinformatics/btp352
41. Piper J, Elze MC, Cauchy P, Cockerill PN, Bonifer C, Ott S. Wellington: A Novel Method for the Accurate Identification of Digital Genomic Footprints From DNase-seq Data. *Nucleic Acids Res* (2013) 41:e201. doi: 10.1093/nar/gkt850
42. Kent WJ, Sugnet CW, Furey TS, Roskin KM, Pringle TH, Zahler AM, et al. The Human Genome Browser at UCSC. *Genome Res* (2002) 12:996–1006. doi: 10.1101/gr.229102
43. Bolger AM, Lohse M, Usadel B. Trimmomatic: A Flexible Trimmer for Illumina Sequence Data. *Bioinformatics* (2014) 30:2114–20. doi: 10.1093/bioinformatics/btu170
44. Kim D, Langmead B, Salzberg SL. HISAT: A Fast Spliced Aligner With Low Memory Requirements. *Nat Methods* (2015) 12:357–60. doi: 10.1038/nmeth.3317
45. Anders S, Pyl PT, Huber W. Htseq–a Python Framework to Work With High-Throughput Sequencing Data. *Bioinformatics* (2015) 31:166–9. doi: 10.1093/bioinformatics/btu638
46. Bindea G, Mlecnik B, Hackl H, Charoentong P, Tosolini M, Kirilovsky A, et al. ClueGO: A Cytoscape Plug-in to Decipher Functionally Grouped Gene Ontology and Pathway Annotation Networks. *Bioinformatics* (2009) 25:1091–3. doi: 10.1093/bioinformatics/btp101
47. Shannon P, Markiel A, Ozier O, Baliga NS, Wang JT, Ramage D, et al. Cytoscape: A Software Environment for Integrated Models of Biomolecular Interaction Networks. *Genome Res* (2003) 13:2498–504. doi: 10.1101/gr.1239303
48. Dose M, Emmanuel AO, Chaumeil J, Zhang J, Sun T, Germar K, et al. beta-Catenin Induces T-Cell Transformation by Promoting Genomic Instability. *Proc Natl Acad Sci USA* (2014) 111:391–6. doi: 10.1073/pnas.1315752111
49. Gokmen MR, Dong R, Kanhere A, Powell N, Perucha E, Jackson I, et al. Genome-Wide Regulatory Analysis Reveals That T-Bet Controls Th17 Lineage Differentiation Through Direct Suppression of IRF4. *J Immunol* (2013) 191:5925–32. doi: 10.4049/jimmunol.1202254
50. Buenrostro JD, Giresi PG, Zaba LC, Chang HY, Greenleaf WJ. Transposition of Native Chromatin for Fast and Sensitive Epigenomic Profiling of Open Chromatin, DNA-Binding Proteins and Nucleosome Position. *Nat Methods* (2013) 10:1213–8. doi: 10.1038/nmeth.2688
51. Arbones ML, Ord DC, Ley K, Ratech H, Maynard-Curry C, Otten G, et al. Lymphocyte Homing and Leukocyte Rolling and Migration Are Impaired in L-Selectin-Deficient Mice. *Immunity* (1994) 1:247–60. doi: 10.1016/1074-7613(94)90076-0
52. Yukawa M, Jagannathan S, Vallabh S, Kartashov AV, Chen X, Weirauch MT, et al. AP-1 Activity Induced by Co-Stimulation Is Required for Chromatin Opening During T Cell Activation. *J Exp Med* (2019) 217:1–16. doi: 10.1101/647388
53. Brignall R, Cauchy P, Bevington SL, Gorman B, Pisco AO, Bagnall J, et al. Integration of Kinase and Calcium Signaling at the Level of Chromatin Underlies Inducible Gene Activation in T Cells. *J Immunol* (2017) 199:2652–67. doi: 10.4049/jimmunol.1602033
54. Goldberg AD, Allis CD, Bernstein E. Epigenetics: A Landscape Takes Shape. *Cell* (2007) 128:635–8. doi: 10.1016/j.cell.2007.02.006
55. Shibukawa Y, Yamazaki N, Kumasawa K, Daimon E, Tajiri M, Okada Y, et al. Calponin 3 Regulates Actin Cytoskeleton Rearrangement in Trophoblastic Cell Fusion. *Mol Biol Cell* (2010) 21:3973–84. doi: 10.1091/mbc.e10-03-0261
56. Ciuba K, Hawkes W, Tojkander S, Kogan K, Engel U, Iskratsch T, et al. Calponin-3 Is Critical for Coordinated Contractility of Actin Stress Fibers. *Sci Rep* (2018) 8:17670. doi: 10.1038/s41598-018-35948-6
57. Melotte V, Qu X, Ongenaert M, van Criekinge W, de Bruine AP, Baldwin HS, et al. The N-myc Downstream Regulated Gene (NDRG) Family: Diverse Functions, Multiple Applications. *FASEB J* (2010) 24:4153–66. doi: 10.1096/fj.09-151464
58. Fouani L, Kovacevic Z, Richardson DR. Targeting Oncogenic Nuclear Factor Kappa B Signaling With Redox-Active Agents for Cancer Treatment. *Antioxid Redox Signal* (2019) 30:1096–123. doi: 10.1089/ars.2017.7387
59. Oh YM, Park HB, Shin JH, Lee JE, Park HY, Kho DH, et al. Ndrg1 Is a T-cell Clonal Anergy Factor Negatively Regulated by CD28 Costimulation and Interleukin-2. *Nat Commun* (2015) 6:1–14. doi: 10.1038/ncomms9698
60. Ai R, Sun Y, Guo Z, Wei W, Zhou L, Liu F, et al. NDRG1 Overexpression Promotes the Progression of Esophageal Squamous Cell Carcinoma Through Modulating Wnt Signaling Pathway. *Cancer Biol Ther* (2016) 17:943–54. doi: 10.1080/15384047.2016.1210734
61. Soon MSF, Lee HJ, Engel JA, Straube J, Thomas BS, Pernold CPS, et al. Transcriptome Dynamics of CD4(+) T Cells During Malaria Maps Gradual Transit From Effector to Memory. *Nat Immunol* (2020) 21:1597–610. doi: 10.1038/s41590-020-0800-8
62. Kakaradov B, Arsenio J, Widjaja CE, He Z, Aigner S, Metz PJ, et al. Early Transcriptional and Epigenetic Regulation of CD8(+) T Cell Differentiation Revealed by Single-Cell RNA Sequencing. *Nat Immunol* (2017) 18:422–32. doi: 10.1038/ni.3688
63. Bartel FO, Higuchi T, Spyropoulos DD. Mouse Models in the Study of the Ets Family of Transcription Factors. *Oncogene* (2000) 19:6443–54. doi: 10.1038/sj.onc.1204038
64. Anderson MK, Hernandez-Hoyos G, Diamond RA, Rothenberg EV. Precise Developmental Regulation of Ets Family Transcription Factors During Specification and Commitment to the T Cell Lineage. *Development* (1999) 126:3131–48. doi: 10.1242/dev.126.14.3131
65. David-Fung ES, Butler R, Buzi G, Yui MA, Diamond RA, Anderson MK, et al. Transcription Factor Expression Dynamics of Early T-Lymphocyte Specification and Commitment. *Dev Biol* (2009) 325:444–67. doi: 10.1016/j.ydbio.2008.10.021
66. Eyquem S, Chemin K, Fasseu M, Bories JC. The Ets-1 Transcription Factor Is Required for Complete Pre-T Cell Receptor Function and Allelic Exclusion at the T Cell Receptor Beta Locus. *Proc Natl Acad Sci USA* (2004) 101:15712–7. doi: 10.1073/pnas.0405546101
67. Leiden JM. Transcriptional Regulation of T Cell Receptor Genes. *Annu Rev Immunol* (1993) 11:539–70. doi: 10.1146/annurev.iy.11.040193.002543
68. Wotton D, Prosser HM, Owen MJ. Regulation of Human T Cell Receptor Beta Gene Expression by Ets-1. *Leukemia* (1993) 7(Suppl 2):S55–60.
69. Giese K, Kingsley C, Kirshner JR, Grosschedl R. Assembly and Function of a TCR Alpha Enhancer Complex Is Dependent on LEF-1-Induced DNA Bending and Multiple Protein-Protein Interactions. *Genes Dev* (1995) 9:995–1008. doi: 10.1101/gad.9.8.995
70. Grenningloh R, Kang BY, Ho IC. Ets-1, a Functional Cofactor of T-Bet, Is Essential for Th1 Inflammatory Responses. *J Exp Med* (2005) 201:615–26. doi: 10.1084/jem.20041330
71. Mouly E, Chemin K, Nguyen HV, Chopin M, Mesnard L, Leite-de-Moraes M, et al. The Ets-1 Transcription Factor Controls the Development and Function of Natural Regulatory T Cells. *J Exp Med* (2010) 207:2113–25. doi: 10.1084/jem.20092153

72. Meixner A, Karreth F, Kenner L, Wagner EF. Jund Regulates Lymphocyte Proliferation and T Helper Cell Cytokine Expression. *EMBO J* (2004) 23:1325–35. doi: 10.1038/sj.emboj.7600133

**Conflict of Interest:** The authors declare that the research was conducted in the absence of any commercial or financial relationships that could be construed as a potential conflict of interest.

frontiers in Immunology

ORIGINAL RESEARCH
published: 28 May 2021
doi: 10.3389/fimmu.2021.635942

# Deconvoluting the T Cell Response to SARS-CoV-2: Specificity Versus Chance and Cognate Cross-Reactivity

*Alexander A. Lehmann*[1], *Greg A. Kirchenbaum*[1], *Ting Zhang*[1], *Pedro A. Reche*[2] *and Paul V. Lehmann*[1]*

[1] Research and Development, Cellular Technology Ltd., Shaker Heights, OH, United States, [2] Laboratorio de Inmunomedicina & Inmunoinformatica, Departamento de Immunologia & O2, Facultad de Medicina, Universidad Complutense de Madrid, Madrid, Spain

SARS-CoV-2 infection takes a mild or clinically inapparent course in the majority of humans who contract this virus. After such individuals have cleared the virus, only the detection of SARS-CoV-2-specific immunological memory can reveal the exposure, and hopefully the establishment of immune protection. With most viral infections, the presence of specific serum antibodies has provided a reliable biomarker for the exposure to the virus of interest. SARS-CoV-2 infection, however, does not reliably induce a durable antibody response, especially in sub-clinically infected individuals. Consequently, it is plausible for a recently infected individual to yield a false negative result within only a few months after exposure. Immunodiagnostic attention has therefore shifted to studies of specific T cell memory to SARS-CoV-2. Most reports published so far agree that a T cell response is engaged during SARS-CoV-2 infection, but they also state that in 20-81% of SARS-CoV-2-unexposed individuals, T cells respond to SARS-CoV-2 antigens (mega peptide pools), allegedly due to T cell cross-reactivity with Common Cold coronaviruses (CCC), or other antigens. Here we show that, by introducing irrelevant mega peptide pools as negative controls to account for chance cross-reactivity, and by establishing the antigen dose-response characteristic of the T cells, one can clearly discern between cognate T cell memory induced by SARS-CoV-2 infection vs. cross-reactive T cell responses in individuals who have not been infected with SARS-CoV-2.

**Keywords: mega peptide pools, ELISPOT, ImmunoSpot, immune monitoring, COVID-19, T cell affinity**

OPEN ACCESS

***Edited by:***
*Peter Katsikis, Erasmus University Rotterdam, Netherlands*

***Reviewed by:***
*Yvonne Mueller, Erasmus Medical Center, Netherlands*
*Amit Awasthi, Translational Health Science and Technology Institute (THSTI), India*

***Correspondence:**
*Paul V. Lehmann*
*paul.lehmann@immunospot.com*

***Specialty section:***
*This article was submitted to Immunological Memory, a section of the journal Frontiers in Immunology*

***Received:*** *30 November 2020*
***Accepted:*** *11 March 2021*
***Published:*** *28 May 2021*

***Citation:***
*Lehmann AA, Kirchenbaum GA, Zhang T, Reche PA and Lehmann PV (2021) Deconvoluting the T Cell Response to SARS-CoV-2: Specificity Versus Chance and Cognate Cross-Reactivity. Front. Immunol. 12:635942. doi: 10.3389/fimmu.2021.635942*

## INTRODUCTION

Traditionally, the assessment of immune memory has relied upon measurements of serum antibodies without queries of the T cell compartment. However, SARS-CoV-2 infection highlights the shortcoming of such a serodiagnostic approach. While the majority of SARS-CoV-2-infected individuals initially develop an antibody response to this virus, false negative results are a concern because not all infected individuals attain high levels of serum antibody reactivity acutely after infection (1–3), and those who do develop detectable antibody reactivity might decline to the limit of detection within a few months (4). In such cases, the detection of T cell memory might be the only evidence of such infection, and is a surrogate of acquired immune protection from SARS-CoV-2 reinfection.

Fueled additionally by evidence that T cell-mediated immunity is required for immune protection against SARS-CoV-2 (5–7), attention has turned to T cell immunodiagnostics trying to establish

whether the detection of T cell memory may be a more sensitive and reliable indicator of SARS-CoV-2 exposure than antibodies (8–11). In most studies published so far, SARS-CoV-2-specific memory T cells were detected in the majority of infected individuals, but such were also found in 20-81% of control subjects who clearly could not have been infected by the SARS-CoV-2 virus (9, 12–18). If generalizable, such results would imply that T cell assays are unsuited to reliably identify who has, or has not, been infected by the SARS-CoV-2 virus, providing false positive results in up to 81% of the individuals tested. It should be noted right away, however, that the notion of cross-reactive SARS-CoV-2 antigen recognition by T cells being common in unexposed subjects might be related to the T cell assay itself and the test conditions used, as it was not observed by others (14, 19, 20). Progress with settling the issue of T cell cross-reactivity in SARS-CoV-2 antigen recognition, and identifying suitable test systems, will decide whether T cell diagnostics can reliably detect specific immune memory to SARS-CoV-2 infection/exposure, and possibly identify the immune protected status of those subjects.

Next to possible cross-reactivity, T cell immune diagnostics of SARS-CoV-2 infection faces the challenge of having to reliably detect antigen-specific T cells in blood that occur in very low frequency. The numbers of SARS-CoV-2-specific T cells in blood post-infection is about one tenth of the numbers of T cells specific for viruses that induce strong responses, such as influenza, Epstein Barr (EBV) or human cytomegalovirus (HCMV) (11, 21), and reliably detecting even the latter is at the border of current technology. Possibly further complicating matters, the frequencies of SARS-CoV-2-specific T cells are even lower in subjects who underwent a mild or asymptomatic SARS-CoV-2 infection as compared to those who developed more severe COVID-19 (12, 20, 22, 23), but this notion has not been supported by others (5, 24). Owing to these low T cell frequencies, and the antigen-induced signal being small in magnitude, any contribution of cross-reactive T cell stimulation will interfere with the reliable detection of genuine SARS-CoV-2-specific T cells. Setting up clear cut-off criteria for identifying antigen-specific T cell memory is therefore paramount.

Because T cell assays rely upon detecting SARS-CoV-2 antigen-specific T cells in blood *via* memory T cell re-activation *ex vivo*, the choice and formulation of the SARS-CoV-2 antigen itself used for the T cell recall will critically define the assay result. As the epitope utilization in the T cell response to SARS-CoV-2 is not yet known, by necessity, the aforementioned T cell diagnostic efforts tailored toward this virus have relied either on pools of hundreds of peptides that cover the entire proteome of the virus, or on pools of a multitude of predicted epitopes (mega peptide pools). Traditional T cell immune monitoring efforts, however, have called for the utilization of select, highly purified individual peptides whose specificity has been carefully established. Presently it is unproven whether pools of hundreds of unpurified peptides are even suited for reliable T cell diagnostics, and whether false positive or false negative results obtained using them are inherent to the recall antigen formulation. The chance for T cell cross-reactivity can be expected to increase with every peptide added into a pool, multiplying the chance for false positive results. Conversely, irrelevant peptides (those not recognized by T cells) also present in the pool can be expected to compete with the actually recognized T cell epitopes for binding to HLA molecules, possibly causing false negative results (25). To our knowledge, it has not yet been systematically addressed whether and how chance cross-reactivity or peptide competition affects T cell immune monitoring results when mega peptide pools are used for testing. Instead of relying on third party mega peptide pools as the proper negative control to establish the background noise of the T cell assay, in all SARS-CoV-2 studies published so far, the mega peptide pool-induced T cell activation has been compared to PBMC cultured in media alone, in the absence of any exogenously added peptide. In this report we introduce suitable negative control mega peptide pools, and using them, we address how to reliably detect even the very low frequency SARS-CoV-2 antigen-specific T cells in subjects who have undergone mild SARS-CoV-2 infection.

Cognate T cell cross-reactivity between related pathogens, such as SARS-CoV-2 and seasonal common cold coronaviruses (CCC), needs to be distinguished from the aforementioned chance cross-reactivities. In cognate cross-reactivity, the TCR binds peptide sequences of two antigens that have sequence similarities. In the majority of documented cases, such cross-reactive peptide sequences differ in only one or two amino acids with an additional requirement being that the exchange of amino acid(s) does not interfere with the peptides' binding to, and folding in, the peptide binding groove of the restricting HLA molecule. Examples of experimentally verified cognate cross-reactivities include T cell recognition of serotypes of the Dengue virus (26, 27), influenza A virus strains (28–31), hepatitis C virus escape variants (32), and HIV epitope variants from different clades (33, 34).

However, it remains controversial how exclusively specific T cell recognition is in general (35). On one hand, there are reports suggesting that T cell recognition might be highly promiscuous with individual T cell clones being able to cross-reactively recognize $10^6$ different peptides (36). On the other hand, changing even a single amino acid in the presented peptide frequently abrogates T cell recognition, in particular if the change affects the binding of the peptide for the restricting MHC molecule, its conformation when bound to the MHC molecule, or when involving a TCR contact residue. While some studies have indicated an extremely low frequency of T cell cross-reactions between unrelated peptides (37–39), other studies (relying on tetramers) claim the opposite (40, 41). Accordingly, it needed to be addressed what impact TCR chance cross-reactivity has on *ex vivo* T cell monitoring when using mega peptide pools in general, and for SARS-CoV-2 antigen recognition in particular.

When T cell activation was seen in SARS-CoV-2-unexposed individuals using SARS-CoV-2 mega peptide pools for recall, the finding was interpreted as cognate cross-reactivity with related coronaviruses that cause harmless, common cold-like epidemies in the human population (42). There are four seasonal coronavirus strains, 229E, NL63, OC43, and HKU1, which cause pandemics in multiyear infection cycles in the human population world-wide (43). Although in any given year only 15-30% of humans displaying symptoms of common cold are indeed infected by one of these seasonal coronaviruses, 90% of the adult human population eventually becomes seropositive for at least three of these coronaviruses (44–46). From the

perspective of T cell immune diagnostics of SARS-CoV-2, such cross-reactive T cell responses would generate false positive results. Another major scope of the present study was to establish to what extent cognate T cell cross-reactions of seasonal coronavirus antigens interferes with the detection of T cell memory induced by the SARS-CoV-2 virus itself.

The SARS-CoV-2 pandemic has made its rounds for nearly a year by now, yet its prevalence in the human population remains unknown as most of those infected go undiagnosed, having developed mild or no clinical symptoms at all (47). By now serum antibodies may no longer be reliable in revealing, in retrospect, who has or has not been infected more than 3 months ago. If measurements of T cell memory would also fail to provide this information, our understanding of SARS-CoV-2's prevalence would remain shrouded. Should vaccines under present development fail, without this information, it will remain guesswork to decide whether and when sufficient herd immunity has developed in a population, or if robust immunity develops at all following natural infection (48). Without knowing who has or has not been infected by SARS-CoV-2, one cannot distinguish whether a candidate vaccine can prime a protective immune response in naïve individuals, or whether it merely boosts immunity that has been pre-established by the natural infection. Without this information, all those individuals – possibly the majority of the population - who already went through an uncomplicated SARS-CoV-2 infection and might be protected from re-infection, or are prone to develop a mild disease if reinfected again, need to continue to live in fear of contracting a potentially lethal disease.

In this report we sought solutions to deconvolute T cell reactivity to SARS-CoV-2 mega peptide pools so as to clearly distinguish between individuals who have or have not been infected with this virus.

# MATERIALS AND METHODS

## Peripheral Blood Mononuclear Cells

Pre-COVID Era Donors. PBMC from healthy human donors were obtained from CTL's ePBMC library (CTL, Shaker Heights, OH, USA) collected prior to Dec 31, 2019. The PBMC were collected in FDA-registered collection centers from IRB-consented healthy human donors by leukapheresis using the Spectra Optia® Apheresis System CMNC collection protocol using ACD-A as the anticoagulant. All PBMC were from healthy adults who had not taken medication within a month of the blood draw that might influence their T cell response. In addition, tests were done on each donor at the collection centers' CLIA-certified laboratories to identify common infections, including Human Immunodeficiency Virus (HIV). Subjects positive for HIV were disqualified from the ePBMC library. The donors' age, sex, and ethnicity are shown in **Supplementary Table 1**. The cryopreservation procedure used fully preserves the thawed PBMC's functionality in T cell assays when compared to the freshly isolated PBMC (49–51).

SARS-CoV-2-Infected Donors. PBMC of subjects were collected under Advarra Approved IRB #Pro00043178, CTL study number: GL20-16 entitled COVID-19 Immune Response Evaluation. All subjects tested positive for SARS-CoV-2 RNA in PCR performed on nasal swabs, and these PCR tests were performed in accredited medical laboratories. All such donors underwent mild COVID infection, from which the subjects fully recovered within one or two weeks. These subjects were bled between 2 weeks and 3 months post recovery (median of 24 days). The donors' age, sex, and ethnicity are shown in **Supplementary Table 1**. SARS-CoV-2 antigen-specific serum antibodies were evaluated for this cohort in parallel with Pre-COVID Era donors to additionally verify their infection (**Supplementary Figure 1**).

The cryopreserved cells were thawed following an optimized protocol (51) resulting in viability exceeding 90% for all samples. The PBMC were resuspended in CTL-Test™ Medium (from CTL). CTL-Test™ Medium is serum-free and has been developed for low background and high signal performance in ELISPOT assays. The number of PBMC plated in the ELISPOT experiments was 2 x $10^5$ viable PBMC per well.

## ELISA Assays

MaxiSorp 96-well microplates (Thermo Fisher) were coated with recombinant SARS-CoV-2 Nucleocapsid (RayBiotech, Peachtree Corners, GA), truncated Spike protein (S1 domain) (The Native Antigen Company, Oxford, UK) or receptor binding domain (RBD) (Center for Vaccines and Immunology (CVI), UGA, Athens, GA) at 2μg/mL in PBS overnight at 4°C. Plates were then blocked with ELISA blocking buffer containing 2% w/v bovine serum albumin in PBS with 0.1% v/v Tween20 (PBS-T) (Sigma-Aldrich) for 1 h at room temperature. Donor plasma were serially diluted in assay plates and incubated overnight at 4°C. Plates were then washed with PBS prior to addition of horseradish peroxidase-conjugated anti-human IgG detection reagents (from CTL) and incubation for 2 h at room temperature. Plates were then washed with PBS prior to development with TMB chromogen solution (Thermo Fisher). 1M HCl was used to stop conversion of TMB and optical density was measured at 450nm ($OD_{450}$) and 540nm ($OD_{540}$) using a Spectra Max 190 plate reader (Molecular Devices, San Jose, CA USA). Optical imperfections in assay plates were corrected through subtraction of $OD_{540}$ values. Antigen-specific IgG concentrations are reported as μg/mL IgG equivalents and were interpolated from a standard curve generated using an IgG reference protein (Athens Research and Technology, Athens, GA) coated directly into designated wells of assay plates.

## Antigens and Peptides

### Mega Peptide Pools

Selecting the right peptides is critical for the detection of *in vivo* primed T cells. In general, T cell immune monitoring has relied on three fundamentally different approaches to accomplish this goal (reviewed in 64). The first approach relies upon peptides that have been experimentally verified as T cell epitopes of an antigen. Such information is scarce for SARS-CoV-2, as it has only recently piqued the interest of the immune monitoring community. In the second approach, there is the option to attempt to predict epitopes *in silico*. The group of A. Sette has been pioneering this approach

for SARS-CoV-2 (13). While HLA binding of peptides can be accurately predicted, this does not necessarily predict the immune dominance of such peptides (52). The third approach, which we selected for this study, relies upon the agnostic use of peptides. Here, peptide libraries are created with the individual peptides, 15 amino acids long, systematically covering the amino acid sequence of the antigen of interest. Such peptides are pooled for each antigen resulting in the mega peptide pools of SARS-CoV-2 as defined in more detail in **Supplementary Table 2**.

All mega peptide pools used in this study are products of, and were purchased from JPT (Berlin, Germany). The peptide pools representing the individual antigens are shown in **Supplementary Table 2**. All these mega peptide pools consisted of 15-mer peptides that covered the entire amino acid (aa) sequence of the respective proteins in steps (gaps of) 4 aa. All mega peptide pools were tested at a final concentration of 1.5 μg/mL of each peptide within the pool at the highest concentration, followed by three 1 + 2 (vol + vol) serial dilutions, as specified in the Tables. All mega peptide pools were delivered as lyophilized powder. The individual peptide pools were initially dissolved following the manufacturer's directions in 40 μl DMSO, followed by addition of 210 μl of PBS generating a "primary peptide stock solution" at 100 μg/mL (0.1mg/mL) with 16% v/v DMSO. From each of these wells, a "secondary peptide stock solution" was prepared in a 96-Well deep well plate, with peptides starting at 3 μg/mL which were then threefold serially diluted. Using a 96-well multichannel pipettor, 100μl was transferred "en block" into pre-coated ImmunoSpot® assay plates. Finally, 100 μL of PBMC (containing 2 x $10^5$ cells) in CTL-Test™ media was added "en block" to achieve the desired final peptide concentrations of 1.5, 0.5, 0.17 and 0.06 μg/mL in the ELISPOT assay. The final concentration of DMSO in the ELISPOT assay at 1.5 μg/ml of peptide was therefore 0.24% vol/vol, a concentration at which DMSO does not interfere with the test result (see **Supplementary Figure 2**).

### Positive Controls

CEFX, by JPT Peptide Technologies, Berlin, Germany (Product Code: PM-CEFX) is a pool of 176 known peptide epitopes for a broad range of HLA subtypes – class I and class II – and different infectious agents, namely *Clostridium tetani*, Coxsackievirus B4, *Haemophilus influenza*, *Helicobacter pylori*, Human adenovirus 5, Human herpesvirus 1, Human herpesvirus 2, Human herpesvirus 3, Human herpesvirus 4, Human herpesvirus 5, Human herpesvirus 6, Human papillomavirus, JC polyomavirus, Measles virus, Rubella virus, *Toxoplasma gondii*, and Vaccinia virus. These peptides are 9-15 amino acids long and have been selected to recall both CD4+ and CD8+ T cells. CEFX was tested at 1 μg/mL.

CPI: protein antigens of CMV, Parainfluenza and Influenza viruses. CPI was from and is available through CTL, Catalog #CTL-CPI-001. CPI was tested at 6.25 μg/mL.

CERI: 124 peptides of CMV, EBV, RSV, and Influenza virus. The individual peptides, 9 amino acids long, were selected based on peptide binding predictions for a broad range of HLA class I alleles expressed in all human races, and diverse ethnic subpopulations. CERI was from and is available through CTL, Catalog # CTL-CERI-300. CERI was tested at 1 μg/mL.

All three positive controls have been introduced recently (53) as a superior alternative to the CEF peptide pool.

## Human IFN-γ ELISPOT Assays

Single-color enzymatic ImmunoSpot® kits from CTL were used for the detection of *in vivo*-primed IFN-γ- producing Th1 type memory T cells. Test procedures followed the manufacturer's recommendations. In brief, peptides were plated at the specified concentrations into capture antibody-precoated ELISPOT assay plates in a volume of 100 μL per well, dissolved in CTL-Test™ Media. The plates with the antigen were stored at 37°C in a $CO_2$ incubator for less than an hour until the freshly thawed PBMC were ready for plating. The PBMC were added at 200,000 viable cells/well in 100 μL CTL-Test™ Media and cultured with the peptides for 24h at 37°C and 9% $CO_2$ in an incubator. After removal of the cells, addition of detection antibody, and enzymatic visualization of plate-bound cytokine, the plates were air-dried prior to scanning and counting of spot forming units (SFU). ELISPOT plates were analyzed using an ImmunoSpot® S6 Ultimate Reader, by CTL. SFU numbers were automatically calculated by the ImmunoSpot® Software for each stimulation condition using the Autogate™ function of the ImmunoSpot® Software that enables scientifically validated, objective counting (54). Stringent gating to attain low background inherently reduces the antigen-induced spot count, but increases the signal to noise performance of the ELISPOT test. Occasional subjects have an elevated background that results from increased IFN-γ production by cells of the innate immune system due to underlying cellular activity in such subjects at the time of the blood draw (55). The above statistics-based gating and analysis approach is suited to dissect the antigen-triggered T cell signal from the respective background.

## Statistical Analysis

As ELISPOT counts follow Gaussian (normal) distribution among replicate wells (56), the use of parametric statistics was justified to identify positive and negative responses, respectively. Positive responses were defined as SFU counts exceeding 3 SD of the mean SFU counts of the specified negative control, identifying such at 99.7% confidence.

# RESULTS AND DISCUSSION

## Experimental Design for Assessment of T Cell Memory to SARS-CoV-2

### The Rationale for Selecting IFN-γ ELISPOT for Detecting SARS-CoV-2-Specific Memory T cells

T cell immune monitoring aims at detecting *in vivo* expanded and differentiated antigen-specific T cell populations directly *ex vivo*, either in freshly isolated PBMC, or in PBMC that have been cryopreserved following protocols that maintain full T cell functionality upon thawing the cells (50). The number (frequency) and functions (e.g. cytokine signature) of antigen/peptide-specific T cells need to be measured as present in the body without inducing additional clonal expansions or T cell differentiation *in vitro* during the short-term *ex vivo* antigen stimulation that is required to detect the antigen-reactive T cells. In ELISPOT/ImmunoSpot® assays, antigen- (peptide)-specific T

cells present in the PBMC become activated, and start producing cytokine. This cytokine is captured on a membrane around each secreting T cell, resulting in a cytokine spot (a spot forming unit, SFU). Counting of SFUs permits to establish, at single-cell resolution, the number of antigen-triggered cytokine-producing T cells (55), and thus the frequency of such cells in PBMC. In this study we focused on IFN-γ measurements because, in subjects who successfully overcome SARS-CoV-2 infection, Th1 cells have been reported to prevail by far (5, 9, 18, 57, 58). Th1 cells have been implicated as a protective class of response while Th2 and Th17 have been linked to immune pathology (57, 59). Furthermore, the standard 24h IFN-γ ELISPOT assay detects *in vivo*-primed Th1 effector memory cells only; naïve T cells or central memory cells are not detected in this assay as the latter require several days of differentiation following antigen encounter before they begin secreting IFN-γ (60, 61).

We also selected the *ex vivo* ELISPOT platform because it requires as few as 200,000 peripheral blood mononuclear cells (PBMC) per antigen stimulation condition, and this assay lends itself to high-throughput analysis. Utilizing only 32 million PBMC per subject (obtainable from 32 mL of blood), we established 155 T cell reactivity datapoints per subject, testing 37 mega peptide pools (see **Supplementary Table 2**), each at four concentrations, plus 4 media and 3 positive control wells, all in a single high-throughput experiment. In the mega peptide pools, the individual peptides were present at 1.5 μg/mL at the highest concentration tested, and in 0.5 μg/mL, 0.17 μg/mL, and 0.06 μg/mL in the subsequent 1 + 2 (vol + vol, 3-fold) serial dilutions. Instead of using replicates, these serial antigen dilutions served not only to confirm positive results, but additionally permitted us to establish the affinity/avidity of the responding T cells. Distinguishing between high and low affinity SARS-CoV-2-specific T cells might help shed light on T cell immunity operational in individuals undergoing alternative outcomes following infection (62).

### The Rationale for Using Mega Peptide Pools for Detecting SARS-CoV-2-Specific Memory T cells

Due to the highly individualized nature of T cell epitope recognition in general, for which evidence is also starting to accumulate for SARS-CoV-2 (11–13, 16, 20, 58), and due to the size of the virus whose genome is approximately 29.8 kb (63), there are only two viable options for selecting peptides for a comprehensive assessment of T cell immunity to SARS-CoV-2. One option is to perform *in silico* epitope predictions, and such has already been reported for SARS-CoV-2 (64), but their accuracy has recently been convincingly called into question (52, 65). Moreover, for a comprehensive assessment, the epitope predictions would need to be customized for each test subject, accounting for all HLA class I and class II molecules expressed in each individual. Because it is impractical to individualize predicted peptide epitopes for each subject, we have elected to take the agnostic route, in which the entire sequence of each protein antigen is covered by a series of overlapping peptides. However, this means that, dependent upon the length of the protein, hundreds of peptides need to be combined into mega pools (see **Supplementary Table 2**). While, in theory, the mega peptide pool approach permits systematic coverage of all possible T cell epitopes within a virus, it introduces an as yet undefined dimension: chance cross-reactivity between unrelated peptides.

We tested 15-mer peptides which, based upon their length, preferentially stimulate CD4+ T cells but *via* cross-presentation also recall antigen-specific CD8+ T cells (66). The activation of T cells *vs.* cells of the innate immune system is internally controlled in such recall assays using unpurified PBMC because possible contaminations of peptides, e.g. with LPS, would trigger IFN-γ production in all subjects irrespective of their immune memory status.

### The Rationale for Selecting Negative Control Mega Peptide Pools

To account for chance T cell cross-reactivity, we tested mega peptide pools covering foreign antigens to which it is unlikely that the test subjects have been exposed (one Ebola virus peptide pool, five HIV antigen pools) and a self-antigen, Actin, that due to its abundance in the body is likely to have established self-tolerance. These mega peptide pools are defined in **Supplementary Table 2**, including the number of peptides contained in each.

### Avoiding Inter-Assay Variations

To reduce assay variables, all peptide pools used in this study were from the same vendor, were synthesized, stored, dissolved and tested the same way, and had the exact same formulation consisting of 15 amino acid-long peptides that systematically walk the entire sequence of the respective proteins in steps of 11 amino acids. Taking advantage of the high-throughput suitability of ELISPOT, all the peptide pools (**Supplementary Table 2**) and their dilutions were tested on each PBMC donor in a single experiment, which rendered the peptides the only assay-dependent variable. This approach therefore permitted us to firmly establish within each PBMC sample the number of Th1 T cells responding to the different mega peptide pools, and thus to compare the frequencies of the respective mega peptide pool-reactive T cells within each PBMC donor, and among donors in the cohorts.

We compared T cell reactivity to all the above mega peptide pools in 18 healthy Pre-COVID-19 Era Subjects and in the 9 individuals who recovered from mild SARS-CoV-2 infection as verified by PCR. In the following we describe and interpret the results.

## Classic Single Antigen and Single Antigen Dose-Based Data Analysis Does Not Permit to Distinguish Between SARS-CoV-2-Infected Subjects and Controls

**Figure 1** shows the test results comparing frequencies of SARS-CoV-2 antigen-reactive IFN-γ-producing T cells in the SARS-CoV-2 PCR-verified (also referred to as COVID-recovered) and Pre-SARS-CoV-2 (hereafter referred to as Pre-COVID) cohorts when tested at a single antigen concentration, 1.5 μg/mL of peptide within each peptide pool. Essentially identical results have been reported by others (9, 12–18) showing that, as a cohort, the frequency of SARS-CoV-2 antigen-specific T cells is significantly elevated in COVID-recovered individuals versus the cohort that has not been infected with the SARS-CoV-2 virus. In all these aforementioned studies, and for T cell immune monitoring in general, it has been of concern however, that such results are inconclusive for the individuals, as a large fraction of COVID-recovered subjects show similar or even

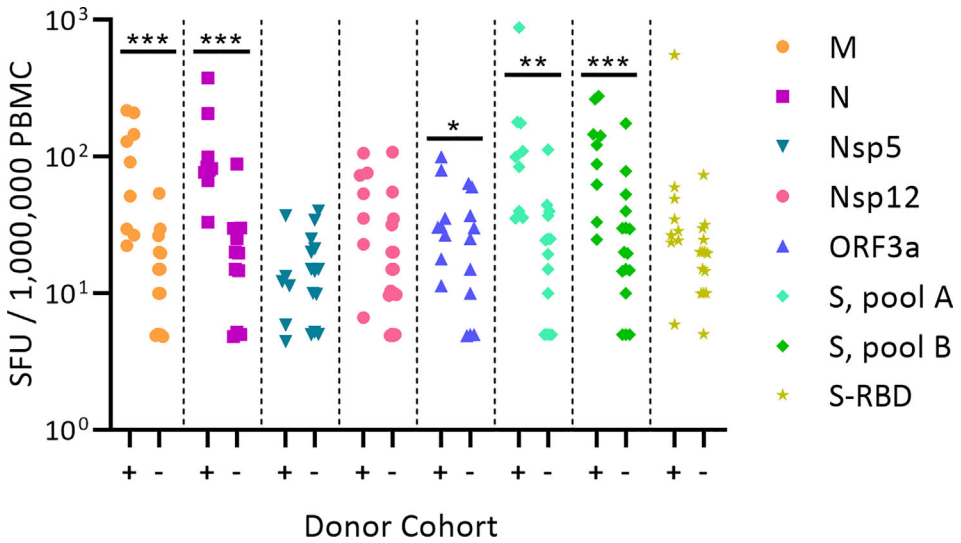


**FIGURE 1** | Classic representation of SARS-CoV-2 antigen-specific T cell frequencies in SARS-CoV-2 PCR verified subjects(+) versus Pre-COVID Era individuals(-). PBMC of each individual within the cohort is represented by a dot. The PBMC were challenged with peptide pools covering the SARS-CoV-2 antigens specified on the right. (These peptide pools are closer defined in **Supplementary Table 2**). The individual peptides in each pool were tested at 1.5 μg/ml. An ELISPOT assay was performed measuring the numbers of antigen-induced IFN-γ-secreting T cells (spot forming units, SFU) in 200,000 PBMC; following convention, the numbers have been normalized to per million PBMC, as shown on the Y axis. Statistical significance between the two cohorts was determined using an independent samples t test. Significant differences between SARS-CoV-2-infected vs. non-exposed cohorts are marked with * denoting $p < 0.05$, ** $p < 0.01$, and *** $p < 0.001$, respectively.

lower frequencies of SARS-CoV-2 antigen-specific T cells than the Pre-COVID control subjects. Simple T cell frequency measurements using single SARS-CoV-2 antigens at a single antigen concentration therefore do not permit to reliably distinguish whether an individual has or has not been infected by SARS-CoV-2. This finding, along with the low frequency of SARS-CoV-2 antigen-reactive T cells, may come as a surprise because massive clonal expansions are typically seen initially after infections and vaccinations (61). There is increasing evidence that the SARS-CoV-2 virus actively disrupts the engagement of an immune response (67–73) explaining its weak immunogenicity. The low frequencies of SARS-CoV-2 antigen-reactive T cells in COVID-recovered individuals in turn makes it challenging to unambiguously detect them.

## Accounting for Chance Cross-Reactivity When Testing Suitable Control Mega Peptide Pools to Establish the Background Noise in ELISPOT Assays

The challenge with selecting mega peptide pools that are suited for negative controls (PP. Neg. Contr.) was that we needed to identify antigens to which the test population had not been exposed. As one such antigen we selected the Ebola virus nucleoprotein, and five HIV antigens, as the participating subjects needed to be HIV-seronegative to qualify for this study. In addition, we tested a peptide pool that covered the sequence of the self-antigen, Actin, as a negative control. These candidate PP. Neg. Contr. antigens are listed in **Supplementary Table 2** including the number of 15-mer peptides they contained. Just as for the SARS-CoV-2 peptide pools, all these negative control peptide pool candidates were tested at four concentrations: 1.5 μg/mL, 0.5 μg/mL, 0.17 μg/mL, and 0.06 μg/mL of each peptide within the pool. The number of PP. Neg Contr. candidate-induced IFN-γ-producing cells was compared to the media control, the latter of which was measured in quadruplicate wells. CPI, CERI, and CEFX antigens were measured in singlet, and served as positive controls, respectively (53). For each PBMC sample, the mean and standard deviation (SD) of four replicate media control wells was established and compared to the SFU counts induced by the candidate negative control peptide pools. SFU counts greater than 3 SD of the mean media control counts are highlighted in **Supplementary Table 3**.

The peptide pool covering HIV's gp160protein induced vigorous SFU formation (> 100 SFU/200,000 PBMC) in 3 subjects' PBMC, and relatively strong SFU formation (17-42 SFU/200,000 PBMC) in two additional subjects, recalling positive responses at 3-4 consecutive peptide dilutions. At the highest concentration, this peptide pool also elicited elevated SFU numbers in 4 additional subjects. All these subjects who responded to gp160 were HIV-seronegative as established by the blood banks that collected them. The gp160 protein belongs to the p24 superfamily, which shares conserved sequences with related proteins expressed by many retroviruses (74). Thus, cognate cross-reactivity with T cells primed by such retroviruses, rather than chance cross-reactivity, struck us as the likely explanation for the gp160 mega peptide pool-triggered recall responses seen in HIV-seronegative subjects. Be that as it may, the gp160 peptide pool was clearly unsuited as a negative control peptide pool.

The six remaining candidate negative control peptide pools occasionally triggered elevated SFU counts, but these occurred at

relatively low frequencies, and predominantly at only the highest peptide concentration (**Supplementary Table 3**). The data therefore provide evidence for low-level chance cross-reactivity when mega peptide pools are tested in ELISPOT assays. In theory, at higher peptide concentrations, this chance cross-reactivity might increase, however, as T cells with low affinity for the peptides might also reach their activation threshold.

Therefore, when analyzing the following SARS-CoV-2 peptide pool-triggered T cell responses, we used and compared two negative controls. One was the conventional "Media control", established as the mean and SD of 4 replicate wells in which PBMC were cultured with media alone. The second was the PP Neg. Control., calculated as the mean and SD of each donor's SFU count induced by the six negative control peptide pools at 1.5 μg/mL. Again, these six negative control pools encompassed Ebola, Actin, and the 4 HIV antigen pools (excluding gp160). The mean and SD for the PP Neg. Control, Media control, and the raw data from which these were derived, are specified for each subject in **Supplementary Table 3**.

## Chance Cross-Reactivity Accounts for Most of SARS-CoV-2 Peptide Reactivity in Pre-COVID Era Subjects

We compared the SFU counts induced by SARS-CoV-2 mega peptide pools in the subjects who recovered from mild COVID-19, and those who were bled prior to the COVID era. The SARS-CoV-2 peptide-induced SFU counts were analyzed vs. either the Media control or the PP. Neg. Control in each case, highlighting positive SFU counts as defined by exceeding 3 SD of the respective mean control count, a threshold that identifies positive responses with > 99.6% confidence. As can be seen in **Supplementary Table 4**, in Pre-COVID subjects, the number of SARS-CoV-2 peptide-induced positive SFU counts was significantly lower when control peptide pools were used as to establish the background noise level. Thus, chance cross-reactivity, rather than cognate cross-reactivity with seasonal coronaviruses, accounted for most of the positive responses detected in Pre-COVID control subjects. The few apparently positive cross-reactive responses left after filtering for chance cross-reactivity in this cohort could be discerned from cognate T cell responses to SARS-CoV-2 peptides in SARS-CoV-2 PCR-verified individuals when taking the affinity of the T cell response into account, as will be shown below.

## Affinity for SARS-CoV-2 Peptides Distinguishes Cognate From Cross-Reactive T Cell Recognition

Testing peptide pools in four serial dilutions not only permits generation of confirmatory results without using replicate wells, but also permits one to gain insights into the affinity of the T cells recognizing the respective peptides. In the context of this study, we will distinguish between Level 4 affinity (high affinity, with all four peptide concentrations recalling T cells, color coded in red), Level 3 affinity (intermediate affinity, eliciting a recall response across 3 consecutive peptide dilutions, highlighted in orange), Level 2 affinity (low affinity, only the two highest peptide concentrations elicit a T cell response, color coded in yellow), and Level 1 affinity (borderline low, eliciting a significant T cell response at the highest peptide concentration only, color coded in beige).

As seen in **Table 1**, most COVID-recovered subjects displayed Level 4 (red) affinity T cell responses to several SARS-CoV-2 antigens, while this level was absent in the Pre-COVID Era controls. In the latter, only occasional Level 3 (orange) and Level 2 affinities (yellow) were seen. Thus, high affinity responses to several SARS-Cov-2 antigens (unlike responses detected against individual antigens at a single antigen concentration, see **Figure 1**) appear to be suited to distinguish cognate SARS-CoV-2 specific T cells in COVID-recovered subjects from cross-reactive T cells in subjects infected by other coronaviruses in the Pre-COVID Era. The frequency of SARS-CoV-2 mega peptide pool-specific T cells was low, but clearly elevated > 3 SD over the negative control mega peptide pool control level. As ELISPOT SFU counts follow normal distribution (56), the mean of background plus ≥ 3 SD positivity cut-off definition sets the chances for a single datapoint being a false positive at ≤0.4%; for four responses in a row being false positive, the chances are negligible at a probability of < 0.0256%.

These types of affinity measurements, which rely on serial dilution of peptides and are simple to perform, also require high-throughput suitable test platforms that are frugal with regards to PBMC utilization, such as ELISPOT. To our knowledge, such T cell affinity measurements have so far not been applied systematically to characterize virus-specific T cell responses, thus permitting to compare the above affinity distributions observed for SARS-CoV-2 with other viruses. To compare the SARS-CoV-2 antigen-induced T cell responses with T cell reactivity to a better characterized virus, we also tested mega peptide pools that covered 14 antigens of Epstein Barr Virus (EBV), which commonly infects most humans by the time they have reached adulthood. The raw data are shown in **Supplementary Table 6**. As summarized in **Table 2**, the percentage of EBV mega peptide pools recognized at affinity Levels 1-4 was comparable in both cohorts to the percentage of SARS-CoV-2 peptide pools eliciting Level 1-4 T cell recall responses in the COVID-recovered subjects. SARS-CoV-2 infection, therefore, seems to induce a T cell response that, at least as far as the affinity of nominal antigen-recognition goes, is comparable to the T cell response to EBV.

## Fine Specificity of SARS-CoV-2 Antigen Recognition in COVID-19-Recovered Subjects

The SARS-CoV-2 peptide pools we used in our study encompassed eight major viral proteins, and systematically covered the respective antigens. Comparing within each donor the SFU counts triggered by these peptide pools permits therefore to assess, first, the total T cell mass mobilized against the virus, and second, which antigens are preferentially targeted by the T cells, i.e., the T cell immune dominance hierarchy within SARS-CoV-2 antigen recognition. As shown in **Table 3**, Spike protein (S) was dominant, or co-dominant, in all COVID-recovered subjects, with 24-51% of all SARS-CoV-2-specific T cells targeting this protein in the individual subjects (it was

**TABLE 1** | Affinity analysis of SFU counts triggered by SARS-CoV-2 peptides in PBMC of donors who recovered from PCR-verified SARS- CoV-2 infection **(A)** and in Pre-Covid Era subjects **(B)**.

**A**

| ID. | ORF3a | N | Nsp12 | Nsp5 | S(A) | S(B) | S-RBD | M |
|---|---|---|---|---|---|---|---|---|
| dC1 | | | | | | | | |
| dC2 | | | | | | | | |
| dC3 | | | | | | | | |
| dC4 | | | | | | | | |
| dC5 | | | | | | | | |
| dC6 | | | | | | | | |
| dC7 | | | | | | | | |
| dC8 | | | | | | | | |
| dC9 | | | | | | | | |

**B**

| ID. | ORF3a | N | Nsp12 | Nsp5 | S(A) | S(B) | S-RBD | M |
|---|---|---|---|---|---|---|---|---|
| dP1 | | | | | | | | |
| dP2 | | | | | | | | |
| dP3 | | | | | | | | |
| dP4 | | | | | | | | |
| dP5 | | | | | | | | |
| dP6 | | | | | | | | |
| dP7 | | | | | | | | |
| dP8 | | | | | | | | |
| dP9 | | | | | | | | |
| dP10 | | | | | | | | |
| dP11 | | | | | | | | |
| dP12 | | | | | | | | |
| dP13 | | | | | | | | |
| dP14 | | | | | | | | |
| dP15 | | | | | | | | |
| dP16 | | | | | | | | |
| dP17 | | | | | | | | |
| dP18 | | | | | | | | |

*PBMC of 9 subjects with SARS-CoV-2-PCR-verified infection **(A)** and PBMC from 18 subjects from the Pre-Covid Era **(B)** where tested in an ELISPOT assay for reactivity to the specified SARS-CoV-2 mega peptide pools. (These peptide pools are closer defined in **Supplementary Table 2**). All peptide pools were tested in 4 serial dilutions on each PBMC sample at 1.5 ug/mL, 0.5 ug/mL, 0.17 ug/mL, and 0.06ug/mL. Affinity levels are color-coded. Red: high affinity, defined as four consecutive peptide dilutions eliciting a positive recall response with SFU counts exceeding 3 SD of the negative peptide pool-based background. Orange: intermediate affinity, defined as three consecutive peptide dilutions eliciting a positive recall response. Yellow: low affinity, with only the two highest peptide concentrations eliciting positive SFU counts. Beige: only the highest concentration of peptide is positive. The raw counts are provided in **Supplementary Table 5**.*

40 ± 9% for the cohort). The recognition of Nucleoprotein (N) (18 ± 6%) and the Membrane Protein (M) (16 ± 12%) was next most abundant for the COVID-recovered cohort, while S-RBD (9 ± 6%), Nsp12 (8 ± 6%) and ORF3a (6 ± 4%) peptide pools constituted third tier targets for T cells. There was therefore a clear T cell response hierarchy at the level of the cohort, but it did not always hold up for each individual within the cohort. For subject dC9, for example, only 24% of the SARS-CoV-2-specific T cells targeted S vs. 49% being specific for M, 19% for N, and 8% targeting S-RBD. An immune monitoring effort that focused only on the "immune dominant" S protein would have detected only 24% of the relevant T cells in this subject. In Subject dC2, 40% of the SARS-CoV-2-specific T cells targeted S protein, but these T cells were of lower affinity than the 25% that recognized N. T cell immune monitoring efforts for SARS-CoV-2 therefore ideally should include several, ideally all antigens of the virus, tested in serial dilutions. **Supplementary Table 6** shows for EBV how inaccurate the assessment of T cell immunity to this virus would be if it was restricted to a single antigen, and at a single peptide dose. The same holds for HCMV (75).

One possible explanation for the relative immune dominance of S protein over the other SARS-CoV-2 proteins is its size relative to the others. The longer a protein, the more potential T cell epitopes it contains. S protein was covered by 315 peptides vs. for example N, one third as long, which was covered by 102 peptides, and M, half as long as N, with 53 peptides. Indeed, for these three antigens, and also for S-RBD and ORF3a, the percentage of T cells targeting them divided by the number of peptides present in each pool (corresponding to the length of the respective protein) gave numbers in the same ballpark: 0.13%, 0.18%, 0.3%, 0.17%, and 0.09% for S, N, M, S-RBD, and ORF3a, respectively (**Table 3**). For these SARS-CoV-2 antigens, therefore, the magnitude of T cell response targeting each appeared to be a mere function of the proteins' respective sizes. With this ratio substantially lower, at 0.03%, Nsp12and Nsp5 were under-targeted relative to their size, possibly suggesting that the expression levels of these two antigens is lower during SARS-CoV-2 replication than that of the other SARS-CoV-2 antigens.

## Non-Cross-Reactive T Cell Recognition of Seasonal Coronavirus Spike Proteins

People around the world commonly get infected with seasonal coronaviruses causing common cold (CCC) such as 229E, NL63, OC43, and HKU1, and over the years most adults can be expected to have been infected with several of these CCC

**TABLE 2 |** Affinity distributions of T cells recognizing SARS-CoV-2- **(A)** vs. EBV peptides **(B)**.

| **A** | | | **SARS-CoV-2 Peptide Pool Positive (%)** | |
|---|---|---|---|---|
| **Aff. Level** | **Definition** | **Color Code** | **COVID-Recovered Subjects** | **Pre-COVID Era Subjects** |
| 4 | 4 serial positives | | 34% | 0% |
| 3 | 3 serial positives | | 7% | 1% |
| 2 | 2 serial positives | | 11% | 3% |
| 1 | First positive only | | 11% | 3% |
| **B** | | | **EBV Peptide Pool Positive (%)** | |
| **Aff. Level** | **Definition** | **Color Code** | **COVID-Recovered Subjects** | **Pre-COVID Era Subjects** |
| 4 | 4 serial positives | | 31% | 17% |
| 3 | 3 serial positives | | 7% | 6% |
| 2 | 2 serial positives | | 7% | 6% |
| 1 | First positive only | | 10% | 12% |

*Peptide pools eliciting positive T cell recall responses in the specified affinity level categories are shown as the percentage of all positive responses within the cohort. The raw data are shown in* ***Supplementary Table 5*** *for the SARS-CoV-2 peptides, and in* ***Supplementary Table 6*** *for the EBV peptides.*

**TABLE 3 |** T cell immune dominance of SARS-CoV-2 proteins.

| **ID.** | **∑ SFU** | **ORF3a** | **N** | **Nsp12** | **Nsp5** | **S (A & B)** | **S-RBD** | **M** |
|---|---|---|---|---|---|---|---|---|
| dC1 | 191 | 10% | 12% | 13% | 0% | 40% | 7% | 18% |
| dC2 | 267 | 12% | 25% | 12% | 0% | 40% | 2% | 10% |
| dC3 | 230 | 10% | 13% | 3% | 5% | 50% | 10% | 10% |
| dC4 | 264 | 3% | 21% | 6% | 3% | 47% | 7% | 13% |
| dC5 | 216 | 1% | 16% | 0% | 2% | 49% | 23% | 9% |
| dC6 | 332 | 5% | 31% | 11% | 2% | 35% | 4% | 14% |
| dC7 | 253 | 12% | 10% | 9% | 1% | 51% | 3% | 15% |
| dC8 | 184 | 6% | 21% | 17% | 1% | 31% | 16% | 7% |
| dC9 | 81 | 0% | 19% | 0% | 0% | 24% | 8% | 49% |
| $\bar{x}$ | na | 6% | 18% | 8% | 2% | 40% | 9% | 16% |
| σ | na | 4% | 6% | 6% | 3% | 9% | 6% | 12% |
| # Pept. | na | 66 | 102 | 231 | 74 | 315 | 53 | 53 |
| $\bar{x}$/(# Pept.) | na | 0.09% | 0.18% | 0.03% | 0.03% | 0.13% | 0.17% | 0.30% |

*The total SARS-CoV-2-specific T cell mass (∑SFU) was calculated by adding up for each SARS-CoV-2-recovered donor the numbers of SFU elicited by all SARS-CoV-2 peptide pools in that donor at 1.5 μg/mL (see the raw data in* ***Supplementary Table 5****). In the top panel, the percentage of T cells targeting each of the SARS-CoV-2 antigens is shown relative to the total clonal SARS-CoV-2-specific T cell mass in that individual, representing an immune dominance index. The superimposed heatmap specifies the affinity level of the respective T cell population, with the color code defined in* ***Table 2****. The lower panel shows the mean percentage ($\bar{x}$) and SD of this immunodominance index for the cohort. Addressing the hypothesis that T cell immune dominance of a SARS-CoV-2 antigen is related to its size, the number of peptides in each pool is shown (# Pept.) and the mean immune dominance index ($\bar{x}$) is normalized for the number of peptides ($\bar{x}$/(# Pept).*

strains. T cell reactivity induced by SARS-CoV-2 mega peptide pools in individuals who clearly have not been exposed to SARS-CoV-2 have therefore been attributed to cognate cross-reactivity with CCC. By introducing negative control mega peptide pools to account for noise created by chance cross-reactivity (**Supplementary Table 3**), and by adding the requirement for high affinity T cell recognition (**Table 1**), we show that SARS-CoV-2 antigens are not recognized by subjects in the Pre-COVID cohort as a consequence of cross-reactivity with CCC antigens. We therefore asked the reverse question: do mega peptide pools that specifically cover CCC antigens detect T cell memory in both cohorts?

We tested Spike proteins of 229E, NL63, OC43, and HKU1, which, due to their size, were each represented in two mega peptide pools (as was the SARS-CoV-2 Sprotein itself). These CCC peptide pools were also tested at four concentrations, following exactly the same protocol as specified above for the SARS-CoV-2 S protein, and all other peptide pools tested in this study. While no Level 4 affinity response to SARS-CoV-2 S protein peptides were seen in Pre-COVID-19 subjects (**Table 1B**), eight of eighteen subjects in this cohort (44%) displayed high affinity T cell responses to at least one of these CCC peptide pools with seven of eighteen (39%) showing no response at all (**Table 4B**). In the PCR-verified cohort seven of nine subjects (78%) showed high

**TABLE 4** | T cell recall responses to Spike proteins of the four Common Cold Coronaviruses, 229E, NL63, OC43, and HKU1, each represented due to size in two peptide pools.

**A**

| ID. | HKU1 S (A) | HKU1 S (B) | 229E S (A) | 229E S (B) | NL63 S (A) | NL63 S (B) | OC43 S (A) | OC43 S (B) |
|---|---|---|---|---|---|---|---|---|
| dC1 | | | | | | | | |
| dC2 | | | | | | | | |
| dC3 | | | | | | | | |
| dC4 | | | | | | | | |
| dC5 | | | | | | | | |
| dC6 | | | | | | | | |
| dC7 | | | | | | | | |
| dC8 | | | | | | | | |
| dC9 | | | | | | | | |

**B**

| ID. | HKU1 S (A) | HKU1 S (B) | 229E S (A) | 229E S (B) | NL63 S (A) | NL63 S (B) | OC43 S (A) | OC43 S (B) |
|---|---|---|---|---|---|---|---|---|
| dP1 | | | | | | | | |
| dP2 | | | | | | | | |
| dP3 | | | | | | | | |
| dP4 | | | | | | | | |
| dP5 | | | | | | | | |
| dP6 | | | | | | | | |
| dP7 | | | | | | | | |
| dP8 | | | | | | | | |
| dP9 | | | | | | | | |
| dP10 | | | | | | | | |
| dP11 | | | | | | | | |
| dP12 | | | | | | | | |
| dP13 | | | | | | | | |
| dP14 | | | | | | | | |
| dP15 | | | | | | | | |
| dP16 | | | | | | | | |
| dP17 | | | | | | | | |
| dP18 | | | | | | | | |

*Each peptide pools has been tested in the specified four concentrations in a standard IFN-γELISPOT assay. SFU counts exceeding 3 SD of the mean of the negative peptide pool control are highlighted according to T cell affinity levels, as specified in* ***Table 2****. The original counts can be found in* ***Supplementary Table 7****.*

affinity responses for CCC peptide pools and none displayed no response at all (**Table 4A**). In isolation, these data could be interpreted as evidence for T cells primed by SARS-CoV-2 infection being cross-reactively recalled by CCC S antigens. However, Pre-COVID-19 donors do not show SARS-CoV-2 S-antigen reactivity (**Table 1B**) in spite of their reactivity to CCC S antigens (**Table 4B**), and the frequency of CCC S antigen-specific T cells is not elevated in the recently SARS-CoV-2-infected cohort (SFU counts in **Table 4A** vs. **B**) as would be expected in the case of a cross-reactive boost. Therefore, we conclude that cross-reactivity does appear to play a major role in shaping the respective S-antigen-specific T cell repertoires.

Our data showing the specificity of T cell responses to SARS-CoV-2 and CCC in the absence of major cross-reactivities are in line with other reports that also relied on IFN-γ ELISPOT assays for T cell detection (14, 19, 20) and contradict publications that claim high cross-reactivity using general T cell activation measurements. It therefore seems possible that the method of observation itself might affect the results. While these T cell assays have, to our knowledge, not been thoroughly compared so far, a recent study might shed light on this discrepancy (19). This group relied on different T cell assays to study SARS-CoV-2-infected subjects vs. individuals without known exposure to the virus. Using IFN-γ ELISPOT, SARS-CoV-2 antigen-triggered responses were found to be specific, commonly occurring in those who had been infected but rarely in unexposed subjects. By contrast, over 90% of individuals in both groups showed proliferation and cellular lactate responses to S subunits S1/S2. The authors concluded that the detection of T cell responses to SARS-CoV-2 is therefore critically dependent on the choice of assay and antigen. The ELISPOT assay used detects IFN-γ-producing effector memory cells that can directly engage in defense reactions, but it does not detect the precursor cells for effector memory cells such as naïve and stem cell-like memory cells, which do not produce effector cytokines (61, 76). Assays that measure T cell activation in general do not distinguish between such T cell subpopulations.

## CONCLUDING REMARKS

The overall question that we addressed was whether test conditions can be established that permit to clearly identify SARS-CoV-2-specific T cell memory engaged in individuals who underwent a mild infection vs. humans who have not been infected with this virus. Previous publications on this subject matter reported up to 80% false positive results for uninfected individuals due to alleged T cell cross-reactivity. Here we have established criteria by which false positive results can be reduced to 0% (0 of 18 Pre-COVID Era test subjects), while permitting the detection of SARS-CoV-2-reactive T cells in eight of nine (89%) SARS-CoV-2 PCR-verified subjects. To accomplish this discrimination, a combination of four criteria needed to be used. First, the detection of *ex vivo* IFN-γ-producing effector memory T cells was required. Second, we introduced negative control mega peptide pools, instead of media Suppl alone, to establish the background noise level caused by chance

cross-reactivity. Third, we introduced the criterion that a T cell response scores positive only if it has sufficient affinity, being triggered by at least four 1 + 2 (vol + vol) (3-fold) serial dilutions of the test peptides. Lastly, as COVID-recovered donors responded to several SARS-CoV-2 antigens, a broad, multi-antigen-specific T cell response profile was established as a requirement for scoring a subject positive. In addition to exhibiting a high affinity T cell response to at least one mega peptide pool, a second high or intermediate affinity level T cell response was also identified in 89% our SARS-CoV-2 PCR-verified cohort. To meet the latter requirement of multi-specificity, several SARS-CoV-2 antigens need to be tested, as there is no fixed immune dominance pattern among them, reminiscent of the T cell response to EBV (**Supplementary Table 6**) and HCMV (75).

Following infection with the original SARS coronavirus (SARS-CoV), antibody and B cell memory wanes, but evidence for T cell memory remains (77). Antibody titers, and potentially B cell memory, also appear to be short-lived after SARS-CoV-2 infection (78), but it is presently not known whether T cell memory to this virus will be durably maintained. If serum antibody reactivity fails to provide reliable information on previous exposure to SARS-CoV-2, then potentially T cell diagnostics could fill this gap.

Even though we report here that SARS-CoV-2- and EBV-specific T cells occur in similar frequencies in COVID-recovered subjects (See **Table 1** vs. **Supplementary Table 6**), it might be premature to conclude that such findings signify the induction of a robust cognate T cell response following SARS-CoV-2 infection. Cognate T cell responses in general show a typical kinetic: in the first weeks after the onset of infection, the frequency of the antigen-specific T cells reaches a peak, after which the frequencies drop to a substantially lower steady state level (78). We measured frequencies of SARS-CoV-2 antigen-specific T cells near their expected peak in our COVID-recovered cohort, while the frequencies of the EBV-specific T cells were assessed in steady state. Therefore, in light of the typical T cell response kinetic, the data reported here, and supported by existing literature, may also signify that mild/asymptomatic SARS-CoV-2 infection induces a much weaker T cell response than natural EBV infection, or other viruses against which we develop protective immunity. The already low numbers of SARS-CoV-2-specific T cells early on after a mild/asymptomatic infection might further decrease with time, which needs to be established. Being able to accurately detect such rare SARS-CoV-2-specific T cells is an important step for immune diagnostics, but is just the first step toward understanding their role in host defense.

## DATA AVAILABILITY STATEMENT

The datasets generated in this study will be made available by the authors, without undue reservation, to any qualified researcher.

## ETHICS STATEMENT

The studies involving human participants were reviewed and approved by Advarra IRB Approved # Pro00043178, CTL study number: GL20-16 entitled COVID 19 Immune Response Evaluation. The patients/participants provided their written informed consent to participate in this study.

## AUTHOR CONTRIBUTIONS

Experiments were designed by AAL, PL, and PR. Experimental data were generated by AAL, TZ, and GK. This publication serves as part of AAL's doctoral thesis to be submitted to the Universidad Complutense de Madrid, Madrid, Spain. All authors contributed to the article and approved the submitted version.

## FUNDING

This study was funded by the R&D budget of Cellular Technology Limited.

## ACKNOWLEDGMENTS

We thank Ruliang Li of Cellular Technology Limited for expert technical assistance, Drs. Magdalena Tary-Lehmann, Nicholas Tomko, and Alexey Y. Karulin for valuable discussions, and Diana Roen for expert editorial assistance. We also thank Melisa Sebok, Malachi Wickman, and Jennifer Penfold from American Red Cross, as well as Tibor Baki and Victoria Gaidaenko of CTL for helping us access blood from COVID-19-recovered subjects.

## SUPPLEMENTARY MATERIAL

The Supplementary Material for this article can be found online at: https://www.frontiersin.org/articles/10.3389/fimmu.2021.635942/full#supplementary-material

## REFERENCES

1. Long QX, Tang XJ, Shi QL, Li Q, Deng HJ, Yuan J, et al. Clinical and Immunological Assessment of Asymptomatic SARS-CoV-2 Infections. *Nat Med* (2020) 26(8):1200–4. doi: 10.1038/s41591-020-0965-6
2. Mallapaty S. Will Antibody Tests For The Coronavirus Really Change Everything? *Nature* (2020) 580(7805):571–2. doi: 10.1038/d41586-020-01115-z
3. Woloshin S, Patel N, Kesselheim AS. False Negative Tests For SARS-CoV-2 Infection — Challenges And Implications. *N Engl J Med* (2020) 383(6):e38. doi: 10.1056/NEJMp2015897
4. Seow J, Graham C, Merrick B, Acors S, Pickering S, Steel KJA, et al. Longitudinal Observation And Decline Of Neutralizing Antibody Responses In The Three Months Following SARS-CoV-2 Infection in Humans. *Nat Microbiol* (2020) 5 (12):1598–607. doi: 10.1038/s41564-020-00813-8
5. Rydyznski Moderbacher C, Ramirez SI, Dan JM, Grifoni A, Hastie KM, Weiskopf D, et al. Antigen-Specific Adaptive Immunity To SARS-CoV-2 In Acute COVID-19 And Associations With Age And Disease Severity. *Cell* (2020) 183(4):996–1012.e19. doi: 10.1016/j.cell.2020.09.038
6. Xu B, C-Y F, Wang A-L, Zou Y-L, Yu Y-H, He C, et al. Suppressed T Cell-Mediated Immunity In Patients With COVID-19: A Clinical Retrospective

Study In Wuhan, China. *J Infect* (2020) 81(1):e51–60. doi: 10.1016/j.jinf.2020.04.012
7. Zhao J, Zhao J, Mangalam AK, Channappanavar R, Fett C, Meyerholz DK, et al. Airway Memory CD4+ T Cells Mediate Protective Immunity Against Emerging Respiratory Coronaviruses. *Immunity* (2016) 44(6):1379–91. doi: 10.1016/j.immuni.2016.05.006
8. Gallais F, Velay A, Nazon C, Wendling M, Partisani M, Sibilia J, et al. Intrafamilial Exposure To SARS-CoV-2 Associated With Cellular Immune Response Without Seroconversion, France. *Emerg Infect Dis* (2021) 27 (1):113–21. doi: 10.1101/2020.06.21.20132449
9. Sekine T, Perez-Potti A, Rivera-Ballesteros O, Strålin K, Gorin JB, Olsson A, et al. Robust T Cell Immunity In Convalescent Individuals With Asymptomatic or Mild COVID-19. *Cell* (2020) 183(1):158–68.e14. doi: 10.1101/2020.06.29.174888
10. Thieme CJ, Anft M, Paniskaki K, Blazquez-Navarro A, Doevelaar A, Seibert FS, et al. Robust T cell response toward spike, membrane, and nucleocapsid SARS-CoV-2 proteins is not associated with recovery in critical COVID-19 patients. *Cell Rep Med* (2020) 1(6):100092. doi: 10.1016/j.xcrm.2020.100092
11. Schwarzkopf S, Krawczyk A, Knop D, Klump H, Heinold A, Heinemann F, et al. Cellular Immunity in COVID-19 Convalescents With PCR-Confirmed Infection But With Undetectable SARS-CoV-2–Specific IgG. *Emerg Infect Dis* (2021) 27(1):122–9. doi: 10.3201/2701.203772
12. Braun J, Loyal L, Frentsch M, Wendisch D, Georg P, Kurth F, et al. SARS-CoV-2-reactive T Cells in Healthy Donors and Patients With COVID-19. *Nature* (2020) 587(7833):270–4. doi: 10.1038/s41586-020-2598-9
13. Grifoni A, Weiskopf D, Ramirez SI, Mateus J, Dan JM, Moderbacher CR, et al. Targets of T Cell Responses To SARS-CoV-2 Coronavirus In Humans With COVID-19 Disease And Unexposed Individuals. *Cell* (2020) 181(7):1489–501.e15. doi: 10.1016/j.cell.2020.05.015
14. Le Bert N, Tan AT, Kunasegaran K, Tham CYL, Hafezi M, Chia A, et al. SARS-CoV-2-Specific T Cell Immunity In Cases of COVID-19 and SARS, and Uninfected Controls. *Nature* (2020) 584(7821):457–62. doi: 10.1038/s41586-020-2550-z
15. Mateus J, Grifoni A, Tarke A, Sidney J, Ramirez SI, Dan JM, et al. Selective and Cross-Reactive SARS-CoV-2 T Cell Epitopes in Unexposed Humans. *Science* (2020) 370(6512):89–94. doi: 10.1126/science.abd3871
16. Nelde A, Bilich T, Heitmann JS, Maringer Y, Salih HR, Roerden M, et al. SARS-CoV-2-Derived Peptides Define Heterologous and COVID-19-Induced T Cell Recognition. *Nat Immunol* (2021) 22(1):74–85. doi: 10.1038/s41590-020-00808-x
17. Ni L, Ye F, Cheng ML, Feng Y, Deng YQ, Zhao H, et al. Detection of SARS-CoV-2-Specific Humoral and Cellular Immunity in COVID-19 Convalescent Individuals. *Immunity* (2020) 52(6):971–7.e3. doi: 10.1016/j.immuni.2020.04.023
18. Weiskopf D, Schmitz KS, Raadsen MP, Grifoni A, Okba NMA, Endeman H, et al. Phenotype and Kinetics of SARS-CoV-2–Specific T Cells in COVID-19 Patients With Acute Respiratory Distress Syndrome. *Sci Immunol* (2020) 5 (48):eabd2071. doi: 10.1126/sciimmunol.abd2071
19. Ogbe A, Kronsteiner B, Skelly DT, Pace M, Brown A, Adland E, et al. T Cell Assays Differentiate Clinical And Subclinical SARS-CoV-2 Infections From Cross-Reactive Antiviral Responses. *medRxiv* (2020) 2020.09.28.20202929. doi: 10.1101/2020.09.28.20202929
20. Peng Y, Mentzer AJ, Liu G, Yao X, Yin Z, Dong D, et al. Broad and Strong Memory CD4(+) and CD8(+) T Cells Induced by SARS-CoV-2 in UK Convalescent Individuals Following COVID-19. *Nat Immunol* (2020) 21 (11):1336–45. doi: 10.1038/s41590-020-0782-6
21. Habel JR, Nguyen THO, van de Sandt CE, Juno JA, Chaurasia P, Wragg K, et al. Suboptimal SARS-CoV-2–Specific CD8+ T cell Response Associated With The Prominent HLA-A*02:01 Phenotype. *PNAS* (2020) 117(39):24384–91. doi: 10.1073/pnas.2015486117
22. Mathew D, Giles JR, Baxter AE, Oldridge DA, Greenplate AR, Wu JE, et al. Deep Immune Profiling of COVID-19 Patients Reveals Distinct Immunotypes With Therapeutic Implications. *Science* (2020) 369(6508):eabc8511. doi: 10.1126/science.abc8511
23. Pepper M, Rodda L, Netland J, Shehata L, Pruner K, Morawski P, et al. Functional SARS-CoV-2-specific Immune Memory Persists After Mild COVID-19. *Cell* (2021) 184(1):169–83.e17. doi: 10.1016/j.cell.2020.11.029
24. Le Bert N, Clapham HE, Tan AT, Chia WN, Tham CY, Lim JM, et al. Highly Functional Virus-Specific Cellular Immune Response In Asymptomatic SARS-CoV-2 Infection. *J Exp Med* (2021) 218(5):e20202617. doi: 10.1084/jem.20202617
25. Adorini L, Muller S, Cardinaux F, Lehmann PV, Falcioni F, Nagy ZA. In Vivo Competition Between Self Peptides And Foreign Antigens in T-Cell Activation. *Nature* (1988) 334(6183):623–5. doi: 10.1038/334623a0
26. Friberg H, Bashyam H, Toyosaki-Maeda T, Potts JA, Greenough T, Kalayanarooj S, et al. Cross-Reactivity And Expansion of Dengue-Specific T Cells During Acute Primary And Secondary Infections in Humans. *Sci Rep* (2011) 1:51. doi: 10.1038/srep00051
27. Friberg H, Burns L, Woda M, Kalayanarooj S, Endy TP, Stephens HA, et al. Memory CD8+ T Cells From Naturally Acquired Primary Dengue Virus Infection Are Highly Cross-Reactive. *Immunol Cell Biol* (2011) 89(1):122–9. doi: 10.1038/icb.2010.61
28. Gras S, Kedzierski L, Valkenburg SA, Laurie K, Liu YC, Denholm JT, et al. Cross-Reactive CD8+ T-Cell Immunity Between The Pandemic H1N1-2009 and H1N1-1918 Influenza A Viruses. *PNAS* (2010) 107(28):12599–604. doi: 10.1073/pnas.1007270107
29. Haanen JB, Wolkers MC, Kruisbeek AM, Schumacher TN. Selective Expansion of Cross-Reactive CD8(+) Memory T Cells By Viral Variants. *J Exp Med* (1999) 190(9):1319–28. doi: 10.1084/jem.190.9.1319
30. Roti M, Yang J, Berger D, Huston L, James EA, Kwok WW. Healthy Human Subjects Have CD4+ T Cells Directed Against H5N1 Influenza Virus. *J Immunol* (2008) 180(3):1758–68. doi: 10.4049/jimmunol.180.3.1758
31. Townsend AR, Skehel JJ. The Influenza A Virus Nucleoprotein Gene Controls The Induction of Both Subtype Specific And Cross-Reactive Cytotoxic T Cells. *J Exp Med* (1984) 160(2):552–63. doi: 10.1084/jem.160.2.552
32. Urbani S, Amadei B, Cariani E, Fisicaro P, Orlandini A, Missale G, et al. The Impairment of CD8 Responses Limits The Selection of Escape Mutations In Acute Hepatitis C Virus Infection. *J Immunol* (2005) 175(11):7519–29. doi: 10.4049/jimmunol.175.11.7519
33. Conrad JA, Ramalingam RK, Smith RM, Barnett L, Lorey SL, Wei J, et al. Dominant Clonotypes Within HIV-Specific T Cell Responses Are Programmed Death-1high and CD127low and Display Reduced Variant Cross-Reactivity. *J Immunol* (2011) 186(12):6871–85. doi: 10.4049/jimmunol.1004234
34. Lee JK, Stewart-Jones G, Dong T, Harlos K, Di Gleria K, Dorrell L, et al. T cell cross-Reactivity And Conformational Changes During TCR Engagement. *J Exp Med* (2004) 200(11):1455–66. doi: 10.1084/jem.20041251
35. Petrova G, Ferrante A, Gorski J. Cross-Reactivity of T Cells And Its Role In The Immune System. *Crit Rev Immunol* (2012) 32(4):349–72. doi: 10.1615/CritRevImmunol.v32.i4.50
36. Wooldridge L, Ekeruche-Makinde J, van den Berg HA, Skowera A, Miles JJ, Tan MP, et al. A Single Autoimmune T Cell Receptor Recognizes More Than a Million Different Peptides. *J Biol Chem* (2012) 287(2):1168–77. doi: 10.1074/jbc.M111.289488
37. Ishizuka J, Grebe K, Shenderov E, Peters B, Chen Q, Peng Y, et al. Quantitating T cell Cross-Reactivity For Unrelated Peptide Antigens. *J Immunol* (2009) 183(7):4337–45. doi: 10.4049/jimmunol.0901607
38. Oseroff C, Kos F, Bui HH, Peters B, Pasquetto V, Glenn J, et al. HLA Class I-Restricted Responses To Vaccinia Recognize a Broad Array of Proteins Mainly Involved In Virulence And Viral Gene Regulation. *PNAS* (2005) 102 (39):13980–5. doi: 10.1073/pnas.0506768102
39. Sylwester AW, Mitchell BL, Edgar JB, Taormina C, Pelte C, Ruchti F, et al. Broadly Targeted Human Cytomegalovirus-Specific CD4+ and CD8+ T Cells Dominate The Memory Compartments of Exposed Subjects. *J Exp Med* (2005) 202(5):673–85. doi: 10.1084/jem.20050882
40. Campion SL, Brodie TM, Fischer W, Korber BT, Rossetti A, Goonetilleke N, et al. Proteome-Wide Analysis of HIV-Specific Naive And Memory CD4(+) T Cells in Unexposed Blood Donors. *J Exp Med* (2014) 211(7):1273–80. doi: 10.1084/jem.20130555
41. Su LF, Davis MM. Antiviral Memory Phenotype T Cells In Unexposed Adults. *Immunol Rev* (2013) 255(1):95–109. doi: 10.1111/imr.12095
42. Cui J, Li F, Shi ZL. Origin and Evolution of Pathogenic Coronaviruses. *Nat Rev Microbiol* (2019) 17(3):181–92. doi: 10.1038/s41579-018-0118-9
43. Killerby ME, Biggs HM, Haynes A, Dahl RM, Mustaquim D, Gerber SI, et al. Human Coronavirus Circulation In The United States 2014-2017. *J Clin Virol* (2018) 101:52–6. doi: 10.1016/j.jcv.2018.01.019
44. Gorse GJ, Patel GB, Vitale JN, O'Connor TZ. Prevalence of Antibodies to Four Human Coronaviruses is Lower in Nasal Secretions Than in Serum. *CVI* (2010) 17(12):1875–80. doi: 10.1128/CVI.00278-10

45. Severance EG, Bossis I, Dickerson FB, Stallings CR, Origoni AE, Sullens A, et al. Development of a Nucleocapsid-Based Human Coronavirus Immunoassay and Estimates of Individuals Exposed to Coronavirus In a U.S. Metropolitan Population. *CVI* (2008) 15(12):1805–10. doi: 10.1128/CVI.00124-08
46. Zhou W, Wang W, Wang H, Lu R, Tan W. First Infection By All Four Non-Severe Acute Respiratory Syndrome Human Coronaviruses Takes Place During Childhood. *BMC Infect Dis* (2013) 13(1):433. doi: 10.1186/1471-2334-13-433
47. Guan WJ, Ni ZY, Hu Y, Liang WH, Ou CQ, He JX, et al. Clinical Characteristics of Coronavirus Disease 2019 in China. *N Engl J Med* (2020) 382(18):1708–20. doi: 10.1056/NEJMoa2002032
48. Tillett RL, Sevinsky JR, Hartley PD, Kerwin H, Crawford N, Gorzalski A, et al. Genomic Evidence For Reinfection With SARS-CoV-2: A Case Study. *Lancet Infect Dis* (2021) 21(1):52–8. doi: 10.1016/S1473-3099(20)30764-7
49. Tary-Lehmann M, Hamm CD, Lehmann PV. Validating Reference Samples For Comparison in a Regulated ELISPOT Assay. In: U Prabhakar and M Kelley, editors. *Validation of Cell-Based Assays In The GLP Setting: A Practical Guide*. John Wiley ∓ Sons, Ltd (2008). p. 127–46. doi: 10.1002/9780470987810.ch9
50. Kreher CR, Dittrich MT, Guerkov R, Boehm BO, Tary-Lehmann M. CD4+ and CD8+ Cells In Cryopreserved Human PBMC Maintain Full Functionality in Cytokine ELISPOT Assays. *J Immunol Methods* (2003) 278(1):79–93. doi: 10.1016/S0022-1759(03)00226-6
51. Ramachandran H, Laux J, Moldovan I, Caspell R, Lehmann PV, Subbramanian RA. Optimal Thawing of crYopreserved Peripheral Blood Mononuclear Cells For Use In High-Throughput Human Immune Monitoring Studies. *Cells* (2012) 1(3):313–24. doi: 10.3390/cells1030313
52. Mei S, Li F, Leier A, Marquez-Lago TT, Giam K, Croft NP, et al. A Comprehensive Review And Performance Evaluation of Bioinformatics Tools for HLA Class I Peptide-Binding Prediction. *Brief Bioinform* (2020) 21(4):1119–35. doi: 10.1093/bib/bbz051
53. Lehmann AA, Reche PA, Zhang T, Suwansaard M, Lehmann PV. CERI. CEFX, and CPI: Largely Improved Positive Controls For Testing Antigen-Specific T Cell Function in PBMC Compared to CEF. *Cells* (2021) 10(2):248. doi: 10.3390/cells10020248
54. Zhang W, Lehmann PV. Objective, User-Independent ELISPOT Data Analysis Based On Scientifically Validated Principles. *Methods Mol Biol* (2012) 792:155–71. doi: 10.1007/978-1-61779-325-7_13
55. Hesse MD, Karulin AY, Boehm BO, Lehmann PV, Tary-Lehmann M. A T Cell Clone's Avidity Is A Function Of Its Activation State. *J Immunol* (2001) 167 (3):1353–61. doi: 10.4049/jimmunol.167.3.1353
56. Karulin AY, Caspell R, Dittrich M, Lehmann PV. Normal Distribution of CD8+ T-Cell-Derived ELISPOT Counts Within Replicates Justifies The Reliance on parametric Statistics For Identifying Positive Responses. *Cells* (2015) 4(1):96–111. doi: 10.3390/cells4010096
57. Janice Oh HL, Ken-En Gan S, Bertoletti A, Tan YJ. Understanding the T Cell Immune Response in SARS Coronavirus Infection. *Emerg Microbes Infect* (2012) 1(9):e23. doi: 10.1038/emi.2012.26
58. Neidleman J, Luo X, Frouard J, Xie G, Gill G, Stein ES, et al. SARS-CoV-2-Specific T Cells Exhibit Phenotypic Features of Helper Function, Lack of Terminal Differentiation, and High Proliferation Potential. *Cell Rep Med* (2020) 1(6):100081. doi: 10.1016/j.xcrm.2020.100081
59. Hotez PJ, Bottazzi ME, Corry DB. The Potential Role of Th17 Immune Responses In Coronavirus Immunopathology And Vaccine-Induced Immune Enhancement. *Microb Infect* (2020) 22(4):165–7. doi: 10.1016/j.micinf.2020.04.005
60. O'Garra A. Cytokines Induce The Development of Functionally Heterogeneous T Helper Cell Subsets. *Immunity* (1998) 8(3):275–83. doi: 10.1016/S1074-7613(00)80533-6
61. Pepper M, Jenkins MK. Origins of CD4(+) Effector And Central Memory T Cells. *Nat Immunol* (2011) 12(6):467–71. doi: 10.1038/ni.2038
62. Bacher P, Rosati E, Esser D, Martini GR, Saggau C, Schiminsky E, et al. Low-Avidity CD4(+) T Cell Responses to SARS-CoV-2 In Unexposed Individuals And Humans With Severe COVID-19. *Immunity* (2020) 53(6):1258–71.e5. doi: 10.1016/j.immuni.2020.11.016
63. Jiang HW, Li Y, Zhang HN, Wang W, Yang X, Qi H, et al. SARS-CoV-2 Proteome Microarray For Global Profiling of COVID-19 Specific IgG and IgM Responses. *Nat Commun* (2020) 11(1):3581. doi: 10.1038/s41467-020-17488-8
64. Grifoni A, Sidney J, Zhang Y, Scheuermann RH, Peters B, Sette A. A Sequence Homology And Bioinformatic Approach Can Predict Candidate Targets For Immune Responses to SARS-CoV-2. *Cell Host Microbe* (2020) 27(4):671–80.e2. doi: 10.1016/j.chom.2020.03.002
65. Lehmann AA, Zhang T, Reche PA, Lehmann PV. Discordance Between the Predicted vs. The Actually Recognized CD8+ T Cell Epitopes of HCMV pp65 Antigen and Aleatory epiTope Dominance. *Front Immunol* (2021) 11:618428. doi: 10.3389/fimmu.2020.618428
66. Tel J, Schreibelt G, Sittig SP, Mathan TSM, Buschow SI, Cruz LJ, et al. Human Plasmacytoid Dendritic Cells Efficiently Cross-Present Exogenous Ags to CD8 + T Cells Despite Lower Ag Uptake Than Myeloid Dendritic Cell Subsets. *Blood* (2013) 121(3):459–67. doi: 10.1182/blood-2012-06-435644
67. Jewett A. The potential effect of novel coronavirus SARS-CoV-2 on NK cells; a perspective on potential therapeutic interventions. *Front Immunol* (2020) 11:1692. doi: 10.3389/fimmu.2020.01692
68. Kaneko N, Kuo HH, Boucau J, Farmer JR, Allard-Chamard H, Mahajan VS, et al. Loss of Bcl-6-Expressing T Follicular Helper Cells and Germinal Centers in COVID-19. *Cell* (2020) 183(1):143–57.e13. doi: 10.1016/j.cell.2020.08.025
69. Olagnier D, Farahani E, Thyrsted J, Blay-Cadanet J, Herengt A, Idorn M, et al. SARS-CoV2-Mediated Suppression of NRF2-Signaling Reveals Potent Antiviral and Anti-Inflammatory Activity of 4-Octyl-Itaconate and Dimethyl Fumarate. *Nat Commun* (2020) 11(1):4938. doi: 10.21203/rs.3.rs-31855/v1
70. Remy KE, Mazer M, Striker DA, Ellebedy AH, Walton AH, Unsinger J, et al. Severe Immunosuppression and Not a Cytokine Storm Characterizes COVID-19 Infections. *JCI Insight* (2020) 5(17). doi: 10.1172/jci.insight.140329
71. Schub D, Klemis V, Schneitler S, Mihm J, Lepper PM, Wilkens H, et al. High Levels of SARS-CoV-2-Specific T Cells With Restricted Functionality In Severe Courses of COVID-19. *JCI Insight* (2020) 5(20). doi: 10.1172/jci.insight.142167
72. Zhang X, Tan Y, Ling Y, Lu G, Liu F, Yi Z, et al. Viral and Host Factors Related to the Clinical Outcome of COVID-19. *Nature* (2020) 583(7816):437–40. doi: 10.1038/s41586-020-2355-0
73. Zhou R, To KK, Wong YC, Liu L, Zhou B, Li X, et al. Acute SARS-CoV-2 Infection Impairs Dendritic Cell and T Cell Responses. *Immunity* (2020) 53 (4):864–77.e5. doi: 10.1016/j.immuni.2020.07.026
74. Campos-Olivas R, Newman JL, Summers MF. Solution Structure and Dynamics of the Rous Sarcoma Virus Capsid Protein and Comparison With Capsid Proteins of Other Retroviruses. *J Mol Bio* (2000) 296(2):633–49. doi: 10.1006/jmbi.1999.3475
75. Lehmann PV, Suwansaard M, Zhang T, Roen DR, Kirchenbaum GA, Karulin AY, et al. Comprehensive Evaluation of the Expressed CD8+ T Cell Epitope Space Using High-Throughput Epitope Mapping. *Front Immunol* (2019) 10:655. doi: 10.3389/fimmu.2019.00655
76. Jarjour NN, Masopust D, Jameson SC . T Cell Memory: Understanding COVID-19. *Immunity* (2021) 54(1):14–8. doi: 10.1016/j.immuni.2020.12.009
77. Tang F, Quan Y, Xin ZT, Wrammert J, Ma MJ, Lv H, et al. Lack of Peripheral Memory B Cell Responses in Recovered Patients With Severe Acute Respiratory Syndrome: A Six-Year Follow-Up Study. *J Immunol* (2011) 186 (12):7264–8. doi: 10.4049/jimmunol.0903490
78. Bevan MJ. Understand Memory, Design Better Vaccines. *Nat Immunol* (2011) 12(6):463–5. doi: 10.1038/ni.2041


**Conflict of Interest:** PL is Founder, President and CEO of Cellular Technology Ltd., a company that specializes in immune monitoring by ELISPOT testing, producing high-throughput-suitable readers, test kits, and GLP-compliant contract research. AAL, GK, and TZ are employees of CTL. This study was funded by CTL, and the funder directed the study design, collection, analysis, interpretation of data, the writing of this article, and made the decision to submit it for publication.

frontiers in Immunology

ORIGINAL RESEARCH
published: 13 July 2021
doi: 10.3389/fimmu.2021.677824

# PSGL-1 Is a T Cell Intrinsic Inhibitor That Regulates Effector and Memory Differentiation and Responses During Viral Infection

*Roberto Tinoco[1]*, Emily N. Neubert[1], Christopher J. Stairiker[2], Monique L. Henriquez[1] and Linda M. Bradley[2]**

[1] Department of Molecular Biology and Biochemistry, University of California, Irvine, Irvine, CA, United States, [2] Infectious and Inflammatory Disease Center, NCI Designated Cancer Center, Sanford Burnham Prebys Medical Discovery Institute, La Jolla, CA, United States

OPEN ACCESS

**Edited by:**
Ramon Arens,
Leiden University Medical Center, Netherlands

**Reviewed by:**
Markus Johannes Hofer,
The University of Sydney, Australia
Kim Klonowski,
University of Georgia, United States
Bertram Bengsch,
University of Freiburg Medical Center, Germany

***Correspondence:**
Roberto Tinoco
rtinoco@uci.edu
Linda M. Bradley
lbradley@spbdiscovery.org

**Specialty section:**
This article was submitted to Immunological Memory, a section of the journal Frontiers in Immunology

**Received:** 08 March 2021
**Accepted:** 21 June 2021
**Published:** 13 July 2021

**Citation:**
Tinoco R, Neubert EN, Stairiker CJ, Henriquez ML and Bradley LM (2021) PSGL-1 Is a T Cell Intrinsic Inhibitor That Regulates Effector and Memory Differentiation and Responses During Viral Infection. Front. Immunol. 12:677824. doi: 10.3389/fimmu.2021.677824

Effective T cell differentiation during acute virus infections leads to the generation of effector T cells that mediate viral clearance, as well as memory T cells that confer protection against subsequent reinfection. While inhibitory immune checkpoints have been shown to promote T cell dysfunction during chronic virus infections and in tumors, their roles in fine tuning the differentiation and responses of effector and memory T cells are only just beginning to be appreciated. We previously identified PSGL-1 as a fundamental regulator of T cell exhaustion that sustains expression of several inhibitory receptors, including PD-1. We now show that PSGL-1 can restrict the magnitude of effector T cell responses and memory T cell development to acute LCMV virus infection by limiting survival, sustaining PD-1 expression, and reducing effector responses. After infection, PSGL-1-deficient effector T cells accumulated to a greater extent than wild type T cells, and preferentially generated memory precursor cells that displayed enhanced accumulation and functional capacity in response to TCR stimulation as persisting memory cells. Although, PSGL-1-deficient memory cells did not exhibit inherent greater sensitivity to cell death, they failed to respond to a homologous virus challenge after adoptive transfer into naïve hosts indicating an impaired capacity to generate memory effector T cell responses in the context of viral infection. These studies underscore the function of PSGL-1 as a key negative regulator of effector and memory T cell differentiation and suggest that PSGL-1 may limit excessive stimulation of memory T cells during acute viral infection.

**Keywords: virus infection, PSGL-1, effector T cells, memory T cells, LCMV**

## INTRODUCTION

Immunological memory confers host protection through an immune response that is more robust and effective at neutralizing a previously encountered pathogen. T cell-mediated immunity to virus infections requires differentiation of effector T cells that contribute to pathogen clearance by interfering with viral replication and by direct killing of virus-infected cells. As the infection is

resolved memory T cells are generated that promote long-term host protection against re-infection (1). The signals determining the generation of memory T cells remain incompletely understood, and depend upon contextual cues that include the duration of antigen exposure, the degree of inflammation, as well as the tissue localization and distribution of infection. Both $CD8^+$ and $CD4^+$ T cells can be classified as central memory ($T_{CM}$) and effector memory ($T_{EM}$) cells that are broadly distinguished by their preferential migration through, and responses in lymphoid and non-lymphoid tissues, respectively. An additional subset, designated tissue resident memory cells ($T_{RM}$), that are retained at the sight of initial infection where they locally provide protective immunity (2). It is the integration of a multitude of signals in diverse microenvironments that regulates the transcriptional and epigenetic programming, which determines effector and memory T cell fates (3). The fine-tuning of T cell responses to viral pathogens is in part achieved by appropriate engagement of negative regulatory molecules to prevent excessive T cell responses (4). It is now apparent that signals through PD-1 regulate effector $CD8^+$ T cell responses (5) and both PD-1 and LAG-3 impact the generation and responses of memory T cells in acute viral infections (6–8). We previously identified that the adhesion receptor, P-selectin glycoprotein-1 (PSGL-1), is a key T cell-intrinsic inhibitory receptor that is required for the development of T cell exhaustion in chronic virus infection and determines the expression levels of multiple inhibitory receptors that include PD-1, TIM-3, and LAG-3 among others (9). We now address whether PSGL-1 can also play a fundamental role in the regulation of effector and memory T cell differentiation and responses.

PSGL-1 (encoded by the gene *Selplg*) is expressed on the surface of most hematopoietic cells and well-known for its role in regulating leukocyte migration into sites of infection *via* binding of P-selectin on inflamed vascular endothelium. Selectin-binding requires post-translational modifications that include sulfation and glycosylation, which are constitutively present on PSGL-1 expressed by innate immune cells (10). Naïve T cells lack these modifications and are thus unable to bind selectins, but can acquire selectin binding capacity during effector differentiation (11), although expression is typically transient. On T cells, however, PSGL-1 can engage additional ligands in the absence of, or independently of selectin binding (12). These include the lymphoid tissue chemokines, CCL19 and CCL21 (13), which regulate the entry and positioning of T cells and dendritic cells in secondary lymphoid organs (14), and VISTA (V-type immunoglobulin domain-containing suppressor of T cell activation) (15), a negative regulator of T cell responses, which is primarily expressed on myeloid cells (16), respectively. The role of PSGL-1 as a potential negative regulator of T cells was initially identified in studies showing that PSGL-1-deficient $CD8^+$ T cells displayed greater homeostatic turnover in the absence of overt activation, as well as enhanced persistence as memory cells after acute infection with LCMV Armstrong (Arm) strain (17). However, whether PSGL-1-deficiency cells alters T cell function or differentiation, or secondary responses has not been addressed.

Here we report that PSGL-1 is a negative regulator of T cell responses to LCMV Arm infection that limits the responses of effector and memory T cells. With primary infection, virus-specific $CD8^+$ and $CD4^+$ *Selplg*$^{-/-}$ T cells accumulated to a much greater extent than wild type (WT) cells and displayed greater persistence as memory T cells due to better intrinsic survival. As effectors, *Selplg*$^{-/-}$ T cells expressed increased levels of the receptors, IL-7Rα and IL-2Rβ, as well as lower levels of PD-1 and developed a predominantly memory precursor/progenitor phenotype when compared to WT T cells. We observed greater numbers of cytokine-producing virus-specific $CD4^+$ and $CD8^+$ T cells in *Selplg*$^{-/-}$ mice at both the effector and memory stages after infection. In sharp contrast, however, although *Selplg*$^{-/-}$ memory T cells responded effectively to restimulation by LCMV viral peptides *in vitro* and did not exhibit greater susceptibility to death in the context of TCR engagement *in vivo*, they failed to respond to a secondary challenge with LCMV Arm after adoptive transfer with WT cells into the same naïve host, thus suggesting that inhibition *via* PSGL-1 during memory T cell activation may limit excessive stimulation induced by viral infection. These studies underscore that PSGL-1 has a fundamental role as a regulator of effector and memory T cell differentiation and indicate that PSGL-1-dependent inhibition may be essential for memory effector anti-viral responses.

## MATERIALS AND METHODS

### Mice

C57BL/6J and *Selplg*$^{-/-}$ mice (18) were purchased from Jackson Laboratory and then bred in specific-pathogen-free (SPF) facilities and maintained in biosafety level 2 (BSL-2) facilities after infection in the vivaria at SBP and UC Irvine. *Selplg*$^{-/-}$ mice were backcrossed to C57BL/6J mice for more than ten generations. P14 and SMARTA mice were obtained from The Scripps Research Institute (originally from Dr. Charles D. Surh). These mice were bred to Ly5.1 (B6.SJL-Ptprc$^a$ Pepc$^b$/BoyJ) mice and to Thy1.1 (B6.PL-Thy 1$^a$/CyJ) *Selplg*$^{-/-}$ mice which were purchased from Jackson Laboratory and bred in house. Both male and female mice were used and were greater than 6 weeks of age. All experiments were approved by the animal care and use committees at SBP (A3053-01) and UC Irvine (AUP-18-148).

### Virus Infection and Titers

LCMV Armstrong (Arm) strain was propagated in baby-hamster kidney cells and titrated on Vero African-green-monkey kidney cells (19, 20). Frozen stocks were diluted in Vero cell media and mice were infected by intraperitoneal (i.p.) injection of $2 \times 10^5$ plaque-forming units (PFUs) of LCMV Arm. Virus titers were determined from serial dilutions of sera taken from mice at 4 days post infection (dpi) using a focus forming assay (21).

### Adoptive Transfer

Naïve P14 WT or *Selplg*$^{-/-}$ T cells or SMARTA WT or *Selplg*$^{-/-}$ T cells were isolated from the spleens by magnetic sorting (Stem Cell Technologies, negative selection) according to the

manufacturers protocol. WT and *Selplg*$^{-/-}$ P14 or SMARTA cells were transferred in equal numbers (1000 each) into C57BL/6 mice by i.v. injection. On the same day, the mice were infected with LCMV Arm by i.p. injection. For memory cell adoptive transfer, viable WT and *Selplg*$^{-/-}$ P14 cells were isolated from the spleens of mice at 30dpi by FACS sorting based on the allelic markers. WT and *Selplg*$^{-/-}$ P14 memory cells were coinjected into naïve C57BL/6 recipients in a dose of 2000 each by i.v. injection, followed by i.p. infection with LCMV Arm.

## Flow Cytometry

Cells from the spleens or pooled lymph nodes (inguinal, axial, brachial) were dissociated in HBSS. For cell surface staining, 2x10$^6$ cells were incubated with antibodies in staining buffer (PBS, 2% fetal bovine serum (FBS) and 0.01% $NaN_3$) for 20 minutes at 4°C and with H-2D$^b$-$GP_{33-41}$, H-2D$^b$-$GP_{276-286}$, H-2D$^b$-$NP_{396-404}$, or IA$^b$-$_{66-77}$ tetramers (NIH core facility) for 1 hour and 5 minutes at room temperature. For functional assays, cells from infected animals were cultured for 5 hours at 37°C with 2ug/mL of $GP_{33-41}$, $GP_{276-286}$, $NP_{396-404}$, and $GP_{61-80}$ peptides (AnaSpec) in the presence of brefeldin A (1µg/ml; Sigma-Aldrich). The cells were then stained with antibodies for expression of surface proteins, fixed, permeabilized, and stained with antibodies for intracellular cytokine detection. To evaluate cell degranulation, splenocytes were incubated in the presence of anti-CD107a-FITC (Biolegend). The culture media was RPMI-1640 containing 10 mM HEPES, 1% non-essential amino acids and L-glutamine, 1mM sodium pyruvate, 10% heat-inactivated FBS, and penicillin/streptomycin antibiotics. The following anti-mouse antibodies were used in this study: Biolegend CD4 (RM4-5), CD8 (53-6.7), CD62L (MEL-14), CD127(A7R34), CD122 (TM-β1), CD107a (1D4B), IFN-γ (XMG1.2), TNF-α (MP6-XT22), CD11a (M17/4), CD49d (R1-2), CD45.1 (A20), CD90.1 (OX-7), KLRG-1 (2F1/KLRG1), PD-1 (29F.1A12), CD95 (Fas, SA367H8), CD178 (FasL, MFC3). Caspase-3 staining was done using CaspGLOW Fluorescein Active Caspase-3 staining kit (ThermoFisher) and following manufacturer's instructions.

## *In Vivo* Proliferation

Mice were injected i.p. with 2 mg BrdU (Sigma-Aldrich) 16 hours before removing the spleens at 9dpi to measure proliferation by flow cytometry after intracellular staining with an anti-BrdU antibody. BrdU staining was done using a BrdU Flow kit (BD Biosciences) following the manufacturer's instructions. Cells were acquired with a Novocyte3000 flow cytometer.

## Data Analysis

Flow cytometry data were analyzed with FlowJo software (TreeStar). Graphs were prepared with GraphPad Prism software. GraphPad Prism was used for statistical analysis to compare outcomes using a two-tailed unpaired Student's t test; significance was set to $p < 0.05$ and represented as *<0.05, **<0.005, ***<0.001, and ****<0.0001. Error bars show SEM.

# RESULTS

## *Selplg*$^{-/-}$ Mice Infected With LCMV Have an Increased Accumulation of Effector and Memory T Cells

To investigate whether PSGL-1 expression regulated T cell responses to primary virus infection, we infected WT and *Selplg*$^{-/-}$ mice with LCMV Arm. We first quantified virus-specific T cells in the spleen as indicated by co-expression of CD11a$^+$CD49d$^+$ (22) and found increased numbers of effector CD4$^+$ and CD8$^+$ T cells at 8dpi, indicating a larger population of T cells was responding to the virus (**Figure 1A**). We next quantified the numbers of virus-specific CD8$^+$ T cells in the spleens by staining with the MHC-I tetramers specific for $GP_{33-41}$, $GP_{276-286}$, and $NP_{396-404}$ LCMV epitopes recognized by CD8$^+$ T cells with differing TCR affinities (23). We also observed significant increases in the numbers of virus epitope-specific CD8$^+$ T cells in *Selplg*$^{-/-}$ mice at 8dpi (**Figure 1B**) and importantly, these differences were maintained at 30dpi (**Figure 1C**) long after viral clearance, which occurs by 8dpi. However, the frequencies of virus-specific CD8$^+$ T cells were selectively increased in $NP^+_{396-404}$ cells from *Selplg*$^{-/-}$ mice compared to WT mice (**Figures S1A, B**), suggesting a more pronounced effect of PSGL-1-deficiency on the highest affinity LCMV-specific CD8$^+$ T cell clone (23). We next investigated whether CD4$^+$ T cell responses were different in *Selplg*$^{-/-}$ mice compared to WT mice and found that, like CD8$^+$ T cells, the numbers of virus-specific CD4$^+$ T cells were significantly increased at 8dpi (**Figure 1D**) as well as at 30dpi (**Figure 1E**) in the spleen with *Selplg*-deficiency as were the frequencies (**Figures S1C, D**). Furthermore, longitudinal analyses revealed that the differences in the recovery of virus-specific CD8$^+$ and CD4$^+$ T cells in the spleens of *Selplg*$^{-/-}$ mice were detectable as early as 5dpi and sustained thereafter (**Figures S2A, B**). We found comparable results in the lymph nodes (**Figures S2C, D**), indicating that impaired trafficking into these sites with *Selplg*-deficiency did not account for the differences in recovery that were observed. Together, these findings show that with *Selplg*-deficiency, both virus-specific CD4$^+$ and CD8$^+$ T cells exhibit an enhanced response to acute LCMV infection as indicated by the significant increases in the numbers that accumulated during the effector response, differences that were maintained in the memory stage after viral clearance.

## *Selplg*$^{-/-}$ CD8$^+$ T Cells Exhibit Enhanced Survival but Not Increased Proliferation

To address whether the increased recovery of virus-specific T cells in *Selplg*$^{-/-}$ mice was a result of differences in their proliferation and/or survival, we infected WT and *Selplg*$^{-/-}$ mice and injected BrdU 16 hours prior to analysis at 8dpi. BrdU incorporation by CD8$^+$ T cells *in vivo* showed that both WT and *Selplg*$^{-/-}$ CD8$^+$ tetramer$^+$ cells proliferated; however, *Selplg*$^{-/-}$ CD8$^+$ T cells had decreased frequencies of BrdU$^+$ cells compared to WT at 8dpi (**Figure 2A**). Since we did not observe enhanced proliferation in *Selplg*$^{-/-}$ T cells, we next analyzed apoptosis by evaluating virus-specific CD8$^+$ T cells for their levels of active caspase 3 and propidium iodide (PI) uptake, and found that compared to WT cells, *Selplg*$^{-/-}$ CD8$^+$ T cells had

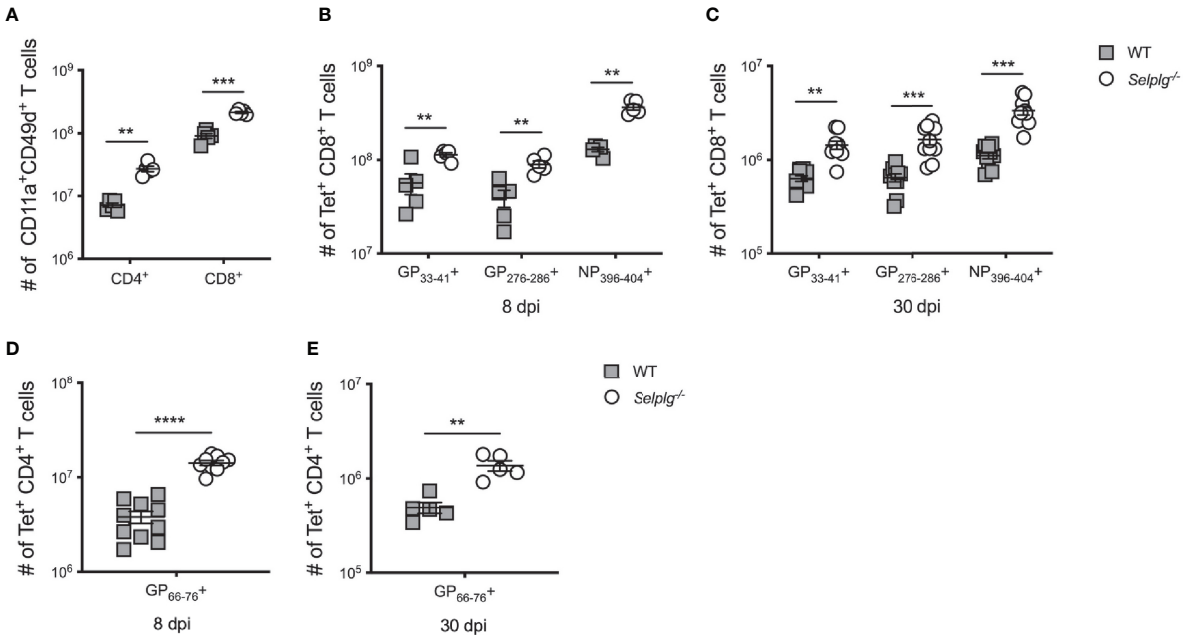


**FIGURE 1** | Increased accumulation of *Selplg-/-* T cells during LCMV infection. WT and *Selplg*$^{-/-}$ mice were infected with LCMV Armstrong by i.p. injection. **(A)** The numbers of antigen responding CD11a$^{+}$CD49d$^{+}$ T cells in spleen at 8dpi. Tetramer$^{+}$ CD8$^{+}$ T cells in the spleens were enumerated at 8dpi **(B)** and 30dpi **(C)**. Tetramer$^{+}$ CD4$^{+}$ T cells were enumerated in the spleens at 8dpi **(D)** and 30dpi **(E)**. Data are representative of four independent experiments (n = 5 or more mice/group). Graphs show the mean ± SEM. $^{**}p < 0.005$, $^{***}p < 0.001$, $^{****}p < 0.0001$ by two-tailed unpaired *t*-test.

lower frequencies of caspase 3$^{+}$PI$^{+}$ cells, indicating that these cells had decreased apoptosis (**Figure 2B**).

Since cytokines such as the γc cytokines, IL-2, IL-7 and IL-15, can promote CD8$^{+}$ T cell survival and can impact the differentiation of effector and memory T cells (24), we examined whether differences in expression of IL-7Rα or CD122 (IL-2Rβ), which is part of both the IL-2 and IL-15 receptors, distinguished WT and *Selplg*$^{-/-}$ CD8$^{+}$ T cells. We found dramatic increases IL-7Rα expression on *Selplg*$^{-/-}$ CD8$^{+}$ T cells by 8dpi and higher expression compared to WT cells up to 30dpi (**Figure 2C**). We also found increased expression of IL-7 Ra (**Figure 2D**) and frequencies of IL-7Rα$^{+}$ virus-specific CD8$^{+}$ T cells (**Figure 2E**) with all 3 tetramer$^{+}$ populations, shown at 8dpi. Increases in CD122 expression on *Selplg*$^{-/-}$ memory CD8$^{+}$ T cells were also found with all three CD8$^{+}$ tetramer$^{+}$ populations (**Figure 2F**), shown at 30dp**i**. These findings indicate that PSGL-1 expression can reduce the expansion of anti-viral effector T cells by limiting their survival, to which lower levels of cytokine receptor expression could contribute.

## Virus-Specific *Selplg*$^{-/-}$ CD8$^{+}$ T Cells Become Enriched in Memory Precursor and Central Memory Phenotype Cells

The increased levels of IL-7Rα on virus-specific CD8$^{+}$ T cells from *Selplg*$^{-/-}$ mice compared to WT mice suggested the possibility of altered differentiation of CD8$^{+}$ T cells during the course of viral infection. Thus, we analyzed virus-specific CD8$^{+}$ T cell subsets by examining the reciprocal expression of IL-7Rα and KLRG-1 which distinguishes memory precursor effectors (MPECs: IL-7Rα$^{+}$, KLRG-1$^{-}$) from more terminally differentiated and more short-lived effectors (SLECs: IL-7Rα$^{-}$, KLRG-1$^{+}$) in the LCMV Arm model (25). *Selplg*$^{-/-}$ mice had an increased accumulation of SLECs as early as 5dpi in both $NP^{+}_{396–404}$ and $GP^{+}_{33–41}$ CD8$^{+}$ T cells (**Figure 3A**). These differences were also evident at later stages of the response (15dpi). A similar pattern was observed with respect to accumulation of virus-specific *Selplg*$^{-/-}$ CD8$^{+}$ T cells that bore a MPEC phenotype (**Figure 3B**), although both $NP^{+}_{396–404}$ and $GP_{33–41}$+ CD8+ T cells showed significantly greater recovery throughout the effector response and after memory formation in *Selplg*$^{-/-}$ mice. Moreover, comparison of the ratios of MPEC to SLEC phenotype cells showed that memory precursors comprised a much greater proportion of virus-specific CD8$^{+}$ T cells in *Selplg*$^{-/-}$ mice (**Figure 3C**). Not only did memory T cells from these mice express higher levels of IL-7Rα than WT cells (**Figures 2C, D**), we also observed higher expression of CD62L on the memory population as a whole, indicating greater representation of $T_{CM}$ phenotype cells (**Figure 3D**). The results show that PSGL-1 expression limited the development of both SLECs and MPECs to regulate the size of the memory T cell pool, but also suggest that the absence of PSGL-1-dependent inhibition could alter the differentiation of CD8$^{+}$ T cells towards a MPEC phenotype or may promote a loss of SLECs due to terminal differentiation. Greater representation of $T_{CM}$ cells, which are also considered to be memory progenitors, supports the concept that CD8$^{+}$ T cells with greater memory

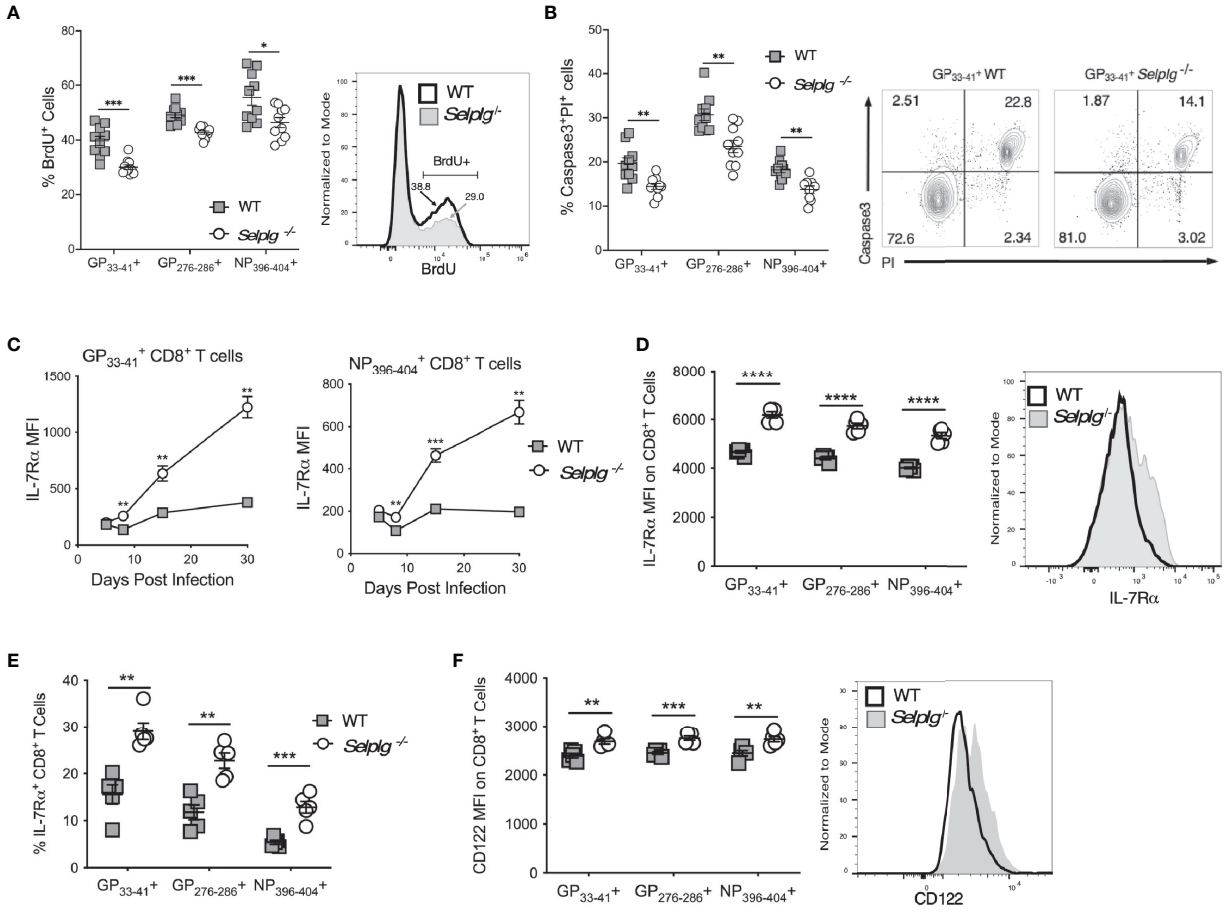


**FIGURE 2** | *Selplg*$^{-/-}$ effector and memory T cells have increased survival. WT and *Selplg*$^{-/-}$ mice were infected with LCMV Armstrong by i.p. injection. **(A)** CD8$^+$ T cells were analyzed for the frequencies of BrdU incorporating CD8$^+$ tetramer$^+$ T cells, with a representative histogram for $GP_{33-41^+}$ cells. **(B)** Frequencies of Caspase 3$^+$PI$^+$ CD8$^+$ tetramer$^+$ T cells at 8dpi, with a representative dot plot showing the frequencies for $GP_{33-41^+}$ T cells. **(C)** Geometric mean fluorescence intensity (MFI) of IL-7Rα levels expressed on CD8$^+$ tetramer$^+$ cells from the blood at the indicated time points and **(D)** at 30dpi from the spleen, with a representative histogram for $GP_{33-41^+}$ cells. **(E)** The frequencies of IL-7Rα$^+$, tetramer$^+$ CD8$^+$ T cells. **(F)** The levels CD122 expressed on tetramer$^+$ cells in spleen at 30dpi expressed as MFI, with a representative histogram for $GP_{33-41^+}$ cells. Data are representative of three independent experiments (n = 5 or more mice/group). Graphs show the mean ± SEM. *$p < 0.05$, **$p < 0.005$, ***$p < 0.001$, ****$p < 0.0001$ by two-tailed unpaired *t*-test **(A–F)**.

potential are generated in the context of PSGL-1-deficiency after LCMV Arm infection.

## Increased Functional Anti-Viral T Cells Are Generated in *Selplg*$^{-/-}$ Mice

We next evaluated whether functional differences existed between WT and *Selplg*$^{-/-}$ T cells in response to LCMV Arm infection. We thus examined cytokine production of anti-viral T cells *via ex vivo* peptide stimulation and found that while both WT and *Selplg*$^{-/-}$ T cells produced effector cytokines, significantly greater numbers of virus-specific CD8$^+$ T cells producing IFN-γ, IFN-γ and TNF-α, and IFN-γ, TNF-α, and IL-2 were detected in *Selplg*$^{-/-}$ mice at 8dpi (**Figure 4A**). Greater frequencies were also observed for $NP^+_{396-404}$ cells (**Figure S3A**). In addition, we detected increased frequencies of CD107$^+$IFN-γ$^+$ CD8$^+$ T cells in *Selplg*$^{-/-}$ mice, indicating that they had increased degranulation capacity, which reflects cytotoxic activity (**Figure 4B**). Consistent with the increase in cytokine-producing T cells in *Selplg*$^{-/-}$ mice, we also observed increased numbers (**Figure 4C**) and frequencies (**Figure S3B**) of cytokine$^+$ CD4$^+$ T cells. There were significant increases in IFN-γ$^+$, IFN-γ$^+$TNF-α$^+$, and IFN-γ$^+$TNF-α$^+$IL-2$^+$ cells in *Selplg*$^{-/-}$ mice and importantly, we detected more virus-specific CD4$^+$ and CD8$^+$ T cells that produced all three cytokines (**Figures 4A, C**). These studies showed that both WT and *Selplg*$^{-/-}$ T cells differentiated into functional effector T cells, but that that greater numbers and frequencies of polyfunctional T cells were generated in *Selplg*$^{-/-}$ mice.

We previously found that *Selplg*$^{-/-}$ CD8$^+$ T cells generated during chronic LCMV infection had reduced expression of PD-1 as well as other inhibitory receptors (9). Since PD-1 is upregulated on effector CD8$^+$ T cells responding to LCMV Arm (5), we examined whether *Selplg*$^{-/-}$ virus-specific CD8$^+$ T cells expressed differences in PD-1 levels during acute infection. We found comparable high frequencies of PD-1$^+$ tetramer$^+$

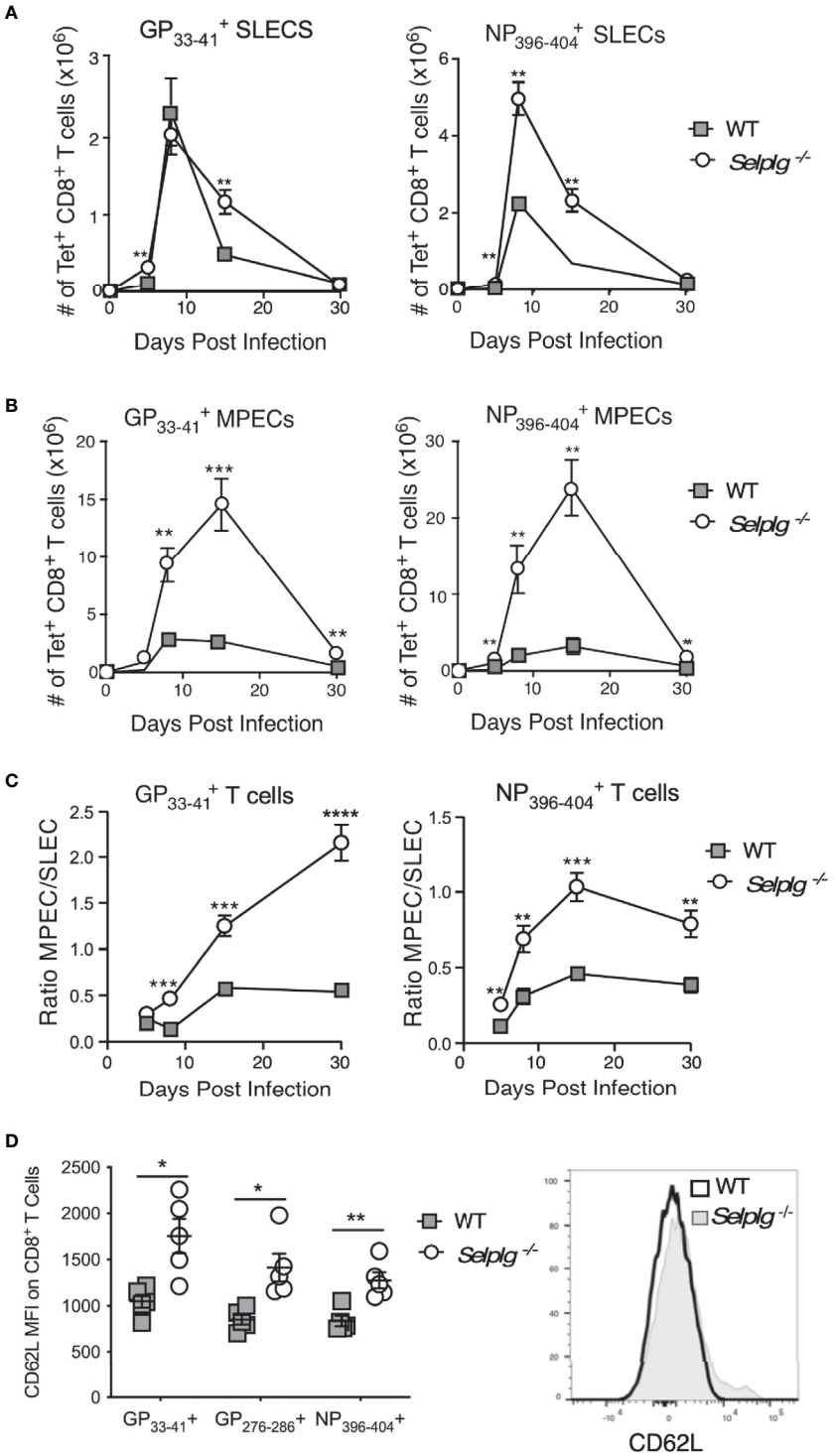


**FIGURE 3** | Virus-specific CD8$^+$ T cells in *Selplg*$^{-/-}$ mice are enriched for memory precursor and central memory phenotype cells. WT and *Selplg*$^{-/-}$ mice were infected with LCMV Arm and the numbers of short-lived effector phenotype cells (SLECs: IL7Rα$^-$, KLRG-1$^+$) **(A)** and memory precursor effector cells (MPECs, IL-7Rα$^+$, KLRG-1$^-$) **(B)** were evaluated for $GP_{33-41^+}$ CD8$^+$ T cells and $NP_{396-404^+}$ CD8$^+$ T cells in the spleens. **(C)** The ratios of MPEC to SLEC phenotype CD8$^+$ T cells for each of the tetramer+ populations. **(D)** Expression levels (MFI) of CD62L on CD8$^+$ tetramer$^+$ T cells from the spleens at 30dpi, with a representative histogram for $GP_{33-41^+}$ CD8$^+$ T cells. Data are representative of three independent experiments (n = 5 or more mice/group). Graphs show the mean ± SEM *$p$ < 0.05, **$p$ < 0.005, ***$p$ < 0.001, ****$p$ < 0.0001 by two-tailed $t$-test.

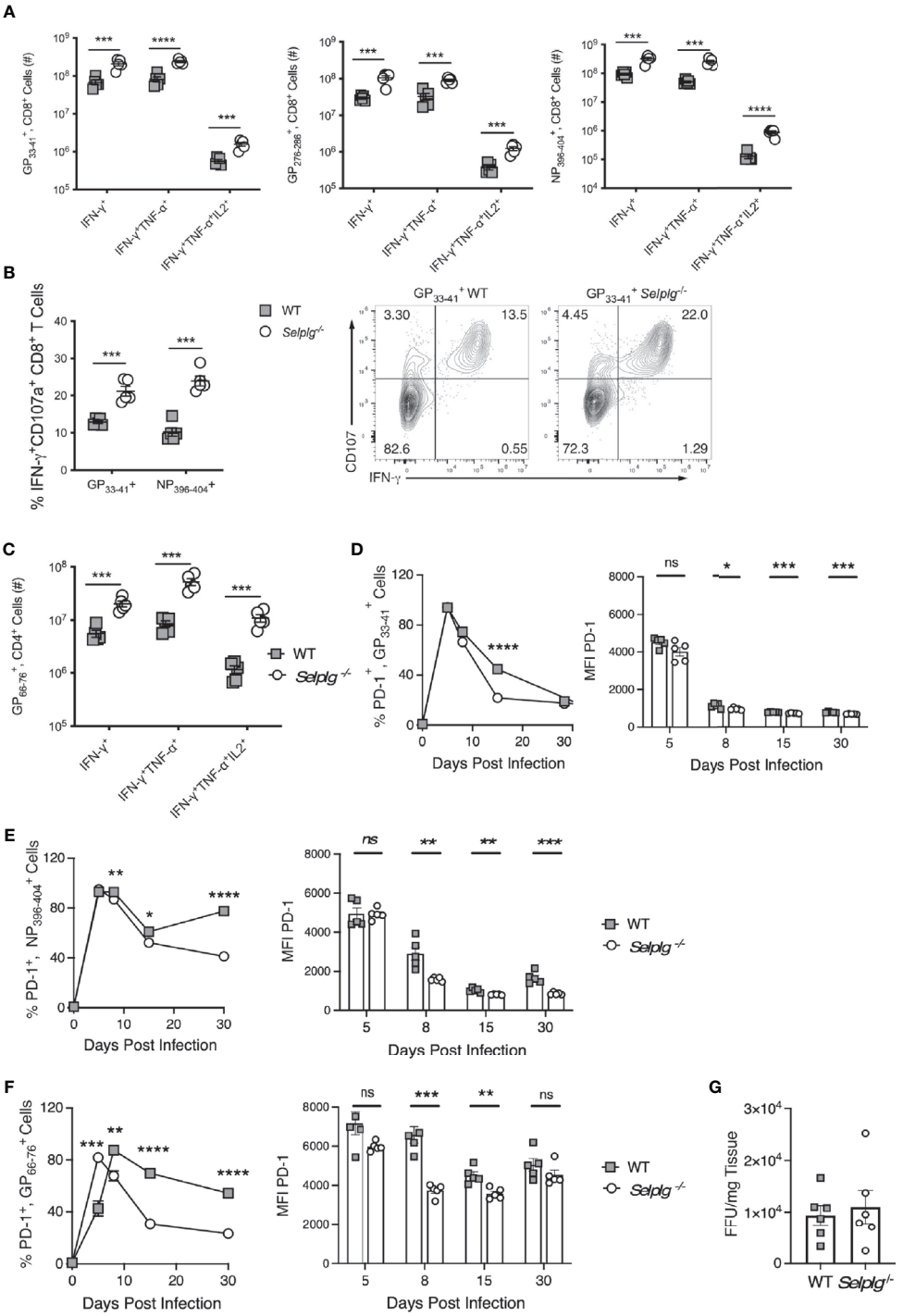


**FIGURE 4** | Virus-specific T cells in *Selplg*$^{-/-}$ mice have increased effector function and altered PD-1 expression. WT and *Selplg*$^{-/-}$ mice were infected with LCMV Arm and their spleens isolated at 8dpi. Splenocytes were stimulated *ex vivo* with the indicated LCMV peptides and assessed for the **(A)** and the numbers of cytokine$^{+}$ CD8$^{+}$ T cells **(B)** and the frequencies of IFN-γ$^{+}$CD107a$^{+}$ CD8$^{+}$ T cells, **(C)** in addition to the numbers of cytokine$^{+}$ CD4$^{+}$ T cells. **(D, E)** % PD-1$^{+}$ tetramer$^{+}$, CD8$^{+}$ T cells and expression of PD-1(MFI). **(F)** % PD-1$^{+}$ tetramer$^{+}$, CD4$^{+}$ T cells and expression of PD-1 (MFI). **(G)** Virus titers measured from the spleens at 4dpi by focus forming units (FFU) and expressed/g of tissue. Data in **(A–F)** are representative of three independent experiments (n = 5 or more mice/group). Data in **(G)** are from one experiment. Graphs show the mean ± SEM *$p < 0.05$, **$p < 0.005$, ***$p < 0.001$, ****$p < 0.0001$ by two-tailed unpaired *t*-test.

$CD8^+$ T cells in WT and *Selplg*$^{-/-}$ mice at 5dpi, and these cells initially upregulated PD-1 expression to similar levels as WT cells. However, by 8dpi, the frequencies of PD-$1^+$ tetramer$^+$ $CD8^+$ T cells in both groups of mice began to drop, with dramatically decreased expression levels on *Selplg*$^{-/-}$ tetramer$^+$ $CD8^+$ T compared to their WT counterparts (**Figures 4D, E**). Greater frequencies of PD-$1^+$ cells were sustained in both WT and *Selplg*$^{-/-}$ mice, particularly in the $NP_{396\text{-}404}$ tetramer$^+$ population up to 30dpi, the length of our analysis in this experiment. Similar outcomes were observed with $GP^+_{66-76}$. $CD4^+$ T cells (**Figure 4F**). However, by 48dpi, PD-1 expression was lost on WT as well as *Selplg*$^{-/-}$ T cells (not shown). Together the data suggest that PSGL-1 impacts PD-1 levels on virus-specific T cells particularly during the transition to memory cells, which may indicate differences in activation status by WT compared to *Selplg*$^{-/-}$ T cells. Overall our results suggest that lower expression of PD-1 with PSGL-1-deficiency could contribute to the greater representation of MPECs and $T_{CM}$ cells at the memory phase (**Figure 3**). Notably, we did not detect differences in expression of other inhibitory receptors (LAG-3 or TIM-3, not shown).

Since greater T cell functionality accompanied PSGL-1 deficiency, we considered the possibility that a more effective response could reduce viral loads, thereby hastening the effector to memory transition and limiting the differentiation of SLECs. Thus, we measured viral load at 4dpi (5) when LCMV Arm is detectable in the spleen although not in the blood. We did not find differences in viral titers at this time (**Figure 4G**), although the virus levels were variable. The results suggest that capacity for early viral containment is not affected by the subsequent greater accumulation of effector T cells with PSGL-1-deficiency.

## Increased Functionality of Memory Anti-Viral T Cells in *Selplg*$^{-/-}$ Mice

We next assessed the functional capacity of virus-specific memory T cells from WT and *Selplg*$^{-/-}$ mice as measured by cytokine production. As observed at 8dpi, at 30dpi we detected increased numbers of $CD8^+$ T cells in *Selplg*$^{-/-}$ mice that were IFN-$\gamma^+$, IFN-$\gamma^+$, TNF-$\alpha^+$, and IFN-$\gamma^+$TNF-$\alpha^+$IL-$2^+$ after restimulation with viral peptides (**Figure 5A**). The *Selplg*$^{-/-}$ $CD4^+$ T cell population also contained more IFN-$\gamma^+$, IFN-$\gamma^+$TNF-$\alpha^+$, and IFN-$\gamma^+$TNF-$\alpha^+$IL-$2^+$ producers at 30dpi (**Figure 5B**). Furthermore, we observed increased frequencies and numbers of cytokine$^+$$CD8^+$ T cells (**Figures S4A, B**) and $CD4^+$ T cells (**Figure S4C**). Together, our findings indicate that with LCMV Arm infection, functional *Selplg*$^{-/-}$ memory T cells persist in greater numbers, and that a greater fraction produce effector cytokines after restimulation with viral antigens.

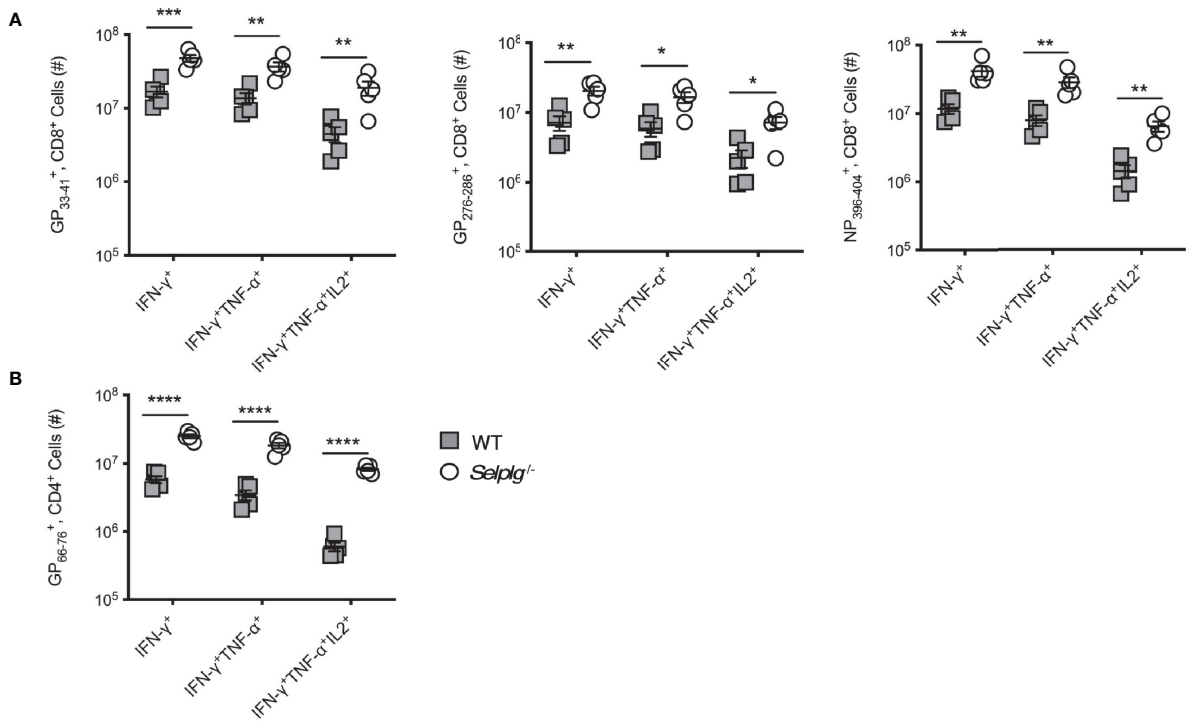


**FIGURE 5** | *Selplg*$^{-/-}$ mice have increased accumulation of cytokine producing memory T cells. WT and *Selplg*$^{-/-}$ mice were infected with LCMV Armstrong and the spleens were isolated at 30dpi. Splenocytes were stimulated with the indicated viral peptides and the numbers of cytokine$^+$ $CD8^+$ T cells **(A)** and $CD4^+$ T cells **(B)** were enumerated. Data are representative of three independent experiments (n = 5 or more mice/group). Graphs show the mean ± SEM *$p < 0.05$, **$p < 0.005$, ***$p < 0.001$, ****$p < 0.0001$ by two-tailed unpaired *t*-test.

## The Accumulation of *Selplg*$^{-/-}$ T Cells During Viral Infection Is Cell-Intrinsic

Since *Selplg*$^{-/-}$ mice mounted a more robust CD8$^+$ T cell response during acute LCMV infection, we next determined whether this accumulation was cell-intrinsic. We co-transferred WT and *Selplg*$^{-/-}$ TCR transgenic (P14) CD8$^+$ T cells at a 1:1 ratio in WT mice and examined their expansion after LCMV Arm infection. We found that *Selplg*$^{-/-}$ P14 T cell frequencies were increased in the blood from 7dpi through 30dpi (**Figure 6A**) during which time a ~1.5 ratio of knockout to WT cells within P14 cells was maintained. However, both WT and *Selplg*$^{-/-}$ P14 cells decayed over time (**Figure S5**). To address whether the survival differences were further sustained, we compared the frequencies of P14 cells in the blood at 7dpi and 156dpi (**Figure 6B**, left panel) as well as the numbers in the spleens 156dpi (**Figure 6B**, right panel). The results demonstrate that consistently greater recovery of *Selplg*$^{-/-}$ P14 cells compared to their WT counterparts. We next co-transferred WT and *Selplg*$^{-/-}$ T cell receptor transgenic CD4$^+$ (SMARTA) T cells at a 1:1 ratio into naive WT mice that were subsequently infected with LCMV Arm. We observed significantly greater recovery of *Selplg*$^{-/-}$ SMARTA cells compared to WT SMARTA cells in the blood from 7dpi to 30dpi, which stabilized at a ~3 fold difference by 15dpi (**Figure 6C**). Both populations decayed with time (**Figure S5**). We also found that increased frequencies of *Selplg*$^{-/-}$ SMARTA$^+$ T cells were sustained at 156dpi in the blood, at which time increased numbers of *Selplg*$^{-/-}$ SMARTA T cells in the spleens were also observed (**Figure 6D**). Our findings show that the greater persistence of *Selplg*$^{-/-}$ virus-specific CD8$^+$ and CD4$^+$ T cells is cell-intrinsic, and that PSGL-1-deficiency increased the numbers of memory T cells that were maintained long-term.

## Greater MPEC Representation Does Not Support *Selplg*$^{-/-}$ Memory T Cell Responses After Secondary Viral Challenge

Since we observed increased representation of memory precursor/progenitor CD8$^+$ T cells after primary LCMV infection in *Selplg*$^{-/-}$ mice, we assessed their whether their altered differentiation was T cell intrinsic. Thus, we followed the recovery of adoptively co-transferred WT and *Selplg*$^{-/-}$ P14 cells in the blood with time after infection and found maintenance of ~2 fold higher *Selplg*$^{-/-}$ cells compared to WT cells (**Figure 7A**). *Selplg*$^{-/-}$ P14 cells displayed greater recovery of MPECs and decreased recovery of SLECs compared to WT P14 cells (**Figure 7B**). At 30dpi, we found PD-1$^+$ cells both the WT and *Selplg*$^{-/-}$ P14 populations, although PD-1 expression by these cells was at low levels (**Figure 7C**). We next assessed the impact of PSGL-1-deficiency on the response of memory P14 cells to viral challenge. In order to avoid the confounding T cell memory response of the initial host, differences in the frequencies of virus-specific T cells and the existence of LCMV-specific antibodies, we sorted WT and *Selplg*$^{-/-}$ P14$^+$ T cells from WT mice at 30dpi after they had that received both populations in a 1:1 ratio at the time of infection. We co-injected these memory populations in equal numbers into naive WT hosts that were then infected with LCMV Arm. We detected robust expansion/recovery of WT P14 T cells at 6dpi, with contraction occurring by 8dpi in the spleens. However, few

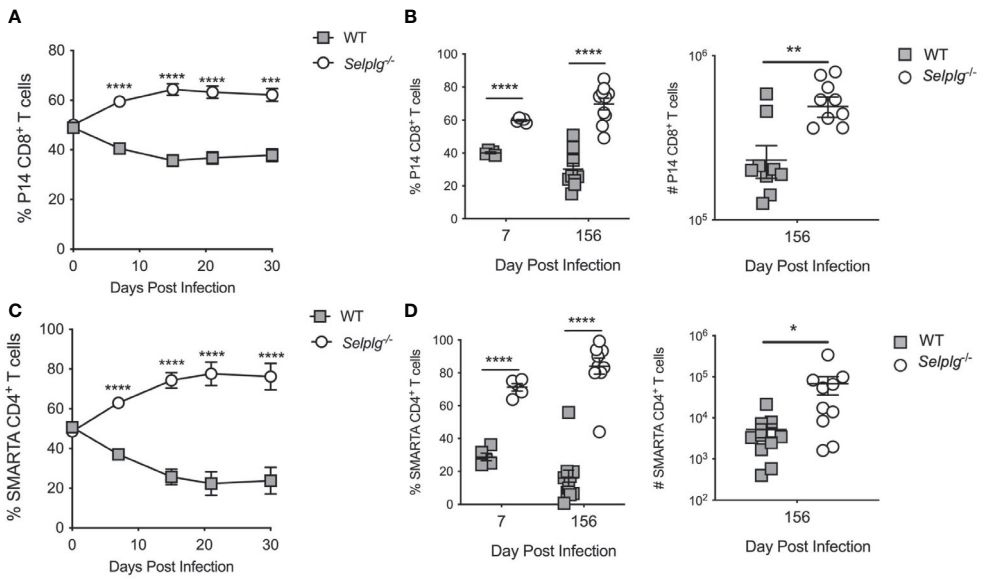


**FIGURE 6** | *Selplg*$^{-/-}$ T cells display increased cell-intrinsic accumulation as effector and memory T cells. **(A)** Frequencies of WT and *Selplg*$^{-/-}$ P14 T cells in the blood after adoptive transfer into naïve WT recipients and infection with LCMV Arm. **(B)** Frequencies and numbers of P14 T cells in the spleens at 7- and 156dpi. **(C)** Frequencies of WT and *Selplg*$^{-/-}$ SMARTA T cells in the blood after adoptive transfer and infection with LCMV Arm. **(D)** Frequencies and numbers of SMARTA T cells in the spleens at 7- and 156dpi. Data are representative of three independent experiments (n = 5 or more mice/group). Graphs show the mean ± SEM $^*p < 0.05$, $^{**}p < 0.005$, $^{***}p < 0.001$, $^{****}p < 0.0001$ by two-tailed unpaired *t*-test.

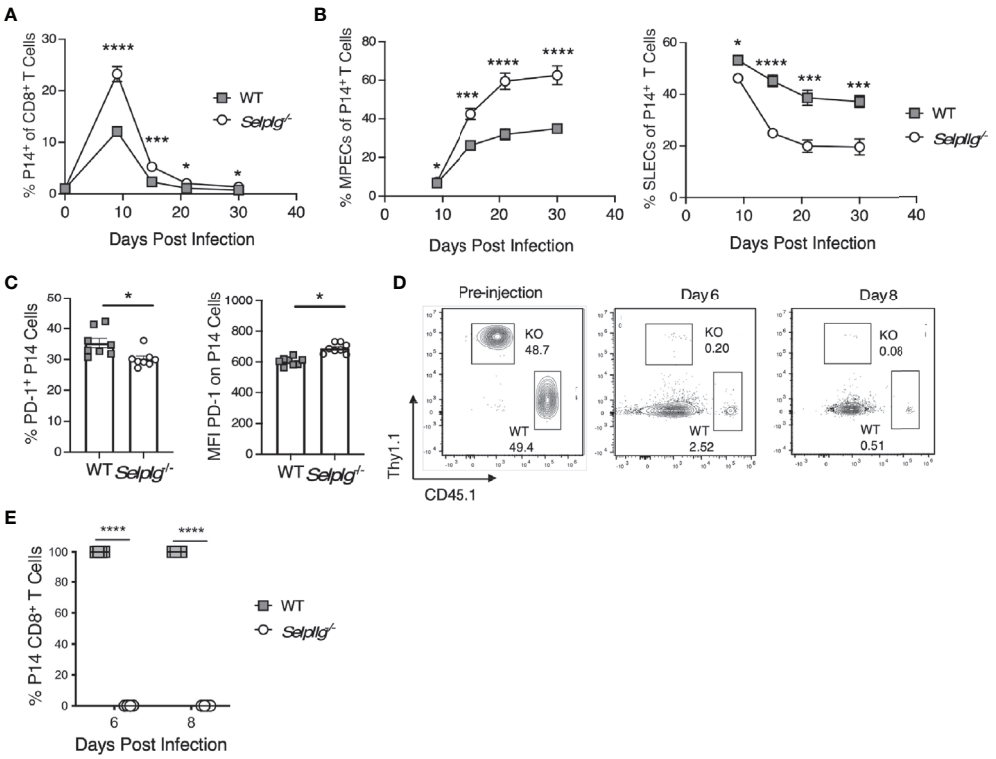


**FIGURE 7** | Greater MPEC representation does not support *Selplg*$^{-/-}$ memory T cell responses after secondary viral challenge. WT and *Selplg*$^{-/-}$ memory P14 CD8$^{+}$ T cells were isolated from the spleens of WT mice at 30 days after cotransfer in a 1:1 ratio and infection with LCMV Armstrong. These cells were then re-injected in equivalent numbers into WT naïve hosts and mice that were then infected with LCMV Armstrong. **(A)** The frequencies of WT and *Selplg*$^{-/-}$ P14 T cells in the blood with time. **(B)** The frequencies of the memory precursor effector cells (MPECs, IL-7R$\alpha^{+}$, KLRG-1$^{-}$) and short-lived effector phenotype cells (SLECs: IL7R$\alpha^{-}$, KLRG-1$^{+}$) as a % of WT and *Selplg*$^{-/-}$ P14 cells. **(C)** Frequencies PD-1$^{+}$ cells and their and expression levels of PD-1 (MFI). **(D)** representative flow cytometry plots for the pre-injection populations of P14 cells, and **(E)** their recovery at 6 and 8 dpi **(B)**. Data are representative of three independent experiments (n = 5 or more mice/group). Graphs show the mean ± SEM *$p < 0.05$, ***$p < 0.001$, ****$p < 0.0001$ by two-tailed unpaired *t*-test.

*Selplg*$^{-/-}$ P14 T cells were recovered (**Figures 7D, E**). *Selplg*$^{-/-}$ memory T cells were also not detected at 4- or 6dpi in in the peripheral lymph nodes, mesenteric lymph nodes, Peyer's patches, lungs or liver (not shown). These data indicate that redistribution of P14 memory T cells is not likely to account for their lack of accumulation upon viral challenge.

To address the potential for preferential cell death by *Selplg*$^{-/-}$ P14 cells, we assessed the impact of TCR restimulation *in vivo* by injecting $GP_{33-41}$ peptide together with LPS as an adjuvant. As observed previously, *Selplg*$^{-/-}$ P14 cells were recovered in greater frequencies than WT P14 cells at 30dpi. However, there were no differences in the frequencies of Caspase 3$^{+}$ cells (**Figure S6B**), or of CD95$^{+}$ and CD95L$^{+}$ cells (**Figure S6C**) after TCR stimulation *in vivo*. These findings suggest that TCR-induced cell death or death receptor-mediated cell death does not account for the disappearance of PSGL-1-deficient memory T cells. The data support the possibility that PSGL-1 expression by memory T cells is required to limit memory effector CD8$^{+}$ T cell stimulation and responses, thereby sustaining effector activity in the context of the extensive inflammatory milieu that develops with acute LCMV infection.

## DISCUSSION

In this study we demonstrated that PSGL-1, in its function as a T cell-intrinsic inhibitory receptor, limits the magnitude of CD4$^{+}$ and CD8$^{+}$ T cell responses to acute infection with LCMV Arm, and correspondingly constrains the size of the memory cell pool. Accordingly, *Selplg*$^{-/-}$ mice had notable increases in the numbers of virus-specific CD4$^{+}$ and CD8$^{+}$ T cells following acute LCMV infection that were evident by 5dpi as well as at the peak of the effector T cell response (8dpi), and they maintained increased numbers of persisting memory T cells (≥30dpi). Phenotypic analyses of CD8$^{+}$ T cells indicated that there were greater numbers of effector cells in both the SLEC and MPEC populations in *Selplg*$^{-/-}$ mice compared to WT mice, but that the representation of MPECs compared to SLECs was significantly increased. Previous studies showed that dendritic cells from *Selplg*$^{-/-}$ mice have a greater capacity to stimulate naïve T cells *in vitro* (26), which suggests that changes P innate immune cells could also impact the magnitude of T cell responses in the context of germ-line deficiency of PSGL-1. However CD8$^{+}$ T cells displayed intrinsic greater generation of

MPECs, supporting a conclusion that PSGL-1-deficiency favors the differentiation of cells with memory progenitor potential. This conclusion is supported by our finding of increased representation of $CD8^+$ $T_{CM}$ compared to $T_{EM}$ phenotype cells with PSGL-1-deficiency, as indicated by expression of CD62L. Importantly, the accumulation of greater numbers of *Selplg*$^{-/-}$ T cells was a result of increased survival and not proliferation, as shown in our previous study of LCMV Clone 13 infection (9). In addition, *Selplg*$^{-/-}$ T cell survival was cell-intrinsic as both $CD4^+$ and $CD8^+$ virus-specific T cells exhibited greater persistence as memory cells in WT hosts after viral infection.

Consistent with this result, memory T cells from *Selplg*$^{-/-}$ mice had increased expression IL-7Rα and IL-2Rβ, components of the receptors that regulate responses to the γc cytokines IL-7, IL-2 and IL-15, which regulate T cell survival (27). These results corroborate a previous study showing that *Selplg*$^{-/-}$ T cells exhibit elevated homeostatic turnover in WT mice, and are in partial agreement with the finding in that study which showed that *Selplg*$^{-/-}$ T cells proliferate in response to high levels of IL-2 or IL-15 *in vitro*. Importantly, we did not find differences in expression levels of IL-7Rα on naïve T cells from WT and *Selplg*$^{-/-}$ mice (not shown), indicating that the inhibitory function of PSGL-1, which impacts the expression levels of γc cytokine receptors, occurs in the context of T cell activation.

The effects on survival that led to an overall increase in the availability of effector T cells after infection thereby increased the numbers of cytokine-producing T cells in *Selplg*$^{-/-}$ mice that were maintained during memory development. Polyfunctionality was also exhibited by greater frequencies of T cells from *Selplg*$^{-/-}$ mice compared to those from WT mice. To a large extent, this outcome was linked to a more rapid decrease in PD-1 expression on virus-specific *Selplg*$^{-/-}$ T cells. PD-1, which is induced T cells shortly after activation, was previously shown to inhibit the P14 effector T cell response during the first few days after LCMV Arm infection (5). Since virus-specific WT and *Selplg*$^{-/-}$ cells expressed comparable high levels of PD-1 at the peak of viral replication at 5dpi, but then more quickly lost expression, our results imply that PSGL-1-deficiency supports a more rapid effector to memory transition. The results also show that PSGL-1 does not directly regulate PD-1 at the peak of the viral replication, and possibly thereafter. Our finding that PD-1 expression is retained by virus-specific cells for an extended period after viral clearance suggests that maintenance of PD-1 is not likely to be due to residual antigen. However, PD-1 expression is linked to antigen recognition by the TCR, and different affinities might be expected lead to changes in PD-1 expression as shown by the different LCMV epitopes examined. It is possible that PSGL-1 signals sustain PD-1 expression on WT cells ($NP396^+$ $CD8^+$ cells as well as WT $GP66^+$ $CD4^+$ cells), but this will require further study. Overall, we conclude that PSGL-1 could potentially contribute to effector T cell death during the contraction phase of the response by sustaining greater activation, and thus PD-1 expression.

Other studies of PD-1 regulation of T cell anti-viral responses support the conclusion that inhibitory signals function to limit the magnitude of effector T cell responses. In response to acute infection with Friend's Virus, PD-1- or PD-L1-deficiency resulted in enhanced effector $CD8^+$ T cell development that was associated with greater survival and polyfunctionality (28). A study of acute vaccinia virus infection showed that PD-1-deficiency not only dramatically increased virus-specific T cell recovery at the effector and memory stages, but in contrast to our study, that memory effector $CD8^+$ T cell responses after adoptive transfer and challenge of naïve hosts were also significantly greater. Yet another study of PD-1-axis deficiency with influenza virus infection showed greater effector responses, but more dramatic effector contraction and decreased memory $CD8^+$ T cell function (8). Together the data imply that the fine tuning of T cell effector responses by inhibitory receptors is influenced by the tissue sites of infection, viral loads, and/or inflammatory conditions engendered by individual viruses.

Our results showing that effector generation is greater in *Selplg*$^{-/-}$ mice indicates that PSGL-1 dampens the response with LCMV Arm infection. Greater numbers of virus-specific effector $CD4^+$ and $CD8^+$ T cells in *Selplg*$^{-/-}$ mice were found early after infection, and MPEC phenotype T cells with significantly elevated expression of IL-7R predominated by 8dpi. Interestingly, PD-1 blockade during LCMV Arm infection also demonstrated increased numbers of MPECs possibly due to earlier viral control (5). Thus, we anticipated that the virus might be more rapidly controlled in *Selplg*$^{-/-}$ mice thereby limiting the extent of antigen stimulation and hastening the effector to memory transition. However, we did not detect differences in viral titers in the spleens of WT and PSGL-1-deficient mice at 4dpi, implying that differences in the regulation of T cell differentiation with PSGL-1-deficiency rather than earlier viral control had a greater impact on the memory development. Our finding of increased expression of CD62L on *Selplg*$^{-/-}$ T cells at this time further supports an interpretation that differentiation of $T_{CM}$ phenotype cells with memory progenitor potential (29) are favored with PSGL-1-deficiency.

Although strong TCR stimulation is typically identified with terminal T cell differentiation (30), a recent study demonstrated that greater TCR stimulation can favor $T_{CM}$ differentiation when coupled to high levels of Bim and Bcl2 (31), which would not be dependent on differences in viral loads. However, it is also possible that PSGL-1-deficiency allows for greater activation of SLECs due to more limited PD-1 expression, thereby driving their terminal differentiation and promoting increased representation of MPECs. In contrast to our results, a recent study identified a key role for PD-1 in combination with LAG-3 in maintaining memory $CD8^+$ T cell precursors early during infection (7). As additional evidence for roles of inhibitory receptors in regulating T cell responses, both CTLA-4 and PD-1 were found to restrain aberrant effector T cell differentiation and profound inflammation that occurs with their genetic deficiency either early or late in life, respectively (32). However, CTLA-4 primarily prevented the generation of aberrant $CD4^+$ T cell phenotypes whereas PD-1 restricted $CD8^+$ T cell differentiation. It is noteworthy that PSGL-1 appears to regulate both $CD4^+$ and $CD8^+$ T cells comparably with respect to survival and function, and we do not find that *Selplg*$^{-/-}$ mice develop spontaneous inflammatory responses or signs of autoimmunity as do mice that are deficient in PD-1 and CTLA-4.

Implicit in our results is the conclusion that limiting PSGL-1-signaling during T cell priming after infection or vaccination would favor a generation of a larger memory cell pool, but we were unable to identify a PSGL-1 blocking reagent to directly test this concept. Our data showing significantly better functionality of effector and persisting memory *Selplg*$^{-/-}$ CD8$^{+}$ T cells in response to TCR stimulation *in vitro* further support a conclusion that the capacity for high quality memory responses is potentially improved when the contributions of PSGL-1-dependent inhibition are removed. However, although *Selplg*$^{-/-}$ mice sustained greater numbers and frequencies of effector and memory T cells throughout the course of viral infection, with an adoptive transfer approach to prime WT and *Selplg*$^{-/-}$ T cells together in a PSGL-1-sufficient environment by LCMV Arm infection, they failed to mount a detectable memory effector response to a secondary viral challenge in naïve hosts as indicated by a failure to recover *Selplg*$^{-/-}$ T cells compared to WT T cells. This outcome reveals that despite an intrinsic survival advantage of *Selplg*$^{-/-}$ T cells even under conditions of competition with WT cells during their responses to the virus in WT hosts, the inhibitory effects of PSGL-1 resulted in a memory population with greater potential for secondary effector responses. Our results indicate that PSGL-1 can be a critical inhibitor of memory effector T cell responses as was also recently shown with the combined deficiency of both PD-1 and LAG-3 on memory CD8$^{+}$ T cells with LCMV Arm where deficiency in these receptors supported greater recovery of effector T cells (7). We propose that *Selplg*$^{-/-}$ memory T cells may be less inhibited than their WT memory counterparts, as indicated by their increased cytokine responses to peptide restimulation *in vitro*. In the context of TCR signals, diminished inhibition could result in enhanced responses to stimulatory signals (e.g., CD28 or proinflammatory cytokines) that would potentially be detrimental to memory T cell survival and ultimately their function if overstimulation occurred. Importantly, we did not detect greater susceptibility of *Selplg*$^{-/-}$ memory T cells to TCR/peptide-mediated activation-induced cell death *in vivo*, suggesting that the virus challenge is coupled to their impaired memory effector responses in WT hosts.

Since we previously showed that PSGL-1 inhibitory signaling promoted the generation of exhausted T cells (9), it is significant that this inhibitory axis also regulates T cell differentiation during acute viral infection. Overall our results indicate that PSGL-1 is a fundamental negative regulator of T cells that ensures that TCR signals are fine-tuned to promote the generation of memory T cells that respond optimally to confer protection upon re-exposure to previously encountered viral pathogens. But importantly in the acute setting, PSGL-1 could be uniquely required to limit the responses of memory T cells, which are considered to be more readily activated by lower levels of antigen stimulation and costimulation than naïve T cells. Further studies will be required to identify how PSGL-1 contributes to the integration of co-inhibitory and co-stimulatory signals, cytokines, and the strength of TCR signals that together dictate the quantity and quality of the memory T cell pool.

## DATA AVAILABILITY STATEMENT

The raw data supporting the conclusions of this article will be made available by the authors, without undue reservation.

## ETHICS STATEMENT

The animal study was reviewed and approved by IACUC committees at the Sanford Burnham Prebys Medical Discovery Institute and at the University of California, Irvine.

## AUTHOR CONTRIBUTIONS

RT and LB initiated and designed the study as well as analyzed and interpreted experiments. EN and MH helped with *in vivo* experiments at UC Irvine, CS contributed to the *in vivo* experiments and performed virus analyses at SBP. RT and LB wrote the manuscript. RT and LB are corresponding authors. All authors contributed to the article and approved the submitted version.

## FUNDING

The authors would like to acknowledge funding from the NIH Grant R01 AI137239 to RT; NIH T32 AI007319 to EN, and R01 AI106895 and R21 AI15916 to LB. The work at SBP was also supported by the NIH NCI Cancer Center Support Grant P30 CA030199.

## ACKNOWLEDGMENTS

We thank Dr. Florent Carrette (Aix Marseille Université and Innate Pharma, Marseilles, France) for critical review of the manuscript.

## SUPPLEMENTARY MATERIAL

The Supplementary Material for this article can be found online at: https://www.frontiersin.org/articles/10.3389/fimmu.2021.677824/full#supplementary-material

## REFERENCES

1. Kaech SM, Wherry EJ. Heterogeneity and Cell-Fate Decisions in Effector and Memory CD8+ T Cell Differentiation During Viral Infection. *Immunity* (2007) 27:393–405. doi: 10.1016/j.immuni.2007.08.007
2. Hope JL, Stairiker CJ, Bae EA, Otero DC, Bradley LM. Striking a Balance-Cellular and Molecular Drivers of Memory T Cell Development and Responses to Chronic Stimulation. *Front Immunol* (2019) 10:1595. doi: 10.3389/fimmu.2019.01595
3. Chen Y, Zander R, Khatun A, Schauder DM, Cui W. Transcriptional and Epigenetic Regulation of Effector and Memory Cd8 T Cell Differentiation. *Front Immunol* (2018) 9:2826. doi: 10.3389/fimmu.2018.02826
4. Attanasio J, Wherry EJ. Costimulatory and Coinhibitory Receptor Pathways in Infectious Disease. *Immunity* (2016) 44:1052–68. doi: 10.1016/j.immuni.2016.04.022

5. Ahn E, Araki K, Hashimoto M, Li W, Riley JL, Cheung J, et al. Role of PD-1 During Effector CD8 T Cell Differentiation. *Proc Natl Acad Sci USA* (2018) 115:4749–54. doi: 10.1073/pnas.1718217115
6. Allie SR, Zhang W, Fuse S, Usherwood EJ. Programmed Death 1 Regulates Development of Central Memory CD8 T Cells After Acute Viral Infection. *J Immunol* (2011) 186:6280–6. doi: 10.4049/jimmunol.1003870
7. Johnnidis JB, Muroyama Y, Ngiow SF, Chen Z, Manne S, Cai Z, et al. Inhibitory Signaling Sustains a Distinct Early Memory CD8(+) T Cell Precursor That Is Resistant to DNA Damage. *Sci Immunol* (2021) 6(55): eabe3702. doi: 10.1126/sciimmunol.abe3702
8. Pauken KE, Godec J, Odorizzi PM, Brown KE, Yates KB, Ngiow SF, et al. The PD-1 Pathway Regulates Development and Function of Memory Cd8(+) T Cells Following Respiratory Viral Infection. *Cell Rep* (2020) 31:107827. doi: 10.1016/j.celrep.2020.107827
9. Tinoco R, Carrette F, Barraza ML, Otero DC, Magana J, Bosenberg MW, et al. Psgl-1 Is an Immune Checkpoint Regulator That Promotes T Cell Exhaustion. *Immunity* (2016) 44:1190–203. doi: 10.1016/j.immuni.2016.04.015
10. Carlow DA, Gossens K, Naus S, Veerman KM, Seo W, Ziltener HJ. PSGL-1 Function in Immunity and Steady State Homeostasis. *Immunol Rev* (2009) 230:75–96. doi: 10.1111/j.1600-065X.2009.00797.x
11. Lord GM, Rao RM, Choe H, Sullivan BM, Lichtman AH, Luscinskas FW, et al. T-Bet is Required for Optimal Proinflammatory CD4+ T-Cell Trafficking. *Blood* (2005) 106:3432–9. doi: 10.1182/blood-2005-04-1393
12. DeRogatis JM, Viramontes KM, Neubert EN, Tinoco R. Psgl-1 Immune Checkpoint Inhibition for CD4(+) T Cell Cancer Immunotherapy. *Front Immunol* (2021) 12:636238. doi: 10.3389/fimmu.2021.636238
13. Veerman KM, Williams MJ, Uchimura K, Singer MS, Merzaban JS, Naus S, et al. Interaction of the Selectin Ligand PSGL-1 With Chemokines CCL21 and CCL19 Facilitates Efficient Homing of T Cells to Secondary Lymphoid Organs. *Nat Immunol* (2007) 8:532–9. doi: 10.1038/ni1456
14. Hauser MA, Legler DF. Common and Biased Signaling Pathways of the Chemokine Receptor CCR7 Elicited by Its Ligands CCL19 and CCL21 in Leukocytes. *J Leukoc Biol* (2016) 99:869–82. doi: 10.1189/jlb.2MR0815-380R
15. Johnston RJ, Su LJ, Pinckney J, Critton D, Boyer E, Krishnakumar A, et al. VISTA Is an Acidic pH-Selective Ligand for PSGL-1. *Nature* (2019) 574:565–70. doi: 10.1038/s41586-019-1674-5
16. Wang L, Rubinstein R, Lines JL, Wasiuk A, Ahonen C, Guo Y, et al. VISTA, a Novel Mouse Ig Superfamily Ligand That Negatively Regulates T Cell Responses. *J Exp Med* (2011) 208:577–92. doi: 10.1084/jem.20100619
17. Veerman KM, Carlow DA, Shanina I, Priatel JJ, Horwitz MS, Ziltener HJ. PSGL-1 Regulates the Migration and Proliferation of CD8(+) T Cells Under Homeostatic Conditions. *J Immunol* (2012) 188:1638–46. doi: 10.4049/jimmunol.1103026
18. Yang J, Hirata T, Croce K, Merrill-Skoloff G, Tchernychev B, Williams E, et al. Targeted Gene Disruption Demonstrates That P-Selectin Glycoprotein Ligand 1 (PSGL-1) Is Required for P-Selectin-Mediated But Not E-Selectin-Mediated Neutrophil Rolling and Migration. *J Exp Med* (1999) 190:1769–82. doi: 10.1084/jem.190.12.1769
19. Ahmed R, Salmi A, Butler LD, Chiller JM, Oldstone MB. Selection of Genetic Variants of Lymphocytic Choriomeningitis Virus in Spleens of Persistently Infected Mice. Role in Suppression of Cytotoxic T Lymphocyte Response and Viral Persistence. *J Exp Med* (1984) 160:521–40. doi: 10.1084/jem.160.2.521
20. Borrow P, Evans CF, Oldstone MB. Virus-Induced Immunosuppression: Immune System-Mediated Destruction of Virus-Infected Dendritic Cells Results in Generalized Immune Suppression. *J Virol* (1995) 69:1059–70. doi: 10.1128/jvi.69.2.1059-1070.1995
21. Battegay M, Cooper S, Althage A, Banziger J, Hengartner H, Zinkernagel RM. Quantification of Lymphocytic Choriomeningitis Virus With an Immunological Focus Assay in 24- or 96-Well Plates. *J Virol Methods* (1991) 33:191–8. doi: 10.1016/0166-0934(91)90018-U
22. McDermott DS, Varga SM. Quantifying Antigen-Specific CD4 T Cells During a Viral Infection: CD4 T Cell Responses are Larger Than We Think. *J Immunol* (2011) 187:5568–76. doi: 10.4049/jimmunol.1102104
23. Wherry EJ, Blattman JN, Murali-Krishna K, van der Most R, Ahmed R. Viral Persistence Alters CD8 T-Cell Immunodominance and Tissue Distribution and Results in Distinct Stages of Functional Impairment. *J Virol* (2003) 77:4911–27. doi: 10.1128/JVI.77.8.4911-4927.2003
24. D'Cruz LM, Rubinstein MP, Goldrath AW. Surviving the Crash: Transitioning From Effector to Memory CD8+ T Cell. *Semin Immunol* (2009) 21:92–8. doi: 10.1016/j.smim.2009.02.002
25. Joshi NS, Cui W, Chandele A, Lee HK, Urso DR, Hagman J, et al. Inflammation Directs Memory Precursor and Short-Lived Effector CD8(+) T Cell Fates *Via* the Graded Expression of T-bet Transcription Factor. *Immunity* (2007) 27:281–95. doi: 10.1016/j.immuni.2007.07.010
26. Urzainqui A, Martinez del Hoyo G, Lamana A, de la Fuente H, Barreiro O, Olazabal IM, et al. Functional Role of P-Selectin Glycoprotein Ligand 1/P-Selectin Interaction in the Generation of Tolerogenic Dendritic Cells. *J Immunol* (2007) 179:7457–65. doi: 10.4049/jimmunol.179.11.7457
27. Rochman Y, Spolski R, Leonard WJ. New Insights Into the Regulation of T Cells by Gamma(C) Family Cytokines. *Nat Rev Immunol* (2009) 9:480–90. doi: 10.1038/nri2580
28. David P, Megger DA, Kaiser T, Werner T, Liu J, Chen L, et al. The PD-1/PD-L1 Pathway Affects the Expansion and Function of Cytotoxic Cd8(+) T Cells During an Acute Retroviral Infection. *Front Immunol* (2019) 10:54. doi: 10.3389/fimmu.2019.00054
29. Obar JJ, Lefrancois L. Early Signals During CD8 T Cell Priming Regulate the Generation of Central Memory Cells. *J Immunol* (2010) 185:263–72. doi: 10.4049/jimmunol.1000492
30. Snook JP, Kim C, Williams MA. TCR Signal Strength Controls the Differentiation of CD4(+) Effector and Memory T Cells. *Sci Immunol* (2018) 3 (25):eaas9103. doi: 10.1126/sciimmunol.aas9103
31. Li KP, Ladle BH, Kurtulus S, Sholl A, Shanmuganad S, Hildeman DA. T-Cell Receptor Signal Strength and Epigenetic Control of Bim Predict Memory CD8(+) T-Cell Fate. *Cell Death Differ* (2020) 27:1214–24. doi: 10.1038/s41418-019-0410-x
32. Wei SC, Sharma R, Anang NAS, Levine JH, Zhao Y, Mancuso JJ, et al. Negative Co-stimulation Constrains T Cell Differentiation by Imposing Boundaries on Possible Cell States. *Immunity* (2019) 50:1084–98.e10. doi: 10.1016/j.immuni.2019.03.004


**Conflict of Interest:** The authors declare that the research was conducted in the absence of any commercial or financial relationships that could be construed as a potential conflict of interest.

frontiers in Immunology

REVIEW
published: 20 July 2021
doi: 10.3389/fimmu.2021.715234

# CD8$^+$ T Cell Exhaustion in Cancer

*Joseph S. Dolina, Natalija Van Braeckel-Budimir, Graham D. Thomas and Shahram Salek-Ardakani* *

*Cancer Immunology Discovery, Pfizer, San Diego, CA, United States*

A paradigm shift in the understanding of the exhausted CD8$^+$ T cell ($T_{ex}$) lineage is underway. Originally thought to be a uniform population that progressively loses effector function in response to persistent antigen, single-cell analysis has now revealed that CD8$^+$ $T_{ex}$ is composed of multiple interconnected subpopulations. The heterogeneity within the CD8$^+$ $T_{ex}$ lineage is comprised of immune checkpoint blockade (ICB) permissive and refractory subsets termed stem-like and terminally differentiated cells, respectively. These populations occupy distinct peripheral and intratumoral niches and are characterized by transcriptional processes that govern transitions between cell states. This review presents key findings in the field to construct an updated view of the spatial, transcriptional, and functional heterogeneity of anti-tumoral CD8$^+$ $T_{ex}$. These emerging insights broadly call for (re-)focusing cancer immunotherapies to center on the driver mechanism(s) underlying the CD8$^+$ $T_{ex}$ developmental continuum aimed at stabilizing functional subsets.

**Keywords: T cell exhaustion, PD-1/PD-L1, T cell trafficking, tumor immunity, cancer immunotherapy, CXCR3, co-stimulatory/inhibitory receptors, stem-like CD8+ T cells**

OPEN ACCESS

***Edited by:***
*Vandana Kalia, University of Washington, United States*

***Reviewed by:***
*Sang-Jun Ha, Yonsei University, South Korea*
*Jianxun J. Song, Texas A&M Health Science Center, United States*

***Correspondence:**
*Shahram Salek-Ardakani*
*shahram.salek-ardakani@pfizer.com*

***Specialty section:***
*This article was submitted to Immunological Memory, a section of the journal Frontiers in Immunology*

***Received:*** *26 May 2021*
***Accepted:*** *02 July 2021*
***Published:*** *20 July 2021*

***Citation:***
*Dolina JS, Van Braeckel-Budimir N, Thomas GD and Salek-Ardakani S (2021) CD8$^+$ T Cell Exhaustion in Cancer. Front. Immunol. 12:715234. doi: 10.3389/fimmu.2021.715234*

## INTRODUCTION

T cell exhaustion is a blanket term covering all of the dysfunctional states that exist within antigen-specific CD8$^+$ T lymphocytes as first described in the framework of chronic viral infection, where these cells persist but are unsuccessful in clearing a pathogenic threat (1). Blockade of surface co-inhibitory receptors such as programmed death 1 (PD-1) expressed by CD8$^+$ $T_{ex}$ was shown to reinvigorate cytolytic cell-mediated immune responses leading to the eradication of some persistent viruses (2). Later found in cancer, CD8$^+$ $T_{ex}$ are found to be equally hyporesponsive to anti-tumor immunotherapies (3). Cells expressing PD-1 were thought to be rescued by ICB *via* simple unidirectional reversion from the unresponsive, exhausted state (2). In cancer, this was also believed to involve dysfunctional CD8$^+$ $T_{ex}$ expressing high levels of PD-1, primarily residing in the tumor microenvironment (TME) (3).

Recent advances in single-cell transcriptomics and genome-wide epigenetic profiling comparing normal tissue, peripheral blood, and the lymphoid compartment to tumor parenchyma have challenged this view. New insights have been made regarding the spatial arrangement and heterogeneity of CD8$^+$ $T_{ex}$ and their modulation by ICB (3). We now understand that PD-1 expression is not an absolute measure of cellular dysfunction and senescence. Instead, PD-1 intensity reflects a complex heterogeneity existing within CD8$^+$ $T_{ex}$ (4). Emergent data now casts CD8$^+$ $T_{ex}$ as a developmental continuum, where the lineage is comprised of stem-like PD-1$^{lo}$CD8$^+$ $T_{ex}$ precursors/progenitors that ultimately give rise to terminally dysfunctional PD-1$^{hi}$CD8$^+$ $T_{ex}$ (3). In cancer, these CD8$^+$ $T_{ex}$ subsets appear to be unevenly spread amongst normal peripheral versus tumoral tissues and are differentially responsive to ICB (3).

This review discusses the original works that first identified CD8$^+$ $T_{ex}$ and more contemporary reports describing this population as a developmentally distinct lineage using chronic viral infection. We draw on these data as a basis to further our understanding of CD8$^+$ $T_{ex}$ function during anti-tumor immune responses and elucidate the cellular dynamics and molecular pathways underlying the success and limitations of ICB. Throughout this review, we highlight fundamental knowledge gaps regarding the factors underlying control over CD8$^+$ $T_{ex}$ heterogeneity.

## TRANSLATING CD8$^+$ T CELL EXHAUSTION FROM CHRONIC INFECTION TO CANCER: A COMMON ROLE OF PERSISTENT ANTIGEN

The origin of the term T cell exhaustion goes back to the notable decay of T cell responses first documented in human immunodeficiency virus (HIV)-infected patients (5). It was speculated that viral persistence was linked with loss of function observed in these declining T cell subsets. CD8$^+$ T cell functionality (the ability to rapidly expand after priming, produce effector cytokines and cytolytic molecules, and contract to form memory) characterizes acute recognition of cognate antigen during vaccination or natural, but eventually cleared, viral/bacterial infections (6, 7). Throughout the expansion phase, naïve CD8$^+$ T cells differentiate into short-lived effector cells (SLEC) or memory precursor effector cells (MPEC) (6). Upon contraction and antigen clearance, most SLECs die while MPECs survive to form memory CD8$^+$ T cells for long-term protective immunity (**Figure 1A**) (6, 8). The existence of a CD8$^+$ $T_{ex}$ counterpart to the conventional acute immune response was formally realized at the height of the HIV pandemic when Zinkernagel et al. exposed mice to acute (Armstrong and WE) versus chronic (Clone 13 and DOCILE) strains of lymphocytic choriomeningitis virus (LCMV), a rodent-borne negative-stranded RNA arenavirus (9). In this seminal work, Clone 13 and DOCILE strains persisted in infected mice for greater than 200 days at high inocula while transferred T cell receptor (TCR) transgenic virus-specific CD8$^+$ T cells disappeared or crashed without contraction to memory (9). Initial exposure of select viral strains and doses thus appeared to scale cellular immunity towards protection or completely 'exhausted' the response, as it was coined.

This finding was later examined by two teams [Zajac, Wherry, and Ahmed et al. (10, 11) along with Gallimore and Rammensee et al. (12)] concurrent with the advent of major histocompatibility complex class I (MHC I) tetramer staining technology to track endogenous antigen-specific CD8$^+$ T cells. It was found that initially dominant cytolytic CD8$^+$ T cell responses against LCMV-derived peptides with high MHC I affinity ($NP_{396-404}$ and $GP_{34-42}$) were rapidly deleted, just as Zinkernagel initially observed (9). However, functionally inadequate responses against low/moderate affinity peptides ($GP_{33-41}$ and $GP_{276-286}$) persisted for greater than 60 days post-infection (**Figure 1B**) (10–12). These results showed that constantly elevated viral load and peptide affinity for MHC I strongly correlated with the degree of exhaustion and determined deletion versus persistence of CD8$^+$ $T_{ex}$ (10, 11). Low avidity persisting cells exhibited a hierarchical loss of functionality at relatively low viral loads, which manifested as a dramatic decrease in proliferation, cytotoxicity, and cytokine production (2, 10, 11). Interleukin-2 (IL-2) and tumor necrosis factor (TNF) were lost early, whereas interferon-γ (IFN-γ) production persisted longer after infection (2, 10, 11). At elevated viral doses or with depletion of CD4$^+$ T cell help, these gradual losses of functionality (or dysfunction) resulted in a nearly complete reduction in effector function followed by cell death/deletion (9–11). This process translated to HIV infection and other chronic or latent viral infections in humans, including hepatitis B and C viruses (HBV/HCV), herpes simplex virus (HSV), cytomegalovirus (CMV), human papillomaviruses (HPV), Epstein-Barr virus (EBV), and others (2, 13).

A common feature of chronic viral infection and cancer is that both are prolonged diseases characterized by an overt persistence of antigen (4). CD8$^+$ tumor-infiltrating lymphocytes (TILs) are similarly hyporesponsive as those found during chronic viral infection but are instead caught in an *in vivo* détente against the progressively growing tumor (14). Patient TILs are also tumor antigen-specific and MHC-

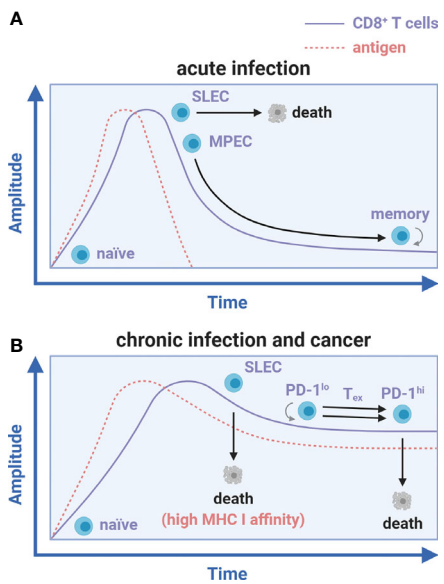


**FIGURE 1** | Antigen load differentially influences CD8$^+$ T cell memory and exhaustion fates. CD8$^+$ T cell differentiation during acute infection versus chronic infection and cancer. **(A)** Activation of naïve CD8$^+$ T cells during acute infection leads to SLEC and MPEC differentiation. Upon antigen clearance, SLECs undergo apoptosis while MPECs survive and differentiate into long-lived, self-renewing memory CD8$^+$ T cells. **(B)** With chronic infection and cancer, SLEC specific to peptides of high MHC I affinity develop and prematurely die while the MPEC subset does not form. Instead of memory formation, CD8$^+$ T cells against peptides of low MHC I affinity expand, exhaust (in a unidirectional PD-1$^{lo}$ to PD-1$^{hi}$ transition), and die in a continued stalemate against persistent antigen.

restricted, supporting the role of chronic antigen persistence in driving T cell exhaustion (15, 16). Importantly, antigen displayed in the TME appears to fully drive CD8+ TIL exhaustion towards completion, whereas the periphery does not, as shown in preclinical models (17, 18). These data imply that the periphery may be an active reservoir of functional precursors to CD8+ $T_{ex}$ (**Figures 2A, B**) before the physical invasion of tumors and chronic exposure to tumor-derived antigen (**Figure 2C**)—a spatial feature distinct from Clone 13 infection. Although persistent antigen plays a significant role in sustaining CD8+ $T_{ex}$ for terminal differentiation in the tumor, other early events in CD8+ T cell activation may also be critical for the initial programming of exhaustion in the periphery or specialized tumor niches, including TCR signal quality/strength (NFAT versus NFAT/AP-1 signaling, discussed below), co-stimulation, IL-2 availability (with associated CD4+ T cell helper signals), and inflammatory cues in the first few divisions (**Figure 3A**) (1, 10, 19–22).

Contemporary studies comparing chronic viral infection to cancer have sought to identify common CD8+ $T_{ex}$ transcriptional signatures. At first glance, both tumor- and chronic virus-specific CD8+ T cells possess significant enrichment of genes related to recent TCR signaling (*Batf*, *Egr2*, *Ezh2*, *Irf4*, *Nfatc1*, *Nfatc2*, *Nr4a1*, *Nr4a2*, and *Nr4a3*) (17, 18, 23–25). This observation reinforces that constant engagement of persistent antigen is a dominant driver of exhaustion. These dominant transcriptional features are notably shared in a direct comparison of CD8+ $T_{ex}$ isolated from HIV-infected and melanoma patients. They can also be recapitulated in CD8+ T cells given repeated cognate peptide stimulations *in vitro* (26, 27). However, significant disparities in CD8+ $T_{ex}$ transcriptional phenotypes also exist between cancer and viral settings. These appear to be unrelated to exhaustion *per se*, where TIL uniquely retain gene ontologies associated with the suppressive TME and are devoid of pathways linked with virally-induced inflammation (3, 18, 28).

## REVERSING T CELL EXHAUSTION: LESSONS LEARNED FROM IMMUNE CHECKPOINT BLOCKADE

The onset of exhaustion coincides with the surface expression of co-inhibitory receptors, which control CD8+ T cell function (2). It has been considered that these immune checkpoints, which include PD-1 (among others), evolved to constrain T cell activation, preventing excessive adverse inflammatory and autoimmune events (29, 30). They also seem to function throughout exhaustion and not merely correlate with loss-of-function, as blocking interactions between PD-1 and its ligand (PD-L1) can restore the function and survival of CD8+ $T_{ex}$ (2, 31). With Clone 13 infection, ICB of PD-(L)1 was initially shown by Barber and Ahmed et al. to reinvigorate CD8+ $T_{ex}$ (31). Importantly, restoration of the response originated from PD-1+CD8+ $T_{ex}$ and not from *de novo* naïve PD-1−CD8+ T cell priming (31). This early study led to the idea that reinvigoration

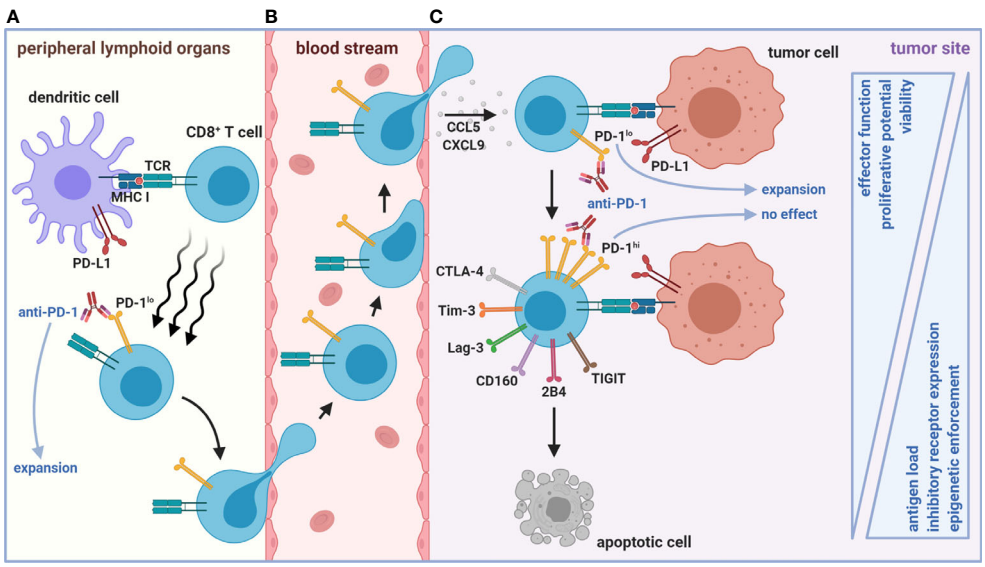


**FIGURE 2** | Spatiotemporal organization of early versus late stages of tumor-mediated CD8+ T cell dysfunction. **(A)** Naïve CD8+ T cell priming against tumor antigen in peripheral LNs (or intratumoral TLS, not depicted) results in the formation of a stem-like PD-1loCD8+ T cell population with self-renewing properties. **(B)** This population represents an active reservoir of cells that can give rise to effector-like PD-1loCD8+ $T_{ex}$ after chemokine-mediated trafficking to and positioning within the TME via CCL5 and CXCL9. **(C)** However, persistent antigen load in the TME eventually forces continued differentiation of these cells into terminally dysfunctional PD-1hiCD8+ $T_{ex}$. The PD-1hi state is accompanied by heightened co-inhibitory receptor expression (including Tim-3, Lag-3, CD160, 2B4, TIGIT, and CTLA-4) and progressive loss of effector functions. Once CD8+ $T_{ex}$ enter a PD-1hi state, epigenetic enforcement prevents de-differentiation back to functional stem-like and effector-like PD-1lo states. Anti-tumoral responses facilitated by ICB (*e.g.*, anti-PD-1) arise from expansion from only lymphoid or intratumoral PD-1loCD8+ $T_{ex}$ subsets. The functionally inferior, ICB-resistant PD-1hiCD8+ $T_{ex}$ fate ultimately culminates in apoptosis.

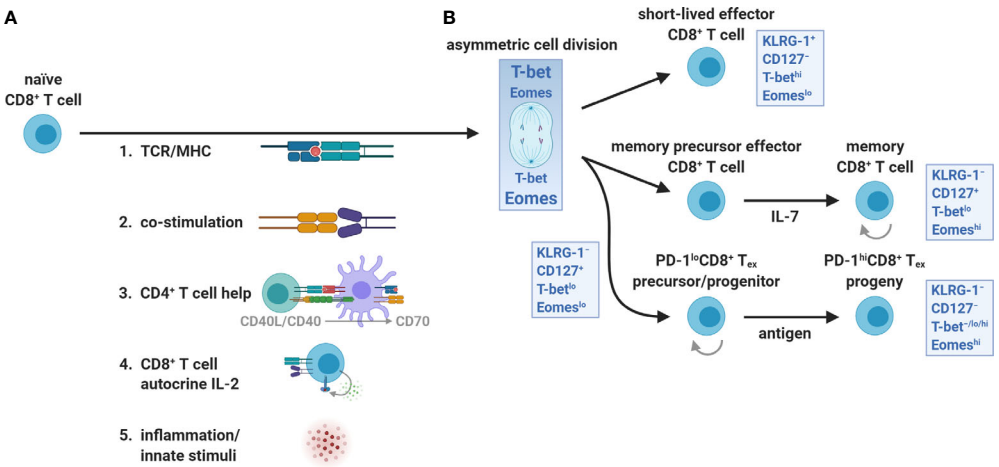


**FIGURE 3** | T-bet and Eomes partitioning during CD8+ T cell priming and expansion. **(A)** The orientation and strength of TCR/MHC ligation, co-stimulation (*e.g.*, CD28 interaction with CD80 and CD86), CD4+ T cell help (CD40L/CD40 licensing of DCs including up-regulation of MHC I, CD80/CD86, CD70, and third signal cytokines), autocrine IL-2 exposure, and innate inflammatory stimuli (danger- and pathogen-associated molecular patterns) all influence the activation, survival, and differentiation of naïve CD8+ T cells. **(B)** CD8+ T cells integrate these input events at priming and during the first division. The uneven partitioning of T-bet and Eomes favors SLEC (effector) versus MPEC (memory) differentiation early after activation, respectively. In contrast, the CD8+ $T_{ex}$ lineage requires both transcription factors and retains some features of memory cells including self-renewal of PD-$1^{lo}$ subsets and expression of memory-associated transcription factors and survival molecules. The reliance on homeostatic cytokines (predominantly IL-7) versus persistent antigen for development and self-renewal distinguishes memory from PD-$1^{lo/hi}$ exhaustion lineages, respectively.

of CD8+ $T_{ex}$ was practically synonymous with 'reversal' of exhaustion. At this time, ICB was rapidly advanced into the clinic and established a new paradigm for cancer treatment, leading to durable responses in a limited set of patients (32, 33). Despite its early success and first recordings of tails in long-term endpoint survival curves, the mechanism of action behind ICB remained elusive.

Blackburn and Wherry et al. uncovered an underlying complexity within the presumed homogenous PD-$1^{+}$CD8+ $T_{ex}$, where this population could be further separated into PD-$1^{lo}$ and PD-$1^{hi}$ subsets (34). A hypothesis emerged from this that proposed PD-$1^{lo}$ cells differentiate into the PD-$1^{hi}$ subset as CD8+ T cells exhaust. Inherent in this theory, reinvigoration did not equate to the reversal of exhaustion (herein defined as a PD-$1^{hi}$ to PD-$1^{lo/-}$ transition). Beneficial responses rather arose solely from the mobilization of less exhausted, permissive PD-$1^{lo}$ cells instead of PD-$1^{hi}$ terminally exhausted counterparts. After transferring day 30 Clone 13-generated PD-$1^{lo}$ and PD-$1^{hi}$ sorted cells into naïve mice subsequently re-challenged with Clone 13 in the presence or absence of anti-PD-L1, Blackburn and Wherry et al. showed that only PD-$1^{lo}$CD8+ $T_{ex}$ could proliferate in response to ICB (34). Similar transfer experiments also revealed that PD-$1^{lo}$CD8+ $T_{ex}$ were more effective at controlling viral load and remained less apoptotic compared to PD-$1^{hi}$CD8+ $T_{ex}$ (34). The PD-$1^{hi}$ subset was later associated with expression of additional co-inhibitory receptors, including T cell immunoglobulin domain and mucin domain protein 3 (Tim-3), lymphocyte activation gene 3 (Lag-3), natural killer cell receptor BY55 (CD160), signaling lymphocytic activation molecule 4 (2B4), cytotoxic T-lymphocyte-associated protein 4 (CTLA-4), and T cell immunoreceptor with immunoglobulin and ITIM domains (TIGIT), where cells having heightened co-expression appeared more exhausted (**Figure 2C**) (24, 35–38).

## DAWN OF STEM-LIKE PRECURSORS AND PROGENITORS OF EXHAUSTED CD8+ T CELLS

It also became apparent that heterogeneity existed at a deeper level than surface PD-1, where CD8+ $T_{ex}$ appeared to use the same T-box family transcription factors, T-box expressed in T cells (T-bet) and eomesodermin (Eomes), for SLEC and MPEC lineage commitment, respectively, but with different expression patterns, nuclear localization, and developmental connectivity (4, 39–41). In response to TCR/MHC ligation and orientation of the immune synapse, a naïve CD8+ T cell will asymmetrically divide and unequally partition T-bet and Eomes, separately dictating effector versus memory fates from the first division (22, 42–45). Distinct from SLECs and MPECs, T-bet and Eomes were shown to be dually required for CD8+ $T_{ex}$ development (41). In addition, these transcription factors appeared to arise at different stages of CD8+ $T_{ex}$, where PD-$1^{lo}$T-bet$^{lo}$CD8+ $T_{ex}$ were found to increase Eomes expression and sustain its nuclear localization, divide, and differentiate into PD-$1^{hi}$T-bet$^{-/lo/hi}$ Eomes$^{hi}$CD8+ $T_{ex}$ (**Figures 3B** and **4A**) (40, 41, 46). This differential usage of T-bet and Eomes also suggested that CD8+ $T_{ex}$ was a distinct lineage.

Ahmed et al., therefore, reexamined the Clone 13 model and the underlying CD8+ $T_{ex}$ transcriptional heterogeneity at the

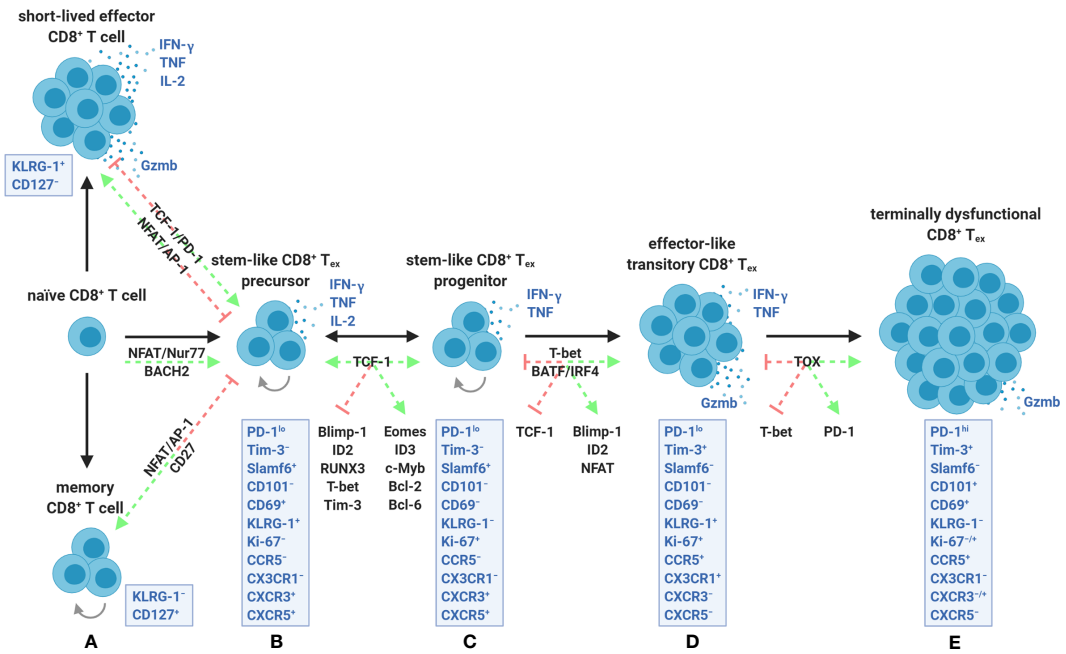


**FIGURE 4** | The CD8$^+$ T cell exhaustion lineage is comprised of a continuum of transcriptionally and epigenetically controlled states. **(A)** Activation of naïve CD8$^+$ T cells for SLEC and MPEC/memory differentiation is optimally driven by transcription factors such as NFAT/AP-1 and sufficient co-stimulation (*e.g.*, CD27). Early development of stem-like CD8$^+$ $T_{ex}$ precursors instead involves partnerless NFAT, lack of co-stimulation/help, constant Nur77 activity, and/or strict dependence on BACH2. These events appear to be stabilized by TCF-1 activity and PD-1 dampening of chronic TCR ligation. **(B, C)** TCF-1 further supports stemness (ability to survive, self-renew, and proliferate) by promoting Eomes, ID3, c-Myb, Bcl-2, and Bcl-6 expression while antagonizing effector-associated transcription factors including Blimp-1, ID2, RUNX3, and T-bet. Stem-like CD8$^+$ $T_{ex}$ precursors **(B)** and progenitors **(C)** are collectively marked by a PD-1$^{lo}$Tim-3$^-$Slamf6$^+$ surface profile and varied expression of CXCR3 and CXCR5 in specific tumor settings. Although equally stabilized by TCF-1, precursors can be distinguished from progenitors as being quiescent, LN-resident, less reliant on antigen, and having a CD69$^+$KLRG-1$^+$Ki-67$^-$ profile. **(C, D)** TCF-1 down-regulation coupled with ongoing exposure to persistent antigen drives constant BATF and IRF4 signaling (which positively feedback on partnerless NFAT activity) and T-bet expression. T-bet additionally overrides a TCF-1 memory-like program by supporting Blimp-1 and ID2 activity leading to an effector-like transitory PD-1$^{lo}$Tim-3$^+$ state marked by initiation of granzyme B production. **(D, E)** Continued NFAT activity ultimately leads to TOX upregulation within this subpopulation, which epigenetically enforces terminal exhaustion, inhibits T-bet-mediated effector programming, and promotes heightened PD-1 expression. Transitory cells **(D)** are discriminated from terminally dysfunctional cells **(E)** by a PD-1$^{lo}$Tim-3$^+$CD101$^-$KLRG-1$^+$CX3CR1$^+$ surface phenotype, remnant IFN-γ and TNF production, and having high proliferative potential. Terminally dysfunctional PD-1$^{hi}$Tim-3$^+$CD8$^+$ $T_{ex}$ co-express multiple co-inhibitory receptors (not depicted), cannot proliferate, have diminished polyfunctionality, but retain granzyme-based cytolytic potential. PD-1$^{lo}$ precursors, progenitors, and transitory CD8$^+$ $T_{ex}$ subpopulations are amenable to ICB **(B–D)**, whereas terminally dysfunctional PD-1$^{hi}$CD8$^+$ $T_{ex}$ are not **(E)**. Precursors and progenitors may interconvert, whereas differentiation into transitory and terminally dysfunctional subsets is unidirectional.

core of the PD-1$^{lo/hi}$ dichotomy (47). Transcriptional analyses of the PD-1$^{lo}$ population revealed an association with *Icos* (inducible T cell co-stimulator; ICOS), *Cxcr5* (C-X-C motif chemokine receptor 5; CXCR5), *Bcl6* (B cell lymphoma 6; Bcl-6), and *Tcf7* (T cell factor 1; TCF-1) expression reminiscent of CD4$^+$ T follicular helper cells ($T_{fh}$), which is why CD8$^+$ $T_{ex}$ are sometimes referred to as $T_{fh}$-like (47, 48). TCF-1 acts as the main transcription factor downstream of Notch receptors as part of the evolutionarily conserved Wnt signaling pathway, known to be critical for T cell thymic development and memory formation (49). TCF-1, together with forkhead box protein O1 (FOXO1), promotes stemness in CD8$^+$ T cells by inhibiting expression of effector-associated genes including *Prdm1* (B lymphocyte-induced maturation protein-1; Blimp-1), *Runx3* (Runt-related transcription factor 3; RUNX3), *Id2* (inhibitor of DNA binding 2; ID2) and *Tbx21* (T-bet) and favoring central memory by promoting *Eomes* and *Bcl6* expression (50, 51). Blimp-1, in particular, is known to act as a rheostat balancing the promotion of cytolytic granzyme B production and terminal dysfunction in CD8$^+$ $T_{ex}$—events directly countered by TCF-1 (**Figures 4B, C**) (49, 51, 52). Other associations of PD-1$^{lo}$CD8$^+$ $T_{ex}$ with the high affinity IL-7 receptor chain (IL-7Rα), L-selectin (CD62L), and mitochondrial β-oxidation (fatty acid metabolism) pathway enrichment suggested shared common features with self-renewing CD8$^+$ T memory precursors (47). Moreover, PD-1$^{hi}$Tim-3$^+$CD8$^+$ $T_{ex}$ did not produce effector cytokines but did retain cytolytic *Gzma* (granzyme A), *Gzmb* (granzyme B), and *Prf1* (perforin) expression (47, 53, 54). Sorting and transferring PD-1$^{lo/hi}$ subsets into infection-matched hosts based upon CXCR5 positivity validated that PD-1$^{lo}$Tim-3$^-$CXCR5$^+$CD8$^+$ $T_{ex}$ marked a self-renewing population that gave rise to PD-1$^{hi}$Tim-3$^+$CXCR5$^-$CD8$^+$ $T_{ex}$ (47). Further and

more critical, anti-PD-L1 blockade triggered a proliferative burst only within the stem-like PD-1$^{lo}$Tim-3$^{-}$ subset and facilitated transitions to the treatment-refractory PD-1$^{hi}$Tim-3$^{+}$ fate (47).

Since TCF-1 expression was generally known to maintain stemness in hematopoietic stem cells, its role in the PD-1$^{lo/hi}$ $T_{ex}$ progenitor/progeny relationship was determined (47). In *Tcf7*$^{-/-}$ mice, PD-1$^{lo}$CD8$^{+}$ $T_{ex}$ fail to develop and cannot seed the exhaustion lineage (47). In contrast, transgenic overexpression of *Tcf7* was found to stabilize PD-1$^{lo}$ stem-like cells and lead to more durable CD8$^{+}$ T cell responses during Clone 13 infection and within the B16-GP$_{33-41}$ melanoma models, implicating TCF-1 as a critical factor for the inception of $T_{ex}$ (55). TCF-1 was later shown to support the expression of *Id3* (ID3), *Eomes*, *Myb* (transcriptional activator Myb; c-Myb), and *Bcl2* (Bcl-2), allowing PD-1$^{lo}$CD8$^{+}$ $T_{ex}$ to survive negative downstream signals from PD-1 early after priming (**Figures 4B, C**) (56, 57).

The factors governing the expression of TCF-1 within stem-like PD-1$^{lo}$CD8$^{+}$ $T_{ex}$ have only recently been investigated. During chronic DOCILE infection of mice, the amount of antigen but not inflammation rapidly promotes the formation of the TCF-1$^{+}$ population (57). Inconsistent with the need for chronic antigen during its establishment, some elements of the exhaustion program (maintenance of a PD-1$^{hi}$ dysfunctional profile) were paradoxically shown to be stable after CD8$^{+}$ $T_{ex}$ transfer to antigen-free conditions (58). This suggests that the CD8$^{+}$ $T_{ex}$ lineage has some component(s) shared with memory CD8$^{+}$ T cells, including slow homeostatic self-renewal by IL-7 and IL-15 (4, 58). In support of this, GP$_{33-41}$-specific CD8$^{+}$ T cells deficient in BACH2 (a transcription factor that promotes memory cell development by limiting TCR-mediated transcriptional changes) fail to form any stem-like PD-1$^{lo}$TCF-1$^{+}$CD8$^{+}$ $T_{ex}$ (57, 59). Conversely, the progression of the stem/memory-like PD-1$^{lo}$TCF-1$^{+}$ state to the TCF-1$^{-}$PD-1$^{hi}$ terminally exhausted fate is halted by deleting BATF and IRF4 (two transcription factors linked with constant TCR signaling and known to destabilize TCF-1) (**Figures 4C, D**) (25, 57). Therefore, T cell-intrinsic TCF-1 expression appears to rely on a low but brief TCR signaling threshold compromised by ongoing antigenic exposure.

Other studies have oppositely shown that PD-1$^{hi}$CD8$^{+}$ $T_{ex}$ generated from Clone 13 infection are less stable without antigen, where these cells inevitably decline and cannot mount a recall response (21, 60). Discrepancies regarding CD8$^{+}$ $T_{ex}$ stability in the presence/absence of antigen may be due to the frequency and quality of TCF-1$^{+}$ stem-like cells at hand. A unified atlas of 12 studies spanning cancer and chronic viral infection has recently revealed that bifurcation of memory commitment from a dysfunctional program occurs early (in less than 7 days following antigen encounter) (61). With preclinical cancer models, the time of initial antigen encounter is less controlled for compared to viral infection. Nevertheless, it has been shown that PD-1$^{lo}$CD8$^{+}$ TIL removed early after tumor injection (likely containing an increased frequency of TCF-1$^{+}$ cells) followed by transfer into naïve hosts and infection with *Listeria monocytogenes* 3-4 weeks later can mount a memory response whereas fully exhausted PD-1$^{hi}$CD8$^{+}$ TIL isolated at later time points cannot (18). In addition, stem-like PD-1$^{lo}$TCF-1$^{+}$CD8$^{+}$ $T_{ex}$ can be divided into CD69$^{+}$Ki-67$^{-}$ precursor cell and CD69$^{-}$Ki-67$^{+}$ progenitor cell subsets (and are thus differentiated as such in this review) (**Figures 4B, C**) (46). Precursors are lymph node (LN)-resident, speculated to depend less on antigen for a low baseline level of proliferation, and remain quiescent compared to a circulating progenitor pool (46). In healthy human subjects, TCF-1$^{+}$ precursors specific to common chronic diseases such as latent EBV and CMV were shown to be present in the periphery and co-express PD-1, TIGIT, and granzyme K (62). These precursors are also embedded within steady-state stem-like/central memory CD8$^{+}$ T cell populations traditionally defined as CCR7$^{+}$CD45RO$^{+/-}$CD95$^{+}$ (62). Yet, no known mediator has been identified to date which controls functional memory versus stem-like PD-1$^{lo}$CD8$^{+}$ $T_{ex}$ precursor differentiation (**Figures 4A, B**) (62). Precursors and progenitors have also been documented to reside in TIL fractions of murine B16 tumors and human melanoma (46). However, it remains to be determined if these small populations are biased in tumor versus LN organization and if CD69 positivity/negativity within the bulk TCF-1$^{+}$PD-1$^{lo}$ population determines true stemness and reactivity to ICB and/or antigen.

## TRANSCRIPTIONAL AND EPIGENETIC EVENTS CRITICAL FOR THE ESTABLISHMENT OF TERMINAL EXHAUSTION

Complementing these approaches, total CD8$^{+}$ $T_{ex}$ were shown to possess a fixed chromatin state distinct from effector and memory cells by ~6,000 open chroman regions before or after exposure to anti-PD-L1 (21, 63, 64). This reinforces that terminal CD8$^{+}$ $T_{ex}$ represents a distinct lineage unable to differentiate into *bona fide* memory cells. Second, ICB-mobilized stem/effector-like PD-1$^{lo}$ populations themselves exhaust and eventually mirror pre-treatment PD-1$^{hi}$CD8$^{+}$ $T_{ex}$. The unique epigenetic signature of CD8$^{+}$ $T_{ex}$ in Clone 13-infected mice was also shown to be conserved in HIV-infected and melanoma patients (26, 63). Although both acutely activated CD8$^{+}$ T cells and CD8$^{+}$ $T_{ex}$ generally express PD-1, assay for transposase-accessible chromatin sequencing (ATAC-Seq) distinguishes these populations, with CD8$^{+}$ $T_{ex}$ possessing many unique features, including *de novo* accessibility of the region at −22.4 kb upstream of the murine *Pdcd1* (PD-1) locus containing a *Nr4a1* (Nur77) binding motif (17, 63).

Downstream from TCF-1-mediated subsistence of PD-1$^{lo}$CD8$^{+}$ $T_{ex}$, thymocyte selection-associated high-mobility group (HMG) box protein, TOX, becomes co-upregulated alongside PD-1 and is associated with the epigenetic signatures demarcating terminal lineage commitment within PD-1$^{hi}$CD8$^{+}$ $T_{ex}$ (24, 56, 65–67). TOX is a nuclear protein that binds DNA in a structure-dependent manner (not sequence-dependent) (64). TOX directly interacts with histone acetyltransferase binding to ORC1 (HBO1) and indirectly coordinates activity with DNA

methyltransferases 3A (DNMT3A), 3B (DNMT3B), and enhancer of zeste homolog 2 (EZH2) to epigenetically fix $CD8^+$ $T_{ex}$ towards terminal exhaustion (64). Ectopic TOX expression is sufficient to induce a full exhaustion transcriptional program in effector $CD8^+$ T cells *in vitro* (65). In contrast, deletion of *Tox* in $CD8^+$ TIL prevents exhaustion *via* decreased chromatin accessibility and expression of *Pdcd1*, *Havcr2* (Tim-3), *Cd244* (2B4), and *Tigit* (TIGIT) in the SV40-Tag-driven autochthonous liver cancer model (65). In the Clone 13 system, $Tcf7^{flox/flox}Cd4^{cre}$ and $Tox^{flox/flox}Cd4^{cre}$ mice (lacking TCF-1 and TOX in all T cells, respectively) results in favored development of effector-like KLRG-$1^+CD8^+$ T cells over the formation of PD-$1^{hi}CD8^+$ $T_{ex}$ (**Figures 4A, D**) (24, 57, 68).

Recent findings by Ahmed (69) and Wherry (46) jointly demonstrate that stem-like cells are initially stable during Clone 13 infection. However, upon ICB treatment, these cells rapidly enter a T-bet-driven effector-like transitory state marked as $CX3CR1^+$KLRG-$1^+CD101^-$PD-$1^{lo}$Tim-$3^+$ (**Figure 4D**), which rapidly proliferate, temporarily produce granzyme B, and eventually digress to fully exhausted $CX3CR1^-$KLRG-$1^-CD101^+$PD-$1^{hi}$Tim-$3^+CD8^+$ $T_{ex}$ (**Figure 4E**) (46, 69). CD101 is not expressed at baseline in $CD8^+$ T cells from healthy humans (70). Conversely, terminally differentiated $CD101^+$PD-$1^{hi}CD8^+$ $T_{ex}$ have recently been observed to correlate negatively with tumor grade and regional LN metastasis within epithelial ovarian cancer patients (70). Transcriptional analyses of murine and human TIL corroborate these results linking changes in naïve-like PD-$1^-$Tim-$3^-CD8^+$ TIL before and after ICB (71). ICB appears to bifurcate PD-$1^-$Tim-$3^-CD8^+$ TIL into a self-renewing stem-like state (expressing *Tcf7*, *Lef1*, and *Sell*) and an effector-like program (expressing *Klrg1*, *Cx3cr1*, *Slamf7*, and *Ifng*) farther downstream along a developmental trajectory to full exhaustion (71). These phenotypic changes (stem-like > effector-like transitory > terminal exhaustion) coincide with chromatin accessibility shifts controlled by multiple transcription factors including NFAT, Nur77, BATF, IRF4, TCF-1, T-bet, and TOX that appear to be coordinated with PD-1-mediated TCR dampening (**Figures 4A–E**) (25, 46, 69, 72). In other words, $CD8^+$ $T_{ex}$ seem to represent a lineage with limited differentiation capacity, existing within a series of fixed sequential epigenetic landscapes. Although reinvigoration of PD-$1^{lo}CD8^+$ $T_{ex}$ can result in a detectable wave of transcriptionally 're-wired' effector-like activity, the cells appear to be limited because they eventually exhaust in response to ICB and are unable to de-differentiate into *bona fide* effector or memory cells present during acute infection (21, 46, 63). In the context of tumor immunity, understanding where these transitions occur *in vivo* (LN versus TME) and how to stabilize the transitory effector-like state is key to maximizing the cytolytic potential of stem-like $CD8^+$ $T_{ex}$.

What governs late-stage cell fate decisions of stem-like PD-$1^{lo}CD8^+$ $T_{ex}$ progenitors to commit to a terminally exhausted PD-$1^{hi}CD8^+$ $T_{ex}$ fate is partially clear at best. Constant TCR signaling is likely involved as enforced nuclear factor of activated T cells (NFAT) activity in antigen-specific $CD8^+$ T cells directly leads to *Tox* transcription (20, 24). Conversely, lack of *Nfatc1* (NFAT2) phenocopies loss of TOX (24). Further, TCR-responsive transcription factors, including BATF and IRF4, appear to positively feedback on *Nfatc1* transcription promoting PD-$1^{hi}$Tim-$3^+$ $T_{ex}$ development (25). In contrast to NFAT1, NFAT2 itself is also known to favor the development of MPECs over SLECs (73). Imbalanced NFAT1 versus NFAT2 may also relate to skewing early T-bet and Eomes segregation in a primed $CD8^+$ T cell to seed TCF-$1^+$ stem-like progenitors even before ongoing direct downstream effects on TOX, and other exhaustion-associated genes are enforced. At a higher level, the overall balance between NFAT and CD28/AP-1 activity upon original and/or continued antigen encounter may be critical as anergic $CD8^+$ T cells and $CD8^+$ T cells primed in the absence of $CD4^+$ T cell help or co-stimulation mirror many of the major transcriptional and epigenetic events that occur in PD-$1^{lo/hi}CD8^+$ $T_{ex}$ in both chronic viral infection and cancer (19, 20, 26, 66, 74–80). Exposure to microenvironmental stressors (low glucose, high lipid) in the TME may also orchestrate the TOX-centric epigenetic program that characterizes the PD-$1^{hi}$ dysfunctional phenotype by disrupting metabolic/mitochondrial fitness (81–83). Mitochondria tend to produce elevated amounts of reactive oxygen species (ROS) in $CD8^+$ $T_{ex}$, which was shown to facilitate nuclear entry of NFAT downstream of a $Ca^{++}$ flux in both $CD4^+$ and $CD8^+$ T cells (81–84). How constant PD-1 signaling, TCR engagement, and altered metabolism control the transition from a TCF-$1^+$ to $TOX^+$ state *via* constant NFAT activity in $CD8^+$ $T_{ex}$ is an area where current knowledge is limited and is only starting to be investigated.

## THERAPEUTIC POTENTIAL OF $CD8^+$ T CELL PROGENITORS IN CANCER

The significance of stem-like TCF-$1^+$PD-$1^{lo}CD8^+$ $T_{ex}$ in governing ICB outcomes may lie in their pre-treatment frequency and crosstalk between other immune cell types during cancer. Surveys of TIL heterogeneity using single-cell RNA sequencing (scRNA-Seq) have indicated that activated, expanded, and exhausted $CD8^+$ T cell subsets are variably present in different tumor samples and effectively cluster based on *Tcf7* expression (53, 85). For instance, Sade-Feldman et al. profiled 48 metastatic melanoma tumor biopsies, comprising 17 responder and 31 non-responder patients receiving ICB (85). scRNA-Seq phenotyping of $CD8^+$ T cell clusters identified 6 clusters that were putatively annotated as belonging to early-activated, memory, effector, and exhausted lineages based upon cell surface marker expression profiles (85). All $CD8^+$ T cell populations were observed in most patients, albeit to differing degrees (85). However, the relative frequency of intratumoral $Tcf7^{hi}$ versus $Tcf7^{lo}$ TIL clusters was predictive of patient responsiveness to ICB (85). It has since then been confirmed in preclinical models that small populations of stem-like PD-$1^{lo}$Slamf6$^+$TCF-$1^+CD8^+$ $T_{ex}$ (with Slamf6 being a surrogate for TCF-1) and PD-$1^{hi}TOX^+CD8^+$ $T_{ex}$ indeed exist in the TME (86). In murine B16 melanoma, TILs retained some features of the

epigenetic profile seen in $CD8^+$ $T_{ex}$ following Clone 13 infection, and anti-PD-1 treatment specifically drove stem-like PD-$1^{lo}$ TILs to divide and convert into terminally exhausted PD-$1^{hi}$ $T_{ex}$ (86). In humans, stem-like TCF-$1^+CD8^+$ $T_{ex}$ progenitors and terminally exhausted TCF-$1^-CD8^+$ $T_{ex}$ have similarly been observed in multiple tumor indications (71, 86, 87).

As noted, Ahmed initially found that stem-like PD-$1^{lo}CD8^+$ $T_{ex}$ express CXCR5; however, these cells co-express high amounts of *Ccr7* transcripts, migrate in response to a CCL19/21 gradient *in vitro*, and localize to the splenic T cell zone *in vivo* after Clone 13 infection (47). In this system, CXCR5 is expressed by both stem-like $CD69^+$Ki-$67^-$ precursors and $CD69^-$Ki-$67^+$ progenitors (46). The function of CXCR5 is less well known in cancer immunology but may relate to stem-like $CD8^+$ $T_{ex}$ positioning. Stem-like PD-$1^{lo}CD8^+$ TILs have been found to sporadically express CXCR5 depending on the tumor type (86, 88). In murine and human melanomas, CXCR5 positivity has thus far not tracked with stem-like PD-$1^{lo}CD8^+$ TIL (86). In contrast, $CXCR5^+$ TILs can be found in non-small-cell lung carcinoma (NSCLC) tumors and may uniquely associate with intratumoral tertiary lymphoid structures (TLS) (88). More work is needed to understand any potential association between $CXCR5^+$ TILs and tumoral TLS. It is tempting to speculate that CXCR5 facilitates localization within these structures, similar to the role of CXCR5 in positioning $CD4^+$ $T_{fh}$ within secondary LNs (48). While only a minority of intratumoral stem-like cells express CXCR5, TCF-$1^+$PD-$1^{lo}CD8^+$ $T_{ex}$ also seem to localize as crude clusters in the TME, implying that there may be additional niche microenvironments within the tumor that support anti-tumor immunity (87). In a histological analysis of prostate, bladder, and kidney cancer biopsies, TCF-$1^+CD8^+$ TILs were predominantly observed within MHC II dense regions, whereas the presumably exhausted TCF-$1^-CD8^+$ TIL appeared to be dispersed (87). Little is known about the role of these MHC II dense niches, which may influence stem-like T cell recruitment and/or dendritic cell (DC) Wnt signaling, thereby maintaining TCF-1 expression and stemness. Stem-like PD-$1^{lo}CD8^+$ $T_{ex}$ are also preferentially found within tumor-draining secondary LNs over non-draining LNs (89). In contrast, terminally exhausted PD-$1^{hi}CD8^+$ $T_{ex}$ are predominantly confined to the TME (89). Regardless, if TCF-$1^+$PD-$1^{lo}CD8^+$ $T_{ex}$ infiltrate or expand locally within tumors after systemic delivery of ICB, the intratumoral frequency of these cells can serve as a valuable biomarker to discriminate responders against non-responders (and/or survival within the responder cohort) (85, 90).

## TISSUE DISTRIBUTION AND INTRATUMORAL POSITIONING OF EXHAUSTED $CD8^+$ T CELLS

Tumor PD-L1 expression would logically seem to be a relevant prognostic factor to rationalize the usage of PD-(L)1-based ICB. PD-$L1^+$ tumors tend to respond more frequently to anti-PD-(L)1; however, there is only a weak correlation with overall treatment efficacy (33, 91, 92). A significant number of PD-$L1^+$ tumors do not respond to ICB, and durable responses are observed in PD-$L1^-$ tumors (33, 91). In other analyses, ICB was found to closely align with the raw amount of neoantigens broadly amongst cancers regardless of PD-L1 expression (91, 93–95). Following the completion of The Cancer Genome Atlas (TCGA), a strong correlation was observed between ICB-responsiveness and a $T_h1$/IFN-γ inflammatory signature, tumor mutational burden (TMB), and leukocyte infiltration (96). Thus, a combination of a T cell-inflamed gene signature with TMB may currently be the best predictor of ICB-responsiveness (91). PD-L1 expression in the tumor (known to be upregulated by IFN-γ) may reflect tumor inflammation status and thus rather passively indicate an overall immune system status rather than mechanistically predict the response of the tumor to ICB (91).

If inflammation and TMB underlie the response, does ICB act directly in the TME or periphery (97)? Immuno-positron emission tomography (immuno-PET) coupled with blockade of LN egress shows a large portion of effector-like $CD8^+$ TIL are derived from the periphery in mice bearing MC38 colorectal tumors systemically treated with anti-PD-1 (98). In the AC29 mesothelioma preclinical model, blockade of LN egress likewise severely compromises the number of $CD8^+$ TIL after systemic anti-PD-L1 (89). In the absence of ICB and irrespective of primary tumor PD-L1 expression, enhanced PD-1/PD-L1 contacts between stem-like PD-$1^{lo}CD8^+$ $T_{ex}$ and migratory PD-$L1^+$ DCs entering the paracortex of tumor-draining LNs negatively correlates with survival of mice exposed to AC29 tumors and non-metastatic melanoma patients following resection (89). Localized delivery of anti-PD-L1 to tumor-draining LNs is sufficient to block these interactions and mobilize stem-like $CD8^+$ $T_{ex}$ from the lymphatics for proliferation, migration to the TME, and preservation of stemness, leading to an increase in host survival comparable to systemic delivery (89). Further, LN-primed $CD8^+$ $T_{ex}$ seem better able to respond to model antigen and proliferate upon *ex vivo* re-stimulation than systemically primed cells (89). These data suggest that LN-primed stem-like $CD8^+$ $T_{ex}$ are a critical component of the response to ICB.

Additional studies involving scRNA/TCR-Seq have allowed a more in-depth look at the intratumoral versus peripheral counterparts of immune responses underlying ICB in patients. In a study by Yost et al., scRNA/TCR-Seq analysis of metastatic basal/squamous cell carcinoma patient TIL before and after ICB indicated that clonal replacement dominated the response where upwards of 84% of $CD8^+$ T cell clonotypes (having a single TCR specificity) present after treatment were novel (*i.e.*, not present in the tumor before treatment) (72). Intratumoral stem-like TCF-$1^+CD8^+$ $T_{ex}$ did contribute a minor fraction to the population of ICB-activated, tumoricidal clonotypes; however, all cells that attacked tumors again eventually became exhausted (72). Therefore, ICB seems to predominantly mobilize functional $CD8^+$ T cells from the periphery into the tumor. A comparison of tumors to normal adjacent tissue (NAT) and peripheral blood *via* scTCR-Seq corroborated these findings across various cancers (99). Patients displaying extratumoral-intratumoral linked clonal expansion across blood/NAT and tumor responded more favorably to ICB (99). However, the action of

ICB on stem-like or effector like CD8$^+$ $T_{ex}$ inside the tumor cannot be dismissed. Despite the lack of a significant correlation between intratumoral PD-L1 expression and survival, PD-1/PD-L1 interactions in the tumor as measured by immune-Förster resonance energy transfer (iFRET) is more predictive of survival in metastatic melanoma and NSCLC patients receiving ICB, in line with findings in draining LNs (89, 100).

Emergent data suggest that the CCR5 and CXCR3 chemokine receptor pathways are needed for anti-PD-(L)1-mediated CD8$^+$ $T_{ex}$ tumor recruitment and/or intratumoral positioning (101–104). Heightened dual expression of the ligands for CCR5 and CXCR3 (CCL5 and CXCL9, respectively) positively correlates with the amount of tumor *CD8a* transcripts and patient survival in cancers of the ovary, breast, lung, colon, as well as melanoma (103). CCL5 from tumor cells or tumor-associated myeloid cells appears to license CXCL9 production almost exclusively from inflammatory CD68$^+$ macrophages and CD11c$^+$ DCs within the TME (98, 103, 105, 106). Genetic deletion or antibody-mediated blockade of either CCL5 and CXCL9 significantly compromises CD8$^+$ T cell recruitment to the TME; however, only CXCL9 correlates with ICB efficacy in multiple preclinical models (102–105). Revisiting CD8$^+$ $T_{ex}$ CCR5 and CXCR3 progenitor/progeny expression patterns in the Clone 13 and preclinical tumor models may clarify this. In both settings, CXCR3 is predominantly expressed on stem-like PD-1$^{lo}$CD8$^+$ $T_{ex}$ (**Figures 4B, C**), whereas CCR5 is oppositely elevated on terminally exhausted PD-1$^{hi}$CD8$^+$ $T_{ex}$ (**Figure 4E**) (46, 69, 102). These axes may be necessary for the positioning and stability of stem-like PD-1$^{lo}$CD8$^+$ $T_{ex}$ in the previously mentioned intratumoral MHC II dense clusters by undescribed mechanisms or serve as markers for recent PD-1$^{lo}$ versus PD-1$^{hi}$CD8$^+$ $T_{ex}$ CXCR3-mediated trafficking (87, 107, 108). With LN egress blocked, anti-PD-1 was shown to directly increase the expansion of intratumoral wild type but not *Cxcr3*$^{-/-}$ CD8$^+$ T cells, which may be related to localization of these cells within the TME or intrinsic effects (102). CXCR3 itself is known to support T-bet expression and favor SLEC differentiation during acute infection and may play a direct role in dictating stem-like to transitory CD8$^+$ $T_{ex}$ differentiation (109, 110). Therapies centered on CXCR3 agonism may augment CD8$^+$ T cell trafficking, positioning, and priming/expansion depending on the exact intersection with the $T_{ex}$ lineage.

## CLINICAL PERSPECTIVES

Despite the undisputed success of ICB in the clinic, it may one day be replaced or combined with other immunotherapies due to its inherent failure in preventing exhaustion. Our increasingly granular understanding of CD8$^+$ $T_{ex}$ and the underlying regulatory mechanisms may present novel therapeutic avenues that include alternative ways to stimulate and stabilize stem/effector-like states along the exhaustion continuum or enhance memory cell lineage commitment. Simple amplification of CD8$^+$ T cell responses by modulating trafficking and tumor positioning may stabilize stem-like and effector-like transitory CD8$^+$ $T_{ex}$. Durable responses may also be possible if effector-like CD8$^+$ T cells can instead be directly coerced to persist in the transitory cytolytic state, for instance, by pharmacologically antagonizing TOX or related mediators of exhaustion. In addition, as stem-like PD-1$^{lo}$CD8$^+$ $T_{ex}$ exhibit heightened expression of several members of the immunoglobulin and tumor-necrosis factor receptor (TNFR) superfamily, including *Tnfrsf4* (OX40) and *Tnfrsf9* (4-1BB), combining ICB with TNFR superfamily member agonism may further support long-lived CD8$^+$ T cell reinvigoration by preferentially targeting the stem-like subset (47). Inhibiting other known or unknown transcriptional components or downstream effector pathways of the exhaustion program may offer other therapeutic avenues.

If maintaining stabilized anti-tumoral CD8$^+$ T cells is impossible, maximal amplification of the response *via* focused neoantigen vaccination or repetitive infusions of adoptive cellular therapies (ACT) may be warranted. Today, it is possible to administer autologous CD8$^+$ T cells genetically engineered to express neoantigen-specific TCRs or chimeric antigen receptors (CARs) (111, 112). This may allow for an unlimited source of artificially generated anti-tumoral CD8$^+$ T cells, thus bypassing the challenge that exhaustion may be unavoidable. ACT may also be designed to be exhaustion-resistant or to maintain stemness through gene-editing technologies (112). Alternatively, neoantigen vaccination might be a more promising strategy, either as part of a patient-shared or fully personalized therapeutic approach (113, 114). Neoantigen vaccines carrying both CD4$^+$ and CD8$^+$ T cell epitopes as long peptides, RNA/DNA vectors, or within viral constructs may better support robust, helper-primed CD8$^+$ T cell responses able to resist exhaustion upon repeated antigen encounter (115–121). Neoantigen vaccination can also strategically address tumor immunoediting. Even if persistent antigens are effectively cleared, some residual tumor cells can unavoidably become resistant to first-line ICB and/or neoantigen vaccination by altering MHC I-displayed tumor antigens *via* deletion or mutation (122). Neoantigen vaccination can solve this by applying booster regimens modified in real-time against resistant tumor cell clonal outgrowth.

## CONCLUSION

Understanding how tumors shape CD8$^+$ T cell exhaustion is needed to effectively program the immune system to destroy cancer—the professed 'emperor of all maladies' (123). An exciting parallel journey between chronic viral infection and cancer has thus been embarked upon to bypass exhaustion and identify the causative molecular cues, new cell types/lineages permissive to ICB, and innovative paths for immunotherapeutic strategies. It is currently clear that reversing exhaustion in PD-1$^{hi}$CD8$^+$ $T_{ex}$ is unlikely. Selective mobilization of stem-like CD8$^+$ $T_{ex}$ is instead called for and lies at the crux of generating functional and stable anti-tumor immune responses. Besides re-shaping the CD8$^+$ $T_{ex}$ developmental continuum, scientists are dually challenged with directing specificity of the responding population as ICB also relies on the endogenous immune system for spontaneous

recognition of select neoantigens from an initially broad TCR repertoire (90, 124, 125). Can stem-like and effector-like $CD8^+$ $T_{ex}$ fates be stabilized to act as a continuous source to deliver an unending supply of tumoricidal $CD8^+$ T cells? Can exhaustion itself be prevented in response to ICB? Can chemokine receptor pathways be exploited to control TME positioning and differentiation status of intratumoral $CD8^+$ $T_{ex}$? Or should immunologists accept the demise of $CD8^+$ $T_{ex}$ and deploy patient-tailored neoantigen and ACT strategies? The answers to these outstanding questions undoubtedly lay forth the path of future clinical trials.

## AUTHOR CONTRIBUTIONS

All authors conceived, discussed content, and contributed to researching data for the article. JD produced the primary drafts of the manuscript and designed the figures. NB-B, GT, and SS-A. provided writing and editorial contributions. All authors contributed to the article and approved the submitted version.

## FUNDING

The authors declare that this study received funding from Pfizer. The funder was not involved in the study design, collection, analysis, interpretation of data, the writing of this article, or the decision to submit it for publication.

## ACKNOWLEDGMENTS

We thank Robert Rickert and the rest of the Cancer Immunology Discovery team at Pfizer for their useful discussions. All figures in this review were created with BioRender.com.

## REFERENCES

1. Blank CU, Haining WN, Held W, Hogan PG, Kallies A, Lugli E, et al. Defining 'T Cell Exhaustion'. *Nat Rev Immunol* (2019) 14:768. doi: 10.1038/s41577-019-0221-9
2. Virgin HW, Wherry EJ, Ahmed R. Redefining Chronic Viral Infection. *Cell* (2009) 138:30–50. doi: 10.1016/j.cell.2009.06.036
3. Thommen DS, Schumacher TN. T Cell Dysfunction in Cancer. *Cancer Cell* (2018) 33:547–62. doi: 10.1016/j.ccell.2018.03.012
4. McLane LM, Abdel-Hakeem MS, Wherry EJ. Cd8 T Cell Exhaustion During Chronic Viral Infection and Cancer. *Annu Rev Immunol* (2019) 37:457–95. doi: 10.1146/annurev-immunol-041015-055318
5. Klein MR, van der Burg SH, Pontesilli O, Miedema F. Cytotoxic T Lymphocytes in HIV-1 Infection: A Killing Paradox? *Immunol Today* (1998) 19:317–24. doi: 10.1016/s0167-5699(98)01288-2
6. Obar JJ, Lefrançois L. Memory CD8+ T Cell Differentiation. *Ann NY Acad Sci* (2010) 1183:251–66. doi: 10.1111/j.1749-6632.2009.05126.x
7. Seder RA, Ahmed R. Similarities and Differences in CD4+ and CD8+ Effector and Memory T Cell Generation. *Nat Immunol* (2003) 4:835–42. doi: 10.1038/ni969
8. Joshi NS, Cui W, Chandele A, Lee HK, Urso DR, Hagman J, et al. Inflammation Directs Memory Precursor and Short-Lived Effector Cd8+ T Cell Fates Via the Graded Expression of T-Bet Transcription Factor. *Immunity* (2007) 27:281–95. doi: 10.1016/j.immuni.2007.07.010
9. Moskophidis D, Lechner F, Pircher H, Zinkernagel RM. Virus Persistence in Acutely Infected Immunocompetent Mice by Exhaustion of Antiviral Cytotoxic Effector T Cells. *Nature* (1993) 362:758–61. doi: 10.1038/362758a0
10. Wherry EJ, Blattman JN, Murali-Krishna K, van der Most R, Ahmed R. Viral Persistence Alters CD8 T-Cell Immunodominance and Tissue Distribution and Results in Distinct Stages of Functional Impairment. *J Virol* (2003) 77:4911–27. doi: 10.1128/JVI.77.8.4911-4927.2003
11. Zajac AJ, Blattman JN, Murali-Krishna K, Sourdive DJ, Suresh M, Altman JD, et al. Viral Immune Evasion Due to Persistence of Activated T Cells Without Effector Function. *J Exp Med* (1998) 188:2205–13. doi: 10.1084/jem.188.12.2205
12. Gallimore A, Dumrese T, Hengartner H, Zinkernagel RM, Rammensee HG. Protective Immunity Does Not Correlate With the Hierarchy of Virus-Specific Cytotoxic T Cell Responses to Naturally Processed Peptides. *J Exp Med* (1998) 187:1647–57. doi: 10.1084/jem.187.10.1647-b
13. Klenerman P, Hill A. T Cells and Viral Persistence: Lessons From Diverse Infections. *Nat Immunol* (2005) 6:873–9. doi: 10.1038/ni1241
14. Hellström I, Hellström KE, Pierce GE, Yang JP. Cellular and Humoral Immunity to Different Types of Human Neoplasms. *Nature* (1968) 220:1352–4. doi: 10.1038/2201352a0
15. Tran E, Robbins PF, Lu Y-C, Prickett TD, Gartner JJ, Jia L, et al. T-Cell Transfer Therapy Targeting Mutant KRAS in Cancer. *N Engl J Med* (2016) 375:2255–62. doi: 10.1056/NEJMoa1609279
16. Rosenberg SA. Progress in the Development of Immunotherapy for the Treatment of Patients With Cancer. *J Intern Med* (2001) 250:462–75. doi: 10.1046/j.1365-2796.2001.00911.x
17. Mognol GP, Spreafico R, Wong V, Scott-Browne JP, Togher S, Hoffmann A, et al. Exhaustion-Associated Regulatory Regions in CD8+ Tumor-Infiltrating T Cells. *Proc Natl Acad Sci USA* (2017) 114:E2776–85. doi: 10.1073/pnas.1620498114
18. Schietinger A, Philip M, Krisnawan VE, Chiu EY, Delrow JJ, Basom RS, et al. Tumor-Specific T Cell Dysfunction Is a Dynamic Antigen-Driven Differentiation Program Initiated Early During Tumorigenesis. *Immunity* (2016) 45:389–401. doi: 10.1016/j.immuni.2016.07.011
19. Ahrends T, Spanjaard A, Pilzecker B, Bąbała N, Bovens A, Xiao Y, et al. CD4+ T Cell Help Confers a Cytotoxic T Cell Effector Program Including Coinhibitory Receptor Downregulation and Increased Tissue Invasiveness. *Immunity* (2017) 47:848–61.e5. doi: 10.1016/j.immuni.2017.10.009
20. Martinez GJ, Pereira RM, Äijö T, Kim EY, Marangoni F, Pipkin ME, et al. The Transcription Factor NFAT Promotes Exhaustion of Activated $CD8^+$ T Cells. *Immunity* (2015) 42:265–78. doi: 10.1016/j.immuni.2015.01.006
21. Pauken KE, Sammons MA, Odorizzi PM, Manne S, Godec J, Khan O, et al. Epigenetic Stability of Exhausted T Cells Limits Durability of Reinvigoration by PD-1 Blockade. *Science* (2016) 354:1160–5. doi: 10.1126/science.aaf2807
22. Pipkin ME, Sacks JA, Cruz-Guilloty F, Lichtenheld MG, Bevan MJ, Rao A. Interleukin-2 and Inflammation Induce Distinct Transcriptional Programs That Promote the Differentiation of Effector Cytolytic T Cells. *Immunity* (2010) 32:79–90. doi: 10.1016/j.immuni.2009.11.012
23. Ashouri JF, Weiss A. Endogenous Nur77 Is a Specific Indicator of Antigen Receptor Signaling in Human T and B Cells. *J Immunol* (2017) 198:657–68. doi: 10.4049/jimmunol.1601301
24. Khan O, Giles JR, McDonald S, Manne S, Ngiow SF, Patel KP, et al. TOX Transcriptionally and Epigenetically Programs CD8+ T Cell Exhaustion. *Nature* (2019) 571:211–8. doi: 10.1038/s41586-019-1325-x
25. Man K, Gabriel SS, Liao Y, Gloury R, Preston S, Henstridge DC, et al. Transcription Factor Irf4 Promotes CD8+ T Cell Exhaustion and Limits the Development of Memory-Like T Cells During Chronic Infection. *Immunity* (2017) 47:1129–41.e5. doi: 10.1016/j.immuni.2017.11.021
26. Chen J, López-Moyado IF, Seo H, Lio C-WJ, Hempleman LJ, Sekiya T, et al. NR4A Transcription Factors Limit CAR T Cell Function in Solid Tumours. *Nature* (2019) 567:530–4. doi: 10.1038/s41586-019-0985-x
27. Zhao M, Kiernan CH, Stairiker CJ, Hope JL, Leon LG, van Meurs M, et al. Rapid In Vitro Generation of Bona Fide Exhausted CD8+ T Cells Is

Accompanied by Tcf7 promotor Methylation. *PloS Pathog* (2020) 16: e1008555. doi: 10.1371/journal.ppat.1008555
28. Thommen DS, Koelzer VH, Herzig P, Roller A, Trefny M, Dimeloe S, et al. A Transcriptionally and Functionally Distinct PD-1+ CD8+ T Cell Pool With Predictive Potential in Non-Small-Cell Lung Cancer Treated With PD-1 Blockade. *Nat Med* (2018) 24:994–1004. doi: 10.1038/s41591-018-0057-z
29. Keir ME, Freeman GJ, Sharpe AH. PD-1 Regulates Self-Reactive CD8+ T Cell Responses to Antigen in Lymph Nodes and Tissues. *J Immunol* (2007) 179:5064–70. doi: 10.4049/jimmunol.179.8.5064
30. Sharpe AH, Wherry EJ, Ahmed R, Freeman GJ. The Function of Programmed Cell Death 1 and Its Ligands in Regulating Autoimmunity and Infection. *Nat Immunol* (2007) 8:239–45. doi: 10.1038/ni1443
31. Barber DL, Wherry EJ, Masopust D, Zhu B, Allison JP, Sharpe AH, et al. Restoring Function in Exhausted CD8 T Cells During Chronic Viral Infection. *Nature* (2006) 439:682–7. doi: 10.1038/nature04444
32. de Miguel M, Calvo E. Clinical Challenges of Immune Checkpoint Inhibitors. *Cancer Cell* (2020) 38:326–33. doi: 10.1016/j.ccell.2020.07.004
33. Postow MA, Callahan MK, Wolchok JD. Immune Checkpoint Blockade in Cancer Therapy. *J Clin Oncol* (2015) 33:1974–82. doi: 10.1200/JCO.2014.59.4358
34. Blackburn SD, Shin H, Freeman GJ, Wherry EJ. Selective Expansion of a Subset of Exhausted CD8 T Cells by alphaPD-L1 Blockade. *Proc Natl Acad Sci USA* (2008) 105:15016–21. doi: 10.1073/pnas.0801497105
35. Blackburn SD, Shin H, Haining WN, Zou T, Workman CJ, Polley A, et al. Coregulation of CD8+ T Cell Exhaustion by Multiple Inhibitory Receptors During Chronic Viral Infection. *Nat Immunol* (2009) 10:29–37. doi: 10.1038/ni.1679
36. Jin H-T, Anderson AC, Tan WG, West EE, Ha S-J, Araki K, et al. Cooperation of Tim-3 and PD-1 in CD8 T-Cell Exhaustion During Chronic Viral Infection. *Proc Natl Acad Sci USA* (2010) 107:14733–8. doi: 10.1073/pnas.1009731107
37. McMahan RH, Golden-Mason L, Nishimura MI, McMahon BJ, Kemper M, Allen TM, et al. Tim-3 Expression on PD-1+ HCV-Specific Human CTLs Is Associated With Viral Persistence, and its Blockade Restores Hepatocyte-Directed In Vitro Cytotoxicity. *J Clin Invest* (2010) 120:4546–57. doi: 10.1172/JCI43127DS1
38. Nakamoto N, Cho H, Shaked A, Olthoff K, Valiga ME, Kaminski M, et al. Synergistic Reversal of Intrahepatic HCV-Specific Cd8 T Cell Exhaustion by Combined PD-1/CTLA-4 Blockade. *PloS Pathog* (2009) 5:e1000313. doi: 10.1371/journal.ppat.1000313
39. Chung HK, McDonald B, Kaech SM. The Architectural Design of CD8+ T Cell Responses in Acute and Chronic Infection: Parallel Structures With Divergent Fates. *J Exp Med* (2021) 218:e20201730. doi: 10.1084/jem.20201730
40. McLane LM, Ngiow SF, Chen Z, Attanasio J, Manne S, Ruthel G, et al. Role of Nuclear Localization in the Regulation and Function of T-Bet and Eomes in Exhausted CD8 T Cells. *CellReports* (2021) 35:109120. doi: 10.1016/j.celrep.2021.109120
41. Paley MA, Kroy DC, Odorizzi PM, Johnnidis JB, Dolfi DV, Barnett BE, et al. Progenitor and Terminal Subsets of CD8+ T Cells Cooperate to Contain Chronic Viral Infection. *Science* (2012) 338:1220–5. doi: 10.1126/science.1229620
42. Chang JT, Palanivel VR, Kinjyo I, Schambach F, Intlekofer AM, Banerjee A, et al. Asymmetric T Lymphocyte Division in the Initiation of Adaptive Immune Responses. *Science* (2007) 315:1687–91. doi: 10.1126/science.1139393
43. Chang JT, Ciocca ML, Kinjyo I, Palanivel VR, McClurkin CE, DeJong CS, et al. Asymmetric Proteasome Segregation as a Mechanism for Unequal Partitioning of the Transcription Factor T-Bet During T Lymphocyte Division. *Immunity* (2011) 34:492–504. doi: 10.1016/j.immuni.2011.03.017
44. Obar JJ, Lefrancois L. Early Events Governing Memory CD8+ T-Cell Differentiation. *Int Immunol* (2010) 22:619–25. doi: 10.1093/intimm/dxq053
45. Rao RR, Li Q, Odunsi K, Shrikant PA. The Mtor Kinase Determines Effector Versus Memory CD8+ T Cell Fate by Regulating the Expression of Transcription Factors T-bet and Eomesodermin. *Immunity* (2010) 32:67–78. doi: 10.1016/j.immuni.2009.10.010
46. Beltra J-C, Manne S, Abdel-Hakeem MS, Kurachi M, Giles JR, Chen Z, et al. Developmental Relationships of Four Exhausted CD8+ T Cell Subsets Reveals Underlying Transcriptional and Epigenetic Landscape Control Mechanisms. *Immunity* (2020) 52:825–41.e8. doi: 10.1016/j.immuni.2020.04.014
47. Im SJ, Hashimoto M, Gerner MY, Lee J, Kissick HT, Burger MC, et al. Defining CD8+ T Cells That Provide the Proliferative Burst After PD-1 Therapy. *Nature* (2016) 537:417–21. doi: 10.1038/nature19330
48. Crotty S. Follicular Helper CD4 T Cells (TFH). *Annu Rev Immunol* (2011) 29:621–63. doi: 10.1146/annurev-immunol-031210-101400
49. Escobar G, Mangani D, Anderson AC. T Cell Factor 1: A Master Regulator of the T Cell Response in Disease. *Sci Immunol* (2020) 5:eabb9726. doi: 10.1126/sciimmunol.abb9726
50. Pais Ferreira D, Silva JG, Wyss T, Fuertes Marraco SA, Scarpellino L, Charmoy M, et al. Central Memory CD8+ T Cells Derive From Stem-Like Tcf7hi Effector Cells in the Absence of Cytotoxic Differentiation. *Immunity* (2020) 53:985–1000. doi: 10.1016/j.immuni.2020.09.005
51. Wu T, Ji Y, Moseman EA, Xu HC, Manglani M, Kirby M, et al. The TCF1-Bcl6 Axis Counteracts Type I Interferon to Repress Exhaustion and Maintain T Cell Stemness. *Sci Immunol* (2016) 1:eaai8593–eaai8593. doi: 10.1126/sciimmunol.aai8593
52. Hwang S, Cobb DA, Bhadra R, Youngblood B, Khan IA. Blimp-1-mediated Cd4 T Cell Exhaustion Causes CD8 T Cell Dysfunction During Chronic Toxoplasmosis. *J Exp Med* (2016) 213:1799–818. doi: 10.1084/jem.20151995
53. Tirosh I, Izar B, Prakadan SM, Wadsworth MH, Treacy D, Trombetta JJ, et al. Dissecting the Multicellular Ecosystem of Metastatic Melanoma by Single-Cell RNA-Seq. *Science* (2016) 352:189–96. doi: 10.1126/science.aad0501
54. Wherry EJ, Ha S-J, Kaech SM, Haining WN, Sarkar S, Kalia V, et al. Molecular Signature of CD8+ T Cell Exhaustion During Chronic Viral Infection. *Immunity* (2007) 27:670–84. doi: 10.1016/j.immuni.2007.09.006
55. Shan Q, Hu S, Chen X, Danahy DB, Badovinac VP, Zang C, et al. Ectopic Tcf1 Expression Instills a Stem-Like Program in Exhausted CD8+ T Cells to Enhance Viral and Tumor Immunity. *Cell Mol Immunol* (2020) 58:89. doi: 10.1038/s41423-020-0436-5
56. Alfei F, Kanev K, Hofmann M, Wu M, Ghoneim HE, Roelli P, et al. TOX Reinforces the Phenotype and Longevity of Exhausted T Cells in Chronic Viral Infection. *Nature* (2019) 571:265–9. doi: 10.1038/s41586-019-1326-9
57. Utzschneider DT, Gabriel SS, Chisanga D, Gloury R, Gubser PM, Vasanthakumar A, et al. Early Precursor T Cells Establish and Propagate T Cell Exhaustion in Chronic Infection. *Nat Immunol* (2020) 21:1256–66. doi: 10.1038/s41590-020-0760-z
58. Utzschneider DT, Legat A, Fuertes Marraco SA, Carrié L, Luescher I, Speiser DE, et al. T Cells Maintain an Exhausted Phenotype After Antigen Withdrawal and Population Reexpansion. *Nat Immunol* (2013) 14:603–10. doi: 10.1038/ni.2606
59. Yao C, Lou G, Sun H-W, Zhu Z, Sun Y, Chen Z, et al. BACH2 Enforces the Transcriptional and Epigenetic Programs of Stem-Like CD8+ T Cells. *Nat Immunol* (2021) 22:370–80. doi: 10.1038/s41590-021-00868-7
60. Lugli E, Galletti G, Boi SK, Youngblood BA. Stem, Effector, and Hybrid States of Memory CD8+ T Cells. *Trends Immunol* (2020) 41:17–28. doi: 10.1016/j.it.2019.11.004
61. Pritykin Y, van der Veeken J, Pine AR, Zhong Y, Sahin M, Mazutis L, et al. A Unified Atlas of CD8 T Cell Dysfunctional States in Cancer and Infection. *Mol Cell* (2021) 81:2477–93. doi: 10.1016/j.molcel.2021.03.045
62. Galletti G, De Simone G, Mazza EMC, Puccio S, Mezzanotte C, Bi TM, et al. Two Subsets of Stem-Like CD8+ Memory T Cell Progenitors With Distinct Fate Commitments in Humans. *Nat Immunol* (2020) 2:251. doi: 10.1038/s41590-020-0791-5
63. Sen DR, Kaminski J, Barnitz RA, Kurachi M, Gerdemann U, Yates KB, et al. The Epigenetic Landscape of T Cell Exhaustion. *Science* (2016) 354:1165–9. doi: 10.1126/science.aae0491
64. Zeng Z, Wei F, Ren X. Exhausted T Cells and Epigenetic Status. *Cancer Biol Med* (2020) 17:923–36. doi: 10.20892/j.issn.2095-3941.2020.0338
65. Scott AC, Dündar F, Zumbo P, Chandran SS, Klebanoff CA, Shakiba M, et al. TOX Is a Critical Regulator of Tumour-Specific T Cell Differentiation. *Nature* (2019) 571:270–4. doi: 10.1038/s41586-019-1324-y
66. Seo H, Chen J, González-Avalos E, Samaniego-Castruita D, Das A, Wang YH, et al. TOX and TOX2 Transcription Factors Cooperate With NR4A

Transcription Factors to Impose CD8+ T Cell Exhaustion. *Proc Natl Acad Sci USA* (2019) 116:12410–5. doi: 10.1073/pnas.1905675116
67. Yao C, Sun H-W, Lacey NE, Ji Y, Moseman EA, Shih H-Y, et al. Single-Cell RNA-Seq Reveals TOX as a Key Regulator of CD8+ T Cell Persistence in Chronic Infection. *Nat Immunol* (2019) 20:890–901. doi: 10.1038/s41590-019-0403-4
68. Chen Z, Ji Z, Ngiow SF, Manne S, Cai Z, Huang AC, et al. Tcf-1-Centered Transcriptional Network Drives an Effector Versus Exhausted CD8 T Cell-Fate Decision. *Immunity* (2019) 51:1–16. doi: 10.1016/j.immuni.2019.09.013
69. Hudson WH, Gensheimer J, Hashimoto M, Wieland A, Valanparambil RM, Li P, et al. Proliferating Transitory T Cells With an Effector-like Transcriptional Signature Emerge From PD-1+ Stem-Like CD8+ T Cells During Chronic Infection. *Immunity* (2019) 51:1043–58. doi: 10.1016/j.immuni.2019.11.002
70. Zhou J, Wang W, Liang Z, Ni B, He W, Wang D. Clinical Significance of CD38 and CD101 Expression in PD-1+CD8+ T Cells in Patients With Epithelial Ovarian Cancer. *Oncol Lett* (2020) 20:724–32. doi: 10.3892/ol.2020.11580
71. Kurtulus S, Madi A, Escobar G, Klapholz M, Nyman J, Christian E, et al. Checkpoint Blockade Immunotherapy Induces Dynamic Changes in PD-1-CD8+ Tumor-Infiltrating T Cells. *Immunity* (2019) 50:181–94. doi: 10.1016/j.immuni.2018.11.014
72. Yost KE, Satpathy AT, Wells DK, Qi Y, Wang C, Kageyama R, et al. Clonal Replacement of Tumor-Specific T Cells Following PD-1 Blockade. *Nat Med* (2019) 348:56. doi: 10.1038/s41591-019-0522-3
73. Xu T, Keller A, Martinez GJ. NFAT1 and NFAT2 Differentially Regulate Ctl Differentiation Upon Acute Viral Infection. *Front Immunol* (2019) 10:184. doi: 10.3389/fimmu.2019.00184
74. Ahrends T, Bąbała N, Xiao Y, Yagita H, van Eenennaam H, Borst J. Cd27 Agonism Plus PD-1 Blockade Recapitulates CD4+ T-Cell Help in Therapeutic Anticancer Vaccination. *Cancer Res* (2016) 76:2921–31. doi: 10.1158/0008-5472.CAN-15-3130
75. Borst J, Ahrends T, Bąbała N, Melief CJM, Kastenmüller W. CD4+ T Cell Help in Cancer Immunology and Immunotherapy. *Nat Rev Immunol* (2018) 18:635–47. doi: 10.1038/s41577-018-0044-0
76. Croft M. Co-Stimulatory Members of the TNFR Family: Keys to Effective T-Cell Immunity? *Nat Rev Immunol* (2003) 3:609–20. doi: 10.1038/nri1148
77. Kong K-F, Yokosuka T, Canonigo-Balancio AJ, Isakov N, Saito T, Altman A. A Motif in the V3 Domain of the Kinase PKC-θ Determines Its Localization in the Immunological Synapse and Functions in T Cells Via Association With CD28. *Nat Publishing Group* (2011) 12:1105–12. doi: 10.1038/ni.2120
78. Kong K-F, Altman A. In and Out of the Bull's Eye: Protein Kinase Cs in the Immunological Synapse. *Trends Immunol* (2013) 34:234–42. doi: 10.1016/j.it.2013.01.002
79. Macian F, García-Rodríguez C, Rao A. Gene Expression Elicited by NFAT in the Presence or Absence of Cooperative Recruitment of Fos and Jun. *EMBO J* (2000) 19:4783–95. doi: 10.1093/emboj/19.17.4783
80. Macián F, García-Cózar F, Im S-H, Horton HF, Byrne MC, Rao A. Transcriptional Mechanisms Underlying Lymphocyte Tolerance. *Cell* (2002) 109:719–31. doi: 10.1016/s0092-8674(02)00767-5
81. Franco F, Jaccard A, Romero P, Yu Y-R, Ho P-C. Metabolic and Epigenetic Regulation of T-Cell Exhaustion. *Nat Metab* (2020) 2:1001–12. doi: 10.1038/s42255-020-00280-9
82. Vardhana SA, Hwee MA, Berisa M, Wells DK, Yost KE, King B, et al. Impaired Mitochondrial Oxidative Phosphorylation Limits the Self-Renewal of T Cells Exposed to Persistent Antigen. *Nat Immunol* (2020) 21:1022–33. doi: 10.1038/s41590-020-0725-2
83. Yu Y-R, Imrichova H, Wang H, Chao T, Xiao Z, Gao M, et al. Disturbed Mitochondrial Dynamics in CD8+ Tils Reinforce T Cell Exhaustion. *Nat Immunol* (2020) 16:425. doi: 10.1038/s41590-020-0793-3
84. Sena LA, Li S, Jairaman A, Prakriya M, Ezponda T, Hildeman DA, et al. Mitochondria Are Required for Antigen-Specific T Cell Activation Through Reactive Oxygen Species Signaling. *Immunity* (2013) 38:225–36. doi: 10.1016/j.immuni.2012.10.020
85. Sade-Feldman M, Yizhak K, Bjorgaard SL, Ray JP, de Boer CG, Jenkins RW, et al. Defining T Cell States Associated With Response to Checkpoint Immunotherapy in Melanoma. *Cell* (2018) 175:998–1013. doi: 10.1016/j.cell.2018.10.038
86. Miller BC, Sen DR, Abosy Al R, Bi K, Virkud YV, LaFleur MW, et al. Subsets of Exhausted CD8+ T Cells Differentially Mediate Tumor Control and Respond to Checkpoint Blockade. *Nat Immunol* (2019) 20:326–36. doi: 10.1038/s41590-019-0312-6
87. Jansen CS, Prokhnevska N, Master VA, Sanda MG, Carlisle JW, Bilen MA, et al. An Intra-Tumoral Niche Maintains and Differentiates Stem-Like CD8 T Cells. *Nature* (2019) 576:465–70. doi: 10.1038/s41586-019-1836-5
88. Brummelman J, Mazza EMC, Alvisi G, Colombo FS, Grilli A, Mikulak J, et al. High-Dimensional Single Cell Analysis Identifies Stem-Like Cytotoxic CD8+ T Cells Infiltrating Human Tumors. *J Exp Med* (2018) 215:2520–35. doi: 10.1084/jem.20180684
89. Dammeijer F, van Gulijk M, Mulder EE, Lukkes M, Klaase L, van den Bosch T, et al. The PD-1/PD-L1-Checkpoint Restrains T Cell Immunity in Tumor-Draining Lymph Nodes. *Cancer Cell* (2020) 38:685–700. doi: 10.1016/j.ccell.2020.09.001
90. Ott PA, Hu-Lieskovan S, Chmielowski B, Govindan R, Naing A, Bhardwaj N, et al. A Phase Ib Trial of Personalized Neoantigen Therapy Plus Anti-PD-1 in Patients With Advanced Melanoma, Non-small Cell Lung Cancer, or Bladder Cancer. *Cell* (2020) 183:347–62.e24. doi: 10.1016/j.cell.2020.08.053
91. Cristescu R, Mogg R, Ayers M, Albright A, Murphy E, Yearley J, et al. Pan-Tumor Genomic Biomarkers for PD-1 Checkpoint Blockade-Based Immunotherapy. *Science* (2018) 362:eaar3593. doi: 10.1126/science.aar3593
92. Davis AA, Patel VG. The Role of PD-L1 Expression as a Predictive Biomarker: An Analysis of All US Food and Drug Administration (FDA) Approvals of Immune Checkpoint Inhibitors. *J Immunother Cancer* (2019) 7:278. doi: 10.1186/s40425-019-0768-9
93. Rizvi NA, Hellmann MD, Snyder A, Kvistborg P, Makarov V, Havel JJ, et al. Mutational Landscape Determines Sensitivity to PD-1 Blockade in non-Small Cell Lung Cancer. *Science* (2015) 348:124–8. doi: 10.1126/science.aaa1348
94. Schumacher TN, Schreiber RD. Neoantigens in Cancer Immunotherapy. *Science* (2015) 348:69–74. doi: 10.1126/science.aaa4971
95. Snyder A, Makarov V, Merghoub T, Yuan J, Zaretsky JM, Desrichard A, et al. Genetic Basis for Clinical Response to CTLA-4 Blockade in Melanoma. *N Engl J Med* (2014) 371:2189–99. doi: 10.1056/NEJMoa1406498
96. Thorsson V, Gibbs DL, Brown SD, Wolf D, Bortone DS, Ou Yang T-H, et al. The Immune Landscape of Cancer. *Immunity* (2018) 48:812–30.e14. doi: 10.1016/j.immuni.2018.03.023
97. Yost KE, Chang HY, Satpathy AT. Recruiting T Cells in Cancer Immunotherapy. *Science* (2021) 372:130–1. doi: 10.1126/science.abd1329
98. Rashidian M, LaFleur MW, Verschoor VL, Dongre A, Zhang Y, Nguyen TH, et al. Immuno-PET Identifies the Myeloid Compartment as a Key Contributor to the Outcome of the Antitumor Response Under PD-1 Blockade. *Proc Natl Acad Sci USA* (2019) 116:16971–80. doi: 10.1073/pnas.1905005116
99. Wu TD, Madireddi S, de Almeida PE, Banchereau R, Chen Y-JJ, Chitre AS, et al. Peripheral T Cell Expansion Predicts Tumour Infiltration and Clinical Response. *Nature* (2020) 579:274–8. doi: 10.1038/s41586-020-2056-8
100. Sánchez-Magraner L, Miles J, Baker CL, Applebee CJ, Lee D-J, Elsheikh S, et al. High PD-1/PD-L1 Checkpoint Interaction Infers Tumor Selection and Therapeutic Sensitivity to Anti-PD-1/PD-L1 Treatment. *Cancer Res* (2020) 80:4244–57. doi: 10.1158/0008-5472.CAN-20-1117
101. Chen IX, Newcomer K, Pauken KE, Juneja VR, Naxerova K, Wu MW, et al. A Bilateral Tumor Model Identifies Transcriptional Programs Associated With Patient Response to Immune Checkpoint Blockade. *Proc Natl Acad Sci USA* (2020) 2:202002806. doi: 10.1073/pnas.2002806117
102. Chow MT, Ozga AJ, Servis RL, Frederick DT, Lo JA, Fisher DE, et al. Intratumoral Activity of the CXCR3 Chemokine System Is Required for the Efficacy of Anti-PD-1 Therapy. *Immunity* (2019) 50:1498–512.e5. doi: 10.1016/j.immuni.2019.04.010
103. Dangaj D, Bruand M, Grimm AJ, Ronet C, Barras D, Duttagupta PA, et al. Cooperation Between Constitutive and Inducible Chemokines Enables T Cell Engraftment and Immune Attack in Solid Tumors. *Cancer Cell* (2019) 35:885–900.e10. doi: 10.1016/j.ccell.2019.05.004
104. House IG, Savas P, Lai J, Chen AXY, Oliver AJ, Teo ZL, et al. Macrophage-Derived CXCL9 and CXCL10 Are Required for Antitumor Immune

Responses Following Immune Checkpoint Blockade. *Clin Cancer Res* (2020) 26:487–504. doi: 10.1158/1078-0432.CCR-19-1868
105. Qu Y, Wen J, Thomas G, Yang W, Prior W, He W, et al. Baseline Frequency of Inflammatory Cxcl9-Expressing Tumor-Associated Macrophages Predicts Response to Avelumab Treatment. *CellReports* (2020) 32:107873. doi: 10.1016/j.celrep.2020.107873
106. Zilionis R, Engblom C, Pfirschke C, Savova V, Zemmour D, Saatcioglu HD, et al. Single-Cell Transcriptomics of Human and Mouse Lung Cancers Reveals Conserved Myeloid Populations Across Individuals and Species. *Immunity* (2019) 50:1317–34.e10. doi: 10.1016/j.immuni.2019.03.009
107. Abboud G, Desai P, Dastmalchi F, Stanfield J, Tahiliani V, Hutchinson TE, et al. Tissue-Specific Programming of Memory CD8 T Cell Subsets Impacts Protection Against Lethal Respiratory Virus Infection. *J Exp Med* (2016) 213:2897–911. doi: 10.1084/jem.20160167
108. Desai P, Tahiliani V, Stanfield J, Abboud G, Salek-Ardakani S. Inflammatory Monocytes Contribute to the Persistence of CXCR3hi CX3CR1lo Circulating and Lung-Resident Memory CD8+ T Cells Following Respiratory Virus Infection. *Immunol Cell Biol* (2018) 96:370–8. doi: 10.1111/imcb.12006
109. Kurachi M, Kurachi J, Suenaga F, Tsukui T, Abe J, Ueha S, et al. Chemokine Receptor CXCR3 Facilitates CD8(+) T Cell Differentiation Into Short-Lived Effector Cells Leading to Memory Degeneration. *J Exp Med* (2011) 208:1605–20. doi: 10.1084/jem.20102101
110. Tokunaga R, Zhang W, Naseem M, Puccini A, Berger MD, Soni S, et al. Cxcl9, CXCL10, CXCL11/CXCR3 Axis for Immune Activation - A Target for Novel Cancer Therapy. *Cancer Treat Rev* (2018) 63:40–7. doi: 10.1016/j.ctrv.2017.11.007
111. Jin BY, Campbell TE, Draper LM, Stevanović S, Weissbrich B, Yu Z, et al. Engineered T Cells Targeting E7 Mediate Regression of Human Papillomavirus Cancers in a Murine Model. *JCI Insight* (2018) 3:5715. doi: 10.1172/jci.insight.99488
112. Waldman AD, Fritz JM, Lenardo MJ. A Guide to Cancer Immunotherapy: From T Cell Basic Science to Clinical Practice. *Nat Rev Immunol* (2020) 3:250. doi: 10.1038/s41577-020-0306-5
113. Ott PA, Hu Z, Keskin DB, Shukla SA, Sun J, Bozym DJ, et al. An Immunogenic Personal Neoantigen Vaccine for Patients With Melanoma. *Nature* (2017) 547:217–21. doi: 10.1038/nature22991
114. Sahin U, Derhovanessian E, Miller M, Kloke B-P, Simon P, Löwer M, et al. Personalized RNA Mutanome Vaccines Mobilize Poly-Specific Therapeutic Immunity Against Cancer. *Nature* (2017) 547:222–6. doi: 10.1038/nature23003
115. Alspach E, Lussier DM, Miceli AP, Kizhvatov I, DuPage M, Luoma AM, et al. Mhc-II Neoantigens Shape Tumour Immunity and Response to Immunotherapy. *Nature* (2019) 574:696–701. doi: 10.1038/s41586-019-1671-8
116. Castle JC, Kreiter S, Diekmann J, Lower M, van de Roemer N, de Graaf J, et al. Exploiting the Mutanome for Tumor Vaccination. *Cancer Res* (2012) 72:1081–91. doi: 10.1158/0008-5472.CAN-11-3722
117. Gubin MM, Zhang X, Schuster H, Caron E, Ward JP, Noguchi T, et al. Checkpoint Blockade Cancer Immunotherapy Targets Tumour-Specific Mutant Antigens. *Nature* (2014) 515:577–81. doi: 10.1038/nature13988
118. Khanolkar A, Badovinac VP, Harty JT. CD8 T Cell Memory Development: CD4 T Cell Help Is Appreciated. *Immunol Res* (2007) 39:94–104. doi: 10.1007/s12026-007-0081-4
119. Kreiter S, Vormehr M, van de Roemer N, Diken M, Löwer M, Diekmann J, et al. Mutant MHC Class II Epitopes Drive Therapeutic Immune Responses to Cancer. *Nature* (2015) 520:692–6. doi: 10.1038/nature14426
120. Kumai T, Lee S, Cho H-I, Sultan H, Kobayashi H, Harabuchi Y, et al. Optimization of Peptide Vaccines to Induce Robust Antitumor Cd4 T-Cell Responses. *Cancer Immunol Res* (2017) 5:72–83. doi: 10.1158/2326-6066.CIR-16-0194
121. Melief CJM, van der Burg SH. Immunotherapy of Established (Pre) Malignant Disease by Synthetic Long Peptide Vaccines. *Nat Rev Cancer* (2008) 8:351–60. doi: 10.1038/nrc2373
122. Kluger HM, Tawbi HA, Ascierto ML, Bowden M, Callahan MK, Cha E, et al. Defining Tumor Resistance to PD-1 Pathway Blockade: Recommendations From the First Meeting of the SITC Immunotherapy Resistance Taskforce. *J Immunother Cancer* (2020) 8:e000398. doi: 10.1136/jitc-2019-000398
123. Mukherjee S. *The Emperor of All Maladies: A Biography of Cancer*. Scribner (2010).
124. Fairfax BP, Taylor CA, Watson RA, Nassiri I, Danielli S, Fang H, et al. Peripheral CD8+ T Cell Characteristics Associated With Durable Responses to Immune Checkpoint Blockade in Patients With Metastatic Melanoma. *Nat Med* (2020) 26:193–9. doi: 10.1038/s41591-019-0734-6
125. Valpione S, Galvani E, Tweedy J, Mundra PA, Banyard A, Middlehurst P, et al. Immune-Awakening Revealed by Peripheral T Cell Dynamics After One Cycle of Immunotherapy. *Nat Cancer* (2020) 1:210–21. doi: 10.1038/s43018-019-0022-x

**Conflict of Interest:** All authors are employees of Pfizer, Inc. and hold stock/stock options in the company.

frontiers in Immunology

REVIEW
published: 19 August 2021
doi: 10.3389/fimmu.2021.706583

# The Effects of Trained Innate Immunity on T Cell Responses; Clinical Implications and Knowledge Gaps for Future Research

*Dearbhla M. Murphy*[1], *Kingston H. G. Mills*[2] *and Sharee A. Basdeo*[1]*

[1] Human and Translational Immunology Group, Department of Clinical Medicine, Trinity Translational Medicine Institute, St James's Hospital, Trinity College Dublin, The University of Dublin, Dublin, Ireland, [2] Immune Regulation Research Group, School of Biochemistry and Immunology, Trinity Biomedical Sciences Institute, Trinity College Dublin, The University of Dublin, Dublin, Ireland

The burgeoning field of innate immune training, also called trained immunity, has given immunologists new insights into the role of innate responses in protection against infection and in modulating inflammation. Moreover, it has led to a paradigm shift in the way we think about immune memory and the interplay between innate and adaptive immune systems in conferring immunity against pathogens. Trained immunity is the term used to describe the medium-term epigenetic and metabolic reprogramming of innate immune cells in peripheral tissues or in the bone marrow stem cell niche. It is elicited by an initial challenge, followed by a significant period of rest that results in an altered response to a subsequent, unrelated challenge. Trained immunity can be associated with increased production of proinflammatory mediators, such as IL-1β, TNF and IL-6, and increased expression of markers on innate immune cells associated with antigen presentation to T cells. The microenvironment created by trained innate immune cells during the secondary challenge may have profound effects on T cell responses, such as altering the differentiation, polarisation and function of T cell subtypes, including Th17 cells. In addition, the Th1 cytokine IFN-γ plays a critical role in establishing trained immunity. In this review, we discuss the evidence that trained immunity impacts on or can be impacted by T cells. Understanding the interplay between innate immune training and how it effects adaptive immunity will give insights into how this phenomenon may affect the development or progression of disease and how it could be exploited for therapeutic interventions or to enhance vaccine efficacy.

**Keywords: trained immunity, T cells, adaptive, innate, BCG, beta-glucan**

OPEN ACCESS

***Edited by:***
*Francesca Di Rosa, Italian National Research Council, Italy*

***Reviewed by:***
*Lionel Le Bourhis, Institut National de la Santé et de la Recherche Médicale (INSERM), France*
*Roberta Zappasodi, Memorial Sloan Kettering Cancer Center, United States*

***Correspondence:**
*Sharee A. Basdeo*
*basdeos@tcd.ie*

***Specialty section:***
*This article was submitted to Immunological Memory, a section of the journal Frontiers in Immunology*

***Received:*** *07 May 2021*
***Accepted:*** *30 July 2021*
***Published:*** *19 August 2021*

***Citation:***
*Murphy DM, Mills KHG and Basdeo SA (2021) The Effects of Trained Innate Immunity on T Cell Responses; Clinical Implications and Knowledge Gaps for Future Research. Front. Immunol. 12:706583. doi: 10.3389/fimmu.2021.706583*

## INTRODUCTION

In their seminal paper in 2011, Netea and colleagues proposed the idea of trained immunity (also called innate memory or innate immune training) (1) which directly challenged the dogma that only the adaptive immune system had the capacity for immune memory in humans. Trained immunity in mammals is an epigenetic and metabolic reprogramming of innate immune cells, which can occur locally in tissues and in the stem cell niche of the bone marrow, causing altered innate

immune responses (2–4). Trained immunity is induced by a primary insult, where innate immune cells are activated and then return to homeostatic function during a period of rest, but maintain the epigenetic and metabolic reprogramming caused by the primary insult. This reprogramming results in an altered immune response to a subsequent, usually unrelated, insult (2–4). It has been reported that β-glucan (a fungal cell wall component), lipopolysaccharide (LPS), the bacillis Clamette-Guérin (BCG) vaccine, adenoviruses and secretory products from helminths can act as the primary stimulus to elicit trained immunity (5–7) (**Table 1**). In addition, there is evidence that endogenous compounds such as oxidised low density lipoprotein (ox-LDL) can also induce trained immunity (17) (**Table 1**).

Trained immunity has been well documented in monocytes but can also occur in differentiated macrophages, dendritic cells (DC) and natural killer (NK) cells (19–23). Since many innate immune cells are short-lived, the functional effects of trained immunity, which can last several weeks (5, 24), and in some cases, up to a year (8, 25), are attributed to immune reprogramming of the haematopoietic stem cells in the bone marrow (10, 24–26). This results in newly generated myeloid cells exhibiting the features of trained immunity when they egress from the bone marrow into the circulation (24, 26).

Innate immune training is a medium-term phenomenon which can mediate non-specific or specific immunity against pathogens. This is distinct from adaptive immune memory, which generates specific long-term memory, in the form of memory T and B cells that clonally expand and rapidly respond upon re-exposure to the same pathogen. The effect of trained immunity on adaptive immune responses has not been thoroughly explored. Trained immunity is likely to impact on the adaptive immune response due to the heightened production of T cell polarizing cytokines and increased expression of markers associated with antigen presentation. In addition to polarising naive T cells, cytokines produced by innate cells also regulate memory T cell function and lineage commitment. Therefore, trained immunity may have an impact on T cell plasticity and may alter the Th1/Th2 or Treg/Th17 balance. In addition, T cell responses may have an upstream effect on trained immunity through activation or modulation of innate immune cells.

Understanding the influence of trained immunity on adaptive immune responses will help us to better understand the impact of trained immunity in the control of infectious diseases or in promoting pathology in immune-mediated diseases. It may also

**TABLE 1** | Summary of the type of trained immunity induced by different stimuli, their proposed effect on the T cell response and clinical associations.

| Ligand | Training Type | Cytokines | Proposed effect on T Cell Response | Effect of T Cell on the Induction of Trained Immunity | Clinical Associations | Ref |
|---|---|---|---|---|---|---|
| BCG | Pro-inflammatory | ↑IL-1β | ↑Th1 | T cells downregulate trained immunity | Protection against infection | (5) |
| | | ↑TNF | ↑Th17 | | | (8) |
| | | ↑IL-6 | ↓Tregs | | | (9) |
| | | ↑IL-8 | | | | |
| | | ↓IL-10 | | | | |
| β-glucan | Pro-inflammatory | ↑IL-1β | ↑Th1 | Unknown | Protection against infection | (6) |
| | | ↑TNF | ↑Th17 | | | (10) |
| | | ↑IL-6 | ↓Tregs | | | |
| | | ↓IL-10 | | | | |
| FHTE | Anti-inflammatory | ↑IL-10 | ↑Tregs | Unknown | Protection against EAE | (11) |
| | | ↑IL-1RA | ↓Th1 | | | (12) |
| | | ↓TNF | ↓Th17 | | | |
| | | ↓IL-12p40 | | | | |
| Adenovirus | Pro-inflammatory | ↑MIP-2 | ↑Th17 | CD8 T cell IFN-γ required to induce trained immunity | Protection against infection (via enhanced neutrophilia) | (13) |
| | | ↑KC | | | | |
| | | ↑IL-1β | | | | |
| LPS | Tolerance | ↑IL-10 | ↑Tregs | Unknown | Sepsis Immunoparalysis | (14) |
| | | ↓TNF | ↓Th1 | | | (15) |
| | | ↓IL-6 | ↓Th17 | | | (16) |
| oxLDL | Pro-Inflammatory | ↑TNF | ↑Th-1 | Unknown | Athersclerosis | (17) |
| | | ↑IL-6 | ↑Th-17 | | | |
| | | ↑IL-8 | | | | |
| MuHV-4 | Anti-inflammatory | ↓IL-5 | | | | |
| | | ↓IL-13 | ↓Th2 | Unknown | Reduced allergic reaction to HDMs | (18) |
| | | ↓IL-4 | ↑Th1 | | | |
| | | ↓IL-6 | | | | |
| | | ↓IL-10 | | | | |

aid the design of more effective vaccine strategies that combine the induction of trained immunity with the generation of traditional adaptive immune memory.

## EVIDENCE FOR TRAINED IMMUNITY IMPACTING T CELL RESPONSES

Monocytes that undergo innate immune training with adenovirus or BCG have enhanced antigen presenting function due to increased expression of MHC-II and the co-stimulatory molecules CD80 and CD86 (13, 27). These two signals are critical to the immune synapse between antigen presenting cells (APC) and T cells (**Figure 1A**). A third signal, cytokine production by the APC, directs the polarisation of naïve T cells into discrete subsets and can alter the function of effector T cells that are already lineage committed. Therefore, altered cytokine production in myeloid cells following trained immunity is likely to impact T cell polarisation and lineage fate (**Figure 1B**). Indeed, Kleinnijenhuis et al., suggested that the increased expression of pathogen recognition receptors and increased production of pro-inflammatory cytokines by innate immune cells contributes to enhanced T cell responses (8). However, there is a paucity of data examining the effects of trained immunity on the polarisation of effector T cell subtypes and Treg cells. Since DC are the key APC in triggering naïve T cell activation, identifying the effects trained immunity on DC maturation and function will be critical to understanding the interplay between trained immunity and adaptive immune responses. Further elucidation of the effects of trained monocytes and macrophages on tissue-resident memory T cell responses will also be beneficial in understanding the impact of trained immunity during a subsequent insult.

Monocytes from BCG-vaccinated adults have increased production of IL-1β, TNF and IL-6 upon restimulation *ex vivo* with unrelated pathogens, *Staphylococcus aureus*, *Candida albicans* and the yellow fever virus vaccine strain (5, 8, 9). IL-1β and IL-6 are key drivers of Th17 cell responses and can promote functional plasticity towards the more pro-inflammatory ex-Th17 cell fate, where Th17 lineage cells produce IFN-γ, which is associated with protection against certain infections (28) but also with immune-mediated pathology (29). This suggests that altered innate cytokine production induced by trained immunity is likely to impact on T cell differentiation and fate. Consistent with this, BCG vaccination is associated with elevated IFN-γ and IL-17 production from PBMC stimulated *ex vivo* with *Mycobacterium tuberculosis* and unrelated pathogens (5) (8) (**Table 1**). Taken together, these findings suggest that vaccination with BCG may enhance Th1 and Th17 cell responses to unrelated stimuli, although the evidence does not definitively show that the IFN-γ and IL-17 are produced by T cells (8). In addition, this study did not mechanistically link the increased innate IL-1β and TNF produced by monocytes in BCG vaccinated individuals to the longer-term effect on Th1 or Th17 cells. We propose that this heterologous Th1 and Th17 immunity

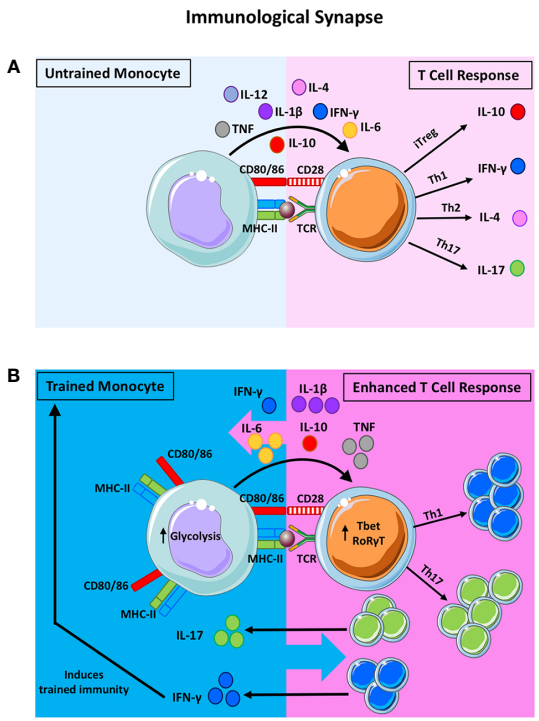


**FIGURE 1** | The potential impact of trained immunity on the bidirectional innate-adaptive immune synapse. The traditional synapse between antigen-presenting cells (APC) and naïve T helper cells is depicted in **(A)**. The innate APC processes and presents antigen on the MHC-II molecule to provide the first signal to activate the T cell. Upregulation of co-stimulatory molecules on the APC and their ligation to the cognate receptors on the T cells provide the second signal required for T cell activation. Cytokine production by the innate APC then polarises the naïve T cell into discreet subsets. For example, the presence of IL-10 will induce the formation of T regulatory cells (Treg) whereas IL-12 and IFN-γ will polarise T cells towards a Th1 lineage. IL-4 promotes Th2 polarisation and IL-1β and IL-6 (along with other innate cytokines) promote Th17 development. This synapse is often viewed as unidirectional, however, there is evidence to suggest that T cell cytokines can impact also APC function. In addition to being the critical control point in the polarization of naïve T cells, this synapse is also crucial for reactivating memory T cells in tissues. Under these circumstances, innate cytokine production can alter the functional profile of previously lineage committed T cells. When trained immunity is induced in innate cells, their APC function and cytokine production is markedly enhanced **(B)**. Trained innate cells exhibit increased expression of MHC-II, costimulatory molecules (CD80/CD86) and an upregulation of aerobic glycolysis. Moreover, trained monocytes produce significantly more TNF, IL-1β and IL-6 compared with untrained monocytes. These features of proinflammatory innate immune training suggest that T cell polarization may be skewed in favour of Th17/Th1 responses, as indicated by the expression of the master transcription factors RORγT and Tbet, respectively. In the same manner, lineage committed T cells that are prone to functional plasticity, such as the Th17 and Treg lineages, may be altered by trained immunity and directed down alternative lineage fates. Enhanced IFN-γ and IL-17 production from T cells can impact innate cell function. In fact, IFN-γ production has been shown to induce trained immunity in tissue resident macrophages. Notably, alternative types of trained immunity that result in enhanced IL-10, for example, will alter T cell fate towards Treg cells, which may in turn impact innate APC function. We propose that, trained immunity alters T cell fate and function which may in turn alter innate cell function. Depending on the primary insult that induces trained immunity, the pro-inflammatory versus anti-inflammatory nature of this bi-directional synapse will be altered depending on the cytokine milieu and the cellular functions that are induced by trained immunity.

generated by the BCG vaccine may, at least in part, be mediated by the altered function of innate cells that have undergone trained immunity. We also hypothesise that trained immunity may promote Th17 cell plasticity towards an 'ex-Th17' phenotype (which means that they start producing IFN-γ), therefore, the increased IFN-γ secretion in this system may be produced by both Th1 and Th17 lineage cells.

The precise role that T cells play during the induction of trained immunity is unclear. Yao et al. reported that trained immunity can be induced in tissue resident alveolar macrophages (AM) following infection with a respiratory adenovirus vector *in vivo* in a mouse model (13) (**Table 1**). These 'trained' AM exhibited heightened MHC II expression, increased glycolytic metabolism and a "defence-ready" gene signature at 4 and 16 weeks post infection (13). Interestingly, the depletion of T cells completely abrogated the expression of MHC-II, chemokine production and metabolic reprogramming in the AM. Consistent with this, SCID mice infected with the adenoviral vector failed to induce trained immunity in the AM population, however, transfer of IFN-γ-producing CD8 T cells to the airways of the SCID mice restored the phenotype and function of the memory AM (13). By depleting T cells at different timepoints, this study established that T cells were required initially to generate the memory AM, but are not required later on to maintain this cell population (13). In addition, they showed that IFN-γ deficiency diminished trained immunity in the AM. To definitively show that IFN-γ production from the CD8 T cell was required for the induction of trained immunity in the AM, CD8 T cells from wild type mice infected with adenovirus vector were transferred to RAG mice and this rescued the trained immunity phenotype in the AM, whereas CD8 T cells from IFN-γ-defective mice did not alter the AM (13). These findings indicate that IFN-γ production by T cells plays a critical role in establishing trained immunity in tissue resident AM and supports the hypothesis that trained immunity can be influenced by T cell responses. This study did not investigate if these "memory" AM modulated T cell responses in the lung during the subsequent infection with *Streptococcus pneumoniae*. However, when T cells were depleted after the memory AM population were established but before challenge with *S. pneumoniae*, these mice were also protected against the bacterial infection (13). This indicates that the T cell response is not necessary to mediate protection against bacterial infection after induction of trained innate immunity by the adenoviral vector. It is possible that the T cell population may be altered in the lung by the enhanced function of these "trained" AM and this may influence disease outcomes in humans.

Conversely, there is evidence to suggest that T cells may play a role in downregulating trained immunity since monocyte function can be enhanced in the absence of T cells (5, 6, 24). It is plausible that T cells have distinct effects on trained immunity depending on the initial training stimulus, the context of inflammation or at different sites. For example, the presence of T cells in the bone marrow appears to downregulate trained immunity, resulting in monocytes with reduced bactericidal capacity compared with T cell-depleted bone marrow (24). Interestingly, there is a requirement for IFN-γ in reprogramming the haematopoietic stem cells in the bone marrow to elicit trained immunity in cells undergoing myelopoiesis (24), underscoring the prominence of its role in this process but the cellular source of IFN-γ may be innate or adaptive, depending on the context.

### Anti-Inflammatory Trained Immunity

The majority of studies to date describe trained immunity as enhancing pro-inflammatory responses, however, it was recently reported that myeloid cells can be trained towards an anti-inflammatory phenotype following exposure to helminth products (11, 12). Macrophages trained *in vitro* with *Fasciola hepatica* total extract (FHTE; **Table 1**) or *F. hepatica* excretory secretory products (FHES) showed heightened production of the anti-inflammatory cytokines IL-1RA and IL-10, but reduced production of the pro-inflammatory cytokines TNF and IL-12p40 (11). IL-10 induces Treg cells while IL-1RA acts as natural inhibitor of IL-1β signalling, stunting the Th17 response (30, 31). Suppressed IL-12p40 and TNF dampens the Th1 cell response (11, 32). FHES administered to mice *in vivo* altered the hematopoietic stem cell niche in the bone marrow and resulted in hyporesponsive monocytes at different sites in the mice (12). These data also showed that this anti-inflammatory trained immunity induced by FTHE or FHES was associated with reduced Th1 and Th17 responses and attenuated EAE (11, 12), the animal model of autoimmune multiple sclerosis, which is mediated by pathogenic Th1, Th17 and ex-Th17 cells (33).

## INNATE IMMUNE TRAINING AND HETEROLOGOUS T CELL IMMUNITY

Many vaccines that are known or postulated to induce trained immunity are also associated with promoting heterologous T cell immunity; a phenomenon whereby T cells can cross-react and promote immunity against unrelated pathogens. Deleterious effects of cross-reactive T cells causing pathology post infection are well documented in humans; for example, dengue virus-induced haemorrhagic fever and Epstein-Barr virus (EBV)-induced mononucleosis (34–36). However, the beneficial effects of heterologous T cell immunity are harder to recognise clinically.

Heterologous T cell immunity can be mediated through T cell receptors that can bind to two or more MHC-peptide complexes, initiating cross-reactive T cell responses (37). Alternatively, memory T cells can also be activated in a bystander manner by cytokines in the absence of antigen specificity (38–41). Cytokines documented to induce this bystander activation of T cells include type 1 and type 2 interferons (38, 39, 42). Moreover, IL-1β or IL-18 can synergise with IL-23 to induce bystander activation and production of IL-17 and IFN-γ from CD4 T cells in the absence of TCR stimulation (43).

A study using an animal model of respiratory syncytial virus (RSV) demonstrated that previous influenza infection protected mice against illness, weight loss and eosinophilia during RSV (44). When the interval between the two infections was extended

from 3 weeks to 21 weeks, the protective effects of influenza infection mediated by reduced eosinophilia were maintained. An examination of the possible mechanisms of protection found no evidence for cross-reactive T cells (44). However, there was some evidence to support bystander activation. Influenza virus-specific T cells returned to the lung during RSV infection and produced IFN-γ, however, the resident memory T cells in the lung did not confer the same bystander protection against eosinophilia as the influenza virus-specific T cells. The authors concluded that the shift in the Th1/Th2 cytokine balance caused by the presence of influenza virus-specific T cells is likely to mediate protection, since the influenza infection promoted IFN-γ and decreased IL-4 in the lung (44). In addition, previous influenza infection was associated with reduced TNF and increased IL-10, suggesting the enhanced anti-inflammatory cytokine production could be responsible for protecting the animals against immune-mediated pathology during RSV infection (44). This study indicates that the history of infection has an impact on subsequent control of pathogens, even after a significant period of rest (21 weeks). Trained immunity is likely to play a role in this experimental model of heterologous immunity, however, there is no definitive evidence that innate cell function was altered by the primary infection (44). The exact role of innate and adaptive immune responses in heterologous immunity is still unclear and further research is required to establish a cause-and-effect relationship between trained innate immunity and heterologous T cell immunity.

Heterologous immunity generated by the BCG vaccine is well documented and accounts for its protective effects against all-cause mortality in infants (45, 46). This is thought to be mediated by both trained innate immunity and heterologous T cell immunity. BCG vaccination in humans has been shown to induce heterologous Th1 and Th17 cell responses in response to *S. aureus* and *C. albicans in vitro* (8). Likewise, immunisation with the BCG vaccine in mice, conferred protection against a subsequent vaccinia virus infection, which was mediated by CD4 T cells (47). Since there is ample evidence that BCG induces innate immune training in myeloid cells (5, 48), it is plausible that the training of these cells results in the activation of T cell mediated heterologous immunity. T cell activation thresholds or TCR specificity may be altered in the context of hyperresponsive trained innate cells that exhibit increased cytokine outputs in addition to enhanced APC function. However, definitive evidence that BCG-induce trained immunity is directly associated with heterologous T cell immunity remains elusive.

The vaccinia virus, used as the smallpox vaccine, has been shown to reduce susceptibility to various infectious diseases and to promote healing of chronic skin rashes (49, 50). Innate immune training has been suggested as the mechanism responsible for the non-specific effects of vaccinia virus in humans, with both epidemiological and experimental data linking vaccinia virus to trained immunity (51–55). Vaccinia virus has also been associated with heterologous T cell immunity to HIV since $CCR5^+$ T cells from smallpox-vaccinated individuals showed significantly lower HIV-1 replication compared with $CCR5^+$ T cells from unvaccinated controls (56). Moreover, HIV replication was markedly reduced in T cells from people who were immunized with vaccina virus 6 months earlier, similar to the effect observed in cells recovered 3 months post vaccination (56). This prolonged effect on virus replication suggests that the mechanism is different to that observed during an active viral co-infection with measles or dengue fever virus, for example, which are known to competitively inhibit HIV replication (57, 58). In a follow-up study that investigated the non-specific effects of vaccination on protection against HIV replication, increased production of IL-8, MIP-1α and MIP-1β were detected in serum of people who had received multiple vaccinations (59). The authors concluded that the persistently elevated chemokines observed several months post vaccination may play a role in reducing viral replication in T cells from vaccinated people compared with unvaccinated controls (56, 59). Taken together, the evidence that vaccina virus induces trained immunity (51), together with the data demonstrating heterologous T cell immunity to HIV, and the associated role of chemokines, suggests that these phenomena may plausibly be linked.

These data suggest that vaccine or infection induced trained immunity and heterologous T cell immunity occur concomitantly and may be integrally linked, however, definitive evidence for this is yet to be established.

## THE CLINICAL SIGNIFICANCE OF THE LINK BETWEEN INNATE IMMUNE TRAINING AND T CELLS

While the clinical benefit of trained immunity in mediating protection against infection is clear, it is important to note that trained immunity may also induce inflammatory pathology (2, 60), in conditions known to involve the induction of pathogenic T cells. Increasing evidence is emerging in support of this hypothesis, as discussed below, however, a knowledge gap remains as to whether trained immunity affects the induction or propagation of pathological adaptive immune responses in different disease settings.

### Allergy

Food allergy is thought to be a disease of the adaptive immune system, however, there is emerging evidence for dysfunctional innate responses in allergy (61, 62), and a possible role for trained immunity in the development of allergy (63, 64). Infants who are allergic to eggs have increased frequencies of circulating monocytes (which express elevated HLA-DR), reduced numbers of Treg cells and an increased monocyte: CD4 T cell ratio compared with healthy controls (61). Interestingly, T cell-depleted PBMC isolated from egg allergic infants showed significantly increased production of TNF, IL-6, IL-8 and IL-1β in response to LPS stimulation compared with non-allergic controls (61). The increased production of TNF, IL-6, IL-8 and IL-1β by monocytes has been previously associated with a trained immunity phenotype (5, 6, 9, 65). Moreover, the

study compared allergic infants that had been subjected to an oral food challenge with those that did not and found no differences in concentrations of IL-6 or TNF in the serum. Consistent with this, the elevated LPS-induced cytokine production by T cell-depleted PBMC from egg-allergic infants were not significantly different on the day of oral food challenge or on a different day. We postulate that this may indicate a role for trained immunity during allergy. Since allergy is mediated by Th2 responses, a mechanistic role for trained immunity in the induction of Th2 cell mediated allergy remains to be determined. Given that the cytokines reported above are more likely to promote Th1 and Th17 responses, further work is required to determine the link, if any, between trained immunity and the induction of allergen-specific T cells. Interestingly, the authors also report significantly diminished IL-12p70 in allergic infants in resting CD3-depleted PBMC and those stimulated with LPS. Therefore, the purported trained immunity that causes increased TNF, IL-6, IL-8 and IL-1β in these infants while concomitantly decreasing IL-12p70 production compared with non-allergic controls may serve to skew the balance in favour of Th2 cells by the limiting Th1 differentiation induced by IL-12p70.

Studies in a murine asthma model have shown that infection with a murine gamma herpes virus (MuHV-4; **Table 1**) 30 days before induction of experimental asthma using house dust mite (HDM) induced a population of regulatory monocytes in lung that inhibited the development of experimental asthma (18). Virally infected mice had lower amounts of the pro-asthmatic innate cytokines IL-5, IL-13, IL-6 and IL-4 in their lungs compared with uninfected control mice (18). Cells isolated from the mediastinal lymph node had reduced proliferative capacity and had reduced production of IL-5, IL-13, IL-4, IL-6 and IL-10 relative to control mice, whereas IFN-γ production from these cells remained unchanged compared with the control, suggesting that the Th2 response, but not Th1 responses, was specifically affected by the infection with the virus (18).

The trained immunity induced by MuHV-4 resulted in reduced production of Th2 polarising cytokines from monocytes, leading to a decrease in Th2 activation and allergic inflammation. This provided strong evidence supporting a role for infection in the prevention of allergy, as postulated in the hygiene hypothesis.

These data suggest a role for trained immunity in influencing the pathogenic T cell responses observed during allergy. However, there is a lack of empirical evidence showing that trained immunity in innate cells modulates T cell responses during allergy.

## Atherosclerosis

Atherosclerosis is a chronic inflammatory disease of the arterial wall, mediated by CD4 T cells that recognise ox-LDL and are commonly found within atherosclerotic plaques (66, 67). Trained immunity has been proposed as an underlying driver of atherosclerosis (17, 68, 69). Ox-LDL enhances pro-inflammatory cytokine production and foam cell formation through the epigenetic reprogramming of monocytes (**Table 1**) (17, 70). While the role of monocytes in the pathogenesis of atherosclerosis has been well established, the mechanism behind persistent vascular inflammation has remained elusive. The long-lasting hyperinflammatory monocytes, which display epigenetic reprogramming following exposure to ox-LDL and increased capacity to produce IL-6, IL-8, TNF and MCP-1 upon restimulation with pathogen associated molecular patterns, provide a plausible mechanism for vascular inflammation. There is also evidence of an association between infection and atherosclerotic cardiovascular disease (ASCVD) (71, 72), and trained immunity is postulated to provide that mechanistic link (73).

Since T cells have an established role in the pathogenesis of atherosclerosis, it is plausible that the emerging role for trained immunity during ASCVD may potentiate pathogenic T cell responses. Conversely, pathogenic T cell responses may also serve to amplify trained immunity in monocytes; for example, IL-17A has been shown to increase the adhesion of monocytes to endothelial cells and increase the gene expression of IL-6 in monocytes during atherosclerosis (74). Direct evidence linking trained immunity to pathological T cell responses during ASCVD remains elusive.

## Rheumatoid Arthritis

The aetiology and pathogenesis of rheumatoid arthritis (RA), like most autoimmune disorders, is complex and remains unclear (75). The roles of pathogenic T cells with a loss of self-tolerance have been extensively studied in RA, but more recently the focus is increasingly on innate immune cells as drivers of this disease (76–80). It has already been proposed that trained immunity may have a role in the induction of RA (60, 81), with evidence that hyperplasia in the RA joint is mediated by epigenetic reprogramming (81).

McGarry and Hanlon et al. reported that $CD14^+$ monocytes in the peripheral blood of RA patients are metabolically reprogrammed towards glycolysis (82), a key feature of trained immunity (48, 65). Furthermore, when compared with healthy controls, monocytes from the blood of RA patients produced more TNF, IL-6 and IL-1β in response to LPS stimulation *in vitro* (82). These are key cytokines that are enhanced in cells that have undergone pro-inflammatory innate immune training with BCG or β-glucan (5, 6). The frequency of $CD14^+$ monocytes is also increased in the blood of RA patients compared with controls, indicative of enhanced myelopoiesis, which is also strongly associated with trained immunity (10, 24, 82). In the setting of established RA disease, the enhanced inflammatory function of monocytes may not be indicative of trained immunity, but it could also reflect chronic inflammation. To determine if these hyperinflammatory monocytes were a precipitating factor for inappropriate inflammation in people with RA, the study examined monocytes in people who were identified as being at increased risk of developing RA (82). The hyperinflammatory $CD14^+$ cell phenotype was present in these individuals at risk of developing RA, suggesting that this trained immunity phenotype may precede clinical signs of disease and may therefore be implicated in pathology (82). This study provides empirical evidence that monocytes in the circulation of people with established RA and in those at risk of developing RA are "primed" towards a hyper-inflammatory

and hyper-metabolic state, akin to that observed in monocytes that have undergone innate immune training. These data support the hypothesis that trained immunity may contribute to the pathogenesis of autoimmune inflammation, however; whether or not these hyperinflammatory monocytes promote autoimmune T cells responses remains unclear.

RA is a disease with a strong pathogenic T cell response, with plastic Th17-lineage cells implicated in the propagation of inflammation (29, 83). Since Th17 cell plasticity is directed by innate cytokines, trained immunity may have a key role in promoting pathological ex-Th17 cells. Interestingly both pathological Th17 lineage cells and monocytes displaying the features of trained immunity in RA patients are dependent on STAT3 signalling (82, 83). There is evidence that activated monocytes from the joints of patients with RA specifically promote Th17 cell responses, and this is mediated by elevated production TNF and IL-1β in the RA monocytes (84).

There is emerging evidence to suggest that trained immunity may be an underlying feature that promotes the pathogenic phenotype of the hyperinflammatory myeloid cells found in RA patients, and precedes the clinical diagnosis of RA (82). These innate immune responses may subsequently drive a pathogenic T cell response. We hypothesise that trained immunity may therefore contribute to the initiation of disease and the propagation of inappropriate inflammation during relapse.

Since autoimmune diseases more than double the risk of CVD, we postulate that this may be mediated by systemic trained immunity that precedes clinical onset of disease. However, the initial stimuli that induce trained immunity in this setting are unknown. Infectious agents, such EBV, cytomegalovirus (CMV) and *Escherichia coli* have been linked with the induction of RA, although their precise role remains elusive (75). This echoes the link between infectious burden and ASCVD, with trained immunity postulated as the common mechanism (73).

### Sepsis

Sepsis is one of the leading causes of preventable death (85). There is evidence that $CD4^+$ T helper cell responses are impaired during sepsis (86) and persistent failure of T cell activation in sepsis is associated with attenuated IFN-γ-producing $CD8^+$ cytotoxic T cells and Th17 cell responses (87).

Interestingly, the absence or reduction cell surface expression of the MHC-II molecule, HLA-DR, on monocytes is a common biomarker used to predict disease outcome (88, 89). Furthermore, low HLA-DR expression has been correlated with an impaired TNF response (89, 90).

LPS or endotoxin tolerance occurs in myeloid cells exposed to LPS, resulting in hypo-responsiveness to a second stimulation (7), and is often used to model sepsis. Endotoxin tolerance, although not considered to be a bona fide type of trained immunity, exhibits marked similarities with trained immunity including induction in the bone marrow and a distinct resting period between the primary and secondary stimulation for its generation (**Table 1**) (3). In addition, LPS-tolerized macrophages exhibit metabolic reprogramming that results in reduced glucose metabolism (91, 92), and tolerised monocytes have increased mitochondrial respiratory activity (93). The bone marrow cells of LPS-tolerised mice have decreased TNF production (14) and macrophages exhibit increased IL-10 production (15). This change in cytokine profile may promote the induction of Treg cells (94). This is in keeping with the finding that after the induction of sepsis, tolerant animals had significantly and persistently higher numbers of Treg cells (95). β-glucan has been shown to reverse the epigenetic state of LPS-induced immunological tolerance (16, 91, 96). Trained immunity induced by BCG, adenovirus or β-glucan has been shown to promote MHC-II expression and TNF production, providing further support that these training molecules may be promising therapeutic interventions in sepsis patients and may help to restore both innate and adaptive immunoparalysis.

In summary, defining the effect of trained immunity on T cell responses in discreet disease settings will be key to determining the clinical relevance of trained immunity in mediating protective or pathological immune responses. We acknowledge that identifying trained immunity and discriminating it from chronic inflammation or immune dysfunction is difficult in settings of clinically established disease. **Figure 2** summarises how different types of trained immunity may promote differential T cell responses and the disease context with which these are associated.

## CONCLUSIONS

In this review, we sought to examine the emerging evidence that trained immunity may affect and be affected by T cell responses. Recent studies have indicated that T cells play a role in modulating trained immunity and there is a clear rationale to support the hypothesis that innate immune training will affect adaptive responses *via* the modulation of innate proinflammatory cytokine production and APC function (**Table 1**). Knowledge gaps remain in understanding the impact of trained immunity on the adaptive immune response, both in settings of acute and chronic inflammation. More specifically, there is still limited information on how specific drivers of trained immunity may differentially affect subpopulations of T cells and disrupt the delicate Treg/Th17 or Th1/Th2 balance, for example. Conversely, understanding how certain populations of T cells regulate the induction of trained immunity may help to identify cell targets for therapeutic interventions. A direct cause and effect relationship between trained immunity and T cell responses remains to be determined, however, there is evidence from current literature, discussed in this review, to suggest that this relationship may exist, at least in the contexts of certain inflammatory conditions.

Although evidence is emerging to suggest that trained immunity may precipitate autoimmune, autoinflammatory and allergic diseases, BCG vaccination has been paradoxically associated with reduced risk of allergy and autoimmune disease (97–101). This raised the question of how trained immunity induced by different stimuli may result in divergent health or disease outcomes. Since T cells play a critical role in mediating pathological inflammation in these settings, the effects

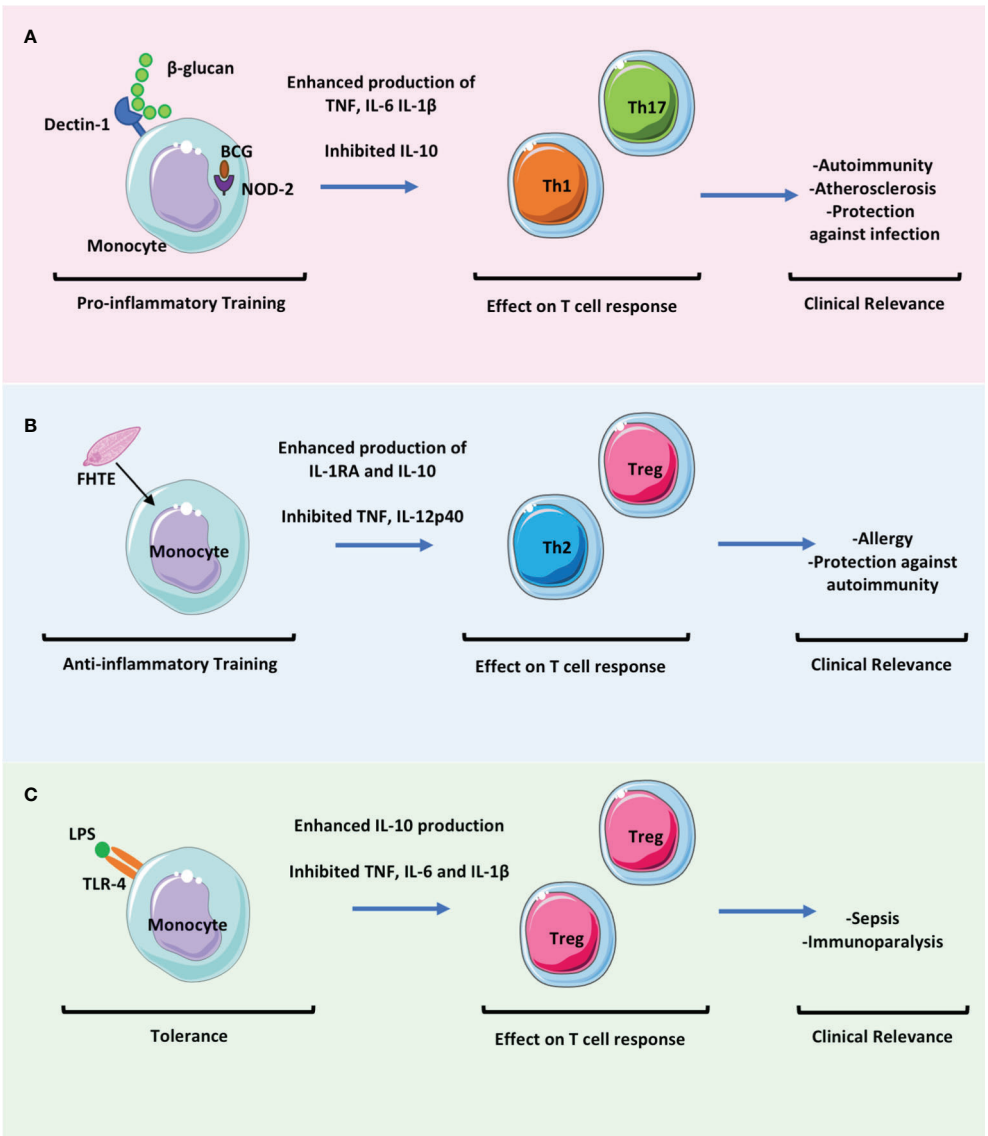


**FIGURE 2** | The effect of trained immunity on T cell responses will be key to determining the clinical relevance of trained immunity in mediating protection versus pathology. Trained immunity likely has an impact in many settings of infectious diseases and in immune mediated pathology. These clinically relevant effects may be mediated directly by the altered immune responses of myeloid cells but also indirectly by the effects of these myeloid cells on adaptive immune responses. **(A)** Trained immunity induced by β-glucan or BCG results in enhanced proinflammatory monocyte function which may promote the activation and differentiation of Th1 and Th17 cells whilst concomitantly downregulating Treg cell responses. This may be beneficial in promoting protection against infection but may be pathogenic in settings of immune mediated pathology such as in autoimmunity or atherosclerosis. **(B)** Fasciola hepatica total extract (FHTE) induces trained immunity which results in enhanced anti-inflammatory responses. This may be beneficial in attenuating autoimmune diseases but may promote cancer or allergy. **(C)** LPS induced trained immunity followed by restimulation with LPS results in tolerance. This induces Treg cells and is thought be pathological during sepsis.

of trained immunity on the T cell response may be a key to determining how the balance falls in favour of inflammation versus resolution in different settings.

Since protective and deleterious nonspecific effects of vaccines are associated with sex (46, 102–105), sex differences may be another key factor in determining outcomes of trained immunity. Interestingly, in a recent trained immunity study on healthy adults, BCG vaccination was associated with significantly reduced inflammatory markers in males only (106). This is in keeping with observations that neonatal BCG vaccination elicits a strong protective effect against all-cause mortality early in boys but later in girls (104). This is also consistent with the evidence that pre-term male neonates are at higher risk of mortality compared with their female counterparts (107). This trend follows through life, with males being more likely to die from sepsis than females (108, 109), an observation associated with altered ratios of proinflammatory IL-6 and anti-inflammatory IL-10. Conversely, females are at increased risk of developing

autoimmune disease, with a role for IFN-γ postulated to be central to this predisposition (110, 111). IFN-γ is produced by both innate and adaptive immune cells and plays a critical role in the induction of trained immunity (13, 25). Therefore, IFN-γ production may be a key determinant in inducing trained immunity in males and females. IFN-γ may also be a critical influence on the outcome of trained immunity; tipping the balance from protection to immune-mediated pathology.

The ability to induce trained immunity may change over a human lifetime. Since defects in immunity leave people uniquely susceptible to infections at the extremes of life, better understanding of how trained immunity can impact the immune response to infection in the very young and the very old will be critical to translating this knowledge towards the design of vaccines specifically for these vulnerable populations. It is noteworthy that the T cell repertoire is small in infancy and increases over time as lymphoid progenitor cells egress from the bone marrow and mature in the thymus. At the other extreme of the lifespan, the diversity of the T cell repertoire is reduced due to thymic involution and the predominance of clonally expanded populations due to previously encountered pathogens (112). This is thought to result in a shift to rely on innate immune cell function in the very young and the very old. Trained immunity has been implicated in processes driving 'inflammageing' and in age-associated neurodegenerative disease such as Alzheimer's disease (2, 113). Since a skewing of haematopoiesis occurs during trained immunity (12, 25), resulting in increased ratios of myelopoiesis to lymphopoieses, it is worthwhile considering how this may affect the T cell repertoire in the long-term. Further work elucidating the kinetics of these skewed ratios over time and what it means for lymphoid cell function will be critical, especially in infants who are forming a T cell repertoire in the thymus from cells that egress from the bone marrow. Conversely, trained immunity may serve as a necessary protective measure in infants to bridge the gap until the T cell repertoire is established.

We postulate that better understanding of the impact of trained immunity on adaptive immune responses will help to determine who benefits from different forms of immune memory; when, how and why.

## AUTHOR CONTRIBUTIONS

DM: conceptualisation, investigation, writing- original draft, and visualisation. KM: conceptualisation, writing- review and editing, and funding acquisition. SB: conceptualisation, investigation, writing -original draft, review and editing, and funding acquisition. All authors contributed to the article and approved the submitted version.

## FUNDING

HRB Emerging Investigator Award EIA-2019-010 (awarded to SB).

## REFERENCES

1. Netea MG, Quintin J, van der Meer JWM. Trained Immunity: A Memory for Innate Host Defense. *Cell Host Microbe* (2011) 9(5):355–61. doi: 10.1016/j.chom.2011.04.006
2. Netea MG, Domínguez-Andrés J, Barreiro LB, Chavakis T, Divangahi M, Fuchs E, et al. Defining Trained Immunity and its Role in Health and Disease. *Nat Rev Immunol* (2020) 20(6):375–88. doi: 10.1038/s41577-020-0285-6
3. Divangahi M, Aaby P, Khader SA, Barreiro LB, Bekkering S, Chavakis T, et al. Trained Immunity, Tolerance, Priming and Differentiation: Distinct Immunological Processes. *Nat Immunol* (2021) 22(1):2–6. doi: 10.1038/s41590-020-00845-6
4. Netea MG, Joosten LAB, Latz E, Mills KHG, Natoli G, Stunnenberg HG, et al. Trained Immunity: A Program of Innate Immune Memory in Health and Disease. *Science* (2016) 352(6284):aaf1098–aaf1098. doi: 10.1126/science.aaf1098
5. Kleinnijenhuis J, Quintin J, Preijers F, Joosten LAB, Ifrim DC, Saeed S, et al. Bacille Calmette-Guerin Induces NOD2-Dependent Nonspecific Protection From Reinfection via Epigenetic Reprogramming of Monocytes. *Proc Natl Acad Sci* (2012) 109(43):17537–42. doi: 10.1073/pnas.1202870109
6. Quintin J, Saeed S, Martens JHA, Giamarellos EJ, Ifrim DC, Logie C, et al. Candida Albicans Infection Affords Protection Against Reinfection via Functional Reprogramming of Monocytes. *Cell Host Microbe* (2012) 12 (2):223–32. doi: 10.1016/j.chom.2012.06.006
7. Seeley JJ, Ghosh S. Molecular Mechanisms of Innate Memory and Tolerance to LPS. *J Leukoc. Biol* (2017) 101(1):107–19. doi: 10.1189/jlb.3mr0316-118rr
8. Kleinnijenhuis J, Quintin J, Preijers F, Benn CS, Joosten LAB, Jacobs C, et al. Long-Lasting Effects of BCG Vaccination on Both Heterologous Th1/Th17 Responses and Innate Trained Immunity. *J Innate Immun* (2014) 6(2):152–8. doi: 10.1159/000355628
9. Arts RJW, Moorlag SJCFM, Novakovic B, Li Y, Wang SY, Oosting M, et al. BCG Vaccination Protects Against Experimental Viral Infection in Humans Through the Induction of Cytokines Associated With Trained Immunity. *Cell Host Microbe* (2018) 23(1):89–100.e5. doi: 10.1016/j.chom.2017.12.010
10. Moorlag SJCFM, Khan N, Novakovic B, Kaufmann E, Jansen T, van Crevel R, et al. β-Glucan Induces Protective Trained Immunity Against Mycobacterium Tuberculosis Infection: A Key Role for IL-1. *Cell Rep* (2020) 31(7):107634. doi: 10.1016/j.celrep.2020.107634
11. Quinn SM, Cunningham K, Raverdeau M, Walsh RJ, Curham L, Malara A, et al. Anti-Inflammatory Trained Immunity Mediated by Helminth Products Attenuates the Induction of T Cell-Mediated Autoimmune Disease. *Front Immunol* (2019) 10:1109(MAY). doi: 10.3389/fimmu.2019.01109
12. Cunningham KT, Finlay CM, Mills KHG. Helminth Imprinting of Hematopoietic Stem Cells Sustains Anti-Inflammatory Trained Innate Immunity That Attenuates Autoimmune Disease. *J Immunol* (2021) 206 (7):1618–30. doi: 10.4049/jimmunol.2001225
13. Yao Y, Jeyanathan M, Haddadi S, Barra NG, Vaseghi-Shanjani M, Damjanovic D, et al. Induction of Autonomous Memory Alveolar Macrophages Requires T Cell Help and Is Critical to Trained Immunity. *Cell* (2018) 175(6):1634–50. doi: 10.1016/j.cell.2018.09.042
14. Fitting C, Dhawan S, Cavaillon JM. Compartmentalization of Tolerance to Endotoxin. *J Infect Dis* (2004) 189(7):1295–303. doi: 10.1086/382657
15. Frankenberger M, Pechumer H, Ziegler-Heitbrock HWL. Interleukin-10 is Upregulated in LPS Tolerance. *J Inflamm* (1995) 45(1):56–63.
16. Novakovic B, Habibi E, Wang SY, Arts RJW, Davar R, Megchelenbrink W, et al. β-Glucan Reverses the Epigenetic State of LPS-Induced Immunological Tolerance. *Cell* (2016) 167(5):1354–68.e14. doi: 10.1016/j.cell.2016.09.034

17. Bekkering S, Quintin J, Joosten LAB, van der Meer JWM, Netea MG, Riksen NP. Oxidized Low-Density Lipoprotein Induces Long-Term Proinflammatory Cytokine Production and Foam Cell Formation via Epigenetic Reprogramming of Monocytes. *Arterioscler Thromb Vasc Biol* (2014) 34(8):1731–8. doi: 10.1161/ATVBAHA.114.303887
18. Machiels B, Dourcy M, Xiao X, Javaux J, Mesnil C, Sabatel C, et al. A Gammaherpesvirus Provides Protection Against Allergic Asthma by Inducing the Replacement of Resident Alveolar Macrophages With Regulatory Monocytes. *Nat Immunol* (2017) 18(12):1310–20. doi: 10.1038/ni.3857
19. Hole CR, Wager CML, Castro-Lopez N, Campuzano A, Cai H, Wozniak KL, et al. Induction of Memory-Like Dendritic Cell Responses *In Vivo*. *Nat Commun* (2019) 10(1):1–13. doi: 10.1038/s41467-019-10486-5
20. Kleinnijenhuis J, Quintin J, Preijers F, Joosten LAB, Jacobs C, Xavier RJ, et al. BCG-Induced Trained Immunity in NK Cells: Role for Non-Specific Protection to Infection. *Clin Immunol* (2014) 155(2):213–9. doi: 10.1016/j.clim.2014.10.005
21. Brillantes M, Beaulieu AM. Memory and Memory-Like NK Cell Responses to Microbial Pathogens. *Front Cell Infection Microbiol* (2020) 10:102. doi: 10.3389/fcimb.2020.00102
22. Romee R, Schneider SE, Leong JW, Chase JM, Keppel CR, Sullivan RP, et al. Cytokine Activation Induces Human Memory-Like NK Cells. *Blood* (2012) 120(24):4751–60. doi: 10.1182/blood-2012-04-419283
23. O'Leary JG, Goodarzi M, Drayton DL, von Andrian UH. T Cell- and B Cell-Independent Adaptive Immunity Mediated by Natural Killer Cells. *Nat Immunol* (2006) 7(5):507–16. doi: 10.1038/ni1332
24. Kaufmann E, Sanz J, Dunn JL, Khan N, Mendonça LE, Pacis A, et al. BCG Educates Hematopoietic Stem Cells to Generate Protective Innate Immunity Against Tuberculosis. *Cell* (2018) 172(1–2):176–90.e19. doi: 10.1016/j.cell.2017.12.031
25. Khan N, Downey J, Sanz J, Kaufmann E, Blankenhaus B, Pacis A, et al. M. Tuberculosis Reprograms Hematopoietic Stem Cells to Limit Myelopoiesis and Impair Trained Immunity. *Cell* (2020) 183(3):752–70.e22. doi: 10.1016/j.cell.2020.09.062
26. Mitroulis I, Ruppova K, Wang B, Chen LS, Grzybek M, Grinenko T, et al. Modulation of Myelopoiesis Progenitors Is an Integral Component of Trained Immunity. *Cell* (2018) 172(1–2):147–61.e12. doi: 10.1016/j.cell.2017.11.034
27. Jeljeli M, Riccio LGC, Doridot L, Chêne C, Nicco C, Chouzenoux S, et al. Trained Immunity Modulates Inflammation-Induced Fibrosis. *Nat Commun* (2019) 10:5670. doi: 10.1038/s41467-019-13636-x
28. Uchiyama R, Yonehara S, Taniguchi S, Ishido S, Ishii KJ, Tsutsui H. Inflammasome and Fas-Mediated IL-1β Contributes to Th17/Th1 Cell Induction in Pathogenic Bacterial Infection In Vivo. *J Immunol* (2017) 199(3):1122–30. doi: 10.4049/jimmunol.1601373
29. Basdeo SA, Cluxton D, Sulaimani J, Moran B, Canavan M, Orr C, et al. Ex-Th17 (Nonclassical Th1) Cells Are Functionally Distinct From Classical Th1 and Th17 Cells and Are Not Constrained by Regulatory T Cells. *J Immunol* (2017) 198(6):2249–59. doi: 10.4049/jimmunol.1600737
30. Hsu P, Santner-Nanan B, Hu M, Skarratt K, Lee CH, Stormon M, et al. IL-10 Potentiates Differentiation of Human Induced Regulatory T Cells *via* STAT3 and Foxo1. *J Immunol* (2015) 195(8):3665–74. doi: 10.4049/jimmunol.1402898
31. Santarlasci V, Cosmi L, Maggi L, Liotta F, Annunziato F. IL-1 and T Helper Immune Responses. *Front Immunol* (2013) 4:182. doi: 10.3389/fimmu.2013.00182
32. Zhu J. T Helper Cell Differentiation, Heterogeneity, and Plasticity. *Cold Spring Harb. Perspect Biol* (2018) 10(10):a030338. doi: 10.1101/cshperspect.a030338
33. Fletcher JM, Lalor SJ, Sweeney CM, Tubridy N, Mills KHG. T Cells in Multiple Sclerosis and Experimental Autoimmune Encephalomyelitis. *Clin Exp Immunol* (2010) 162(1):1–11. doi: 10.1111/j.1365-2249.2010.04143.x
34. Mongkolsapaya J, et al. T Cell Responses in Dengue Hemorrhagic Fever: Are Cross-Reactive T Cells Suboptimal? *J Immunol* (2006) 176(6):3821–9. doi: 10.4049/jimmunol.176.6.3821
35. Aslan N, Watkin LB, Gil A, Mishra R, Clark FG, Welsh FM, et al. Severity of Acute Infectious Mononucleosis Correlates With Cross-Reactive Influenza CD8 T-Cell Receptor Repertoires. *MBio* (2017) 8(6):e01841–17. doi: 10.1128/mBio.01841-17
36. Clute SC, et al. Cross-Reactive Influenza Virus-Specific CD8+ T Cells Contribute to Lymphoproliferation in Epstein-Barr Virus-Associated Infectious Mononucleosis. *J Clin Invest*. (2005) 115(12):3602–12. doi: 10.1172/JCI25078
37. Petrova G, Ferrante A, Gorski J. Cross-Reactivity of T Cells and its Role in the Immune System. *Crit Rev Immunol* (2012) 32(4):349–72. doi: 10.1615/CritRevImmunol.v32.i4.50
38. Tough DF, Borrow P, Sprent J. Induction of Bystander T Cell Proliferation by Viruses and Type I Interferon *In Vivo*. *Science* (1996) 272(5270):1947–50. doi: 10.1126/science.272.5270.1947
39. Tough DF, Sun S, Sprent J. T Cell Stimulation In Vivo by Lipopolysaccharide (LPS). *J Exp Med* (1997) 185(12):2089–94. doi: 10.1084/jem.185.12.2089
40. Gilbertson B, Germano S, Steele P, Turner S, Barbara BF, Cheers C. Bystander Activation of CD8+ T Lymphocytes During Experimental Mycobacterial Infection. *Infect Immun* (2004) 72(12):6884–91. doi: 10.1128/IAI.72.12.6884-6891.2004
41. Raué H-P, Brien JD, Hammarlund E, Slifka MK. Activation of Virus-Specific CD8 + T Cells by Lipopolysaccharide-Induced IL-12 and IL-18. *J Immunol* (2004) 173(11):6873–81. doi: 10.4049/jimmunol.173.11.6873
42. Tough DF, Zhang X, Sprent J. An IFN-γ-Dependent Pathway Controls Stimulation of Memory Phenotype CD8 + T Cell Turnover In Vivo by IL-12, IL-18, and IFN-γ. *J Immunol* (2001) 166(10):6007–11. doi: 10.4049/jimmunol.166.10.6007
43. Lalor SJ, Dungan LS, Sutton CE, Basdeo SA, Fletcher JM, Mills KHG. Caspase-1–Processed Cytokines IL-1β and IL-18 Promote IL-17 Production by γδ and CD4 T Cells That Mediate Autoimmunity. *J Immunol* (2011) 186(10):5738–48. doi: 10.4049/jimmunol.1003597
44. Walzl G, Tafuro S, Moss P, Openshaw PJM, Hussell T. Influenza Virus Lung Infection Protects From Respiratory Syncytial Virus-Induced Immunopathology. *J Exp Med* (2000) 192(9):1317–26. doi: 10.1084/jem.192.9.1317
45. Biering-Sørensen S, Aaby P, Napirna BM, Roth A, Ravn H, Rodrigues A, et al. Small Randomized Trial Among Low-Birth-Weight Children Receiving Bacillus Calmette-Guéerin Vaccination at First Health Center Contact. *Pediatr Infect Dis J* (2012) 31(3):306–8. doi: 10.1097/INF.0b013e3182458289
46. Roth A, Sodemann M, Jensen H, Poulsen A, Gustafson P, Weise C, et al. Tuberculin Reaction, BCG Scar, and Lower Female Mortality. *Epidemiology* (2006) 17(5):562–8. doi: 10.1097/01.ede.0000231546.14749.ab
47. Mathurin KS, Martens GW, Kornfeld H, Welsh RM. CD4 T-Cell-Mediated Heterologous Immunity Between Mycobacteria and Poxviruses. *J Virol* (2009) 83(8):3528–39. doi: 10.1128/jvi.02393-08
48. Arts RJW, et al. Immunometabolic Pathways in BCG-Induced Trained Immunity. *Cell Rep* (2016) 17(10):2562–71. doi: 10.1016/j.celrep.2016.11.011
49. Mayr A. Taking Advantage of the Positive Side-Effects of Smallpox Vaccination. *J Vet Med Ser B* (2004) 51(5):199–201. doi: 10.1111/j.1439-0450.2004.00763.x
50. Sørup S, et al. Smallpox Vaccination and All-Cause Infectious Disease Hospitalization: A Danish Register-Based Cohort Study. *Int J Epidemiol.* (2011) 40(4):955–63. doi: 10.1093/ije/dyr063
51. Blok BA, Arts RJW, van Crevel R, Benn CS, Netea MG. Trained Innate Immunity as Underlying Mechanism for the Long-Term, Nonspecific Effects of Vaccines. *J Leukoc. Biol* (2015) 98(3):347–56. doi: 10.1189/jlb.5ri0315-096r
52. Scherer CA, et al. Distinct Gene Expression Profiles in Peripheral Blood Mononuclear Cells From Patients Infected With Vaccinia Virus, Yellow Fever 17D Virus, or Upper Respiratory Infections. *Vaccine* (2007) 25(35):6458–73. doi: 10.1016/j.vaccine.2007.06.035
53. Jensen ML, Dave S, van der Loeff MS, da Costa C, Vincent T, Leligdowicz A, et al. Vaccinia Scars Associated With Improved Survival Among Adults in Rural Guinea-Bissau. *PloS One* (2006) 1(1):e101. doi: 10.1371/journal.pone.0000101
54. Kristensen I, Aaby P, Jensen H. Routine Vaccinations and Child Survival: Follow Up Study in Guinea-Bissau, West Africa. *BMJ* (2000) 321(7274):1435–8. doi: 10.1136/bmj.321.7274.1435
55. Rieckmann A, Villumsen M, Sørup S, Haugaard LK, Ravn H, Roth A, et al. Vaccinations Against Smallpox and Tuberculosis are Associated With Better Long-Term Survival: A Danish Case-Cohort Study 1971-2010. *Int J Epidemiol* (2017) 46(2):695–705. doi: 10.1093/ije/dyw120

56. Weinstein RS, Weinstein MM, Alibek K, Bukrinsky MI, Brichacek B. Significantly Reduced CCR5-Tropic HIV-1 Replication In Vitro in Cells From Subjects Previously Immunized With Vaccinia Virus. *BMC Immunol* (2010) 11:23. doi: 10.1186/1471-2172-11-23
57. Moss WJ, Ryon JJ, Monze M, Cutts F, Quinn TC, Griffin DE. Suppression of Human Immunodeficiency Virus Replication During Acute Measles. *J Infect Dis* (2002) 185(8):1035–42. doi: 10.1086/340027
58. Watt G, Kantipong P, Jongsakul K. Decrease in Human Immunodeficiency Virus Type 1 Load During Acute Dengue Fever. *Clin Infect Dis* (2003) 36 (8):1067–9. doi: 10.1086/374600
59. Brichacek B, et al. Long-Term Changes of Serum Chemokine Levels in Vaccinated Military Personnel. *BMC Immunol* (2006) 7(1):1–6. doi: 10.1186/1471-2172-7-21
60. Arts RJW, Joosten LAB, Netea MG. The Potential Role of Trained Immunity in Autoimmune and Autoinflammatory Disorders. *Front Immunol* (2018) 9:298. doi: 10.3389/fimmu.2018.00298
61. Neeland MR, Koplin JJ, Dang TD, Dharmage SC, Tang ML, Prescott SL, et al. Early Life Innate Immune Signatures of Persistent Food Allergy. *J Allergy Clin Immunol* (2018) 142(3):857–64.e3. doi: 10.1016/j.jaci.2017.10.024
62. Zhang GQ, Hu HJ, Liu CY, Zhang Q, Shakya S, Li ZY. Probiotics for Prevention of Atopy and Food Hypersensitivity in Early Childhood A PRISMA-Compliant Systematic Review and Meta-Analysis of Randomized Controlled Trials. *Med (United States)* (2016) 95(8). doi: 10.1097/MD.0000000000002562
63. Imran S, Neeland MR, Shepherd R, Messina N, Perrett KP, Netea MG, et al. A Potential Role for Epigenetically Mediated Trained Immunity in Food Allergy. *iScience* (2020) 23(6):101171. doi: 10.1016/j.isci.2020.101171
64. Martino DJ, Prescott SL. Silent Mysteries: Epigenetic Paradigms Could Hold the Key to Conquering the Epidemic of Allergy and Immune Disease. *Allergy: Eur J Allergy Clin Immunol* (2010) 65(1):7–15. doi: 10.1111/j.1398-9995.2009.02186.x
65. Cheng SC, Quintin J, Cramer RA, Shepardson KM, Saeed S, Kumar V, et al. MTOR- and HIF-1α-Mediated Aerobic Glycolysis as Metabolic Basis for Trained Immunity. *Science* (2014) 345(6204). doi: 10.1126/science.1250684
66. Saigusa R, Winkels H, Ley K. T Cell Subsets and Functions in Atherosclerosis. *Nat Rev Cardiol* (2020) 17(7):387–401. doi: 10.1038/s41569-020-0352-5
67. Stemme S, Faber B, Holm J, Wiklund O, Witztum JL, Hansson GK. T Lymphocytes From Human Atherosclerotic Plaques Recognize Oxidized Low Density Lipoprotein. *Proc Natl Acad Sci USA* (1995) 92(9):3893–7. doi: 10.1073/pnas.92.9.3893
68. Riksen NP. Trained Immunity and Atherosclerotic Cardiovascular Disease. *Curr Opin Lipidol.* (2019) 30(5):395–400. doi: 10.1097/MOL.0000000000000628
69. Zhong C, Yang X, Feng Y, Yu J. Trained Immunity: An Underlying Driver of Inflammatory Atherosclerosis. *Front Immunol* (2020) 11:284. doi: 10.3389/fimmu.2020.00284
70. Christ A, Günther P, Lauterbach MAR, Duewell P, Biswas D, Pelka K, et al. Western Diet Triggers NLRP3-Dependent Innate Immune Reprogramming. *Cell* (2018) 172(1–2):162–75.e14. doi: 10.1016/j.cell.2017.12.013
71. Pothineni NVK, Subramany S, Kuriakose K, Shirazi LF, Romeo F, Shah PK, et al. Infections, Atherosclerosis, and Coronary Heart Disease. *Eur Heart J* (2017) 38(43):3195–201. doi: 10.1093/eurheartj/ehx362
72. Corrales-Medina VF, Musher DM, Shachkina S, Chirinos JA. Acute Pneumonia and the Cardiovascular System. *Lancet* (2013) 381(9865):496–505. doi: 10.1016/S0140-6736(12)61266-5
73. Leentjens J, Bekkering S, Joosten LAB, Netea MG, Burgner DP, Riksen NP. Trained Innate Immunity as a Novel Mechanism Linking Infection and the Development of Atherosclerosis. *Circ Res* (2018) 122(5):664–9. doi: 10.1161/CIRCRESAHA.117.312465
74. Erbel C, Akhavanpoor M, Okuyucu D, Wangler S, Dietz A, Zhao L, et al. IL-17a Influences Essential Functions of the Monocyte/Macrophage Lineage and Is Involved in Advanced Murine and Human Atherosclerosis. *J Immunol* (2014) 93(9):4344–55. doi: 10.4049/jimmunol.1400181
75. Mcinnes IB, Schett G. The Pathogenesis of Rheumatoid Arthritis. *N Engl J Med* (2011) 365(23):2205–19. doi: 10.1056/NEJMra1004965
76. Waldner H. The Role of Innate Immune Responses in Autoimmune Disease Development. *Autoimmun Rev* (2009) 8(5):400–4. doi: 10.1016/j.autrev.2008.12.019
77. Theofilopoulos AN, Gonzalez-Quintial R, Lawson BR, Koh YT, Stern ME, Kono DH, et al. Sensors of the Innate Immune System: Their Link to Rheumatic Diseases. *Nat Rev Rheumatol* (2010) 6(3):146–56. doi: 10.1038/nrrheum.2009.278
78. Stuhlmüller B, Ungethüm U, Scholze S, Martinez L, Backhaus M, Kraetsch HG, et al. Identification of Known and Novel Genes in Activated Monocytes From Patients With Rheumatoid Arthritis. *Arthritis Rheumatol* (2000) 43(4):775–90. doi: 10.1002/1529-0131(200004)43:4<775::AID-ANR8>3.0.CO;2-7
79. Häupl T, ØStensen M, Grützkau A, Radbruch A, Burmester G-R, Villiger PM. Reactivation of Rheumatoid Arthritis After Pregnancy: Increased Phagocyte and Recurring Lymphocyte Gene Activity. *Arthritis Rheumatol* (2008) 58(10):2981–92. doi: 10.1002/art.23907
80. Lioté F, Boval-Boizard B, Weill D, Kuntz D, Wautier JL. Blood Monocyte Activation in Rheumatoid Arthritis: Increased Monocyte Adhesiveness, Integrin Expression, and Cytokine Release. *Clin Exp Immunol* (1996) 106 (1):13–9. doi: 10.1046/j.1365-2249.1996.d01-820.x
81. Włodarczyk M, Druszczyńska M, Fol M. Trained Innate Immunity Not Always Amicable. *Int J Mol Sci* (2019) 20(10):2565. doi: 10.3390/ijms20102565
82. McGarry T, Hanlon MM, Marzaioli V, Cunningham CC, Krishna V, Murray K, et al. Rheumatoid Arthritis CD14 + Monocytes Display Metabolic and Inflammatory Dysfunction, A Phenotype That Precedes Clinical Manifestation of Disease. *Clin Transl Immunol* (2021) 10(1):e1237. doi: 10.1002/cti2.1237
83. Basdeo SA, Moran B, Cluxton D, Canavan M, McCormick J, Connolly M, et al. Polyfunctional, Pathogenic CD161 + Th17 Lineage Cells Are Resistant to Regulatory T Cell–Mediated Suppression in the Context of Autoimmunity. *J Immunol* (2015) 195(2):528–40. doi: 10.4049/jimmunol.1402990
84. Evans HG, Gullick NJ, Kelly S, Pitzalis C, Lord GM, Kirkham BW, et al. In Vivo Activated Monocytes From the Site of Inflammation in Humans Specifically Promote Th17 Responses. *Proc Natl Acad Sci USA* (2009) 106(15):6232–7. doi: 10.1073/pnas.0808144106
85. Ryan T, Coakley JD, Martin-Loeches I. Defects in Innate and Adaptive Immunity in Patients With Sepsis and Health Care Associated Infection. *Ann Trans Med* (2017) 5(22):447. doi: 10.21037/atm.2017.09.21
86. Cabrera-Perez J, Condotta SA, Badovinac VP, Griffith TS. Impact of Sepsis on CD4 T Cell Immunity. *J Leukoc Biol* (2014) 96(5):767–77. doi: 10.1189/jlb.5mr0114-067r
87. Coakley JD, Breen EP, Moreno-Olivera A, Al-Harbi AI, Melo AM, O'Connell B, et al. Dysregulated T Helper Type 1 (Th1) and Th17 Responses in Elderly Hospitalised Patients With Infection and Sepsis. *PloS One* (2019) 14(10):e0224276. doi: 10.1371/journal.pone.0224276
88. Lekkou A, Karakantza M, Mouzaki A, Kalfarentzos F, Gogos CA. Cytokine Production and Monocyte HLA-DR Expression as Predictors of Outcome for Patients With Community-Acquired Severe Infections. *Clin Diagn. Lab Immunol* (2004) 11(1):161–7. doi: 10.1128/CDLI.11.1.161-167.2004
89. Winkler MS, Rissiek A, Priefler M, Schwedhelm E, Robbe L, Bauer A, et al. Human Leucocyte Antigen (HLA-DR) Gene Expression Is Reduced in Sepsis and Correlates With Impaired Tnfα Response: A Diagnostic Tool for Immunosuppression? *PloS One* (2017) 12(8):e0182427. doi: 10.1371/journal.pone.0182427
90. Grealy R, White M, Stordeur P, Kelleher D, Doherty DG, McManus R, et al. Characterising Cytokine Gene Expression Signatures in Patients With Severe Sepsis. *Mediators Inflamm* (2013) 2013:164246. doi: 10.1155/2013/164246
91. Cheng SC, Scicluna BP, Arts RJW, Gresnigt MS, Lachmandas E, Giamarellos-Bourboulis EJ, et al. Broad Defects in the Energy Metabolism of Leukocytes Underlie Immunoparalysis in Sepsis. *Nat Immunol* (2016) 17 (4):406–13. doi: 10.1038/ni.3398
92. Lang CH, Bagby GJ, Spitzer JJ. Glucose Kinetics and Body Temperature After Lethal and Nonlethal Doses of Endotoxin. *Am J Physiol - Regul Integr Comp Physiol* (1985) 248(4 Pt 2):R471–8. doi: 10.1152/ajpregu.1985.248.4.r471
93. Widdrington JD, Gomez-Duran A, Pyle A, Ruchaud-Sparagano MH, Scott J, Baudouin SV, et al. Exposure of Monocytic Cells to Lipopolysaccharide

Induces Coordinated Endotoxin Tolerance, Mitochondrial Biogenesis, Mitophagy, and Antioxidant Defenses. *Front Immunol* (2018) 9:2217. doi: 10.3389/fimmu.2018.02217
94. Patente TA, Pelgrom LR, Everts B. Dendritic Cells are What They Eat: How Their Metabolism Shapes T Helper Cell Polarization. *Curr Opin Immunol* (2019) 58:16–23. doi: 10.1016/j.coi.2019.02.003
95. Andrade MMC, Ariga SSK, Barbeiro DF, Barbeiro HV, Pimentel RN, Petroni RC, et al. Endotoxin Tolerance Modulates TREG and TH17 Lymphocytes Protecting Septic Mice. *Oncotarget* (2019) 10(37):3451–61. doi: 10.18632/oncotarget.26919
96. Domínguez-Andrés J, Novakovic B, Li Y, Scicluna BP, Gresnigt MS, Arts RJW, et al. The Itaconate Pathway Is a Central Regulatory Node Linking Innate Immune Tolerance and Trained Immunity. *Cell Metab* (2019) 29 (1):211–20.e5. doi: 10.1016/j.cmet.2018.09.003
97. Aaby P, Shaheen SO, Heyes CB, Goudiaby A, Hall AJ, Shiell AW, et al. Early BCG Vaccination and Reduction in Atopy in Guinea-Bissau. *Clin Exp Allergy* (2000) 30(5):644–50. doi: 10.1046/j.1365-2222.2000.00803.x
98. Marks GB, Ng K, Zhou J, Toelle BG, Xuan W, Belousova EG, et al. The Effect of Neonatal BCG Vaccination on Atopy and Asthma at Age 7 to 14 Years: An Historical Cohort Study in a Community With a Very Low Prevalence of Tuberculosis Infection and a High Prevalence of Atopic Disease. *J Allergy Clin Immunol* (2003) 111(3):541–9. doi: 10.1067/mai.2003.171
99. Kowalewicz-Kulbat M, Locht C. BCG and Protection Against Inflammatory and Auto-Immune Diseases. *Expert Rev Vaccines* (2017) 16(7):699–708. doi: 10.1080/14760584.2017.1333906
100. Steenhuis TJ, Van Aalderen WMC, Bloksma N, Nijkamp FP, Van Der Laag J, Van Loveren H, et al. Bacille-Calmette-Guerin Vaccination and the Development of Allergic Disease in Children: A Randomized, Prospective, Single-Blind Study. *Clin Exp Allergy* (2008) 38(1):79–85. doi: 10.1111/j.1365-2222.2007.02859.x
101. Thøstesen LM, Kjærgaard J, Pihl GT, Birk NM, Nissen TN, Aaby P, et al. Neonatal BCG Vaccination and Atopic Dermatitis Before 13 Months of Age: A Randomized Clinical Trial. *Allergy Eur J Allergy Clin Immunol* (2018) 73 (2):498–504. doi: 10.1111/all.13314
102. Stensballe LG, Nante E, Jensen IP, Kofoed PE, Poulsen A, Jensen H, et al. Acute Lower Respiratory Tract Infections and Respiratory Syncytial Virus in Infants in Guinea-Bissau: A Beneficial Effect of BCG Vaccination for Girls: Community Based Case-Control Study. *Vaccine* (2005) 23(10):1251–7. doi: 10.1016/j.vaccine.2004.09.006
103. Garly ML, Jensen H, Martins CL, Balé C, Baldé MA, Lisse IM, et al. Hepatitis B Vaccination Associated With Higher Female Than Male Mortality in Guinea-Bissau: An Observational Study. *Pediatr Infect Dis J* (2004) 23 (12):1086–92. doi: 10.1097/01.inf.0000145700.77286.94
104. Biering-Sørensen S, Jensen KJ, Monterio I, Ravn H, Aaby P, Benn CS. Rapid Protective Effects of Early BCG on Neonatal Mortality Among Low Birth Weight Boys: Observations From Randomized Trials. *J Infect Dis* (2018) 217 (5):759–66. doi: 10.1093/infdis/jix612
105. Aaby P, Ravn H, Fisker AB, Rodrigues A, Benn CS. Is Diphtheria-Tetanus-Pertussis (DTP) Associated With Increased Female Mortality? A Meta-Analysis Testing the Hypotheses of Sex-Differential Non-Specific Effects of DTP Vaccine. *Trans R Soc Trop Med Hyg* (2016) 110(10):570–81. doi: 10.1093/trstmh/trw073
106. Koeken VACM, Charlotte L, Mourits VP, Moorlag SJCFM, Walk J, Cirovic B, et al. BCG Vaccination in Humans Inhibits Systemic Inflammation in a Sex-Dependent Manner. *J Clin Invest* (2020) 130(10):5591–602. doi: 10.1172/JCI133935
107. O'Driscoll DN, McGovern M, Greene CM, Molloy EJ. Gender Disparities in Preterm Neonatal Outcomes. *Acta Paediatrica Int J Paediatrics* (2018) 107 (9):1494–9. doi: 10.1111/apa.14390
108. Nasir N, Jamil B, Siddiqui S, Talat N, Khan FA, Hussain R. Mortality in Sepsis and its Relationship With Gender. *Pakistan J Med Sci* (2015) 31 (5):1201–6. doi: 10.12669/pjms.315.6925
109. Schröder J, Kahlke V, Staubach KH, Zabel P, Stüber F. Gender Differences in Human Sepsis. *Arch Surg* (1998) 133(11):1200. doi: 10.1001/archsurg.133.11.1200
110. Bae HR, Leung PSC, Tsuneyama K, Valencia JC, Hodge DL, Kim S, et al. Chronic Expression of Interferon-Gamma Leads to Murine Autoimmune Cholangitis With a Female Predominance. *Hepatology* (2016) 64(4):1189–201. doi: 10.1002/hep.28641
111. Green DS, Young HA, Valencia JC. Current Prospects of Type II Interferon γ Signaling & Autoimmunity. *J Biol Chem* (2017) 292(34):13925–33. doi: 10.1074/jbc.R116.774745
112. Egorov ES, Kasatskaya SA, Zubov VN, Izraelson M, Nakonechnaya TO, Staroverov DB, et al. The Changing Landscape of Naive T Cell Receptor Repertoire With Human Aging. *Front Immunol* (2018) 9:1618. doi: 10.3389/fimmu.2018.01618
113. Salani F, Sterbini V, Sacchinelli E, Garramone M, Bossù P. Is Innate Memory a Double-Edge Sword in Alzheimer's Disease? A Reappraisal of New Concepts and Old Data. *Front Immunol* (2019) 10:1768. doi: 10.3389/fimmu.2019.01768

**Conflict of Interest:** The authors declare that the research was conducted in the absence of any commercial or financial relationships that could be construed as a potential conflict of interest.

**Publisher's Note:** All claims expressed in this article are solely those of the authors and do not necessarily represent those of their affiliated organizations, or those of the publisher, the editors and the reviewers. Any product that may be evaluated in this article, or claim that may be made by its manufacturer, is not guaranteed or endorsed by the publisher.

frontiers in Immunology

ORIGINAL RESEARCH
published: 09 September 2021
doi: 10.3389/fimmu.2021.728669

# CD49a Identifies Polyfunctional Memory CD8 T Cell Subsets that Persist in the Lungs After Influenza Infection

*Emma C. Reilly[1†], Mike Sportiello[1†], Kris Lambert Emo[1], Andrea M. Amitrano[1], Rakshanda Jha[1], Ashwin B. R. Kumar[1], Nathan G. Laniewski[1,2], Hongmei Yang[3], Minsoo Kim[1,4] and David J. Topham[1,4*]*

[1] Center for Vaccine Biology and Immunology, University of Rochester Medical Center, Rochester, NY, United States, [2] Department of Pediatrics, University of Rochester Medical Center, Rochester, NY, United States, [3] Department of Biostatistics and Computational Biology, University of Rochester Medical Center, Rochester, NY, United States, [4] Department of Microbiology and Immunology, University of Rochester Medical Center, Rochester, NY, United States

OPEN ACCESS

**Edited by:**
*Shahram Salek-Ardakani, Pfizer, United States*

**Reviewed by:**
*Georges Abboud, University of Florida, United States*
*Ross M. Kedl, University of Colorado Denver, United States*

***Correspondence:**
*David J. Topham*
*david_topham@urmc.rochester.edu*

*[†]These authors have contributed equally to this work*

**Specialty section:**
*This article was submitted to Immunological Memory, a section of the journal Frontiers in Immunology*

**Received:** *21 June 2021*
**Accepted:** *23 August 2021*
**Published:** *09 September 2021*

**Citation:**
*Reilly EC, Sportiello M, Emo KL, Amitrano AM, Jha R, Kumar ABR, Laniewski NG, Yang H, Kim M and Topham DJ (2021) CD49a Identifies Polyfunctional Memory CD8 T Cell Subsets that Persist in the Lungs After Influenza Infection. Front. Immunol. 12:728669. doi: 10.3389/fimmu.2021.728669*

CD8 T cell memory offers critical antiviral protection, even in the absence of neutralizing antibodies. The paradigm is that CD8 T cell memory within the lung tissue consists of a mix of circulating $T_{EM}$ cells and non-circulating $T_{RM}$ cells. However, based on our analysis, the heterogeneity within the tissue is much higher, identifying $T_{CM}$, $T_{EM}$, $T_{RM}$, and a multitude of populations which do not perfectly fit these classifications. Further interrogation of the populations shows that $T_{RM}$ cells that express CD49a, both with and without CD103, have increased and diverse effector potential compared with CD49a negative populations. These populations function as a one-man band, displaying antiviral activity, chemokine production, release of GM-CSF, and the ability to kill specific targets *in vitro* with delayed kinetics compared with effector CD8 T cells. Together, this study establishes that CD49a defines multiple polyfunctional CD8 memory subsets after clearance of influenza infection, which act to eliminate virus in the absence of direct killing, recruit and mature innate immune cells, and destroy infected cells if the virus persists.

**Keywords: resident memory $T_{RM}$, viral immunology, influenza A virus, CD49a, polyfunctionality, CD8 T cells, CD103**

## INTRODUCTION

CD8 T cell memory is critical for host protection from previously encountered and related pathogens (1, 2). After the primary exposure to antigen, multiple classes of memory T cells develop, including circulating ($T_{CM}$ and $T_{EM}$) and resident ($T_{RM}$) populations (3–5). $T_{RM}$ are heralded for their ability to rapidly respond upon instances of reinfection, limiting disease severity and improving survival (2, 6–8). They are predominantly observed at epithelial barrier surfaces of non-lymphoid tissues, maintained in close proximity to the cells often targeted by viruses (2, 8). This memory population has been described in many organs including, but not limited to skin, intestines, lung, female reproductive tract, salivary glands, and tonsils (9–14).

$T_{RM}$ express a range of surface markers, which promote their persistence within the site and facilitate direct interaction with the tissue (15–17). These include CD69, an S1PR1 antagonist, CD103/integrin β7, an integrin that attaches to the E-cadherin junction protein between epithelial cells, and CD49a/CD29, a collagen binding integrin (18–21). The requirement for these surface receptors differs between organs, with CD69 playing critical roles in the development and maintenance of kidney $T_{RM}$, but with less reliance in other sites including lung (15, 22). CD103 contributes to the accumulation of $T_{RM}$ early during the resolution phase, with minimal effects on long term persistence in the intestines, salivary glands, and lung, though maintained expression may be critical in other organs or for functions other than retention within the tissue (12, 15, 22, 23). A dependence on CD49a for the survival of $T_{RM}$ and subsequent protection has been demonstrated in the pulmonary system and intestines, and a role for increased effector capacity has been shown in both skin and tumor $T_{RM}$ (13, 24–26). The observed heterogeneity in the surface phenotype of $T_{RM}$ in different organs is likely driven by microenvironmental differences and the composition of the immune response elicited by the infecting pathogen.

One of the main immune contributors to these differences is the cytokine milieu that results from infection and resolution. TGFβ is known to mediate expression of CD103 and CD49a and a role for IL-12 in promoting surface CD49a while limiting CD103 has been demonstrated *in vitro* (27, 28). While it makes sense that differences exist between organs, variations in features including the immune cell composition, cytokine levels and antigen load also differ within discrete niches in a given organ. With this understanding, we hypothesized that the population of cells in the lungs referred to as $T_{RM}$, which arises after resolution of influenza A virus infection, actually represents a heterogenous mix of multiple subpopulations. To address this, surface phenotyping and RNAseq analyses were performed after resolution of disease in the presence or absence of stimulation. Within these memory populations, the question still remained as to whether certain populations display higher effector capabilities. Using a combination of RNAseq and flow cytometry, this study set out to determine which memory cell(s) offer the most potent protection potential during secondary encounter with antigen.

# MATERIALS AND METHODS

## Mice

All mice were housed in university-approved microisolator cages, within a pathogen-free facility. C57BL/6J mice (Jackson Laboratories) used for experiments were infected at 8-10 weeks of age. This study was carried out in strict accordance with the recommendations in the *Guide for the Care and Use of Laboratory Animals* as defined by the NIH (29). Animal protocols were reviewed and approved by the Institutional Animal Care and Use Committee of the University of Rochester. All animals were housed in a centralized and Association for Assessment and Accreditation of Laboratory Animal Care accredited research animal facility that is fully staffed with trained husbandry, technical, and veterinary personnel.

## Virus and Infection

Mice were anesthetized with 3,3,3-tribromoethanol (Avertin). Upon verification of sedation, mice were placed in the supine position and infected intranasally with $10^5$ $EID_{50}$ of HKx31 human influenza A virus or $3x10^3$ $EID_{50}$ HKx31-OVAI expressing the $OVA^{257-264}$ SIINFEKL peptide in the stalk of the neuraminidase in 30uL volume. Mice were observed until they recovered from anesthesia and monitored daily for weight and overall morbidity.

## Tissue Harvesting and Processing

Mice were anesthetized with Avertin and upon sedation mice were injected intravenously with 0.2ug labeled CD45 antibody in 100uL sterile 1x PBS (30). For **Figures 2–7**, after 3 minutes, the peritoneal cavity was opened, the aorta was cut, and the lungs were harvested. For **Figure 1**, bronchoalveolar lavage (BAL) and cardiac puncture were performed prior to opening the peritoneal cavity and the organs were harvested in the following order: spleen, MLN, lung. BAL and blood cells were spun down at 300xg for 6 minutes, lysed with 0.5mL or 3mL, respectively 1x ammonium-chloride-potassium (ACK) lysis buffer for 5 minutes at room temperature, and washed with 14mLs 1x PBS with 1% FBS (PBS serum). Spleen and MLN were dissociated using the frosted ends of frosted glass slides. These samples were put through 100um filters and spun at 300xg for 6 minutes, followed by ACK lysis with 3mL or 0.5mL, respectively. Samples were washed with PBS serum. Lungs were separated into the left and right lobes prior to dissociation in a Miltenyi Biotec C tube containing 2mL [2mg/mL] collagenase II (Worthington) in RPMI with 8% FBS (RPMI serum) using the Miltenyi Biotec GentleMACs Lung01 program. Collagenase II volume was increased to a total of 5mLs and samples were incubated upside down with gentle shaking at 37C for 30 minutes. Lung samples were further dissociated using the GentleMACs Heart01 program. These samples were filtered through 100um strainers and run on a discontinuous 75/40% Percoll (Cytiva) gradient. Cells were harvested from the interface and washed with PBS serum for immediate staining or RPMI serum for *in vitro* stimulation.

## *In Vitro* Stimulation

For *in vitro* culture, 96-well dishes were used. Wells were pre-coated with αCD3 and αCD28 purified antibodies at [5ug/well] in 1x PBS where indicated. NP and PA peptides were added at 1ug/mL. GolgiPlug™ (Brefeldin A) and GolgiStop™ (Monensin) were used as indicated by BD Biosciences (1uL/mL and 4μL/6mL respectively) for 6 hours prior to staining. Anti-Lamp-1 antibody was added as indicated by manufacturer (4μL/well for 4 hours) prior to staining. GM1006 MMP inhibitor was used as indicated by Millipore Sigma (25μM) for FasL staining.

## *In Vitro* Killing

$1x10^6$ GFP OT-I splenocytes were transferred IV to naïve C57BL/6 males aged 8-10 weeks. Mice were infected with

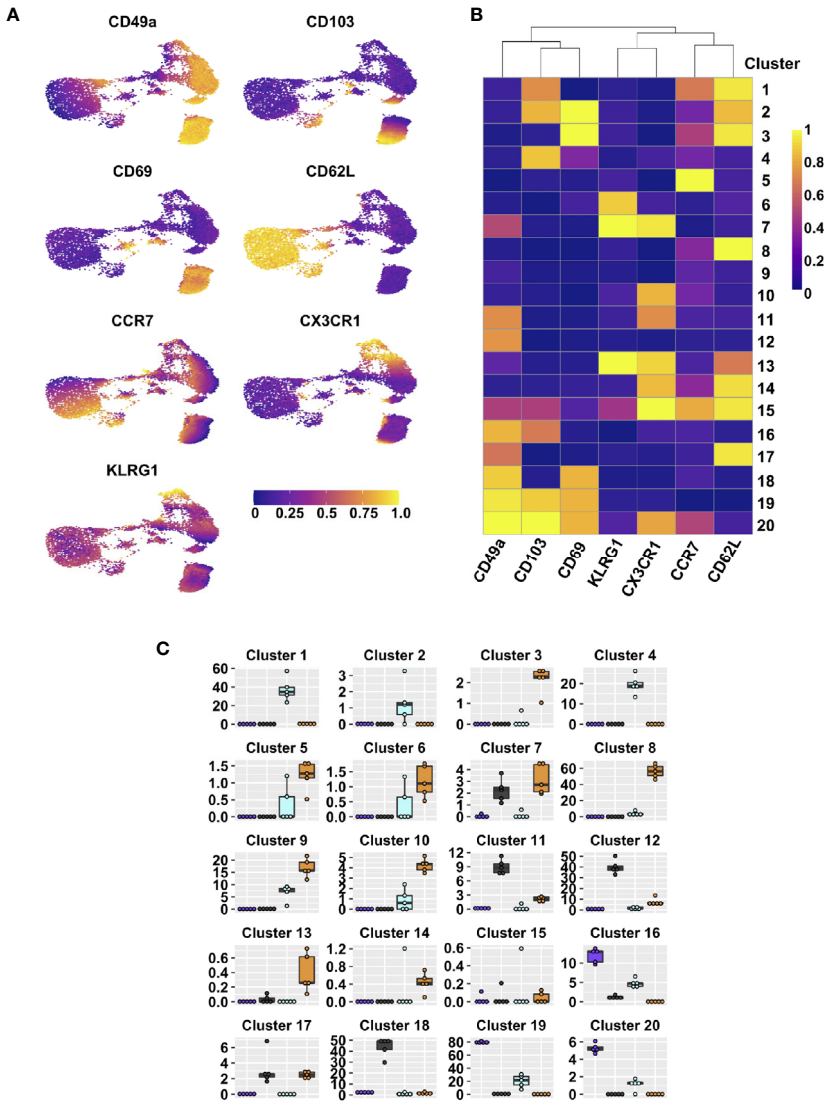


**FIGURE 1** | Integrin subsets are heterogenous based on classical memory T cell markers. UMAPs displaying expression level of different effector and memory markers on lung tissue CD44$^+$ CD8 T cells **(A)**. FlowSOM clusters based on expression of indicated markers; heat map indicates range scaled (0-1) median expression levels **(B)**. Frequencies within lung tissue DP (purple), CD49a (grey), CD103 (aqua), and DN (orange) populations that contribute to each cluster **(C)**. See **Supplementary Table 2** for statistical comparisons of clusters. Data is from 1 representative experiment of 2 independent experiments with n≥3 mice/experiment.

HKx31-OVAI the following day. Cells were harvested from the lung tissue of IV labeled mice at day 21 or day 28 and processed to a single cell suspension. Cells negative for IV labeling were sorted based on integrin phenotype into CD49a single positive, CD49a CD103 double positive, and double negative groups. EL4 cells were counted and incubated at 1x10$^6$ cells/mL in RPMI with CellTrace$^{TM}$ Violet as recommended by the company, and 10ug SIINFEKL peptide or equivalent amount of vehicle ($dH_2O$) for 45 minutes at 37C (31). All cells were washed three times with volumes of 15 mL RPMI serum. Sorted cells and EL4 cells were plated at a 1:1 ratio in U-bottom plates for 11hours. An additional 5ug of SIINFEKL peptide or an equivalent amount of vehicle were added to wells for 2 hours prior to harvest. Cells were transferred to V-bottom dishes, washed with cold PBS, and resuspended in 100uL Annexin V Binding Buffer containing 5uL Annexin V per sample, and transferred to 5mL FACs tubes. After 30 minutes, 200uL cold Binding Buffer added to each tube, and samples were evaluated by flow cytometry, in pairs of SIINFEKL and vehicle controls per sample.

## Flow Cytometry

Cells were spun down at 800xg for 5 minutes in 96-well V-bottom plates. Supernatant was flicked off and cells were resuspended in a master mix of FC-block, surface antibodies,

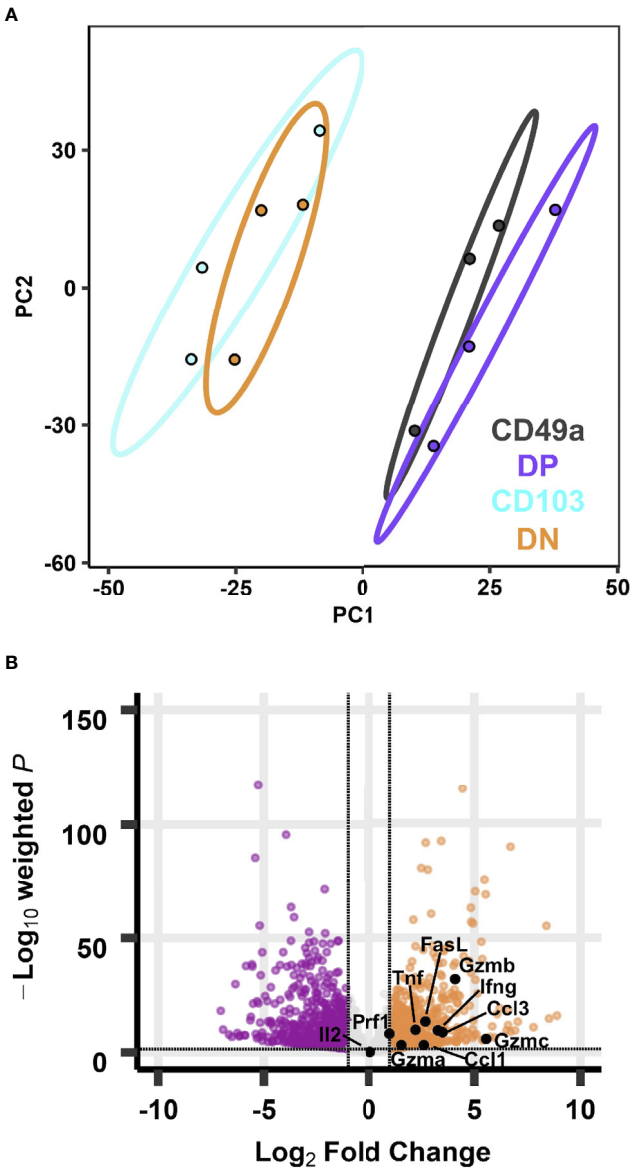


**FIGURE 2** | Transcriptional profiles of CD49a expressing memory CD8 T cell subsets are distinct from CD49a negative counterparts at baseline. PCA of transcripts from CD49, DP, CD103, and DN populations **(A)**. Effector genes overlaid on the volcano plot of differentially expressed genes comparing DP with DN **(B)**. Data is from three groups of five mice pooled and sorted based on integrin phenotype.

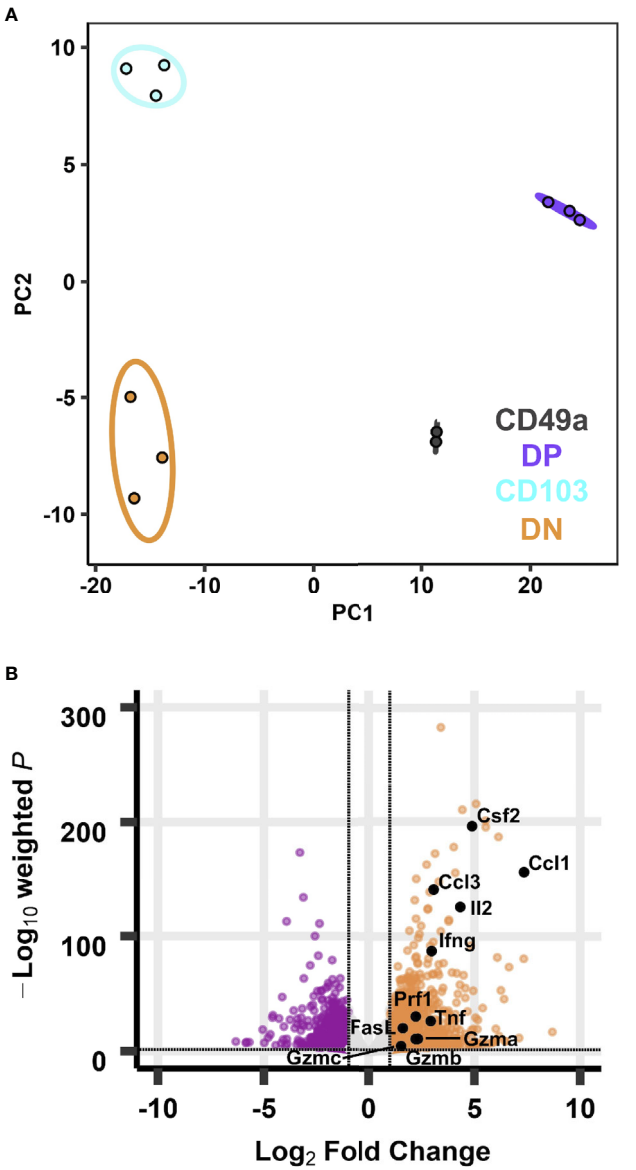


**FIGURE 3** | Transcriptional profiles of integrin memory subsets are all distinct after *in vitro* re-stimulation. PCA of transcripts from CD49, DP, CD103, and DN populations **(A)** after five hours *in vitro* αCD3/CD28 stimulation. Effector genes overlaid on the volcano plot of differentially expressed genes comparing DP with DN **(B)**. Data are from three groups of five mice pooled and sorted based on integrin phenotype. One CD49a sample did not reach RNA quality cutoff and was excluded from the analysis.

and Aqua Fixable Viability Dye. Antibodies were added at 1:200 unless otherwise indicated and viability dye was added as suggested by manufacturer. Cells were incubated in the dark at room temperature for 30 minutes. The BD intracellular staining kit was used as indicated including recommended washes. Briefly, cells were fixed and permeabilized in 1x Fix/Perm for 25 minutes, followed by washing and intracellular staining in Permwash at room temperature for 30 minutes. After washes in Permwash and PBS serum, cells were resuspended in PBS serum and data was captured on an 18 color LSRFortessa with 5 laser lines (Blue, Green, Red, Violet, UV). All antibodies were purchased from BD Biosciences, Biolegend, or Invitrogen (**Supplementary Table 1**).

## Bulk RNA Sequencing

For each experiment, lungs were harvested from three pools of 5 mice each and processed as described. Cells were negatively

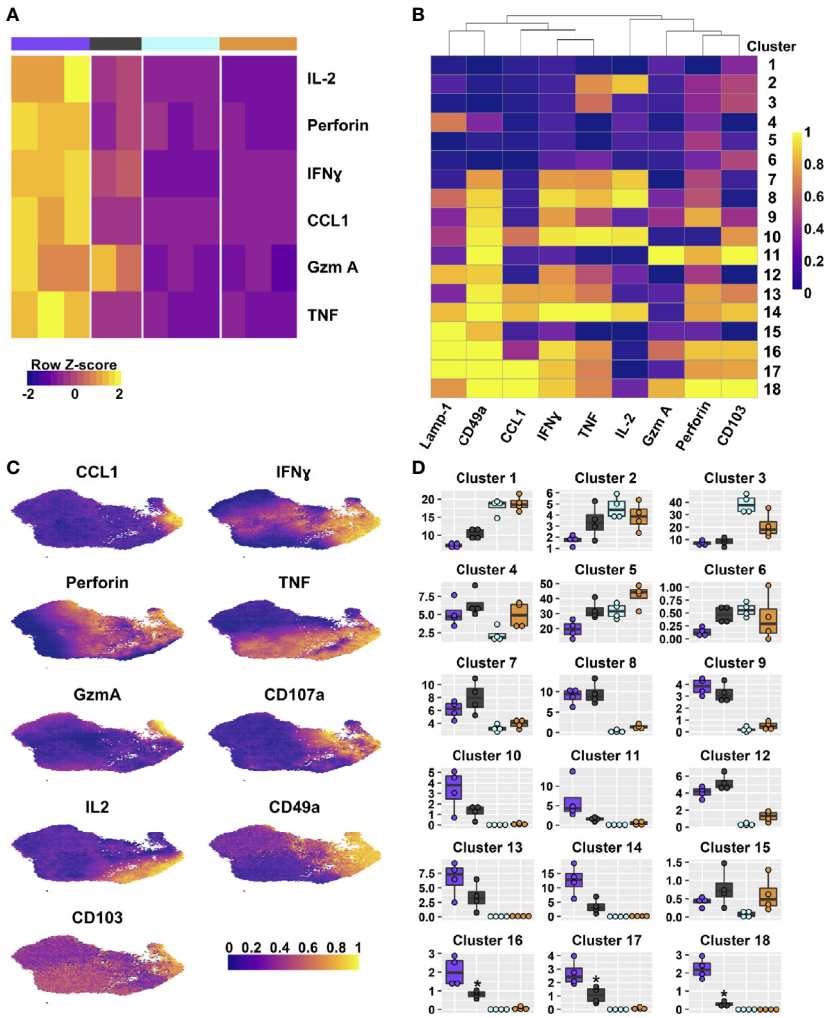


**FIGURE 4** | DP and CD49a CD8 memory T cell subsets are polyfunctional. Heat maps show the transcriptional differences between the four T cell subsets **(A)** and the clusters based on protein staining for Lamp-1, CCL1, IFNγ, TNF, IL-2, Granzyme A, and Perforin after 6 hours of *in vitro* stimulation; heat map **(B)**. UMAPs are based on the effector molecules evaluated **(C)**. Percentage of the integrin subset that is found within each cluster **(D)**. See **Supplementary Table 7** for statistical comparisons of clusters. Data shown is one experiment representative of at least three for B–D with an n≥3 mice/experiment. DP – purple CD49a – grey CD103 – aqua DN – orange.

enriched for CD8 cells using the Miltenyi Biotec mouse CD8$^+$ T Cell Isolation Kit (Miltenyi Biotec, Bergisch Gladbach, North Rhine-Westphalia). For the restimulated group, cells were plated on αCD3/28 coated plates for 5 hours. CD8 T cells were sorted for live, singlet, IV$^{neg}$CD45IV$^{neg}$CD8$^+$CD44$^+$ cells followed by the four CD49a CD103 quadrants into RPMI + serum + penicillin/streptomycin. Cells were spun down and resuspended in RNAeasy buffer containing beta mercaptoethanol. Total RNA was isolated using the RNeasy Plus Micro Kit (Qiagen, Valencia, CA). RNA concentration was determined with the NanopDrop 1000 spectrophotometer (NanoDrop, Wilmington, DE) and RNA quality assessed with the Agilent Bioanalyzer 2100 (Agilent, Santa Clara, CA). 1ng of total RNA was pre-amplified with the SMARTer Ultra Low Input kit v4 (Clontech, Mountain View, CA) per manufacturer's recommendations. The quantity and quality of the subsequent cDNA was determined using the Qubit Flourometer (Life Technologies, Carlsbad, CA) and the Agilent Bioanalyzer 2100 (Agilent, Santa Clara, CA). 150pg of cDNA was used to generate Illumina compatible sequencing libraries with the NexteraXT library preparation kit (Illumina, San Diego, CA) per manufacturer's protocols. The amplified libraries were hybridized to the Illumina flow cell and sequenced using the NextSeq 550 sequencer (Illumina, San Diego, CA). Single end reads of 75nt were generated for each sample. Reads were aligned with STAR-2.7.0 and reads quantified with Subread-1.6.4. DESeq2-1.26.0 was used to generate normalized count matrices and to assess differential expression. Enrichr-2.1 was used for pathway analysis to assess independent hypothesis weighting to correct p values. Final, adjusted, weighted p values were used to assess differential expression. A cutoff of $p<0.05$ was

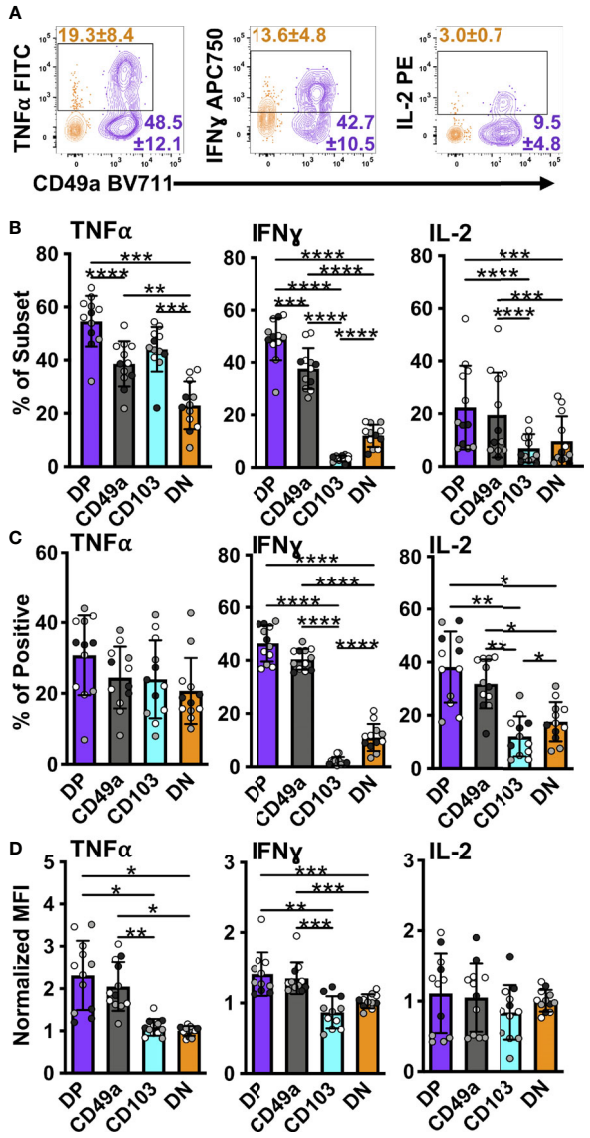


**FIGURE 5** | DP and CD49a CD8 memory T cells express a higher frequency of antiviral and survival proteins. Representative flow cytometry plots showing DP cells compared with DN cells after 6 hours of *in vitro* stimulation **(A)**. Percentage of each subset positive for the cytokine **(B)** and percentage within the cytokine positive populations **(C)**. MFI normalized to DN **(D)**. Data for **(B–D)** shown as mean with standard deviation and each individual sample. *p < 0.05 **p < 0.01 ***p < 0.001 ****p < 0.0001 based on a repeated measures one-way ANOVA with Greenhouse-Geisser correction, followed by *post-hoc* testing comparing all groups through Tukey's multiple comparisons test. Data is three experiments combined with black, grey, or white indicating the individual experiment. n=12 total DP CD49a CD103 DN. DP-purple, CD49a-grey, CD103-aqua, DN-orange.

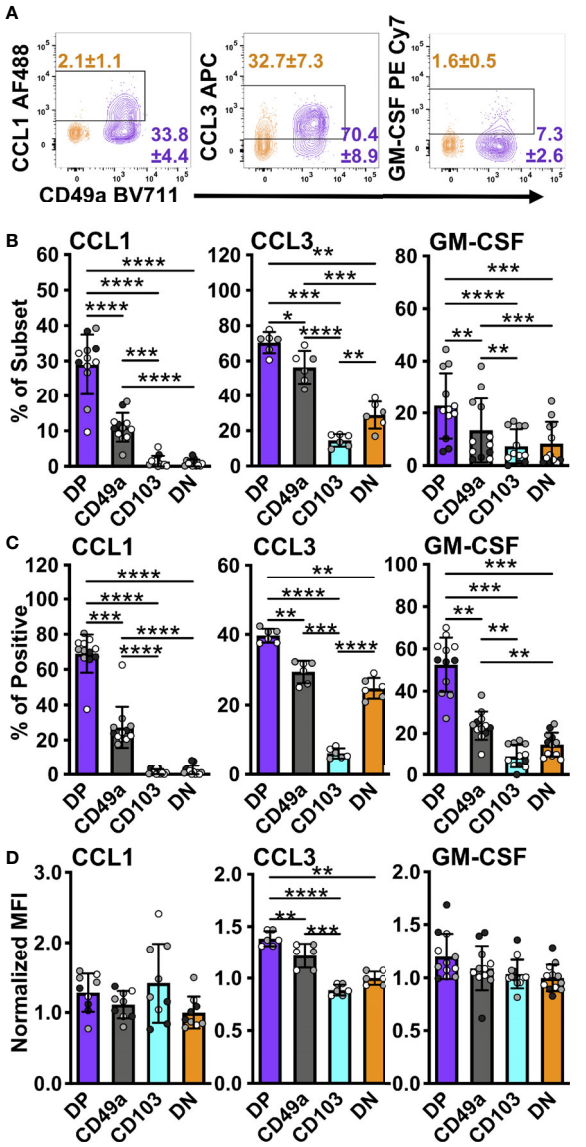


**FIGURE 6** | DP and CD49a CD8 memory T cells express higher frequencies of chemokine and growth factor producing cells. Representative flow cytometry plots showing DP cells compared with DN cells after 6 hours of stimulation *in vitro* stimulation **(A)**. Percentage of each subset positive for the chemokine **(B)** and percentage within the chemokine positive populations **(C)**. MFI normalized to DN (D Data for **(B–D)** shown as mean with standard deviation and each individual sample. *p < 0.05 **p < 0.01 ***p < 0.001 ****p < 0.0001 based on a repeated measures one-way ANOVA with Greenhouse-Geisser correction, followed by *post-hoc* testing comparing all groups through Tukey's multiple comparisons test. Data is two (CCL3) or three experiments combined with black, grey, or white indicating the individual experiment. n=6 for CCL3 n=12 for CCL1 and GM-CSF DP CD49a CD103 DN. DP-purple, CD49a-grey, CD103-aqua, DN-orange.

used. Enrichr-2.1 was used for gene set enrichment analysis to assess for enrichment of pathways from the Kyoto Encyclopedia of Genes and Genomes (KEGG), for which a p<.05 was used. EnhancedVolcano-2.1 was used to plot volcano plots. ggplot2-3.3.2 was used for a variety of plots. Pheatmap-1.0.12 and gplot-3.1.1 were used for heatmap plotting. A full list of packages, version numbers, and software citations can be found on github: (https://github.com/sportiellomike).

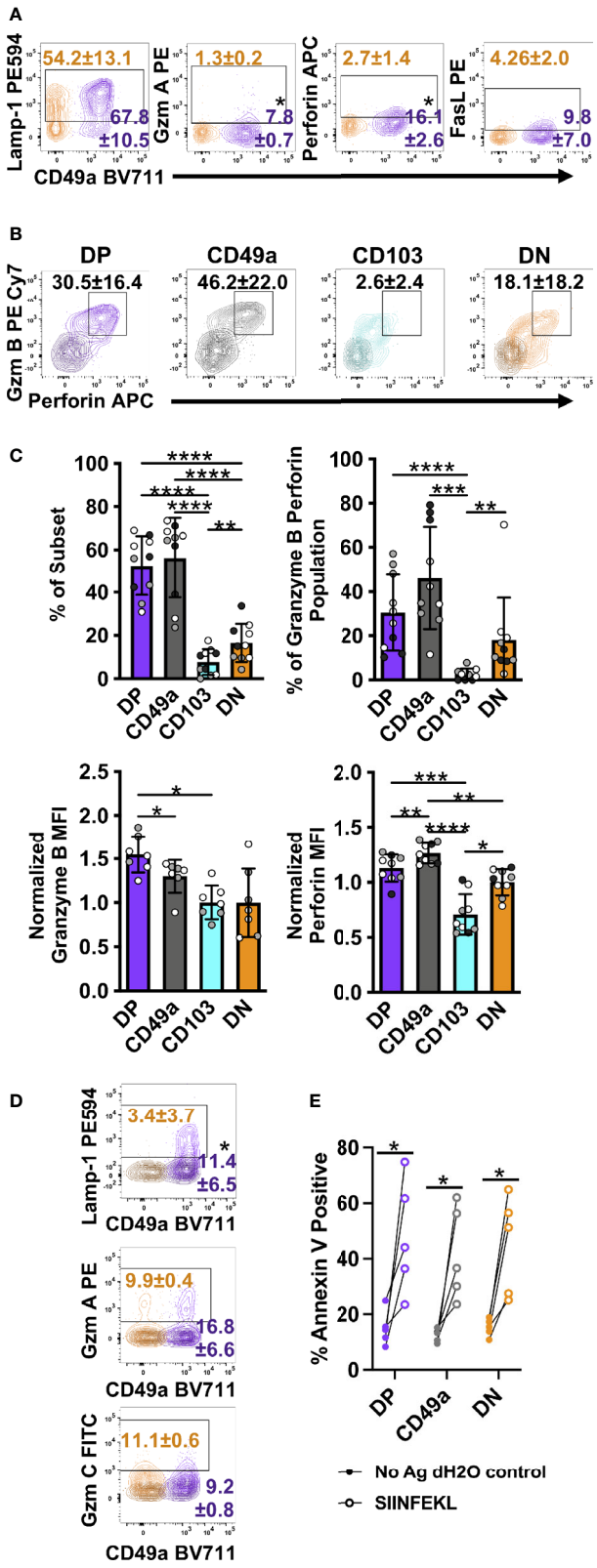


**FIGURE 7** | Continued

**FIGURE 7** | DP and CD49a CD8 memory T cells express a higher frequency cytolytic granules. Representative flow cytometry plots showing DP cells compared with DN cells after 6 hours of *in vitro* stimulation **(A)** and 30 hours of stimulation with media control overlaid **(B)** (Mean and standard deviation). Mean of each subset and individual samples positive for granzyme B and perforin **(C)** and percentage within the granzyme B/perforin double positive population **(C)**. MFI normalized to DN for granzyme B and perforin **(C)**. Comparison of DP and DN cells after 24 hours of stimulation with the mean and standard deviation of the percentage shown. Media control is overlaid in darker shade of the subset color **(D)**. Percentage of Annexin V+ EL4 cells with vehicle control or antigen loading after 13 hour co-culture with T cell subsets sorted from lung tissue CD8 T cells at day 21+ post-infection. *p < 0.05 based on a paired T test on one experiment representative of 3 independent experiments **(A, D)**, p < 0.05 based on paired T test on two combined experiments **(E)**, or *p < 0.05 **p < 0.01 ***p < 0.001 ****p < 0.0001 based on a repeated measures one-way ANOVA with Greenhouse-Geisser correction, followed by *post-hoc* testing comparing all groups through Tukey's multiple comparisons test **(B, C)** of three experiments combined with black, grey, or white indicating the individual experiment. DP CD49a CD103 DN. DP-purple, CD49a-grey, CD103-aqua, DN-orange.

## Statistical Analysis of Flow Cytometry Data

Statistics were performed using Prism analysis software (GraphPad 9). Percentage data was log2 transformed prior to statistical analysis. Repeated measures one-way ANOVA were performed with Greenhouse-Geisser correction, followed by *post-hoc* testing comparing groups to DN using Dunnett's multiple comparisons test. When comparing *in vitro* treatment to control, a paired T-test was performed on log2 transformed data. MFI data were normalized to the DN population per mouse. Only samples with cells in all four quadrants were included. Significance was defined as a p-value<0.05 (or adjusted p-value when appropriate).

## RESULTS

After influenza infection, the lung is home to multiple types of CD8 T cells. Based on the established paradigm, CD8 T cells in the tissue (IV-label negative) constitute circulating $T_{EM}$ ($CD44^{pos}CD62L^{neg}KLRG1^{neg}CCR7^{neg}CX3CR1^{pos/neg}$) and predominantly non-circulating $T_{RM}$ ($CD44^{pos}CD69^{pos}CD49a^{pos}CD103^{pos}$) (2, 5, 8, 32, 33). To verify the presence of these two main subsets and determine the level of heterogeneity within each memory type, cells were examined directly *ex vivo* after clearance of influenza virus at day 21 post-infection by flow cytometry. The cells were stained for classical effector and memory surface markers, allowing for the discrimination of $T_{EFF}$ ($CD44^{pos}CD62L^{neg}KLRG1^{pos}$), $T_{CM}$ ($CD44^{pos}CD62L^{pos}$), $T_{EM}$ ($CD44^{pos}CD62L^{neg}KLRG1^{neg}CCR7^{neg}CX3CR1^{pos/neg}$), and $T_{RM}$ ($CD44^{pos}CD69^{pos}CD49a^{pos}CD103^{pos}$) (2, 5, 8, 32, 33). Dimensional reduction and visualization of data from $TCR\beta^{pos}CD8^{pos}CD44^{pos}$ cells was achieved through Uniform Manifold Approximation and Projection (UMAP) (**Figure 1A**) (34). Data were subsequently clustered using FlowSOM, resulting in 20 distinct clusters (**Figure 1B**) (35). Unexpectedly, some of the cells expressed CD62L, resulting in multiple $CD62L^{pos}$ clusters. While this would be anticipated in

the vasculature associated population and lymphoid organs, it is not well established that these cells would also be present in peripheral non-lymphoid tissues, or perhaps suggests the tissue includes some lymphatic structures (**Figure 1B** and **Supplementary Figure 1**). Clusters 1 and 2 co-express CD103, along with CCR7 and CD69, respectively. Cluster 3 co-expresses CD69 alone, cluster 13 also stains for KLRG1 and CX3CR1, suggesting that they may represent a transition state between effector and memory. Classical $T_{EM}$ ($CD44^{pos}CD62L^{neg}$ $KLRG1^{neg}CCR7^{neg}CX3CR1^{pos/neg}CD49a^{neg}CD103^{neg}$) are found in clusters 9 and 10, in the absence and presence of CX3CR1 staining, respectively. Clusters 11 and 20 both have CX3CR1, but co-express CD49a alone or CD49a, CD103, and CD69, supporting that some subsets of "$T_{RM}$" phenotype cells may have the capacity to leave the tissue (36). Alternatively, CX3CR1 can bind its chemokine ligand fractalkine (CX3CL1) expressed on the surface of epithelial and endothelial cells, potentially aiding in micropositioning within different niches throughout the tissue (37). Finally, cluster 19, expressing the combination of CD49a, CD103, and CD69 contains the cells considered to be classical $T_{RM}$. No subsets expressing only CD103 and CD69 were found, however cluster 4 represents CD103 single positive cells. On the contrary, cluster 18 expresses both CD49a and CD69. Clusters 12 (CD49a only) and 16 (CD49a and CD103) may also indicate CD69 negative $T_{RM}$ subsets.

Since CD69 did not appear to be the defining feature of lung $T_{RM}$, we focused on further subsetting the memory CD8 T cells based on CD49a and CD103 expression. $CD49a^{pos}CD103^{neg}$ (CD49a), $CD49a^{pos}CD103^{pos}$ (Double Positive DP), $CD103^{pos}CD49a^{neg}$ (CD103), and $CD49a^{neg}CD103^{neg}$ (Double Negative DN) were examined for their contribution to each of the twenty clusters (**Figure 1C** and **Supplementary Table 2**). CD103 was represented across clusters 1 and 4, and based on phenotype, has the potential to function as $T_{CM}$ and possibly CD103 single positive $T_{RM}$. However, similar analysis at three months post-infection demonstrates that the CD103 single positive $T_{RM}$ population does not persist long-term. The DN population is accounted for by a number of clusters (3, 5, 6, 8, 9, and 10), and in addition to the hypothesized $T_{EM}$ phenotype, these cells also represent $T_{CM}$ and effector-like populations. As a whole, these subsets likely represent "circulating" CD8 T cell memory. The CD49a population is predominantly found in clusters 11, 12, and 18, with the potential ability to recirculate based on CX3CR1 expression in cluster 11. DP cells are distributed across clusters 16, 19, and 20, with a small subset expressing CX3CR1 (cluster 20).

The phenotyping data suggest that as a whole, the DN and CD103 subsets represent circulating memory cells and the CD49a and DP subsets are likely the predominantly resident populations. Each memory population is presumed to be capable of performing immune surveillance, and the cells expressing CD49a are highly motile, yet their functions in the homeostatic state are unclear (24). To further characterize these subsets, non-naive CD8 T cells from the lung tissue ($CD45IV^{neg}/TCR\beta^{pos}/CD8^{pos}/CD44^{pos}$) of day 21 infected mice were sorted based on their CD49a/CD103 profile, and bulk RNA sequencing was performed on these four subsets to determine if there were intrinsic baseline differences under homeostatic conditions (**Supplementary Figure 2**). Principle component analysis demonstrated that transcript expression stratifies the CD49a expressing subsets (CD49a and DP) from the CD49a negative populations (CD103 and DN), but it is insufficient to further distinguish the subsets into CD103 positive and negative (**Figure 2A**). PC1, which accounts for over 40% of the variance is driven in part by *Itga1* (CD49a) which serves as an internal control for sorting (**Supplementary Figures 3A, B**). PCA excluding *Itga1* did not alter the patterns observed suggesting additional genes define these subsets (**Supplementary Figures 3C–E**). Additionally, PC1 shows upregulation of *Ifitm1*, adhesion molecule *Tjp1* (ZO-1), and *Csf1* (**Supplementary Figure 3A**). Since the DP population demarcates the canonical $T_{RM}$ cells and DN are circulating memory, the initial analysis compared these two populations to investigate any transcriptional differences. Using independent hypothesis weighting and adjusted p-values, over 700 genes were found to be differentially expressed when comparing DP to DN populations (38). Examination of the top 500 genes that displayed differential regulation further supported that the CD103 and DN cells are almost transcriptionally indistinguishable at baseline (**Supplementary Figures 4A, B**). CD49a cells also display significantly different transcript levels from CD103 and DN cells, and to a smaller degree compared with DP (**Supplementary Figures 4A, B**). In fact, a small subset of genes is uniquely upregulated in CD49a cells compared with DP cells (**Supplementary Figure 4A**).

To further appreciate the cellular programs which are the foundation for these observed transcriptional differences, Kyoto Encyclopedia of Genes and Genomes (KEGG) pathway analysis was performed to reveal differentially regulated biological pathways (39–42). Despite over 700 genes with differential expression between DP and DN cells, no pathways were significantly different (padj<0.05). Using a less strict level of significance (padj<0.1) two pathways were identified: *cytokine-cytokine receptor interaction*s and *steroid biosynthesis* (**Supplementary Figure 4C**). With the goal of defining the population(s) that are most effective at limiting re-infection, the *cytokine-cytokine receptor interactions* pathway was more closely scrutinized. Directed examination identified a number of transcripts that were differentially

**TABLE 1** | Effector genes that are significantly upregulated in DP cells compared with DN cells, ordered by log2 fold change.

| Gene name | Protein name | Log2 Fold Change | Base Mean | Adj. p-value |
|---|---|---|---|---|
| *Gzmc* | Granzyme C | 5.55 | 17 | 1.65E-06 |
| *Gzmb* | Granzyme B | 4.09 | 9,250 | 1.29E-32 |
| *Ccl3* | CCL3 | 3.50 | 831 | 1.99E-09 |
| *Ifng* | Interferon γ | 3.28 | 3,595 | 2.86E-10 |
| *Ccl1* | CCL1 | 2.62 | 32 | 8.20E-4 |
| *Tnf* | TNF | 2.23 | 888 | 1.82E-10 |
| *Gzma* | Granzyme A | 1.56 | 2063 | 7.87E-04 |
| *Prf1* | Perforin | 1.00 | 6,979 | 9.12E-09 |

expressed at baseline. These include: *Tnf*, *Ifng*, *Gzma*, *Gzmb*, *Gzmc*, *Prf1*, and the chemokine *Ccl3* (**Table 1**; **Supplementary Table 3** and **Figure 2B**). Protein levels for these effector molecules were quantified by flow cytometry. However, despite an increase in transcript levels, only low levels of granzyme A, perforin, and Lamp-1 were detected (**Supplementary Figure 5**). This lack of correlation between cytokine transcript and protein levels has been seen previously in $T_{RM}$ cells (43, 44). To further evaluate with $T_{RM}$ subsets, pathways were compared between the DP and the CD49a populations. However, at baseline, no differentially expressed pathways were identified (**Supplementary Table 4**).

Under homeostasis, the prototypical $T_{RM}$ (DP) and the CD49a population both expressed higher baseline transcript levels for effector genes compared with non-$T_{RM}$ memory. However, it was unclear whether this observation persisted in the different subsets after restimulation. To address this, cells were activated *in vitro* with αCD3 and αCD28, as a mimic for TCR-based stimulation. Briefly, memory CD8 T cells were sorted on day 21 post-infection after 5 hours of *in vitro* stimulation using a similar approach to the unstimulated cells ($CD45IV^{neg}/CD8^{pos}/CD44^{pos}$ and sorted based on CD49a/CD103 expression). PCA of the bulk RNA sequencing results demonstrates that after stimulation, the transcriptional profiles for all subsets are distinct (**Figure 3A**; **Supplementary Table 5** and **Supplementary Figure 6**). Top loadings for the principal component separating CD49a expressing subsets (PC1) from CD49a negative subsets include effector molecule *Ccl1* and junctional protein *Tjp1* (**Supplementary Figure 6A**). Principal component 1 contributes to over 60% of the variance (**Supplementary Figure 6B**). The gene encoding CD49a (*Itga1)* again serves as an internal control for the sorting technique used. Nevertheless, the PCA results are nearly identical when CD49a and CD103 are excluded (**Supplementary Figures 6C–E**). The top loadings of PC2, which separates CD103 expressing subsets from CD103 negative subsets also include both effector-associated genes (*Ccl9* and C*x3cr1*) and structural binding proteins including *Cdh4* and *Itgae* (which encodes CD103 and serves as an internal control). The number of differentially expressed genes, when comparing DP to DN increased to over 1,300, with almost 800 genes uniquely upregulated only in the DP cells (**Figure 3B** and **Supplementary Figure 7**). Pathway analysis of the differentially expressed of the differentially expressed genes revealed over 70 upregulated KEGG pathways when comparing DP to DN. These include pathways related to effector programs with *cytokine-cytokine receptor interactions* as the top enriched pathway (**Supplementary Figure 7C**). Other enriched pathways include *C-type lectin receptor signaling pathway*, *cell adhesion molecules*, *natural killer cell mediated cytotoxicity*, *chemokine signaling pathway*, and *TNF signaling pathway* (**Supplementary Figure 7C** and **Supplementary Table 6**). Within the *cytokine-cytokine receptor interaction* pathway, DP showed increased levels of 54/292 genes and specific evaluation of effector associated genes that were upregulated in the DP compared with the DN population identified 17 genes to further pursue (**Figure 3B** and **Table 2**). Of note, one of the most upregulated genes in the data set was *Ccl1*, the chemokine associated with recruitment of innate myeloid derived cells through binding its cognate receptor CCR8 (45, 46). DP cells also displayed increased transcript levels for genes associated with classical antiviral cytokines (*Ifng*, *Tnf*), T cell survival and activation (*Il2*), chemokines (*Ccl3, Ccl4, Cxcl9*), cell differentiation (*Gmcsf*) and cytolytic components (*Prf1, Gzma, Gzmb,Gzmc, Fasl, Tnfsf10*) (**Table 2**).

**TABLE 2** | Effector genes that are significantly upregulated in DP cells compared with DN cells, ordered by log2 fold change, after *in vitro stimulation*.

| Gene name | Protein name | Log2 Fold Change | Base Mean | Adj. p-value |
|---|---|---|---|---|
| *Ccl1* | CCL1 | 7.34 | 37,106 | 1.26E-156 |
| *Csf1* | CSF | 6.14 | 2,939 | 2.48E-187 |
| *Csf2* | GM-CSF | 4.89 | 2,769 | 1.02E-196 |
| *Il2* | IL-2 | 4.33 | 5,369 | 2.35E-126 |
| *Il10* | IL-10 | 4.22 | 460 | 9.37E-51 |
| *Ccl3* | CCL3 | 3.07 | 129,614 | 1.59E-141 |
| *Ifng* | Interferon γ | 2.98 | 104,386 | 5.95E-88 |
| *Tnf* | TNF α | 2.93 | 12,511 | 4.02E-27 |
| *Tnfsf10* | TRAIL | 2.76 | 565 | 1.47E-41 |
| *Gzma* | Granzyme A | 2.33 | 2,379 | 1.32E-11 |
| *Prf1* | Perforin | 2.23 | 7,903 | 4.38E-31 |
| *Gzmb* | Granzyme B | 2.22 | 86,942 | 1.66E-11 |
| *Il21* | IL-21 | 1.96 | 144 | 4.39E-07 |
| *Fasl* | Fas Ligand | 1.62 | 2,716 | 5.92E-21 |
| *Gzmc* | Granzyme C | 1.53 | 1,205 | 2.40E-05 |
| *Cxcl9* | CXCL9 | 1.26 | 542 | 7.04E-04 |
| *Il17a* | IL-17A | 1.31 | 100 | 8.06E-04 |

$T_{RM}$ derived IFNγ is known to be critical for protection against influenza, so these findings support the contribution of the DP population to the antiviral response (47). Notably, the CD49a population showed similar increases in effector transcript levels compared with DN T cells, suggesting that they may represent a previously unappreciated critical antiviral $T_{RM}$ subset. In fact, a direct comparison between the DP and CD49a showed that genes were more highly enriched for the *natural killer cell mediated cytotoxicity* pathway in CD49a, suggesting that the cytotoxic components may be further enhanced in the CD49a single positive cells compared with DP. Conversely, the majority of effector genes were not differentially expressed between CD103 and DN, and in some cases displayed higher transcript levels in DN, such as *Ifng*.

To determine whether transcript levels equated to protein expression after re-stimulation, flow cytometry was utilized (**Figure 4**). One focus was evaluating whether $T_{RM}$ are polyfunctional, or if separate sub-populations contribute to specific aspects of the antiviral response. To achieve this, T cells were stimulated *in vitro* with αCD3/CD28 in the presence of Golgi and ER transport inhibitors for 6 hours and examined by multi-color intracellular flow cytometry (48). CD8 T cells were surveyed for antiviral cytokines, IL-2, CCL1, and cytolytic components based on (**Table 2** and **Figure 4A**). The multidimensional data from the four integrin subsets were concatenated and reduced down to two dimensions using UMAP to generate a similarity map based on the functional molecules examined (TNF, IFNγ, IL-2, Granzyme A, Perforin, Lamp-1, and CCL1) (**Figure 4C**) (34). FlowSOM clustering was applied to further interrogate the T cell effector profiles (35). This

approach yielded 18 distinct clusters (**Figures 4B**). Given the prior understanding of beneficial effector capabilities, focus was put on examining clusters 10, 13, 14, and 16-18, all of which identify polyfunctional subsets. Cells in these clusters are $CCL1^+$ with co-expression of IFNγ and TNF, but further separated based on the level of these molecules, as well as staining for perforin, IL-2 and Lamp-1 (**Figures 4B, D**). Strikingly, when examining the frequencies of these clusters within the integrin subtypes, DP cells had the highest proportions for all of these clusters (**Figure 4D** and **Supplementary Table 7**). CD49a cells also displayed marked contributions to these clusters (**Figure 4D** and **Supplementary Table 7**). In contrast, the vast majority of CD103 and DN cells could be accounted for with clusters 3 and 5, which displayed low levels of perforin and TNF or low quantities of only perforin, respectively. These data support that CD49a and DP identify multiple polyfunctional $T_{RM}$ subsets.

In an effort to further interrogate the presence of effector molecules in the different memory subsets, the frequency, normalized count, and MFI of the positive fractions were quantified for an expanded panel of cytokines, chemokines, a growth factor, and cytotoxic components. Both DP and CD49a cells showed increases in frequencies for IFNγ and IL-2 compared with DN cells, with DP cells also showing increases in the percentage of TNF positive cells (**Figures 5A, B**). DP and CD49a also had increased MFIs for both IFNγ and TNF compared with both CD103 and DN (**Figure 5D**). This approach demonstrates not only higher proportions of positive cells, but also supports increased protein levels on a per cell basis in DP and CD49a compared with non-$T_{RM}$ cells (**Figures 5B, D**). Among the $IFN\gamma^+$ cells, DP and CD49a were the main contributors, comprising approximately 80% of the response (**Figure 5C**). Despite a strong bias toward CD49a expressing subsets producing more IFNγ and IL-2, an increased percentage of CD103 cells were found to make TNF (as shown in cluster 3) at comparable frequencies with DN, but this was not accompanied by a higher contribution to the $TNF^+$ population or a greater amount produced on a per cell basis (**Figures 5B, D**). To ensure that the outcomes observed with bulk stimulation of CD8 T cells weren't skewed from that of known influenza specific CD8 T cells, the same stimulation experiment was performed using influenza derived NP and PA peptides. Interestingly, upon peptide stimulation, the CD49a subset displayed the highest frequencies of cytokine positive cells, consistent with differences in NP/PA specificity between the subsets (**Supplementary Figure 8**). CD49a cells showed significantly higher levels of both IFNγ and TNF compared with DN, albeit at a lower overall response compared with αCD3/CD28 stimulation (**Supplementary Figure 8**). Of note, IL-17A, IL-21, and IL-10 were also examined within these experiments, however, no protein staining was detected under the stimulation conditions described.

$T_{RM}$ have previously been said to orchestrate both innate and adaptive responses, however, the mechanisms controlling these outcomes were not fully clear (6, 7). Supported by the RNAseq data, we hypothesized that $T_{RM}$ have the capacity to release both chemokines and growth factors to recruit and aid in APC maturation. To determine the breadth of the chemokine response of memory CD8 T cells, CCL3 and CXCL9 were analyzed in addition to CCL1. All of these chemokine genes were upregulated in DP compared with DN at the transcript level (**Table 2**). As suggested by clustering, CCL1 was expressed only in CD49a and DP cells, indicating a unique function of CD49a positive subsets, though these were more frequently found in DP cells than in CD49a (**Figures 6A–C**). This was consistent with results from NP and PA peptide stimulation (**Supplementary Figure 8**). CCL3 was expressed at the highest frequency, overall contribution, and MFI in DP cells and a higher percentage in CD49a versus CD103 and DN (**Figures 6A–D**). Additionally, the growth factor GM-CSF was expressed predominantly in CD49a expressing cells (DP and CD49a), showing both increased percentages within the subsets as well as increased contribution to the GM-CSF positive population (**Figures 6A–C**). We were unable to detect CXCL9 protein within the CD8 T cells using this re-stimulation approach. Overall, this data paints a picture of polyfunctional CD49a expressing cells as signaling hubs, both directing and contributing to an effective antiviral response.

In addition to cytokines and chemokines, the increase in transcript levels of cytotoxic-associated molecules suggested that $T_{RM}$ retain the ability to kill target cells (**Table 2**). DP cells display increases in mRNA for granzymes A, B, and C, and perforin. Furthermore, transcript for apoptosis-inducing FasL and TRAIL were increased (**Table 2**) (49, 50). At 6 hours post-stimulation, memory CD8 T cells were evaluated for Lamp-1 staining, an indicator of vesicle:plasma membrane fusion, granzymes A, B, and C, perforin, FasL, and TRAIL (51). Even at 6 hours post-stimulation, low levels of granzyme A and perforin were detected in DP cells with higher frequencies than in DN cells (**Figure 7A**). TRAIL and granzymes B and C were not detected at this time point (**Supplementary Figure 9** and data not shown). While this was consistent with the idea that the function of $T_{RM}$ is to release IFNγ rather than kill infected targets, it conflicted with mRNA levels (47, 52). To further complicate our understanding, over half of the cells were surface Lamp-1 positive (**Figure 7A**). This suggested that despite the addition of transport inhibitors, vesicular fusion still occurred.

It is possible that $T_{RM}$ cells may be pre-loaded with cytolytic granules that are not blocked from degranulation by ER and Golgi transport inhibitors. Furthermore, in agreement with a paper examining human skin $T_{RM}$ cells, the inability to detect granzymes and high levels of perforin may be due to altered kinetics with increased time necessary for new granules to be formed (**Supplementary Figure 9A**) (13). To test this, cells were incubated for either 12 (data not shown) or 24 hours prior to the addition of transport inhibitors. To stain for degranulation, αLamp-1 was added 2 hours prior to addition of transport inhibitors. Cells were then incubated for an additional 6 hours after addition of the inhibitors, and subsequently stained for granzymes and perforin. Using this protocol, CD49a expressing subsets from the lungs and the airways produced dramatic levels of perforin and granzymes (**Figures 7B, C** and **Supplementary Figures 9B, C**). In fact, CD49a expressed higher levels of perforin per cell compared with DN cells, validating the RNAseq results. Not surprisingly, at this time point, DP cells expressed a higher

proportion of Lamp-1 stained cells compared with DN, however, no increase in either granzymes A or C was observed (**Figure 7D**). Of note, while skin $T_{RM}$ required only IL-15 in culture to produce granzyme B and this effect was additive in the presence of TCR stimulation, exogenous cytokines had no additional effect on the lung CD8 T cells evaluated in this model, and their addition in the absence of TCR stimulation was insufficient to induce cytotoxicity (data not shown) (13). To determine whether granzyme B and perforin were indicative of actual killing ability, an *in vitro* killing assay was set up using EL4 cells as APCs. To minimize the known differences in tetramer positivity between the different subsets, the transgenic OT-I adoptive transfer model was utilized (53, 54). Briefly, one day prior to infection with a SIINFEKL expressing HKx31 influenza A variant, GFP OT-I T cells were transferred intravenously. At greater than 21 days post-infection, lung tissue CD8 T cells were sorted based on their integrin phenotype. In this model, CD103 single positive cells were almost non-existent, so only DP, CD49a, and DN were evaluated. DP, CD49a, and DN cells were cultured with SIINFEKL pulsed Cell Tracker Violet labeled EL4 cells or unloaded Cell Tracker Violet labeled vehicle control EL4 cells. After 13 hours of co-culture, cells were harvested and stained for Annexin 5. All subsets examined displayed increased frequencies of Annexin V positive target cells in the presence of peptide, compared with control cells (**Figure 7E**). Despite the fact that a higher frequency of DP and CD49a populations produced perforin and granzyme B compared with DN, there was no significant difference in the contribution to the population, supporting that both resident and circulating CD8 T cells can kill infected targets (**Figures 7C, E**). Taken together, the data implies that $T_{RM}$ cells may respond in sequence, first limiting the spread of infection through release of antiviral cytokines and recruitment of innate cells, followed by direct elimination of residual virally infected cells. It also suggests that the heterogenous populations of $T_{RM}$, may specialize in discrete responses.

## DISCUSSION

Memory CD8 T cells arise in response to pathogen exposure and are maintained in different locations throughout the body (3–5). The memory cells can be defined by their ability circulate or persist as resident memory at the site of infection. $T_{RM}$ in different organs have discrete requirements for development, maintenance, and the level of effector capacity (55). The requirement for varied responses in the periphery is likely driven in part by the type of invading pathogen and local inflammatory milieu. This study aimed to interrogate the memory population(s) at a single peripheral site and ask whether this diversity was still maintained. CD8 T cells in the lung tissue were examined after resolution of influenza A virus infection, with the hypothesis that the cells referred to as $T_{RM}$ actually present a heterogenous mix of populations which have particular effector capabilities. Surprisingly, the memory CD8 T cell composition in the lung tissue was comprised not only of $T_{RM}$ and $T_{EM}$, but also cells which matched the phenotype of $T_{CM}$. While it cannot be discounted that the approach used captured cells within lymphatics of the lungs, the cells within the airway (through bronchoalveolar lavage), contained similar populations. This suggests that even on the surface, the diversity of the CD8 memory T cells found in lung tissue is much higher than previously appreciated. Within the cells of $T_{RM}$ phenotype, the canonical $CD103^{pos}CD49^{apos}CD69^{pos}$ population was identified, in addition to other subsets which express only one of the integrins or lack CD69. Unexpectedly, CX3CR1 expressing cells were found within both $CD103^{pos}CD49^{apos}$ cells and the CD49a single positive populations. Similar to what is observed within skin draining DCs, we propose that CX3CR1 on these cells may explain the small subset of cells $T_{RM}$ found within lymphatics and the draining lymph nodes (36, 56). Since CX3CL1 can also be expressed by epithelial and endothelial cells, it is also conceivable that receptor expression improves homing to infected cells or reentry into the vasculature (37).

The phenotypic differences observed may be due to the microenvironmental niches in which the cells reside – changes in TGFβ levels alone could account for integrin expression alterations (28).

Other studies have shown that the requirement for CD69 is not present in every organ, however, it is conceivable that it may be more critical for cells in close proximity to afferent lymphatics, than for cells embedded within the epithelial cell layer (15, 22). Similarly, a requirement for CD103:E-cadherin interactions would not exist for a T cell within the parenchyma or migrating along the basement membrane. These findings set up and support the idea that the surface phenotype may be driven by the local microenvironment, and may in turn promote different responses and cell fate within that niche.

It was unclear, however, whether the subsets were truly distinct, or if the cells examined just represent plasticity or phenotypic intermediates. At baseline, the cells phenotypically defined as $T_{RM}$ (DP and CD49a) examined directly *ex vivo* have discrete transcriptional profiles compared with non-CD49a expressing population. In this homeostatic state, the $T_{RM}$ cells contained higher levels of mRNA for effector genes, however, minimal protein, if any, was observed in the absence of stimulation. Although less intensively studied in $T_{RM}$ cells, memory CD8 T cells have been shown to employ different mechanisms through which they repress the translation of accumulated mRNA (44, 57, 58). While the specific processes underlying these observations warrant further research, we hypothesized that the amassed effector gene transcripts provide the ability for $T_{RM}$ cells to rapidly respond upon reactivation.

After *in vitro* restimulation, all four subsets were transcriptionally distinct, and this held true when PCA was performed excluding the genes for CD49a and CD103. Cells expressing both CD103 and CD49a had the highest levels of effector responses overall, spanning antiviral cytokines, T-cell survival genes, chemokines, a growth factor, and cytolytic mediators. CD49a single positive cells, which are intermediate in effector function between DP and DN cells, actually displayed increased enrichment for genes associated with cytotoxicity. Evaluation of protein levels confirmed the majority of the transcript data after *in vitro* reactivation, however, the kinetics for some of these responses were delayed. We hypothesized that these cells may be pre-programmed to respond in sequence, facilitating

viral clearance and recruitment of cells with APC potential, without destroying the epithelial barrier.

Consistent with many other studies, within 6 hours of TCR stimulation, DP and CD49a cells produce copious amounts of protective IFNγ (47). These same populations of cells also secrete T-cell survival factor, IL-2. These immediate responses may enhance the lifespan of the $T_{RM}$ cells or promote proliferation after rechallenge and clear virus with less damage to the airway epithelium.

Within this same time frame, DP cells and CD49a cells release chemokines CCL1 and CCL3 and the growth factor GM-CSF. Interestingly, cells that traffic from the spleen after influenza infection have previously been shown to produce CCL1 and GM-CSF, so it is intriguing that this profile of protection is conserved within the cells already present within the lungs (59). The receptor for CCL1 (CCR8) is expressed on specific subsets of $T_{RM}$, so this mechanism could be in place to recruit $T_{RM}$ at other regions of the tissue to specific niches of infection (60). Concurrently, CCL1 can recruit innate immune cells (myeloid and DC lineages) to the site of infection (60, 61). GM-CSF has roles in both maturation of myeloid and APC populations, but also in the repair of the airway epithelium (62–64). This strengthens the hypothesis that $T_{RM}$ aim to clear infection in the absence of extensive tissue damage.

In line with this, despite high transcript levels for cytolytic mediators granzyme B and perforin, minimal protein can be detected at 6 hours post-stimulation. These data are consistent with the concept that $T_{RM}$ are initially noncytolytic and that control of infection is primarily through release of antiviral molecules. However, similar to $T_{RM}$ in other systems, stimulating the cells for longer time periods results for the accumulation of high levels of granzyme B and perforin and killing of target cells (13, 47). Interestingly, both CD49a single positive and DP cells have comparable positive frequencies for these cytotoxic molecules, but CD49a cells produce higher levels of perforin, and demonstrate a much higher frequency after stimulation with NP/PA peptide. This suggests that during reinfection with a heterosubtypic virus, the CD49a cells may be more predisposed to killing target cells than their DP counterparts.

Overall, this study identified a previously unappreciated level of heterogeneity within the lung CD8 memory subset, even within the populations of cells labelled as $T_{RM}$. Cells expressing CD49a display the highest levels of effector function, and the integrin phenotype may further identify cells capable of cytotoxicity and repair mechanisms. In another study CD49a expression was utilized to sort for downstream RNA sequencing, all integrin positive cells were evaluated, rather than only antigen experienced CD8 T cells. This difference alone makes it difficult to directly compare with the results from this study. However, despite that caveat, they found similar results in regard to transcripts related to cytotoxicity (*GZMB* and *PRF1*), chemokines (*CCL4* and *CCL5*), and antiviral cytokines including *IFNG* (13).

With the knowledge that CD49a similarly defines polyfunctional $T_{RM}$ in human skin and tumor infiltrating lymphocytes in melanoma, and supports cell motility, we propose that the ubiquity of collagen IV in the basement membrane of epithelial surfaces and the data presented here, further substantiate a probable role for CD49a in many, if not all $T_{RM}$ populations (13, 26). As a whole, the memory T cells in the lungs have the capacity to generate antiviral immunity, support T cell survival, enhance recruitment and maturation of other cells to the site of infection, with the potential to aid in repair of the tissue after clearance of the pathogen.

## DATA AVAILABILITY STATEMENT

The datasets presented in this study can be found in online repositories. The names of the repository/repositories and accession number(s) can be found below: Geo with accession GSE17653 (https://www.ncbi.nlm.nih.gov/geo/query/acc.cgi?acc=GSE179653). All code used for data analysis in this manuscript is available at (https://github.com/sportiellomike). Other raw data files are available upon request.

## ETHICS STATEMENT

The animal study was reviewed and approved by Institutional Animal Care and Use Committee of the University of Rochester.

## AUTHOR CONTRIBUTIONS

ECR and MS designed and performed experiments, analyzed and interpreted data, and wrote the manuscript. KLE provided technical support and edited the manuscript. AMA contributed reagents and experimental expertise. RJ provided bioinformatics support. ABRK contributed comments on data interpretation and helped edit the manuscript. NGL assisted with flow cytometry data analyses and bioinformatics support. HY provided statistical support. MK provided reagents and expertise. DJT provided overall direction, procured funding, interpreted data, and edited the manuscript.

## FUNDING

This work was funded by a Program Project grant through the National Institutes of Health, National Institute of Allergy and Infectious Diseases P01-AI102851 and through the National Institutes of Health training grant T32GM007356-46 and the National Institutes of Health training grant T32HL066988-20.

## ACKNOWLEDGMENTS

This work was made possible with the support and contributions of the University of Rochester Medical Center Genomics Research Center (GRC), Flow Cytometry Core, and the Vivarium as well as the NIH Tetramer Core at Emory University.

## SUPPLEMENTARY MATERIAL

The Supplementary Material for this article can be found online at: https://www.frontiersin.org/articles/10.3389/fimmu.2021.728669/full#supplementary-material

## REFERENCES


1. Topham DJ, Tripp RA, Doherty PC. CD8+ T Cells Clear Influenza Virus by Perforin or Fas-Dependent Processes. *J Immunol* (1997) 159:5197–200.
2. Wu T, Hu Y, Lee YT, Bouchard KR, Benechet A, Khanna K, et al. Lung-Resident Memory CD8 T Cells (TRM) Are Indispensable for Optimal Cross-Protection Against Pulmonary Virus Infection. *J Leukocyte Biol* (2014) 95:215–24. doi: 10.1189/jlb.0313180
3. Martin MD, Badovinac VP. Defining Memory CD8 T Cell. *Front Immunol* (2018) 9:2692. doi: 10.3389/fimmu.2018.02692
4. Joshi NS, Cui W, Chandele A, Lee HK, Urso DR, Hagman J, et al. Inflammation Directs Memory Precursor and Short-Lived Effector CD8(+) T Cell Fates *via* the Graded Expression of T-Bet Transcription Factor. *Immunity* (2007) 27:281–95. doi: 10.1016/j.immuni.2007.07.010
5. Sallusto F, Lenig D, Forster R, Lipp M, Lanzavecchia A. Two Subsets of Memory T Lymphocytes With Distinct Homing Potentials and Effector Functions. *Nature* (1999) 401:708–12. doi: 10.1038/44385
6. Ariotti S, Hogenbirk MA, Dijkgraaf FE, Visser LL, Hoekstra ME, Song JY, et al. T Cell Memory. Skin-Resident Memory CD8(+) T Cells Trigger a State of Tissue-Wide Pathogen Alert. *Science* (2014) 346:101–5. doi: 10.1126/science.1254803
7. Schenkel JM, Fraser KA, Beura LK, Pauken KE, Vezys V, Masopust D. T Cell Memory. Resident Memory CD8 T Cells Trigger Protective Innate and Adaptive Immune Responses. *Science* (2014) 346:98–101. doi: 10.1126/science.1254536
8. Ray SJ, Franki SN, Pierce RH, Dimitrova S, Koteliansky V, Sprague AG, et al. The Collagen Binding Alpha1beta1 Integrin VLA-1 Regulates CD8 T Cell-Mediated Immune Protection Against Heterologous Influenza Infection. *Immunity* (2004) 20:167–79. doi: 10.1016/S1074-7613(04)00021-4
9. Masopust D, Jiang J, Shen H, Lefrancois L. Direct Analysis of the Dynamics of the Intestinal Mucosa CD8 T Cell Response to Systemic Virus Infection. *J Immunol* (2001) 166:2348–56. doi: 10.4049/jimmunol.166.4.2348
10. Wakim LM, Woodward-Davis A, Bevan MJ. Memory T Cells Persisting Within the Brain After Local Infection Show Functional Adaptations to Their Tissue of Residence. *Proc Natl Acad Sci United States America* (2010) 107:17872–9. doi: 10.1073/pnas.1010201107
11. Casey KA, Fraser KA, Schenkel JM, Moran A, Abt MC, Beura LK, et al. Antigen-Independent Differentiation and Maintenance of Effector-Like Resident Memory T Cells in Tissues. *J Immunol* (2012) 188:4866–75. doi: 10.4049/jimmunol.1200402
12. Thom JT, Weber TC, Walton SM, Torti N, Oxenius A. The Salivary Gland Acts as a Sink for Tissue-Resident Memory CD8(+) T Cells, Facilitating Protection From Local Cytomegalovirus Infection. *Cell Rep* (2015) 13:1125–36. doi: 10.1016/j.celrep.2015.09.082
13. Cheuk S, Schlums H, Gallais Serezal I, Martini E, Chiang SC, Marquardt N, et al. CD49a Expression Defines Tissue-Resident CD8+ T Cells Poised for Cytotoxic Function in Human Skin. *Immunity* (2017) 46:287–300. doi: 10.1016/j.immuni.2017.01.009
14. Pan Y, Tian T, Park CO, Lofftus SY, Mei S, Liu X, et al. Survival of Tissue-Resident Memory T Cells Requires Exogenous Lipid Uptake and Metabolism. *Nature* (2017) 543:252–6. doi: 10.1038/nature21379
15. Takamura S, Yagi H, Hakata Y, Motozono C, McMaster SR, Masumoto T, et al. Specific Niches for Lung-Resident Memory CD8+ T Cells at the Site of Tissue Regeneration Enable CD69-Independent Maintenance. *J Exp Med* (2016) 213:3057–73. doi: 10.1084/jem.20160938
16. Klonowski KD, Williams KJ, Marzo AL, Blair DA, Lingenheld EG, Lefrancois L. Dynamics of Blood-Borne CD8 Memory T Cell Migration In Vivo. *Immunity* (2004) 20:551–62. doi: 10.1016/S1074-7613(04)00103-7
17. Richter M, Ray SJ, Chapman TJ, Austin SJ, Rebhahn J, Mosmann TR, et al. Collagen Distribution and Expression of Collagen-Binding Alpha1beta1 (VLA-1) and Alpha2beta1 (VLA-2) Integrins on CD4 and CD8 T Cells During Influenza Infection. *J Immunol* (2007) 178:4506–16. doi: 10.4049/jimmunol.178.7.4506
18. Bankovich AJ, Shiow LR, Cyster JG. CD69 Suppresses Sphingosine 1-Phosophate Receptor-1 (S1P1) Function Through Interaction With Membrane Helix 4. *J Biol Chem* (2010) 285:22328–37. doi: 10.1074/jbc.M110.123299
19. Shiow LR, Rosen DB, Brdickova N, Xu Y, An J, Lanier LL, et al. CD69 Acts Downstream of Interferon-Alpha/Beta to Inhibit S1P1 and Lymphocyte Egress From Lymphoid Organs. *Nature* (2006) 440:540–4. doi: 10.1038/nature04606
20. Cepek KL, Shaw SK, Parker CM, Russell GJ, Morrow JS, Rimm DL, et al. Adhesion Between Epithelial Cells and T Lymphocytes Mediated by E-Cadherin and the Alpha E Beta 7 Integrin. *Nature* (1994) 372:190–3. doi: 10.1038/372190a0
21. Cepek KL, Parker CM, Madara JL, Brenner MB. Integrin Alpha E Beta 7 Mediates Adhesion of T Lymphocytes to Epithelial Cells. *J Immunol* (1993) 150:3459–70.
22. Walsh DA, Borges da Silva H, Beura LK, Peng C, Hamilton SE, Masopust D, et al. The Functional Requirement for CD69 in Establishment of Resident Memory CD8(+) T Cells Varies With Tissue Location. *J Immunol* (2019) 203:946–55. doi: 10.4049/jimmunol.1900052
23. Sheridan BS, Pham QM, Lee YT, Cauley LS, Puddington L, Lefrancois L. Oral Infection Drives a Distinct Population of Intestinal Resident Memory CD8(+) T Cells With Enhanced Protective Function. *Immunity* (2014) 40:747–57. doi: 10.1016/j.immuni.2014.03.007
24. Reilly EC, Lambert Emo K, Buckley PM, Reilly NS, Smith I, Chaves FA, et al. TRM Integrins CD103 and CD49a Differentially Support Adherence and Motility After Resolution of Influenza Virus Infection. *Proc Natl Acad Sci USA* (2020) 117:12306–14. doi: 10.1073/pnas.1915681117
25. Richter MV, Topham DJ. The Alpha1beta1 Integrin and TNF Receptor II Protect Airway CD8+ Effector T Cells From Apoptosis During Influenza Infection. *J Immunol* (2007) 179:5054–63. doi: 10.4049/jimmunol.179.8.5054
26. Melssen MM, Olson W, Wages NA, Capaldo BJ, Mauldin IS, Mahmutovic A, et al. Formation and Phenotypic Characterization of CD49a, CD49b and CD103 Expressing CD8 T Cell Populations in Human Metastatic Melanoma. *Oncoimmunology* (2018) 7:e1490855. doi: 10.1080/2162402X.2018.1490855
27. Zhang N, Bevan MJ. Transforming Growth Factor-Beta Signaling Controls the Formation and Maintenance of Gut-Resident Memory T Cells by Regulating Migration and Retention. *Immunity* (2013) 39:687–96. doi: 10.1016/j.immuni.2013.08.019
28. Bromley SK, Akbaba H, Mani V, Mora-Buch R, Chasse AY, Sama A, et al. CD49a Regulates Cutaneous Resident Memory CD8(+) T Cell Persistence and Response. *Cell Rep* (2020) 32:108085. doi: 10.1016/j.celrep.2020.108085
29. N.R. Council. *Guide for the Care and Use of Laboratory Animals*. Washington, DC: National Academies Press (2011).
30. Patel BV, Tatham KC, Wilson MR, O'Dea KP, Takata M. In Vivo Compartmental Analysis of Leukocytes in Mouse Lungs. *Am J Physiol Lung Cell Mol Physiol* (2015) 309:L639–52. doi: 10.1152/ajplung.00140.2015
31. Gays F, Unnikrishnan M, Shrestha S, Fraser KP, Brown AR, Tristram CM, et al. The Mouse Tumor Cell Lines EL4 and RMA Display Mosaic Expression of NK-Related and Certain Other Surface Molecules and Appear to Have a Common Origin. *J Immunol* (2000) 164:5094–102. doi: 10.4049/jimmunol.164.10.5094
32. Gerlach C, Moseman EA, Loughhead SM, Alvarez D, Zwijnenburg AJ, Waanders L, et al. The Chemokine Receptor CX3CR1 Defines Three Antigen-Experienced CD8 T Cell Subsets With Distinct Roles in Immune Surveillance and Homeostasis. *Immunity* (2016) 45:1270–84. doi: 10.1016/j.immuni.2016.10.018
33. Bottcher JP, Beyer M, Meissner F, Abdullah Z, Sander J, Hochst B, et al. Functional Classification of Memory CD8(+) T Cells by CX3CR1 Expression. *Nat Commun* (2015) 6:8306. doi: 10.1038/ncomms9306
34. Becht E, McInnes L, Healy J, Dutertre CA, Kwok IWH, Ng LG, et al. Dimensionality Reduction for Visualizing Single-Cell Data Using UMAP. *Nat Biotechnol* (2019) 37:38–44. doi: 10.1038/nbt.4314
35. Van Gassen S, Callebaut B, Van Helden MJ, Lambrecht BN, Demeester P, Dhaene T, et al. FlowSOM: Using Self-Organizing Maps for Visualization and Interpretation of Cytometry Data. *Cytomet A* (2015) 87:636–45. doi: 10.1002/cyto.a.22625
36. Johnson LA, Jackson DG. The Chemokine CX3CL1 Promotes Trafficking of Dendritic Cells Through Inflamed Lymphatics. *J Cell Sci* (2013) 126:5259–70. doi: 10.1242/jcs.135343
37. Muehlhoefer A, Saubermann LJ, Gu X, Luedtke-Heckenkamp K, Xavier R, Blumberg RS, et al. Fractalkine is an Epithelial and Endothelial Cell-Derived

Chemoattractant for Intraepithelial Lymphocytes in the Small Intestinal Mucosa. *J Immunol* (2000) 164:3368–76. doi: 10.4049/jimmunol.164.6.3368
38. Ignatiadis N, Klaus B, Zaugg JB, Huber W. Data-Driven Hypothesis Weighting Increases Detection Power in Genome-Scale Multiple Testing. *Nat Methods* (2016) 13:577–80. doi: 10.1038/nmeth.3885
39. Kanehisa M. Toward Understanding the Origin and Evolution of Cellular Organisms. *Protein Sci* (2019) 28:1947–51. doi: 10.1002/pro.3715
40. Kanehisa M, Furumichi M, Sato Y, Ishiguro-Watanabe M, Tanabe M. KEGG: Integrating Viruses and Cellular Organisms. *Nucleic Acids Res* (2021) 49: D545–51. doi: 10.1093/nar/gkaa970
41. Kanehisa M, Goto S. KEGG: Kyoto Encyclopedia of Genes and Genomes. *Nucleic Acids Res* (2000) 28:27–30. doi: 10.1093/nar/28.1.27
42. Love MI, Huber W, Anders S. Moderated Estimation of Fold Change and Dispersion for RNA-Seq Data With Deseq2. *Genome Biol* (2014) 15:550. doi: 10.1186/s13059-014-0550-8
43. Hombrink P, Helbig C, Backer RA, Piet B, Oja AE, Stark R, et al. Programs for the Persistence, Vigilance and Control of Human CD8(+) Lung-Resident Memory T Cells. *Nat Immunol* (2016) 17:1467–78. doi: 10.1038/ni.3589
44. Hayward SL, Scharer CD, Cartwright EK, Takamura S, Li ZT, Boss JM, et al. Environmental Cues Regulate Epigenetic Reprogramming of Airway-Resident Memory CD8(+) T Cells. *Nat Immunol* (2020) 21:309–20. doi: 10.1038/s41590-019-0584-x
45. Roos RS, Loetscher M, Legler DF, Clark-Lewis I, Baggiolini M, Moser B. Identification of CCR8, the Receptor for the Human CC Chemokine I-309. *J Biol Chem* (1997) 272:17251–4. doi: 10.1074/jbc.272.28.17251
46. Miller MD, Krangel MS. The Human Cytokine I-309 is a Monocyte Chemoattractant. *Proc Natl Acad Sci USA* (1992) 89:2950–4. doi: 10.1073/pnas.89.7.2950
47. McMaster SR, Wilson JJ, Wang H, Kohlmeier JE. Airway-Resident Memory CD8 T Cells Provide Antigen-Specific Protection Against Respiratory Virus Challenge Through Rapid IFN-Gamma Production. *J Immunol* (2015) 195:203–9. doi: 10.4049/jimmunol.1402975
48. O'Neil-Andersen NJ, Lawrence DA. Differential Modulation of Surface and Intracellular Protein Expression by T Cells After Stimulation in the Presence of Monensin or Brefeldin a. *Clin Diagn Lab Immunol* (2002) 9:243–50. doi: 10.1128/cdli.9.2.243-250.2001
49. Huang DC, Hahne M, Schroeter M, Frei K, Fontana A, Villunger A, et al. Activation of Fas by FasL Induces Apoptosis by a Mechanism That Cannot be Blocked by Bcl-2 or Bcl-X(L). *Proc Natl Acad Sci USA* (1999) 96:14871–6. doi: 10.1073/pnas.96.26.14871
50. Schneider P, Thome M, Burns K, Bodmer JL, Hofmann K, Kataoka T, et al. TRAIL Receptors 1 (DR4) and 2 (DR5) Signal FADD-Dependent Apoptosis and Activate NF-Kappab. *Immunity* (1997) 7:831–6. doi: 10.1016/S1074-7613(00)80401-X
51. Alter G, Malenfant JM, Altfeld M. CD107a as a Functional Marker for the Identification of Natural Killer Cell Activity. *J Immunol Methods* (2004) 294:15–22. doi: 10.1016/j.jim.2004.08.008
52. Mintern JD, Guillonneau C, Carbone FR, Doherty PC, Turner SJ. Cutting Edge: Tissue-Resident Memory CTL Down-Regulate Cytolytic Molecule Expression Following Virus Clearance. *J Immunol* (2007) 179:7220–4. doi: 10.4049/jimmunol.179.11.7220
53. Jenkins MR, Webby R, Doherty PC, Turner SJ. Addition of a Prominent Epitope Affects Influenza A Virus-Specific CD8+ T Cell Immunodominance Hierarchies When Antigen is Limiting. *J Immunol* (2006) 177:2917–25. doi: 10.4049/jimmunol.177.5.2917
54. Lambert Emo K, Hyun YM, Reilly E, Barilla C, Gerber S, Fowell D, et al. Live Imaging of Influenza Infection of the Trachea Reveals Dynamic Regulation of CD8+ T Cell Motility by Antigen. *PloS Pathog* (2016) 12:e1005881. doi: 10.1371/journal.ppat.1005881
55. Topham DJ, Reilly EC. Tissue-Resident Memory CD8(+) T Cells: From Phenotype to Function. *Front Immunol* (2018) 9:515. doi: 10.3389/fimmu.2018.00515
56. Stolley JM, Johnston TS, Soerens AG, Beura LK, Rosato PC, Joag V, et al. Retrograde Migration Supplies Resident Memory T Cells to Lung-Draining LN After Influenza Infection. *J Exp Med* (2020) 217(8):e20192197. doi: 10.1084/jem.20192197
57. Salerno F, Engels S, van den Biggelaar M, van Alphen FPJ, Guislain A, Zhao W, et al. Translational Repression of Pre-Formed Cytokine-Encoding mRNA Prevents Chronic Activation of Memory T Cells. *Nat Immunol* (2018) 19:828–37. doi: 10.1038/s41590-018-0155-6
58. Yang C, Khanniche A, DiSpirito JR, Ji P, Wang S, Wang Y, et al. Transcriptome Signatures Reveal Rapid Induction of Immune-Responsive Genes in Human Memory CD8(+) T Cells. *Sci Rep* (2016) 6:27005. doi: 10.1038/srep27005
59. Brinza L, Djebali S, Tomkowiak M, Mafille J, Loiseau C, Jouve PE, et al. Immune Signatures of Protective Spleen Memory CD8 T Cells. *Sci Rep* (2016) 6:37651. doi: 10.1038/srep37651
60. McCully ML, Ladell K, Andrews R, Jones RE, Miners KL, Roger L, et al. CCR8 Expression Defines Tissue-Resident Memory T Cells in Human Skin. *J Immunol* (2018) 200:1639–50. doi: 10.4049/jimmunol.1701377
61. Reimer MK, Brange C, Rosendahl A. CCR8 Signaling Influences Toll-Like Receptor 4 Responses in Human Macrophages in Inflammatory Diseases. *Clin Vaccine Immunol* (2011) 18:2050–9. doi: 10.1128/CVI.05275-11
62. Opalek JM, Ali NA, Lobb JM, Hunter MG, Marsh CB. Alveolar Macrophages Lack CCR2 Expression and do Not Migrate to CCL2. *J Inflammation (Lond)* (2007) 4:19. doi: 10.1186/1476-9255-4-19
63. Shi Y, Liu CH, Roberts AI, Das J, Xu G, Ren G, et al. Granulocyte-Macrophage Colony-Stimulating Factor (GM-CSF) and T-Cell Responses: What We do and Don't Know. *Cell Res* (2006) 16:126–33. doi: 10.1038/sj.cr.7310017
64. van Riet S, van Schadewijk A, de Vos S, Vandeghinste N, Rottier RJ, Stolk J, et al. Modulation of Airway Epithelial Innate Immunity and Wound Repair by M(GM-CSF) and M(M-CSF) Macrophages. *J Innate Immun* (2020) 12:410–21. doi: 10.1159/000506833

**Conflict of Interest:** The authors declare that the research was conducted in the absence of any commercial or financial relationships that could be construed as a potential conflict of interest.

**Publisher's Note:** All claims expressed in this article are solely those of the authors and do not necessarily represent those of their affiliated organizations, or those of the publisher, the editors and the reviewers. Any product that may be evaluated in this article, or claim that may be made by its manufacturer, is not guaranteed or endorsed by the publisher.

frontiers in Immunology

REVIEW
published: 04 October 2021
doi: 10.3389/fimmu.2021.745332

# Molecular and Cellular Mechanisms Modulating Trained Immunity by Various Cell Types in Response to Pathogen Encounter

*Orlando A. Acevedo*[1], *Roslye V. Berrios*[1], *Linmar Rodríguez-Guilarte*[1], *Bastián Lillo-Dapremont*[1] *and Alexis M. Kalergis*[1,2]*

[1] Millennium Institute of Immunology and Immunotherapy, Departamento de Genética Molecular y Microbiología, Facultad de Ciencias Biológicas, Pontificia Universidad Católica de Chile, Santiago, Chile, [2] Departamento de Endocrinología, Facultad de Medicina, Pontificia Universidad Católica de Chile, Santiago, Chile

OPEN ACCESS

**Edited by:**
Jeffrey C. Nolz,
Oregon Health and Science University, United States

**Reviewed by:**
Georges Abboud,
University of Florida, United States
Umadevi S. Sajjan,
University of Michigan, United States
Valerie Koeken,
Radboud University Nijmegen Medical Centre, Netherlands

***Correspondence:**
Alexis M. Kalergis
akalergis@bio.puc.cl

**Specialty section:**
This article was submitted to Immunological Memory, a section of the journal Frontiers in Immunology

**Received:** 21 July 2021
**Accepted:** 15 September 2021
**Published:** 04 October 2021

**Citation:**
Acevedo OA, Berrios RV, Rodríguez-Guilarte L, Lillo-Dapremont B and Kalergis AM (2021) Molecular and Cellular Mechanisms Modulating Trained Immunity by Various Cell Types in Response to Pathogen Encounter. Front. Immunol. 12:745332. doi: 10.3389/fimmu.2021.745332

The induction of trained immunity represents an emerging concept defined as the ability of innate immune cells to acquire a memory phenotype, which is a typical hallmark of the adaptive response. Key points modulated during the establishment of trained immunity include epigenetic, metabolic and functional changes in different innate-immune and non-immune cells. Regarding to epigenetic changes, it has been described that long non-coding RNAs (LncRNAs) act as molecular scaffolds to allow the assembly of chromatin-remodeling complexes that catalyze epigenetic changes on chromatin. On the other hand, relevant metabolic changes that occur during this process include increased glycolytic rate and the accumulation of metabolites from the tricarboxylic acid (TCA) cycle, which subsequently regulate the activity of histone-modifying enzymes that ultimately drive epigenetic changes. Functional consequences of established trained immunity include enhanced cytokine production, increased antigen presentation and augmented antimicrobial responses. In this article, we will discuss the current knowledge regarding the ability of different cell subsets to acquire a trained immune phenotype and the molecular mechanisms involved in triggering such a response. This knowledge will be helpful for the development of broad-spectrum therapies against infectious diseases based on the modulation of epigenetic and metabolic cues regulating the development of trained immunity.

**Keywords: trained immunity, unspecific cross-protection, epigenetics, metabolic reprogramming, innate memory**

## INTRODUCTION

The immune system represents our main line of defense against infections and other diseases. For centuries, this type of response has been divided into two large branches: innate and adaptive immunity (1). The innate immune system represents the first barrier that aims to limit the ability of pathogens to spread through our body (2, 3). This response involves various innate cells including neutrophils, monocytes, macrophages, dendritic cells (DCs), Natural Killer cells (NK cells), as well

as non-immune cells, such as the epithelium (4). The adaptive immune response corresponds to the second barrier of the immune system. Unlike the innate system, the adaptive response is antigen-specific and generates long-lasting protection, mainly mediated by T and B lymphocytes (1). It has been shown that effective memory immune responses rely on the interaction between cells of the innate and adaptive immune cells (5, 6). While activation of innate immunity provides the first line of defense against infections, it also primes the adaptive immune response *via* antigen presentation and cytokine production (7–10).

Furthermore, adaptive immunity can enhance the antimicrobial machinery of innate cells, making them more effective at clearing pathogenic microorganisms (11, 12). An additional layer of complexity is added to this network of interactions after recent findings showing the ability of innate cells to adopt a memory phenotype upon encountering different kinds of stimuli derived from pathogens (13, 14). During the last decade, such observations led to the establishment of the concept of "trained immunity", which modified the traditional conception of memory responses that only used to apply to adaptive immunity (15). This new evidence suggested that innate-immune cells can adopt a memory-like phenotype through different epigenetic, metabolic and functional changes (16, 17). Furthermore, it has been proposed that non-immune cells can develop some of the features of this memory-like phenotype (18–20). Trained immunity can be triggered by a wide range of stimuli, including the bacteria Bacillus Calmette Guerin (BCG), β-glucan (a fungal cell wall component) and sex-related hormones, such as β-estradiol (19, 21, 22). Notably, the capacity to induce trained immunity is not only restricted to microbial-derived signals and hormones, as other endogenous ligands such as oxidized low-density lipoproteins (oxLDL) can also contribute to initiating this type of response (23). In the current article, we will summarize the mechanism underlying the development of trained immunity, the cells able to develop this response, and their contribution to controlling infectious diseases.

## MECHANISMS UNDERLYING THE ESTABLISHMENT OF TRAINED IMMUNITY

Epigenetic changes on histones that interact with the DNA are one of the fundamental factors for the establishment of trained immunity (24). These epigenetic modifications include changes in histone methylation, which may promote or repress gene transcription (25). Recent studies underscore the contribution of long non-coding RNAs (LncRNAs) in triggering trained immunity due to their ability to promote chromatin remodeling by a direct interaction with chromatin while allowing the assembly of histone-modifying enzymes (26). The 3D arrangement of chromatin and proteins associated during this process occurs in discrete regions of enriched chromosomal contacts known as topologically associated domains (TADs) (27). Within TADs, genes with related functions are brought into proximity through the formation of chromosomal loops, which facilitate clustered regulation of gene transcription (27). A recent study described a novel class of LncRNAs, known as Immune-gene Priming LncRNAs (IPLs) involved in accumulating H3K4me3 at the promoters of trained immune genes (26). Bioinformatic analyses revealed the presence of a single LncRNA associated with TADs in which trained immune transcripts interacted with the histone H3Lys4 methyltransferase (MLL1) to direct local H3K4me3 accumulation (26). The IPL found in this study corresponds to UMLILO (upstream master LncRNA of the inflammatory chemokine locus) and was shown to regulate gene expression in TADs containing the genes encoding for IL8, CXCL1, CXCL2, and CXCL3 on human monocytes (26). This study also described two other important points. First, in mice, the TAD that contains these chemokines lacks UMLILO, therefore the expression of these genes cannot be trained (26). Of note, the insertion of UMLILO in the TAD of murine macrophages comprising these chemokines resulted in the training of such genes. These observations support the notion that LncRNA-mediated regulation is essential in establishing trained immunity (26). Secondly, genetic ablation of UMLILO in human monocytes abrogates the induction of trained immunity in these cells, further supporting the critical role of LncRNA in promoting innate immune training (26). In conclusion, targeting LncRNA appears as an attractive target for modulating the establishment of trained immunity and regulating inflammation (26).

The development of trained immunity also involves metabolic changes that ultimately lead to enhanced cytokine responses (28). Studies performed in mice highlight the ability of *C. albicans* infection in conferring protection against *S. aureus* (21, 29, 30). *In vitro* studies showed that trained immunity induced by *C. albicans* is mediated by the cell wall component β-glucan, which induces monocyte epigenetic remodeling and functional reprogramming (21, 30). In this case, trained monocytes accumulate the metabolite fumarate produced during the tricarboxylic acid cycle (TCA) (31). Fumarate then binds and inhibits histone demethylase 5 (KDM5) activity involved in the demethylation of H3K4 (32). Under this scenario, fumarate accumulation increases H3K4 tri-methylation in the promoters of genes encoding pro-inflammatory cytokines TNF-α and IL-6 (32). Different studies have been carried out to understand the interplay between metabolites and histone-modifying enzymes involved in establishing trained immunity. One example is acetyl-CoA, which is fundamental for the activity of histone acetyltransferases (HATs) (33, 34). Evidence showed that increased activity of metabolic pathways leading to acetyl-CoA production leads to an increased frequency of acetylation marks on histone tails (35). In mammalian cells, these changes are dependent on adenosine triphosphate (ATP)-citrate lyase (ACLY), which converts citrate into acetyl-CoA (36). Therefore, substrates that can be converted into citrate, such as glucose, fatty acids or glutamine, can ultimately lead to ACLY-dependent acetylation of histones (33). Another metabolite modulating trained immunity is itaconate, a derivative from the TCA cycle recognized by the ability to form adducts with glutathione (GSH) (37). Oxidized GSH inhibits the activity of S-adenosyl methionine synthetase, MAT1A involved in the synthesis of s-adenosyl methionine (SAM), the primary substrate of histone methyltransferases (HMTs) which are also modulators of trained

immunity (38, 39). In the worm *C. elegans*, low SAM concentration restricts H3K4me3 accumulation at immune-responsive promoters, limiting the expression of genes necessary for the innate immune response against bacterial infection (40).

Another essential change observed in β-glucan- and BCG-trained cells is the increased ratio of nicotinamide adenine dinucleotide ($NAD^+$) over the reduced form (NADH) (41). $NAD^+$ is a required cofactor for the activity of de-acetylating enzymes known as sirtuins (SIRTs) (42). These enzymes catalyze the removal of lysine acetyl groups from different proteins, including histones (42). By removing acetyl groups, lysine residues of histones recover their positive charge and become more tightly bound to DNA leading to inhibition of gene transcription (43). During the establishment of trained immunity, a higher ratio of $NAD^+$ over NADH promotes the activity of SIRTs, which subsequently influence inflammatory responses (44). *In vivo* studies showed that mice lacking SIRT2 displayed enhanced pro-inflammatory responses in a model of colitis induced by dextran sulfate sodium (DSS) as compared to wild-type mice (44). In this case, SIRT2 deficiency leads to the increased polarization of macrophages toward a pro-inflammatory phenotype (44). Thus, therapies targeting SIRT2 on macrophages could be explored to treat colitis (44). In addition, activity of Sirtuins also represses the expression of genes involved in glycolytic metabolism, including the transcriptional regulator HIF1α, a pivotal modulator for the induction of trained immunity (41). Studies related to other factors that trigger trained immunity showed that administration of BCG vaccine on healthy human volunteers up-regulates the production of IL-6 by monocytes and neutrophils upon exposure to *S. aureus* (45, 46). However, it is still not fully understood how these complex interactions take place in different immune and non-immune cells. The following sections will focus on the currently known drivers of trained immunity on different innate-immune and other non-immune cells and their contribution during infectious diseases.

## TRAINED IMMUNITY IN NEUTROPHILS

Circulating human neutrophils are the most prominent immune cells present in the blood (47). These cells are characterized by their short lifespan (6–10 h) and their rapid recruitment following BCG or *Mycobacterium tuberculosis* (*M. tuberculosis*) infection (48, 49). *In vitro* studies indicate that neutrophils derived from BCG-vaccinated individuals showed a trained immunity phenotype (46, 50). It has been suggested that such phenotype on neutrophils relies on the ability of BCG to train hematopoietic bone marrow stem cells precursors (HSCPs), which subsequently can differentiate into neutrophils (19). In addition, intravenous rather than subcutaneous immunization of mice with BCG results in trained immunity on neutrophils. Such differences may be explained by the access of BCG to the bone marrow through blood circulation (19). Trained immunity induced by BCG on neutrophils is characterized by increased expression of CD11b and Interleukin-8 (IL-8) following re-stimulation with unrelated BCG stimuli, such as *S. aureus* or lipopolysaccharide (LPS) (46). Since both markers were involved in neutrophil activation and chemotaxis, respectively (51), these data suggest that trained immunity induced by BCG on neutrophils promotes neutrophil recruitment and activation, which is also essential for bacterial clearance (52).

Studies using mice vaccinated with BCG *via* the intranasal route showed that neutrophils accumulate in the lungs as early as 1 to 3 days post-inoculation of BCG (29). Interestingly, these recruited neutrophils showed the ability to kill *M. tuberculosis*, supporting a role of BCG in promoting neutrophil antimicrobial responses (49). Furthermore, studies in the mouse model showed that neutrophil depletion before BCG vaccination resulted in increased bacterial loads compared to isotype control-treated mice (50). These data suggest that neutrophils play a significant role in reducing the mycobacterial burden and are necessary for the protection conferred by BCG vaccination (50). Further studies are needed to determine if trained immunity on neutrophils modulates the production of chemokines important to attract other immune cells, which might complement neutrophil-mediated responses.

*In vitro* studies of human-derived neutrophils indicate that BCG vaccination increases reactive oxygen species (ROS) production by these cells upon *C. albicans* stimulation as compared to neutrophils from non-vaccinated individuals (46). In addition, neutrophils derived from BCG-vaccinated subjects showed a higher production of lactate and enhanced killing activity against *C. albicans* in comparison to neutrophils from the non-vaccinated subjects (46). These data suggest that the development of trained immunity induced by BCG is associated with increased glycolytic activity and favors neutrophil-mediated killing of *C. albicans and M.* tuberculosis (46, 50). These results raise new questions, such as the way trained neutrophils may affect the function of other cell types. The contribution of non-trained neutrophils modulating the function of neighboring cells, such as macrophages and T lymphocytes has been documented (53, 54). Therefore, it would be essential to examine whether BCG-trained neutrophils may regulate the responses displayed by these immune cells. Neutrophils have been shown to train macrophages to acquire a long-lasting enhanced protective phenotype against infection (54). Furthermore, it is reported that neutrophils can activate T cells through antigen presentation (55). However, further studies at the single-cell level are needed to elucidate whether the transcriptional landscape of trained neutrophils is present on a particular subset of neutrophils or involves this entire cell population.

## TRAINED IMMUNITY IN MONOCYTES AND MACROPHAGES: GENERAL FEATURES

Monocytes are part of other subset of myeloid cells responsible for producing pro-inflammatory cytokines during an infection (56). These cells circulate in the bloodstream for up to 3 to 5 days, from where they then differentiate into macrophages (57). Monocytes and macrophages are mononuclear phagocytes that mediate fundamental innate immune processes such as pathogen

clearance, inflammatory cytokine production, and tissue repair (58, 59). The ability of monocytes and macrophages to adopt a trained immunity phenotype is an active matter of study (60). Epigenetic changes, such as H3K4me3 were elevated in promoters of genes encoding for pro-inflammatory cytokines after stimulation of monocytes with BCG or β-glucan (61, 62). This notion is supported by the observation that inhibition of histone methyltransferases using 5′-Deoxy-5′-methylthioadenosine (MTA) suppressed monocyte training by *C. albicans* or β-glucan. These data provide additional basis for the role of histone methylation in the training of monocytes (63). H3K4me3 is significantly increased at the Toll-like receptor 4 (TLR4) level in circulating monocytes collected after BCG vaccination as compared to values obtained from monocytes isolated before BCG vaccination (64). In addition to the activation of the Toll-like receptor (TLR) signaling pathway (63), immune training by β-glucan is dependent on the Dectin-1/Raf-1 pathway (65). The interaction between monocytes and β-glucan through Dectin-1 activates the spleen tyrosine kinase and the caspase recruitment domain-containing protein 9 (Syk/CARD9), resulting in the activation of the transcription factor NF-κB (61, 66). The inhibition of Dectin-1 by laminarin in purified peripheral blood monocytes from healthy donors suppressed β-glucan-induced trained immunity (63). These findings suggest that Dectin-1 is a significant driver of trained immunity in monocytes (63).

## METABOLIC PATHWAYS INVOLVED IN THE TRAINING OF MONOCYTES AND MACROPHAGES

Different metabolic pathways are involved in the regulation and development of trained immunity in monocytes (32, 67, 68). Trained monocytes show high glucose consumption, high lactate production, and a high ratio of nicotinamide dinucleotide and reduced adenine (NADH), reflecting a change in metabolism with increased glycolysis (68). These changes depend on signaling through Akt, mTOR (mammalian target of rapamycin), and HIF-1α (hypoxia-inducible factor 1α) (60). In this sense, priming of monocytes with BCG increases the phosphorylation of Akt (68). Inhibition of Akt by Wortmannin during the first 24 hours of training with BCG prevents the increase in the production of cytokines by re-stimulation with LPS (**Table 1**) (67, 68). Inhibition of mTOR by rapamycin leads to similar effects inhibiting the production of TNF-α and IL-6 following re-stimulation of cells with LPS (60) and pre-treatment of cells with ascorbate that inhibits the HIF-1α pathway (**Table 1**) (60). Treatment of cells with metformin or 2-deoxy-glucose abrogates enhanced cytokine production by inhibiting hexokinase-2 (37). Furthermore, inhibition of glycolytic pathways inhibited epigenetic modifications in the promoters of genes encoding IL-6 and TNF-α (**Table 1**) (67). The increased glycolysis observed in trained monocytes promotes the accumulation of fumarate, which inhibits histone demethylase 5 KDM5. Therefore favoring H3K4me3 on the promoters of pro-inflammatory cytokines TNFα and IL-6 (32). Other metabolic pathways involved in the development of trained immunity include the synthesis of cholesterol, which can be inhibited by statins (**Table 1**) (30), which then prevent the enrichment of H3K4me3 in the promoters of genes that encode IL-6 and TNF-α (32, 67, 68). In conclusion, several metabolic pathways could be targeted to increase trained immunity and enhance the mechanisms of immune defense against infections.

During the differentiation of monocytes into macrophages, training induced by β-glucan increases the expression of genes involved in metabolic and inflammatory pathways, and such changes are dependent on cAMP signaling. In this line, cAMP inhibitors including 2 ′, 5′-dideoxyadenosine and propranolol can prevent the increased production of IL-6 and TNF-α induced by β-glucan training (69). Additionally, monocytes and macrophages exposed to β-glucan showed a trained immune phenotype dependent on the metabolism of glutathione, a relevant antioxidant molecule involved in detoxifying free radicals (70). Along these lines, plasma concentration of IL-1β from BCG-vaccinated individuals are positively associated with serum glutathione concentrations (71). Furthermore, trained immunity also up-regulates the expression of genes involved in glutathione metabolism, suggesting an increase in glutathione synthesis and a higher glutathione recycling rate (71). Finally, single nucleotide

**TABLE 1** | Inhibitors of different signaling, metabolic and epigenetic changes are involved in inducing trained immunity against infectious diseases.

| **Inhibitors of signaling pathways** | | | |
|---|---|---|---|
| **Cell type** | **Inhibitor** | **Function** | **Reference** |
| Monocytes | Rapamycin | mTOR inhibitor | (23) |
| | Wortmannin | Akt inhibitor | |
| | Ascorbate | HIF-1α inhibitor | |
| | Metformin | AMPK inhibition | |
| **Inhibitors of metabolic pathways** | | | |
| **Cell type** | **Inhibitor** | **Function** | **Reference** |
| Monocytes | 2-Deoxy Glucose | Inhibits Hexokinase 2 | (68) |
| **Inhibitors of epigenetic modifiers** | | | |
| **Cell type** | **Inhibitor** | **Function** | **Reference** |
| Macrophages | MTA | Methyltransferase inhibitor | (63) |
| Bronchial epithelial cells | Epigallocatechin-3-gallate (EGCG) | Inhibition of histone acetyltransferase | (20) |
| | BIX01294 | Inhibitor of histone Methyltransferase | |

polymorphisms (SNPs) in these genes are associated with changes in pro-inflammatory cytokine production after *in vitro* training by β-glucan and BCG (71). Therefore, enzymes whose activity is dependent on cAMP or glutathione could be used as novel targets to modulate trained immunity.

## HORMONAL CONTROL OF TRAINED IMMUNITY RESPONSES IN MONOCYTES AND MACROPHAGES

Studies *in vivo* have shown that administration of β-glucan in mice attenuates the hallmarks of sepsis-induced by *Escherichia coli* infection in a sex-dependent manner (22). In this regard, β-glucan mediated prevention of lung injury by the induction of trained immunity worked better in females than in males (22). Interestingly, this work showed that female hormones, such as estrogens are involved in the development of trained immunity, which can also explain the increased susceptibility of male over female mice to *E. coli*-induced sepsis (22). Mechanistically the authors showed that exposure of macrophages to β-estradiol, which is a form of the female hormone estrogen (72), polarizes these cells toward a pro-inflammatory M1 phenotype with enhanced ability to kill *E. coli* and therefore more efficient at preventing sepsis (22). Finally, this study also showed that treatment of macrophages with β-estradiol inhibited the nuclear translocation of RelB, a member of the non-canonical pathway of NF-κB, which contributes to macrophage polarization towards the M1 pro-inflammatory phenotype (73).

Remarkably, the role of estradiol and sex-depended hormones in trained immunity remains controversial. *In vitro* studies have shown that sex hormones such as estradiol and dihydrotestosterone (DHT) can inhibit the production of pro-inflammatory cytokines during the trained immune response elicited by BCG (48). Therefore, further research is required to define the specific contribution of sex hormones to trained immunity and how differs from the induction by BCG or β-glucan. To our knowledge, there is only limited studies comparing the metabolic and epigenetic landscape associated with immune training induced by BCG in comparison to β-glucan (67, 74, 75).

## TRAINED IMMUNITY ON ALVEOLAR MACROPHAGES AND INVOLVEMENT OF RESIDENT CELLS

Alveolar macrophages (AMs) are the main sentinels that reside in the alveolar space and represent an example of tissue-resident cells in which trained immunity has been described (76). Most of the current knowledge in innate immune memory comes from systemic infection or immunization data, which induces innate memory in circulating monocytes or macrophages (21, 62). The establishment of trained immunity on AMs provides an example for the involvement of adaptive immunity for the development of trained immunity on innate immune cells (76). Consistently with this notion, a recent study showed that the interaction between alveolar macrophages (AMs) and T cells in the surface mucosal allows the development a memory-like response in macrophages (76).

Evidence showed that *S. pneumoniae* infection following adenovirus vaccination induces trained immunity on AMs *via* a rapid increase of chemokines and neutrophilia (76). In this process, $CD8^+$ T cells are required for the priming of AMs through secretion of IFN-γ (76). Following infection, AMs up-regulate the expression of MHC II (76). Furthermore, when $CD8^+$ T cells were depleted, a loss of AMs memory was observed at 7 and 28 days post depletion, accompanied by a decrease in AMs glycolytic rate (76). Although this type of interaction between an innate and adaptive immune response generates trained immunity phenotype in AMs, it would be important to evaluate whether other resident cell populations, such as DCs can be trained in this manner (76).

## TRAINED IMMUNITY IN NK CELLS

Natural killer (NK) cells are another cell type with the ability to adopt an immune memory-like phenotype for viral pathogens (73). Consistently with this notion, it was shown that NK cells can adopt a memory phenotype against murine cytomegalovirus (MCMV) (77). Studies in mice showed that adoptive transfer of MCMV-induced memory NK cells significantly increased the survival of newborn mice upon MCMV infection as compared to mice transferred with unexperienced NK cells (78). The mechanisms underlying trained immunity, in this case, involved structural changes at the chromatin structure, in which the suppressive DNA methylation is reduced in the locus of genes codifying for antiviral cytokines such as interferon (IFN)-γ (73). Furthermore, regulatory genes important for cell activation become accessible for the transcriptional machinery allowing a faster response upon stimulation (73). Studies from cohort patients showed that cytomegalovirus (CMV) seropositivity was associated with the expansion of memory NK cells (79). Identifying such memory cells was based on the expression of the activating receptor NKG2C, which recognizes MHC-I presented peptides leading to cell activation (80). NK memory-like cells have also been shown to be induced by the BCG vaccine (81). In humans, enhanced IFN-γ production by NK cells from vaccinated volunteers was still present over one year after vaccination, suggesting that BCG induces long-lasting memory in NK cells (81). Furthermore, this BCG-induced memory increased production of IFN-γ, IL-1β, IL-6, and TNF-α following challenges with *M. tuberculosis* and *M. tuberculosis*-unrelated pathogens, such as *C. albicans* and *S. aureus* (**Figure 1**) (81).

Experimental studies have shown that cytokine priming with an antibody cocktail containing IL-12, IL-18, and IL-15 is sufficient to program NK cells to produce higher levels of IFN-γ upon re-challenge with cytokines or antibodies targeting activating receptors, such as Ly49H and NK1.1 (82). Furthermore, the ability to produce IFN-γ is maintained at least for a month and passed from mother to daughter cells, suggesting that this memory is epigenetically controlled (66). This notion is further supported by observation that the pre-activation of NK cells with IL-12, IL-18,

and IL-15 cytokines promoted demethylation of IFN-γ regulatory elements (83). These findings suggest that NK cells can develop non-antigen-specific memory, in a process driven by chromatin remodeling (82, 83).

## TRAINED IMMUNITY IN INNATE LYMPHOID CELLS

Innate lymphoid cells (ILCs) display classical lymphoid cell morphology lacking the diversified antigen receptors expressed on T and B cells (84). ILCs consist of three groups: group 1 ILC (ILC1) producing IFN -γ, group 2 ILC (ILC2) producing IL-4, IL-5, and IL-13, and group 3 ILC (ILC3) that produce IL-17 and IL-22, which have functions similar to their pairs of adaptive immunity, helper T cells (Th) of the type Th1, Th2, and Th17 respectively (84, 85). Thus, the cytokines produced by ILCs contribute to multiple immune pathways, including lymphoid development, metabolic homeostasis, maintenance of appropriate immune responses to commensals and pathogens in mucosal barriers, enhancing adaptive immunity, and regulating tissue inflammation (84, 85).

During infections of humans or mice with *M. tuberculosis*, ILCs are decreased in peripheral blood and migrate to the site of infection in which recruitment is regulated through the CXCL13/CXCR5 axis (86). The IL-22 produced by ILC3 is essential to inhibit excess inflammation and damage to epithelial cells in mice infected by *M. tuberculosis*; these cells also reduce the bacterial load (87). It has recently been shown that ILCs have immune responses that resemble the training observed in other cells of the innate immune system; intranasal injection of BCG can increase the recruitment of ILCs to the lungs and improve IFN-γ production (13). However, it was also documented that exposure of ILC-2 to allergens such as *Aspergillus* induces a pathological trained immunity response characterized by the secretion of Th2 related cytokines such as IL-5 and IL-13 (**Figure 1**) (88). These data suggest that trained immunity can also generate pathological responses depending on the stimuli involved. Further studies are needed to elucidate the epigenetic changes and metabolic factors associated with ILC-2 training (88).

## TRAINED IMMUNITY ON HEMATOPOIETIC STEM CELLS

Hematopoietic stem cells (HSCs) are long-lived cells mainly present in the bone marrow (BM), which can self-renew and generate multipotent and lineage-committed hematopoietic progenitors, which then originate the entire set of cells present in the mammalian blood system (89). Interestingly, a recent study showed that allowing the access of BCG vaccine to the bone marrow employing intravenous immunization rather than subcutaneous (sc) route in mice modified the transcriptomic landscape of HSCs resulting in enhanced myelopoiesis (19). As compared to the standard subcutaneous route, an intravenous administration of BCG favors the expansion of HSC progenitors and the up-regulation of different genes involved in DNA replication, cell division, and cell cycle (19). Among them, various key regulators of cell cycle progression such as Cdk1,

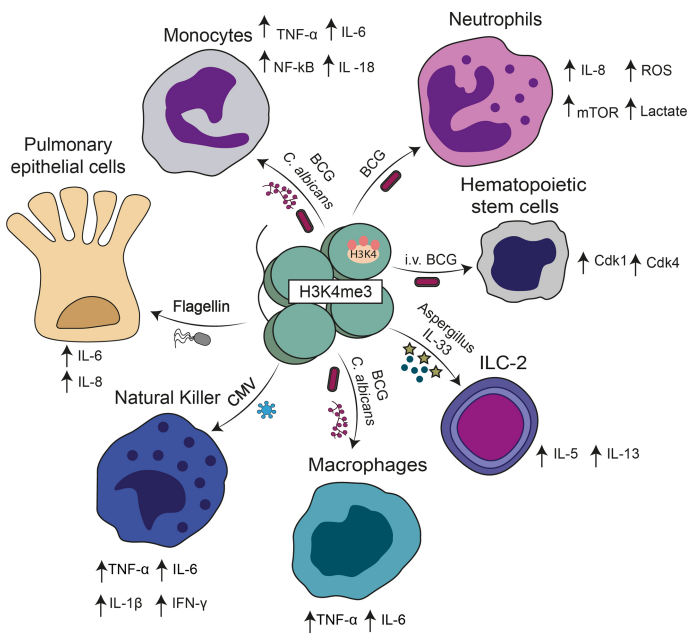


**FIGURE 1** | Cell subsets in which trained immunity has been described. Different stimuli including BCG, β-glucan, cytokines, CMV, and bacterial components can induce a trained immunity phenotype. A common hallmark of trained immunity in these cases is the presence of H3K4me3 in the promoters of genes encoding for different cytokines described in the figure.

Cdk4, and other cyclins were strongly up-regulated in HSCs of mice vaccinated intravenously with BCG as compared with HSCs from animals immunized subcutaneously BCG (**Figure 1**) (19). Interestingly, macrophages derived from the bone marrow of mice immunized intravenously with BCG, but not subcutaneously, showed significantly better protection against an *in vitro M. tuberculosis* challenge (19). Therefore, the outcomes of trained immunity also involved changes in the precursors of innate cells, such as macrophages and neutrophils (19). In the latter case, as mature neutrophils have a short lifespan it was demonstrated that trained immunity can act *via* the modulation of hematopoietic stem cells (HSCs) (90). In this *in vivo* study, intraperitoneal injection of mice with β-glucan increased the numbers and frequency of multipotent progenitors and hematopoietic progenitors in the bone marrow and led to enhanced cell-cycle progression in HSCs (90). This was a beneficial response facing a second heterologous challenge with LPS or chemotherapy-induced myelosuppression (90). However, elevated production of cytokines, such as IFN-γ can also produce unwanted cell survival effects because sustained IFN-γ signaling can have negative consequences on hematopoietic stem cells by increasing susceptibility for secondary stress-induced apoptosis (91). However, is still controversial whether IFN-γ alone induces HSC apoptosis. *In vitro* IFN-γ treatment of human HSCs co-cultured with stromal cells augmented HSC apoptosis (92). In addition, RNA expression studies of HSCs from patients with high IFN-γ levels have indicated an increase in the transcription of apoptosis-related genes (93). Furthermore, stimulation of HSCs with IFN-γ alone showed no increase in apoptosis (94). Therefore, suggesting that interaction of IFN-γ with the action of other cells modulates HSCs apoptosis. These findings provide valuable information to developing new therapeutic approaches to target trained immunity and cytokine production for diseases in which cell cycle disorders play a significant role, such as cancer (95).

## TRAINED IMMUNITY IN BRONCHIAL EPITHELIAL CELLS

Although many reports have shown that trained immunity is triggered in innate immune cells, a recent study highlights the ability of respiratory epithelial cells in acquiring a memory phenotype after exposure to flagellin from *Pseudomonas aeuroginosa* (*P. aeuroginosa*) (20). Specifically, *in vitro* studies showed that pre-exposure of human bronchial epithelial cells (BEAS2-B) to this bacterial component increases their inflammatory response to living conidia from *Aspergillus fumigatus* (*A. fumigatus*) and LPS (20). In this case, trained cells produced increased levels of IL-8 and IL-6 following LPS or *A. fumigatus* challenge in comparison to non-trained controls (**Figure 1**). Trained immune responses were shown to rely on epigenetic modifications. For example, inhibition of histone acetyltransferase with epigallocatechin-3-gallate (EGCG) significantly reduced the flagellin-induced IL-8 trained immune response to *A. fumigates* (**Table 1**) (20). Similarly, treatment of cells with BIX01294, an inhibitor of histone methyltransferase which prevents methylation of H3K4, also reduced flagellin-induced IL-8 trained immune response without affecting the IL-8 levels observed in non-trained cells (**Table 1**) (20).

## TRAINED IMMUNITY IN SKIN STEM CELLS

Skin stem cells have been also shown capable of generating a prolonged memory to acute inflammation, which allows accelerating the restoration after subsequent damage in a model of skin inflammation induced by TLR7 and the NALP3 agonist imiquimod (96). Sequence analyses revealed an increase of inflammation and hyper proliferation-associated pathways, including apoptosis signaling, interleukin signaling, oxidative stress response, and PI3 kinase pathways (96). It was suggested that the memory experienced by the inflammation of skin epithelial stem cells may be the basis for the recurrent skin inflammation exhibited by patients with autoimmune disorders, such as psoriasis and atopic dermatitis, as well as hyperproliferative disorders, including cancer (96).

## TRAINED IMMUNITY IN THE GASTROINTESTINAL TRACT

Evidence from recent studies showed that β-glucan can also influence intestinal inflammation and epithelial barrier function. Experiments in mice showed that oral administration of β-glucan could aggravate intestinal inflammation in a model of dextran sodium sulfate (DSS)-induced colitis (97). In addition, mice lacking dectin-1, the receptor for β-glucan, also showed augmented susceptibility to DSS-induced colitis, a finding recapitulated in humans with specific polymorphisms in dectin-1 (97). Prolonged oral treatment of mice with antifungals increases disease severity in models of chronic colitis and chronic allergic airways disease (98). Such findings highlight the importance of a healthy fungal community in gut homeostasis. Furthermore, these results also suggest that gut microbiota may influence peripheral immune responses and pulmonary allergies. In this line, additional research is needed to further elucidate the role of trained immunity in the gut in health and disease.

## IMMUNITY TRAINING IN AGAINST PROTOZOAN-MEDIATED PATHOLOGIES

The trained immunity also confers protection against protozoan infectious agents, as demonstrated for Leishmaniasis, which is associated with a pro-inflammatory activity in monocytes and macrophages (99–102). A recent study shows that the induction of trained immunity by β-glucan increases the efficiency of phagocytosis and the clearance of *L. braziliensis*, in parallel with increased production of cytokines, specifically IL-6 and

IL-10 (100). Such an increased immune response depends on the enhanced expression of IL-32 that induces antimicrobial peptides (100).

## TRAINED IMMUNITY IN NON-INFECTIOUS PATHOLOGIES

The trained immunity induced by BCG or β-glucan not only confers non-specific protection against infectious agents, but also to other pathologies, such as cancer (39). For example, the BCG vaccine can contribute to the anti-tumor immune response as a treatment in bladder cancer (39). The anti-tumor effect of BCG seem to rely on the ability to induce trained immunity in monocytes in which autophagy plays an essential regulatory role (103, 104). It has been shown during non-muscle-invasive bladder cancer that high expression of histone methyltransferase G9a is associated with poor cancer prognosis (39).The activity of this enzyme inhibits the induction of trained immunity in monocytes (39). In addition pharmacological inhibition of G9a improves trained immune responses, accompanied by a decrease in H3K9me2 marks on pro-inflammatory genes (39). Furthermore, *ex vivo* inhibition of G9a is associated with an amplified trained immune response and altered RNA expression of inflammatory genes in monocytes derived from patients suffering non-muscle-invasive bladder cancer (39).

In contrast, functional and transcriptional reprogramming toward a long-term pro-inflammatory phenotype of monocytes and macrophages after brief *in vitro* exposure to ox-LDL contributes to the progression to atherosclerosis (23, 105). Monocytes from patients with severe symptomatic coronary atherosclerosis display a pro-inflammatory phenotype associated with the epigenetic remodeling at the level of histone methylation and higher expression of speed-limiting enzymes of the glycolysis and pentose phosphate pathways (106). Consistently with this notion, bone marrow-derived and peritoneal macrophages from $ApoE^{-/-}$ mice (a murine model of atherosclerosis) produced more pro-inflammatory cytokines after TLR stimulation by LPS than did saline-treated controls. These data suggest that an ApoE deficiency may lead to the development of trained immunity (107). However, additional research is needed to determine the relationship between trained immunity and this pathology.

## CONCLUDING REMARKS

While the induction of trained immunity has been shown for different types of innate cells, there is increasing evidence showing that other non-immune cells could also contribute to this type of immune/inflammatory response. Important questions that remain to be answered include elucidating the spectrum of cells that can develop a trained immunity phenotype and test if this process depends on the origin of cells. Finally, it will be important to elucidate the mechanism regulating trained immunity to provide an enhanced host defense while preventing a deleterious inflammation on different tissues. Answers to these questions in future studies are crucial to targeting trained immunity to develop broad-spectrum therapeutic approaches against infectious and non-infectious diseases.

## FUTURE PERSPECTIVES

Here we have described and discussed as to how different epigenetic and metabolic changes can lead to the establishment of trained immunity. There is an intricate relationship between the metabolic reprogramming of cells and epigenetic changes given by the ability of multiple metabolites to modulate the activity of histone-modifying enzymes that subsequently regulate gene expression. However, many gaps of knowledge remain in this field. For example, it remains to define how long the changes associated to trained immunity last and if, in addition to epigenetic modulation, there are other post-translational modifications on proteins relevant for the induction of trained immunity. Finally, due to the wide arsenal of epigenetic and metabolic pathways involved in regulation of trained immunity there are several potential targets to modulate the magnitude of trained memory responses and subsequently regulate inflammation. However, because it is currently thought that epigenetic modulators may have pleiotropic unwanted effects, it is possible that using LncRNAs could constitute a more specific therapeutical approach. The knowledge about the factors controlling the folding state of a given LncRNA, as well as the identification of structural motifs involved in interaction with histone modifying enzymes, may contribute to the design of next-generation therapies able to increase the expression of relevant cytokines to enhance antimicrobial responses of different cell sub-sets.

## AUTHOR CONTRIBUTIONS

OA, RB, BL-D, LR-G, and AK wrote the manuscript. AK reviewed the manuscript and approved the version to be published. All authors contributed to the article and approved the submitted version.

## FUNDING

This research was funded by CONICYT PAI project I781902009 Chile, as well as the Millennium Institute on Immunology and Immunotherapy grant number P09/016-F and ICN09_016. CORFO grant #13CTI-21526/P4 and P5; ANID/FONDECYT grants #3180570 (KB); #1190830 (AMK). Biomedical Research Consortium CTU06 (AK). COPEC-UC2019.R.1169. COPEC-UC2020.E.1.

## REFERENCES


1. Sun L, Wang X, Saredy J, Yuan Z, Yang X, Wang H. Innate-Adaptive Immunity Interplay and Redox Regulation in Immune Response. *Redox Biol* (2020) 37:101759. doi: 10.1016/j.redox.2020.101759
2. Zak DE, Aderem A. Systems Integration of Innate and Adaptive Immunity. *Vaccine* (2015) 33:5241–8. doi: 10.1016/j.vaccine.2015.05.098
3. Hato T, Dagher PC. How the Innate Immune System Senses Trouble and Causes Trouble. *Clin J Am Soc Nephrol* (2015) 10:1459–69. doi: 10.2215/CJN.04680514
4. Sarma JV, Ward PA. The Complement System. *Cell Tissue Res* (2011) 343:227–35. doi: 10.1007/s00441-010-1034-0
5. Gasteiger G, Rudensky AY. Interactions Between Innate and Adaptive Lymphocytes. *Nat Rev Immunol* (2014) 14(9):631–9. doi: 10.1038/nri3726
6. Eisenbarth SC. Dendritic Cell Subsets in T Cell Programming: Location Dictates Function. *Nat Rev Immunol* (2019) 2:89–103. doi: 10.1038/s41577-018-0088-1
7. Guermonprez P, Valladeau J, Zitvogel L, Théry C, Amigorena S. Antigen Presentation and T Cell Stimulation by Dendritic Cells. *Annu Rev Immunol* (2002) 20(20):621–767. doi: 10.1146/annurev.immunol.20.100301.064828
8. Meinderts SM, Baker G, Van Wijk S, Beuger BM, Geissler J, Jansen MH, et al. Neutrophils Acquire Antigen-Presenting Cell Features After Phagocytosis of IgG-Opsonized Erythrocytes. *Blood Adv* (2019) 3 (11):1761–73. doi: 10.1182/bloodadvances.2018028753
9. Muntjewerff EM, Meesters LD, van den Bogaart G. Antigen Cross-Presentation by Macrophages. *Front Immunol* (2020) 11:1–11. doi: 10.3389/fimmu.2020.01276
10. Jennings P, Yuan D. NK Cell Enhancement of Antigen Presentation by B Lymphocytes. *J Immunol* (2009) 182(5):2879–87. doi: 10.4049/jimmunol.0803220
11. Liu W, Xiao X, Demirci G, Madsen J, Li XC. Macrophages Licensed by CD4+ T Cells Can Recognize and Reject Allogeneic Cells. *Transplant J* (2012) 188 (6):2703–11. doi: 10.1097/00007890-201211271-00883
12. Ara A, Ahmed KA, Xiang J. Multiple Effects of CD40–CD40L Axis in Immunity Against Infection and Cancer. *ImmunoTargets Ther* (2018) 7:55–61. doi: 10.2147/itt.s163614
13. Wang X, Peng H, Tian Z. Innate Lymphoid Cell Memory. *Cell Mol Immunol* (2019) 16:423–9. doi: 10.1038/s41423-019-0212-6
14. Netea MG, van der Meer JWM. Trained Immunity: An Ancient Way of Remembering. *Cell Host Microbe* (2017) 21:297–300. doi: 10.1016/j.chom.2017.02.003
15. Netea MG, Joosten LAB, Latz E, Mills KHG, Natoli G, Stunnenberg HG, et al. Trained Immunity: A Program of Innate Immune Memory in Health and Disease. *Sci (80- )* (2016) 352:427. doi: 10.1126/science.aaf1098
16. Covián C, Ríos M, Berríos-Rojas RV, Bueno SM, Kalergis AM. Induction of Trained Immunity by Recombinant Vaccines. *Front Immunol* (2021) 11:611946. doi: 10.3389/fimmu.2020.611946
17. Covián C, Fernández-Fierro A, Retamal-Díaz A, Díaz FE, Vasquez AE, Lay MK, et al. BCG-Induced Cross-Protection and Development of Trained Immunity: Implication for Vaccine Design. *Front Immunol* (2019) 10:2806. doi: 10.3389/fimmu.2019.02806
18. Liu GY, Liu Y, Lu Y, Qin YR, Di GH, Lei YH, et al. Short-Term Memory of Danger Signals or Environmental Stimuli in Mesenchymal Stem Cells: Implications for Therapeutic Potential. *Cell Mol Immunol* (2016) 3:369–78. doi: 10.1038/cmi.2015.11
19. Kaufmann E, Sanz J, Dunn JL, Khan N, Mendonça LE, Pacis A, et al. BCG Educates Hematopoietic Stem Cells to Generate Protective Innate Immunity Against Tuberculosis. *Cell* (2018) 172:176–90.e19. doi: 10.1016/j.cell.2017.12.031
20. Bigot J, Guillot L, Guitard J, Ruffin M, Corvol H, Chignard M, et al. Respiratory Epithelial Cells Can Remember Infection: A Proof-Of-Concept Study. *J Infect Dis* (2020) 221(6):1000–5. doi: 10.1093/infdis/jiz569
21. Leonhardt J, Große S, Marx C, Siwczak F, Stengel S, Bruns T, et al. Candida Albicansβ-Glucan Differentiates Human Monocytes Into a Specific Subset of Macrophages. *Front Immunol* (2018) 9:2818. doi: 10.3389/fimmu.2018.02818
22. Sun Z, Pan Y, Qu J, Xu Y, Dou H, Hou Y. 17β-Estradiol Promotes Trained Immunity in Females Against Sepsis via Regulating Nucleus Translocation of RelB. *Front Immunol* (2020) 11:1591. doi: 10.3389/fimmu.2020.01591
23. Bekkering S, Quintin J, Joosten LAB, van der Meer JWM, Netea MG, Riksen NP. Oxidized Low-Density Lipoprotein Induces Long-Term Proinflammatory Cytokine Production and Foam Cell Formation via Epigenetic Reprogramming of Monocytes. *Arterioscler Thromb Vasc Biol* (2014) 34:1731–8. doi: 10.1161/ATVBAHA.114.303887
24. Van Der Heijden CDCC, Noz MP, Joosten LAB, Netea MG, Riksen NP, Keating ST. Epigenetics and Trained Immunity. *Antioxid Redox Signal* (2018) 29(11):1023–40. doi: 10.1089/ars.2017.7310
25. Fanucchi S, Domínguez-Andrés J, Joosten LAB, Netea MG, Mhlanga MM. The Intersection of Epigenetics and Metabolism in Trained Immunity. *Immunity* (2021) 29(11):1023–40. doi: 10.1016/j.immuni.2020.10.011
26. Fanucchi S, Fok ET, Dalla E, Shibayama Y, Börner K, Chang EY, et al. Immune Genes are Primed for Robust Transcription by Proximal Long Noncoding RNAs Located in Nuclear Compartments. *Nat Genet* (2019) 51:138–50. doi: 10.1038/s41588-018-0298-2
27. Gonzalez-Sandoval A, Gasser SM. On TADs and LADs: Spatial Control Over Gene Expression. *Trends Genet* (2016) 8:485–95. doi: 10.1016/j.tig.2016.05.004
28. Kleinnijenhuis J, Quintin J, Preijers F, Benn CS, Joosten LAB, Jacobs C, et al. Long-Lasting Effects of Bcg Vaccination on Both Heterologous Th1/Th17 Responses and Innate Trained Immunity. *J Innate Immun* (2014) 6:152–8. doi: 10.1159/000355628
29. Lilly EA, Yano J, Shannon KE, Hardie E. Spectrum of Trained Innate Immunity Induced by Low-Virulence Candida Species Against Lethal Polymicrobial Intra-Abdominal Infection. *G E N* (1992) 46:43–8. doi: 10.1128/IAI.00348-19
30. Bekkering S, Blok BA, Joosten LAB, Riksen NP, Van Crevel R, Netea MG. In Vitro Experimental Model of Trained Innate Immunity in Human Primary Monocytes. *Clin Vaccine Immunol* (2016) 23:926–33. doi: 10.1128/CVI.00349-16
31. Martínez-Reyes I, Chandel NS. Mitochondrial TCA Cycle Metabolites Control Physiology and Disease. *Nat Commun* (2020) 11(1):102. doi: 10.1038/s41467-019-13668-3
32. Arts RJW, Novakovic B, ter Horst R, Carvalho A, Bekkering S, Lachmandas E, et al. Glutaminolysis and Fumarate Accumulation Integrate Immunometabolic and Epigenetic Programs in Trained Immunity. *Cell Metab* (2016) 24:807–19. doi: 10.1016/j.cmet.2016.10.008
33. Feron O. The Many Metabolic Sources of Acetyl-CoA to Support Histone Acetylation and Influence Cancer Progression. *Ann Transl Med* (2019) 7 (Suppl 8):S277.1–6. doi: 10.21037/atm.2019.11.140
34. Bradshaw PC. Acetyl-Coa Metabolism and Histone Acetylation in the Regulation of Aging and Lifespan. *Antioxidants* (2021) 10(4):572.1–43. doi: 10.3390/antiox10040572
35. Fan J, Krautkramer KA, Feldman JL, Denu JM. Metabolic Regulation of Histone Post-Translational Modifications. *ACS Chem Biol* (2015) 10(1):95–108. doi: 10.1021/cb500846u
36. Wellen KE, Hatzivassiliou G, Sachdeva UM, Bui TV, Cross JR, Thompson CB. ATP-Citrate Lyase Links Cellular Metabolism to Histone Acetylation. *Sci (80- )* (2009) 324(5930):1076–80. doi: 10.1126/science.1164097
37. Mills EL, Ryan DG, Prag HA, Dikovskaya D, Menon D, Zaslona Z, et al. Itaconate is an Anti-Inflammatory Metabolite That Activates Nrf2 via Alkylation of KEAP1. *Nature* (2018) 556(7699):113–7. doi: 10.1038/nature25986
38. Keating ST, Groh L, van der Heijden CDCC, Rodriguez H, dos Santos JC, Fanucchi S, et al. The Set7 Lysine Methyltransferase Regulates Plasticity in Oxidative Phosphorylation Necessary for Trained Immunity Induced by β-Glucan. *Cell Rep* (2020) 31(3):107548.1–22. doi: 10.1016/j.celrep.2020.107548
39. Mourits VP, van Puffelen JH, Novakovic B, Bruno M, Ferreira AV, Arts RJW, et al. Lysine Methyltransferase G9a is an Important Modulator of Trained Immunity. *Clin Transl Immunol* (2021) 10(2):e1253.1–16. doi: 10.1002/cti2.1253
40. Ding W, Smulan LJ, Hou NS, Taubert S, Watts JL, Walker AK. S-Adenosylmethionine Levels Govern Innate Immunity Through Distinct Methylation-Dependent Pathways. *Cell Metab* (2015) 22(4):633–45. doi: 10.1016/j.cmet.2015.07.013
41. Cheng SC, Quintin J, Cramer RA, Shepardson KM, Saeed S, Kumar V, et al. MTOR- and HIF-1α-Mediated Aerobic Glycolysis as Metabolic Basis for Trained Immunity. *Sci (80- )* (2014) 345:1250684–1250684. doi: 10.1126/science.1250684

42. Anderson KA, Madsen AS, Olsen CA, Hirschey MD. Metabolic Control by Sirtuins and Other Enzymes That Sense NAD+, NADH, or Their Ratio. *Biochim Biophys Acta - Bioenerg* (2017) 1858:991–8. doi: 10.1016/j.bbabio.2017.09.005
43. Ali I, Conrad RJ, Verdin E, Ott M. Lysine Acetylation Goes Global: From Epigenetics to Metabolism and Therapeutics Graphical Abstract HHS Public Access. *Chem Rev* (2018) 118:1216–52. doi: 10.1021/acs.chemrev.7b00181.Lysine
44. Sasso GL, Menzies KJ, Mottis A, Piersigilli A, Perino A, Yamamoto H, et al. SIRT2 Deficiency Modulates Macrophage Polarization and Susceptibility to Experimental Colitis. *PloS One* (2014) 9:e103573. doi: 10.1371/journal.pone.0103573
45. Cirovic B, de Bree LCJ, Groh L, Blok BA, Chan J, van der Velden WJFM, et al. BCG Vaccination in Humans Elicits Trained Immunity via the Hematopoietic Progenitor Compartment. *Cell Host Microbe* (2020) 28:322–334.e5. doi: 10.1016/j.chom.2020.05.014
46. Moorlag SJCFM, Rodriguez-Rosales YA, Gillard J, Fanucchi S, Theunissen K, Novakovic B, et al. BCG Vaccination Induces Long-Term Functional Reprogramming of Human Neutrophils. *Cell Rep* (2020) 33:108387. doi: 10.1016/j.celrep.2020.108387
47. Summers C, Rankin SM, Condliffe AM, Singh N, Peters AM, Chilvers ER. Neutrophil Kinetics in Health and Disease. *Trends Immunol* (2010) 31:318–24. doi: 10.1016/j.it.2010.05.006
48. D'avila H, Roque NR, Cardoso RM, Castro-Faria-Neto HC, Melo RCN, Bozza PT. Neutrophils Recruited to the Site of Mycobacterium Bovis BCG Infection Undergo Apoptosis and Modulate Lipid Body Biogenesis and Prostaglandin E 2 Production by Macrophages. *Cell Biol* (2008) 10 (12):2589–604. doi: 10.1111/j.1462-5822.2008.01233.x
49. Lombard R, Doz E, Carreras F, Epardaud M, Le Vern Y, Buzoni-Gatel D, et al. IL-17RA in non-Hematopoietic Cells Controls CXCL-1 and 5 Critical to Recruit Neutrophils to the Lung of Mycobacteria-Infected Mice During the Adaptive Immune Response. *PloS One* (2016) 11:1–18. doi: 10.1371/journal.pone.0149455
50. Bickett TE, McLean J, Creissen E, Izzo L, Hagan C, Izzo AJ, et al. Characterizing the BCG Induced Macrophage and Neutrophil Mechanisms for Defense Against Mycobacterium Tuberculosis. *Front Immunol* (2020) 11:1202. doi: 10.3389/fimmu.2020.01202
51. Paugam C, Chollet-Martin S, Dehoux M, Chatel D, Brient N, Desmonts JM, et al. Neutrophil Expression of CD11b/CD18 and IL-8 Secretion During Normothermic Cardiopulmonary Bypass. *J Cardiothorac Vasc Anesth* (1997) 11:575–9. doi: 10.1016/S1053-0770(97)90007-0
52. Suttmann H, Lehan N, Böhle A, Brandau S. Stimulation of Neutrophil Granulocytes With Mycobacterium Bovis Bacillus Calmette-Guérin Induces Changes in Phenotype and Gene Expression and Inhibits Spontaneous Apoptosis. *Infect Immun* (2003) 71:4647–56. doi: 10.1128/IAI.71.8.4647-4656.2003
53. Li Y, Wang W, Yang F, Xu Y, Feng C, Zhao Y. The Regulatory Roles of Neutrophils in Adaptive Immunity. *Cell Commun Signal* (2019) 17 (1):147.1–11. doi: 10.1186/s12964-019-0471-y
54. Grainger JR, Grencis RK. Neutrophils Worm Their Way Into Macrophage Long-Term Memory. *Nat Immunol* (2014) (10):902–4. doi: 10.1038/ni.2990
55. Minns D, Smith KJ, Findlay EG. Orchestration of Adaptive T Cell Responses by Neutrophil Granule Contents. *Mediators Inflamm* (2019) 8968943:1–16. doi: 10.1155/2019/8968943
56. Chiu S, Bharat A. Role of Monocytes and Macrophages in Regulating Inmmune Reponse Following Lung Transplantation. *Physiol Behav* (2017) 176:139–48. doi: 10.1097/MOT.0000000000000313.Role
57. Joeris T, Müller-Luda K, Agace WW, Mowat AMI. Diversity and Functions of Intestinal Mononuclear Phagocytes. *Mucosal Immunol* (2017) 10:845–64. doi: 10.1038/mi.2017.22
58. Gordon S, Taylor PR. Monocyte and Macrophage Heterogeneity. *Nat Rev Immunol* (2005) 5:953–64. doi: 10.1038/nri1733
59. Hirayama D, Iida T, Nakase H. The Phagocytic Function of Macrophage-Enforcing Innate Immunity and Tissue Homeostasis. *Int J Mol Sci* (2017) 19:1–14. doi: 10.3390/ijms19010092
60. Ieronymaki E, Daskalaki MG, Lyroni K, Tsatsanis C. Insulin Signaling and Insulin Resistance Facilitate Trained Immunity in Macrophages Through Metabolic and Epigenetic Changes. *Front Immunol* (2019) 10:1330. doi: 10.3389/fimmu.2019.01330
61. Wagener M, Hoving JC, Ndlovu H, Marakalala MJ. Dectin-1-Syk-CARD9 Signaling Pathway in TB Immunity. *Front Immunol* (2018) 9:225. doi: 10.3389/fimmu.2018.00225
62. Arts RJW, Joosten LAB, Netea MG. Immunometabolic Circuits in Trained Immunity. *Semin Immunol* (2016) 28:425–30. doi: 10.1016/j.smim.2016.09.002
63. Quintin J, Saeed S, Martens JHA, Giamarellos-Bourboulis EJ, Ifrim DC, Logie C, et al. Candida Albicans Infection Affords Protection Against Reinfection via Functional Reprogramming of Monocytes. *Cell Host Microbe* (2012) 12:223–32. doi: 10.1016/j.chom.2012.06.006
64. Kleinnijenhuis J, Quintin J, Preijers F, Joosten LAB, Ifrim DC, Saeed S, et al. Bacille Calmette-Guérin Induces NOD2-Dependent Nonspecific Protection From Reinfection via Epigenetic Reprogramming of Monocytes. *Proc Natl Acad Sci USA* (2012) 109:17537–42. doi: 10.1073/pnas.1202870109
65. Shi C, Pamer EG. Monocyte Recruitment During Infection and Inflammation. *Nat Rev Immunol* (2011) 11:762–74. doi: 10.1038/nri3070
66. Lee DH, Kim HW. Innate Immunity Induced by Fungal β-Glucans via Dectin-1 Signaling Pathway. *Int J Med Mushrooms* (2014) 16:1–16. doi: 10.1615/IntJMedMushr.v16.i1.10
67. Arts RJW, Carvalho A, La Rocca C, Palma C, Rodrigues F, Silvestre R, et al. Immunometabolic Pathways in BCG-Induced Trained Immunity. *Cell Rep* (2016) 17:2562–71. doi: 10.1016/j.celrep.2016.11.011
68. Kumar V, Giamarellos-bourboulis EJ, Martens JHA, Rao NA, Aghajanirefah A, Manjeri GR, et al. mTOR/Hif1α-Mediated Aerobic Glycolysis as Metabolic Basis for Trained Immunity. *Sci (80- )* (2014) 345:1–18. doi: 10.1126/science.1250684.mTOR/HIF1
69. Saeed S, Quintin J, Kerstens HHD, Rao NA, Aghajanirefah A, Matarese F, et al. Epigenetic Programming of Monocyte-to-Macrophage Differentiation and Trained Innate Immunity. *Science* (2014) 345:1251086. doi: 10.1126/science.1251086
70. Hayes JD, McLellan LI. Glutathione and Glutathione-Dependent Enzymes Represent a Co-Ordinately Regulated Defence Against Oxidative Stress. In *Free Radical Research* (1999) 31(4):273–300. doi: 10.1080/10715769900300851
71. Ferreira AV, Koeken VACM, Matzaraki V, Kostidis S, Alarcon-Barrera JC, de Bree LCJ, et al. Glutathione Metabolism Contributes to the Induction of Trained Immunity. *Cells* (2021) 101–11. doi: 10.3390/cells10050971
72. Mahmoodzadeh S, Dworatzek E. The Role of 17β-Estradiol and Estrogen Receptors in Regulation of Ca2+ Channels and Mitochondrial Function in Cardio Myocytes. *Front Endocrinol (Lausanne)* (2019) 15:1–15. doi: 10.3389/fendo.2019.00310
73. Luetke-Eversloh M, Hammer Q, Durek P, Nordström K, Gasparoni G, Pink M, et al. Human Cytomegalovirus Drives Epigenetic Imprinting of the IFNG Locus in NKG2Chi Natural Killer Cells. *PloS Pathog* (2014) 10:1–13. doi: 10.1371/journal.ppat.1004441
74. Domínguez-Andrés J, Arts RJW, Bekkering S, Bahrar H, Blok BA, de Bree LCJ, et al. In Vitro Induction of Trained Immunity in Adherent Human Monocytes. *STAR Protoc* (2021) 2(1):100365.1–10. doi: 10.1016/j.xpro.2021.100365
75. de Bree CLCJ, Janssen R, Aaby P, van Crevel R, Joosten LAB, Benn CS, et al. The Impact of Sex Hormones on BCG-Induced Trained Immunity. *J Leukoc Biol* (2018) 104:573–8. doi: 10.1002/JLB.5MA0118-027R
76. Yao Y, Jeyanathan M, Haddadi S, Robbins CS, Schertzer JD, Xing Z, et al. Induction of Autonomous Memory Alveolar Macrophages Requires T Cell Help and Is Critical to Article Induction of Autonomous Memory Alveolar Macrophages Requires T Cell Help. *Cell* (2018) 175:1634–50.e17. doi: 10.1016/j.cell.2018.09.042
77. O'Leary JG, Goodarzi M, Drayton DL, Von Andrian UH. Cell- and B Cell-Independent Adaptive Immunity Mediated by Natural Killer Cells. *Nat Immunol* (2006) 7:507–16. doi: 10.1038/ni1332
78. JF B, Jf W GD, RM W. Adoptive Transfer Studies Demonstrating the Antiviral Effect of Natural Killer Cells *In Vivo*. *J Exp Med* (1985) 161:40–52. doi: 10.1084/jem.161.1.40
79. Foley B, Cooley S, Verneris MR, Curtsinger J, Luo X, Waller EK, et al. Human Cytomegalovirus (CMV)-Induced Memory-Like NKG2C + NK Cells Are Transplantable and Expand *In Vivo* in Response to Recipient CMV Antigen. *J Immunol* (2012) 189:5082–8. doi: 10.4049/jimmunol.1201964

80. Della Chiesa M, Sivori S, Carlomagno S, Moretta L, Moretta A. Activating KIRs and NKG2C in Viral Infections: Toward NK Cell Memory? *Front Immunol* (2015) 6:573. doi: 10.3389/fimmu.2015.00573
81. Kleinnijenhuis J, Quintin J, Preijers F, Joosten LAB, Jacobs C, Xavier RJ, et al. BCG-Induced Trained Immunity in NK Cells: Role for non-Specific Protection to Infection. *Clin Immunol* (2014) 155:213–9. doi: 10.1016/j.clim.2014.10.005
82. Leong JW, Chase JM, Romee R, Schneider SE, Sullivan RP, Cooper MA, et al. Preactivation With IL-12, IL-15, and IL-18 Induces Cd25 and a Functional High-Affinity Il-2 Receptor on Human Cytokine-Induced Memory-Like Natural Killer Cells. *Biol Blood Marrow Transplant* (2014) 20:463–73. doi: 10.1016/j.bbmt.2014.01.006
83. Ni J, Hölsken O, Miller M, Hammer Q, Luetke-Eversloh M, Romagnani C, et al. Adoptively Transferred Natural Killer Cells Maintain Long-Term Antitumor Activity by Epigenetic Imprinting and CD4+ T Cell Help. *Oncoimmunology* (2016) 5:1–13. doi: 10.1080/2162402X.2016.1219009
84. Artis D, Spits H. The Biology of Innate Lymphoid Cells. *Nature* (2015) 517:293–301. doi: 10.1038/nature14189
85. Vivier E, Artis D, Colonna M, Diefenbach A, Di Santo JP, Eberl G, et al. Innate Lymphoid Cells: 10 Years on. *Cell* (2018) 174:1054–66. doi: 10.1016/j.cell.2018.07.017
86. Ardain A, Domingo-Gonzalez R, Das S, Kazer SW, Howard NC, Singh A, et al. Group 3 Innate Lymphoid Cells Mediate Early Protective Immunity Against Tuberculosis. *Nature* (2019) 570:528–32. doi: 10.1038/s41586-019-1276-2
87. Tripathi D, Radhakrishnan RK, Thandi RS, Paidipally P, Devalraju KP, Neela VSK, et al. Erratum: IL-22 Produced by Type 3 Innate Lymphoid Cells (ILC3s) Reduces the Mortality of Type 2 Diabetes Mellitus (T2DM) Mice Infected With Mycobacterium Tuberculosis (PLoS Pathogens (2019) 15:12 (E1008140) DOI: 10.1371/Journal.Ppat.1008140). *PloS Pathog* (2021) 17:1–21. doi: 10.1371/journal.ppat.1009578
88. Martinez-Gonzalez I, Mathä L, Steer CA, Ghaedi M, Poon GFT, Takei F. Allergen-Experienced Group 2 Innate Lymphoid Cells Acquire Memory-Like Properties and Enhance Allergic Lung Inflammation. *Immunity* (2016) 45:198–208. doi: 10.1016/j.immuni.2016.06.017
89. Eaves CJ. Hematopoietic Stem Cells: Concepts, Definitions, and the New Reality. *Blood* (2012) 125(17):2605–13. doi: 10.1182/blood-2014-12-570200
90. Mitroulis I, Ruppova K, Wang B, Chen LS, Grzybek M, Grinenko T, et al. Modulation of Myelopoiesis Progenitors Is an Integral Component of Trained Immunity. *Cell* (2018) 172:147–61.e12. doi: 10.1016/j.cell.2017.11.034
91. King K. Interferon Gamma-Mediated Regulation of Hscs: Mechanisms and Role in Clonal Hematopoiesis. *Exp Hematol* (2020) 88:S19. doi: 10.1016/j.exphem.2020.09.009
92. Selleri C, Maciejewski JP, Sato T, Young NS. Interferon-γ Constitutively Expressed in the Stromal Microenvironment of Human Marrow Cultures Mediates Potent Hematopoietic Inhibition. *Blood* (1996) 87(10):4149–57. doi: 10.1182/blood.v87.10.4149.bloodjournal87104149
93. Zeng W, Miyazato A, Chen G, Kajigaya S, Young NS, Maciejewski JP. Interferon-γ-Induced Gene Expression in CD34 Cells: Identification of Pathologic Cytokine-Specific Signature Profiles. *Blood* (2006) 107(1):167–75. doi: 10.1182/blood-2005-05-1884
94. Baldridge MT, King KY, Boles NC, Weksberg DC, Goodell MA. Quiescent Haematopoietic Stem Cells are Activated by IFN-γ in Response to Chronic Infection. *Nature* (2010) 465(7299):793–7. doi: 10.1038/nature09135
95. Lérias JR, de Sousa E, Paraschoudi G, Martins J, Condeço C, Figueiredo N, et al. Trained Immunity for Personalized Cancer Immunotherapy: Current Knowledge and Future Opportunities. *Front Microbiol* (2020) 10:1–12. doi: 10.3389/fmicb.2019.02924
96. Naik S, Larsen SB, Gomez NC, Alaverdyan K, Sendoel A, Yuan S, et al. Inflammatory Memory Sensitizes Skin Epithelial Stem Cells to Tissue Damage. *Nature* (2017) 550:475–80. doi: 10.1038/nature24271
97. Heinsbroek SEM, Williams DL, Welting O, Meijer SL, Gordon S, de Jonge WJ. Orally Delivered β-Glucans Aggravate Dextran Sulfate Sodium (DSS)-Induced Intestinal Inflammation. *Nutr Res* (2015) (12):1106–12. doi: 10.1016/j.nutres.2015.09.017
98. Wheeler ML, Limon JJ, Bar AS, Leal CA, Gargus M, Tang J, et al. Immunological Consequences of Intestinal Fungal Dysbiosis. *Cell Host Microbe* (2016) 19(6):865–73. doi: 10.1016/j.chom.2016.05.003
99. Convit J, Ulrich M, Polegre MA, Avila A, Rodríguez N, Mazzedo MI, et al. Therapy of Venezuelan Patients With Severe Mucocutaneous or Early Lesions of Diffuse Cutaneous Leishmaniasis With a Vaccine Containing Pasteurized Leishmania Promastigotes and Bacillus Calmette-Guerin: Preliminary Report. *Mem Inst Oswaldo Cruz* (2004) 99:57–62. doi: 10.1590/s0074-02762004000100010
100. Dos Santos JC, Barroso de Figueiredo AM, Teodoro Silva MV, Cirovic B, de Bree LCJ, Damen MSMA, et al. β-Glucan-Induced Trained Immunity Protects Against Leishmania Braziliensis Infection: A Crucial Role for IL-32. *Cell Rep* (2019) 28:2659–2672.e6. doi: 10.1016/j.celrep.2019.08.004
101. Arts RJW, Moorlag SJCFM, Novakovic B, Li Y, Wang SY, Oosting M, et al. BCG Vaccination Protects Against Experimental Viral Infection in Humans Through the Induction of Cytokines Associated With Trained Immunity. *Cell Host Microbe* (2018) 23:89–100.e5. doi: 10.1016/j.chom.2017.12.010
102. Netea MG, Domínguez-Andrés J, Barreiro LB, Chavakis T, Divangahi M, Fuchs E, et al. Defining Trained Immunity and its Role in Health and Disease. *Nat Rev Immunol* (2020) 20:375–88. doi: 10.1038/s41577-020-0285-6
103. Buffen K, Oosting M, Quintin J, Ng A, Kleinnijenhuis J, Kumar V, et al. Autophagy Controls BCG-Induced Trained Immunity and the Response to Intravesical BCG Therapy for Bladder Cancer. *PloS Pathog* (2014) 10:e1004485. doi: 10.1371/journal.ppat.1004485
104. Redelman-Sidi G, Glickman MS, Bochner BH. The Mechanism of Action of BCG Therapy for Bladder Cancer–a Current Perspective. *Nat Rev Urol* (2014) 11:153–62. doi: 10.1038/nrurol.2014.15
105. Bekkering S, Joosten LAB, van der Meer JWM, Netea MG, Riksen NP. Trained Innate Immunity and Atherosclerosis. *Curr Opin Lipidol* (2013) 24:487–92. doi: 10.1097/MOL.0000000000000023
106. Bekkering S, van den Munckhof I, Nielen T, Lamfers E, Dinarello C, Rutten J, et al. Innate Immune Cell Activation and Epigenetic Remodeling in Symptomatic and Asymptomatic Atherosclerosis in Humans *In Vivo*. *Atherosclerosis* (2016) 254:228–36. doi: 10.1016/j.atherosclerosis.2016.10.019
107. Noye EC, Bekkering S, Limawan AP, Nguyen MU, Widiasmoko LK, Lu H, et al. Postnatal Inflammation in ApoE-/- Mice is Associated With Immune Training and Atherosclerosis. *Clin Sci (Lond)* (2021) 135:1859–71. doi: 10.1042/CS20210496


**Conflict of Interest:** The authors declare that the research was conducted in the absence of any commercial or financial relationships that could be construed as a potential conflict of interest.

**Publisher's Note:** All claims expressed in this article are solely those of the authors and do not necessarily represent those of their affiliated organizations, or those of the publisher, the editors and the reviewers. Any product that may be evaluated in this article, or claim that may be made by its manufacturer, is not guaranteed or endorsed by the publisher.

frontiers in Immunology

REVIEW
published: 11 October 2021
doi: 10.3389/fimmu.2021.710375

# The Roles of Tissue-Resident Memory T Cells in Lung Diseases

*Rui Yuan[1†], Jiang Yu[1†], Ziqiao Jiao[1†], Jinfei Li[1†], Fang Wu[2], Rongkai Yan[3], Xiaojie Huang[4] and Chen Chen[5,6*]*

[1] Xiangya School of Medicine, Central South University, Changsha, China, [2] Department of Oncology, The Second Xiangya Hospital of Central South University, Changsha, China, [3] Department of Radiology, Johns Hopkins University School of Medicine, Baltimore, MD, United States, [4] Department Cardiovascular Surgery, The Second Xiangya Hospital of Central South University, Changsha, China, [5] Department of Thoracic Surgery, The Second Xiangya Hospital of Central South University, Changsha, China, [6] Hunan Key Laboratory of Early Diagnosis and Precise Treatment of Lung Cancer, The Second Xiangya Hospital of Central South University, Changsha, China

The unique environment of the lungs is protected by complex immune interactions. Human lung tissue-resident memory T cells ($T_{RM}$) have been shown to position at the pathogen entry points and play an essential role in fighting against viral and bacterial pathogens at the frontline through direct mechanisms and also by orchestrating the adaptive immune system through crosstalk. Recent evidence suggests that $T_{RM}$ cells also play a vital part in slowing down carcinogenesis and preventing the spread of solid tumors. Less beneficially, lung $T_{RM}$ cells can promote pathologic inflammation, causing chronic airway inflammatory changes such as asthma and fibrosis. $T_{RM}$ cells from infiltrating recipient T cells may also mediate allograft immunopathology, hence lung damage in patients after lung transplantations. Several therapeutic strategies targeting $T_{RM}$ cells have been developed. This review will summarize recent advances in understanding the establishment and maintenance of $T_{RM}$ cells in the lung, describe their roles in different lung diseases, and discuss how the $T_{RM}$ cells may guide future immunotherapies targeting infectious diseases, cancers and pathologic immune responses.

**Keywords: tissue-resident memory T cells, non-small-cell lung cancer, lung infection, immunotherapy, vaccine**

OPEN ACCESS

***Edited by:***
*Vandana Kalia, University of Washington, United States*

***Reviewed by:***
*Aki Hoji, Indiana University, Purdue University Indianapolis, United States*
*Haina Shin, Washington University in St. Louis, United States*

***Correspondence:**
*Chen Chen*
*chenchen1981412@csu.edu.cn*

*†These authors have contributed equally to this work and share first authorship*

***Specialty section:***
*This article was submitted to Immunological Memory, a section of the journal Frontiers in Immunology*

***Received:*** *16 May 2021*
***Accepted:*** *27 September 2021*
***Published:*** *11 October 2021*

***Citation:***
*Yuan R, Yu J, Jiao Z, Li J, Wu F, Yan R, Huang X and Chen C (2021) The Roles of Tissue-Resident Memory T Cells in Lung Diseases. Front. Immunol. 12:710375. doi: 10.3389/fimmu.2021.710375*

## INTRODUCTION

Tissue-resident memory T ($T_{RM}$) cells comprise a recently identified lymphocyte lineage that occupies tissues without recirculating. They reside in epithelial barrier tissues, such as lung, gastrointestinal tract, reproductive tract, and skin, and in some non-barrier tissues, such as brain, kidney, and joint (1–3). $T_{RM}$ cells are transcriptionally, functionally and phenotypically distinct from circulating effector memory T cells (4).

The human lung is continuously exposed to environmental and microbial antigens (2). $T_{RM}$ cells in lung tissues play a crucial role in both innate and adaptive immune responses to lung infections, such as Respiratory Syncytial Virus (RSV), SARS-CoV-2, Brucella and Mycobacterium tuberculosis (5–7). Growing evidence has revealed that the $T_{RM}$ cells reside in tissues in the absence of antigens and may provide rapid on-site immune protection against previously exposed pathogens in peripheral tissues to accelerate pathogen clearance (5).

Recently, $T_{RM}$ cells have been found to participate in anti-tumor immunity as well. $T_{RM}$ cells can promote intra-tumoral cytotoxic T lymphocytes (CTLs) responses and are correlated with overall survival in lung cancer patients (8–10). Induction of $T_{RM}$ cells can enhance the efficacy of cancer vaccines (11) and increase the response rate when using anti-PD-1 antibodies to reverse tumor-induced T cell exhaustion in NSCLC patients (12, 13).

In addition to the protective roles against diseases, evidence suggests that $T_{RM}$ cells also become activated after sensitization to self-antigens. Aberrantly activated $T_{RM}$ cells can induce autoimmune disorders, such as autoimmune hepatitis and psoriasis (4, 14). In the respiratory system, $T_{RM}$ specifically activated by environmental allergens might underlie the development and worsening of allergic asthma and other airway diseases (15–18). Pathogenic $T_{RM}$ cells may contribute to chronic pulmonary inflammation and fibrosis (2). $T_{RM}$ cells are also recognized as the primary mediator of acute cellular rejection (ACR) after lung transplantation.

This review aims to comprehensively summarize the current understandings of the biology of $T_{RM}$ cells, including the distinguishing molecular markers, regulators, and functions of $T_{RM}$ cells, discuss the contributions of $T_{RM}$ cells to lung diseases, especially infectious diseases and tumors, and highlight potential $T_{RM}$-related therapeutic strategies for respiratory diseases.

## DEFINING LUNG $T_{RM}$ CELLS

Human memory T cells can be broadly categorized into three subsets: central memory T cells ($T_{CM}$), effector memory T cells ($T_{EM}$), and tissue-resident memory T cells ($T_{RM}$). $T_{CM}$ cells are memory T cells that recirculate through secondary lymphoid organs, whereas $T_{EM}$ cells recirculate through nonlymphoid tissues. $T_{RM}$ cells, by contrast, typically reside in specific tissues, especially mucus organs, such as lungs and gastrointestinal tracts, defending against pathogens in peripheral nonlymphoid tissues. Compared with $T_{CM}$ and $T_{EM}$ cells, commitment to the tissue of residence is a defining characteristic of $T_{RM}$ cells, which has been described in almost all organs (19). Most memory T cells in non-lymphoid tissues are $T_{RM}$ cells, either CD4+ or CD8+ (9). $T_{RM}$ cells can be further fractionated by their functional characteristics into epithelial and stromal $T_{RM}$ cells (20, 21).

$T_{RM}$ cells are widely distributed throughout the body, including the skin, lungs, lymphoid organs, etc. However, $T_{RM}$ cells in different organs display distinct properties (21). In healthy human skin, most of the $T_{RM}$ cells are dermal CD4+ CD69+CD103− cells, which express high levels of the cutaneous lymphocyte antigen (CLA) and specific chemokine receptors like CCR4 (22). With increased expression of T cell factor-1 (TCF-1) and lymphoid enhancer factor-1 (LEF-1), human lymph node CD8+ $T_{RM}$ cells exhibit a phenotype of tissue residency as well as an organ-specific signature (23). Human lymph node-specific profile of memory CD8+ T cells is defined by expression of CXCR5 and TCF-1 and high proliferative capacity, which accordingly indicates that human lymph node memory CD8+ T cells display higher proliferative capacity than their counterparts in other tissues (24). Similarly, $T_{RM}$ cells in non-small-cell lung cancer (NSCLC) may be identified by CD39 and CD103 (25). In mice, the formation and maintenance of skin $T_{RM}$ cells is mediated by chemokine receptors like CXCR3, CXCR6, and CCR10 (26). Genetic knockout studies of mice have shown that CD69 deficiency reduces the retention of CD4+ T cells in the bone marrow (27).

Eomes and T-bet are T-box transcription factors (TFs) that restrict the formation of CD103+$T_{RM}$ cells, indicating that downregulation of both transcription factors is crucial for the generation of CD103+ $T_{RM}$ cells. Eomes TF is significantly downregulated in CD8+CD103+$T_{RM}$ cells compared to circulating $T_{EM}$ or $T_{CM}$ cells. The residual T-bet expression upregulates interleukin-15 receptor (IL-15R) β-chain (CD122) expression, which is essential for long-term $T_{RM}$ cell survival. The coordinated downregulation of both T-box TFs optimizes cytokine transforming growth factor-beta (TGF-β) signaling, leading to the efficient development of CD8+CD103+$T_{RM}$ cells (28).

Both CD69 and CD103 are expressed in CD8+ $T_{RM}$ cells and less frequently, CD103 is expressed in CD4+$T_{RM}$ cells (29). CD69, which is an early activation marker involved in lymphocyte proliferation and retention, plays a key role in distinguishing $T_{RM}$ cells from those in circulation. Additionally, CD103 is a key to recognize most CD4+and CD8+$T_{RM}$ cells (30). The expression of CD103 helps $T_{RM}$ cells dock to the E-cadherin-expressed on epithelial cells and prevents them from re-circulating in the blood (31). It is generally accepted that TGF-β is an upstream regulator of $T_{RM}$ transformation. Increasing TGF-β *in vivo* appears to significantly increase the number of local $T_{RM}$ cells (32, 33). It has been revealed that the function and expression of CD103 greatly depends on the TGF-β, indicating that the $T_{EM}$ and other T cells might lack TGF-β cytokines and thus fail to upregulate CD103 (34). CD39 is also highly expressed in $T_{RM}$ cells and is associated with higher $T_{RM}$ cells activities and quantity. CD39 could protect cells from apoptosis induced by adenosine triphosphate (ATP). As a transmembrane glycoprotein and extracellular nucleosidase, CD39 is also present in many biological processes such as adenosine regulation, proliferation, and resident transduction signals (28). While most human CD4+T cells express CD69, a portion of them express CD103+at the same time, especially in the lung. The majority of lung CD4+ $T_{EM}$ phenotype cells express the canonical $T_{RM}$ marker CD69. Comparing the gene expression patterns of CD103+$T_{RM}$ cells in lung and $T_{EM}$ cells in the blood, human lung CD4+CD103+$T_{RM}$ cells express higher levels of *ITGAE* (which encodes CD103), *CTLA4*, *KLRC1* (which encodes the inhibitory receptor NKG2A) (35, 36) and ICOS (31). CD4+CD103+$T_{RM}$ cells express deployment-ready mRNAs encoding effector molecules that rapidly respond to pathogens. Human lung $T_{RM}$ cells express lower levels of *S1PR1* (which encodes the S1P receptor) (37), lymph node-homing molecules, *SELL* (which encodes the lymph node-homing receptor CD62L), *KLRG1* (which encodes the activation marker KLRG1) (35),

*KLF2* (which drives expression of S1PR1) and *CCR7* (31). Additionally, some genes have different expressions between CD103+$T_{RM}$ cells and peripheral $T_{EM}$ cells, including genes that encode heat-shock proteins (HSPA1A, HSPA7, HSPA2, and HSPD1), transcription factors (EGR2, FOSB, ATF3, RBPJ, EPAS1, and BATF) (31, 35), anti-apoptotic factors (PHLDA1 and BIRC3), the tumor necrosis factor (TNF) receptor signaling family (TRAF1 and TANK) (31), chemokine (XCL1), solute carrier family members mediating amino acid transport (SLC7A5 and SLC1A5), chemokine receptor (CXCR6), transforming growth factor (TGF-β1), interleukin (IL-21R), the ligand for the death receptor Fas (FASLG), adhesion G-protein-coupled receptor (CD97), interferon-γ receptors (IFNGR) (35), and fatty-acid-binding protein (FABP5) (38). All the genes mentioned above have higher expression levels in lung CD103+ $T_{RM}$ cells. Characteristically, lung CD4+CD103+$T_{RM}$ cells exhibit high levels of various integrins and adhesion molecules (31, 39). Compared with blood-derived $T_{EM}$ cells, differences in the molecular expression of lung CD103+$T_{RM}$ cells are summarized in **Table 1**.

Several transcription factors play critical roles in the proliferation of $T_{RM}$ cells. The activation of the programmed cell death protein 1(PD-1) signal pathway downregulates the expression of Bhlhe40, which supports mitochondria and chromatin production in $T_{RM}$ cells and is thus essential to the proliferation and maintenance of $T_{RM}$ cells (40). Transcription factors such as BATF, NAB1, and NAB2 are also highly expressed in $T_{RM}$ cells. These factors can regulate T cell metabolisms to maintain their survival and reduce the expression of inhibitory phenotypes (41).

## LUNG $T_{RM}$ CELLS AND PROTECTION AGAINST RESPIRATORY INFECTION

CD8+$T_{RM}$ cells are considered as the first line of defense in peripheral tissues against pathogens. Many studies suggest that some risk factors may interfere with circulating memory CD8+T cell function (**Table 2** and **Figure 1**). Reticular fibroblasts located near T cells around the infection site can transmit long-lasting activation signals to CD8+T cells by upregulating ICOS ligand (ICOSL), CD40, and interleukin-6 (IL-6), which promotes the preferential differentiation of T cells into $T_{RM}$ cells (55). CD8+$T_{RM}$ cells can produce chemokines after local tissue activation and recruit non-antigen-specific T cells, exerting natural effector functions (56, 57). $T_{RM}$ cells promote the production of IL-2 and some pro-inflammatory cytokines, effectively mobilizing inflammatory responses and exert

**TABLE 1** | The differences in integrins and molecule expression between lung $T_{RM}$ cells and $T_{EM}$ cells.

| Classification | Molecules | Function | Expression level in $T_{RM}$ cells compared with $T_{EM}$ cells | Species | References |
|---|---|---|---|---|---|
| Intercellular Adhesion Molecule | ICAM2 (CD102) | lymphocyte activation | Higher | Human | (31, 35) |
| | ICAM1 (CD54) | lymphocyte activation | Lower | Human | (35) |
| Chemokine Receptor | CCR5 | lymphocyte recruitment | Higher | Human | (35) |
| | CCR5 | lymphocyte recruitment | Higher | Human | (35) |
| | CCR7 | impairing T-cell homing to lymph nodes | Lower | Human | (31) |
| | CXCR6 | T-cell recruitment | Higher | Human | (31, 35, 36) |
| | CXCR3 | T-cell recruitment | Higher | Human | (35) |
| | CX3CR1 | transmigration through endothelial layers | Lower | Human | (35) |
| Cytotoxic T-Lymphocyte-Associated Protein | CTLA4 | inhibitory molecules | Higher | Human | (31, 35) |
| Immunoglobulin | LAG3 | inhibitory molecules | Higher | Human | (35) |
| Adenosine Receptor | A2AR | inhibitory molecules | Higher | Human | (35) |
| Interleukin | IL-17 | pro-inflammatory cytokines | Higher | Human | (36) |
| Interferon | IFN-γ | pro-inflammatory cytokines | Higher | Human and Mouse | (31, 36, 38) |
| Integrin | CD103 | retention, adhesion, and migration to tissues | Higher | Mouse | (36, 37) |
| | CD49a | retention, adhesion, and migration to tissues | Higher | Human | (36) |
| Other molecules | CD69 | retention, adhesion, and migration to tissues | Higher | Human | (36) |
| | CD97 | G-protein-coupled receptor | Higher | Human | (35) |
| | CD101 | inhibitory molecules | Higher | Human | (36) |
| | CD279 (PD-1) | inhibitory molecules | Higher | Human | (36) |
| | CD272 (BTLA) | inhibitory molecules | Higher | Human | (35) |
| | SPRY1 | inhibitory molecules | Higher | Human | (31, 35) |

**TABLE 2 |** The features of $T_{RM}$ cells in lung infection or pathological process.

| Infection or pathological process | Phenotype | Function or regulation | References |
|---|---|---|---|
| SARS-CoV-2 infection | tissue-resident memory-like Th1 cells and tissue-resident memory-like Th17 cells | Natural Th17 cells were recruited to the infected site by CCL20 on lung epithelial cells stimulated by IL-17A and expanded in the presence of IL-23, which then were converted to $T_{RM}$ cells, existing as ex-Th17 cells and exerting Th1-like immunity in the event of SARS-CoV-2. | (42) |
| Respiratory Syncytial Virus | CD4+$T_{RM}$ cells and CD8+$T_{RM}$ cells | $T_{RM}$ cells showed gradual differentiation with down-regulated costimulatory molecules and increased CXCR3 expression, which had been implicated in protection against RSV-induced lung pathology in mice *via* dendritic cells and CD8+ T cells. | (43–45) |
| Bordetella Pertussis | CD69+CD4+$T_{RM}$ cells | $T_{RM}$ cells produced IL-17 and IFN-γ, thereby recruiting neutrophils and preventing their colonization in the nose. | (46–49) |
| Influenza Viruses | CD8+$T_{RM}$ cells | The expression of PPAR-γ and dendritic cells with high expression of IRF4 can effectively promote the production of CD8+$T_{RM}$ cells which protect the body from influenza viruses by producing IFN-γ and TNF-α. | (50, 51) |
| Brucella infection | CXCR3lo CD103+CD8+$T_{RM}$ cells and CXCR3hi CD103+CD8+$T_{RM}$ cells | CXCR3hi $T_{RM}$ cells could not be depleted by anti-CD8 mAb, thus inducing protection against Brucella more efficiently. | (52) |
| Pulmonary Inflammation | CD69hiCD103loCD4+$T_{RM}$ cells | Enhance the secretion of IL-5 and IL-13 which can cause pulmonary inflammation and fibrosis. | (15) |
| | CD69hiCD103hiCD4+$T_{RM}$ cells | Improve the fibrosis reaction caused by pulmonary inflammation and reduce lung injury. | (15) |
| Asthma | Th2-$T_{RM}$ cells | Th2-$T_{RM}$ cells expressing high levels of CD44 and ST2 can reside in lung tissues and retain allergen memory. Once re-exposed to an allergen, Th2-$T_{RM}$ cells proliferate near the airway, producing type 2 cytokines that enhance eosinophil activation and promote peribronchial inflammation. | (18, 53, 54) |

immune defenses (58). At the same time, $T_{RM}$ cells produce IL-10 and express inhibitory receptors, thus inhibit excessive inflammatory response and limit tissue damage caused by inflammation (59). CD4+ $T_{RM}$ cells in non-lymphoid tissues, such as lung, skin, and genital mucosa, can influence the immune reaction of various pathogenic microorganisms (60–62).

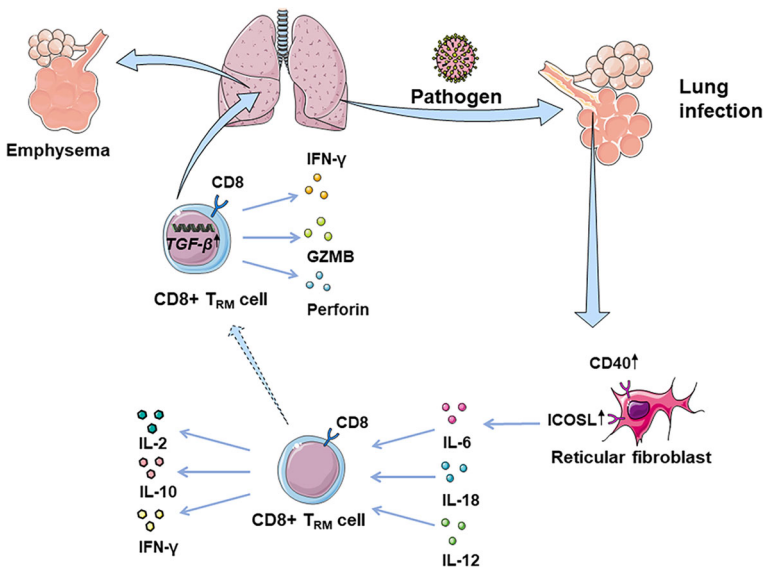


**FIGURE 1** | CD8+ $T_{RM}$ cells in lung infection and immunopathology. CD8+ $T_{RM}$ cells are considered as the first line of defense in peripheral tissues against earlier exposure to antigens. CD8+ $T_{RM}$ cells located in the lung parenchyma could rapidly synthesize IFN-γ following the inhalation of pathogens, driven by exposure to IL-12/IL-18. Fibroblast reticular cells located near T cells around the focus can transmit long-lasting activation signals to CD8+T cells, by upregulating ICOSL, CD40, and IL-6. Additionally, CD8+ $T_{RM}$ cells promote the production of IL-2, mobilizing inflammatory response. At the same time, $T_{RM}$ cells can produce IL-10, thus inhibiting the excessive inflammatory response and limiting tissue damage caused by inflammation. However, CD8+ $T_{RM}$ cells can be abnormally deposited in the lung due to overexpression of TGF-β-related genes, which may damage normal tissues by releasing IFN-γ, GZMB, and perforin, leading to lung emphysema or fibrosis.

## Antivirus Effect

In lungs, follicular tissue-resident CD4+ T helper cells contribute to the defense against virus in conjunction with CD8+ T cells relying on IL-21 (63). These helper T cells can also induce antiviral B cell reactions in bronchus lymphoid tissue in flu virus infection, indicating that $T_{RM}$ cells could promote the protective response of B cells and CD8+T cells in lung infections (63). CD8+$T_{RM}$ cells in the lung act as protective agents against viruses through interferon-γ (IFN-γ) (64). Studies of Coronavirus disease 2019 (COVID-19) have suggested that the disease severity and lung injuries are related to the interaction of tissue-resident memory-like Th17 cells ($T_{RM}$17 cells) with lung macrophages and cytotoxic CD8+T cells. High serum IL-17A and GM-CSF levels in COVID-19 patients are associated with more severe clinical courses (6). Overall, lung $T_{RM}$17 cells are potential coordinators of excessive inflammation in severe COVID-19 (6). Patients recovering from COVID-19 acquire $T_{RM}$ cells with Th1 phenotype against COVID-19 (65). Neutrophils attracted to the site of infection secret IL-17A and stimulate lung epithelial cells to express CCL20. The expression of CCL20 recruits natural Th17 (nTh17) cells to the infected site. In the presence of IL-23, nTh17 are converted to $T_{RM}$ cells (66). COVID-19 prevents the $T_{RM}$ cells from remaining ex-Th17 cells and exerting Th1-like immunity effects (42). Previous studies showed in RSV-immune mice, $T_{RM}$ cells enhanced respiratory syncytial virus clearance, indicating CD8+$T_{RM}$ cells can enhance resistance against secondary RSV infection (43, 44). In RSV-immune mice, CD69 co-expressed heavily with CD38, consistent with its role as an early activation marker. Some CD4+CD69+T cells also expressed integrin CD103, and permanent memory CD4+T cells were enriched in airways. As the infection progressed, these $T_{RM}$ cells were enriched in infection site with increased CXCR3 expression (45). Similarly, $T_{RM}$ cells protect the human body from influenza viruses by producing large amounts of IFN-γ and TNF-α (50). When encountered with influenza A virus, dendritic cells with high expression of IRF4 can effectively promote the production of CD8+$T_{RM}$ cells, thus reducing infection severity (67). PPAR-γ expression accelerates the establishment of CD8+TRM cells, suggesting that PPAR-γ is a positive regulatory factor for $T_{RM}$ cells. Moreover, PPAR-γ deficiency reduces the number of alveolar macrophages residing in tissues during pulmonary infections, indicating that alveolar macrophages might be negative regulators of CD8+$T_{RM}$ cells and could limit the establishment of $T_{RM}$ cells (51).

## Antibacterial Effect

Non-homologous bystander activation can trigger the sensory and alerting functions of lung CD8+$T_{RM}$ cells (68). Unlike memory CD8+T cells in circulating blood, CD8+$T_{RM}$ cells located in the lung parenchyma can rapidly synthesize IFN-γ after the inhalation of heat-killed bacteria or bacterial products, a process-driven by exposure to IL-12/IL-18 (69). Bacterial infection of respiratory tract leads to bystander activation of pulmonary $T_{RM}$ cells, enhancement of the recruitment of neutrophils to the airway and reduction of the severity of bacterial pneumonia (69). These activations suggest that $T_{RM}$ cells innately amplify inflammatory responses and participate in non-homologous responses to bacterial infections (68). Lung CD4+$T_{RM}$ cells remodel epithelial responses to accelerate neutrophil recruitment during pneumonia. During heterotypic immunity, CD4+T cells upregulate CXCL5 and drive neutrophil recruitment in the lung (70). In mice infected with Bordetella pertussis, $T_{RM}$ cells produced IL-17 and IFN-γ, recruiting neutrophils and preventing nasal colonization (46–49). In addition, uninfected mice acquired immunity after receiving adoptive transferred CD4 T cells isolated from either lungs or spleens of convalescent mice (71). Following mucosal znBAZ vaccination, lung CD8+ $T_{RM}$ cells exhibit superior protection against Brucella infections. Mucosal znBAZ immunization induces CD103+ and CD103- CD8+ $T_{RM}$ cells expressing $CXCR3^{lo}$ and $CXCR3^{hi}$ phenotypes in the lung parenchyma and airways, respectively. These CXCR3-expressing CD103+ and CD103-CD8+$T_{RM}$ cells are not depleted by anti-CD8 mAb treatment (52).

## Other Effect

$T_{RM}$ cells also increase resistance to parasite invasions. Both the percentage and absolute numbers of lung CD4+ and CD8+ cells increase after Schistosoma. japonicum infection (72). CD103-expressing pulmonary CD4+ and CD8+ T cells play essential roles in mediating granulomatous inflammation induced by S. japonicum infection (72).

# LUNG $T_{RM}$ CELLS IN ANTI-TUMOR IMMUNITY

Approximately 85% of lung cancers worldwide are non-small cell lung cancer (NSCLC), of which lung adenocarcinoma (LUAD) and lung squamous cell carcinoma (LUSC) are the most common (73). Growing evidence suggested that in human solid tumors, tumor-associated lymphocytes in NSCLC may comprise the function of $T_{RM}$ cells (25). CD8+$T_{RM}$ cells in the tumor microenvironment (TME) are a homogeneous CD103+ CD49+CD69+ population expressing T-bet, porylated (p) STAT-3, and Aiolos transcription factors and a subset of these cells produces IFN-γ and IL-17. In patients with NSCLC, CD8+ $T_{RM}$ cells overexpress several T cell inhibitory receptors and exhaustion surface markers and co-express PD-1 and CD39, implying that they are enriched in activated tumor-antigen reactive T cells (74). Cytotoxic CD8+T lymphocytes (CTLs) in NSCLC with a high level of CD103 display enhanced cytotoxicity and proliferation, suggesting a robust anti-tumor immune response in human lung cancer (41). Compared to T cells from adjacent and tumor-free lung tissues, these cells exhibit more significant heterogeneity in the expression of molecules associated with T cell antigen receptor (TCR) activation and immune checkpoints such as 4-1BB, PD-1, TIM-3. However, in human lung cancer, far from being exhausted, PD-1-expressing $T_{RM}$ cells in tumors are clonally expanded and enriched for transcripts linked to cell proliferation and cytotoxicity (12).

The origination, infiltration, and differentiation of $T_{RM}$ in NSCLC is still unclear. O'Brien and colleagues' model speculated that in patients with early-stage NSCLC, $T_{EM}$ cells encountered antigens during tumor formation and were converted to CD103+ $T_{RM}$ cells that exerted anti-tumor activity (75). However, due to a variety of factors associated with tumor growth in TME, the tumors might not be eliminated. These factors, combined with the chronic antigen stimulation, may trigger an exhaustion program characterized by increased Eomes and CD39 expression. The presence of B7-H4 in tumors or other TME stromal cells might upregulate Eomes expression in T cells. As a tumor grows, this exhaustion program may dominate $T_{RM}$ cells, causing increasing TILs hypofunctionality.

In addition, transcription factors may play a role. Patients suffering from advanced-stage NSCLC exhibit a progressive decrease of NFATc1 in tumor cells and TILs decrease progressively (76). Some CD103+$T_{RM}$ cells may lead to decreased function and cytotoxicity of CD8+T cells, a phenomenon observed in the lungs of tumor-bearing $NFATc1^{\Delta CD4}$ mice, likely promoted by decreased IL-2 in the absence of NFATc1 (77). Runx3 also plays an important part in the differentiation of $T_{RM}$ in NSCLC (78). The Runx3 is required for optimal $T_{RM}$ cell differentiation in the lung parenchyma and maximal expression of granzyme B in $T_{RM}$ cells. Several tissue-residency signature genes are upregulated in Runx3-overexpressing cells and downregulated in Runx3-deficient cells. Conversely, circulating memory cell signatures are enriched in Runx3-deficient cells and depleted from Runx3-overexpressing cells.

Other immune cells such as $M1^{hot}$ tumor-associated macrophages (TAM) can boost the infiltration and survival of $T_{RM}$ cells in patients with NSCLC (32). $M1^{hot}$ TAMs may recruit $T_{RM}$ cells *via* CXCL9 expression and sustain them by producing more essential fatty acids on which $T_{RM}$ cells depend. Monocytes acquire the ability to prime $T_{RM}$ cells *via* IL-10-mediated TGF-β release. IL-10 plays a negative regulatory role in the immune system per classical theory, but it has been found that CD103 was significantly upregulated, and T cells transform into $T_{RM}$ cells when influenced by IL-10 (33). Significantly upregulated CD103 leads to more T cells transforming into $T_{RM}$ cells. Therefore, IL-10-mediated TGF-β signaling may have a critical role in post-vaccination $T_{RM}$ generation (33).

Moreover, chemokine receptors and cytoskeleton proteins contribute to $T_{RM}$ cell infiltration. The focal adhesion-associated protein paxillin binding to the CD103 cytoplasmic tail triggers αEβ7 integrin outside-in signaling that promotes the migration and functions of CD8+T cells (79). This binding process explains the more favorable prognosis associated with more retention of $T_{RM}$ cells in TME (79). In both mice and human lungs, CXCR6 is expressed on the surface of $T_{RM}$ cells with the action of intrapulmonary antigens, aiding the migration of $T_{RM}$ cells from pulmonary interstitium to TME and maintaining the $T_{RM}$ cell pool (80), whereas memory CD8+T cells of the spleen do not express this receptor (81).

Duhen et al. proposed a model in human solid tumors associating $T_{RM}$ cells with tumor growth: CD8+ T cells are primed by dendritic cells presenting tumor antigens within the tumor-draining lymph nodes and then migrate to the tumor where they recognize the cognate antigens then clonally expand (25). The consequence of this TCR activation in a TGF-β-rich environment is the upregulation of CD39 and CD103 on CD8+ TILs. CD103 expressed on some $T_{RM}$ cells may promote immunologic synapse by binding to E-cadherin on tumor cells (82). Activation of these cells also leads to the downregulation of the proteins that are essential for T-cell recirculation, retaining CD8+ TILs within the tumor. In human lung cancer, there are many important anti-tumor costimulatory molecules such as SIRPG and KIR2DL4 on the surface of $T_{RM}$ cells, which help the CTLs kill tumor cells (41). In human, CD103+ $T_{RM}$ cells can also produce granzyme B (GZMB) and IFN-γ, which can restrict tumor cell growth and metastasis by inducing fibronectin production, make antigens available to prime for the priming of new tumor-specific T cells, and enhance recruitment of monocytes, NK cells, and XCR1+ cDC1 to the tumor site (9). However, repetitive TCR stimulations of the CD8+ TILs impair effector function, mediate immune escape, and ultimately tumor progression. CD103+CD39+CD8+$T_{RM}$ cells efficiently kill autologous tumor cells in an MHC-class I-dependent manner. Additionally, the content of cytokine and receptor function influence immune functions (**Figure 2**).

The infiltration of CD8+ T cells in solid tumors is a favorable prognostic marker (83). In the tumors that exhibited a high level of infiltrated CD8+ T cells, the proliferation of CD103+ T cells was correlated with improved long-term survival, indicating that infiltration of CD8+CD103+ $T_{RM}$ cells is a favorable prognostic marker (84). Another study suggested that high intratumoral but not stromal CD103+ TILs were associated with better overall survival in patients with resected LUSC, another significant prognostic implication of CD103 expression in TILs in human LUSC (85). Moreover, CD103 and E-cadherin interaction play a vital role in granule polarization and exocytosis, enhancing recruitment and retention of tumor-antigen-specific TILs in human NSCLC. In human NSCLC, CD28H is mainly expressed in $T_{RM}$ cells and is thus associated with improved tumor prognosis (86). However, other studies conversely demonstrated opposite results that B7-H5 (the ligand of CD28H) was expressed in more than 60% of cases of NSCLC and was associated with worse prognosis. Hence, the expression patterns of CD103 in TILs of NSCLC and the associated prognostic implications are significant and merit further investigation.

In $T_{RM}$ cells in human NSCLC tissues, there are several dysfunctional subtypes, such as NKG2A+CD8+ T cells (87). NKG2A is an inhibitory receptor of both T cells and natural killer (NK) cells. Persistent activation causes T cells and NK cells to express NKG2A and may lead to chronic infection and cancer. Tumor-infiltrating NKG2A+CD8+T cells form the predominant subset of NKG2A+cells in human lung cancer (87). Blockading NKG2A may promote anti-tumor immunity by unleashing dysfunctional CD8+T cells in tumors, and targeting NKG2A+ CD8+T cells is a promising approach for future anti-lung cancer immunotherapy.

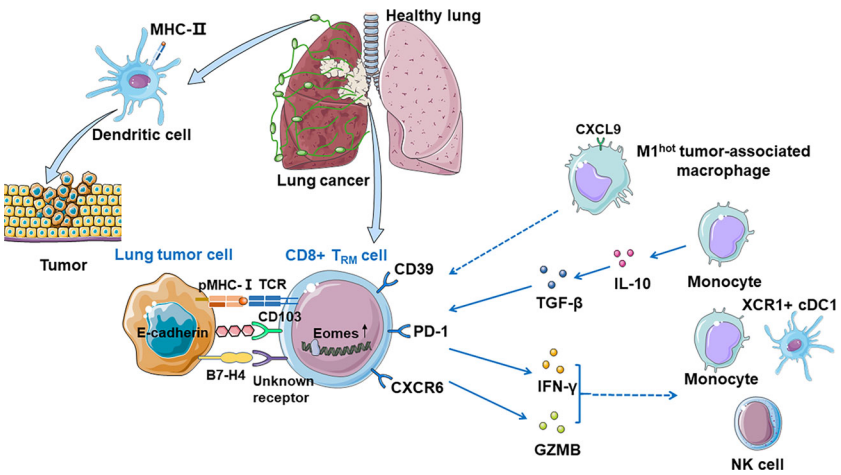


**FIGURE 2** | CD8+ $T_{RM}$ cells in anti-tumor immunity. Dendritic cells present tumor antigens in the tumor-draining lymph nodes and then migrate to the tumor where they recognize their cognate antigens and expand, priming CD8+ T cells significantly. Tumor-associated CD8+ $T_{RM}$ cells can be identified by CD39 and CD103, and CD103 promotes immunologic synapse by binding to E-cadherin on tumor cells. $T_{RM}$ cells which express PD-1 are expanded and enriched for transcripts linked to cell proliferation and cytotoxicity. CXCR6 is expressed on the surface of $T_{RM}$ cells when exposed to tumor antigens, transferring $T_{RM}$ cells from pulmonary interstitium to tumor microenvironment, and maintaining the $T_{RM}$ cell pool. $M1^{hot}$ TAMs recruit $T_{RM}$ cells *via* CXCL9 expression and sustain them by making more essential fatty acids on which $T_{RM}$ cells depend. Monocytes prime $T_{RM}$ cells *via* IL-10-mediated TGF-β release which increases the number of local $T_{RM}$ cells. CD8+ CD103+ $T_{RM}$ cells can also produce GZMB and IFN-γ, which recruits monocytes, NK cells, and XCR1+ cDC1 to the tumor site. B7-H4 on tumor cells might upregulate Eomes in T cells, which may cause growing TILs hypofunctionality.

While numerous studies have reported that the presence of $T_{RM}$-like CD8+T cells in human NSCLC is a favorable prognosis (77), the role of CD4+TILs with a shared phenotype remains unclear. As CD4+$T_{RM}$ cells exhibit phenotypic and functional heterogeneity, different subsets are expected to play different and even opposite roles in TME. CD4+$T_{RM}$ cells are known to be essential for cytotoxic programming of CD8+T cells, and they can also suppress tumor growth through secretion of IFN-γ or direct killing tumor cells in human NSCLC (88).

## POTENTIAL THERAPEUTIC STRATEGIES BASED ON $T_{RM}$ CELLS

Given the remarkable roles of $T_{RM}$ cells in lung diseases, increasing $T_{RM}$ production or reactivating suppressed $T_{RM}$ cells may be a valuable therapeutic strategy (**Table 3**). It is believed that in lung diseases without medical intervention, $T_{RM}$ cells play a less critical role because their function is inhibited and disabled in the focal microenvironment (88). Therefore, current researches focus on reactivating $T_{RM}$ cells that have adapted to the disease microenvironment, increasing the load of $T_{RM}$ cells in the lesions, and mediating immune responses such as cytotoxicity and conditioning, to kill pathogens or slow down disease progression (**Table 4**).

## $T_{RM}$ Cells and Neoadjuvant Chemotherapy

$T_{RM}$ cells may be involved in varied NSCLC therapies. Neoadjuvant chemotherapy was one modality in the treatment of resectable NSCLC. The beneficial effects of neoadjuvant chemotherapy might be mediated partially by CD8+CD103+ mediated tumor cell killing (13). With neoadjuvant chemotherapy, more infiltration of CD4+CD103+PD-1 $T_{RM}$ cells at the time of surgery was associated with longer overall survival. Moreover, $T_{RM}$ cells could be of great importance in TME and in cancer immune checkpoint blockade immunotherapy. In both mice model and human, dual anti-PD-L1/anti-4-1BB immunotherapy increased the number of intratumoral CD103+ CD8+ T cells and altered their distribution (90). Administration of PD-L1 mAb and 4-1BB mAb further increased the cytolytic capacity of CD103+CD8+T cells. Collectively, infiltrated CD103+ CD8+T cells served as a potential effector T cell population.

**TABLE 3** | Strategies to improve the efficacy of vaccines and adoptive cell therapies by targeting $T_{RM}$ cells.

| Strategies | Examples | Ways to improve | References |
|---|---|---|---|
| Transcription Factors | Runx3, Bhlhe40, BATF, NAB1, NAB2 | Up-regulation | (40, 41, 78) |
| Cytokines | TGF-β、IL-10 | Increment | (33, 59) |
| Leukocyte surface antigen | CD39, CXCR6, PPAR-γ, SIRPG, KIR2DL4 | Activation | (41, 51, 81) |
| Cells | $M1^{hot}$ TAM cells, Reticular fibroblasts, Dendritic cells with high expression of IRF4 | Activation | (32, 55, 67) |
| | Alveolar macrophage | Inhibition | (51) |

**TABLE 4** | Molecules in mice or/and humans regulating lung $T_{RM}$ cells.

| The process lung $T_{RM}$ cells participate in | Species | Regulatory molecules | References |
|---|---|---|---|
| Anti-tumor immunity | Mouse | Runx3, NFATc1, CXCR6, TGF-β | (40, 41, 78) |
| | Human | Eomes, CD39, CXCL9, paxillin, TGF-β, SIRPG, KIR2DL4 | (25, 32, 41, 74, 75, 79) |
| Positive role in infection | Human | ICOSL, CD40, IL-6, IL-10 | (55, 59) |
| Negative role in infection | Mouse | TGF-β, IL-5, IL-13 | (15, 89) |
| Antivirus immunity | Mouse | CD69, CD38, CD103, CXCR3, IFN-γ, IRF4, PPAR-γ | (45, 50, 51, 67) |
| | Human | IL-17A, CCL20, IL-23 | (42) |
| Antibacterial Immunity | Mouse | IFN-γ,IL-12,IL-17,IL-18, CXCL5, CXCR3 | (46–49, 68, 70) |
| Association with asthma | Mouse | CD44, ST2, IFN-γ, perforin, granules | (18, 53, 54) |

Combining 4-1BB agonism with PD-L1 blockade may increase tumor-infiltrated CD103+CD8+T cells, facilitating tumor regression. It is also reported that CD103+CD8+$T_{RM}$ cells could be considered potential biomarkers when selecting patients that may benefit from immune checkpoint blockade immunotherapy in patients with multiple primary lung adenocarcinoma after neoadjuvant immunotherapy (91). Yet more evidence is required to determine the clinical practice of potential the therapeutic strategies based on $T_{RM}$ cells, as a more favorable indicator of prognosis or a target of immune therapy.

Several treatments may potentially activate or increase the number of $T_{RM}$ cells. One possible treatment involves promoting the separation and trans-differentiation of T cells to $T_{RM}$ cells in TME, which could inhibit tumor progression. At the same time, in murine models, apoptosis induced by IR increases the number of newly infiltrated T cells and converts them into $T_{RM}$ cells, producing an inflammation-like effect that may assist immunotherapy (92).

## $T_{RM}$ Cells and Radiotherapy

Since $T_{RM}$ cells have a unique survival advantage in radiotherapy, a RT-PD1-MerTK triple therapy based on radiotherapy may also be effective. Promoting $T_{RM}$ cell production from other sources such as traditional radiotherapy may be an equally valuable potential treatment. $T_{RM}$ cells have stronger radiation resistance than tumor cells, and efficient infrared irradiation (IR) makes pre-existing $T_{RM}$ cells survive and mediates the anti-tumor effect of $T_{RM}$ cells (93). In murine models, compared with traditional radiotherapy, anti-PD-1 therapy relieves the inhibitory effect on immune cells such as $T_{RM}$ cells, while anti-MerTK can transform apoptosis caused by radiation into cell necrosis and turn macrophages near tumors from M2 to M1 and reduce tumor load (94). This triple therapy could increase the content of CTLs and promote the differentiation of $T_{RM}$ cells, improving the anti-tumor effect. Adding anti-PD1 and anti-MerTK to radiation could significantly upregulate CD8+CD103+TRM at the abscopal tumors, suppress the abscopal tumor growth and extended the survival rate (95). As for epigenetic and metabolic regulation, a treatment scheme for TA/AC may be considered. TA, or microtubule inhibitor A, is a histone deacetylase inhibitor that can promote the production of IFN- γ in Bhlhe40+CD8+$T_{RM}$ cells (96). Acetic acid (AC) can be used as the substrate of acetyl-CoA synthesis, which is independent from the tricarboxylic acid (TCA) cycle and promotes histone acetylation and cytokine production in Bhlhe40+CD8+ $T_{RM}$ cells (97). The combination of TA and AC can promote tissue retention and functional differentiation of $T_{RM}$ cells (40). TA/Ac treatment not only enhances Bhlhe40−/− CD8+ T cell effector and resident gene expression but also promotes the expression of these genes in WT CD8+ T cells, indicating appropriate combinations of epigenetic modifiers with certain metabolites may represent promising approaches for maximally reinvigorating tissue or tumor-resident CD8+ T cell antiviral or antitumor activities.

## $T_{RM}$ Cells and Vaccines

Another treatment approach involves the induction of persistent $T_{RM}$ cells by vaccines. Phosphatidylserine liposomes are excellent antigen carriers, which can be combined with polyconic adjuvants for the development of new BCG vaccines (71). Because anti-cytomegalovirus response is one of the most powerful and persistent cellular immune responses observed in human bodies, cytomegalovirus is a possible effective $T_{RM}$-cell-inducing vaccine vector (98). Murine models show that other peptide nanofibers with strong immunogenicity may likewise improve the immune response (99), particularly with combined polypeptide antigen and adjuvant (33). Continuous stimulation with local homologous antigens can increase $T_{RM}$ cell population, and zymosan used as an adjuvant could transform CD8+T cells into $T_{RM}$ cells in the absence of antigens. Mice models indicate that adding zymosan adjuvant to a possible vaccine may moderate local inflammation as well as greatly enhance the production of $T_{RM}$ cells (100). Similarly, combining ovalbumin antigen and CpG DNA adjuvant hybridized pH-responsive substances can increase the $T_{RM}$ cells response range and lifespan. This combination can also activate antigen-presenting cells (APCs), and stimulate continuous $T_{RM}$ cell production in mice (101).

Intranasal vaccine administration induces $T_{RM}$ cells in the lung (11). Triggering an appropriate inflammatory response in the immune process may allow $T_{RM}$ cells to bypass antigen recognition. Lung $T_{RM}$ cells are most effectively induced at the memory stage of basic vaccines in murine models (99). In-depth analysis of the phenotypes of the locally induced CD8+T cells showed that after vaccination, $T_{RM}$ cells and CD8+T cells coexist as effector phenotypes and that $T_{RM}$ cells play an important role. Indeed, at the peak of the local immune response, concentrations of $T_{RM}$ are 10-fold higher than those of effector CD8+T cells, and only the $T_{RM}$ cells population persist locally after 30 days. Even when effector CD8+T cells are no longer detectable, tumor resistance is still observed (11).

The CXCR6-CXCL16 axis demonstrably governs the growth of NSCLC in the migration of CD8+ resident memory T cells in lung mucosa after vaccination. CXCR6 deficiency impairs cancer vaccine efficacy and CD8+ resident memory T-cell recruitment in lung tumors (80). Interestingly, intranasal vaccination induces higher and more sustained concentrations of CXCL16 than intramuscular vaccination, particularly compared with other chemokines in the bronchoalveolar lavage fluid and pulmonary parenchyma in both mice and human (81).

Despite it is observed that vaccines can promote the $T_{RM}$ cells population, retention and function and then enhance the anti-tumor immunity both in mice and human, the efficiency and safety of tumor-related vaccines remains unclear thus require further investigations.

## LUNG $T_{RM}$ AND IMMUNOPATHOLOGY

In certain conditions, lung $T_{RM}$ cells may cause excessive inflammatory responses and tissue fibrosis (**Table 4**). After acute influenza infection, abnormal reactivation of $T_{RM}$ cells in the lung may likewise cause lung tissue changes and fibrosis (102). In elderly mice, CD8+ $T_{RM}$ cells can be abnormally deposited in the lung due to overexpression of TGF-β-related genes (103). Low responsive $T_{RM}$ cells not only fail to perform an immune function but may also lead to chronic inflammation and the sequelae of fibrosis (89). $CD69^{hi}CD103^{lo}CD4+$ $T_{RM}$ cells produce effector cytokines and promoted the inflammation and fibrotic responses induced by chronic exposure to Aspergillus fumigatus (15). Studies have shown that pathogenic immune cells like $CD69^{hi}CD103^{lo}CD4+T_{RM}$ cells enhance the secretion of IL-5 and IL-13, which can cause excessive pulmonary inflammation and fibrosis. By contrast, $CD69^{hi}CD103^{hi}CD4+$ TRM cells can improve the fibrosis reaction caused by pulmonary inflammation and reduce lung injury, indicating that lung $CD4^{+}$ $T_{RM}$ cells play crucial roles in the pathology of chronic lung inflammation, and CD103 expression defines pathogenic effector and immunosuppressive $T_{RM}$ cell subpopulations in the the lung (15).

### Association With Asthma

Th2-$T_{RM}$ cells are associated with asthma. These cells release cytokines that recruit eosinophils and sustain mast cells in the airway, leading to an inflammatory response. Th2-$T_{RM}$ cells expressed with high levels of CD44 and ST2 have been observed in lung tissues and can retain allergen memory throughout the life of a host organism (53). Re-exposure to a known allergen causes Th2-$T_{RM}$ cells to proliferate near the airway, producing type 2 cytokines that enhance eosinophil activation and promote peribronchial inflammation (104). Together with circulating memory Th2 cells, they perform non-redundant functions in asthma induction (18, 53, 54). Although these $T_{RM}$ cells eliminate invasive pathogens, the release of pro-inflammatory factors (such as IFN-γ, perforin, and granulose) may damage normal cells, leading to lung damage, emphysema, or fibrosis.

### Participation in Acute Cellular Rejection (ACR) After Lung Transplantation

T cells are mediators of acute cellular rejection (ACR) after lung transplantation (105). The role of pulmonary $T_{RM}$ cells in ACR in lung transplantation remains uncertain. Longitudinal analysis of lung transplant recipients has indicated that $T_{RM}$ cells from recipients gradually formed $T_{RM}$ phenotypes approximating healthy people after 6 months allograft, while donor T cells persisted in the form of $T_{RM}$. The increase in the proportion of recipient-derived $T_{RM}$ cells was associated with ACR, suggesting that $T_{RM}$ cells may influence the inflammatory environment of lung allograft after transplantation (2).

## CONCLUSION

Human lung $T_{RM}$ cells, whether CD8+ or CD4+, persist in lung tissues for decades of human life. The essential role of lung $T_{RM}$ cells is maintaining tissue homeostasis when facing viruses, antigens, and pathogens encountered through respiration, and may also be important in tumor surveillance. Lung $T_{RM}$ cells can also promote pathologic inflammation, inducing chronic airway inflammatory changes leading to asthma and fibrosis. Similarly, lung $T_{RM}$ cells from infiltrating recipient T cells in transplantation may mediate allograft immunopathology and promote lung damage. More comprehensive understanding of the induction and maintenance of $T_{RM}$ cells by cancer vaccines or other immunotherapeutic approaches may provide insights into the innovation of immunotherapies of lung diseases.

## AUTHOR CONTRIBUTIONS

CC provided the concepts and ideas of the article. RY, JY, ZJ, and JL performed literature search and wrote the manuscript's first draft. CC, FW, XH, and RY performed a critical revision of the first draft and the final editing of the manuscript. All authors contributed to the article and approved the submitted version.

## FUNDING

This study was funded by the China National Natural Science Foundation No. 81902351, the Hunan Provincial Natural Science Foundation (No. 2020SK53419, 2021JJ30926 and No. 2019JJ50953), Hunan Provincial Key Area R&D Program NO. 2019SK2253, CSCO Cancer Research Foundation (CSCO-Y-young2019-034 and CSCO-2019Roche-073), and the Changsha Municipal Natural Science Foundation NO. kq2014246.

## ACKNOWLEDGMENTS

The authors greatly appreciate Mr. Jameson Goodman for critical review of the manuscript.

## REFERENCES


1. Clark RA. Resident Memory T Cells in Human Health and Disease. *Sci Transl Med* (2015) 7(269):269rv1. doi: 10.1126/scitranslmed.3010641
2. Snyder ME, Farber DL. Human Lung Tissue Resident Memory T Cells in Health and Disease. *Curr Opin Immunol* (2019) 59:101–8. doi: 10.1016/j.coi.2019.05.011
3. Schenkel JM, Masopust D. Tissue-Resident Memory T Cells. *Immunity* (2014) 41(6):886–97. doi: 10.1016/j.immuni.2014.12.007
4. Wu H, Liao W, Li Q, Long H, Yin H, Zhao M, et al. Pathogenic Role of Tissue-Resident Memory T Cells in Autoimmune Diseases. *Autoimmun Rev* (2018) 17(9):906–11. doi: 10.1016/j.autrev.2018.03.014
5. Gebhardt T, Palendira U, Tscharke DC, Bedoui S. Tissue-Resident Memory T Cells in Tissue Homeostasis, Persistent Infection, and Cancer Surveillance. *Immunol Rev* (2018) 283(1):54–76. doi: 10.1111/imr.12650
6. Zhao Y, Kilian C, Turner JE, Bosurgi L, Roedl K, Bartsch P, et al. Clonal Expansion and Activation of Tissue-Resident Memory-Like Th17 Cells Expressing GM-CSF in the Lungs of Severe COVID-19 Patients. *Sci Immunol* (2021) 6(56):eabf6692. doi: 10.1126/sciimmunol.abf6692
7. Ogongo P, Porterfield JZ, Leslie A. Lung Tissue Resident Memory T-Cells in the Immune Response to Mycobacterium Tuberculosis. *Front Immunol* (2019) 10:992. doi: 10.3389/fimmu.2019.00992
8. Park SL, Gebhardt T, Mackay LK. Tissue-Resident Memory T Cells in Cancer Immunosurveillance. *Trends Immunol* (2019) 40(8):735–47. doi: 10.1016/j.it.2019.06.002
9. Amsen D, van Gisbergen K, Hombrink P, van Lier RAW. Tissue-Resident Memory T Cells at the Center of Immunity to Solid Tumors. *Nat Immunol* (2018) 19(6):538–46. doi: 10.1038/s41590-018-0114-2
10. Djenidi F, Adam J, Goubar A, Durgeau A, Meurice G, de Montpreville V, et al. CD8+CD103+ Tumor-Infiltrating Lymphocytes Are Tumor-Specific Tissue-Resident Memory T Cells and a Prognostic Factor for Survival in Lung Cancer Patients. *J Immunol* (2015) 194(7):3475–86. doi: 10.4049/jimmunol.1402711
11. Nizard M, Roussel H, Diniz MO, Karaki S, Tran T, Voron T, et al. Induction of Resident Memory T Cells Enhances the Efficacy of Cancer Vaccine. *Nat Commun* (2017) 8:15221. doi: 10.1038/ncomms15221
12. Clarke J, Panwar B, Madrigal A, Singh D, Gujar R, Wood O, et al. Single-Cell Transcriptomic Analysis of Tissue-Resident Memory T Cells in Human Lung Cancer. *J Exp Med* (2019) 216(9):2128–49. doi: 10.1084/jem.20190249
13. Gaudreau PO, Negrao MV, Mitchell KG, Reuben A, Corsini EM, Li J, et al. Neoadjuvant Chemotherapy Increases Cytotoxic T Cell, Tissue Resident Memory T Cell, and B Cell Infiltration in Resectable NSCLC. *J Thorac Oncol* (2021) 16(1):127–39. doi: 10.1016/j.jtho.2020.09.027
14. You Z, Li Y, Wang Q, Zhao Z, Li Y, Qian Q, et al. The Clinical Significance of Hepatic CD69(+) CD103(+) CD8(+) Resident Memory T Cells in Autoimmune Hepatitis. *Hepatology* (2021) 74(2):847–63. doi: 10.1002/hep.31739
15. Ichikawa T, Hirahara K, Kokubo K, Kiuchi M, Aoki A, Morimoto Y, et al. CD103(hi) Treg Cells Constrain Lung Fibrosis Induced by CD103(lo) Tissue-Resident Pathogenic CD4 T Cells. *Nat Immunol* (2019) 20(11):1469–80. doi: 10.1038/s41590-019-0494-y
16. Goplen NP, Wu Y, Son YM, Li C, Wang Z, Cheon IS, et al. Tissue-Resident CD8(+) T Cells Drive Age-Associated Chronic Lung Sequelae After Viral Pneumonia. *Sci Immunol* (2020) 5(53):eabc4557. doi: 10.1126/sciimmunol.abc4557
17. Hondowicz BD, An D, Schenkel JM, Kim KS, Steach HR, Krishnamurty AT, et al. Interleukin-2-Dependent Allergen-Specific Tissue-Resident Memory Cells Drive Asthma. *Immunity* (2016) 44(1):155–66. doi: 10.1016/j.immuni.2015.11.004
18. Turner DL, Goldklang M, Cvetkovski F, Paik D, Trischler J, Barahona J, et al. Biased Generation and *In Situ* Activation of Lung Tissue-Resident Memory CD4 T Cells in the Pathogenesis of Allergic Asthma. *J Immunol* (2018) 200(5):1561–9. doi: 10.4049/jimmunol.1700257
19. Wang X, Tian Z, Peng H. Tissue-Resident Memory-Like ILCs: Innate Counterparts of TRM Cells. *Protein Cell* (2020) 11(2):85–96. doi: 10.1007/s13238-019-0647-7
20. Takamura S. Divergence of Tissue-Memory T Cells: Distribution and Function-Based Classification. *Cold Spring Harb Perspect Biol* (2020) 12(10):a037762. doi: 10.1101/cshperspect.a037762
21. Szabo PA, Miron M, Farber DL. Location, Location, Location: Tissue Resident Memory T Cells in Mice and Humans. *Sci Immunol* (2019) 4(34):eaas9673. doi: 10.1126/sciimmunol.aas9673
22. Clark RA, Chong B, Mirchandani N, Brinster NK, Yamanaka K, Dowgiert RK, et al. The Vast Majority of CLA+ T Cells Are Resident in Normal Skin. *J Immunol* (2006) 176(7):4431–9. doi: 10.4049/jimmunol.176.7.4431
23. Miron M, Kumar BV, Meng W, Granot T, Carpenter DJ, Senda T, et al. Human Lymph Nodes Maintain TCF-1(Hi) Memory T Cells With High Functional Potential and Clonal Diversity Throughout Life. *J Immunol* (2018) 201(7):2132–40. doi: 10.4049/jimmunol.1800716
24. Im SJ, Hashimoto M, Gerner MY, Lee J, Kissick HT, Burger MC, et al. Defining CD8+ T Cells That Provide the Proliferative Burst After PD-1 Therapy. *Nature* (2016) 537(7620):417–21. doi: 10.1038/nature19330
25. Duhen T, Duhen R, Montler R, Moses J, Moudgil T, de Miranda NF, et al. Co-Expression of CD39 and CD103 Identifies Tumor-Reactive CD8 T Cells in Human Solid Tumors. *Nat Commun* (2018) 9(1):2724. doi: 10.1038/s41467-018-05072-0
26. Mackay LK, Rahimpour A, Ma JZ, Collins N, Stock AT, Hafon ML, et al. The Developmental Pathway for CD103(+)CD8+ Tissue-Resident Memory T Cells of Skin. *Nat Immunol* (2013) 14(12):1294–301. doi: 10.1038/ni.2744
27. Shinoda K, Tokoyoda K, Hanazawa A, Hayashizaki K, Zehentmeier S, Hosokawa H, et al. Type II Membrane Protein CD69 Regulates the Formation of Resting T-Helper Memory. *Proc Natl Acad Sci USA* (2012) 109(19):7409–14. doi: 10.1073/pnas.1118539109
28. Milner JJ, Goldrath AW. Transcriptional Programming of Tissue-Resident Memory CD8(+) T Cells. *Curr Opin Immunol* (2018) 51:162–9. doi: 10.1016/j.coi.2018.03.017
29. Steel KJA, Srenathan U, Ridley M, Durham LE, Wu SY, Ryan SE, et al. Polyfunctional, Proinflammatory, Tissue-Resident Memory Phenotype and Function of Synovial Interleukin-17a+CD8+ T Cells in Psoriatic Arthritis. *Arthritis Rheumatol* (2020) 72(3):435–47. doi: 10.1002/art.41156
30. Topham DJ, Reilly EC. Tissue-Resident Memory CD8(+) T Cells: From Phenotype to Function. *Front Immunol* (2018) 9:515. doi: 10.3389/fimmu.2018.00515
31. Oja AE, Piet B, Helbig C, Stark R, van der Zwan D, Blaauwgeers H, et al. Trigger-Happy Resident Memory CD4(+) T Cells Inhabit the Human Lungs. *Mucosal Immunol* (2018) 11(3):654–67. doi: 10.1038/mi.2017.94
32. Garrido-Martin EM, Mellows TWP, Clarke J, Ganesan AP, Wood O, Cazaly A, et al. M1(hot) Tumor-Associated Macrophages Boost Tissue-Resident Memory T Cells Infiltration and Survival in Human Lung Cancer. *J Immunother Cancer* (2020) 8(2):e000778. doi: 10.1136/jitc-2020-000778
33. Thompson EA, Darrah PA, Foulds KE, Hoffer E, Caffrey-Carr A, Norenstedt S, et al. Monocytes Acquire the Ability to Prime Tissue-Resident T Cells *via* IL-10-Mediated TGF-Beta Release. *Cell Rep* (2019) 28(5):1127–35.e4. doi: 10.1016/j.celrep.2019.06.087
34. Pizzolla A, Nguyen TH, Sant S, Jaffar J, Loudovaris T, Mannering SI, et al. Influenza-Specific Lung-Resident Memory T Cells Are Proliferative and Polyfunctional and Maintain Diverse TCR Profiles. *J Clin Invest* (2018) 128(2):721–33. doi: 10.1172/JCI96957
35. Hombrink P, Helbig C, Backer RA, Piet B, Oja AE, Stark R, et al. Programs for the Persistence, Vigilance and Control of Human CD8(+) Lung-Resident Memory T Cells. *Nat Immunol* (2016) 17(12):1467–78. doi: 10.1038/ni.3589
36. Snyder ME, Finlayson MO, Connors TJ, Dogra P, Senda T, Bush E, et al. Generation and Persistence of Human Tissue-Resident Memory T Cells in Lung Transplantation. *Sci Immunol* (2019) 4(33):eaav5581. doi: 10.1126/sciimmunol.aav5581
37. Yoshizawa A, Bi K, Keskin DB, Zhang G, Reinhold B, Reinherz EL. TCR-pMHC Encounter Differentially Regulates Transcriptomes of Tissue-Resident CD8 T Cells. *Eur J Immunol* (2018) 48(1):128–50. doi: 10.1002/eji.201747174
38. Pan Y, Tian T, Park CO, Lofftus SY, Mei S, Liu X, et al. Survival of Tissue-Resident Memory T Cells Requires Exogenous Lipid Uptake and Metabolism. *Nature* (2017) 543(7644):252–6. doi: 10.1038/nature21379
39. Hombrink P, Helbig C, Backer RA, Piet B, Oja AE, Stark R, et al. Erratum: Programs for the Persistence, Vigilance and Control of Human CD8(+) Lung-Resident Memory T Cells. *Nat Immunol* (2017) 18(2):246. doi: 10.1038/ni0217-246d

40. Li C, Zhu B, Son YM, Wang Z, Jiang L, Xiang M, et al. The Transcription Factor Bhlhe40 Programs Mitochondrial Regulation of Resident CD8(+) T Cell Fitness and Functionality. *Immunity* (2019) 51(3):491–507.e7. doi: 10.1016/j.immuni.2019.08.013
41. Ganesan AP, Clarke J, Wood O, Garrido-Martin EM, Chee SJ, Mellows T, et al. Tissue-Resident Memory Features Are Linked to the Magnitude of Cytotoxic T Cell Responses in Human Lung Cancer. *Nat Immunol* (2017) 18 (8):940–50. doi: 10.1038/ni.3775
42. Katayama H. Can Immunological Manipulation Defeat SARS-CoV-2? Why G-CSF Induced Neutrophil Expansion Is Worth a Clinical Trial: G-CSF Treatment Against COVID-19. *Bioessays* (2021) 43(2):e2000232. doi: 10.1002/bies.202000232
43. Luangrath MA, Schmidt ME, Hartwig SM, Varga SM. Tissue-Resident Memory T Cells in the Lungs Protect Against Acute Respiratory Syncytial Virus Infection. *Immunohorizons* (2021) 5(2):59–69. doi: 10.4049/immunohorizons.2000067
44. Matyushenko V, Kotomina T, Kudryavtsev I, Mezhenskaya D, Prokopenko P, Matushkina A, et al. Conserved T-Cell Epitopes of Respiratory Syncytial Virus (RSV) Delivered by Recombinant Live Attenuated Influenza Vaccine Viruses Efficiently Induce RSV-Specific Lung-Localized Memory T Cells and Augment Influenza-Specific Resident Memory T-Cell Responses. *Antiviral Res* (2020) 182:104864. doi: 10.1016/j.antiviral.2020.104864
45. Guvenel A, Jozwik A, Ascough S, Ung SK, Paterson S, Kalyan M, et al. Epitope-Specific Airway-Resident CD4+ T Cell Dynamics During Experimental Human RSV Infection. *J Clin Invest* (2020) 130(1):523–38. doi: 10.1172/JCI131696
46. Wilk MM, Borkner L, Misiak A, Curham L, Allen AC, Mills KHG. Immunization With Whole Cell But Not Acellular Pertussis Vaccines Primes CD4 TRM Cells That Sustain Protective Immunity Against Nasal Colonization With Bordetella Pertussis. *Emerg Microbes Infect* (2019) 8 (1):169–85. doi: 10.1080/22221751.2018.1564630
47. Dubois V, Chatagnon J, Thiriard A, Bauderlique-Le Roy H, Debrie AS, Coutte L, et al. Suppression of Mucosal Th17 Memory Responses by Acellular Pertussis Vaccines Enhances Nasal Bordetella Pertussis Carriage. *NPJ Vaccines* (2021) 6(1):6. doi: 10.1038/s41541-020-00270-8
48. Zurita ME, Wilk MM, Carriquiriborde F, Bartel E, Moreno G, Misiak A, et al. A Pertussis Outer Membrane Vesicle-Based Vaccine Induces Lung-Resident Memory CD4 T Cells and Protection Against Bordetella Pertussis, Including Pertactin Deficient Strains. *Front Cell Infect Microbiol* (2019) 9:125. doi: 10.3389/fcimb.2019.00125
49. Raeven RHM, Rockx-Brouwer D, Kanojia G, van der Maas L, Bindels THE, Ten Have R, et al. Intranasal Immunization With Outer Membrane Vesicle Pertussis Vaccine Confers Broad Protection Through Mucosal IgA and Th17 Responses. *Sci Rep* (2020) 10(1):7396. doi: 10.1038/s41598-020-63998-2
50. Paik DH, Farber DL. Influenza Infection Fortifies Local Lymph Nodes to Promote Lung-Resident Heterosubtypic Immunity. *J Exp Med* (2021) 218 (1):e20200218. doi: 10.1084/jem.20200218
51. Goplen NP, Huang S, Zhu B, Cheon IS, Son YM, Wang Z, et al. Tissue-Resident Macrophages Limit Pulmonary CD8 Resident Memory T Cell Establishment. *Front Immunol* (2019) 10:2332. doi: 10.3389/fimmu.2019.02332
52. Wang H, Hoffman C, Yang X, Clapp B, Pascual DW. Targeting Resident Memory T Cell Immunity Culminates in Pulmonary and Systemic Protection Against Brucella Infection. *PloS Pathog* (2020) 16(1):e1008176. doi: 10.1371/journal.ppat.1008176
53. Rahimi RA, Nepal K, Cetinbas M, Sadreyev RI, Luster AD. Distinct Functions of Tissue-Resident and Circulating Memory Th2 Cells in Allergic Airway Disease. *J Exp Med* (2020) 217(9):e20190865. doi: 10.1084/jem.20190865
54. Bosnjak B, Kazemi S, Altenburger LM, Mokrovic G, Epstein MM. Th2-TRMs Maintain Life-Long Allergic Memory in Experimental Asthma in Mice. *Front Immunol* (2019) 10:840. doi: 10.3389/fimmu.2019.00840
55. Brown FD, Sen DR, LaFleur MW, Godec J, Lukacs-Kornek V, Schildberg FA, et al. Fibroblastic Reticular Cells Enhance T Cell Metabolism and Survival *via* Epigenetic Remodeling. *Nat Immunol* (2019) 20(12):1668–80. doi: 10.1038/s41590-019-0515-x
56. Schenkel JM, Fraser KA, Vezys V, Masopust D. Sensing and Alarm Function of Resident Memory CD8(+) T Cells. *Nat Immunol* (2013) 14(5):509–13. doi: 10.1038/ni.2568
57. Ariotti S, Hogenbirk MA, Dijkgraaf FE, Visser LL, Hoekstra ME, Song JY, et al. T Cell Memory. Skin-Resident Memory CD8(+) T Cells Trigger a State of Tissue-Wide Pathogen Alert. *Science* (2014) 346(6205):101–5. doi: 10.1126/science.1254803
58. Haynes L, Eaton SM, Burns EM, Rincon M, Swain SL. Inflammatory Cytokines Overcome Age-Related Defects in CD4 T Cell Responses *In Vivo*. *J Immunol* (2004) 172(9):5194–9. doi: 10.4049/jimmunol.172.9.5194
59. Kumar BV, Ma W, Miron M, Granot T, Guyer RS, Carpenter DJ, et al. Human Tissue-Resident Memory T Cells Are Defined by Core Transcriptional and Functional Signatures in Lymphoid and Mucosal Sites. *Cell Rep* (2017) 20(12):2921–34. doi: 10.1016/j.celrep.2017.08.078
60. Iijima N, Iwasaki A. T Cell Memory. A Local Macrophage Chemokine Network Sustains Protective Tissue-Resident Memory CD4 T Cells. *Science* (2014) 346(6205):93–8. doi: 10.1126/science.1257530
61. Teijaro JR, Turner D, Pham Q, Wherry EJ, Lefrancois L, Farber DL. Cutting Edge: Tissue-Retentive Lung Memory CD4 T Cells Mediate Optimal Protection to Respiratory Virus Infection. *J Immunol* (2011) 187 (11):5510–4. doi: 10.4049/jimmunol.1102243
62. Glennie ND, Volk SW, Scott P. Skin-Resident CD4+ T Cells Protect Against Leishmania Major by Recruiting and Activating Inflammatory Monocytes. *PloS Pathog* (2017) 13(4):e1006349. doi: 10.1371/journal.ppat.1006349
63. Son YM, Cheon IS, Wu Y, Li C, Wang Z, Gao X, et al. Tissue-Resident CD4 (+) T Helper Cells Assist the Development of Protective Respiratory B and CD8(+) T Cell Memory Responses. *Sci Immunol* (2021) 6(55):eabb6852. doi: 10.1126/sciimmunol.abb6852
64. McMaster SR, Gabbard JD, Koutsonanos DG, Compans RW, Tripp RA, Tompkins SM, et al. Memory T Cells Generated by Prior Exposure to Influenza Cross React With the Novel H7N9 Influenza Virus and Confer Protective Heterosubtypic Immunity. *PloS One* (2015) 10(2):e0115725. doi: 10.1371/journal.pone.0115725
65. Grau-Exposito J, Sanchez-Gaona N, Massana N, Suppi M, Astorga-Gamaza A, Perea D, et al. Peripheral and Lung Resident Memory T Cell Responses Against SARS-CoV-2. *Nat Commun* (2021) 12(1):3010. doi: 10.1038/s41467-021-23333-3
66. Getschman AE, Imai Y, Larsen O, Peterson FC, Wu X, Rosenkilde MM, et al. Protein Engineering of the Chemokine CCL20 Prevents Psoriasiform Dermatitis in an IL-23-Dependent Murine Model. *Proc Natl Acad Sci USA* (2017) 114(47):12460–5. doi: 10.1073/pnas.1704958114
67. Ainsua-Enrich E, Hatipoglu I, Kadel S, Turner S, Paul J, Singh S, et al. IRF4-Dependent Dendritic Cells Regulate CD8(+) T-Cell Differentiation and Memory Responses in Influenza Infection. *Mucosal Immunol* (2019) 12 (4):1025–37. doi: 10.1038/s41385-019-0173-1
68. Ge C, Monk IR, Pizzolla A, Wang N, Bedford JG, Stinear TP, et al. Bystander Activation of Pulmonary Trm Cells Attenuates the Severity of Bacterial Pneumonia by Enhancing Neutrophil Recruitment. *Cell Rep* (2019) 29 (13):4236–44 e3. doi: 10.1016/j.celrep.2019.11.103
69. Wu T, Hu Y, Lee YT, Bouchard KR, Benechet A, Khanna K, et al. Lung-Resident Memory CD8 T Cells (TRM) are Indispensable for Optimal Cross-Protection Against Pulmonary Virus Infection. *J Leukoc Biol* (2014) 95 (2):215–24. doi: 10.1189/jlb.0313180
70. Shenoy AT, Wasserman GA, Arafa EI, Wooten AK, Smith NMS, Martin IMC, et al. Lung CD4(+) Resident Memory T Cells Remodel Epithelial Responses to Accelerate Neutrophil Recruitment During Pneumonia. *Mucosal Immunol* (2020) 13(2):334–43. doi: 10.1038/s41385-019-0229-2
71. Wilk MM, Misiak A, McManus RM, Allen AC, Lynch MA, Mills KHG. Lung CD4 Tissue-Resident Memory T Cells Mediate Adaptive Immunity Induced by Previous Infection of Mice With Bordetella Pertussis. *J Immunol* (2017) 199(1):233–43. doi: 10.4049/jimmunol.1602051
72. Zhao Y, Yang Q, Jin C, Feng Y, Xie S, Xie H, et al. Changes of CD103-Expressing Pulmonary CD4(+) and CD8(+) T Cells in S. Japonicum Infected C57BL/6 Mice. *BMC Infect Dis* (2019) 19(1):999. doi: 10.1186/s12879-019-4633-8
73. Herbst RS, Morgensztern D, Boshoff C. The Biology and Management of Non-Small Cell Lung Cancer. *Nature* (2018) 553(7689):446–54. doi: 10.1038/nature25183
74. Corgnac S, Malenica I, Mezquita L, Auclin E, Voilin E, Kacher J, et al. CD103 (+)CD8(+) TRM Cells Accumulate in Tumors of Anti-PD-1-Responder Lung Cancer Patients and Are Tumor-Reactive Lymphocytes Enriched With Tc17. *Cell Rep Med* (2020) 1(7):100127. doi: 10.1016/j.xcrm.2020.100127

75. O'Brien SM, Klampatsa A, Thompson JC, Martinez MC, Hwang WT, Rao AS, et al. Function of Human Tumor-Infiltrating Lymphocytes in Early-Stage Non-Small Cell Lung Cancer. *Cancer Immunol Res* (2019) 7(6):896–909. doi: 10.1158/2326-6066.CIR-18-0713
76. Heim L, Friedrich J, Engelhardt M, Trufa DI, Geppert CI, Rieker RJ, et al. NFATc1 Promotes Antitumoral Effector Functions and Memory CD8(+) T-Cell Differentiation During Non-Small Cell Lung Cancer Development. *Cancer Res* (2018) 78(13):3619–33. doi: 10.1158/0008-5472.CAN-17-3297
77. Corgnac S, Boutet M, Kfoury M, Naltet C, Mami-Chouaib F. The Emerging Role of CD8(+) Tissue Resident Memory T (TRM) Cells in Antitumor Immunity: A Unique Functional Contribution of the CD103 Integrin. *Front Immunol* (2018) 9:1904. doi: 10.3389/fimmu.2018.01904
78. Milner JJ, Toma C, Yu B, Zhang K, Omilusik K, Phan AT, et al. Runx3 Programs CD8(+) T Cell Residency in non-Lymphoid Tissues and Tumours. *Nature* (2017) 552(7684):253–7. doi: 10.1038/nature24993
79. Gauthier L, Corgnac S, Boutet M, Gros G, Validire P, Bismuth G, et al. Paxillin Binding to the Cytoplasmic Domain of CD103 Promotes Cell Adhesion and Effector Functions for CD8(+) Resident Memory T Cells in Tumors. *Cancer Res* (2017) 77(24):7072–82. doi: 10.1158/0008-5472.CAN-17-1487
80. Karaki S, Blanc C, Tran T, Galy-Fauroux I, Mougel A, Dransart E, et al. CXCR6 Deficiency Impairs Cancer Vaccine Efficacy and CD8(+) Resident Memory T-Cell Recruitment in Head and Neck and Lung Tumors. *J Immunother Cancer* (2021) 9(3):e001948. doi: 10.1136/jitc-2020-001948
81. Wein AN, McMaster SR, Takamura S, Dunbar PR, Cartwright EK, Hayward SL, et al. CXCR6 Regulates Localization of Tissue-Resident Memory CD8 T Cells to the Airways. *J Exp Med* (2019) 216(12):2748–62. doi: 10.1084/jem.20181308
82. Dhodapkar MV, Dhodapkar KM. Tissue-Resident Memory-Like T Cells in Tumor Immunity: Clinical Implications. *Semin Immunol* (2020) 49:101415. doi: 10.1016/j.smim.2020.101415
83. Lalos A, Tulek A, Tosti N, Mechera R, Wilhelm A, Soysal S, et al. Prognostic Significance of CD8+ T-Cells Density in Stage III Colorectal Cancer Depends on SDF-1 Expression. *Sci Rep* (2021) 11(1):775. doi: 10.1038/s41598-020-80382-2
84. Amsen D, Hombrink P, van Lier RAW. Tumor Immunity Requires Border Patrol to Fight the Enemy Within. *Nat Immunol* (2017) 18(8):870–2. doi: 10.1038/ni.3792
85. Koh J, Kim S, Kim MY, Go H, Jeon YK, Chung DH. Prognostic Implications of Intratumoral CD103+ Tumor-Infiltrating Lymphocytes in Pulmonary Squamous Cell Carcinoma. *Oncotarget* (2017) 8(8):13762–9. doi: 10.18632/oncotarget.14632
86. Zhong C, Lang Q, Yu J, Wu S, Xu F, Tian Y. Phenotypical and Potential Functional Characteristics of Different Immune Cells Expressing CD28H/B7-H5 and Their Relationship With Cancer Prognosis. *Clin Exp Immunol* (2020) 200(1):12–21. doi: 10.1111/cei.13413
87. Chen Y, Xin Z, Huang L, Zhao L, Wang S, Cheng J, et al. CD8(+) T Cells Form the Predominant Subset of NKG2A(+) Cells in Human Lung Cancer. *Front Immunol* (2019) 10:3002. doi: 10.3389/fimmu.2019.03002
88. Oja AE, Piet B, van der Zwan D, Blaauwgeers H, Mensink M, de Kivit S, et al. Functional Heterogeneity of CD4(+) Tumor-Infiltrating Lymphocytes With a Resident Memory Phenotype in NSCLC. *Front Immunol* (2018) 9:2654. doi: 10.3389/fimmu.2018.02654
89. Wang Z, Wang S, Goplen NP, Li C, Cheon IS, Dai Q, et al. PD-1(Hi) CD8(+) Resident Memory T Cells Balance Immunity and Fibrotic Sequelae. *Sci Immunol* (2019) 4(36):eaaw1217. doi: 10.1126/sciimmunol.aaw1217
90. Qu QX, Zhu XY, Du WW, Wang HB, Shen Y, Zhu YB, et al. 4-1bb Agonism Combined With PD-L1 Blockade Increases the Number of Tissue-Resident CD8+ T Cells and Facilitates Tumor Abrogation. *Front Immunol* (2020) 11:577. doi: 10.3389/fimmu.2020.00577
91. Zhang C, Yin K, Liu SY, Yan LX, Su J, Wu YL, et al. Multiomics Analysis Reveals a Distinct Response Mechanism in Multiple Primary Lung Adenocarcinoma After Neoadjuvant Immunotherapy. *J Immunother Cancer* (2021) 9(4):e002312. doi: 10.1136/jitc-2020-002312
92. Arina A, Beckett M, Fernandez C, Zheng W, Pitroda S, Chmura SJ, et al. Tumor-Reprogrammed Resident T Cells Resist Radiation to Control Tumors. *Nat Commun* (2019) 10(1):3959. doi: 10.1038/s41467-019-11906-2
93. Muroyama Y, Nirschl TR, Kochel CM, Lopez-Bujanda Z, Theodros D, Mao W, et al. Stereotactic Radiotherapy Increases Functionally Suppressive Regulatory T Cells in the Tumor Microenvironment. *Cancer Immunol Res* (2017) 5(11):992–1004. doi: 10.1158/2326-6066.CIR-17-0040
94. Zhuang Y, Li S, Wang H, Pi J, Xing Y, Li G. PD-1 Blockade Enhances Radio-Immunotherapy Efficacy in Murine Tumor Models. *J Cancer Res Clin Oncol* (2018) 144(10):1909–20. doi: 10.1007/s00432-018-2723-4
95. Caetano MS, Younes AI, Barsoumian HB, Quigley M, Menon H, Gao C, et al. Triple Therapy With MerTK and PD1 Inhibition Plus Radiotherapy Promotes Abscopal Antitumor Immune Responses. *Clin Cancer Res* (2019) 25(24):7576–84. doi: 10.1158/1078-0432.CCR-19-0795
96. Williams RJ, Trichostatin A. An Inhibitor of Histone Deacetylase, Inhibits Hypoxia-Induced Angiogenesis. *Expert Opin Investig Drugs* (2001) 10 (8):1571–3. doi: 10.1517/13543784.10.8.1571
97. Li C, Zhu B, Son YM, Wang Z, Jiang L, Xiang M, et al. The Transcription Factor Bhlhe40 Programs Mitochondrial Regulation of Resident CD8(+) T Cell Fitness and Functionality. *Immunity* (2020) 52(1):201–2. doi: 10.1016/j.immuni.2019.12.008
98. Zheng X, Oduro JD, Boehme JD, Borkner L, Ebensen T, Heise U, et al. Mucosal CD8+ T Cell Responses Induced by an MCMV Based Vaccine Vector Confer Protection Against Influenza Challenge. *PloS Pathog* (2019) 15(9):e1008036. doi: 10.1371/journal.ppat.1008036
99. Haddadi S, Vaseghi-Shanjani M, Yao Y, Afkhami S, D'Agostino MR, Zganiacz A, et al. Mucosal-Pull Induction of Lung-Resident Memory CD8 T Cells in Parenteral TB Vaccine-Primed Hosts Requires Cognate Antigens and CD4 T Cells. *Front Immunol* (2019) 10:2075. doi: 10.3389/fimmu.2019.02075
100. Caminschi I, Lahoud MH, Pizzolla A, Wakim LM. Zymosan by-Passes the Requirement for Pulmonary Antigen Encounter in Lung Tissue-Resident Memory CD8(+) T Cell Development. *Mucosal Immunol* (2019) 12(2):403–12. doi: 10.1038/s41385-018-0124-2
101. Knight FC, Gilchuk P, Kumar A, Becker KW, Sevimli S, Jacobson ME, et al. Mucosal Immunization With a pH-Responsive Nanoparticle Vaccine Induces Protective CD8(+) Lung-Resident Memory T Cells. *ACS Nano* (2019) 13(10):10939–60. doi: 10.1021/acsnano.9b00326
102. Wilk MM, Mills KHG. CD4 TRM Cells Following Infection and Immunization: Implications for More Effective Vaccine Design. *Front Immunol* (2018) 9:1860. doi: 10.3389/fimmu.2018.01860
103. Ferguson KT, McQuattie-Pimentel AC, Malsin ES, Sporn PHS. Dynamics of Influenza-Induced Lung-Resident Memory T Cells, Anatomically and Functionally Distinct Lung Mesenchymal Populations, and Dampening of Acute Lung Injury by Neutrophil Transfer of Micro-RNA-223 to Lung Epithelial Cells. *Am J Respir Cell Mol Biol* (2018) 59(3):397–9. doi: 10.1165/rcmb.2018-0047RO
104. Hamelmann E, Gelfand EW. IL-5-Induced Airway Eosinophilia–the Key to Asthma? *Immunol Rev* (2001) 179:182–91. doi: 10.1034/j.1600-065X.2001.790118.x
105. Greer M, Werlein C, Jonigk D. Surveillance for Acute Cellular Rejection After Lung Transplantation. *Ann Transl Med* (2020) 8(6):410. doi: 10.21037/atm.2020.02.127


**Conflict of Interest:** The authors declare that the research was conducted in the absence of any commercial or financial relationships that could be construed as a potential conflict of interest.

**Publisher's Note:** All claims expressed in this article are solely those of the authors and do not necessarily represent those of their affiliated organizations, or those of the publisher, the editors and the reviewers. Any product that may be evaluated in this article, or claim that may be made by its manufacturer, is not guaranteed or endorsed by the publisher.

frontiers in Immunology

ORIGINAL RESEARCH
published: 07 December 2021
doi: 10.3389/fimmu.2021.722320

# The Chemokine Receptor CCR5 Links Memory CD4$^+$ T Cell Metabolism to T Cell Antigen Receptor Nanoclustering

OPEN ACCESS

**Edited by:**
Brian S. Sheridan,
Stony Brook University, United States

**Reviewed by:**
Eva Reali,
University of Milano-Bicocca, Italy
Tim Hand,
University of Pittsburgh, United States

***Correspondence:**
Santos Mañes
smanes@cnb.csic.es
Raquel Blanco
raquel.blancof@gmail.com

†These authors share senior authorship

**Specialty section:**
This article was submitted to Immunological Memory, a section of the journal Frontiers in Immunology

**Received:** 08 June 2021
**Accepted:** 16 November 2021
**Published:** 07 December 2021

**Citation:**
Blanco R, Gómez de Cedrón M, Gámez-Reche L, Martín-Leal A, González-Martín A, Lacalle RA, Ramírez de Molina A and Mañes S (2021) The Chemokine Receptor CCR5 Links Memory CD4$^+$ T Cell Metabolism to T Cell Antigen Receptor Nanoclustering. Front. Immunol. 12:722320. doi: 10.3389/fimmu.2021.722320

*Raquel Blanco*[1*†], *Marta Gómez de Cedrón*[2], *Laura Gámez-Reche*[1,3], *Ana Martín-Leal*[1], *Alicia González-Martín*[3], *Rosa A. Lacalle*[1], *Ana Ramírez de Molina*[2] *and Santos Mañes*[1*†]

[1] Department of Immunology and Oncology, Centro Nacional de Biotecnología (CNB/CSIC), Madrid, Spain, [2] Precision Nutrition and Cancer Program, Molecular Oncology Group, IMDEA Food Institute, CEI UAM+CSIC, Madrid, Spain, [3] Department of Biochemistry, Universidad Autónoma de Madrid, and Instituto de Investigaciones Biomédicas Alberto Sols (IIB/CSIC), Madrid, Spain

The inhibition of anabolic pathways, such as aerobic glycolysis, is a metabolic cornerstone of memory T cell differentiation and function. However, the signals that hamper these anabolic pathways are not completely known. Recent evidence pinpoints the chemokine receptor CCR5 as an important player in CD4$^+$ T cell memory responses by regulating T cell antigen receptor (TCR) nanoclustering in an antigen-independent manner. This paper reports that CCR5 specifically restrains aerobic glycolysis in memory-like CD4$^+$ T cells, but not in effector CD4$^+$ T cells. CCR5-deficient memory CD4$^+$ T cells thus show an abnormally high glycolytic/oxidative metabolism ratio. No CCR5-dependent change in glucose uptake nor in the expression of the main glucose transporters was detected in any of the examined cell types, although CCR5-deficient memory cells did show increased expression of the hexokinase 2 and pyruvate kinase M2 isoforms, plus the concomitant downregulation of Bcl-6, a transcriptional repressor of these key glycolytic enzymes. Further, the TCR nanoclustering defects observed in CCR5-deficient antigen-experienced CD4$^+$ T cells were partially reversed by incubation with 2-deoxyglucose (2-DG), suggesting a link between inhibition of the glycolytic pathway and TCR nanoscopic organization. Indeed, the treatment of CCR5-deficient lymphoblasts with 2-DG enhanced IL-2 production after antigen re-stimulation. These results identify CCR5 as an important regulator of the metabolic fitness of memory CD4$^+$ T cells, and reveal an unexpected link between T cell metabolism and TCR organization with potential influence on the response of memory T cells upon antigen re-encounter.

**Keywords: memory CD4+ T cells, efector CD4+ T cells, metabolic reprogramming, chemokine signaling, CCR5, BCL6, glycolysis**

## INTRODUCTION

The adaptive immune system has the ability to generate immunological memory. This allows for rapid and robust secondary responses upon antigen re-encounter (1). The response of memory T ($T_M$) cells to low antigen concentrations has been linked to the antigen-independent formation of T cell antigen receptor (TCR) oligomers known as nanoclusters (2–4). The nanoscopic organization of the TCR molecules is not exclusive to $T_M$ cells; it also occurs in effector T ($T_E$) cells, although to a lesser extent. Indeed, the antigenic sensitivity gradient in $CD4^+$ and $CD8^+$ T cell subsets ($T_M$>$T_E$>>naive) correlates with the valency of TCR nanoclusters at the cell surface (5, 6). TCR nanoscopic organization allows cooperativity between TCR molecules (7) and increases avidity for multimeric peptide-major histocompatibility complexes (5, 8). TCR nanoclustering in antigen-experienced $T_M$ and $T_E$ lymphoblasts is strongly dependent on the sterol and sphingolipid composition of the plasma membrane (6, 9, 10); the importance of the cell's metabolic state in TCR organization has, however, been left completely unexplored.

A solid body of evidence indicates that dynamic changes in cellular metabolism determine the functionality and fate of $CD4^+$ and $CD8^+$ T cells (11–13). Each differentiation state and lineage subset of T cells has a unique metabolic profile. Quiescent, naive T cells, which have low metabolic needs, are largely dependent on the oxidative phosphorylation (OXPHOS) of small amounts of glucose or fatty acids in the mitochondria to generate ATP (12). Upon antigen stimulation, $T_E$ cells increase both OXPHOS and aerobic glycolysis to fulfill their new ATP and building block demands. The net result is a metabolic switchover that reduces the OXPHOS/glycolytic ratio in these cells. This increase in glycolysis, which occurs in $CD8^+$ and all effector $CD4^+$ T helper (Th) subsets (Th1, Th2 and Th17), is not only important for generating the biomass needed for the expansion of activated cells, it is also required for the expression of cytokines involved in T cell effector function (14–17). In contrast, the metabolism of $CD4^+$ regulatory T cells, and of both $CD4^+$ and $CD8^+$ $T_M$ cells, largely relies on OXPHOS and fatty acid oxidation (FAO) (12, 16, 18). Thus, $T_M$ cells undergo a metabolic switchover that increases the OXPHOS/glycolytic ratio compared to $T_E$ cells. Indeed, the inhibition of glycolysis is a necessary step in preserving the generation of long-lived $CD8^+$ $T_M$ cells, whereas enhanced glycolytic flow prevents $T_M$ cell formation (19).

Switches between these dynamic metabolic programs are orchestrated by the TCR plus co-stimulatory and cytokine signaling. Together, these induce top-down signaling circuits culminating in the expression or repression of specific transcription factors. For instance, interleukin (IL)-2 signaling boosts the transcription of glycolytic genes through the induction of interferon-regulatory factor (IRF)-4, hypoxia-inducible factor (HIF)-1α, and Myc (20). Interestingly, IL-2 also downregulates the glycolysis-inhibiting repressor B-cell lymphoma 6 (Bcl)-6, thus preventing the induction of a Bcl-6-guided transcriptional program more compatible with $T_M$ cell metabolism (21). Other cytokines such as IL-15 and IL-7 promote $T_M$ cell formation by triggering mitochondrial oxidative metabolism through the expression of carnitine palmitoyltransferase-1a (CPT1a) and lipases, which respectively control FAO and the mobilization of intrinsic fatty acids (22). Co-stimulatory and cytokine signaling also control mitochondrial fusion and fission dynamics, and the ultrastructure of the cristae, affecting mitochondrial respiratory capacity and hence the formation of $T_E$ and $T_M$ cells (23–27). Although information on the regulation of T cell metabolism has increased in recent years, much remains to be learnt about the array of signals involved in its reprogramming.

T cells are also exposed to signals provided by chemokines - cytokines that act through seven-transmembrane G-protein-coupled receptors and traditionally catalogued as regulators of leukocyte trafficking (28). Solid evidence exists, however, that some chemokine receptors influence T-cell fate and function in a chemotactic-independent manner (29). In particular, C-C chemokine receptor 5 (CCR5) has been implicated in maximizing $CD4^+$ T cell co-stimulation and the induction of transcriptional programs responsible for cytokine production (30–34). CCR5 transduces signals from CCL3, CCL4 and CCL5, the expression of which is induced upon TCR-mediated activation (35). Recently, CCR5 has been involved in $CD4^+$ $T_M$ cell responses. CCR5 deficiency does not affect $CD4^+$ $T_M$ cell generation, but reduces TCR nanoclustering organization and, consequently, the antigenic sensitivity of $T_M$ cells after antigen re-encounter (6). As a result, $CCR5^{-/-}$ mice show impaired production of high-affinity class-switched antibodies after antigen re-challenge, a phenomenon dependent on $CD4^+$ $T_M$ cell function.

Since CCR5 activity affects $CD4^+$ $T_M$ cell functionality, the present work examines whether it also affects $T_M$ cell metabolism. The information of potential effects of CCR5 on T cell metabolism is, however, limited. In activated $CD4^+$ $T_E$ cells, CCR5 has been reported to increase glucose uptake, glycolysis and AMP-activated protein kinase (AMPK)-α1 activity and, therefore, presumably FAO; indeed, the inhibition of glycolysis and the AMPK pathway prevents CCR5-mediated chemotaxis (36). The CCL5-mediated chemotactic activity of activated and resting $CD4^+$ $T_M$ cells has different metabolic requirements (37), but the involvement of CCR5 activation in metabolic alterations has never before been studied. The present work shows that CCR5 deficiency enhances glycolysis in $CD4^+$ $T_M$ cells, thus hindering the metabolic switch associated with the $T_M$ cell lineage. OXPHOS and glycolysis were found comparable in CCR5-deficient and CCR5-proficient $CD4^+$ $T_E$ cells, indicating the CCR5 effect in $T_M$ cells to be specific to them. CCR5-deficient $CD4^+$ $T_M$ cells showed very little expression of Bcl-6, whereas some key enzymes regulating the glycolytic flow were increased. Strikingly, the inhibition of glycolysis in CCR5-deficient, antigen-experienced $CD4^+$ T lymphoblasts increased the degree of TCR nanoclustering. These results indicate that CCR5 improves the functional and metabolic fitness of $CD4^+$ $T_M$ cells, and reveal an unexpected bond between metabolic reprogramming and TCR nanoscopic organization.

## MATERIALS AND METHODS

### Mice

TCR transgenic OT-II $CCR5^{-/-}$ mice (31) recognizing the peptide $OVA_{323–339}$ (ISQAVHAAHAEINEAGR; I-Ab MHC class II

molecule) were maintained under specific-pathogen-free conditions at the CNB animal facilities, in agreement with Spanish national and EU guidelines. All animal procedures were approved by the ethics committees of the CNB and the *Comunidad de Madrid* (PROEX 277/14; PROEX 090/19).

## Culture of Mouse Primary T Cells

Spleen and lymph nodes from 6 to 12 week-old OT-II WT and $CCR5^{-/-}$ mice were isolated and cell suspensions obtained using 40 μm pore filters. Erythrocytes were lysed with AKT lysis buffer (0.15 M $NH_4Cl$, 10 mM $KHCO_3$, 0.1 mM EDTA) and activated with the $OVA_{323-339}$ peptide for 3 days in complete medium, i.e., RPMI 1640 (Biowest), 10% FBS, 1 mM sodium pyruvate, 2 mM L-glutamine, 1% non-essential amino acids, 100 U/ml penicillin/streptomycin, 10 μM β-mercaptoethanol. The antigen was removed and the cells cultured with IL-2 (5 ng/ml) or IL-15 (20 ng/ml) for four more days.

## Analysis of Cell Bioenergetics

The oxygen consumption rate (OCR) and the extracellular acidification rate (ECAR) were measured using an XF96 Extracellular Flux analyzer (Seahorse Bioscience). $CD4^+$ $T_E/T_M$ cells were seeded ($0.3x10^6$ cells/well) on a XF96 cell culture microplate previously treated with Cell-Tak (Corning). Mitochondrial stress tests were performed by incubating cells for 1 h in the absence of $CO_2$ in non-buffered XF assay medium pH7.4 (Seahorse Bioscience), supplemented with 25 mM glucose, 2 mM glutamine and 1 mM sodium pyruvate. After basal rate measurements, different modulators of mitochondrial respiration were injected sequentially (1): 2.5 μM oligomycin to inhibit ATP-synthase and to calculate the ATP-linked oxygen consumption (2); 1.5 μM carbonyl cyanide-P-trifluoro-methoxy-phenylhydrazone (FCCP; an uncoupling agent) to obtain the maximum respiration under stress conditions; and (3) a mix of 0.5 μM rotenone/antimycin A to completely block mitochondrial respiration by inhibiting complexes I and III respectively.

The oxidation of exogenous fatty acids was measured using palmitate-BSA as a substrate. Briefly, cells were seeded overnight in complete medium. Forty-five minutes prior to the assay, cells were incubated with non-buffered XF assay medium pH7.4 (Seahorse Bioscience) supplemented with palmitate-BSA, 1 mM glucose, 0.5 mM carnitine, and 5 mM HEPES, adjusted to pH 7.4, and incubated (30-45 min, 37°C) in a non-$CO_2$ incubator; etomoxir (40 μM) was added in the corresponding wells 15 min before starting the assay. OCR was measured under basal conditions and after the sequential addition of 2.5 μM oligomycin, 1.5 μM FCCP and 0.5 μM rotenone/antimycin A.

Glycolysis stress tests were performed using cells starved in a non-$CO_2$ incubator for 1 h at 37°C in non-buffered XF assay medium (Seahorse Bioscience) supplemented with 2 mM glutamine and 1 mM sodium pyruvate. After measuring basal ECAR and OCR, 15 mM glucose were injected to stimulate glycolysis, followed by 2.5 μM oligomycin to obtain the maximum glycolytic capacity *via* the inhibition of oxygen consumption. Finally, 100 mM of 2-deoxy-D-glucose (2-DG) were injected to shut down glycolysis. For glycolytic rate assays, cells were incubated in the absence of $CO_2$ for 1 h in non-buffered XF assay medium (Seahorse Bioscience) supplemented with 25 mM glucose, 2 mM glutamine and 1 mM sodium pyruvate. After basal ECAR measurements, 0.5 μM rotenone/antimycin and 100 mM 2-DG were injected.

OCR and ECAR were measured three times after the addition of each drug. At least three animals per condition, run in triplicate, were used in each experiment. Calculations were performed with the Seahorse XF Cell Test Report Generator software (Seahorse Bioscience).

## Chemokine Determination

The supernatant of OT-II cells ($10^6$ cells/well) differentiated under $T_E$ and $T_M$ conditions (as indicated above) was collected on day 7 of culture, and mouse CCL3, CCL4 and CCL5 levels determined using a specific sandwich ELISA (R&D Systems) following the manufacturer's instructions.

## Quantitative Real-Time PCR

Total RNA was extracted from cells using the RNeasy Mini Kit (Qiagen), and cDNA synthesized from 1 μg total RNA using the High Capacity cDNA Reverse Transcription Kit (Promega). Quantitative RT–PCR was performed in a QuantStudio 5 Real-Time PCR System (Applied Biosystems), using FluoCycle II SYBR Master Mix (EuroClone) with the primer pairs listed in **Supplementary Table S1**. Gene expression was normalized using the 18S ribosomal RNA signal.

## Western Blot Analysis

Protein extracts were obtained after cell lysis with RIPA buffer (50 mM Tris-HCl pH 8.0, 150 mM NaCl, 1% NP-40, 0.5% sodium deoxycholate and 1% SDS) supplemented with protease and phosphatase inhibitors (1 mM PMSF, 1 mM $Na_3VO_4$, 10 μg/ml leupeptin, 10 μg/ml aprotinin and 5 mM NaF). Proteins were quantified using the Micro BCA Protein Assay Kit (Pierce). Equal amounts of proteins were resolved on 10% polyacrylamide gels and transferred to PVDF membranes. Membranes were probed with anti-Bcl-6 (BD Pharmingen) and anti-β-actin (Sigma Aldrich) antibodies.

## Flow Cytometry Analysis

WT and $CCR5^{-/-}$ OT-II lymphoblasts ($10^6$) differentiated under $T_E$ or $T_M$ conditions were stained (30 min, 4°C) with LIVE/DEAD™ Fixable Near-IR Dead Cell Stain (Thermofisher Scientific) and, after extensive washing with ice-cold PBS-2% BSA, stained (15 min, 4°C) with anti-CD4-PECy5.5 (clone GK1.5; BioLegend) in the dark. The cells were then fixed and permeabilized using the eBioscience™ Foxp3/Transcription Factor Fixation/Permeabilization Kit (Thermofisher Scientific) following the manufacturer's instructions, and stained (1 h, 20°C, in the dark) with anti-Bcl6-PE (clone K112-91; 2 μg/ml; BD Bioscience). Cells were analyzed using a Gallios Flow Cytometry Analyzer (Beckman Coulter), and data processed using FlowJo software (BD Bioscience).

## Glucose Internalization

Glucose uptake was determined for the whole cell population using the Glucose Uptake-Glo Assay (Promega). Basically, WT

and CCR5$^{-/-}$ OT-II lymphoblasts differentiated under $T_E$ or $T_M$ conditions ($0.5x10^6$) were starved for 30 min in glucose-free RPMI 1640 medium (Biowest) supplemented with 2 mM L-glutamine, 1% non-essential amino acids and 100 U/ml penicillin/streptomycin, and then incubated with 2-DG (20 min, 37°C). Cells were lysed and 2-DG incorporation determined following the manufacturer's instructions.

## Immunogold Labeling, Replica Preparation, and EM Analysis

CCR5$^{-/-}$ and WT OT-II lymphoblasts treated - or not - with 2-DG (2 mM, 24 h) were used to prepare cell surface replicas as previously described (5, 6). Briefly, T cells were fixed in 1% paraformaldehyde and labeled with anti-mouse CD3ϵ mAb (145-2C11), followed by 10 nm gold-conjugated protein A (Sigma-Aldrich). Labeled cells were adhered to poly-L-lysine-coated mica strips and fixed with 0.1% glutaraldehyde. Samples were covered with another mica strip, frozen in liquid ethane (KF-80, Leica), and stored in liquid nitrogen. Cell replicas were prepared with a Balzers 400T freeze fracture (FF) unit, mounted on copper grids, and analyzed using a JEM1010 electron microscope (Jeol) operating at 80 kV. Images were taken with a Bioscan CCD camera (Gatan) and processed with TVIPS software. EM image acquisition and quantification was performed by two researchers, one of them blind to the experiment. The number of TCR molecules in the same cluster was determined when the distance between gold particles was smaller than their diameter (10 nm).

## Re-Stimulation Assays

CCR5$^{-/-}$ OT-II lymphoblasts were treated with vehicle or 2-DG (2mM) for 24 h and, after extensive washing to remove all remnants of 2-DG, co-cultured (24 h) with irradiated (15 Gy) splenocytes loaded (2 h, 37°C) with different concentration of $OVA_{323-339}$ peptide. Supernatants were collected to measure IL-2 by ELISA (ELISA MAX Deluxe, BioLegend). Proliferation was assessed *via* methyl-$^3$[H]-thymidine (1 μCi/well) incorporation into DNA, using a 1450 Microbeta liquid scintillation counter (PerkinElmer).

## Statistical Analysis

Statistical analyses were performed using Prism software (GraphPad). Differences were assessed using the two-tailed Student *t* test with Welch's correction or the Holm-Sidak correction for multiple *t* test comparisons, or, when appropriate, two-way ANOVA with the *post-hoc* Bonferroni test for multiple comparisons. The Chi-square test was used to analyze the overall distribution of gold particles. Variances were compared using the F test. Data are expressed as means ± SEM. Significance was set at $p<0.05$.

# RESULTS

## CCR5 Does Not Alter Mitochondrial Activity in CD4$^+$ T Cells

To analyze whether CCR5 affects the metabolic reprogramming of CD4$^+$ T cells, WT and CCR5$^{-/-}$ OT-II splenocytes were stimulated with cognate antigen and subsequently cultured for four days in the presence of IL-2 or IL-15, but in the absence of antigenic stimulation (**Figure 1A**). In accordance with other studies (6, 23), these culture conditions generated resting CD4$^+$ $T_E$ (IL-2) or $T_M$ (IL-15) lymphoblasts, respectively. Notably, $T_E$ and $T_M$ lymphoblasts expressed comparable levels of the main CCR5 ligands (CCL3, CCL4 and CCL5) and the receptor CCR5 (**Supplementary Figure S1**), suggesting that the differentiation conditions do not affect potential autocrine/paracrine CCR5 signaling (6).

The oxygen consumption rate (OCR) was monitored as an indicator of mitochondrial function in WT and CCR5$^{-/-}$ $T_E$ and $T_M$ cells, using glucose as carbon source. No differences were seen between any cell type in terms of basal or maximum OCR (OCRmax), spare respiratory capacity (SRC; a variable determining the capacity of the cell to respond to an energy demand), or ATP production (**Supplementary Figure S2**). To rule out that the lack of differences was associated with the carbon source, similar experiments were performed using palmitate in a low glucose medium (1 mM). Pre-treatment of the cells with etomoxir, a CPT1a inhibitor, drastically reduced the OCR (**Supplementary Figure S3**), allowing the contribution of FAO to the measured variables to be distinguished. Again, no significant differences were seen between any cell type in terms of OCRmax, SRC or ATP production (**Supplementary Figure S3**). In agreement with the lack of differences in OXPHOS determinations between CCR5 proficient and deficient cells, no relative differences were found in the expression of mitochondrial genes (**Supplementary Figure S4**), including NADH:ubiquinone oxidoreductase subunit A9 (NDUFA9, respiratory complex I), succinate dehydrogenase complex iron sulfur subunit B (SDHB; complex II), cytochrome C Oxidase assembly factor heme A:farnesyltransferase (COX10, complex IV), mitochondrial ATP synthetase (ATP5A1; complex V), mitochondrial pyruvate carrier (MPC)-1, or carnitine palmitoyltransferase 1A (CPT-1A). Nevertheless, NDUFA9 and SDHB were upregulated in $T_M$ compared to $T_E$ cells, independent of CCR5 status. Thus, the absence of CCR5 does not alter mitochondrial activity in CD4$^+$ T cells.

## CCR5 Restrains Glycolysis Specifically in CD4$^+$ $T_M$ Cells

Whether CCR5 affects the glycolytic pathway was next studied, measuring the extracellular acidification rate (ECAR). CCR5 affected none of the glycolytic variables measured in $T_E$ cells (**Supplementary Figure S5**), i.e., no significant differences were found between WT and CCR5$^{-/-}$ CD4$^+$ $T_E$ cells in their glycolytic rate (ECAR after the addition of saturating amounts of glucose), glycolytic capacity (maximum ECAR after oligomycin-induced OXPHOS inhibition) or glycolytic reserve (the capacity to respond to an energetic demand). In contrast, CCR5$^{-/-}$ $T_M$ cells showed a significant increase in all the glycolytic variables measured compared to their WT counterparts (**Figures 1B–E**). This suggests that CCR5 signals restrain the glycolytic activity of $T_M$ cells.

Although extracellular acidification is mainly driven by glycolytic activity, it can also be the consequence of other metabolic processes, such as the production of $CO_2$ by the tricarboxylic acid (TCA) cycle. The relative contribution of

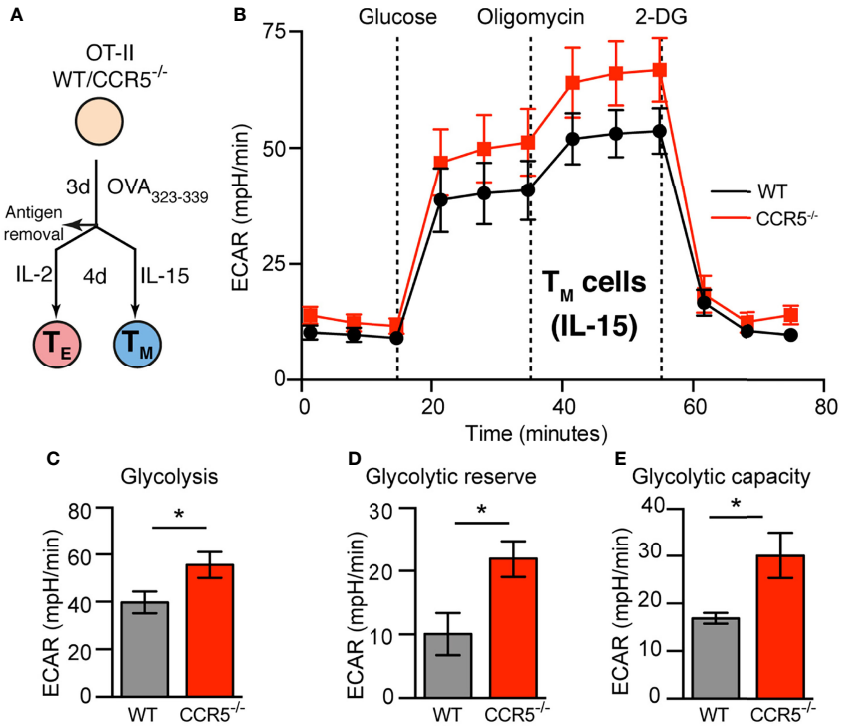


**FIGURE 1** | CCR5 deficiency increases glycolytic metabolism in memory CD4$^+$ T cells. **(A).** Diagram showing the *ex-vivo* activation and differentiation of primary CD4$^+$ T cells (OT-II). **(B)** ECAR profiles of WT and CCR5$^{-/-}$ $T_M$ (IL-15-expanded) lymphoblasts differentiated as in **(A)**, incubated in XF assay medium supplemented with 2 mM glutamine and 1 mM sodium pyruvate in the absence of $CO_2$, and subsequently inoculated with glucose, oligomycin and 2-DG as indicated. **(C–E).** Determination of glycolysis **(C)**, glycolytic reserve **(D)** and glycolytic capacity **(E)** (details in *Results*) from the ECAR curves obtained as in **(B)**. Data represent means ± SEM (n≥9 from three independent experiments). *p < 0.05, two-tailed Student *t* test.

glycolysis and the TCA cycle activity to ECAR was therefore measured using the glycolytic rate assay. This assay determines the glycolytic proton efflux rate (glycoPER), which represents acidification due solely to glycolysis. Both the WT and CCR5$^{-/-}$ $T_E$ cells showed comparable glycoPER values under untreated conditions (basal glycolysis), and after the addition of rotenone/antimycin A to inhibit mitochondrial activity (compensatory glycolysis; **Supplementary Figure S6**). However, the values recorded for both basal and compensatory glycolysis were significantly higher in CCR5$^{-/-}$ than in CCR5-proficient $T_M$ cells (**Figures 2A–C**). Further, CCR5 deficiency in $T_M$ cells caused a significant reduction in OXPHOS/glycolytic activity (i.e., the mitoOCR/glycoPER ratio) compared to the WT $T_M$ cells (**Figure 2D**). Indeed, whereas the WT $T_M$ cells showed a higher mitoOCR/glycoPER ratio than did the WT $T_E$ cells, the CCR5$^{-/-}$ $T_M$ and $T_E$ cells showed comparable mitoOCR/glycoPER ratios (**Figure 2D**). Together, these results indicate that the metabolic switch associated with CD4$^+$ $T_M$ cell formation is impaired in CCR5$^{-/-}$ cells due to their enhanced glycolytic metabolism.

## CCR5 Does Not Affect Glucose Uptake in CD4$^+$ $T_M$ Cells

Given that the CCR5$^{-/-}$ $T_M$ cells were substantially more glycolytic than CCR5-proficient cells, a detailed inspection was made of the different elements involved in the glycolytic route. Glucose internalization in WT and CCR5$^{-/-}$ $T_E$ and $T_M$ cells was examined using 2-DG as a probe, and an increased uptake of glucose was seen in the $T_E$ cells but of both backgrounds. This is consistent with the reduced glycolysis seen in the $T_M$ compared to the $T_E$ cells. Nonetheless, differences in 2-DG internalization were not associated with CCR5 expression (**Figure 3A**).

The expression of glucose transporters was also determined at the mRNA level. Glut-1, Glut-3, Glut-6 and Glut-8 mRNA were detected in WT and CCR5$^{-/-}$ $T_E$ and $T_M$ cells. Glut-1 and Glut-6 mRNAs were differentially expressed between $T_E$ and $T_M$ cells, independent of their WT or CCR5$^{-/-}$ genetic background (**Figure 3B**). The mRNA levels for Glut-3 and Glut-8 were associated with no remarkable differences between the cells of any type (**Supplementary Figure S7A**). Collectively, these results indicate that CCR5 does not affect the expression of glucose transporters, which is consistent with the lack of difference seen in glucose uptake between the WT and CCR5$^{-/-}$ cells.

## CCR5 Downregulates Specific Glycolytic Genes in CD4$^+$ $T_M$ Cells

To study how CCR5 expression regulates the glycolytic flow in $T_M$ cells, mRNA levels were determined in WT and CCR5$^{-/-}$ $T_E$ and $T_M$ cells for enzymes proposed to be rate-limiting in the glycolytic cascade: hexokinase 2 (HK2) and isoform M2 of pyruvate kinase (PKM2) (38). In addition, the relative

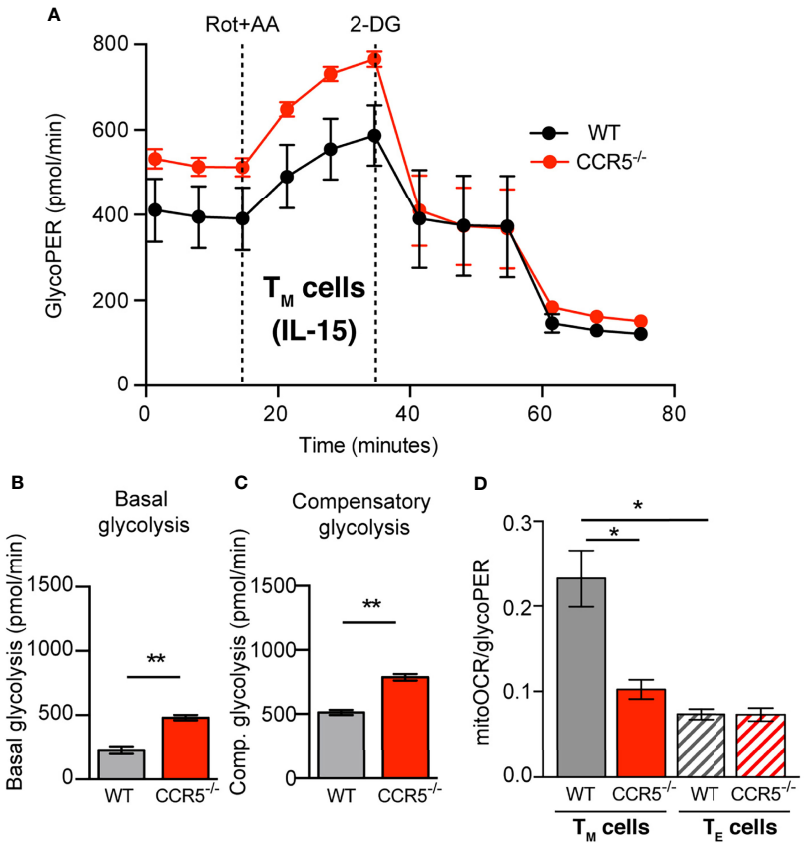


**FIGURE 2** | CCR5 deficiency prompts glycolytic metabolism over OXPHOS in memory CD4$^+$ T cells. **(A)** GlycoPER profiles in WT and CCR5$^{-/-}$ $T_M$ cells under basal condition (non-buffered XF assay medium pH 7.4, containing 25 mM glucose and 2 mM glutamine 1 mM sodium pyruvate, in the absence of $CO_2$), and following addition of rotenone/antimycin A (Rot+AA) and 2-DG. **(B, C)** Basal glycolysis **(B)** and compensatory glycolysis **(C)** determined from profiles as in **(A)**. **(D)** Basal mitoOCR/glycoPER ratio in WT and CCR5$^{-/-}$ $T_M$ (solid bars) and $T_E$ (hatched bars) cells. Data are means ± SEM (n≥9 from three independent experiments). **p < 0.01, *p < 0.05, two-tailed Student *t* test **(B, C)**, or two-way ANOVA with Bonferroni *post-hoc* test **(D)**.

expression of glyceraldehyde-3-phosphate dehydrogenase (GAPDH) and lactate dehydrogenase (LDHA) was determined. The mRNA levels for HK2 and PKM2 were significantly upregulated in CCR5$^{-/-}$ CD4$^+$ $T_M$ cells compared to their WT counterparts, but both enzymes were equally expressed in CCR5$^{-/-}$ and WT $T_E$ cells (**Figure 3C**). Moreover, both HK2 and PKM2 mRNA levels were higher in the WT $T_E$ than in the WT $T_M$ cells (**Figure 3C**), confirming the existence of the $T_E$/$T_M$ metabolic switchover. The expressions of GAPDH and LDHA were not affected by CCR5 status in either the $T_E$ and $T_M$ cells (**Supplementary Figure S7B**). These results indicate that CCR5 activity in $T_M$ cells affects the regulation of key glycolytic enzymes, explaining the glycolytic differences observed between CCR5-proficient and -deficient $T_M$ cells.

## Differential Expression of Bcl-6 in WT and CCR5$^{-/-}$ $T_M$ Cells

The mechanism behind the deregulation of glycolysis in CCR5$^{-/-}$ $T_M$ cells was next investigated. Since glycolysis is not affected by CCR5 in $T_E$ cells, it was reasoned that the glycolytic differences between in CCR5$^{-/-}$ and WT CD4$^+$ $T_M$ cells might be associated with the different cytokines used in $T_E$ and $T_M$ cell differentiation. Bcl-6 is a transcriptional repressor of genes involved in glycolysis, the expression of which is increased in CD4$^+$ T cells cultured under low IL-2 concentrations (21). In agreement with published data, Bcl-6 protein was very low in IL-2-differentiated $T_E$ cells, independent of the CCR5 genotype (**Figures 4A–E**). In contrast, Bcl-6 was clearly upregulated in the WT $T_M$ cells but remained low in the CCR5$^{-/-}$ $T_M$ cells, both by flow cytometry and immunoblotting (**Figures 4A–E**). In agreement with the protein data, Bcl-6 mRNA levels were also significantly higher in the WT than in the CCR5$^{-/-}$ $T_M$ cells (**Figure 4F**), whereas no differences were seen between the WT and CCR5$^{-/-}$ $T_E$ cells. These results suggest that CCR5 deficiency downregulates Bcl-6 expression at the transcriptional and translational level.

## Glycolytic Repression Promotes TCR Nanoclustering

Finally, experiments were performed to see whether the metabolic changes driven by CCR5 affect the nanoscopic organization of the TCR in CD4$^+$ T cells, a process in which

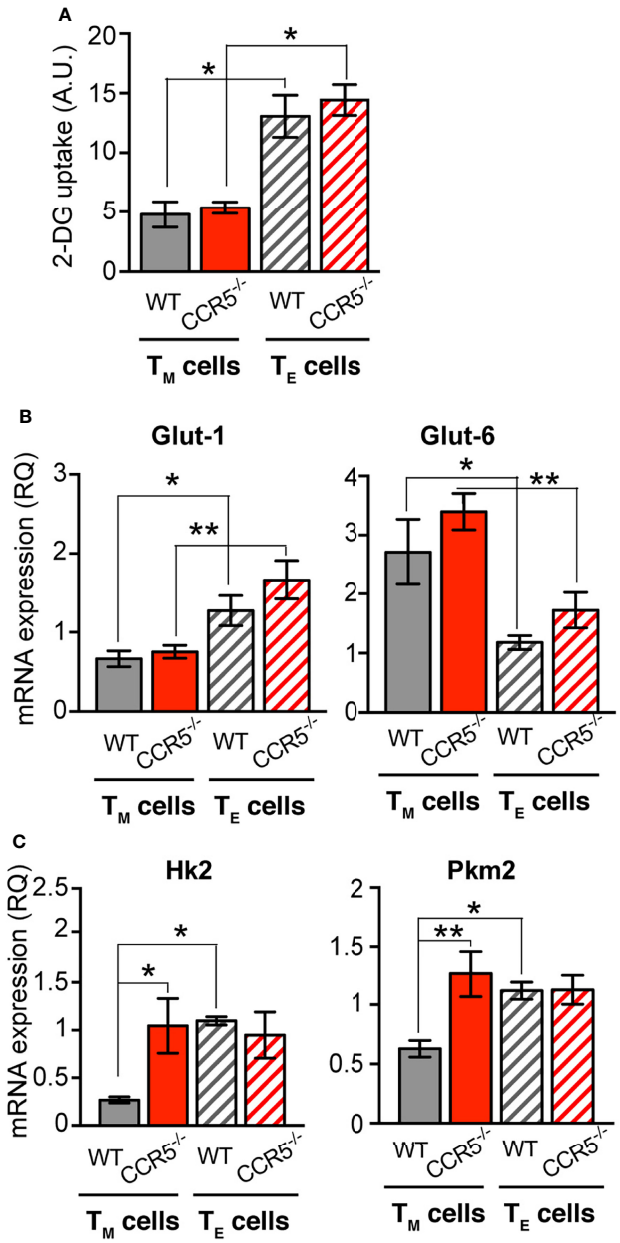


**FIGURE 3** | CCR5 regulates glucose uptake and rate-limiting glycolytic enzymes specifically in CD4$^+$ $T_M$ cells. **(A)** Determination of 2-DG uptake in WT and CCR5$^{-/-}$ $T_M$ (solid bars) and $T_E$ (hatched bars) cells ($n$=3). **(B, C)** Relative mRNA expression of the glucose transporters Glut-1 and Glut-6 **(B)**, and the glycolytic enzymes Hk2 and Pkm2 **(C)** in WT and CCR5$^{-/-}$ $T_M$ and $T_E$ lymphoblasts ($n$=12). Data are means ± SEM. **p < 0.01, *p < 0.05, two-way ANOVA with Bonferroni *post-hoc* test.

CCR5 signaling is also determinant (6). Electron microscopy (EM) was used to analyze surface replicas of antigen-experienced OT-II WT and CCR5$^{-/-}$ CD4$^+$ lymphoblasts after labeling with anti-CD3ϵ antibody and 10 nm gold-conjugated protein A. In agreement with earlier findings (6), TCR nanoclustering was reduced in CCR5$^{-/-}$ compared to WT lymphoblasts (**Figure 5A**). The percentage of monovalent TCRs was significantly higher among CCR5$^{-/-}$ than WT lymphoblasts, whereas the percentage of TCR nanoclusters larger than four TCR molecules was higher in WT than in CCR5$^{-/-}$ cells. To determine if the TCR nanoclustering differences could be ascribed to the enhanced glycolytic activity of CCR5$^{-/-}$ lymphoblasts, TCR organization was analyzed in CCR5$^{-/-}$ lymphoblasts cultured for one day in the presence of the glycolytic inhibitor 2-deoxyglucose (2-DG). 2-DG significantly increased TCR nanocluster number and size in CCR5$^{-/-}$ lymphoblasts, whereas the percentage of monovalent TCRs was drastically reduced (**Figure 5B**). These results suggest that the inhibition of the glycolytic pathway is important in the formation of TCR nanoclusters in antigen-experienced T cells.

The valency of TCR nanoclusters has been related to their sensitivity to antigenic stimulation (5, 6). Given that glycolysis inhibition with 2-DG increased the valency of TCR nanoclusters in CCR5$^{-/-}$ lymphoblasts, tests were made to determine whether 2-DG would increase their antigenic re-stimulation. OT-II WT and CCR5$^{-/-}$ lymphoblasts were incubated for 24 h with 2-DG, and the inhibitor then removed before co-incubation with irradiated splenocytes pre-loaded with different doses of the $OVA_{323-339}$ peptide. Since glycolysis activation is required for complete T cell activation (14–17), IL-2 production and T cell proliferation were analyzed shortly after re-stimulation. IL-2 production was seen to increase significantly in the 2-DG-treated CCR5$^{-/-}$ lymphoblasts compared to controls in an antigen dose-dependent manner (**Figure 5C**). A similar trend (i.e., not significant) towards enhanced IL-2 production was observed in the 2-DG-treated WT lymphoblasts. In contrast, 2-DG treatment tended to inhibit WT and CCR5$^{-/-}$ lymphoblast proliferation at all antigen doses (**Figure 5D**), suggesting that 2-DG interferes with cell proliferation in an antigen- and CCR5-independent manner.

## DISCUSSION

Long-term memory mediated by CD4$^+$ T cells is central to the recall response of the adaptive immune system to antigens. CD4$^+$ $T_M$ cells expand after antigen exposure and begin to make cytokines (which direct immune cell function), provide help in the B cell and CD8$^+$ T cell responses, and directly exert effector functions (39, 40). A major characteristic of CD4$^+$ $T_M$ cells is their ability to respond to lower doses of antigen and/or to reduced levels of co-stimulation compared to naive CD4$^+$ T cells (41, 42). This enhanced antigenic sensitivity has been associated with the organization of the TCR into nanoclusters (5, 6) and to the onset of a bioenergetic program in which OXPHOS dominates over glycolysis (43). This work shows CCR5 to be a key regulator of both TCR nanoclustering and the $T_M$ cell metabolic program, revealing its importance in the maximization of CD4$^+$ $T_M$ immune responses (6).

CCR5 deficiency in mice and humans (homozygous carriers for the *ccr5Δ32* polymorphism) causes no significant change in the frequency of the different CD4$^+$ $T_M$ cell subtypes either in the

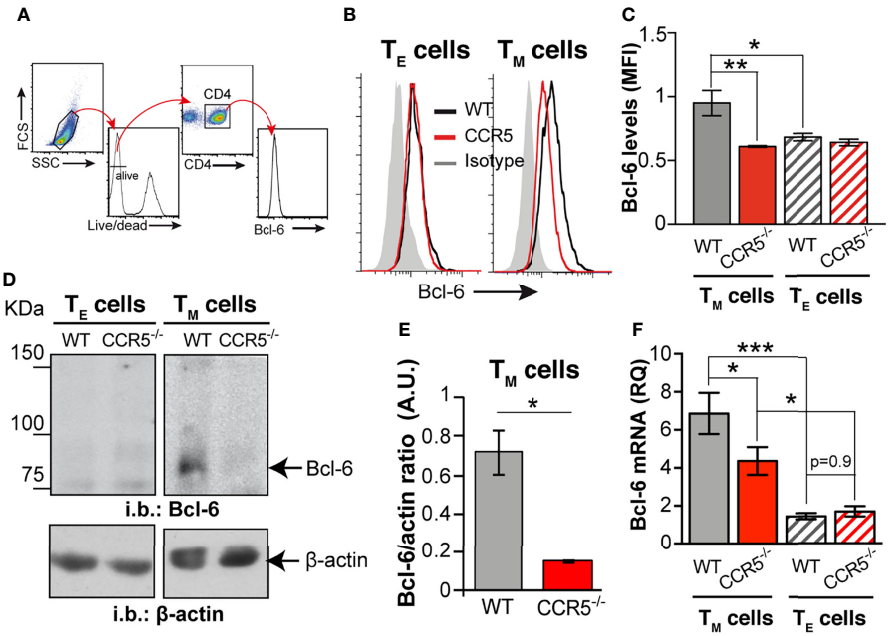


**FIGURE 4** | CCR5 deficiency downregulates the glycolytic repressor Bcl-6 in CD4$^+$ $T_M$ cells. **(A)** Gating strategy for determination of relative Bcl-6 levels by flow cytometry. **(B)** Representative histograms for Bcl-6 levels in WT (black lines) and CCR5$^{-/-}$ (red lines) $T_E$ (left) and $T_M$ (right) cells; the isotype control histogram is also shown (gray). **(C)** Quantification of the mean fluorescent intensity (MFI) for Bcl-6 staining in WT and CCR5$^{-/-}$ $T_E$ (hatched bars) and $T_M$ (solid bars) cells ($n$=3) **(D)**. Representative immunoblots of Bcl-6 and β-actin (loading control) in total cell extracts from WT and CCR5$^{-/-}$ $T_E$ and $T_M$ cells ($n$=3). **(E)** Bcl-6: β-actin densitometry ratio from immunoblots as in **(A)**. **(F)** Relative expression of *Bcl-6* mRNA in WT and CCR5$^{-/-}$ $T_E$ (hatched bars) and $T_M$ (solid bars) cells ($n$=12). Data are means ± SEM. ***p < 0.001, **p < 0.01 *p < 0.05, two-tailed Student *t* test **(E)**, or two-way ANOVA with Bonferroni *post-hoc* test **(C, F)**.

periphery or in the secondary lymphoid organs. However, the functionality of CCR5-deficient $T_M$ cells is lessened, as demonstrated by the reduced expression of cytokines after re-stimulation, or their impaired helper function in the B cell-mediated humoral response (6). This functional deficit is linked to an enrichment of long-chain ceramides in the membrane of antigen-experienced CCR5$^{-/-}$ cells, caused by the increased GATA-1-induced expression of specific ceramide synthases. High levels of ceramides most likely rigidify the plasma membrane, which interferes with TCR nanoclustering and, hence, the ability to respond to low doses of antigen and/or co-stimulation. Here, we show that CCR5$^{-/-}$ $T_M$ cells also experience an aberrant increase in glycolysis compared to CCR5-proficient cells. The OXPHOS/glycolytic ratio in the former is reduced, altering the bioenergetic program associated with $T_M$ cell differentiation. Importantly, the inhibition of glycolysis increased TCR nanoclustering in antigen-experienced CCR5$^{-/-}$ cells, suggesting a link between high glycolytic activity and reduced TCR nanoclustering. We therefore propose that autocrine/paracrine stimulation of CCR5 enhances TCR nanoclustering in CD4$^+$ $T_M$ cells through two signals (**Figure 5E**): (i) the reduction of GATA-1 translocation to the nucleus, which restrains the expression of enzymes involved in ceramide biosynthesis (a negative signal for TCR nanoclustering), and (ii) the stabilization of the repressor Bcl-6, which dampens the expression of rate-limiting enzymes for glycolysis (here detected as a negative signal for TCR nanoclustering).

The inhibition of glycolysis seems to be important for the generation of long-lived CD8$^+$ $T_M$ cells (19, 20), but it also has a negative impact on CD4$^+$ and CD8$^+$ T cell activation (14–17). This renders it counterintuitive to associate the increased TCR nanoclustering induced by 2-DG treatment in CCR5$^{-/-}$ lymphoblasts with increased sensitivity upon antigen recall. We nonetheless addressed this experimentally by limiting the 2-DG treatment time (to enhance TCR nanoclustering prior to antigen recall), and by analyzing lymphoblast re-stimulation shortly after antigen exposure. This strategy revealed the enhanced production of IL-2 in 2-DG-treated compared to control (vehicle-treated) re-stimulated CCR5$^{-/-}$ lymphoblasts. This occurred in an antigen-dose-dependent manner, suggesting increased antigenic sensitivity in the 2-DG-treated lymphoblasts. The 2-DG treatment also increased IL-2 production in re-stimulated WT lymphoblasts, although the effect was less notable, probably because CCR5 signals already attenuate glycolysis in these cells. In contrast to IL-2, 2-DG treatment impaired WT and CCR5$^{-/-}$ lymphoblast proliferation, another effect of antigenic re-stimulation. The discrepancy between IL-2 and proliferation results might indicate that glycolysis is essential for the generation of the biomass necessary for cell division, but not for the initial TCR-induced signaling involved in IL-2 transcription - at least at the time point analyzed. More studies are needed to confirm this.

The present results suggest that the functional link between CCR5 and Bcl-6 is central for the inhibition of glycolysis in CD4$^+$ $T_M$ cells. Bcl-6 expression is repressed when IL-2 signaling is

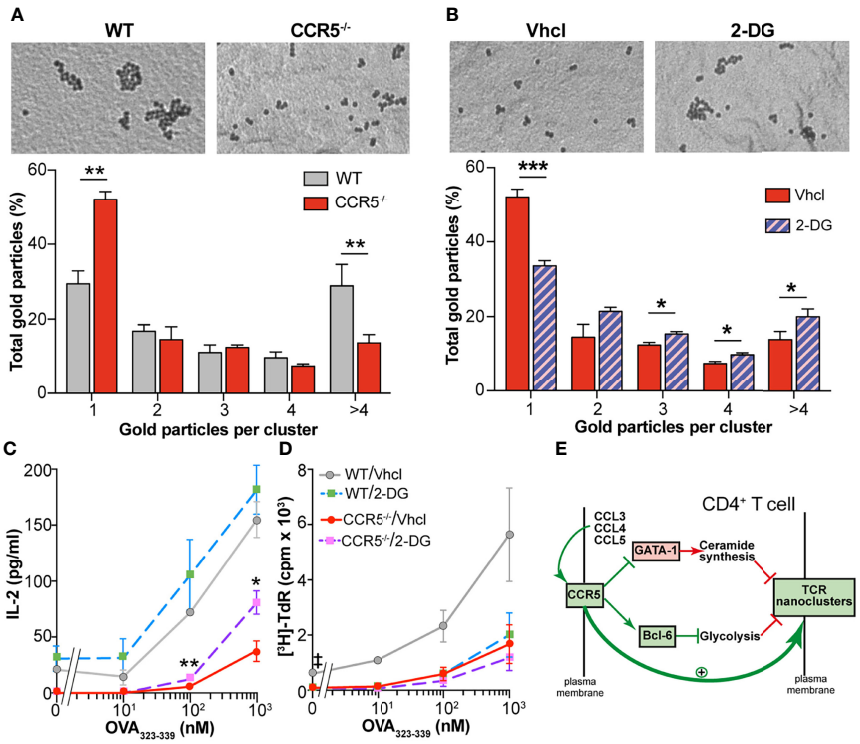


**FIGURE 5** | Inhibition of glycolysis increases TCR nanoclustering in CCR5$^{-/-}$ cells. **(A)** Analysis of TCR nanoclustering by EM in OT-II WT and CCR5$^{-/-}$ lymphoblasts (WT, *n*=5 cells, 11,339 particles; CCR5$^{-/-}$, *n*=5 cells, 9,347 particles). Top: A representative small field image shows gold particle distribution in the cell surface replicas of anti-CD3ε-labeled cells. Bottom: quantification (means ± SEM) of gold particles in clusters of the indicated size in WT (gray) and CCR5$^{-/-}$ cells (red). **(B)** OT-II CCR5$^{-/-}$ lymphoblasts were expanded in the presence of IL-2 (see Figure 1A), and incubated with the glycolysis inhibitor 2-DG over the last 24 h of expansion (day 7). Lymphoblast surface replicas were stained with anti-CD3ε and TCR nanoclustering analyzed by EM. Top: representative small field images show gold particle distribution in the cell surface replicas. Bottom: quantification (means ± SEM) of gold particles in clusters of the indicated size in vehicle- (solid red; *n*=5, 9,347 particles) and 2-DG-treated cells (hatched violet; *n*=5, 11,993 particles). Data are means ± SEM. ***p < 0.001, **p < 0.01, *p < 0.05 one-tailed Student *t* test **(A, B)**. **(C, D)** OT-II WT and CCR5$^{-/-}$ lymphoblasts were incubated with 2-DG over the last 24 h of expansion, washed extensively to remove the inhibitor, and then co-cultured with irradiated splenocytes previously loaded with the $OVA_{323-339}$ peptide. IL-2 **(C)** and cell proliferation **(D)** were determined after 24 h of re-stimulation-Data are means ± SEM (*n*=3). **p<0.01, *p<0.05 (for comparisons between Vhcl- and 2-DG-treated CCR5$^{-/-}$ cells), ‡p < 0.05 (for comparisons between Vhcl- and 2-DG-treated WT cells); two-tailed Student *t* test with Holm-Sidak correction for multiple comparisons. **(E)** Model proposed for the regulation of TCR nanoclustering by CCR5. It is here proposed that autocrine/paracrine activation of CCR5 fosters TCR nanoclustering by triggering two independent signals in CD4$^+$ $T_M$ cells: (i) the inhibition of GATA-1 translocation into the nucleus, and (ii) the stabilization of the glycolytic repressor Bcl-6. More details are available in the text.

elevated (21). Since IL-2 signaling is limited in the $T_M$ cell differentiation conditions (driven by IL-15), it is coherent that Bcl-6 levels should be higher in $T_M$ than in $T_E$ cells, but curiously, this only occurred in CCR5-proficient $T_M$ cells. Previous studies have reported no difference in IL-2 expression between CCR5$^{-/-}$ and WT $T_M$ lymphoblasts; indeed, IL-2 expression is reduced in antigen-experienced CCR5$^{-/-}$ cells after re-stimulation ( (6) and this study). It is therefore unlikely that the low Bcl-6 levels in CCR5$^{-/-}$ $T_M$ lymphoblasts should be a consequence of negative signals provided by autocrine IL-2 production.

How CCR5 signaling induces and/or stabilizes Bcl-6 levels deserves investigation. STAT3 deletion in CD8$^+$ T cells reduces Bcl-6 expression during the transition of effector to memory cells (44), and low Bcl-6 levels and impaired $T_M$ cell function have been found in humans with dominant-negative STAT3 mutations (45). Since CCR5 triggers STAT signaling (28), CCR5-proficient $T_M$ cells might increase Bcl-6 mRNA levels through a STAT3 pathway not operative in CCR5-deficient cells. Nevertheless, preliminary experiments have shown no major differences in phospho-STAT3 levels between WT and CCR5$^{-/-}$ $T_M$ cells (data not shown).

An intriguing point is that the enhanced glycolysis of CCR5$^{-/-}$ $T_M$ cells is not associated with any increased glucose uptake. Whereas the $T_E$ and $T_M$ lymphoblasts showed clear divergence in their 2-DG uptake and the expression of some glucose transporters, these differences were independent of CCR5 expression. The upregulation of HK2 and PKM2 might explain the increased glycolytic flow in CCR5$^{-/-}$ $T_M$ cells while having no effect on glucose transporter expression. Glucose uptake in lymphocytes might occur by facilitated diffusion through GLUT transporters following a concentration gradient (46). HK2 catalyzes the rate-limiting phosphorylation of glucose to glucose-6-phosphate, which not only provides the initial substrate for glycolysis but removes glucose from equilibrium, favoring its continued diffusion through GLUTs. Pyruvate kinases catalyze the irreversible transphosphorylation between phosphoenolpyruvate and

adenosine diphosphate to form pyruvate, another rate-limiting step in glycolysis. There are several isoforms expressed in mammals, which differ in terms of substrate affinity and catalytic efficiency (47). PKM2 is upregulated in cells with a high anabolic profile since its dimeric form is less active. This not only leads to the accumulation of glycolytic intermediates and their diversion to other biosynthetic pathways, but also to the reduced import of pyruvate into the mitochondria.

In summary, CCR5 signaling appears to be a key regulator of glycolytic metabolism specifically in $CD4^+$ $T_M$ cells. Mechanistically this regulatory activity relies on the stabilization of the glycolytic repressor Bcl-6, which controls the expression of rate-limiting glycolytic enzymes. More important is the observation that the inhibition of glycolysis enhances the valency and frequency of TCR nanoclusters, a factor determining the re-stimulation response of $CD4^+$ $T_M$ cells to low doses of antigen (6). By hampering the glycolytic pathway and modulating ceramide biosynthesis, CCR5 may foster TCR nanoclustering in $CD4^+$ $T_M$ cells, making them more efficient in responding to antigen re-exposure. In humans, *ccr5Δ32* homozygosity, which leads to functional CCR5 deficiency, does not cause immunodeficiency but is linked to a greater probability of certain pathogens, including influenza (48), causing fatal infections. Interestingly, $CD4^+$ $T_M$ cell function seems to be very important in the protective response against these pathogens (40, 49). Thus, CCR5 might decisively maximize $CD4^+$ $T_M$ cell responses by inhibiting glycolytic metabolism, and increase antigenic sensitivity through the induction of TCR nanoclustering.

## DATA AVAILABILITY STATEMENT

The raw data supporting the conclusions of this article will be made available by the authors, without undue reservation.

## ETHICS STATEMENT

The animal study was reviewed and approved by CNB and the Comunidad de Madrid (PROEX 277/14; PROEX 090/19).

## AUTHOR CONTRIBUTIONS

SM and RB conceived the study.RB, MGdC and RAL designed the metabolic experiments. AM-L performed EM analyses. RB and LR-G performed most of the experiments and interpreted the data. AG-M contributed materials and technical support. ARdM contributed ideas and technical support. SM and RB wrote the manuscript. All authors read, discussed and edited the manuscript. All authors contributed to the article and approved the submitted version.

## FUNDING

This research was funded by the Spanish Ministerio de Economía y Competitividad (SAF2017–83732-R to SM), the projects PID2020-116303RB-I00/MCIN/AEI/10.13039/501100011033 (to SM) and PID2019-110183RB-C21/MCIN/AEI/10.13039/501100011033 (to AR), the Comunidad de Madrid (B2017/BMD-3733/IMMUNOTHERCAN-CM to SM; P2018/BAA-4343-ALIBIRD2020-CM to AR), and the Merck-Salud Foundation (to SM). AM-L was a recipient of the *Formación del Personal Universitario* predoctoral fellowship from the Spanish Ministry of Education (FPU13/04430).

## ACKNOWLEDGMENTS

We thank D. Sancho (CNIC) for providing reagents, RM Peregil (CNB) for technical assistance, MC Moreno and M.A. Sánchez for flow cytometry services (CNB), and MT Rejas and M Guerra for assistance with EM (CBM-SO).

## SUPPLEMENTARY MATERIAL

The Supplementary Material for this article can be found online at: https://www.frontiersin.org/articles/10.3389/fimmu.2021.722320/full#supplementary-material

## REFERENCES

1. Luqman M, Bottomly K. Activation Requirements for $CD4^+$ T Cells Differing in CD45R Expression. *J Immunol* (1992) 149:2300–6.
2. Lillemeier BF, Mortelmaier MA, Forstner MB, Huppa JB, Groves JT, Davis MM. TCR and Lat Are Expressed on Separate Protein Islands on T Cell Membranes and Concatenate During Activation. *Nat Immunol* (2010) 11:90–6. doi: 10.1038/ni.1832
3. Schamel WW, Arechaga I, Risueño RM, van Santen HM, Cabezas P, Risco C, et al. Coexistence of Multivalent and Monovalent TCRs Explains High Sensitivity and Wide Range of Response. *J Exp Med* (2005) 202:493–503. doi: 10.1084/jem.20042155
4. Schamel WW, Alarcon B, Minguet S. The TCR Is an Allosterically Regulated Macromolecular Machinery Changing Its Conformation While Working. *Immunol Rev* (2019) 291:8–25. doi: 10.1111/imr.12788
5. Kumar R, Ferez M, Swamy M, Arechaga I, Rejas MT, Valpuesta JM, et al. Increased Sensitivity of Antigen-Experienced T Cells Through the Enrichment of Oligomeric T Cell Receptor Complexes. *Immunity* (2011) 35:375–87. doi: 10.1016/j.immuni.2011.08.010
6. Martín-Leal A, Blanco R, Casas J, Sáez ME, Rodríguez-Bovolenta E, Rojas I, et al. CCR5 Deficiency Impairs $CD4^+$ T-Cell Memory Responses and Antigenic Sensitivity Through Increased Ceramide Synthesis. *EMBO J* (2020) 39:e104749. doi: 10.15252/embj.2020104749
7. Martín-Blanco N, Blanco R, Alda-Catalinas C, Bovolenta ER, Oeste CL, Palmer E, et al. A Window of Opportunity for Cooperativity in the T Cell Receptor. *Nat Commun* (2018) 9:2618. doi: 10.1038/s41467-018-05050-6
8. Molnar E, Swamy M, Holzer M, Beck-Garcia K, Worch R, Thiele C, et al. Cholesterol and Sphingomyelin Drive Ligand-Independent T-Cell Antigen Receptor Nanoclustering. *J Biol Chem* (2012) 287:42664–74. doi: 10.1074/jbc.M112.386045
9. Beck-Garcia K, Beck-Garcia E, Bohler S, Zorzin C, Sezgin E, Levental I, et al. Nanoclusters of the Resting T Cell Antigen Receptor (TCR) Localize to Non-Raft Domains. *Biochim Biophys Acta* (2015) 1853:802–9. doi: 10.1016/j.bbamcr.2014.12.017
10. Wang F, Beck-Garcia K, Zorzin C, Schamel WW, Davis MM. Inhibition of T Cell Receptor Signaling By Cholesterol Sulfate, A Naturally Occurring Derivative of Membrane Cholesterol. *Nat Immunol* (2016) 17:844–50. doi: 10.1038/ni.3462

11. Buck MD, O'Sullivan D, Pearce EL. T Cell Metabolism Drives Immunity. *J Exp Med* (2015) 212:1345–60. doi: 10.1084/jem.20151159
12. Maciver NJ, Michalek RD, Rathmell JC. Metabolic Regulation of T Lymphocytes. *Annu Rev Immunol* (2013) 31:259–83. doi: 10.1146/annurev-immunol-032712-095956
13. Ohradanova-Repic A, Boes M, Stockinger H. Role of Metabolism in Regulating Immune Cell Fate Decisions. *Front Immunol* (2020) 11:527. doi: 10.3389/fimmu.2020.00527
14. Chang CH, Curtis JD, Maggi LB, Faubert B, Villarino AV, O'Sullivan D, et al. Posttranscriptional Control of T Cell Effector Function by Aerobic Glycolysis. *Cell* (2013) 153:1239. doi: 10.1016/j.cell.2013.05.016
15. Wang R, Dillon CP, Shi LZ, Milasta S, Carter R, Finkelstein D, et al. The Transcription Factor Myc Controls Metabolic Reprogramming Upon T Lymphocyte Activation. *Immunity* (2011) 35:871–82. doi: 10.1016/j.immuni.2011.09.021
16. Stark JM, Tibbitt CA, Coquet JM. The Metabolic Requirements of Th2 Cell Differentiation. *Front Immunol* (2019) 10:2318. doi: 10.3389/fimmu.2019.02318
17. De Oca MM, De Labastida Rivera F, Winterford C, Frame TCM, Ng SS, Amante FH, et al. IL-27 Signalling Regulates Glycolysis in Th1 Cells to Limit Immunopathology During Infection. *PloS Pathog* (2020) 16:e1008994. doi: 10.1371/journal.ppat.1008994
18. O'Sullivan D, van derWindt GWJ, Huang SCC, Curtis JD, Chang CH, Buck MDL, et al. Memory $CD8^+$ T Cells Use Cell-Intrinsic Lipolysis to Support the Metabolic Programming Necessary for Development. *Immunity* (2014) 41:75–88. doi: 10.1016/j.immuni.2014.06.005
19. Sukumar M, Liu J, Ji Y, Subramanian M, Crompton JG, Yu Z, et al. Inhibiting Glycolytic Metabolism Enhances $CD8^+$ T Cell Memory and Antitumor Function. *J Clin Invest* (2013) 123:4479–88. doi: 10.1172/JCI69589
20. Man K, Kallies A. Synchronizing Transcriptional Control of T Cell Metabolism and Function. *Nat Rev Immunol* (2015) 15:574–84. doi: 10.1038/nri3874
21. Oestreich KJ, Read KA, Gilbertson SE, Hough KP, McDonald PW, Krishnamoorthy V, et al. Bcl-6 Directly Represses the Gene Program of the Glycolysis Pathway. *Nat Immunol* (2014) 15:957–64. doi: 10.1038/ni.2985
22. Zhang J, Bi G, Xia Y, Li P, Deng X, Wei Z, et al. Transcriptional Regulation of T Cell Metabolism Reprograming. In: *Advances in Experimental Medicine and Biology*. New York LLC: Springer. (2017). 131–52. doi: 10.1007/978-94-024-1170-6_3
23. Buck MDD, O'Sullivan D, Klein Geltink R II, Curtis JDD, Chang CH, Sanin DEE, et al. Mitochondrial Dynamics Controls T Cell Fate Through Metabolic Programming. *Cell* (2016) 166:63–76. doi: 10.1016/j.cell.2016.05.035
24. Sena LA, Li S, Jairaman A, Prakriya M, Ezponda T, Hildeman DA, et al. Mitochondria Are Required for Antigen-Specific T Cell Activation Through Reactive Oxygen Species Signaling. *Immunity* (2013) 38:225–36. doi: 10.1016/j.immuni.2012.10.020
25. Li W, Zhang L. Rewiring Mitochondrial Metabolism for $CD8^+$ T Cell Memory Formation and Effective Cancer Immunotherapy. *Front Immunol* (2020) 11:1834. doi: 10.3389/fimmu.2020.01834
26. Ogando J, Saéz ME, Santos J, Nuevo-Tapioles C, Gut M, Esteve-Codina A, et al. PD-1 Signaling Affects Cristae Morphology and Leads to Mitochondrial Dysfunction In Human $CD8^+$ T Lymphocytes. *J Immunother Cancer* (2019) 7:151. doi: 10.1186/s40425-019-0628-7
27. Paik S, Jo EK. An Interplay Between Autophagy and Immunometabolism for Host Defense Against Mycobacterial Infection. *Front Immunol* (2020) 11:603951. doi: 10.3389/fimmu.2020.603951
28. Lacalle RA, Blanco R, Carmona-Rodríguez L, Martín-Leal A, Mira E, Mañes S. Chemokine Receptor Signaling and the Hallmarks of Cancer. *Int Rev Cell Mol Biol* (2017) 331:181–244. doi: 10.1016/bs.ircmb.2016.09.011
29. Matti C, Legler DF. CCR5 Deficiency/CCR5Δ32: Resistant to HIV Infection at the Cost of Curtailed $CD4^+$ T Cell Memory Responses. *EMBO J* (2020) 39: e105854. doi: 10.15252/embj.2020105854
30. Molon B, Gri G, Bettella M, Gomez-Moutón C, Lanzavecchia A, Martinez AC, et al. T Cell Costimulation by Chemokine Receptors. *Nat Immunol* (2005) 6:465–71. doi: 10.1038/ni1191
31. González-Martín A, Gómez L, Lustgarten J, Mira E, Mañes S. Maximal T Cell-Mediated Antitumor Responses Rely Upon CCR5 Expression in Both CD4(+) and CD8(+) T Cells. *Cancer Res* (2011) 71:5455–66. doi: 10.1158/0008-5472.CAN-11-1687
32. Floto RA, MacAry PA, Boname JM, Mien TS, Kampmann B, Hair JR, et al. Dendritic Cell Stimulation by Mycobacterial Hsp70 Is Mediated Through Ccr5. *Science* (2006) 314:454–8. doi: 10.1126/science.1133515
33. Franciszkiewicz K, Le Floc'h A, Jalil A, Vigant F, Robert T, Vergnon I, et al. Intratumoral Induction of CD103 Triggers Tumor-Specific CTL Function and CCR5-Dependent T-Cell Retention. *Cancer Res* (2009) 69:6249–55. doi: 10.1158/0008-5472.CAN-08-3571
34. Camargo JF, Quiñones MP, Mummidi S, Srinivas S, Gaitan AA, Begum K, et al. CCR5 Expression Levels Influence NFAT Translocation, IL-2 Production, and Subsequent Signaling Events During T Lymphocyte Activation. *J Immunol* (2009) 182:171–82. doi: 10.4049/jimmunol.182.1.171
35. Choi WT, An J. Biology and Clinical Relevance of Chemokines and Chemokine Receptors CXCR4 and CCR5 in Human Diseases. *Exp Biol Med* (2011) 236:637–47. doi: 10.1258/ebm.2011.010389
36. Chan O, Burke JD, Gao DF, Fish EN. The Chemokine CCL5 Regulates Glucose Uptake and AMP Kinase Signaling in Activated T Cells to Facilitate Chemotaxis. *J Biol Chem* (2012) 287:29406–16. doi: 10.1074/jbc.M112.348946
37. Taub DD, Hesdorffer CS, Ferrucci L, Madara K, Schwartz JB, Goetzl EJ. Distinct Energy Requirements for Human Memory CD4 T-Cell Homeostatic Functions. *FASEB J* (2013) 27:342–9. doi: 10.1096/fj.12-217620
38. Soto-Heredero G, Gómez de las Heras MM, Gabandé-Rodríguez E, Oller J, Mittelbrunn M. Glycolysis – A Key Player in the Inflammatory Response. *FEBS J* (2020) 287:3350–69. doi: 10.1111/febs.15327
39. MacLeod MKL, Clambey ET, Kappler JW, Marrack P. CD4 Memory T Cells: What Are They and What Can They Do? *Semin Immunol* (2009) 21:53–61. doi: 10.1016/j.smim.2009.02.006
40. McKinstry KK, Strutt TM, Kuang Y, Brown DM, Sell S, Dutton RW, et al. Memory $CD4^+$ T Cells Protect Against Influenza Through Multiple Synergizing Mechanisms. *J Clin Invest* (2012) 122:2847–56. doi: 10.1172/JCI63689
41. Rogers PR, Dubey C, Swain SL. Qualitative Changes Accompany Memory T Cell Generation: Faster, More Effective Responses at Lower Doses of Antigen. *J Immunol* (2000) 164:2338–46. doi: 10.4049/jimmunol.164.5.2338
42. London CA, Lodge MP, Abbas AK. Functional Responses and Costimulator Dependence of Memory $CD4^+$ T Cells. *J Immunol* (2000) 164:265–72. doi: 10.4049/jimmunol.164.1.265
43. Van Der Windt GJW, O'Sullivan D, Everts B, Huang SCC, Buck MD, Curtis JD, et al. CD8 Memory T Cells Have a Bioenergetic Advantage That Underlies Their Rapid Recall Ability. *Proc Natl Acad Sci USA* (2013) 110:14336–41. doi: 10.1073/pnas.1221740110
44. Cui W, Liu Y, Weinstein JS, Craft J, Kaech SM. An Interleukin-21-Interleukin-10-STAT3 Pathway Is Critical for Functional Maturation of Memory $CD8^+$ T Cells. *Immunity* (2011) 35:792–805. doi: 10.1016/j.immuni.2011.09.017
45. Siegel AM, Heimall J, Freeman AF, Hsu AP, Brittain E, Brenchley JM, et al. A Critical Role for STAT3 Transcription Factor Signaling in the Development and Maintenance of Human T Cell Memory. *Immunity* (2011) 35:806–18. doi: 10.1016/j.immuni.2011.09.016
46. Marko AJ, Miller RA, Kelman A, Frauwirth KA. Induction of Glucose Metabolism in Stimulated T Lymphocytes Is Regulated by Mitogen-Activated Protein Kinase Signaling. *PloS One* (2010) 5:e15425. doi: 10.1371/journal.pone.0015425
47. Ruiz-Iglesias A, Mañes S. The Importance of Mitochondrial Pyruvate Carrier in Cancer Cell Metabolism and Tumorigenesis. *Cancers (Basel)* (2021) 13:1488. doi: 10.3390/cancers13071488
48. Falcon A, Cuevas MT, Rodriguez-Frandsen A, Reyes N, Pozo F, Moreno S, et al. CCR5 Deficiency Predisposes to Fatal Outcome in Influenza Virus Infection. *J Gen Virol* (2015) 96:2074–8. doi: 10.1099/vir.0.000165
49. Nelson SA, Sant AJ. Imprinting and Editing of the Human CD4 T Cell Response to Influenza Virus. *Front Immunol* (2019) 10:932. doi: 10.3389/fimmu.2019.00932


**Conflict of Interest:** The authors declare that the research was conducted in the absence of any commercial or financial relationships that could be construed as a potential conflict of interest.

# Advantages of publishing in Frontiers

**OPEN ACCESS**
Articles are free to read for greatest visibility and readership

**FAST PUBLICATION**
Around 90 days from submission to decision

**HIGH QUALITY PEER-REVIEW**
Rigorous, collaborative, and constructive peer-review

**TRANSPARENT PEER-REVIEW**
Editors and reviewers acknowledged by name on published articles

**Frontiers**
Avenue du Tribunal-Fédéral 34
1005 Lausanne | Switzerland

**Visit us:** www.frontiersin.org
**Contact us:** frontiersin.org/about/contact

**REPRODUCIBILITY OF RESEARCH**
Support open data and methods to enhance research reproducibility

**DIGITAL PUBLISHING**
Articles designed for optimal readership across devices

**FOLLOW US**
@frontiersin

**IMPACT METRICS**
Advanced article metrics track visibility across digital media

**EXTENSIVE PROMOTION**
Marketing and promotion of impactful research

**LOOP RESEARCH NETWORK**
Our network increases your article's readership